DEVELOPMENT OF A THIN STEEL STRIP CASTING PROCESS

Final Report

April 1994

Work Performed Under Contract No. FC07-92ID13086

For
U.S. Department of Energy
Assistant Secretary for
Energy Efficiency and Renewable Energy
Washington, DC

By
Armco Research and Technology
Armco, Inc.

DEVELOPMENT OF A THIN STEEL STRIP CASTING PROCESS

Final Report

April 1994

R. C. Sussman, Program Manager
R. S. Williams, Principal Investigator

Prepared for the
U.S. Department of Energy
Assistant Secretary for
Energy Efficiency and Renewable Energy
Washington, DC

Prepared by
Armcor Research and Technology
Armcor, Inc.
Middletown, OH 45043

DISCLAIMER

TABLE OF CONTENTS

APPENDICES

1.0   EXECUTIVE SUMMARY

This project was a comprehensive effort to develop the promising technology of direct strip casting to the point where a pilot scale program for casting carbon steel strip could be initiated. All important aspects of the technology were being investigated so that requirements of the pilot program could be accurately estimated, as well as the prospects for technical and economic success. The program was terminated early due to a change in business strategy of the primary contractor, Armco Inc., whereby the focus of most future business development is to be directed at specialty steels and not low carbon steel. At the time of termination, the project was on target of all technical milestones and under budget.

The major part of the project was on the casting of strip at the experiment casting facility. A newly commission caster, capable of producing direct cast strip of up to 12 inches wide in heats of 1000 and 3000 lbs was employed for the development work. A total of 81 1000-1200 lbs heats were cast as well as one test heat of 3000 lbs. Most produced strip of from .016 to .085 inches in thickness. Reliability of the process was excellent for the short casting times involved. Quality was generally poor from modern hot strip mill standards, but the technologies and practices necessary for good surface quality were identified and steady progress was being made.

The experimental effort followed a three part experimental plan:

1. Get control of the critical process variables;

2. Develop practices which permitted casting of complete heats with reasonable strip properties;

3. Perform an experiment design to explore the critical process variables.

Parts 1 and 2 where complete when the program terminated. Several key technologies where developed. These include the "gapless" casting technique using abradable refractory materials, the flexible mounting system for the nozzle components to reduce thermal distortion and cracking, continuous wheel surface conditioning using an array of grit blasting nozzles, a new "jet nozzle" design to reduce freezing in the nozzle channel,

1

thermal imaging of the solidified strip surface to ascertain the proper heat transfer conditions, and several mathematical and physical models used to improve equipment and operating practices.

Armco Inc., Research & Technology, requests approval from the U.S. Department of Energy of this proposal and allocation of funds for accomplishment.

2.0 **BACKGROUND: DEVELOPMENT OF THIN STRIP CASTING**

An important new frontier is being opened in steel processing--the emergence of thin strip casting. Casting steel directly to thin strip has enormous benefits in energy savings by potentially eliminating the need for hot reduction in a hot strip mill. This has been the driving force for numerous current research efforts into the direct strip casting of steel.

One of the processes with considerable promise is the casting of steel onto a single cooling substrate. The process has already led to the production of thin foil (0.001 to 0.005" thick) by the planar flow casting process at speeds of up to 75 ft/sec. If a derivative of this process could be developed to cast steel, particularly carbon steel, in the thickness range of 0.030 - 0.125", a method of thin strip casting might be realized.

The U.S. Department of Energy initiated a program to evaluate the development of thin strip casting in the steel industry. In earlier phases of this program, planar flow casting on an experimental caster was studied by a team of engineers from Westinghouse Electric Corporation and Armco Inc. The results of that program are described in Report DOE/ID/12443-2 (DE88013689). It was concluded by the engineers and the DOE monitors that further work was warranted on both the planar flow casting process and also on a related single wheel technique, the melt overflow casting process, that was briefly investigated at the end of the product.

A subsequent research program, DE-FC07-88ID12712, was designed as a fundamental and developmental study of both casting processes. The goal of the full program was to ascertain the potential of these processes for further research effort on a pilot plant scale. Casting experiments were to be conducted on a small diameter casting wheel and a large 7 ft diameter integrally cooled wheel. The original experimental plan and focus is shown in Table I with a "go/no-go" decision point as Task 4.3 about 9 months into the program. This decision point was extended for 3.5 months when problems developed with the operation of the 7 ft diameter casting wheel and the wheel had to be fully disassembled and redesigned.

After the water modeling and substrate studies were completed, planar flow casting trials were made on the 7 ft diameter caster. The ideal substrate and nozzle design were used in one of the trials. From the results, it was concluded that the method could not be used successfully for carbon steel without major modifications. A new design of the pouring box and nozzle was conceived and constructed. This combined the best features of the melt overflow and planar flow methods. This

3

design was used on one trial before the program was halted due to exhausting allocated funds. Continuous strip about 0.045 in. thick was cast at a very high productivity rate of 360 ft/min. Although the strip had a more ripply surface than the strip produced by the melt overflow method on the small wheel caster, the process has definite promise for further investigation.

Sixty-one trial heats were cast to thoroughly evaluate the melt overflow casting process on the small wheel caster. The initial strip was very poor in both top and bottom surface quality. Other problems encountered were freezing at the melt pool/wheel interface, leakage of liquid steel under the wings of the nozzle, gap control between the nozzle and wheel, and others. Many step-by-step improvements were made to overcome these problems. Eventually, the process evolved to the point where silicon-killed carbon steel strip that had very attractive surface quality on both the top and bottom could be consistently produced. This process was chosen for the go/no-go trial heats and five consecutive heats of carbon steel were successfully cast. Equipment and refractory supply limitations restricted the thickness of the strip that could be produced in this phase of the program to a maximum of around 0.035". A modest amount of the strip was cold rolled with no apparent quality problem. Cup expansion tests demonstrated very good formability.

The experimental work demonstrated the feasibility of casting carbon steel strip by either the melt overflow process or the modified planar flow process. Further experimental work was needed to increase the thickness of the cast strip, improve top surface quality, gauge control, and increase the process productivity.

TABLE 1

PROCESS DEVELOPMENT OF THIN STRIP STEEL CASTINGS

Task	1988				1989		
	1/18	4/18	7/18	10/18	1/18	4/18	7/18
1. Investigate Fundamental Casting Parameters							
1.1 Water Modeling of Planar Flow Nozzle	-|-|-|-|-|-						
1.2 Analytical Investigation of Planar Flow and Overflow Feeding Systems	-|-|-|-|-|-						
2. Establish the Effects of Casting Wheel Substrate	-|-|-|-|-						
3. Design and Perform Preliminary Casting Experiments for Screening Purposes							
3.1 Melt Overflow Casting Experiments	-|-|-|-|-|-|-|-						
3.2 Planar Flow Casting Experiments		-|-|-|-|-|-					
4. Go/No Go Decision and Selection of Candidate Process for Final Evaluation							
4.1 Establish Criteria for Making Go/No Go Decision and for Candidate Process Approval				-			
4.2 Go/No Go Decision				-			
4.3 Selection of Candidate Process				-			
5. Optimization of Candidate Process and Evaluation of Electromagnetic Casting Devices							
5.1 Development of Experimental Plan				-|-			
5.2 Investigation of Electromagnetic Enhancement of Nozzle Exit Flow				-|-|-|-|-|-|-|-			
5.3 Conduct Casting Experiments				-|-|-|-|-|-|-|-			
6. Processing & Characterization of Cast Material							
6.1 Development of Experimental Plan			-				
6.2 Characterization of As-Cast Material				-|-|-|-|-|-|-			
6.3 Characterization of Processed Material				-|-|-|-|-|-|-|-			
7. Techno-Economic Analysis of Candidate Process					-|-|-		
8. Specification of Scaled-Up Technology							
8.1 Specification of Scaled-Up Equipment and Facility Size					-		
8.2 Conceptual Design of Scaled-Up Equipment					-|-|-|-|-|-		
8.3 Establish Program Costs to Evaluate Scaled-Up Process					-|-|-|-		
9. Project Management							
9.1 Management Plan	-						
9.2 Program Management	-|-|-|-|-|-|-|-|-|-|-|-|-|-|-|-|-|-						
9.3 Reporting	-|-|-|-|-|-|-|-|-|-|-|-|-|-|-|-|-|-						
9.4 Review Meetings	-|-|-|-|-|-|-|-|-|-|-|-|-|-|-|-|-|-						
9.5 Technology Transfer						-|-|-	
9.6 Critical Review of Single-Wheel Casting Technologies	-|-|-						

```
        0       3       6       9       12      15      18
```

2/25/88
JWY069A

3.0 JUSTIFICATION FOR WORK

The cost reduction potential for any direct thin steel strip casting technique includes at least three important areas:

- Energy and Yield Savings
- Operating Cost Savings
- Process Capital Cost Savings

If the proposed direct strip casting process using a single water cooled quench wheel can be successfully developed from a technical and operational standpoint, it has potential for cost savings over conventional hot rolled strip production practice in each of the three areas.

Extensive detail on cost reduction and energy assessment for direct steel strip casting is contained in the initial Armco Inc. proposal for this program, "Process Development of Thin Strip Steel Casting", Volume I - Technical Proposal, March 27, 1987.

As further justification for the continuance of this direct steel strip casting project, a report was prepared assessing the state of the art in single wheel strip casting technology. This report is included as "Volume 3 - Critical Review of Single Wheel Casting Technologies" of this Proposal.

4.0 TECHNICAL APPROACH

1. Current Status

A a result of the previous work sponsored by DOE on open channel strip casting, as well as subsequent studies funded by Armco Inc., low carbon steel strip of good surface quality and properties can be routinely cast in the thickness range of 0.025 - 0.035 in, at rates of about 150 fpm. This success is the primary motivation for continued development of open channel casting. The current upper limit in thickness appears to be determined by equipment and material restrictions, and is not a fundamental process limitation. Specifically, we have verified that cast thickness can be increased by increasing the contact length of the melt pool to the wheel or by lowering the casting speed. The primary effect in both cases is the increase of time for solidification to occur. The melt pool height is currently limited by the available refractory brick and wheel diameter and the lower casting speed by the motor and drive assembly. Increasing melt pool contact length on the substrate and decreasing casting speed should result in thicker strip.

Additionally, several important casting parameters such as wheel diameter, nozzle geometry, and casting angle, were fixed during the previous trials. A systematic study of these parameters should produce more optimum conditions for thick strip casting. Finally, because the pool height is approaching the 3 inch channel width, significant edge effects are being observed, the most damaging being an increased tendency to freeze-off at the nozzle due to the reduced heat flow from the melt at the edges.

All of these limitations, with the exception of the narrow width problem, were to be addressed in the original contract under Task 5 Optimization of Candidate Process and Evaluation of Electromagnetic Casting Devices. During the time since work was stopped on the previous contract, Armco has completed much of the work originally proposed for the 3 inch wide casting machines and an upgrade to a 12 inch wide caster is currently underway. We propose to continue that work under the new Steel Initiative program, following much the same path set forth by the original DOE strip casting research program. In order to facilitate the experimental trials, we would limit the initial electromagnetic evaluation to a study involving model experiments only. Furthermore, in order to insure that the encouraging results thus far lead to a timely and successful commercialization of direct strip casting, development of the key technologies that must be addressed at the start of a future pilot plant project will be initiated in this proposed phase of the research. This requires some new work on specific technologies as well as an increased schedule for process development. The additional work is discussed below.

2. New Work

As the results already obtained support the technical feasibility of direct strip casting of carbon steels, we propose to address several capabilities which would be required to proceed to a pilot plant program. Namely, we would initiate design and construction of a strip coiler, determine the requirements for a pouring box heater to maintain melt temperature, and establish the unique sensing requirements for control of the open channel casting process. Additionally, the analysis of data from the casting trials must be strengthened and incorporated into a set of design tools consisting of simple parametric models of the process. Refractory materials and techniques must be developed which will allow for reliable, continuous operation for long durations and commercial strip widths. These new areas will be discussed further below.

Coiler: While the design of the coiler is not seen as involving any advances in current technology, it is required in order to conduct a systematic investigation of the metallurgical properties of as-cast and processed strip. An "off-the shelf" design might not be available for the widths and speeds of interest. Furthermore, special considerations must be given to the cooling of the coil in order to control the metallurgical properties.

Pouring Box Heater: The pouring box heater would be necessary for longer casting trials, as many trials now end in nozzle freeze-off when the steel temperature superheat falls too low. This will be of greater concern for larger heats. The heating requirements for the high throughput box will be fairly demanding and thus may involve some engineering innovation. Several techniques such as plasma and induction heating will be explored.

Sensing and Control: As demonstrated by the nozzle gap control technique developed during the last contract period, the sensing and control requirements for open channel casting are likely to be unique. The residence time for the material once it enters the open channel is very short and, because the process is near-net-shape, there is a limited amount of down stream processing possible to correct such things as poor gauge control or metallurgical structure problems. Tight, precise control of the process is therefore paramount. Melt delivery temperature is one aspect already mentioned Additionally, there are the metal level control in the nozzle, the overall gauge control, maintenance of substrate finish, and cooling rate as determined by the substrate temperature and finish. A separate subtask will incorporate sensing and control development for each of the critical areas.

Model Development The experimental data, along with further mathematical modeling of the heat transfer and solidification, will be used to formulate parametric relationships which will serve as design tools for further caster development. While the original analysis may require somewhat sophisticated mathematical techniques such as finite difference models, the final formulation will be a simple system of formulas which shall be suitable for inclusion into an engineering spreadsheet. This will allow quick evaluation of tradeoffs in the design of casting devices for specific product ranges and productivities.

Refractory Development: As expected, there have been many critical refractory problems in the development of thin strip casting, particularly with the material for the nozzles. As previously stated, the primary limitation on the cast thickness is currently the availability of suitably sized refractories. Furthermore, the materials and practices necessary for fabricating nozzles with widths in the range of commercial strip must be developed. Therefore, we propose to include in the program a refractory supplier as a subcontractor. This would give us access to the required engineering and production capabilities. Incorporating the refractory vendor as a subcontractor will forge a closer relationship, with the commitment to insure the availability of the components needed for the completion of this program and for eventual production supplies. Such commitment by all participants is required if the technology is to achieve commercial success.

Large Width Casting: In addition to the specific process improvements listed above, we propose to construct a large casting wheel. The design is complete and construction is underway. When completed, this modified wheel will be used to further optimize the process with reduced edge effects, and would allow questions vital to a pilot scale design, to be examined. Examples of scaling problems are: design of a melt feeding system for large widths, refractory fabrication techniques for wide nozzles, mechanical stability for increased widths and durations, and strip handling.

In order to fully exploit the additional capabilities of the wider casting wheel and to allow for a reasonable period of process development, the experimental program will be extended to a total of three years. This will permit nearly 2-1/2 years of experimental work at the larger strip widths and thus advance the technology to the point where a reasonable assessment can be made of the risks and benefits of a full scale pilot program.

3. Technology Assessment and Pilot Plant Specification

The technology review and economic analysis will occur toward the end of the experimental casting trials. This review will evaluate the status of the strip

9

casting technology with respect to competing technologies. Furthermore, any deficiencies in the current development will be flagged and possible approaches for resolution outlined. This study will form the basis of a recommendation for a full pilot plant program, which will be included in the final report for this program.

5.0 STATEMENT OF WORK

This research was to establish the technical and economic feasibility of casting low carbon steels on a single wheel caster utilizing the Open Channel Casting Process (OCC). The program included the following elements:

(1)   Establish the ability of the OCC process to produce commercial quality steel strip throughout the range of 0.030 in. to 0.125 in. thickness with widths up to 12 in., and to determine the scalability for full pilot production. This work involved experimental trials on the 12 in. wide casting wheel at the Armco Research Casting Laboratory, using heat sizes of 1000 lb. The early termination of the program precluded the planned move to 3000 lb. heats.

(2)   Perform a technical and economic assessment of the OCC process including a comparison with competing thin strip, thin slab, and conventional continuous slab casting processes. Establish technical and commercial thresholds for proceeding to a pilot installation.

(3)   Determine requirements for a pilot scale program including a conceptual design and costs.

TASK 1: MODEL DEVELOPMENT

1.1 Tundish and Nozzle Fluid Flow

- Extend the mathematical model developed on the previous program to the conditions existing for the 12 in. wide caster.

- Using a combination of mathematical simulation as developed above, and physical modeling with water in a full scale tundish mockup, establish the requirements for consistent liquid metal feeding of the OCC nozzle.

1.2 Heat Transfer and Solidification

- Develop a mathematical model of heat transfer through the substrate. The model will predict heat flux and solidified shell thickness as a function of position on the cast substrate, for casting parameters such as melt pool length, heat transfer coefficient.

- Analyze the substrate temperature data from Task 2.2 using the above model to obtain heat flux information. Use this information to establish the heat transfer coefficient and solidification rate. Issue a topical report on the modeling work.

1.3 Parametric Model Development

- Create a parametric model, through a synthesis of the data from the 12" casting trials, the model results of Tasks 1.1 and 1.2, and fundamental analysis. This model will serve as a design tool by establishing the relationship between the desired casting rate and thickness and basic design parameters such as casting speed, rim thickness and diameter, cooling flow, and melt pool depth.

TASK 2: PROCESS DEVELOPMENT

2.1 Experimental Plan for 12" Casting Trials

- Define the target strip qualities and the most important process parameters, taking into consideration the possibility of post cast thermo-mechanical treatments. Develop an experimental plan for the 12" wide casting trials to improve strip quality and thickness.

2.2 Open Channel Casting of up to 12" Widths

- Modify pouring box and nozzle designs to improve strip quality.

- Develop nozzle designs and casting techniques which result in increased strip thickness.

- Explore effects of the substrate and substrate condition on the uniformity of heat extraction.

- Using the local temperature sensing in the 12" wheel substrate, vary the cooling flow in order to determine the effect of substrate temperature on the process and product.

- Enhance metal cleanliness through improved shielding and pouring box modifications to reduce slag formation and accumulation in the melt pool.

TASK 3: PROCESS ENHANCEMENTS

3.1 Pouring Box Heating

- Determine cooling rates in ladle and pouring box, and project to larger heat sizes (i.e. 1000 and 3000 LB and eventual production). Establish the degree of temperature control required for the OCC casting process. Select a heating technology (induction, plasma arc, radiation, etc.) for experimental study.

- Design and fabricate a heating device and establish its effectiveness on melt pool temperature stabilization using either a tundish mockup, or by incorporating into the actual cast trials.

3.2 Electromagnetic Devices

- Examine the feasibility of electromagnetic devices to enhance the containment of the sides and bottom of the liquid metal pool, in order to allow greater ferrostatic head pressures for a given nozzle to wheel gap.

- Perform low temperature metal simulations to test concepts.

- Prepare a topical report and meet with DOE for a go/no decision on the application of MFD to the caster.

3.3 Measurement and Control

- Identify critical sensing and control requirements and specify possible solutions. Include:

    - Gap control,
    - Metal level control in the pool,
    - Substrate temperature sensing and control,
    - Melt temperature measurement,
    - On-line strip gauge measurement.
    - On-line substrate profile measurement

- Implement sensing and control as required by the casting program.

TASK 4: REFRACTORY DEVELOPMENT

- Develop pressed zirconia material for use in OCC nozzles; include both monolithic and composite designs.

- Design nozzle mounting mechanism and refractory retainer.

- Develop operating practices for the experimental nozzles.

- Explore alternative methods for producing zirconia nozzles, such as casting, extrusion, etc.

- Explore use of other traditional steelmaking refractories (e.g. high purity alumina, slide gate material) for OCC nozzles.

TASK 5: Process Enhancement with MFD Device

- Design MFD device based on evaluation of Task 3.2.

- Fabricate and install MFD device on 12 in. caster.

- Establish test procedures for evaluation of MFD.

- Incorporate MFD device into process development trials.

TASK 6: PROCESSING AND CHARACTERIZATION OF CAST MATERIAL

- Define the important finished product properties, and develop an experimental plan to enhance these values by modification of the casting process, melt chemistry, and post cast thermo-mechanical treatments.

- Characterize the material produced in Task 2.2. Key properties will be the thickness and gauge consistency, surface finish, and formability. Establish the necessary post cast treatments to achieve improved finished properties.

- Modify the casting procedure and alloy composition to improve the final strip properties. The objective is to establish the potential of the strip cast material as a commercially viable, high tonnage product.

TASK 7: TECHNOLOGICAL AND ECONOMIC ASSESSMENT OF DIRECT STRIP CASTING

7.1 Technical and Economic Analysis

- Conduct a technical assessment analysis of the direct strip casting process that includes, but is not limited to, the following items: Product quality, process economics (product yield, maintenance, consumables, capital, labor, casting rate, and energy costs), scalability, and competitive technologies. Issue topical report.

7.2 Selection of Product

- Select a target product or products which offer the most promise of success for a pilot plant venture and which are consistent with the goals of the Metals Initiative. Include an analysis of the customer requirements for delivery of material from the pilot plant.

7.3 Specification of Pilot Plant

- Determine machine requirements and facility size for a pilot scale casting operation.

- Develop a conceptual design for the scaled-up equipment and an experimental plan for the advancement of strip casting technology.

- Establish the costs for implementing the pilot scale project.

- Conduct a review with the U.S. Dept. of Energy of the program results and the pilot plan to determine if further work is justified.

TASK 8.0: PROJECT MANAGEMENT

8.1 Management Plan

- Produce a specific management and manpower plan for the project and review with DOE.

- Review existing recording and reporting forms and procedures.

8.2 Program Management

- Perform all necessary oversight of the project to insure that budget and schedule are on target.

- Initiate any changes necessary to achieve the primary objectives of this contract, with notification and approval from DOE where required.

8.3 Reporting

- File quarterly progress reports to DOE as well as monthly telephone reports to the technical monitor.

- Provide written annual reports for distribution to the public by DOE. The annual report will include information on the current scope, schedule, and budget, and progress achieved to date. Proprietary information will not be included unless protected by patent. A complete written final report will be submitted to DOE soon after the contract expires.

- Provide additional informal communication with DOE as requested, as well as produce individual topical reports whenever they are deemed appropriate.

15

8.4 Review Meetings

-   Conduct a kick-off meeting with DOE and all contractual parties after the establishment of the manpower plan.

-   Hold semiannual on-site review meetings with DOE contract and technical monitors.

-   Conduct a final project review at the end of the contract period.

8.6 Technology Transfer

-   Do all necessary and normal outside reporting to maintain industry awareness of the program, including attending conferences and publishing technical papers, following established external reporting approval procedures.

-   Perform any additional activities requested by DOE to inform the industry and the public of the program, with due consideration of proprietary rights.

8.7 Holding Company

-   Form a holding company to own and license all background and new intellectual property derived from this and subsequent government supported, Metals Initiative projects. Complete an intellectual property agreement including background patents.

6.0 TASK-BY-TASK REPORT

6.1 Task 1.0 Model Development

The ultimate goal of the mathematical modeling was to develop tools to assist the other tasks; specifically, models to predict the results of Open Channel Casting given a set of operating parameters, as well as design tools based on the mathematical description of the process. These tools would be used for specification of the pilot plant facility.

Several model were successful in this role. A physical model of the tundish and nozzle fluid flow was used to make modification in flow control systems in both the nozzle and tundish. A transient thermal model of the nozzle gave some insights which were key to developing a material design and operating practice which nearly eliminated this danger of freezing in the nozzle. Finally, a solidification model was used to redesign the casting substrate and eventually to establish the feasibility commercial production rates on reasonably sized single wheel casting machines.

6.1.1 Tundish and Nozzle Fluid Flow

A combination of physical modeling using water and finite difference mathematical modeling has been applied to the problem of developing uniform feeding of molten metal to the open channel casting nozzle. A full scale Plexiglas model of the pouring box and wheel was constructed. In order to be certain of similarity, the geometry, the volumetric flow, and the wheel surface speed were all matched to the actual cast values. This presented some difficulty, as the mechanism for pick up of material by the wheel is different. Metal leaves the melt pool by solidification; for a fixed pool geometry, increasing the cast speed decreases the thickness of material leaving the pool, as there is less time for solidification to occur. The thickness is roughly proportional to the inverse of the square-root of the residence time in the pool. The linear feet per unit time of strip increases proportionally with the speed. The overall effect of speed on material flow through the caster is thus proportional to the square root of the speed.

In the case of the water model, liquid water exits the pool by viscous drag, which increases with wheel speed. The thickness of the layer extracted increases with casting speed, and hence the overall material throughput of the water model increases faster than a linear relationship. It should then be possible to match the volumetric flow rate of the caster to that of the water model for a certain speed wheel. For the smooth Plexiglas wheel of the water model, this speed where the flows matched occurred over 300 fpm, was much higher than that used for OCC. Therefore, the drag of water out of the pool was enhanced by covering the smooth wheel with cloth. It was then possible to match the volumetric flow and the wheel speed to experimental values from the strip caster at 200 fpm at 2.5 inch head. These conditions were then used in the actual tests.

A series of die flow studies investigated variations on the flow control configuration of the pouring box. The original dam design resulted in very poor mixing in the box. An improved dam design was found, but the best mixing was with no dam installed, using instead a receiving cup for the submerged entry nozzle from the ladle (Fig. 1). The original purpose of the cup was to control the initial splash during fill of the box.

The water model was used to study the effects of weir modifications on the flow in the melt pool. Specifically, the dog-bone style weir, which have notches in the weir next to the wall to increase flow near the wall, was modeled to determine if flow into the corners of the melt pool was enhanced as desired. While the velocity of the melt stream along the corner past the weir was not noticeably greater than that in the center portion, the quantity of flow was increased. This was confirmed quantitatively using a colorimeter mounted on a track to allow the measurement point to be scanned across the width of the flow after exit from the pool. The increased flow into the corner regions acted to prevent corner freeze-up, a frequent problem during open channel casting. Additional water model trials were used to evaluate the effect of weir to nozzle lip positioning. The weir forms the back portion of the melt pool, so that this positioning establishes the aspect ratio of the pool. Positioning the weir closer to the wheel enhances the effect of the dog-bone style channels in directing flow into the relatively cool corners of the nozzle. However, smaller weir to wheel distances result in larger aspect ratios which might create a less stable flow pattern in the melt pool. We have seen from our casting experiments that any disruption in the flow near the meniscus of melt connecting the nozzle lip to the wheel is likely to result in a defect in the strip, due to the uneven heat transfer conditions across the width which result (See Section 6.2.2).

Three weir to wheel spacings were examined, starting from the position then in used in the experimental trials of 1.75 inches, and moving forward to 1.25 and 0.75 inches. The results, which were corroborated using the mathematical model, showed that the overall flow pattern was unchanged at 1.25 inches, but became unstable at 0.75 inch separation (Fig. 2). At the larger spacings, the moving substrate causes a rolling action in the pool. At the top surface, the flow is toward the back, in the direction of the weir. This has been verified for the actual casts by observing the motion of slag and refractory on the pool surface. At the smallest weir spacing, this stable rolling action was disturbed. The flow would vary with time, and it was impossible to predict with certainty the direction of flow. For the remainder of the casting trials, the weir was positioned at the intermediate position, as the best compromise between aggressive corner flow and pool stability.

Another series of water modeling trials examined the idea of a ported weir design. Rather than a continuous opening beneath the weir for flow, the weir is brought down to contact the nozzle floor, and holes or ports are placed at regular intervals in the weir to allow for fluid flow (Fig. 3). One motivation for this study was the desire to stiffen the nozzle assembly by bringing the weir down to restrain the nozzle floor from bowing up in the center. Water models trials of several ported weir designs revealed dead spots in the flow

in the regions between the ports. These dead zones could only be removed by reducing the spacing between the weir ports to something less than the nozzle to weir gap.

A finite difference model of flow in the box and nozzle was created and verified using the water model. This model verified that the new jet stream nozzle design was very effective in directing a stream of fresh metal at the lower lip of the nozzle where freeze-ups are most likely to originate. Several variations in jet geometry were modeled and the best candidate was selected for trial.

The original plan was to use the mathematical model to guide the pilot scale tundish and nozzle design. This still appears a very workable approach. Full details of tundish modeling are given in Appendix I.

6.1.2   Heat Transfer and Solidification

Freeze-up Prediction: A transient thermal model of the nozzle was developed to predict freeze-up conditions in the OCC nozzle. The model showed that no reasonable casting conditions resulted in freezing in the nozzle under steady state conditions. The danger exists in the initial stages as the relatively cold nozzle extracts heat from the molten metal. The most significant controllable factors in avoiding freezing were the nozzle preheating, which acted to reduce the heat load from the nozzle, and the casting speed, which determined the rate at which fresh, hot metal is supplied to the nozzle. Contrary to our previous notions, nozzle conductivity, heat transfer from the nozzle to wheel, and surface radiation have very little effect on the probability for freeze-off. Weir height above the nozzle floor was seen to be significant, however, as it affected the velocity of metal in the critical freezing area.

In order to make the model useful for designing casting conditions, a parameter was needed to quantitatively rank casting conditions as to the probability of freezing, It seemed reasonable to assume that freezing would no longer be possible once the temperature of the liquid at the nozzle wall, as predicted by the heat transfer coefficient and the transient heat flux into the wall, was equal to or greater than the liquidus. Accordingly, each case modeled was ranked by the time required to reach this balancing heat flux. Separate times are calculated for the center of the nozzle floor and the corner. The corner region is more susceptible to freezing because each volume element of metal flow loses heat to both the floor and the wall of the nozzle. More details are given in Appendix I, and the development of a guide to casting procedure based on this model is discussed below in section 6.1.3.

Solidification and Thermal Model: One of the critical requirements of this program was a capability to predict strip thickness as a function of casting parameters. A solidification model could determine the size and speed of a wheel capable of casting strip of the required gages at commercially acceptable productivities. Moreover, an accurate thermal model can be used to determine operating windows for a given casting machine, such as

the experimental 12 inch wide caster. Accordingly, a transient, finite difference model of the OCC process called STRIP1D was developed (see Appendix II).

Fig. 4 is a schematic of the OCC process showing how the model was divided into five zones: Zone I, the melt pool; Zone II, out of the pool where no solidification takes place, but contact with the wheel is maintained; Zone III, where the strip has left the substrate and the inside surface of the wheel is still being spray cooled; Zone IV, which has no spray cooling, but a water pool exists, and Zone V, where spray cooling resumes prior to reentry into Zone I. Zone 1 is where all solidification occurs. The melt pool is considered semi-infinite, though nozzle convection effects can be modeled using an option to specify heat flux along the solidification front. Heat transfer from the solidified strip to the substrate is determined by an interfacial heat transfer coefficient. The determination of this coefficient, which is not constant, is discussed in the next paragraph. Heat transfer from the substrate to the water follows well establish spray and pool cooling formula. Radiant and convective cooling to the air is included, though their effect is small. The substrate can be multi-layered, which allows oxide or clad layers to be modeled. The output includes not only thermal profiles of the substrate and the strip, but also cast thickness, which is determined by the position where the portion of the material of a given element below the solidus temperature is at least 70%.

The heat transfer coefficient between the solidified strip and the substrate is always a difficulty in these models, and is often determined by matching predicted thickness to cast thickness to yield an average coefficient. In this model, different rules were developed for the Zone I and Zone II. Based on observations of the cast trials, a small air gap is assumed to exist in Zone II, and an appropriate heat transfer coefficient is used. Much effort went into determining the best approach for Zone I. It is expected that the heat transfer coefficient varies greatly in this region because of the rapid thermal shrinkage of the solidified shell. An imperical formula was adopted which assumed an initial period of very high thermal contact, then a decay proportional to the inverse of the contact time (Appendix II, eqn. [6]). The adjustable constants of this model were fitted to the thickness data from the cast trials. Experiments, described in detail in Appendix II, were conducted using chill blocks with thermocouples at various depths to determine the substrate heat flux directly. The measured thermal profiles were then compared to those predicted by the solidification model and found to agree. Other results from the literature were also successfully predicted, using these parameters, even for contact times several orders of magnitude greater. We feel that the resulting model is more robust than prior models in the literature, where a single, average heat transfer coefficient is used. Our model accurately reflects the decrease in heat transfer efficiency with contact time. We can thus make predictions for larger casting wheel with deeper pools and hence longer contact times with more confidence.

6.1.3   Parametric Study

The most important requirement of our modeling work on this program was that it remain relevant to experimental work in progress and would develop into tools for the design and operation of the pilot equipment. Our modeling capabilities proved to be very flexible and responsive to the needs of the casting program. The water model was a very valuable tool as we made modifications in the flow control devices in the tundish. The early efforts in solidification modeling were shifted somewhat to address the freeze-up problem which was plaguing the experimental effort at the time. The model results eliminated some possible solutions by revealing the negligible effect of nozzle conductivity and nozzle to wheel heat transfer. The same insight resulted in the jet stream nozzle design described in Section 6.2.2 to reduce the amount of heat extracted from the metal before it reaches the critical region. Also, the time-to-heat balance freeze-up parameter discussed above suggested a reasonable casting strategy of starting fast and dropping the speed as the nozzle heated up.

The most fully developed of the design tools is STRIP1D. The model was transferred to a PC platform for ease of use. The program was modified to allow for change of speed during the simulation to model the operating strategy used to defeat the freeze-ups. Multicomponent substrate wheels were included to aid in the selection of cladded wheels. Output files were added to predict the temperature of thermocouple which were installed on the casting wheel to control surface temperature, a critical variable. Finally, STRIP1D was used extensively to develop the basic design of the pilot cast for Task 7.

6.2   Task 2.0   Casting Process Development

6.2.1   Experimental Plan

Process development does not generally proceed in a linear fashion, particularly in leapfrog efforts such as direct casting of steel strip. Rather, it is expected that the development will proceed in relatively abrupt steps. We considered three stages of competence required for our twelve inch casting development, which resulted in three separate phases for the experimental plan. Of course, the boundaries between the phases were fuzzy, with up to six months of transition time.

Phase I: The goal of this phase was to establish control over the basic parameters of Open Channel Casting (OCC): melt temperature and chemistry, cooling substrate, casting speed, and nozzle geometry. Many of our early trials were aborted due to cracking or distortion of the nozzle during preheat. Some casts terminated early due to cracking of the nozzle. In short, we could not maintain the desired nozzle geometry for the full trial. Achieving this capability was the objective of Phase I.

Experiments to achieve this objective required discrete changes in nozzle geometry and refractory joint design, or more radical changes such as the use of refractory board liners.

21

These experimental parameters are not continuous and the results (cracked or not cracked) are also of a qualitative nature which dictates a different experimental methodology from the response surface technique employed for optimization of well established processes. The direction is provided by the skillful interpretation of the results by the experimenter, who must determine the most important areas to seek improvement in order to make the next step in proficiency. Sufficient boldness in proposing new approaches and competence of execution is essential to avoid blind alleys and overlooked solutions.

Phase II: This phase was to establish casting parameters which consistently yield acceptable product for a full trial heat. Qualitative changes were still required, but there would be fewer branches of the decision tree, and each was more thoroughly explored by a set of trials varying the major OCC controlling variables of speed, temperature, and melt pool depth.

Phase III: In this phase, the casting parameters which were established to produce complete casts in Phase II will be optimized using the techniques of statistically designed experiments. We were at the beginning of Phase III when the project terminated. For more details of the method developed for formulating the Experimental Plan, please refer to Appendix III.

6.2.2   Open Channel Casting

Equipment upgrade and Startup: A general, somewhat chronological discussion of the 12 inch casting trials follows. The casting logs for all heats are included in Appendix IV.

The OCC experiments were all performed on the newly commissioned, Armco Wide Strip Casting Facility. While the equipment performed well, the Phase I problem of maintaining cast geometry was proving very difficult to solve by the means identified in the project proposal. We had good success on the 3 inch casting program with nozzles machined from high quality, pressed zirconia brick. This material is very hard, resistant to slag attack, non-wetting to steel, and a good insulator. The original intent was to develop pressed zirconia brick, learn how to construct nozzles from multiple pieces, machine nozzles to fit our wheel radius and cast as before with a small gap between the nozzle and the wheel. The gap would be maintained using the electric sensors developed on the last program. Good material in the form of pressed zirconia brick became available from NARCO, a project partner. Techniques were developed to machine the complex shapes required to form a multipiece OCC nozzle from the brick. Support mechanisms were altered to accommodate the thermal expansion of the material without compromising the critical geometric constraints of close fit to wheel and no leaks at joints. Preheat practices were developed to minimize the danger of freeze-up while controlling the nozzle distortion.

In the end, only very marginal success could be claimed. Few full heats where cast, and most were aborted before or just after start due to nozzle breakup or distortion. A radical change in practice was suggested.

Other than the materials themselves, many incremental improvements were made during the course of this program in the mounting systems used to hold the refractory components in place. The overriding theme was to minimize unnecessary mechanical restraints to allow the materials to expand, while maintaining pressure in the joints which defined the critical geometry, i.e. the nozzle lip and the joints between the sidewalls and the floor. The weir was constructed to sit directly on the floor of the nozzle. Two equally spaced, semicircular slots were machined in the weir to allow fluid flow to the melt pool (see discussion in Section 6.1.1). It was hoped that the floor of the nozzle would be constrained from bowing by the pressure of the weir. This was not successful, as the bow occurred regardless and opened the joints at the walls. A system of spring loaded hold downs was developed to keep moderate compressive stresses on the joints. This proved very successful and was adapted as the nozzle was redesigned for longer contact lengths and jet stream flow devices (Fig. 5).

Another area of improvement was in the preheat practice. By softening and diverting the preheat gas burners, a more even heating of the structure was obtained. Preheating temperature was increased to reduce the potential for initial freeze-up. Insulating backup material was added behind all external surfaces to reduce thermal gradients. High conductivity inserts in the backup lining were tried in an attempt to homogenize the temperature on the working face, but with limited success. Electric preheaters adapted from a high temperature furnace proved inadequate: A a major investment in time and expense would have been required to deliver the required thermal power to the nozzle piece (see Section 6.3.1). Many problems were associated with the cool down which occurred after the burners where shut off as the wheel moved into contact with the wheel just prior to casting. Many refractory materials crack from thermal shock when quickly cooled from the very hot temperature at the end of preheat. Much effort was made to reduce this cool down period, and a major improvement came by leaving the nozzle in contact with the wheel during the entire preheat, making position adjustments to avoid crushing the nozzle as the temperature increased. The practice of long (6 hour), soft preheating, high preheat temperatures (2100°F), and minimal, flexible mounting, along with the developments in nozzle refractory, resulted in nearly 100% success rate for

23

casting. At the end of the project, only damage caused by debris on the wheel caused nozzle failure during a run.

Strip Cracking

Once we began to produce strip in reasonable quantities, it became very apparent that the cracking problem noted on the 3 inch cast material was very much worse on the 12 inch strip. Cracks in cast material are well known problems in conventional casting. They are usually formed in the region of the advancing solidification front where the material is very weak. Only a few tenths of a percent strain is required to create a crack. External strains on the material must be avoided, and the thermal strains must also be controlled. One approach is to increase the hot strength of the solidified strip. This we did through additions of columbium and titanium to refine the grain structure. These elements form very fine oxide in the melt, which serve as nucleation sites for the primary solidification. The thickness of the interdendritic, mushy zone is thus reduced. The first heat with these additions, #858, was the first to be fully cast without breaking up. This practice, with some adjustment in addition levels, was continued through the rest of the experimental trials. Additions were made of .08% Columbium to the furnace for an aim content of 0.05%, while .29% titanium was added to the ladle to achieve an aim content of .20%. Five sources of strain to the strip were identified:

1. Non-homogeneous heat transfer to the substrate;
2. Stresses imparted by strip handling;
3. Disruptions in the meniscus at the nozzle lip.
4. Holes and cavities formed by gas evolution from the steel or the substrate;
5. Thermal stresses from the temperature gradient in the solidified strip;

Our efforts to reduce problems will be discussed in turn below.

Control of Heat Transfer: When the heat transfer varies significantly across the strip, regions of lower cooling remain hotter and thinner, and are pulled apart by surrounding cooler regions, which have higher strength and are shrinking faster. A major source of the non-homogeneity for our trials were scratches in the substrate. These were often caused by imperfections in the nozzle which lead to finning of metal between the nozzle and the wheel, or by material carried around the wheel and back into the nozzle. Improved nozzles helped this problem.

Wheel dressing during casting was also improved. The original system used a stack of 2 inch abrasive flapper wheels in contact across the wheel at the bottom dead center. The joints between the flapper wheels was not sufficiently cleaned so that longitudinal cracks appeared in the strip at every joint. A single piece abrasive wheel with staggered joints showed improvement, but every joint could still be distinguished and served as sites of

longitudinal cracks. An unsegmented abrasive wheel was better still, but the uniformity of the dressing action was poor, and the wheels failed frequently.   Consequently, an in-situ system was developed which allowed the entire surface of the casting wheel to be conditioned each revolution. The finish achieved by this system was very consistent, and the roughness could be adjusted over a wide range.

Another, more fundamental cause of inhomogeniety in heat transfer occurred due to the inevitable shrinkage of the solidified strip as it cooled on the substrate. In the region of the nozzle, where very high heat fluxes are present, any large decrease in heat transfer such as would be expected when a gap is formed between the strip and the wheel would have a dramatic impact on the local solidified thickness and temperature. Strip cast on a smooth substrate would show 1 to 5 dark longitudinal bands, indicating areas of good contact, with brighter, poor contact regions in between where the cracks where found. A rougher substrate reduced this tendency, particularly if grooves where machined into the wheel. It is felt that the rougher substrate controls the scale of the gap formation to be less than the strip thickness, and hence results in a more even heat transfer. The rougher surface also provides something of an escape path for gases released by the solidifying metal and rapidly heated substrate. The   conditioner allowed the roughness to be fixed at around 120 μ inches. Experiments using rougher substrates where planned to confirm these observations and to determined the optimum level of roughness.

Another approach to achieve improved thermal homogeneity is to reduce the shrinkage in the strip by maintaining a higher surface temperature. This not only decreases the total amount of shrinkage in the critical pool area, but also allows for increased creep in the strip to accommodate some of the strain. It was observed from a review of the video tapes of the exiting strip that streaking was not seen whenever the substrate surface temperature exceeded 700°F, measured prior to entry into the melt pool. The practice was established to maintain the surface temperature above 700°F, by adjustment of cast speed and cooling water. When this was done, streaking did not occur, though a more finely spaced pattern of light on dark patches would sometime be present and could be identified with the occurrence of small hot tears. The move from copper to steel substrate wheels permitted slower casting speeds while maintaining the desired surface temperature, thus permitting us to cast thicker strip without loss of quality. A combination of hotter surface temperatures and rougher wheel conditioning is seen as the proper direction to move for improved strip quality.

In order to work for direct strip casting, a very thin, uniform layer of flux would be required. A low temperature flux was procured from a vendor of conventional casting fluxes (CHIVIT) and deposited on the substrate after the dressing wheel using an electrostatic powder spray gun. Unfortunately, only one brief interval of casting using the flux was tried and no definitive results can be reported at this time.

Strip Handling: Video records of the casts revealed frequent forced movement of the strip as it lay on the wheel. Side-to-side movement was caused by the manual strip handling efforts downstream. Other times, the strip would impact the floor or other impediment and the entire arc from floor to pool would lift up. These events could readily be traced to cracks in the strip. A pinch roll system was installed on the floor close to the caster with speed synchronized to the primary caster drive. The practice was to operate with a catenary between the exit point on the wheel and the coiler. This eliminated the problems associated with downstream handling. Problems still persisted in that breaks in the strip from other causes required retreading the pinch roll, which was not always accomplished. At the thicker gages, the weight of the strip in the catenary could sometime result in strip breaks. This arrangement also left the strip on the wheel for more than 20 inches after leaving the melt pool; a time when the uneven cooling would be accentuated.

To further increase the mechanical support of the strip exiting the melt pool, a system consisting of a refractory stripper bar, a driven split roll runout table, and an upper pinch roll was added to the caster (Fig. 6). The drive was synchronized to the caster, with provision made for a slight offset of speed to adjust for shrinkage effects. Also, with the upper pinch roll disengaged, the table could be run at a slight overspeed or under speed to control the tension or compression imparted on the strip.

Operation of the runout table system proved very tricky. Because of the close coupling with the melt pool, there was very little margin of error in the speed setting of the upper pinch roll. If the roll was moving too fast the strip was pulled apart, too slow and a cobble occurred with disastrous consequences for the stripper bar and the wheel surface. Only the lower roll of this pair were driven, which might have accentuated the problem. The top roll of the pair rotated solely due to contact with the moving strip. The top roll could not be lowered after the start of cast because of the inertia of the stationary top roll and the vibrations associated with the action of lowering the roll. A design change was in progress to drive the upper pinch rolls separately from the runout table, and to provide power to both rolls. On the positive side, when the system worked, it provided some of the best strip with very stable operating conditions.

Disruptions of the Meniscus: The area of first contact of the molten metal to the substrate wheel is the most critical area for control of strip quality. A meniscus extends

between the bottom lip of the nozzle and the substrate. Any disruption in the meniscus causes a corresponding change in the thermal contact between the solidifying material and the substrate, which as discussed earlier, usually leads to cracking problems.

Premature solidification along the lower lip of the nozzle, referred to as "dams", was one common source of meniscus disruption. Even a small solid lump close to the lip can cause a variation in the normally planar flow pattern feeding the solidification zone. Two distinct causes of dams were penetration of metal into the region between the lower face of the nozzle and the wheel referred to as "finning", and freezing along the bottom runner caused by excessive thermal loading from the relatively cold nozzle material during the transient heat up phase (the "freeze-up" discussed early in Section 6.2.1 on modeling).

One cause of finning were cracks and shifts in the nozzle components. This was eliminated through the refractory development (Section 6.4) and improvements in the nozzle construction. The key design principle was to use simple butt joints and keep them under compression using spring loading at the critical region near the substrate. All joints were caulked with a refractory sealant which stayed pliable until very high temperatures. Also, the preheat procedure was lengthened to reduce thermal gradients, and the subsequent cooling period just before start of cast was minimized. The net result of these developments was that the geometry of the nozzle was very stable, and joints did not open up to allow finning near the lip. Along with the increase in preheat temperature and quick casting procedure to eliminate freeze-ups, this practice resulted in nearly 100% reliability of the nozzle performance during casting.

Once the more severe problems of freeze-up and finning where solved, more subtle effects of meniscus disruption became apparent. The mechanical stability of the caster was a major concern on a number of points. The effect of vibration could be seen in the thermal pattern of the strip exiting the melt pool. Vibration at low speeds was eliminated by a change in motor drives and reduction gearing.

Longer period variation in strip temperature distribution was caused by the variation in wheel radius with rotation, known as run-out. Run-out resulted in a variation in nozzle to wheel gap from near zero for gapless casting to the maximum run-out for the wheel. To minimize this, the maximum run-out on a cold wheel was set at .002 inches. Copper substrate wheels exceeding this run-out would be turned true by machining in place using a customized lathe. Steel substrates required off-line machining at a machine shop. Unfortunately, the run-out generally increased dramatically as the wheel heated up during casting. This was particularly true of the copper substrates where a .002 inch cold run-out could increase to .020-.030 inches, as measured by the capacitive gap sensors mounted at 135° BTDC position. Steel wheels would increase to only .006-.008 inches. Most of the hot run-out would disappear after cool down, but some increased permanent distortion would always appear so that the condition of the wheels would get increasingly bad.

27

Copper wheels would last anywhere from 3 to 6 heats before needing to be machined, depending on how high a surface temperature was allowed. Steel wheels could go longer if the external surface temperature was kept below 800°F, but we did not have enough trials on steel wheels to give a firm estimate of life.

The presence of run-out was apparent from the alternating light and dark image of the gap region as seen on video camera mounted to the side of the nozzle. The multiple camera recording made it possible to correlate the changes in gap to changes in the appearance of the strip exiting the pool. The effect was most noticeable when operating at low speeds where the outer surface temperature fell below 600°F. Dark bands would appear on the strip corresponding to areas of higher adhesion. These bands, numbering from two to five, would wander back and forth across the strip until a region of minimal gap was reached. The bands would then become mingled into a confused pattern, then re-emerge as separate bands. These patterns were evident on the cast strip and could be related to changes in surface quality, thickness, and cracking. In general, the minimum gap areas were thinner, with somewhat smoother top surface, and more prone to cracks. The effect on cast strip was less evident for conditions of more uniform heat transfer (substrate temperature >700°F).

Efforts to control the wheel distortion and lessen the variation of nozzle to wheel gap included stiffening the wheel assembly, controlling the maximum temperature rise, improving the high temperature strength of the substrate material, and adjusting the gap to compensate for the variation in wheel radius. Various schemes to stiffen the mount did not make much difference in the run-out. Changing from copper to steel wheels dramatically decreased the hot run-out as previously mentioned; but an order for high hot strength copper wheels was canceled at program termination. A modified design for mounting the rim which would change the constraint from inner to the outer faces was fabricated but not tested. Similarly, a the nozzle positioning system upgraded to fast servo motors and control software written to allow tracking of the wheel growth was not tested due to the premature termination of the program.

Increased Thickness

Increased thickness requires increased contact time between the melt pool and substrate for more solidification to occur. The interface heat transfer coefficient between the strip and the substrate is quite high (20,000 kW/C/M^2 initially from the fit of the mathematical model to the data) so that the major component of thermal resistance for casting thick strip is heat conduction through the solidified shell. For instance, doubling the interface coefficient used in the STRIP-1D model results in only a 25% increase in thickness when casting 2 to 3 mm thickness. It is also apparent from the videos of the cast trials, as well as the mathematical model from the previous program that the amount of molten material dragged from the melt pool and carried over on top of the solidified strip exiting the pool

is negligible for typical OCC conditions. Therefore, the only avenue for increasing cast thickness is increased contact time with the melt pool.

The contact time with the pool can be increased by either slowing the cast speed or by increasing the length of contact of the melt pool to the wheel. Initial attempts to use slower speeds were unsuccessful due to limitation of the wheel drive systems. Once these were corrected, the minimum cast speed was lowered from 75 to 28 FPM and the maximum thickness increase from .030 to .045 inches. These trials use 2-1/2 inch nozzles at 60° which results in 3.2 inches of pool contact. Unfortunately, lower cast speed implies lower material throughput, which means lower heat fluxes and hence lower temperatures. Lower temperatures in the nozzle resulted in an increase tendency for freeze-up. Lower temperatures of the substrate caused an increase in the inhomogenious heat transfer with the associated cracking problem as described previously.

Improved preheating practice reduced the tendency for freeze-up at low cast speeds, as did improved casting strategies where the speed was lowered more gradually. The addition of the surface sensing thermocouple (Section 6.3) allowed a more sophisticated casting strategy whereby the speed of casting was lowered only after the substrate had heated to the target temperature and then lowered only as long as the substrate temperature did not drop below the desired minimum. Also, the water cooling system for the caster was modified to operate initially with only one of three cooling zones active. The other two zones would turn on whenever the exit water temperature exceeded set limits. These limits where adjusted so that the inner surface temperature of the wheel, as measured with embedded thermocouples, would not exceed 230 F, which experience had shown was a safe limit with regards to wheel distortion. The best strip produced using these procedures was from .033 to .039 inch thick, with little or no cracks, produced at 135 to 150 FPM, using a 2 1/2 inch extended nozzle (4 to 5.9 inch melt pool contact).

The Jet Stream nozzle design allowed for a full heat to be cast at very low speeds (50 to 75 FPM), and very thick material was produced (.064 inch). The lower limit on the wheel surface temperature was ignored for this trial (Heat 000900), so that quality was poor. Also, while dam formation was not enough to stop the cast, small dams where found along the edges of the cast strip. Refinements in the nozzle design to increase flow into the corners might have prevented this problem.

Several casts of austenitic stainless steel were performed at the end of the program to take advantage of the decreased crack sensitivity to test the limits of the experimental caster for strip thickness. In order to facilitate the speedy termination of the program, the limitation on the casting wheel runout of .002 inch was relaxed; The steel wheel used had a runout of .009 inch. Also, the runout table and upper pinch rolls was not use because its operation was still not reliable. In spite of this, the cast was successful and a coil of material produced. Thickness averaged .043 inch at 150 FPM. A microstructural examination of the material reveal small cracks extending to the free surface on the upper side (away from wheel) of the strip. These cracks are interdendritic hot tears, indicating

29

that a the upper surface of the solidified strip is in tension (see Section 6.6). This is not surprising given large wheel runout and lack of secondary mechanical support. A second stainless trial, where the speed was quickly drop to the minimum of 28 FPM produced strip .065 to .080 inch thick, but of poor uniformity of gage and significant cracking.

6.3. Task 3.0 Process Enhancements

As with any extended process development, many improvements are made during the course of a series of experimental trials. This was particularly true of the Phase I and II portions of the Experimental Plan. Many of these modifications have been discussed in Section 6.2.2 which chronicled the experimental trials. However, several areas were recognized from the beginning as requiring special emphasis, for which separate sub tasks were formed. These were Task 3.1 Pouring Box Heating, Task 3.2 Electro-magnetic Devices, and Task 3.3 Measurement and Control. Specific engineering personnel were assigned to each of these tasks, or in the case of the Task 3.2, a subcontract was initiated with one of the program partners (Westinghouse). A separate topical report was generated for each subtask which have been included as an appendix. A brief review of each is follows.

6.3.1 Pouring Box Heating

The temperature of the liquid metal is a primary variable for all casting processes, and strip casting will be no exception. In a modern carbon steel melt shop, molten steel is poured from a ladle into a casting tundish. The variation in steel temperature from start to finish pour may be as much as 30 F, depending on casting rate and temperature stratification in the ladle. One of the goals of Phase III of the Experimental Plan was to determine the operating window of cast temperature for Open Channel Casting of quality strip. While this work was cut short, we did confirm that it was possible to cast over a relatively wide range of temperatures; 2805 to 3050°F, representing superheats of 45 to 290°F, though no assurance of quality can be made.

The situation for the experimental caster was much different due to the much larger ratio of surface area to volume of the ladles. Cast temperature dropped 30 to 40°F per minute or as much as 150°F over a full 1000 LB trial heat.. To improve control over this important cast parameter, an equipment modification was planned to add pouring box heating to the experimental caster. The sub task goal then became two-fold: To determine the technology necessary to achieve control over casting temperature for a pilot scale facility, and to select and install equipment to provide stable casting temperatures on the experimental caster.

One final additional goal of Task 3.1 was added due to the problems experienced early in the casting trials with adequate preheating of the box and nozzle. The transient freeze-up model discussed in Section 6.1.2 revealed the importance of preheating to reduce the amount of heat extracted from the melt as the internal surfaces of the box comes up to

molten steel temperatures. The target box preheat temperature was increased from 1900 to 2200°F to reduce the incidence of freeze-ups. This required very long, gentle preheat procedures to avoid thermal shock and distortion of the nozzle materials. A means was sought to automate the preheat cycle and to provide for higher effective preheat temperatures. Accordingly, increased benefit was assessed to those heating technologies which could provide preheating of the box as well as metal temperature control during casting.

Five commercially available technologies were considered:

1. Radiant Tube Heaters;

2. Radiant Electric Heaters;

3. Other Gas and Electric Heaters;

4. Induction Heaters;

5. Plásma Arc Torches.

Additionally, one non-commercial approach (forced air ovens) was investigated. For reasons of costs and flexibility, induction heating was selected. For a full discussion, please refer to Appendix V. An induction heated pouring box was designed and fabricated just as the decision was made to terminate the program. Because much of the expense for performing the pouring box heating trial already been incurred, approval was given for a trial to test the design. As discussed in the Appendix V, problems with stray field heating prevented a full test of the box.

Some conclusions can be drawn, however: Due to the limited residence time of the melt in the pouring box of a strip caster, a large power input is required and the equipment to control cast temperature would be fairly complex and expensive. A more likely approach for commercial production would be to provide for good metal temperature control in the ladle, with cooling and heating capability. Such technology exists in the form of ladle argon stirring, ladle arc furnaces, and Continuous Argon Stirred-Oxygen Blown ladle treatment stations. This would reduce the requirements at the caster to those available for continuous casting tundishes now, e.g. insulating tundish covers, plasma arc torches, etc.. which can maintain constant tundish temperatures for an extended cast, but are not designed to increase steel temperature in the box.

6.3.2   Electromagnetic Devices

While there are a number of areas where electrodynamic forces generated in the liquid metal could possibly benefit the Open Channel Casting Process, control of the meniscus at the nozzle gap to prevent leakage was identified at the start as the most important

31

application. The initial OCC nozzle concept, which required very precise control of the hot nozzle geometry and positioning, was seen as a potentially insurmountable challenge for the refractory development. To succeed, the gap between the lip of the nozzle and the casting wheel would have to be such that the surface tension of the molten steel would support the meniscus spanning the gap. The calculated maximum was around .02-.03 inches for the molten pool heights of interest. Maintaining such tight dimensional control over the hot refractory surface is not easy. If magneto-hydrodynamic forces could be use to stabilize the meniscus at larger gaps, the requirements on the refractory would be correspondingly reduced.

It was decided to break the investigation into electromagnetic enhancement into two components: A feasibility study was undertaken as part of Task 3 to select and evaluate gap containment concept; A separate Task 5 was added to provide for installation on the experimental caster, contingent on a positive result from the feasibility study. Westinghouse Electric Science and Technology Center was subcontracted as a program partner to conduct both parts of the study.

A careful, structured process for idea generation and selection resulted in five distinct concepts for electromagnet gap containment:

- Currents injected into the substrate wheel transverse to the cast direction along the gap;
- Current sheet (plate conductor) behind gap with current flowing perpendicular to the cast surface;
- Low frequency coil inside the casting wheel;
- Concentrated coil with current flowing transverse to the cast direction behind the gap;
- Two frequency approach combining the concentrated coil with a more remote, low frequency coil to provide more support.

For more details see Appendix VI.

A finite element model of each concept established the basic feasibility and design parameters. Each concept was then ranked according to effectiveness as an electromagnetic machine and for the mechanical complexity and ruggedness. The concentrated coil approach was the choice, with the two frequency approach seen as a possible enhancement if performance was marginal.

A bench top experiment confirmed the ability of the concentrated coil to impart forces on the metal at the nozzle lip in the correct direction. A more rigorously scaled physical modeling experiment was then constructed to prove the concept. Mathematical modeling was also used in the design process to select fundamental parameters such as number of conductors, frequency, and shape of coil.

The physical modeling experiments failed to show any ability of the design to enhance the containment of the metal at the nozzle lip. The experimental result appears to be correct and reflects unforeseen dynamic interactions of the magnetic field, the fluid flow, and the shape of the metal surface as it protrudes into the gap between the nozzle and wheel. Simply stated, while forces are apparently generated in the metal at the meniscus which are directed away from the gap, these forces rapidly diminish in any metal which extrudes into the gap region. Sufficient forces are not generated to prevent the turbulent flow from penetrating at times, and hence sealing of the nozzle is not improved. As a consequence of the negative result of the feasibility study, a "No-Go" decision was made for Task 5.

6.3.3 Sensor Development

As with any process, success in Open Channel Casting will depend on achieving control over critical process parameters. This implies a sufficient capability to sense these key variables, determine operating ranges, and establish these conditions during the course of a casting trial. Moreover, because of the speed of the OCC solidification, control response time must be much shorter than for conventional continuous casting. In conventional casters, 20 to 30 seconds is required to establish the outer shell of the strand, a major portion of which can be scarfed off if required for surface quality reasons. The entire solidification process for direct cast steel strip occurs in .5 to 2 seconds, and no further process steps are available to remove major flaws. Thus, some stringent control requirements are expected for OCC and Sub task 3.3 was initiated to develop the necessary capabilities.

Many aspects of the OCC process where examined for this task and some developments have been mentioned above in the discussion on Task 2.2, the casting trials. Seven areas will be discussed individually:

1. Gap Sensing, Gap Control, and Nozzle Positioning;;
2. Metal Level Sensing and Control
3. Substrate Temperature Sensing and Control;
4. Melt Temperature Measurement;
5. On-Line Strip Measurement;
6. Substrate Condition;
7. Thermal Imaging of the Strip.

Gap Sensing originally was expected to be a major requirement of OCC. In fact, a pneumatic sensor was developed which could measure gaps of up to .100 inch between the hot refractory face of the nozzle and the substrate wheel. Additionally, an outside vendor was in the final stages of development of a capacitance gauge with similar range and temperature capability. These developments might have played an important role in extending the life of the nozzle for longer casting trials. The nozzle positioning system underwent

several revisions. The final system was capable of actually tracking the wheel growth and the runout caused by the out-of-roundness of the wheel at elevated temperatures.

Metal level sensing and control is a critical area for OCC, as it directly determines the solidification length of the process and hence the cast strip thickness. A commercially available, optical triangulation sensor was selected along with a computer control package for stopper rod control. The mechanical actuator for rod positioning was developed by Armco and integrated with the purchased components to create a feedback control system for metal level control. Successful operation of the sensor required some additional development by Armco and the vendor in order to correctly sense the very bright, very low emissivity surface of molten carbon steel. Sensing was accurate to within +/- 1 mm and control was accurate to +/- 2 mm. This would correspond to around .5% variation in gage for a commercially sized caster (1 meter radius, 30° pool contact angle). With improved control over wave action in the melt pool, this control would undoubtedly improve. Finally, while the laser triangulation sensor was found to be most convenient for our experimental caster, the more conventional techniques of radiation and eddy current level sensing would probably be acceptable for a full size production caster.

As discussed in Section 6.2.2, substrate temperature appears to be a critical variable for OCC. Initially, only inner wall substrate temperatures were measured using thermocouples brazed into copper blocks made flush with the inside surface of the copper substrates. The thermocouple signals were converted to 4-20 ma signals before being transmitted via slip rings to the data acquisition computer. This technique allowed very accurate temperature measurement on a rotating device. Fig. 7 shows a typical trace from one of the five thermocouples in a row across the substrate. The periodic rise in temperature occurred as the instrumented portion of the inner surface passed through the bottom quadrant of the rotation where there was no spray cooling. This periodic increase in average substrate wall temperature may have contributed to the chronic problem of permanent wheel distortion mentioned in 6.2.2.

The outer wheel temperature was measured using a foil thermocouple in sliding contact with the wheel just before the nozzle. The accuracy of the measurement was verified by the agreement with the preheated water temperature after the wheel had come to thermal equilibrium with the water prior to casting. At the start of cast, the casting speed was used to control wheel temperature. Once the desired range of 500 to 800°F was reached, the speed was reduced to the predetermined test speed. The cooling water flows where then used to control outer wheel temperature. This was done manually by shutting and opening flow to one or more cooling zones. During the later trials, this function was automated by proportional controllers.

Melt temperature is considered an key variable in all casting processes. The superheat in the melt generally determines the relative sizes of the equiaxed and columnar solidification regions. Modeling results discussed in Section 6.1.2 suggest that the degree of initial superheat plays a major role in nozzle freeze-up. Unfortunately, this program was

34

terminated before Phase III of the experimental plan was executed, where a systematic exploration of key variables, including melt temperature would have revealed the range and degree of control required of the melt temperature sensing and control system. As it was, platinum based thermocouples in fused silica sleeves served well for the casting trials. Some commercially available temperature systems where reviewed and are discussed in Appendix VII.

On-line strip thickness measurement is considered absolutely essential to any direct strip casting project. Thickness variations across the width and along the width must be minimized to for successful cold rolling to final gauge. Accuracy of +/- 25 μm with a response time under .5 sec. is needed. Feed back could be to the metal level control system for long term (slow response) small variations, or to the casting speed control for quicker response. Sonar, eddy current, capacitive, radiation, x-ray, and optical triangulation methods were considered. X-ray, radiation, and optical methods are all suitable for the application, but optical methods were considered more practical for the experimental facility. A system was purchased, but not installed before the end of the program.

The substrate condition is probably the most enigmatic of the important process variables of Open Channel Casting. It is multidimensional as it encompasses chemical and mechanical properties, each of which can have multiple characteristic properties. However it is characterized, it undoubtedly plays a key role in the process, as all heat transfer occurs through this extended surface. The approach taken here was to avoid as much surface variation as possible with aggressive surface conditioning as discussed in Section 6.2.2. The effort was largely successful with the development of the on-line system. A laser scanning method of measuring multiple aspects of surface geometry and to a limited extend, oxide film development was briefly explored. The technique showed very good promise, but would require substantial development in signal processing and analysis systems.

Thermal imaging of the strip as it exits the melt pool is one way to determine the degree of uniformity of heat transfer required by the direct strip casting process as discussed in Section 6.2.2. A two dimensional imaging system was built to Armco specifications by a vendor in thermal imaging systems. Special attention to wavelength sensitivity is required to get accurate measurements at high temperature on a surface of varying emissivity. The real time false color video image produced could be video taped for analysis (see Fig. 8). The increased sensitivity of the system to thermal variations was beneficial for the determination of the desired substrate surface temperature. In principal, quantitative temperature measurement are possible, but the system was not fully exploited during the abbreviated casting program.

35

6.4   Task 4.0:   Refractory Development

As discussed in Section 6.2.2, the development of special refractories to meet the demands of Open Channel Casting was an important part of the program. A subcontractor, North American Refractories Company, was brought in at the start as a full program partner. Additionally, a significant allotment of Armco engineering hours and support committed to this task is indicative of the importance given to achieving refractory solutions to the OCC nozzle problem. This breathe of this program and the diligence of the team made possible the pursuit of several promising avenues. This development was a key to our successfully completing Phases I and II of the experimental program. In progress at the time of program termination was a broad investigation into the factors affecting component life and the requirements for OCC nozzles for longer casting times. Appendix VIII gives a complete description of the technical developments of the Refractories Development task; A discussion of the unique requirements for OCC nozzles and a brief summary of the program advancements follows.

The primary requirement of the nozzle is that it contain molten steel. The nozzle is an extension of the pouring box or tundish and hence is a steel containment vessel. Furthermore, because of the "open channel" nature of the process, the nozzle materials will also see a steel/slag/air interface. While this is a very corrosive environment, it is found in every steel plant and refractories such as alumina/graphite, zirconia, boron nitride, etc. have been developed for these areas. The OCC nozzles, however must also contain the molten pool which is held against the moving, cold substrate. This necessitates sufficient insulating properties to maintain the inner walls at molten steel temperatures while the face of the nozzle edge is exposed to the substrate which is 2000F cooler, with a gap no more than can be supported by the surface tension of the metal forming the meniscus which connects the nozzle lip and the substrate. This also implies a high degree of precision in the geometry of the nozzle lip, which must fit against the substrate. This precise geometry must be maintained at the high temperatures and high thermal gradients existing at the edge of the nozzle. The material must be substantially nonwetting to steel and oxides of iron so that the meniscus between the lip and the substrate is not destablized. Finally, because the preheat temperature is unlikely to equal steel making temperatures for the entire inner surface of the nozzle, a low thermal diffusivity is desired to minimize the transient heat loss at the start of cast.

At the conclusion of the previous program, hot pressed, partially stabilized zirconia brick was by far the most successful of the materials used for nozzles on the 3 inch wide caster. The material is nonwetting with respect to steel and most steel slags. It is a reasonably good insulator, especially at 80 to 85% of theoretical density to which our brick were fired. Boron nitride, which is the only material equally nonwetting in the steel/slag environment, is a very poor insulator. More conventional nozzle materials such as

aluminum graphite must be protected from contact with air at high temperature to prevent loss of the graphite component.

Accordingly, the refractory effort on the current program was focused initially on developing zirconia nozzles for 12 inch and wider casts. NARCO, who along with their parent company Didier Taylor, are leaders in zirconia technology and supplied the brick use for 3 inch nozzles. As a program partner, they began an effort to increase the size and homogeneity of the hot pressed brick. Armco began an extensive development of machining and fabrication techniques to build the OCC nozzles from the new, larger bricks. As it took some time for the new NARCO materials to become available, Armco constructed some nozzles from coated fire brick and fully stabilized zirconia slide gate material in order to begin testing. These nozzles consistently failed either prior to casting during preheat, or soon after casting started. While some complete heats were poured through fire brick nozzles, the quality was very poor because the nozzle was deeply fissured and falling apart during the run.

The design of 12 inch nozzles from the larger hot pressed brick presented several problems. The original 3 inch, shallow nozzles could be machined from a single 3 by 4 by 9 inch brick. An increase in the depth of the melt pool above the $1 \frac{1}{2}$ inch maximum of the early nozzles required separate side walls with joints which do not allow molten steel penetration. To eliminate the need for a segmented bottom, the cast width was initially limited to 8 inches. Furthermore, the outer lip of the nozzle must conform to the radius of the casting wheel so that the maximum gap between nozzle and wheel is less than around .020 inches.

Diamond tooling allows very precise machining of intricate shapes of the zirconia material. Complicated joints were designed to allow for sealing even after considerable thermal expansion. A key design rule was to provide the least restrain to the movement of the pieces consistent with the minimum geometrical requirements of the nozzle. This resulted in a mounting system designed to put the joints in spring loaded compression. Also, the sides were registered to the bottom by the weir, and expansion was allowed toward the pouring box, so that the surfaces of the sides and bottom facing the wheel would remained aligned as the nozzle expanded during preheat and casting.

After four months of development, the performance of the pressed zirconia nozzles was still very poor. The inevitable thermal gradient through the thickness of the zirconia caused bowing, which opened the nozzle gaps. High temperature sealant, Krojok from NARCO, which remains flexible until very high temperatures somewhat relieved this problem, as did more gentle preheat practices. In some cases, the nozzle would look excellent until the point just before casting when the preheating burners are extinguished and the nozzle brought to final position close to the wheel. The nozzle would then crack from the thermal shock of the momentary cooling, causing the cast to be aborted. In other cases, the distortion of nozzle geometry would be too great to obtain a fit with the wheel.

It was an attempt to recover from one such failure that led to a complete revision of the approach to OCC nozzle design and practice.

Heat 000817 used a nozzle machined from fully stabilized zirconia slide gate material. The increased thermal expansion of the fully stabilized material resulted in excessive bowing of the bottom plate during preheating, such that contact with the substrate wheel was made in the center of the nozzle before the side plates where at the maximum allowable gap. The cast was thus aborted before it started.

Further refractory development efforts were aimed at improving the life, decreasing the cost, and simplifying the design and assembly of the nozzle components. Single piece, gunned or pressure cast tundish materials were tried, but consistently failed due to the cooling which occurs after the preheat burners are shut off. No preheat resulted in immediate freezing in the nozzle, or to failure associated with residual moisture in the lining. A quick evaluation procedure was established to test potential nozzle materials in contact with flowing molten steel.

6.5   Task 5.0   Process Improvement with Electromagnetic Devices

This task was never activated due to the "No-Go" decision reached by the feasibility study of Task 3.2. The feasibility study focused only on enhancement of liquid metal containment at the Open Channel Casting nozzle. Other potential process improvements using electromagnetic devices were not explored.

6.6 Task 6.0   Characterization of Cast Material

Direct strip casting technologies are intended to supplant the conventional route of thick section casting with subsequent hot rolling. The elimination of the capital and energy intensive hot mill is a prime motivation for developing strip casting. If this effort is to succeed, however, material properties of the finished strip must be comparable to that of the conventionally processed product. With this in mind, a large effort was planned for this program to determine the post cast processing steps of annealing and cold rolling necessary to yield acceptable final properties. The bulk of this work was to have begun once Phase III of the experimental was in progress, so that large quantities of acceptable quality strip would be available for post processing. As Phase III had not begun at the time of the decision to withdraw from the program, not much progress can be reported on the original goals of this task. Instead, a concerted effort to analysis the causes of the strip cracking problem was mounted, so that cast conditions could be devised which would eliminated the problem. An additional process engineer experienced in solving casting related problems (Lowry) was added to assist in this effort.

The initial characterization task was to specify the gross physical properties of the as cast strip. These include the width, thickness, variation in thickness, surface finish, and the presence of defects such as cracks and porosity. Additionally, some items specific to the strip casting process were noted, such as the apparent degree of adhesion of the strip to the wheel, and the occurrence of certain patterns on the strip surface associated with slag carryover from the pool, or vibrations of the meniscus. Figure 1 shows the form used to characterize the strip samples, and a description of each column is given below.

Each sample is a roughly one foot square sheared from the strip and is identified by its position in the cast strip. Standard Weight refers to the weight of a section of strip. A conversion of area density to thickness for this alloy was determined by measurements of seven 1 inch diameter punched strip samples from two casting trials. The thickness of each sample was determined in ten locations using point micrometers, then averaged, and divided by the normalized weight of the punching. The conversion factor thus computed: 25.75 mils per LB per square foot, was used to calculate an average thickness for all the sheared samples. In other words, for each sheared sample:

$$\text{Calc. Thickness (.001 inches)} = 25.75 \times (\text{Weight [lbs]} / \text{Area [sq ft]})$$

Additionally, ten micrometer readings where taken across the width of the sample and the high/low reading recorded to give some indication of the uniformity of gauge. Length and width of the sample were recorded for normalization of the weight and the Percent Adhesion, which was determined from the percentage across the width of the sample which had a very fine grain, tightly adhered oxide pattern on the substrate (bottom) side of the strip. This has been associated from the videos with the darker, cooler portions of the strip exiting the pool. The pattern to the light and dark regions was either random, or

biased in the longitudinal direction, so that a simple measure across the width gave a fair representation for the entire sample surface.

Cracks were divided into three categories: L, T, and S type depending on their orientation. In all cases, it is assumed that the cracks represent hot tears caused by the imposition of stress on the partially solidified, or just solidified strip (Appendix IX). The crack types and origins are discussed below, along with a quick review of possible corrective actions.

L or longitudinal cracks had a definite orientation along the length of the strip. These were most often associated with scratches in the substrate wheel, or disturbances of the meniscus at the nozzle lip caused by cracks in the nozzle or fins of metal penetrating the nozzle to wheel gap. Harder substrates (steel vs. copper, platings), and more aggressive surface dressing (shot blast) reduced the likelihood of scratches. The improvements in nozzle materials and nozzle positioning had nearly eliminated the problem of imperfect nozzle lips or leakage. T or transverse cracks which ran across the sample, could be caused by freezing metal adhering to the nozzle lip for some length (dams), or by disturbances in the meniscus caused by vibrations or movement of the substrate wheel. Improved nozzles, preheat and caster startup practices had eliminated the occurrence of dams, unless the casting speed was very low. Eliminating the flapper dresser wheel, improving the wheel motor drive, and refinements in the runout table and practice had greatly reduced the vibration of the melt pool and hence the disruptions of the top and bottom meniscus. Better substrate mounting with less wheel runout and improved nozzle positioning with dynamic tracking was expected to reduce the meniscus disturbance further. S or spider cracks had no particular orientation and usually were curved. They occurred in the regions of poor adhesion, which cooled slower than the surrounding areas. Tension develops as the surrounding areas cool and shrink faster, which can lead to hot tearing. In general, there was little or no difference in thickness between the good and poorly adhered regions, which indicates that the poorly adhered regions developed near the exit from the metal pool after most of the solidification had occurred. This raised the hope that if means could be found to delay the deterioration in the adhesion slightly, the strip would cool to the point where the hot strength would be sufficient to avoid cracking. This was the basis for the hot substrate development. Additionally, fluxes were considered for the wheel to reduce the overall heat transfer as well as the tractions imparted by the substrate on the solidified strip.

Each crack category was rated 0 to 5:

       0 = no visible cracks;
       1 = just visible;
       2 = visible, fairly numerous;
       3 = cracks are through thickness, but not visibly open;
       4 = light shows through cracks;
       5 = crack opened up.

Pits and holes where noted. Bits of refractory from the nozzle where the most common cause of holes for the casts using copper substrates. The steel substrate produced strip which had many areas with large collections of smooth holes. A metallurgical evaluation of these holes, detailed in Appendix X, showed these to be blow holes formed by gas evolution from the substrate side of the strip. It is speculated that small particles of iron from the wheel dressing operation adhere to the wheel and oxide before being carried back into the nozzle region. Many are trapped by the nozzle lip. The iron oxide particles are reduced by the carbon in the melt, forming carbon monoxide gas. This gas forms a bubble which elongates in the cast direction as it is pulled by the substrate while still attached to the nozzle lip. Eventually, these bubbles either break loses and break through to the top surface of the strip, or collapse as the gas evolution decreases as the oxide particle is consumed. This explains the streaking of the holes which occurred in some cases. Nickel plated steel substrates were expected to eliminate the blow holes.

On some samples, surface roughness and flatness of the strip were given qualitative ratings. Bottom surface roughness reflected the substrate condition, while the top surface was locally smooth, but wavy. The top surface could be rough if the dendrites tips growing from the bottom where exposed. Flatness seemed to be a function of casting speed: Slower casting rates meant less flat strip, presumably due to the increased thermal gradient through the solidified shell caused by the extended contact with the substrate after completing solidification. The pinch rolls, particularly the upper pinch rolls when in use, greatly reduced the waviness of the as cast strip.

Austenitic Trials: The last two heats cast on the experimental caster were 304 austenitic stainless compositions. Using an alloy which does not undergo the normal fcc to bcc transition of low carbon alloys preserves more of the initial solidification structure. We hoped to determine if the cracking problem, which we had reduced but not eliminated, was chiefly due to the volume change associated with the austenite to ferrite solid state phase transition, or if stresses generated by the thermal gradient or other mechanically applied stresses were the cause of the hot tears.

The casts trials were successful and some strip with no visible cracking was produced. A metallographic and mechanical property analysis (Appendix XI) revealed, however, that interdendritic cracking was still present. This is reflected in the large scatter in the tensile properties; For instance % elongation varied from 17.0 to 61.5%. The higher figure compares favorably to conventionally produced material.

Is it clear from these results that excessive tensile stresses sometime occur on the upper portion of the solidifying strip during the OCC process. It should be noted that the austenitic trials were conducted after the decision to the program was made. Consequently, some of the established limits for good casting practice were violated to avoid additional expense; Specifically, the runout on the casting wheel was >.009 inches (normal limit .002 inches) and the minimum substrate temperature was allowed to fall below 500 F in order to obtain maximum cast thickness. Nevertheless, some good

43

material was produced, as evidenced by the samples which produced good tensile properties. Much of what was produced was of poor quality. Clearly, single wheel direct strip casting processes must address the question of whether stresses in the last to freeze portion of the strip can be kept low so as to avoid cracking (<.2% strain is the accepted value to avoid hot tearing).

6.7   Task 7.0   Assessment of Direct Strip Casting:

This task was originally scheduled to start during the last 6 months of the project when the potential success of our technology development would be more clear and comparisons to conventional and other new steel strip technologies could be made. As part of that assessment, the scope of a pilot scale program was to be explored. Our sponsors requested in June 93 at our last semi-annual review that we begin to develop the specification for the pilot program early, so that sufficient funds could be budgeted for a follow on pilot program.

Task 7.3   Specifications for Pilot Plant

For the widest possible applicability, the caster for a pilot program should be able to cast material of commercially important width and thickness. Furthermore, the production rate must be such that a full scale facility would match the typical output of a carbon steel melt shop (about 300 tons per hour). As with current continuous casters, it is reasonable to assume that multiple casting wheels could be supplied by a single steel ladle, which reduces the required throughput per caster. Four thick slab strands are currently cast a some conventional casters today, and six or more billet strands are routinely cast.

Current slab casters have cast material from 28 to 80 inches wide. A reasonable target for a pilot plant would be 48 inches wide (50 inch with allowance for trim), which matches the maximum width of some modern casters and is sufficiently wide to give confidence in the scalablity to 80 inches. A lower limit on cast thickness might be .080 inches, which would allow around 50% reduction to obtain the popular cold finish thickness range of .030 to .040 inches. A reasonable upper limit would be .125 inches, which would cover most of the hot band market.

The Strip1D mathematical model of Open Channel Casting was used to determine the size and operating conditions of the casting wheels required. The wheel diameter was estimated by assuming that no more than 60° of arc could be exposed to the molten pool. The maximum diameter required would be around 80 inches with a 28 inch molten metal head. This is somewhat less diameter than the casting wheel first developed on the DOE sponsored strip casting program (FC07-88ID12712 & AC07-83ID12443). Though large when compared to twin roll casting drums in use for aluminum and reported by the various stainless steel casting development projects around the world, the OCC wheel does not have to withstand rolling pressures. Furthermore, the development of abradable nozzles and gapless casting makes large molten pool depths feasible. The wheel shape is also not as critical as with twin roll casting, which must maintain tight control over the interwheel gap.

The results of the productivity calculations are given in Table 2. A four wheel OCC caster producing 80 inch wide material, 0.125 inches thick at 74 fpm would yield the 300 tph productivity. At 48 inches wide, six wheels would be needed. Reducing the cast

thickness to 0.080 inches reduces the number of wheels required to two and four for 80 and 48 inch widths, respectively. If we allow that 48 inch wide is sufficient to demonstrate commercial feasibility, then a single 80 inch diameter casting wheel for up to 48 inch widths of 0.125 inch material would fulfill the requirements for the pilot program. A 20 ton melt shop would be needed in order to have a reasonable length of time to cast a heat, around 25 minutes.

The specifications for the Pilot Strip Caster would be:

Melt Shop: 20 Ton Induction Furnace w/Vacuum Degas or
20 Ton Vacuum Induction Furnace

Ladle Support: A ladle support or car must be designed to support a 20 Ton capacity ladle over the Pouring Box and provide a shroud to protect the metal into the Pouring Box.

Pouring Box: The Pouring Box and melt delivery system must be capable of maintaining the temperature of the heat exiting the box at a constant temperature ($\pm 25F°$). Total capacity of the box when filled to the 28" head exposed to the wheel would be approximately 4-1/2 ton.

The Pouring Box must be capable of being accurately positioned in both the vertical and horizontal directions as well as tilt and wag. It must have an abort feature which quickly empties the molten steel in case of a nozzle failure.

Caster:

Wheel Diameter	80"
Wheel Width	58"
Arc of Contact	60°
Head of Molten Steel (max.)	28 $^1/_4$"
Drive System	30 HP variable speed
Wheel speed	25-200 fpm
Cooling Water - Wheel	2250 gpm @ 120_F
Cooling Water - Other	250 gpm
Surface Conditioning	

The Caster must have an exit conveyor which removes the strip at approximately TDC and conveys it to a set of pinch rolls which are synchronized with the casting wheel and/or capable of applying a slight tension to the strip coming off the wheel

46

Strip Handling: A 40' space should be provided between the Caster and the Coiler to allow for either a spray mist cooling or a Holding Furnace since the temperature treatment of the strip coming off the Caster has not been determined yet.

                                    The strip collection system should include a set of pinch rolls, a shear and a 20 ton coiler.

The Belcan Engineering Group, Inc. Cincinnati, Ohio: an experience designer of steel plant equipment and facilities, was contracted to develop an estimate for a "greenfield" site construction of a 20 ton Melt Shop and a 48" wide pilot strip caster. The shop requirements were developed over several meeting with the project team and Belcan engineers. The total facility cost would be $27,000,000. This does not include the operating costs for the pilot program. Estimating was based on past engineering reports on.similar installations, verbal estimates from vendors and educated ball park figures. The estimates should be accurate for budget planning. The complete engineering study is included as Appendix XII

Table 2

PRODUCTIVITY OF SINGLE WHEEL CASTER

THICKNESS	0.08 Inches

48 WIDE		80 WIDE	
PRODUCTIVITY	**300 TPH**	PRODUCTIVITY	**300 TPH**
WIDTH	48 INCHES	WIDTH	80 INCHES
THICKNESS	0.08 INCHES	THICKNESS	0.08 INCHES
NUMBER WHEELS	4	NUMBER WHEELS	2
SPEED	194 FPM	SPEED	233 FPM
WHEEL RADIUS	41 INCHES	WHEEL RADIUS	49 INCHES
PRODUCTIVITY	**150 TPH**	PRODUCTIVITY	**150 TPH**
WIDTH	48 INCHES	WIDTH	80 INCHES
THICKNESS	0.08 INCHES	THICKNESS	0.08 INCHES
NUMBER WHEELS	2	NUMBER WHEELS	1
SPEED	194 FPM	SPEED	233 FPM
WHEEL RADIUS	41 INCHES	WHEEL RADIUS	49 INCHES
PRODUCTIVITY	**100 TPH**	PRODUCTIVITY	**100 TPH**
WIDTH	48 INCHES	WIDTH	80 INCHES
THICKNESS	0.08 INCHES	THICKNESS	0.08 INCHES
NUMBER WHEELS	2	NUMBER WHEELS	1
SPEED	129 FPM	SPEED	155 FPM
WHEEL RADIUS	27 INCHES	WHEEL RADIUS	32 INCHES
PRODUCTIVITY	**75 TPH**	PRODUCTIVITY	**75 TPH**
WIDTH	48 INCHES	WIDTH	80 INCHES
THICKNESS	0.08 INCHES	THICKNESS	0.08 INCHES
NUMBER WHEELS	1	NUMBER WHEELS	1
SPEED	194 FPM	SPEED	116 FPM
WHEEL RADIUS	41 INCHES	WHEEL RADIUS	24 INCHES
PRODUCTIVITY	**50 TPH**	PRODUCTIVITY	**50 TPH**
WIDTH	48 INCHES	WIDTH	80 INCHES
THICKNESS	0.08 INCHES	THICKNESS	0.08 INCHES
NUMBER WHEELS	1	NUMBER WHEELS	1
SPEED	129 FPM	SPEED	78 FPM
WHEEL RADIUS	27 INCHES	WHEEL RADIUS	16 INCHES

K   1.985 (mm/(sec^.5))
    0.07815 (in./(sec^.5))

Table 2 (contd.)

PRODUCTIVITY OF SINGLE WHEEL CASTER

THICKNESS	0.125 inches

48 WIDE		80 WIDE	
PRODUCTIVITY	**300 TPH**	**PRODUCTIVITY**	**300 TPH**
WIDTH	48 INCHES	WIDTH	80 INCHES
THICKNESS	0.125 INCHES	THICKNESS	0.125 INCHES
NUMBER WHEELS	6	NUMBER WHEELS	4
SPEED	83 FPM	SPEED	74 FPM
WHEEL RADIUS	42 INCHES	WHEEL RADIUS	38 INCHES
PRODUCTIVITY	**150 TPH**	**PRODUCTIVITY**	**150 TPH**
WIDTH	48 INCHES	WIDTH	80 INCHES
THICKNESS	0.125 INCHES	THICKNESS	0.125 INCHES
NUMBER WHEELS	3	NUMBER WHEELS	2
SPEED	83 FPM	SPEED	74 FPM
WHEEL RADIUS	42 INCHES	WHEEL RADIUS	38 INCHES
PRODUCTIVITY	**100 TPH**	**PRODUCTIVITY**	**100 TPH**
WIDTH	48 INCHES	WIDTH	80 INCHES
THICKNESS	0.125 INCHES	THICKNESS	0.125 INCHES
NUMBER WHEELS	2	NUMBER WHEELS	2
SPEED	83 FPM	SPEED	50 FPM
WHEEL RADIUS	42 INCHES	WHEEL RADIUS	25 INCHES
PRODUCTIVITY	**75 TPH**	**PRODUCTIVITY**	**75 TPH**
WIDTH	48 INCHES	WIDTH	80 INCHES
THICKNESS	0.125 INCHES	THICKNESS	0.125 INCHES
NUMBER WHEELS	2	NUMBER WHEELS	1
SPEED	62 FPM	SPEED	74 FPM
WHEEL RADIUS	32 INCHES	WHEEL RADIUS	38 INCHES
PRODUCTIVITY	**50 TPH**	**PRODUCTIVITY**	**50 TPH**
WIDTH	48 INCHES	WIDTH	80 INCHES
THICKNESS	0.125 INCHES	THICKNESS	0.125 INCHES
NUMBER WHEELS	1	NUMBER WHEELS	1
SPEED	83 FPM	SPEED	50 FPM
WHEEL RADIUS	42 INCHES	WHEEL RADIUS	25 INCHES

K   1.985 (mm/(sec^.5))
0.07815 (in./(sec^.5))

49

Figure 1: Pouring Box Cup

The figure is labeled with the following callouts: Submerge Entry Nozzle, Overflow, Metal Level, Refractory Cup, Casting Wheel.

1.25 INCH

1.00 INCH

0.75 INCH
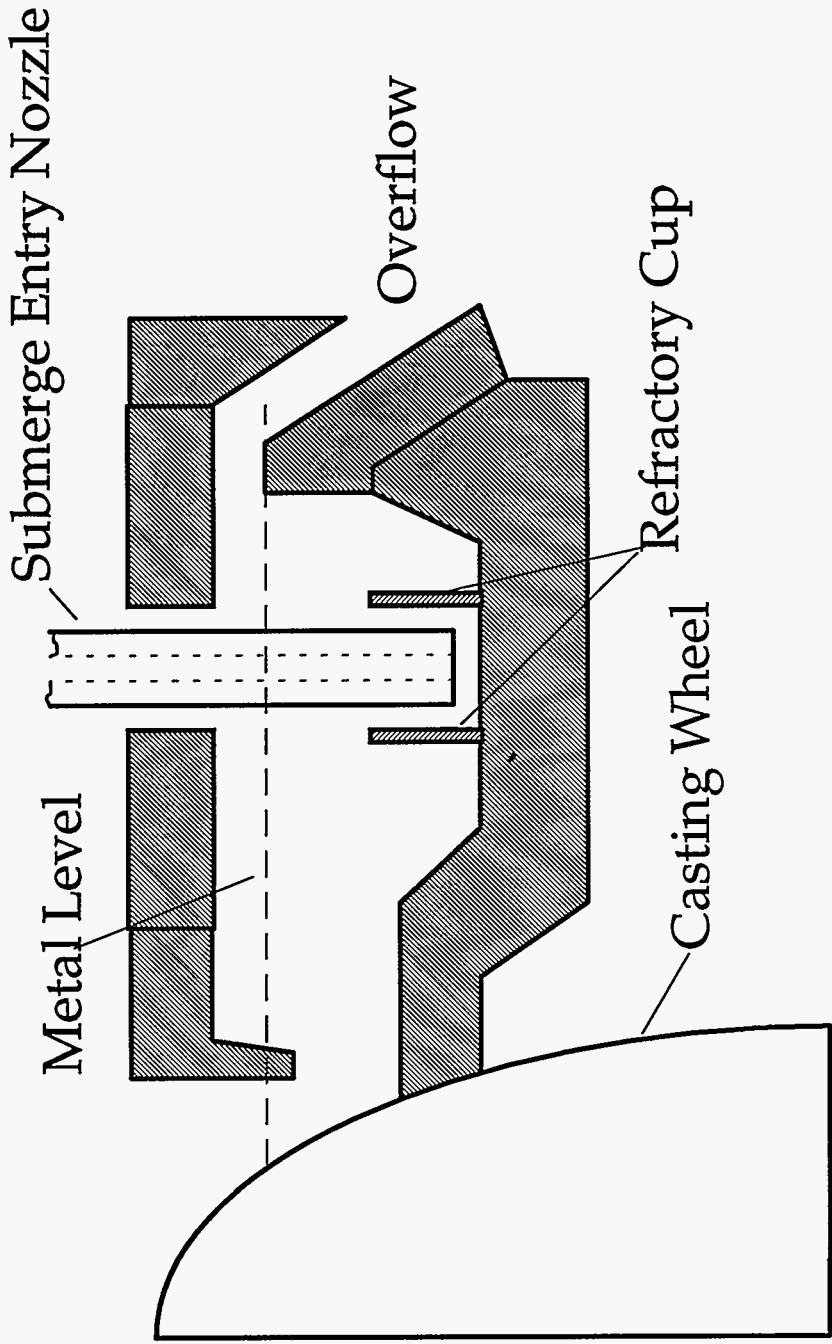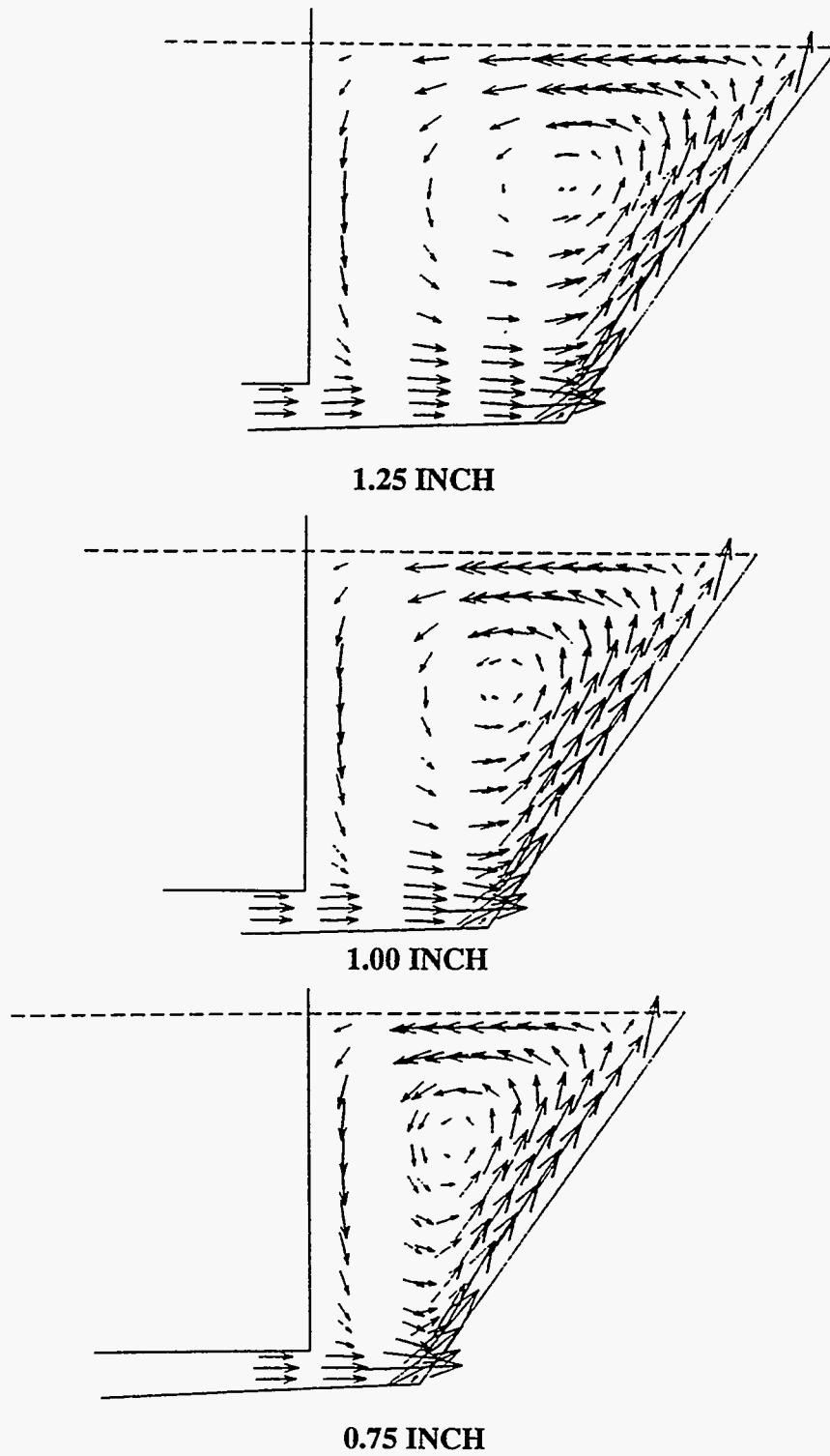
Figure 2: Flow For Different Weir Positions

51
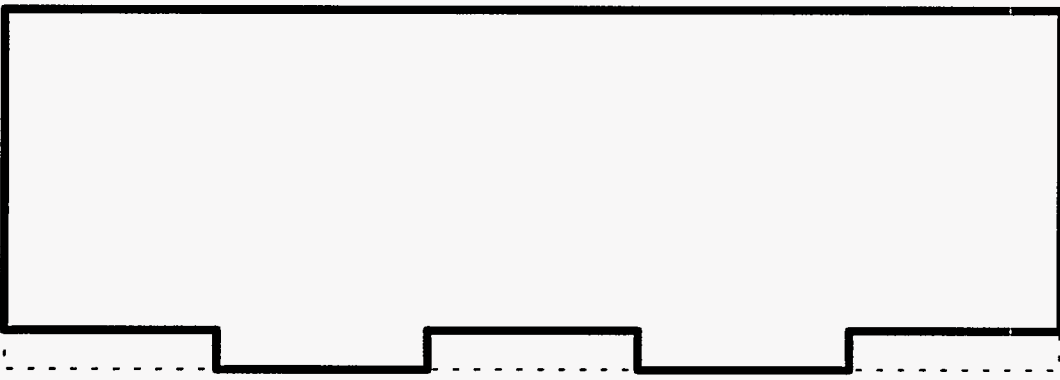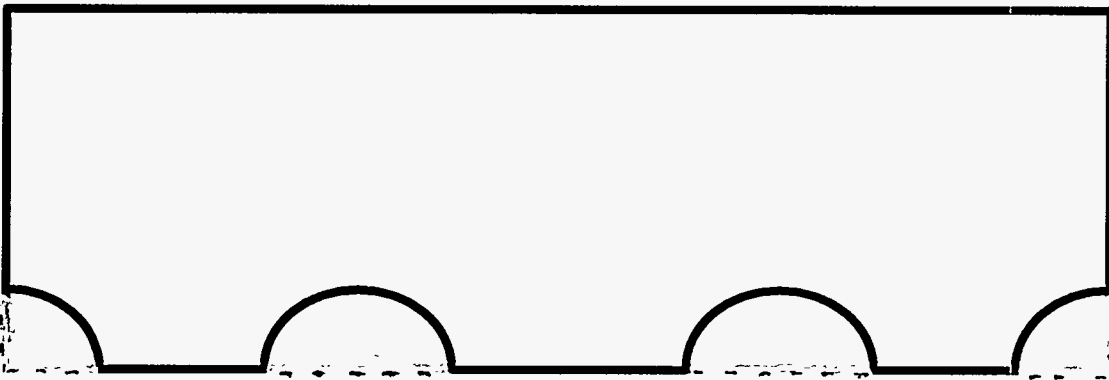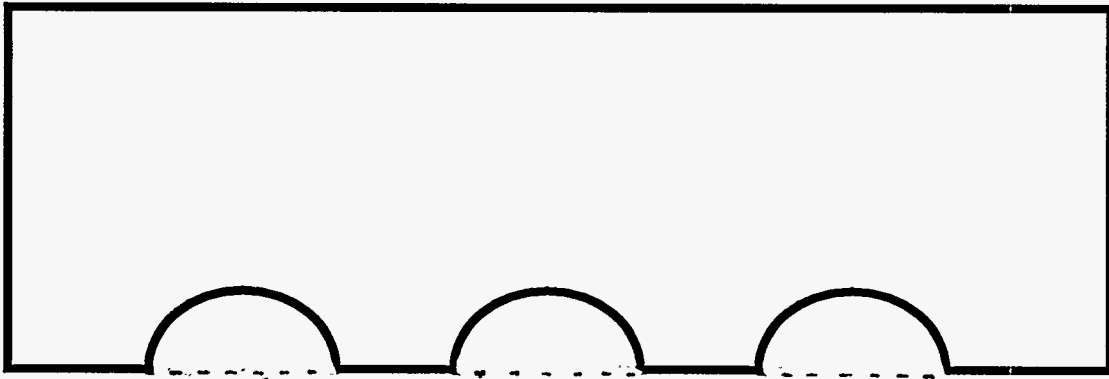
Figure 3: Ported Weir Designs
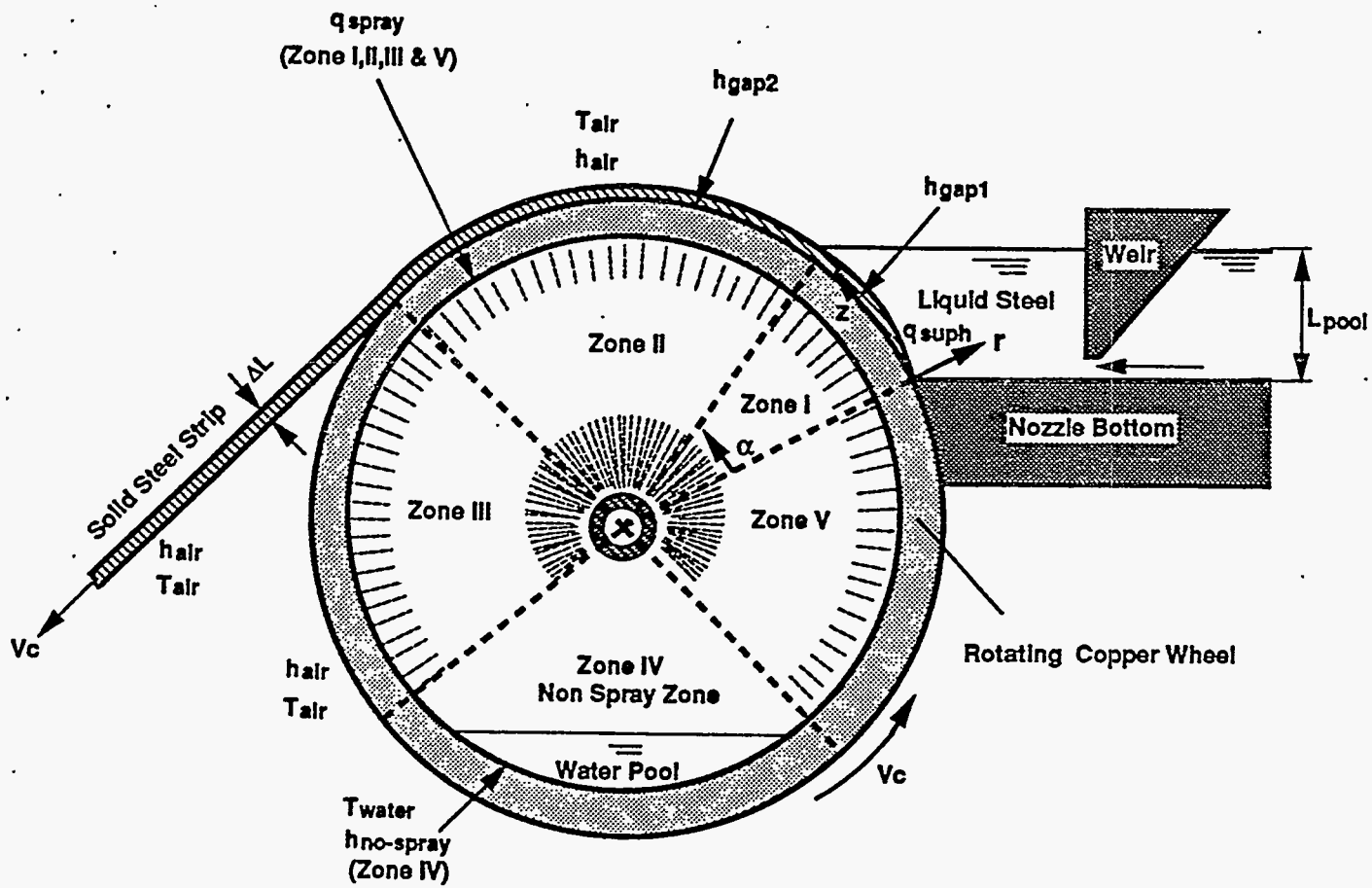
Figure 4. Schematic of Open Channel Casting Process

TOP VIEW

FRONT VIEW OF NOZZLE
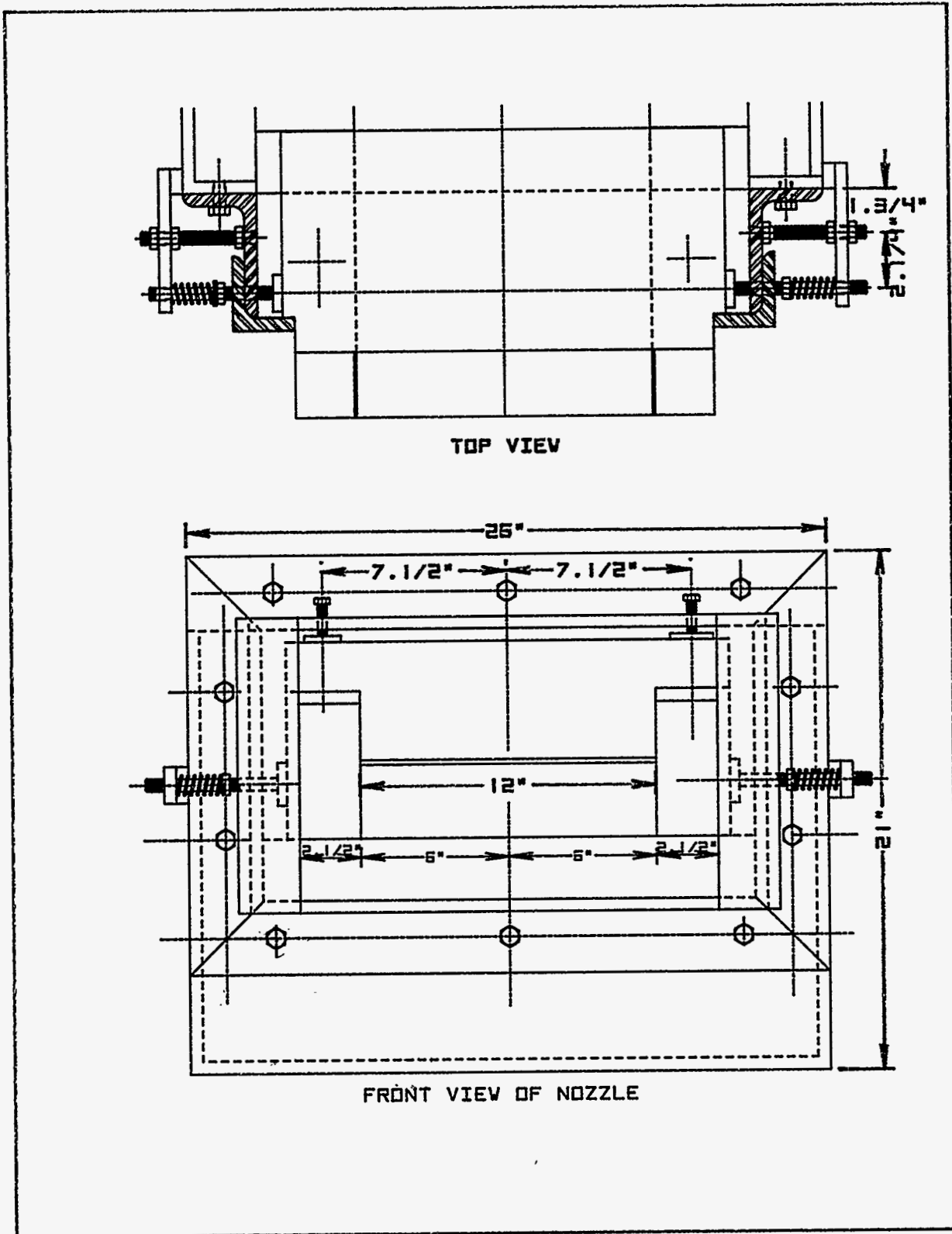
Figure 5a: Spring Loaded Nozzle Mounting System

2.1/2" HEAD
EXTENDED NOZZLE

28.955°

9.235°

4.0285"

12.000 R

2.1/2"
HEAD

4"

8.1/2"

2.1/2" HEAD

44.877°

5.123"

3.166"

11.996 R

2.1/2"
HEAD

3.1/2"

8.1/2"
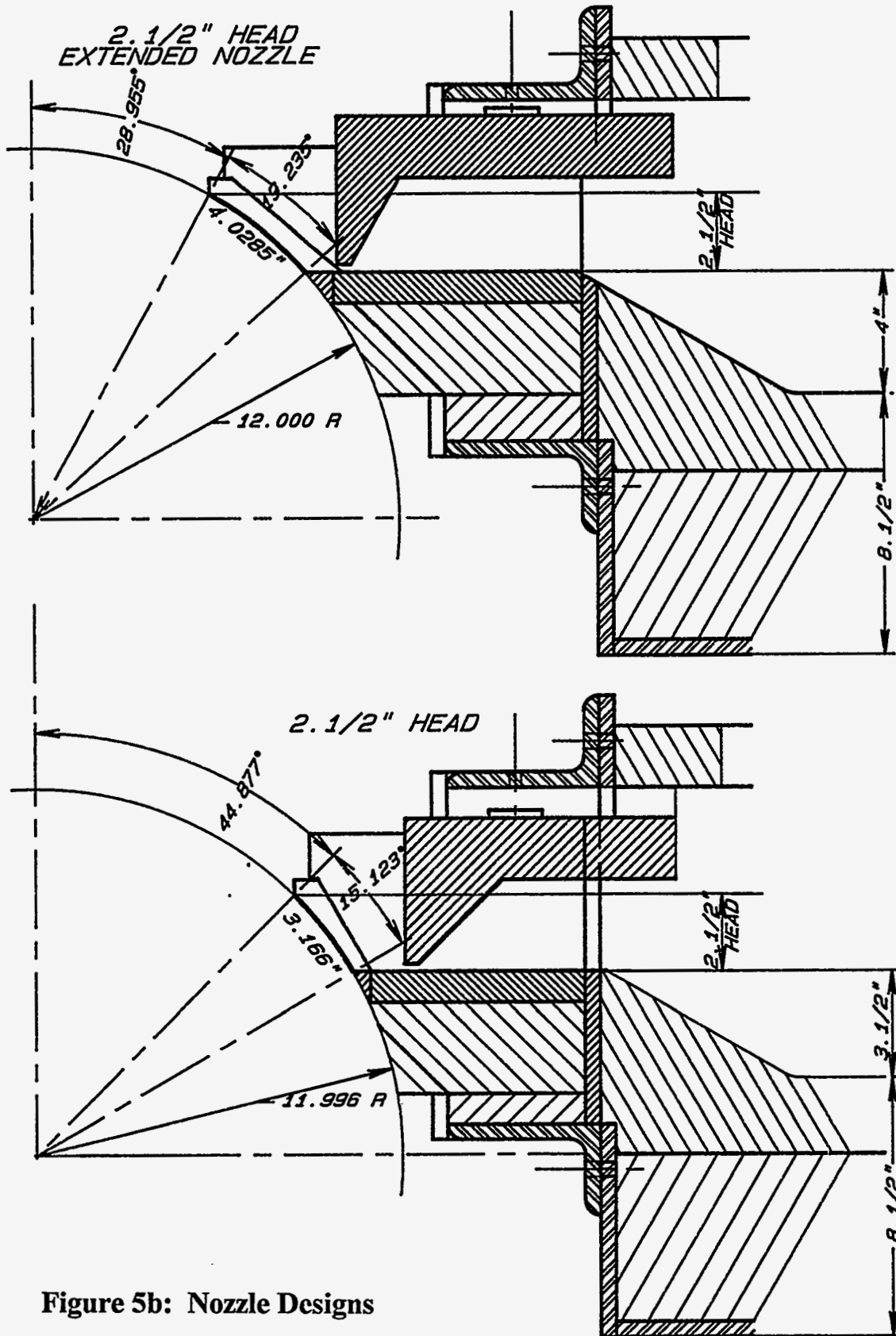
Figure 5b: Nozzle Designs

Figure 6: Caster Elevation

EXIT CONVEYOR

DRIVEN DISC CONVEYOR

BOTTOM DRIVEN PINCH ROLL

24" DIA

20"

12"

56
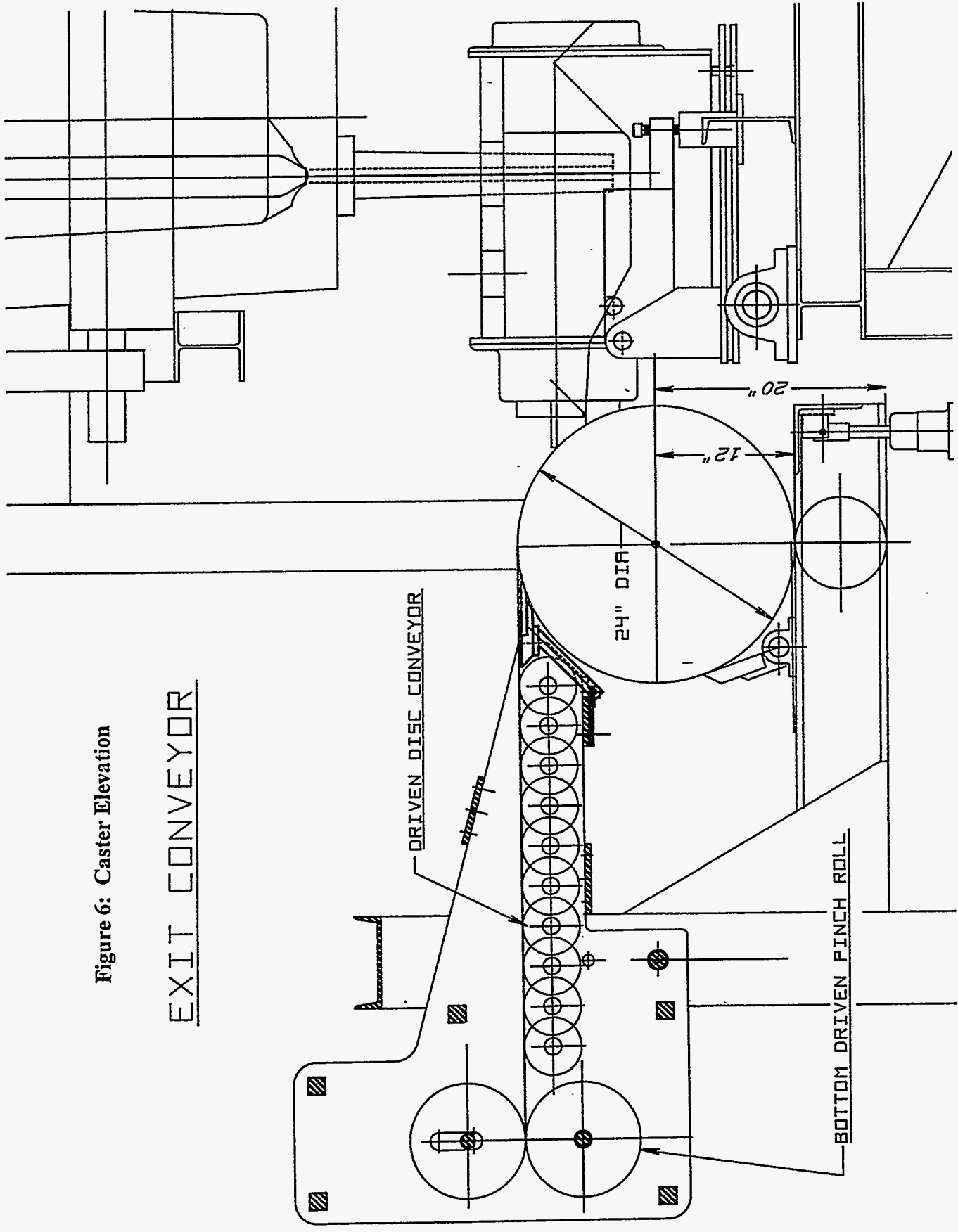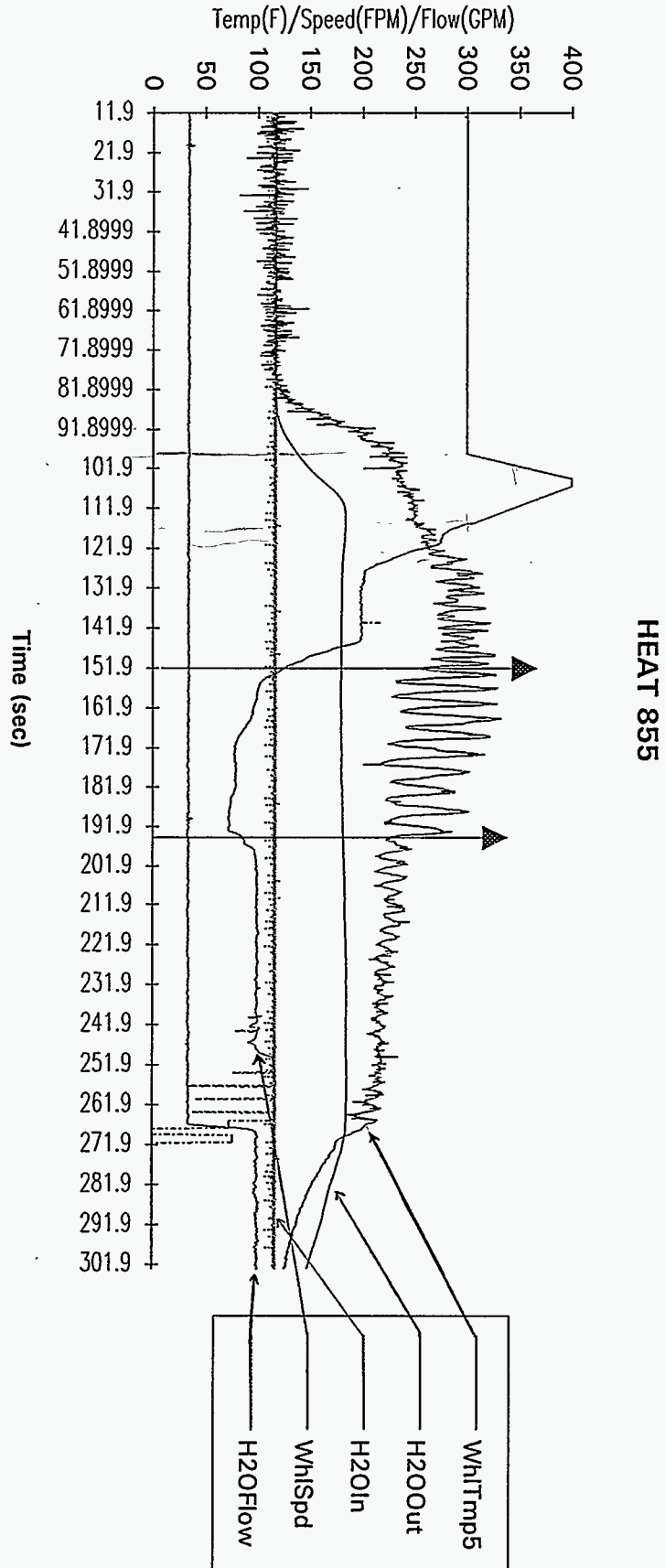
Figure 7: Trace From Embedded Substrate Thermocouple

HEAT 855

Temp(F)/Speed(FPM)/Flow(GPM)

Time (sec)

H2OFlow
WhlSpd
H2OIn
H2OOut
WhlTmp5
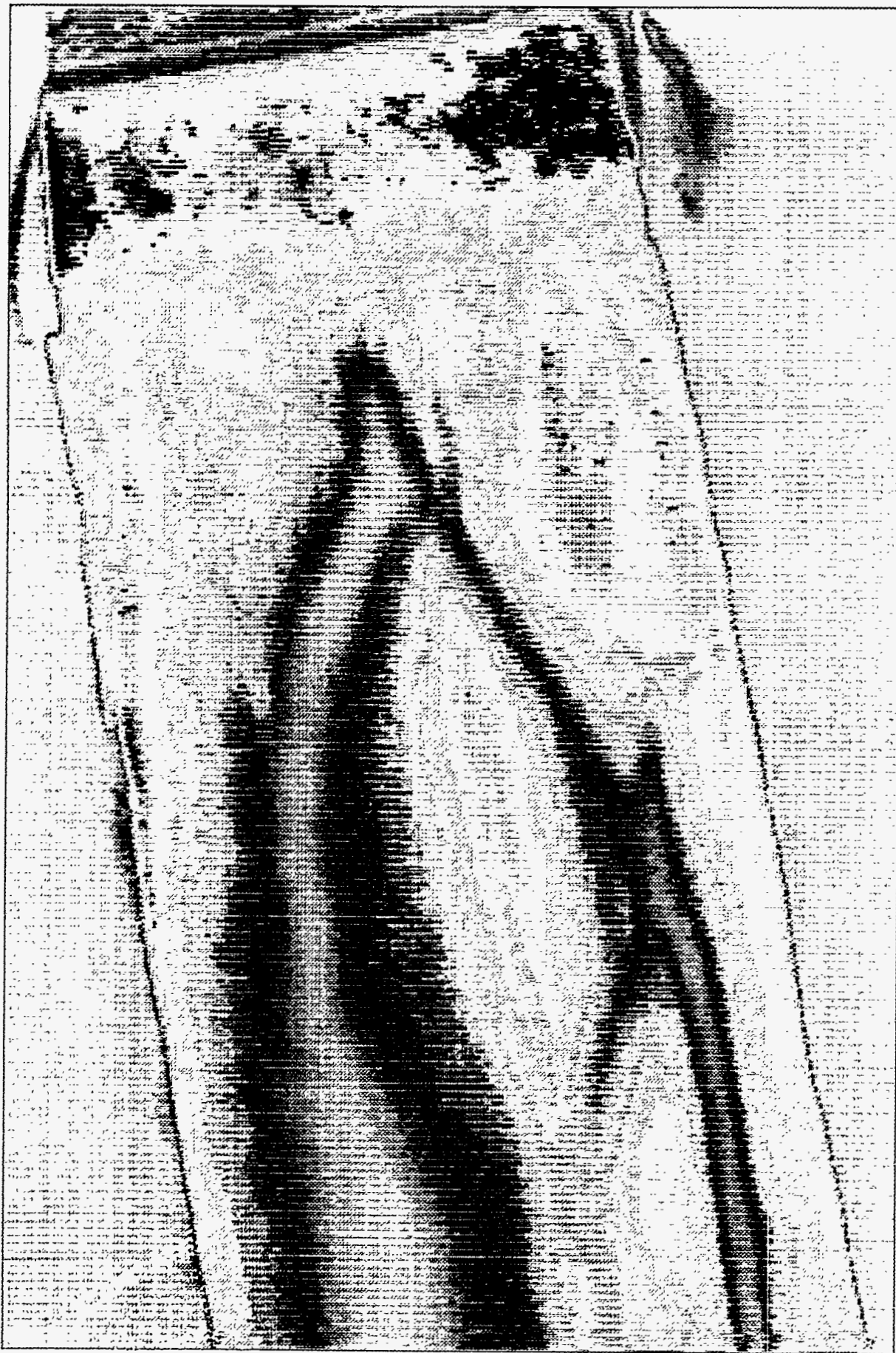
Figure 8a: Thermal Image Showing Inhomogeneous Heat Transfer
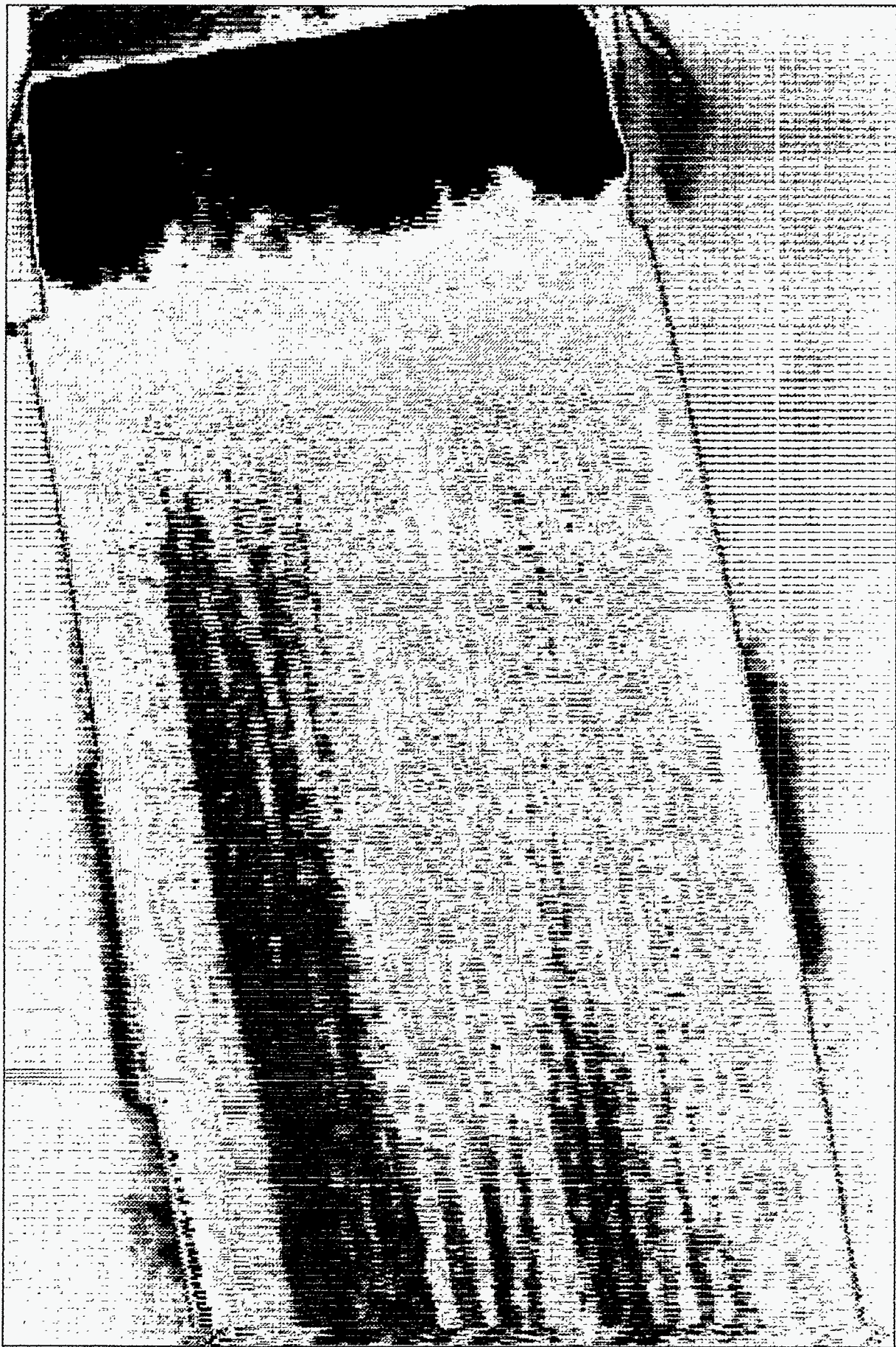
Figure 8b: Thermal Image of Improved Heat Transfer

59
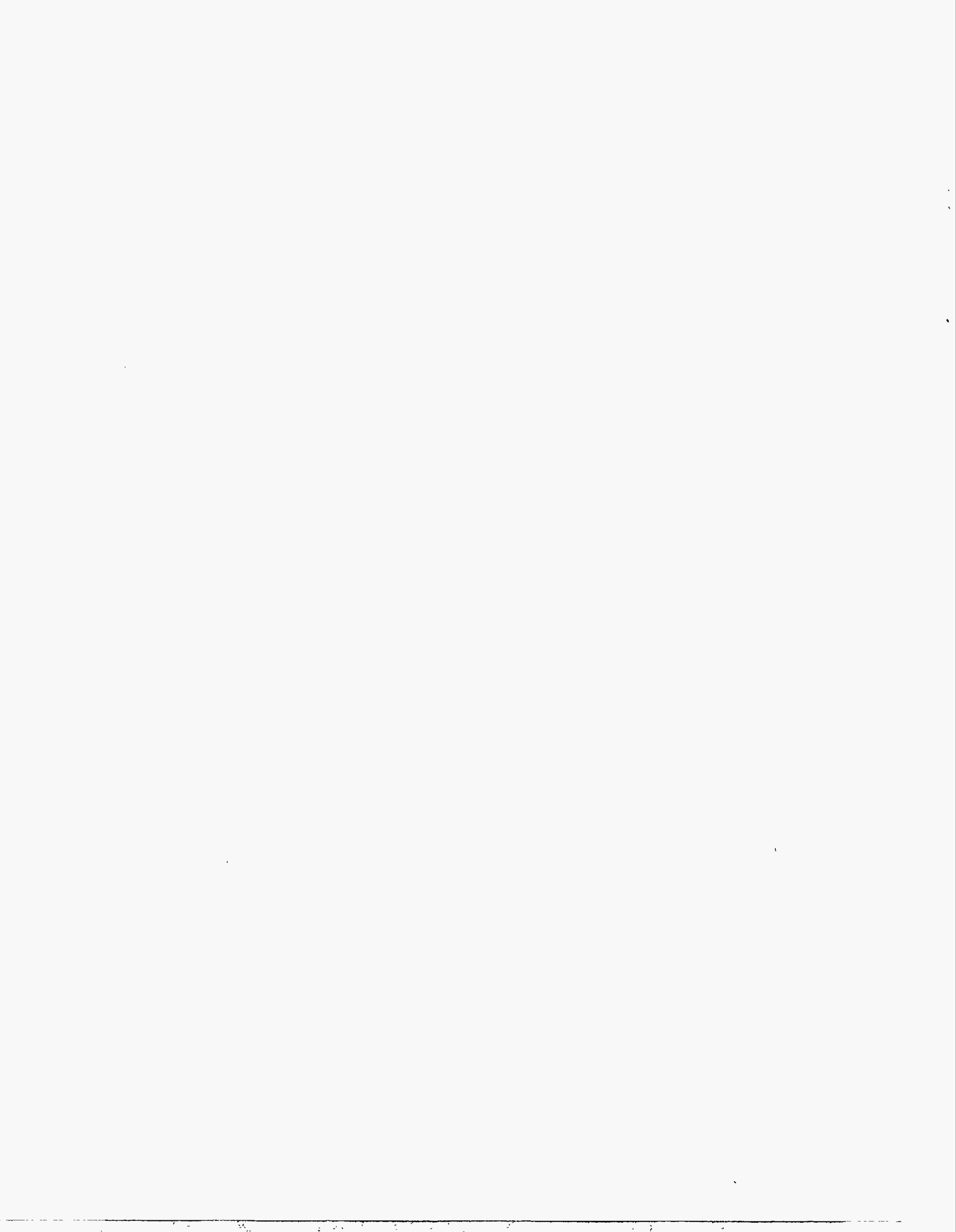
Appendix I

Water and Mathematical
Modeling of Tundish and Nozzle
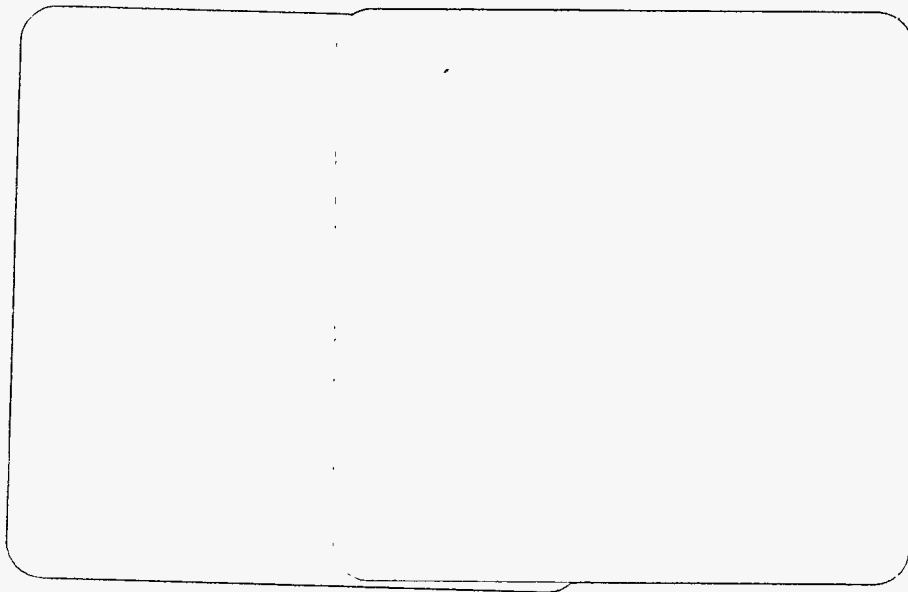
Final Report

on

Modeling of Melt Flow in

Armco/DOE's Strip Casting Tundish

by

Yogesh Sahai, Professor
Materials Science & Engineering Department
The Ohio State University
Columbus, OH 43210

submitted to

Mr. Robert Williams
Armco Research and Technology
Armco, Inc.
705 Curtis St.
Middletown, OH 45043

March 13, 1994

EXECUTIVE SUMMARY

Water and mathematical modeling studies were made at The Ohio State University to optimize the single wheel Armco/DOE's strip caster tundish design, a) to provide the optimum flow conditions for consistent production of good quality strip, and b) to understand the factors that influence the melt flow and to use the developed model(s) for the scale up to the larger width process.

A full scale water model was used as it satisfied the Reynolds as well as Froude similarity criteria. The model was considered to provide a faithful simulation of the melt flow but thermal effects could not be simulated by the isothermal water model. The model was used as a tool to quickly and effectively test any changes in tundish design on the melt flow. Following is a summary of conditions studied in the optimization process.

- Dam configurations
- "Dog Bone" weir geometry - gap under the weir was reduced to 0.25"
- Position of weir - 1.9, 3.2, and 4.5 cm from the wheel
- Splash guard addition
- Angle of contact at wheel
- Head height - 2.5 and 4.0 inch
- New weir designs - weir resting at the spout bottom with semicircular holes

The optimum design conditions were with no dam, new weir design with three holes and "dog bone" configuration resting at the bottom, with splash guard, and 4" head height. These were determined by flow visualization and residence time distribution measurements.

Fluid flow in the tundish was modeled by two- and three- dimensional programs. The results were in good agreement with water modeling experimental results. The computer program was also used to model water as fluid where water was picked up at the wheel and was compared with the conditions where molten steel was used and was solidified at the wheel. This simulation established the validity of a water model for the strip casting situation.

Computer model was used to optimize a new weir metal delivery design system to avoid any possible freezing problems.

Finally, coupled heat transfer and melt flow were modeled to predict the melt flow and temperature distribution in the system. The results also provided the thickness of the solidified shell. Detailed results are provided in this report.

Modeling of Melt Flow in

Armco/DOE's Strip Casting Tundish

This final report contains work done at the Ohio State University for approximately one year period from July 1992 to August 1993. The objectives of the work were as follows:

a) to optimize the melt flow in single wheel Armco/DOE strip casting tundish in order to produce a good quality strip of uniform thickness, and

b) to develop fundamental understanding of the factors affecting the flow so that the knowledge and the model(s) developed could be used to scale up the process from the current 12 inch strip width to much larger width.

Generally melt flow can be modeled using a physical or water model as well as a mathematical or computer model. A full scale water model satisfies the Reynolds as well as Froude similarity criteria. With these similarity conditions, the flow in water model and actual caster could be assumed to be identical. Thus, a water model is a very convenient tool to study the changes in melt flow due to design changes or incorporation of flow control devices in the tundish. Since water used in the present model was at room temperature, the changes in melt flow arising from the temperature differential in actual caster could not be modeled with isothermal water model. The coupled fluid flow and heat transfer could be easily modeled using a mathematical model. A validated mathematical model becomes a useful tool for scale up of the system. In the present work, both models were used and some of the results of the work are presented in the following section.

Water Modeling

A full scale plexiglas model of the strip casting tundish was provided by Armco to the Department of Materials Science and Engineering at The Ohio State University in July, 1992. A large water proof tank was made out of plywood to contain water carried with the rotating wheel. After assembling the model, it was found that water was badly leaking in the area where wheel touched the tundish. As the first task these water leaks were successfully stopped. In actual strip casting, at 2.5" depth of metal at the wheel contact rotating at 100 ft/min (fpm) linear speed a 40 mil strip thickness is observed. A 12" strip width at 40 mil thickness corresponds to about 2.5 gallons per minute (gpm) of volumetric flow rate. Unfortunately in the model, at 2.5 gpm water inlet flow and 100 fpm of wheel speed, the wheel picked up only about 0.6 gpm. In other words, the steady state conditions could not be achieved. Even at higher wheel speeds the increase in water pick up by the wheel was found to be minimal. In

these modeling experiments, it was important to attain a steady state. In an attempt to modify the surface roughness of the wheel, the surface of the wheel was covered by cloth. This was found to be quite effective method and cloth covered wheel picked up more and more water at higher speeds. At 100 fpm water pick up rate went up to 1.1 gpm but more importantly, at 200 fpm the wheel picked up 1.8 gpm, and at 230 fpm wheel speed the pick up increased to 2.5 gpm. It was decided to use 200 fpm wheel speed as standard condition. The 1.8 gpm water pick up at this speed corresponds to about 29 mil thickness. This corresponds very closely to the steel casting conditions.

Figure 1 shows the dimensions and a longitudinal cross section of the tundish. The original configuration of flow control devices, as provided by Donald Follstaedt of Armco Research, was a full baffle with two holes near the bottom. This configuration was found to create a large dead volume at the downstream of the baffle above the holes. Thus, liquid exiting from the two holes directly moved downstream towards the wheel. In the first set of experiments, dye was injected at the inlet in the incoming water for flow visualization with different flow control configurations. Figure 2 shows schematic drawing and dimensions of six flow control configurations studied. In these qualitative trials, the configuration A had no flow control device at all and was found to be the most satisfactory. The dye dispersed very uniformly and was found to give a uniform flow through the tundish to the wheel. There was good mixing throughout the entire volume of the tundish and no stagnant areas were found. The entire baffle was made of three parts each covered the entire width of 30 cm and the height of each piece was 10.1 cm. In configurations B, C, and D only one piece with holes was used. With three holes of equal size (3.2 cm diameter) at the bottom, configuration C, flow through the middle hole was delivered faster and before dye could reach the other two end holes. Water flow was also found on top of the dam. However, the region above the holes and below the top of dam on the downstream side of the dam was found to be stagnant. In configuration B, the middle hole diameter was reduced to 1.3 cm and this provided a uniform flow through the three holes. There was a little stagnant area behind the dam in the space between the holes and above the holes, yet this configuration was found to be the next best geometry to the no dam, configuration A. In configuration D, the dam of configuration C was placed upside down so the holes were located much above the floor of the tundish. This created a large stagnant area behind the dam below the holes. In configuration E, the depth of dam was 20.2 with two rows of holes. There was uniform flow through the bottom two holes but large stagnant areas existed above and between the holes. Liquid flow was very slow through the top set of holes. In configuration F, uniform flow existed through the two holes but very large stagnant areas existed above and between the holes. The configuration F is the original geometry being used at the Armco Strip caster.

4

In conclusion, a tundish without any control device provided the most uniform flow. In these qualitative trials, dye was injected in the inlet tube and flow of colored water in the entire tundish was observed and recorded on a video tape. These studies provided the general characteristics of the flow but to observe flow in local areas and near the wheel, dye was spot injected with a syringe at certain locations and flow of colored water through the tundish was observed and recorded.

Residence Time Distribution (RTD) Studies:

In order to quantitatively study the uniformity with which the melt was delivered to the wheel, the residence time distribution of dye reaching the center and near an outer edge of wheel were measured. Water was delivered to the wheel at approximately 10 or 11 o'clock position depending upon the depth of water. A small boat with a spectrophotometer probe was placed in contact with the wheel at about 3 o'clock position to continuously collect colored water and measure the on-line dye concentration. The RTD curves obtained at the center position of the wheel were compared to the location near edge. These curves provided the uniformity of liquid delivery to the wheel and flow through the tundish. Again, these measurements verified that a tundish without any control device provided the most uniform flow.

"Dog Bone" Geometry of Weir:

As shown in figure 1, a weir was placed in the tundish near the wheel. The purpose of the weir was to deliver more fluid near the bottom of the spout closer to the wheel to avoid any possible freezing of metal near the bottom. This weir was successful in achieving its objective, however, the corner regions of the spout suffered more heat losses. In order to provide more flow near the corners or ends of the weir, a modification known as "dog bone" geometry was adopted. The first change involved an addition to the bottom of the weir of a 0.25" thick strip of plexiglas that reduced the distance between the floor of the tundish and the bottom of the weir from 0.5" to 0.25". The addition of a "dog bone" geometry i.e. a diagonal cut of the weir end of 0.75" height and 0.75" length to the outer edges provided more flow to the outer regions of the tundish, which was confirmed through dye trials as well as concentration curves. Visual dye trials using spot injections were also performed and recorded in the region between the wheel and the weir to test the results obtained from computer modeling.

Position of Weir:

Visual dye trials were also done while varying the position of the weir with respect to the wheel (1.9cm., 3.2cm., and 4.5cm. from the wheel). Concentration curves were also recorded for these changes using a "no dam" geometry in the tundish. The intermediate position was found to provide the optimum flow in terms of turbulence and uniform delivery of liquid to the wheel.

Splash Guard:

A plexiglas cylindrical piece was added to the floor of the tundish directly under the inlet tube to serve as a "splash guard" against water (molten metal) rushing out from the bottom of the inlet tube and splashing up onto the wheel. The cylindrical splash guard was 4" high with 6" diameter. The unit also had a notch cut out of the region facing the back wall of the tundish in the direction opposite of the wheel. The notch provided an outlet for incoming water and resulted in uniform flow patterns. The semicircular notch was cut down to 1.5" from the top of the splash guard.

Head Height:

The head height of the water in contact with the wheel was increased from 2.5" to 4" to more accurately simulate the prototype caster at Armco through the use of a 1.5" high plexiglas addition to the bottom of the tundish. All additional experiments and RTD studies were done with this new design of the tundish. The increased depth provided larger contact length of melt to the wheel and resulted in thicker strip.

New Weir Design:

Three new weir designs (as shown in figure 2B) were tested for the uniformity of flow delivery to the wheel. All these weir touched and rested at the bottom of the tundish spout, and liquid was delivered through the semicircles and the "dog bone" openings in the weir. It was considered that if these designs provided an acceptable flow for the production of a good quality strip, the scale up of the system from the current 12 inch width to either 48 inch or 60 inch wide strip will be logical extension of these design. The flow visualization and the RTD measurements concluded that the third configuration in figure 2B with three openings provided the flow with optimum characteristics. Figure 2C and 2D show RTD curves for the center and near the outer edge of the wheel, respectively. It can be seen that these measurements provide a quantitative measure of the fluid flow through the tundish under these conditions.

Mathematical Modeling

Water flow through the entire tundish was modeled mathematically by solving the following equations:

(a) Equation of Continuity,

(b) Momentum Balance Equations in three dimensions, and

(c) K-Epsilon Turbulence Model Equations.

The symmetrical one half of the tundish was used in this modeling. The length was divided in 52 grids, the half width in 13 grids, and the depth of liquid was divided in 27 grids. The moving wheel boundary was considered at the end of tundish. Typical flow profile results for one case are shown in figure 3. Figure 3A shows flow in selected longitudinal vertical planes. The plane at J = 2 is near the vertical symmetry plane and J = 10 is towards the wall and has a hole in the baffle. A large stagnant region behind the baffle is apparent where fluid velocities are very low. The scale vector of 0.01 m/s is shown. The grid near the moving wheel was very fine and thus the vectors in figure 3A are not clear. Figure 3B shows the enlarged view of the nozzle and wheel region only in six selected planes. A very uniform two-dimensional flow is evident. Figure 3C shows flow in selected horizontal planes. The predicted velocity profiles were in good qualitative agreement with that found in water model for the same conditions.

The similarity between the water flow in plexiglas model tundish with water pick up by the wheel and the steel flow in actual tundish with solidified steel strip pick up by the wheel was considered. The flow in bulk of the tundish would be same in the two cases if the heat transfer aspects were neglected. However, water and steel flow near the nozzle may be different. To clarify this aspect, two cases were mathematically modeled.

As a test case, due to ease of calculations, a rectangular domain was considered. The liquid depth was 6.4 cm and distance between the inlet to the moving vertical wall was 6.8 cm. Water entered the domain at the bottom of the left side and the vertical wall at the right side was moving such that it picked up water to maintain a steady state flow. The predicted velocity profile is shown in figure 4. Figures 5 and 6 show the mean velocity and turbulent velocity fluctuations at four dimensionless depths. Z = 0.98 is very close to the top surface. The velocity fluctuation near the surface is about 1 cm/s. In the next case presented in figures 7, 8, and 9 the grid near the moving wall at the right side was fine. The predicted results were not different.

The next case is for steel with the same grid density as for water in figure 7. In this case liquid steel entered the system but liquid did not leave the domain. Hence, the equations of continuity and momentum balance were modified to account for the solidification taking place.

7

The predicted velocities (see figure 10) away from the moving vertical wall are very small. Comparison of figures 11 and 8 also shows this result. The turbulent fluctuation near the wheel is less for the metal case (compare figures 12 and 9).

In the following four cases the rotating wheel geometry was simulated. However, the rotating wheel in contact with the liquid was replaced by an inclined plane moving at the same velocity as the wheel. Since the diameter of the wheel was sufficiently large, the curvature of the wheel has been ignored in these calculations. Figure 13 shows the predicted velocity field with wheel moving at 100 fpm and water was picked up by the wheel to maintain a steady state. It is interesting to note that at the free surface near the wheel liquid is drawn towards the wheel and rest of the liquid flows back to the weir. Figure 14 and 15 are the mean and turbulent fluctuating velocities plots. In the next case, the wheel speed was increased to 200 fpm. As can be seen in figure 16, the velocity field is similar to the previous case except at the free surface. Figures 17 and 18 are the mean and turbulent fluctuating velocities plots. They are also similar to the previous case.

The next case is for steel being solidified at the wheel and no liquid was drawn out of the system. Thus, liquid at the free surface is not drawn towards the wheel as can be seen in figure19. The wheel speed in this case is 100 fpm. Figures 20 and 21 are the mean and turbulent fluctuating velocities plots. Finally, the wheel speed is increased to 200 fpm and flow rate is 1.8 gpm which corresponds to 29 mil strip thickness. The free surface and downward flow near the weir have higher velocities (see figure 22). The increased velocities can also be found on comparing figures 23 with 20. The last figure 24 is the turbulent fluctuating velocity at different heights. This is not different from the previous case.

Metal Delivery System Design:

Various other innovative designs were considered to deliver metal near and on to the wheel which would avoid the freezing problems. One such concept was mathematically modeled and the results are shown in figures 25 through 29. In this design, the region near the wheel was kept lower than the previous case, and metal was delivered impinging at one location. It was found that by moving the weir location with respect to the bottom well location near the wheel, the region where the fresh hot metal is delivered could be moved. Figure 25 shows the back of bottom well wall and the lowest point of the weir are vertically above each other, thus, is called 0 mm location. In the next four figures (figs. 26 through 29) the weir is moved 1.75, 3, 5, and 7 mm towards the wheel. This weir movement causes the lower melt recirculation to decrease in size and the location of the metal impingement location on to the wheel had moved down. Thus, the design provided a way to control the metal delivery to the wheel.

Coupled Fluid Flow and Heat Transfer Modeling:

Most of the modeling results presented above were obtained by neglecting the heat transfer aspect in the system. These results could be directly compared with the water modeling results and thus, provide a validation of the results. In some preliminary work which started in July 1993, coupled heat transfer and fluid flow modeling was made. Figure 30 and 31 represent the predicted streamline and temperature profiles in the spout/rotating wheel region. Figure 30 clearly shows the recirculation in the melt near the wheel. The contours A, B, C, and D in figure 31 are non-dimensional temperature contours where contour C corresponds to the solidified layer.

Approximately, at this time we were informed of immediately stopping the work. There is no doubt that the modeling work at The Ohio State University was extremely successful in achieving its stated objectives.
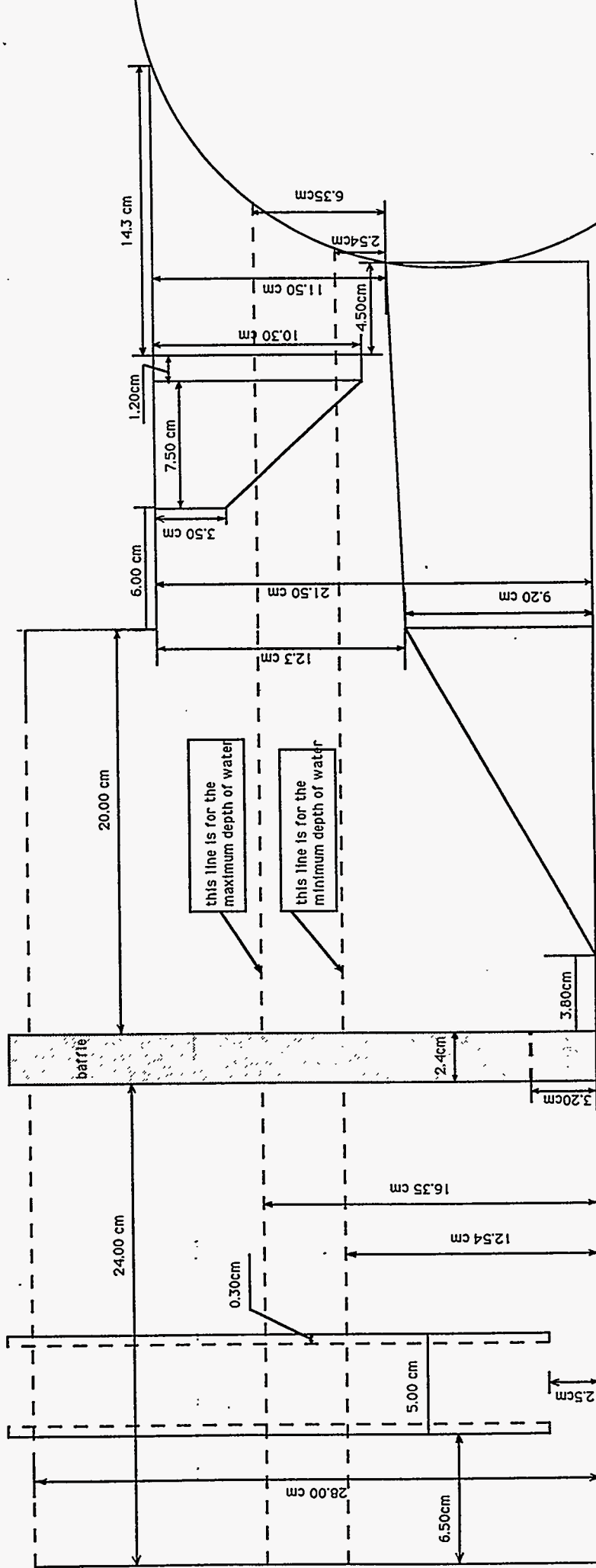
Figure 1

CONFIGURATION DRAWINGS

(ALL DAMS REST ON FLOOR OF TUNDISH)

A.   NO DAM EXISTS.

B.

C.

D.

E.

F.
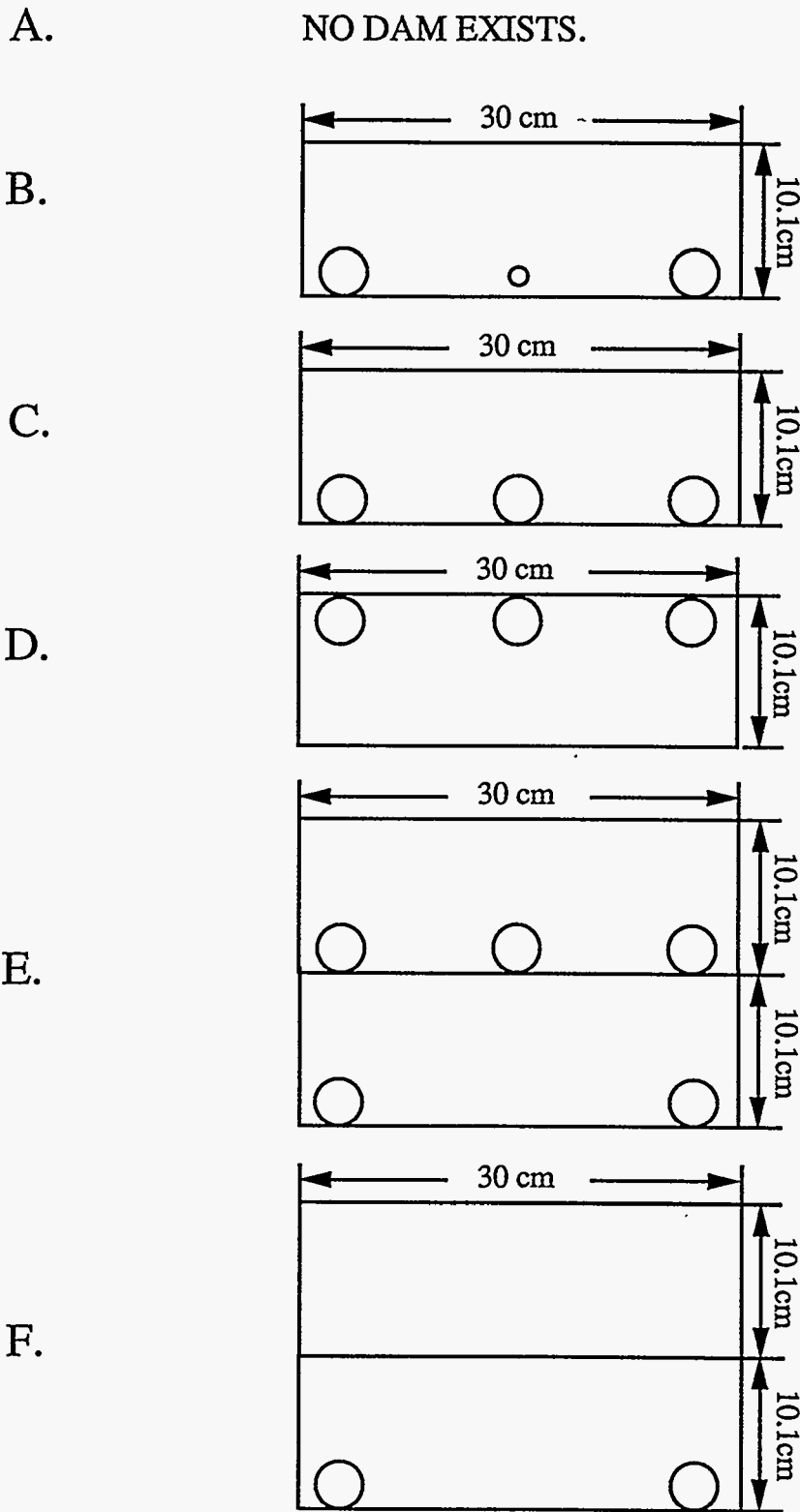
Figure 2A

Hole Diameter = 3.2 cm

Small Hole Diameter = 1.3 cm

FIGURE 2 β

11.5 IN.
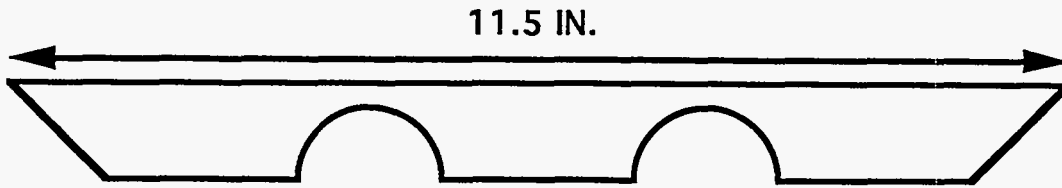
HEIGHT = .8 IN.
HOLE DIAMETER = 1 IN.
DISTANCE BETWEEN HOLES = 2.7 IN.

11.5 IN.
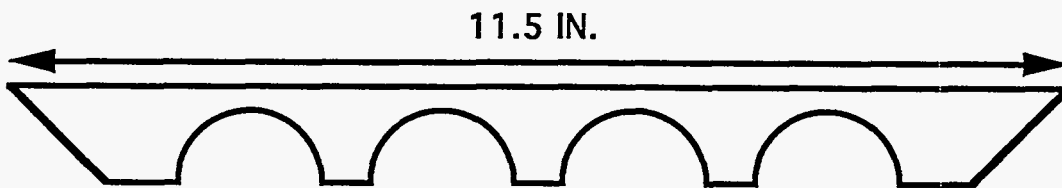
HEIGHT = .8 IN.
HOLE DIAMETER = 1 IN.
DISTANCE BETWEEN HOLES = 1.2 IN.

11.5 IN.
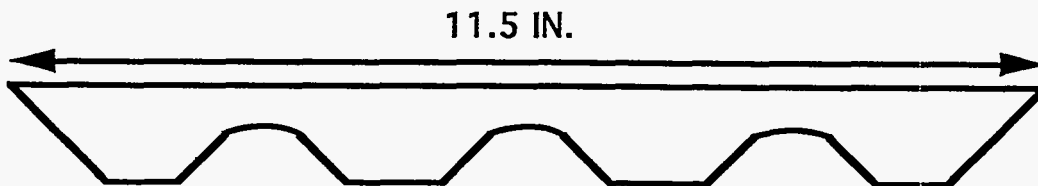
HEIGHT = .8 IN.
HOLE WIDTH = 1.8 IN.
HOLE HEIGHT = .375 IN.
DISTANCE BETWEEN HOLES = 1.2 IN.

Residence Time Distribution of Water
Weir with Three Holes
(Center of Wheel)
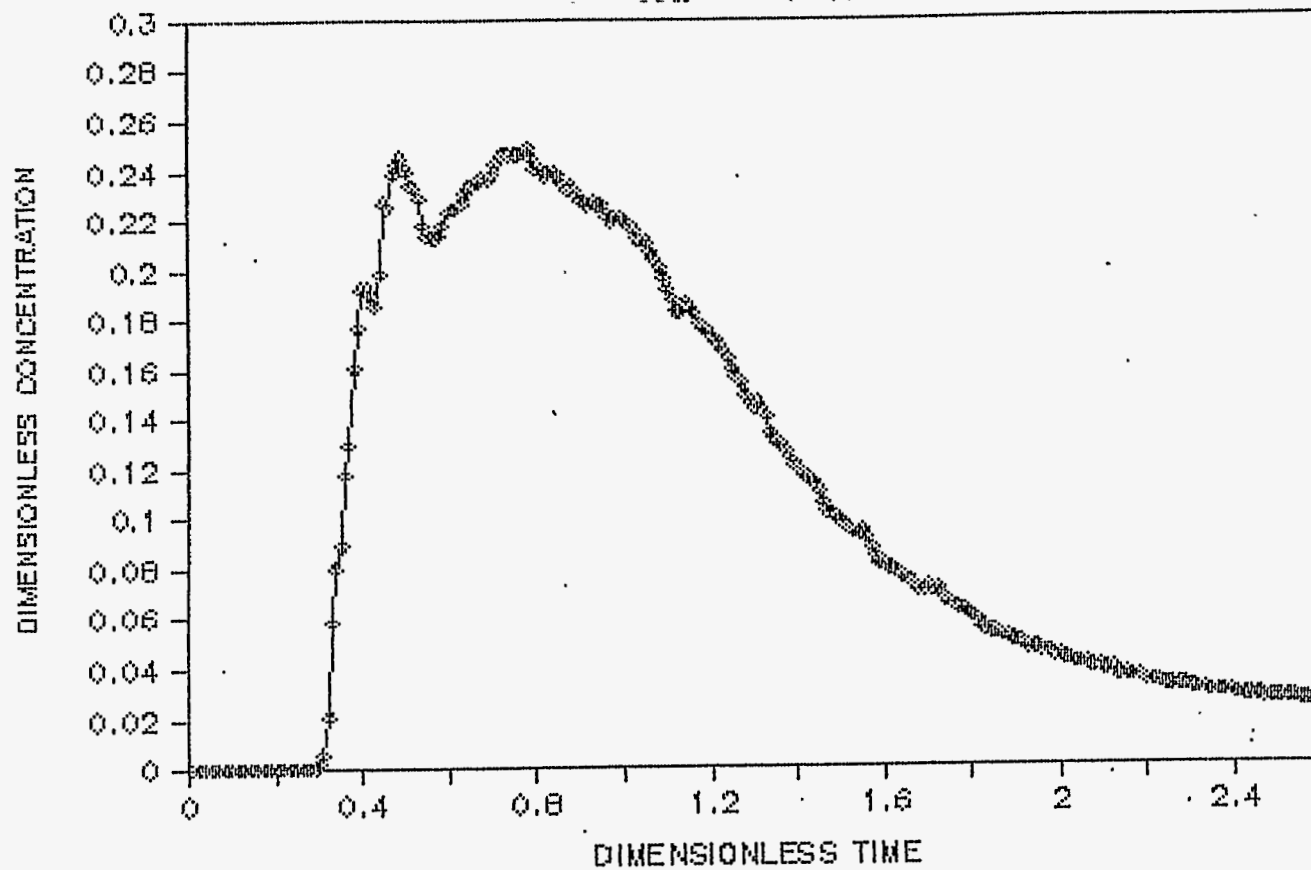
Figure 2C

Residence Time Distribution of Water
Weir with Three Holes
(One End of Wheel)

DIMENSIONLESS TIME

DIMENSIONLESS CONCENTRATION
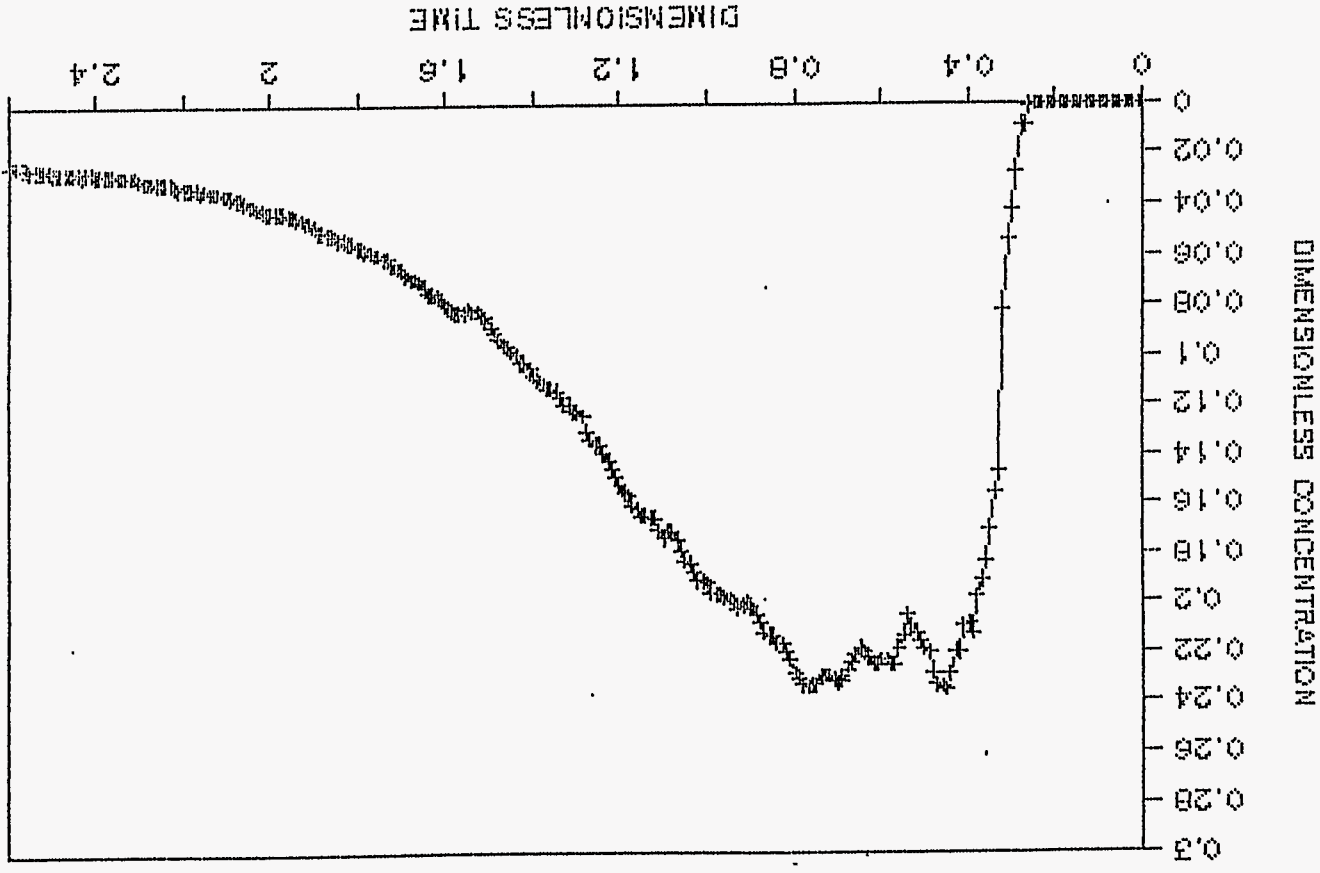
Figure 2D

FLOW IN LONGITUDINAL VERTICAL PLANES

$J = 2$

0.01 m/s

$J = 10$
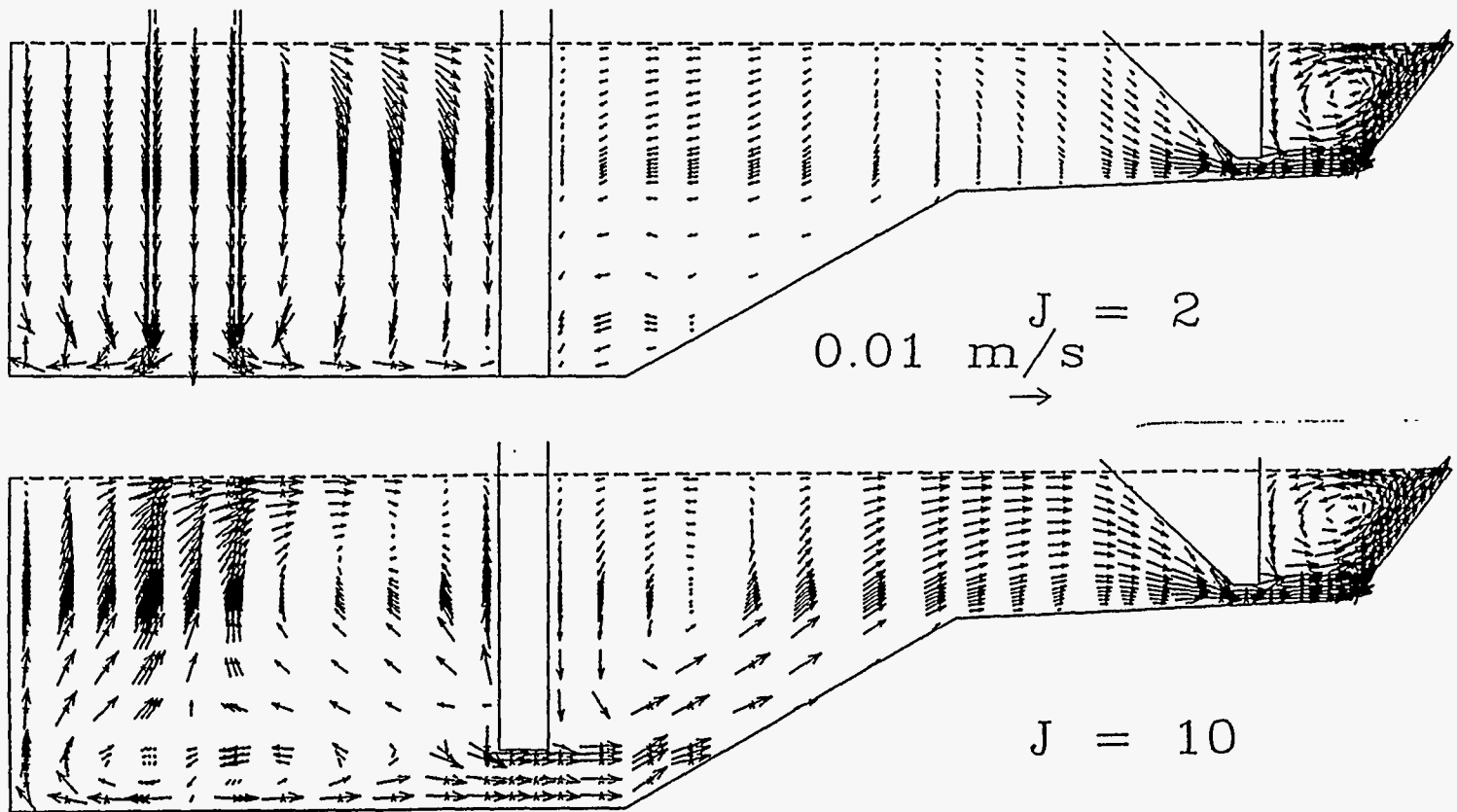
Figure 3A

LIQUID FLOW PROFILE IN POOL
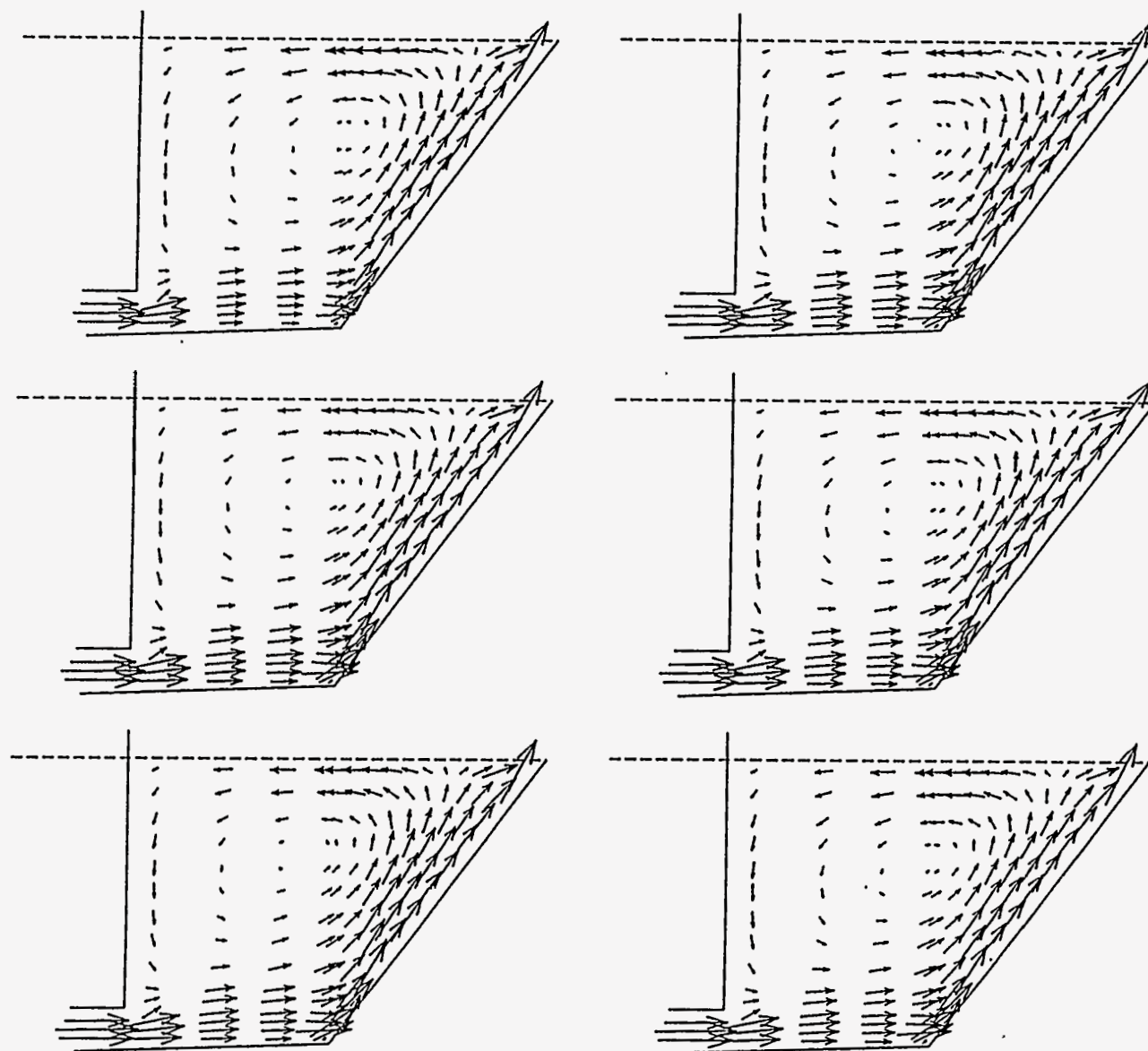
Figure 3B

FLOW IN SELECTED HORIZONTAL PLANES

Figure 3C

0.083 m/s

Figure 4

Figure 5

MEAN VELOCITY cm/s

DISTANCE FROM DAM (mm)

Z*=0.984

Z*=0.734

Z*=0.484

Z*=0.234

Figure 6

DISTANCE FROM DAM (mm)

Z*=0.984

Z*=0.734

Z8=0.484

Z*=0.234

VELOCITY FLUCTUATION TURBULENCE cm/s

0.083 m/s
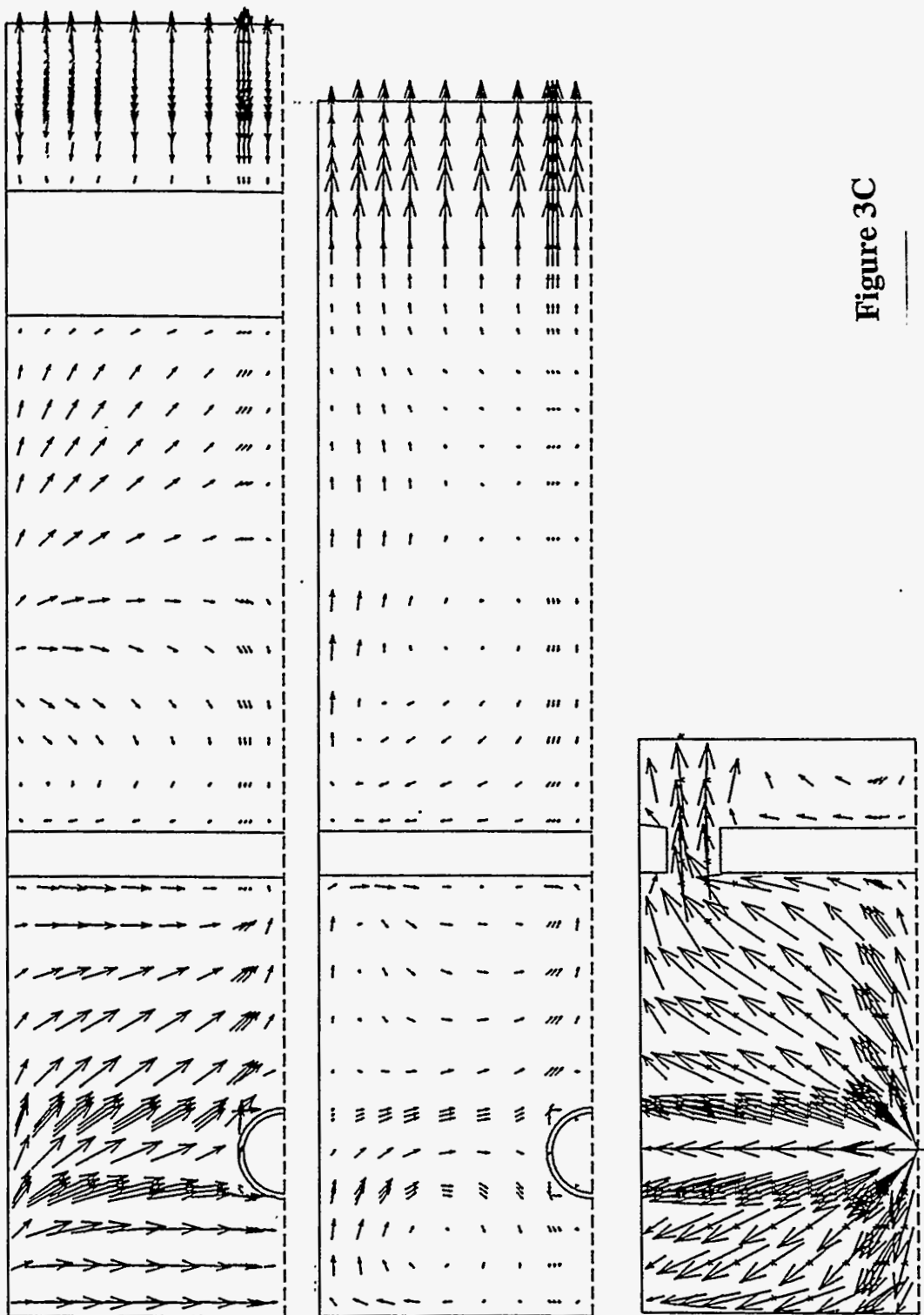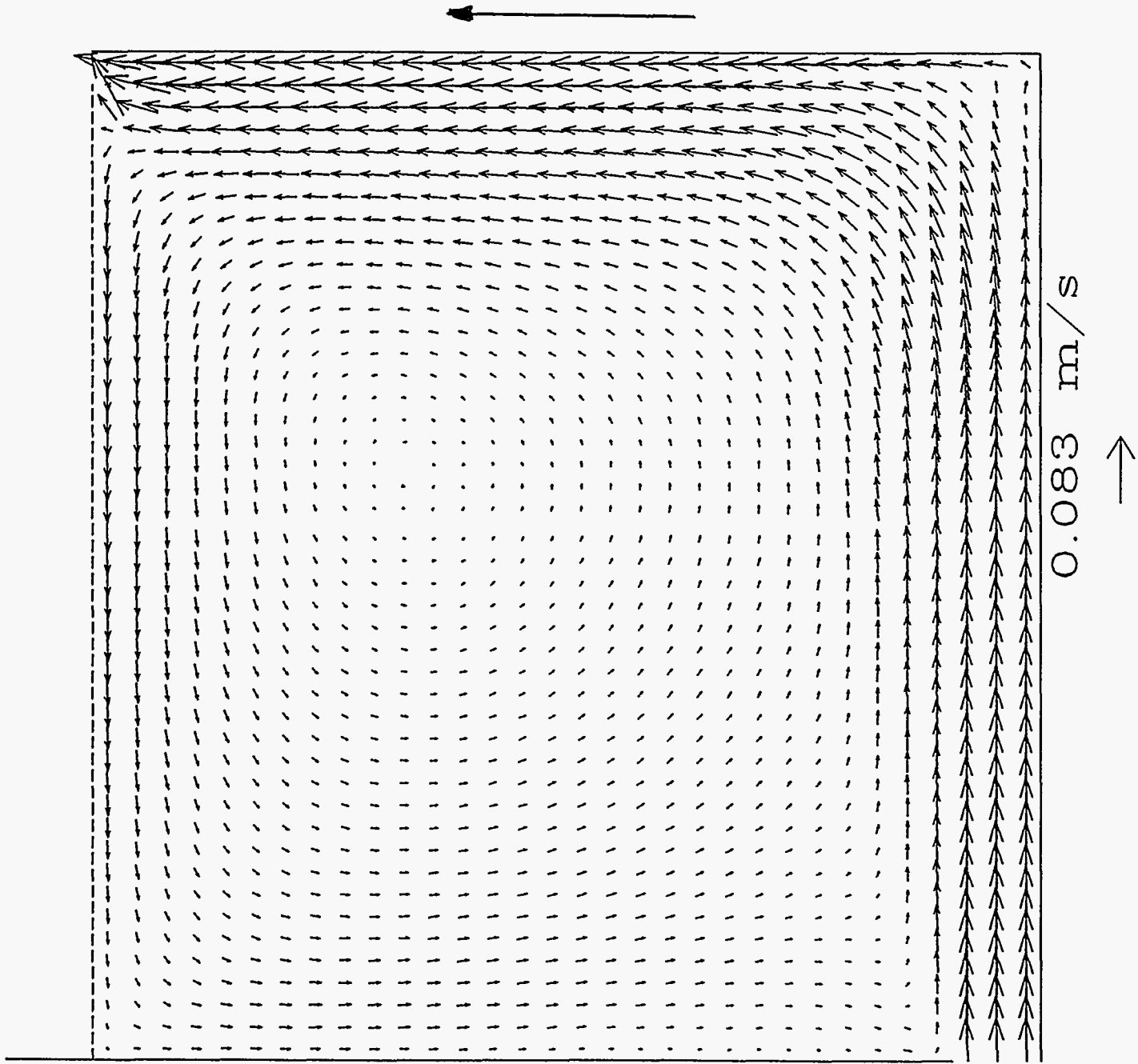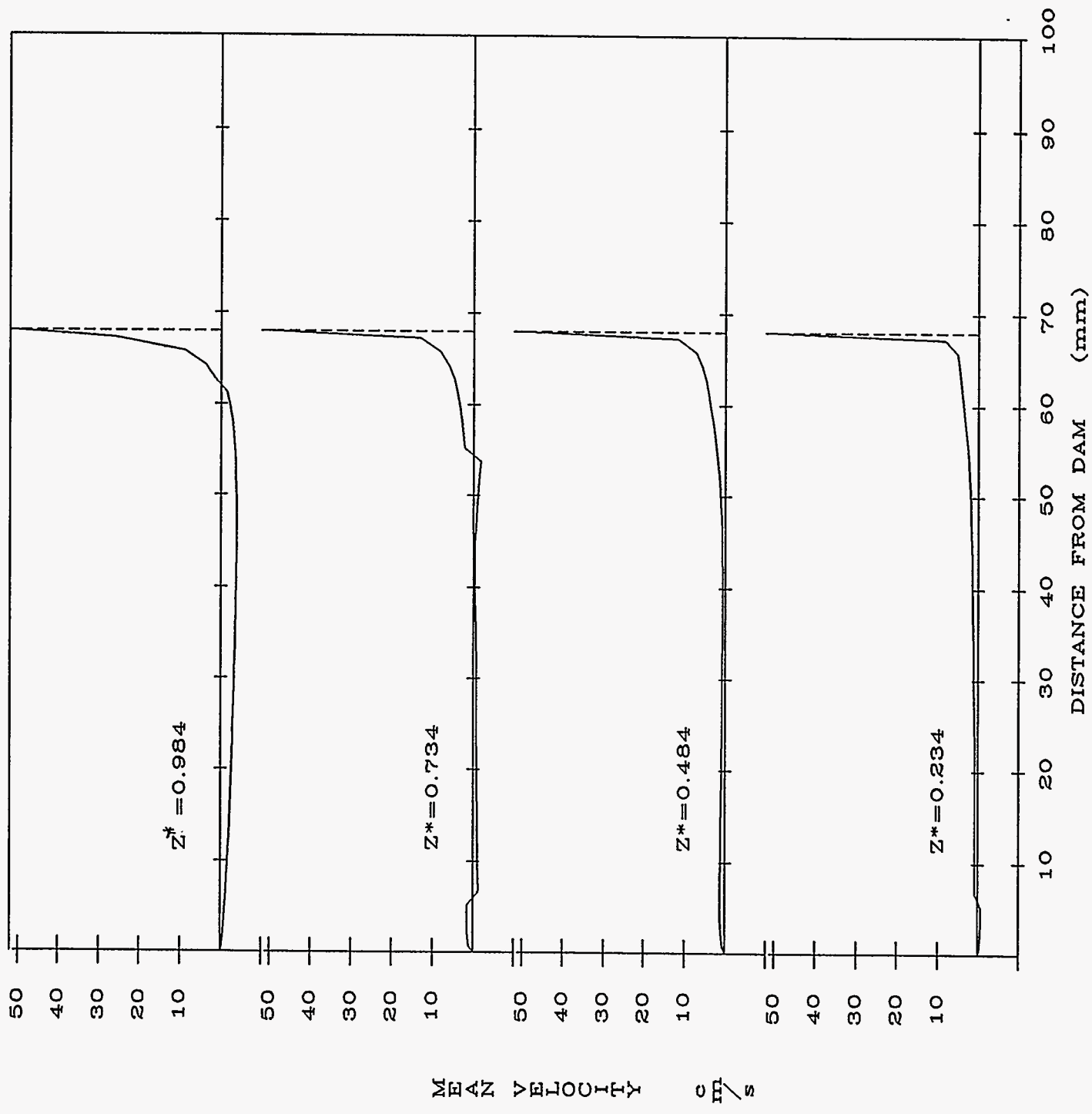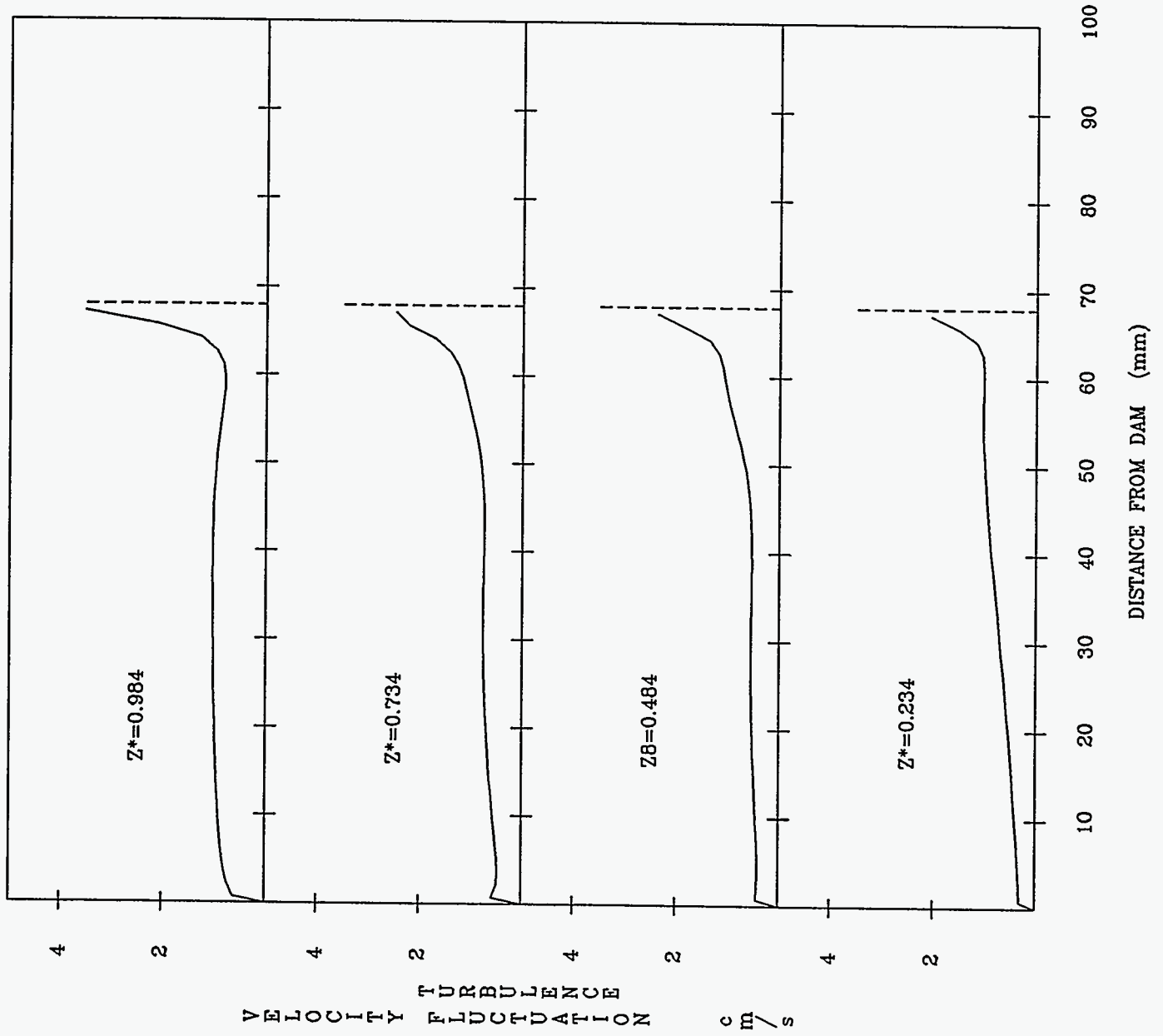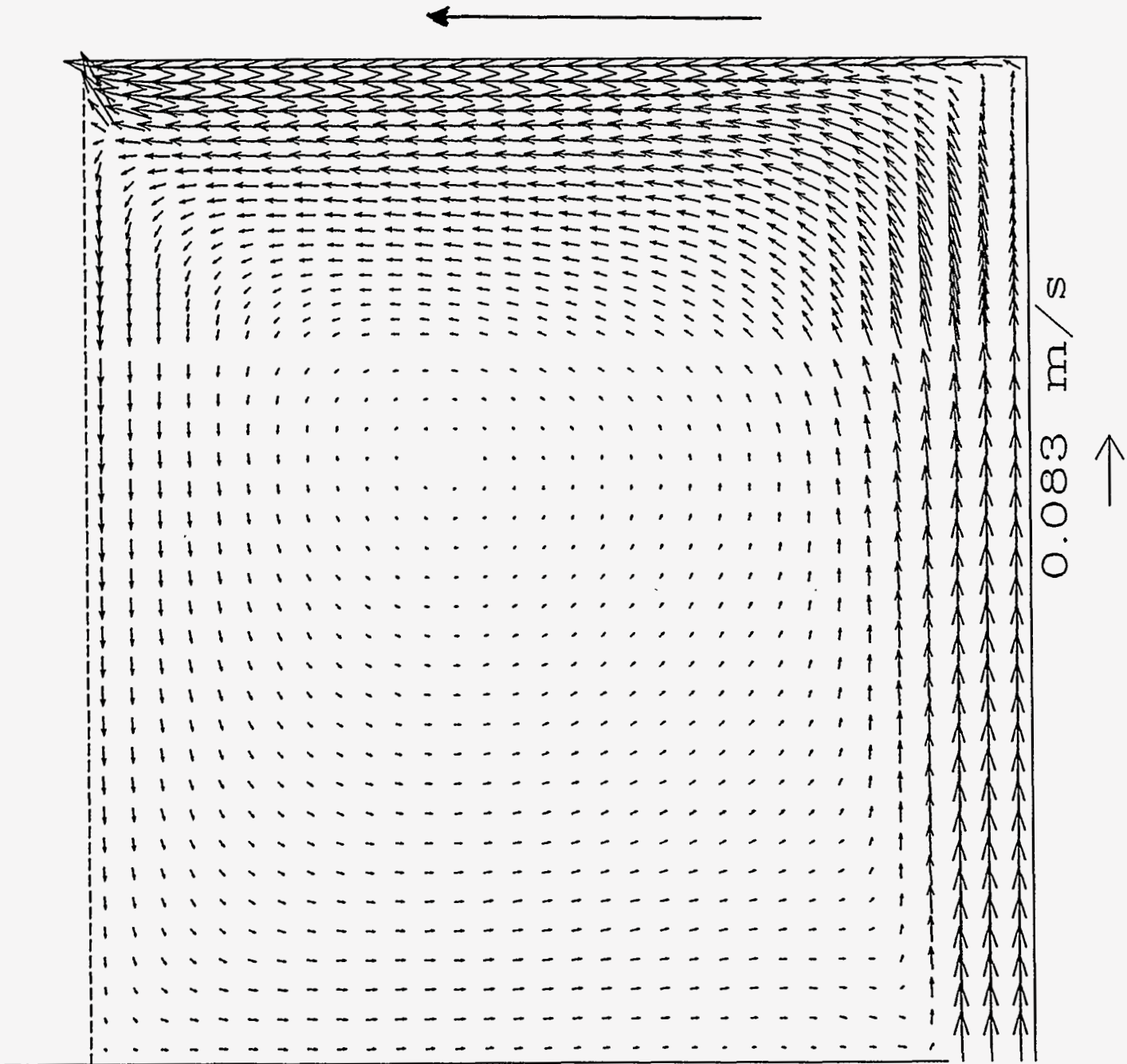
Figure 7

Figure 8

Figure 9

SOLIDIFIED STEEL

0.083 m/s
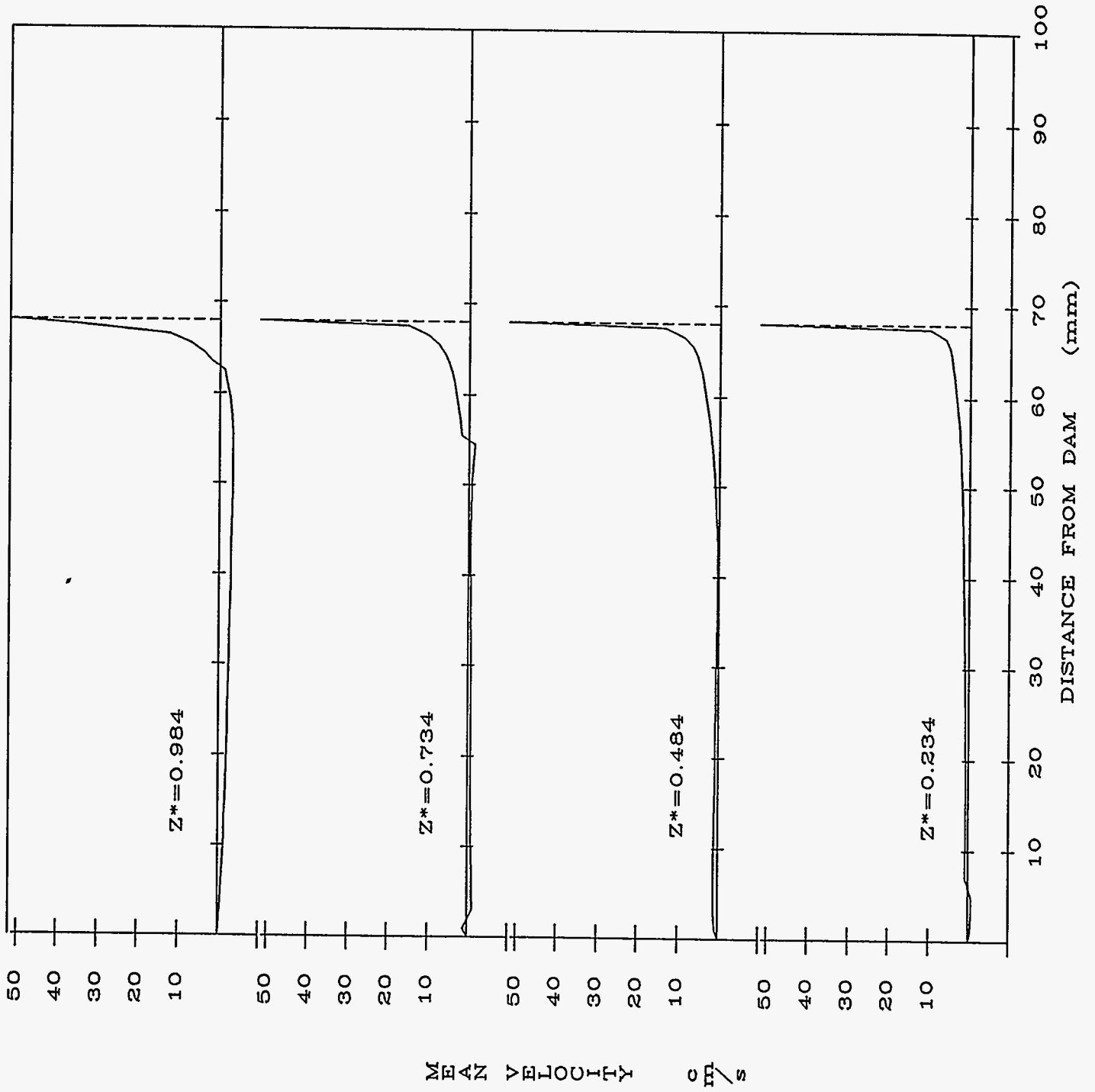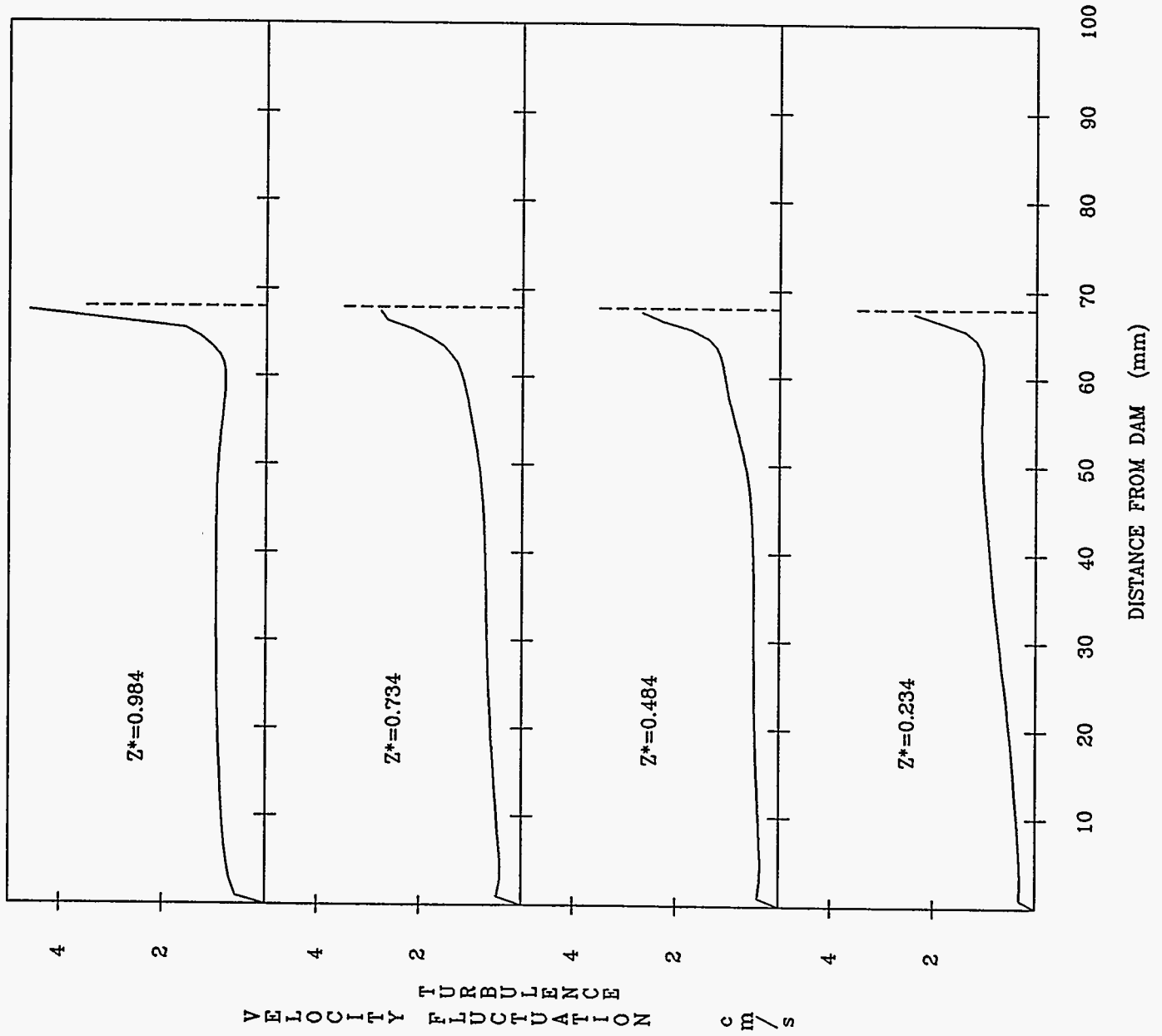
Figure 10

Figure 11

Figure 12

DISTANCE FROM DAM (mm)

VELOCITY FLUCTUATION cm/s
TURBULENCE

Z*=0.984

Z*=0.734

Z*=0.484

Z*=0.234

WHEEL

0.083 m/s

→
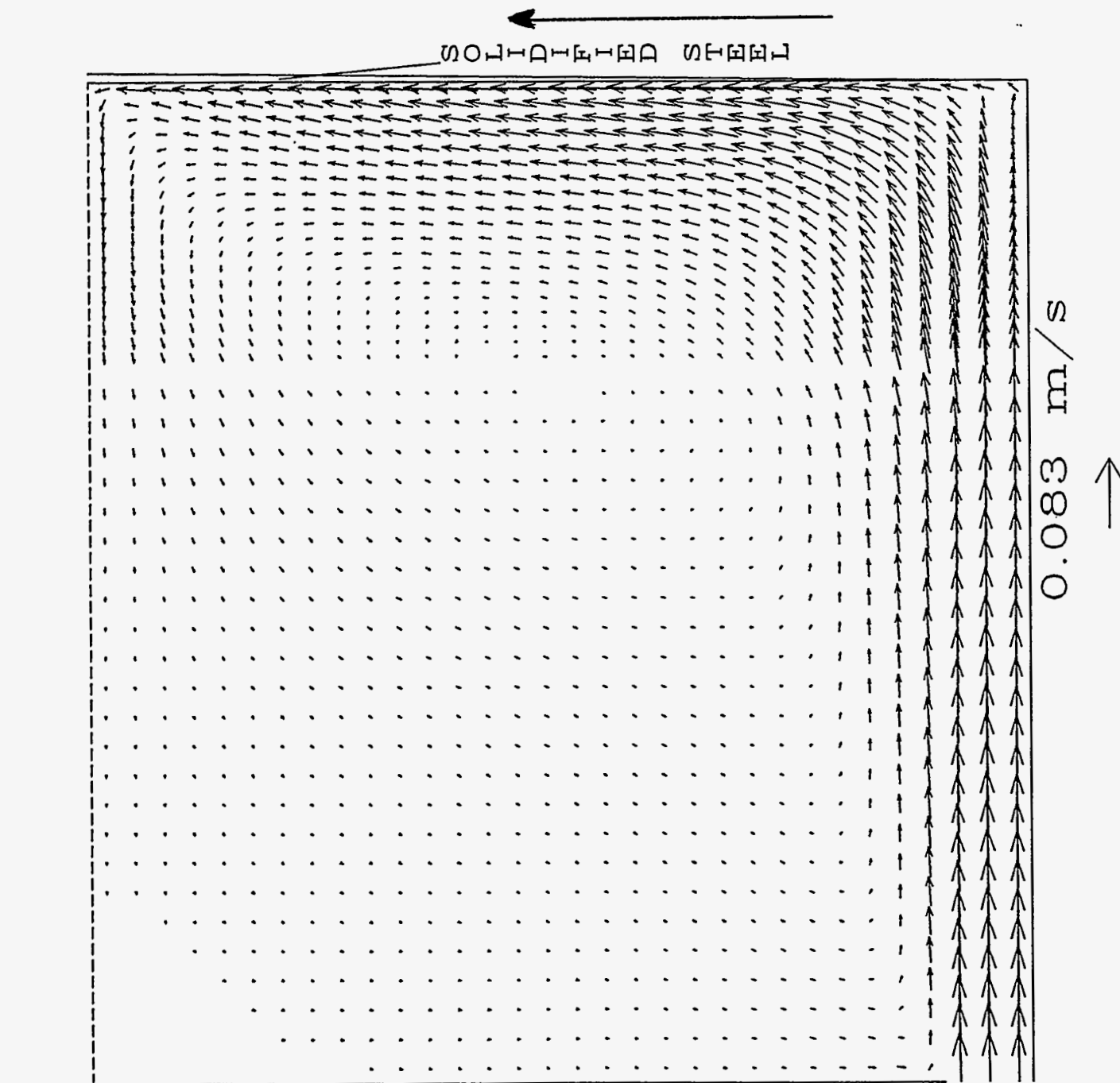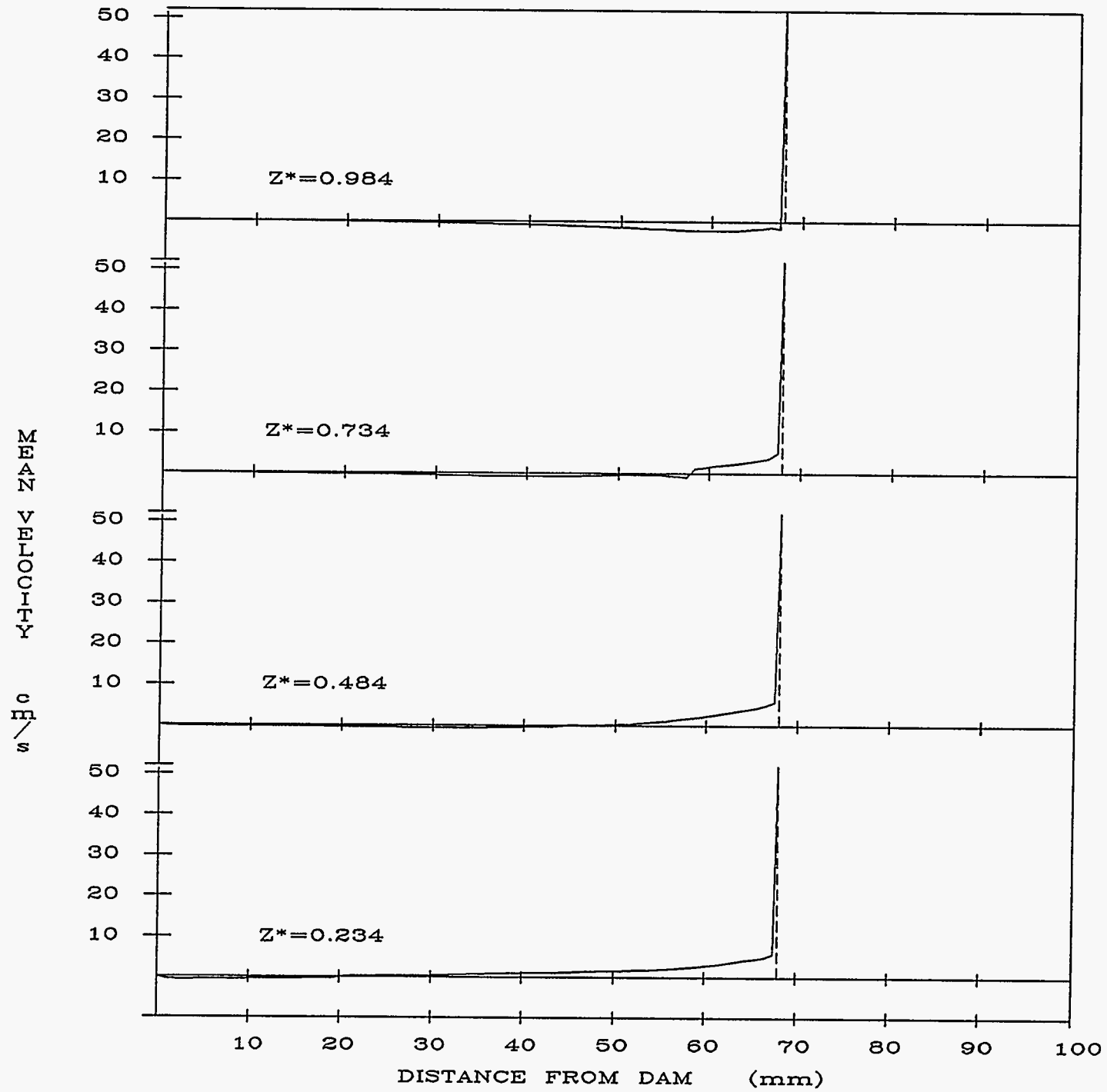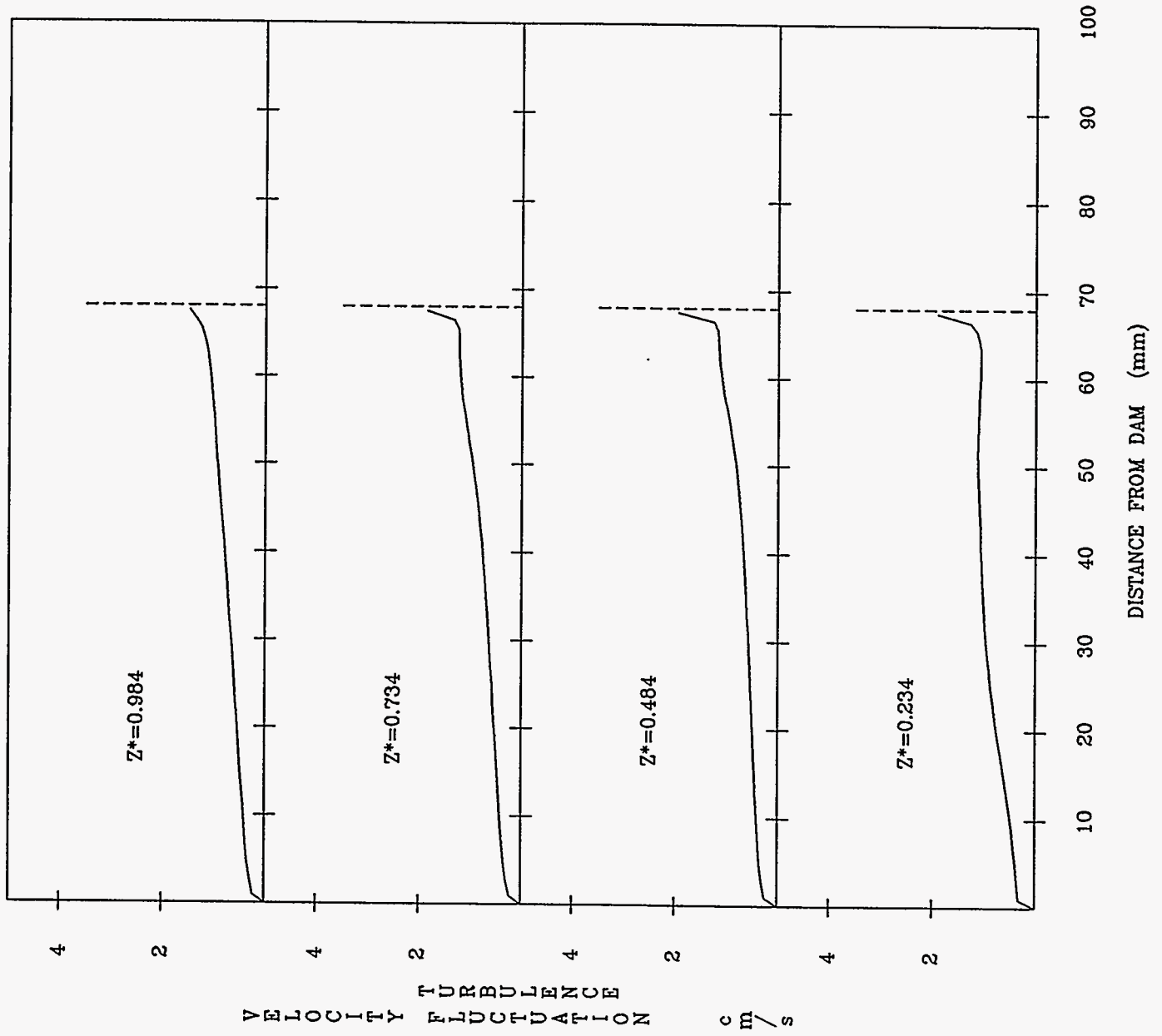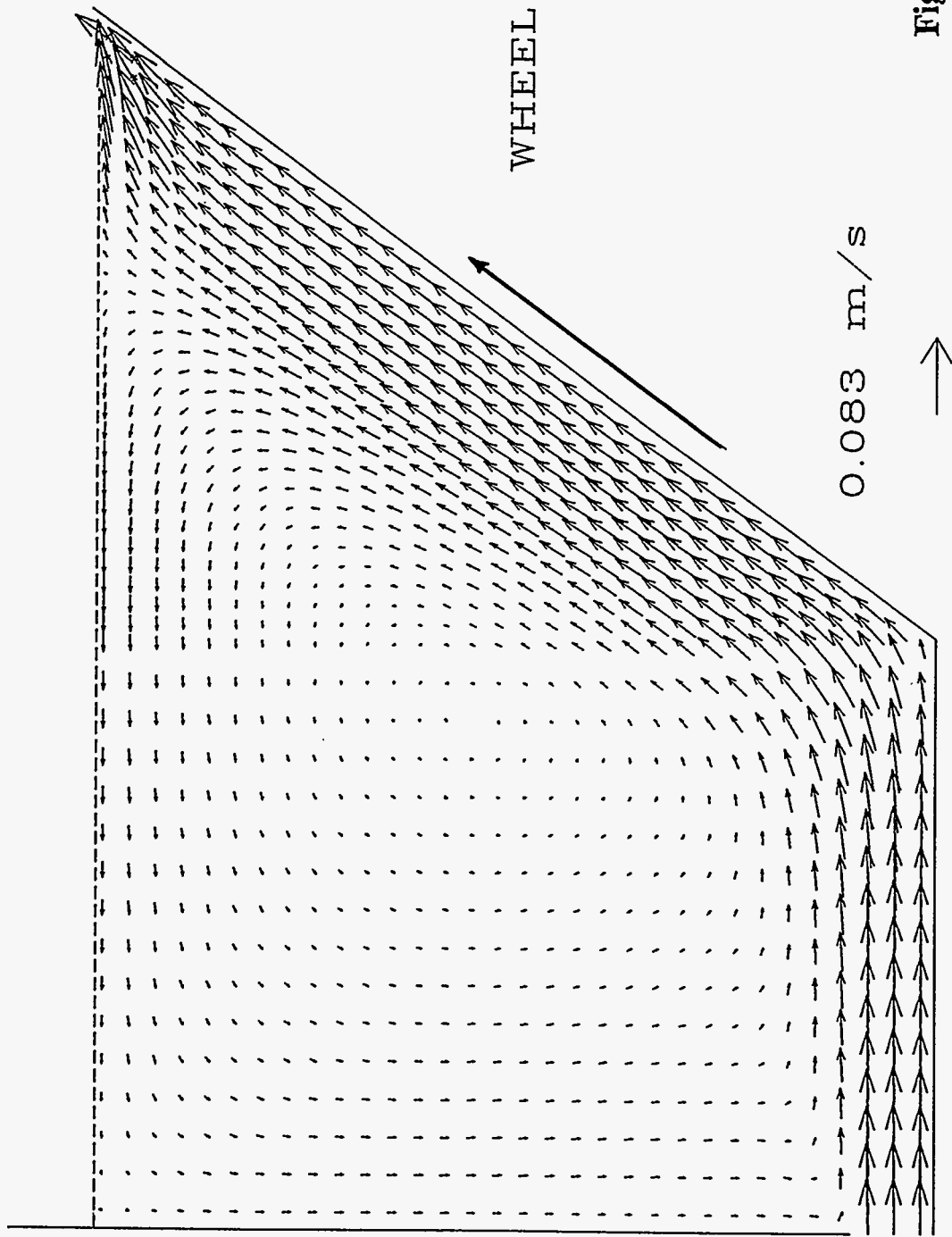
Figure 13

Figure 14

Figure 15

VELOCITY FLUCTUATION cm/s

Z*=0.984

Z =0.734

Z*=0.484

Z*=0.234

DISTANCE FROM DAM (mm)

WHEEL

0.083 m/s
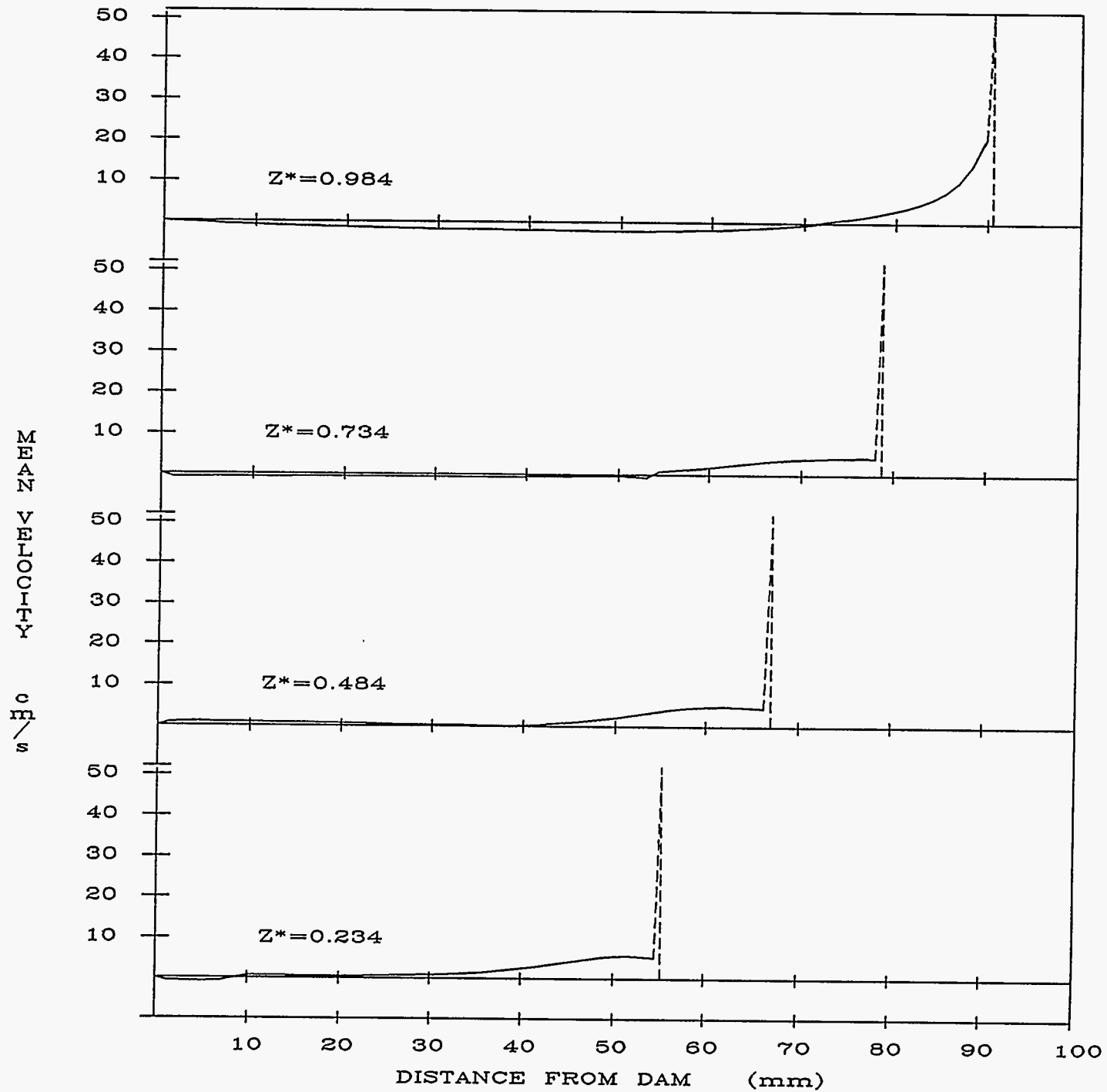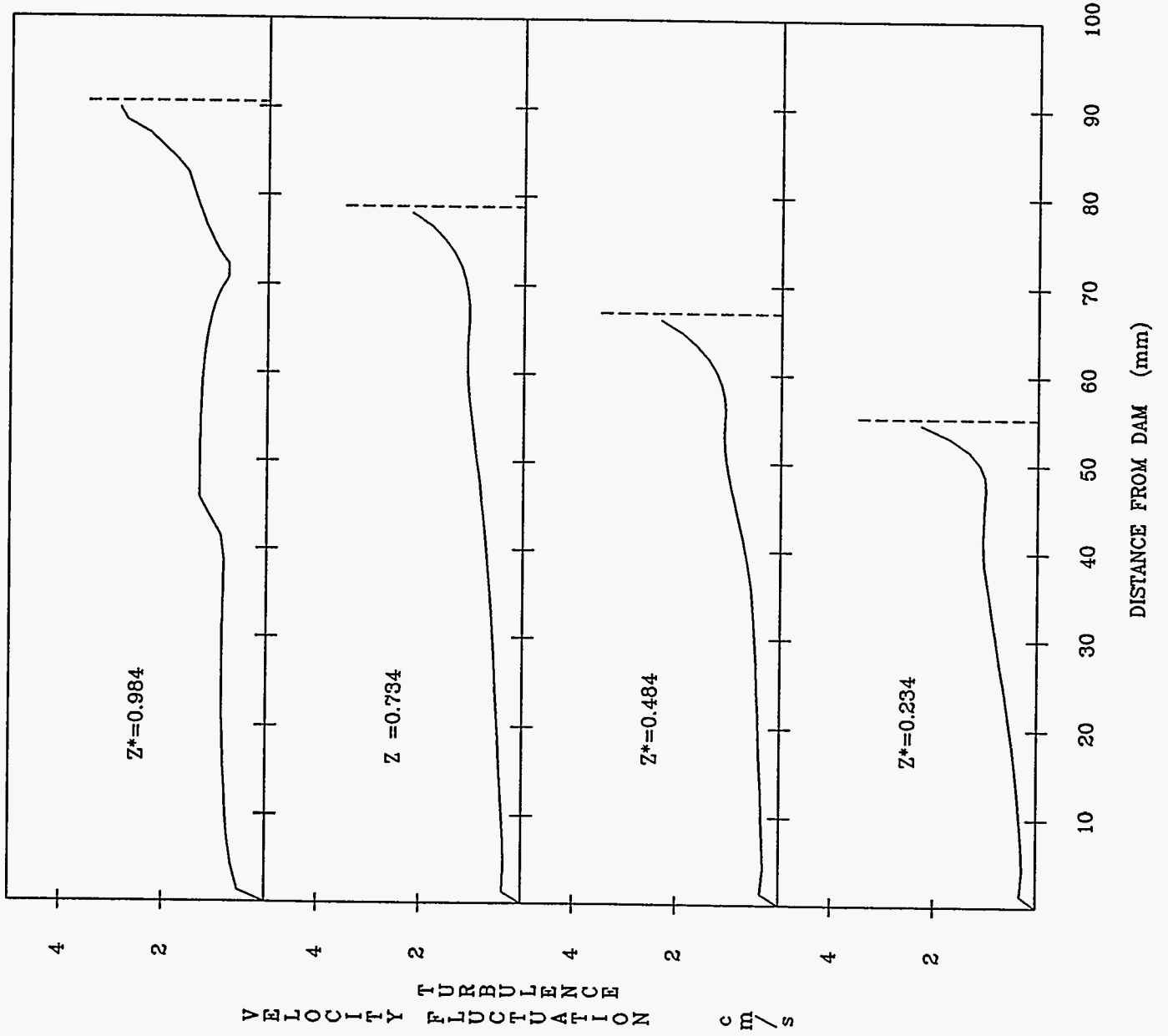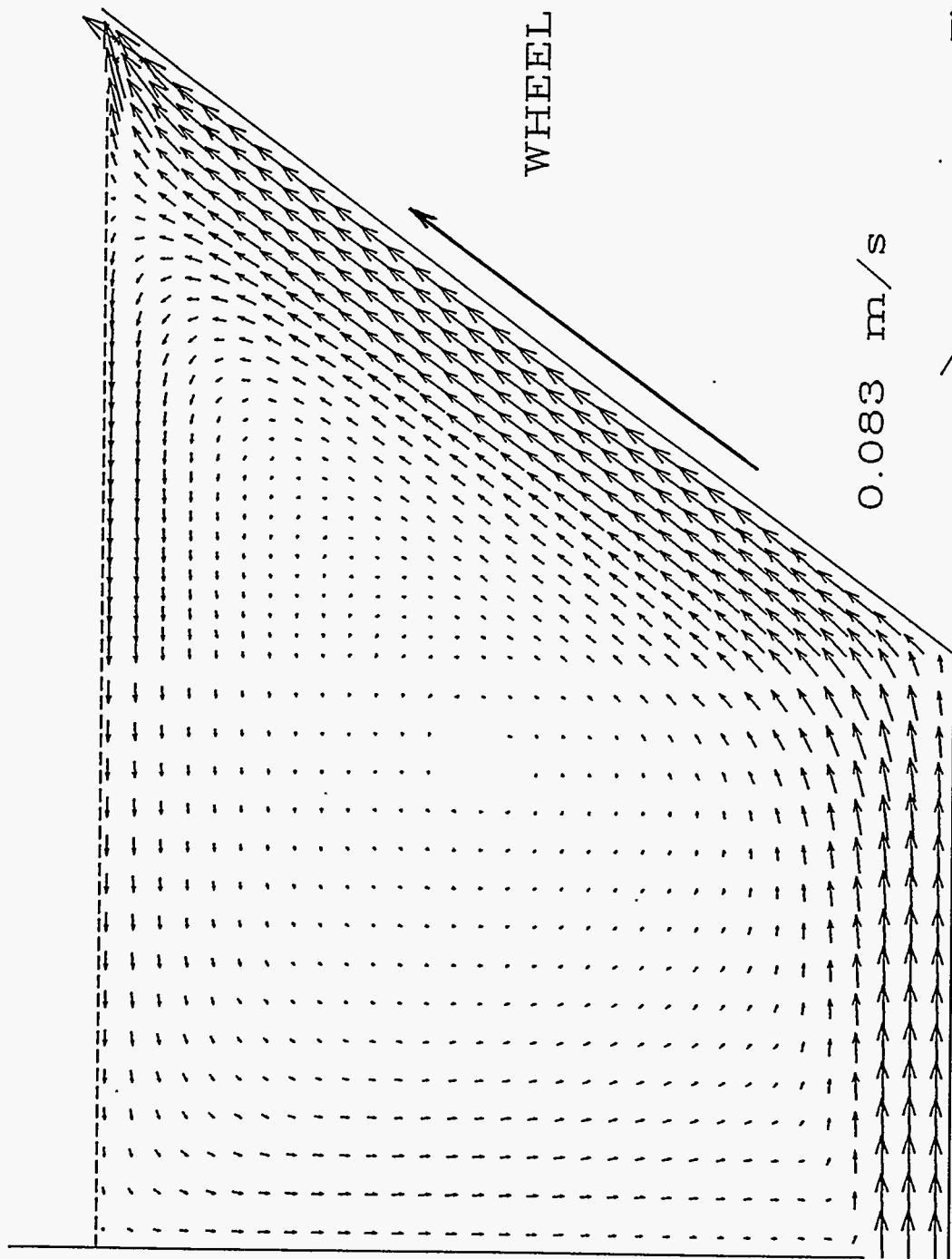
Figure 16

Figure 17

Figure 18

0.083 m/s

→

WHEEL

SOLIDIFIED
STEEL
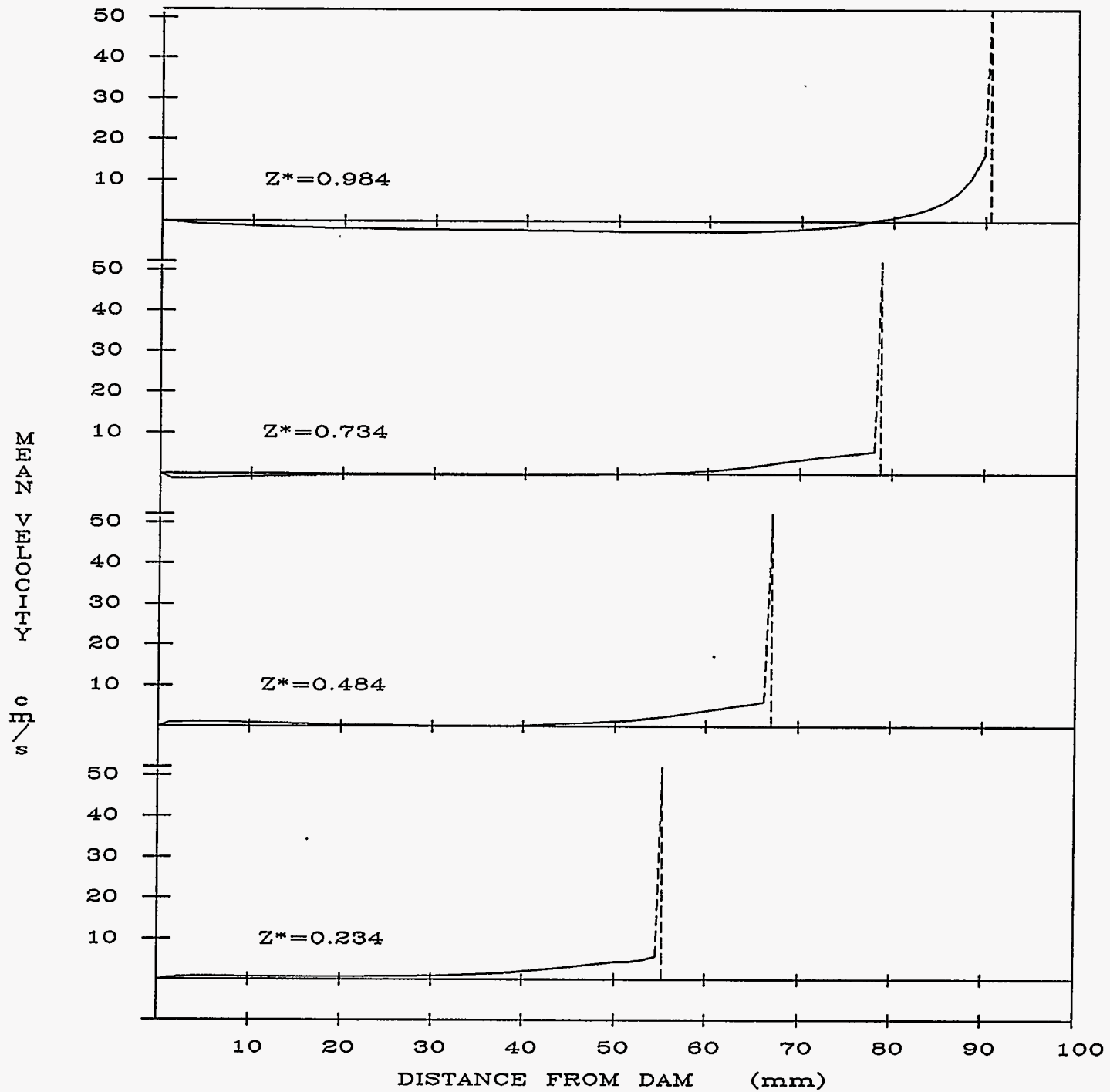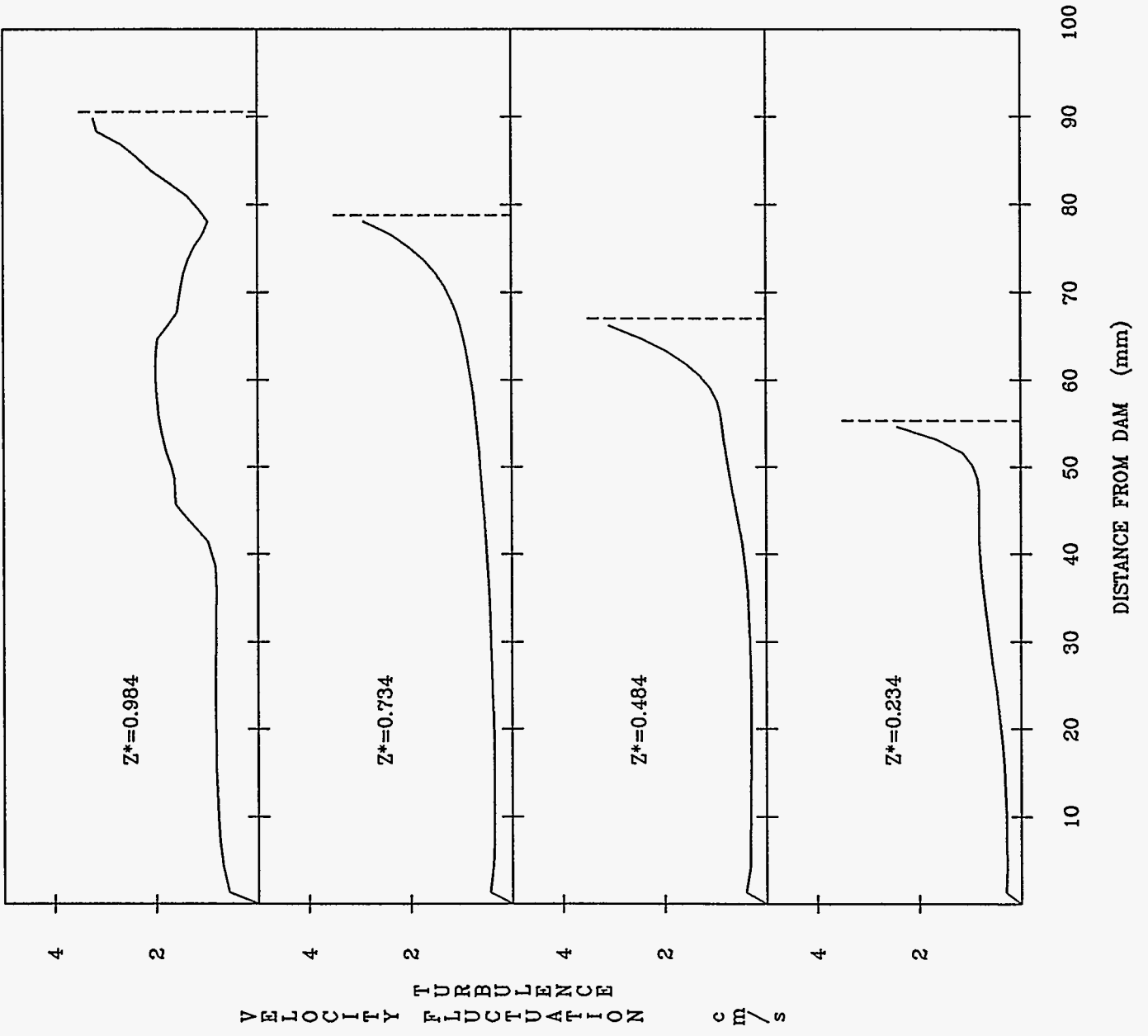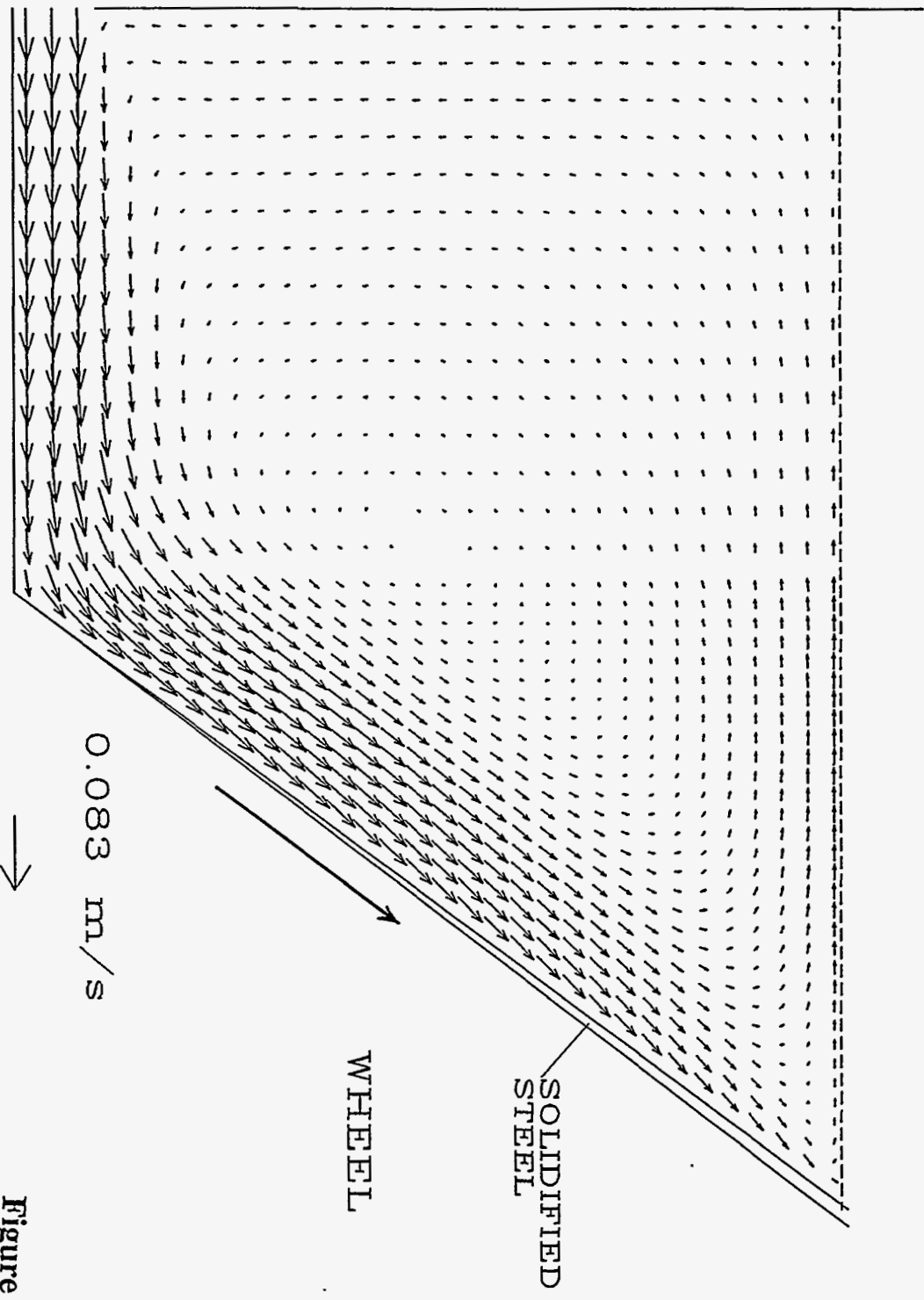
Figure 19

Figure 20

Figure 21

0.083 m/s

WHEEL

SOLIDIFIED
STEEL
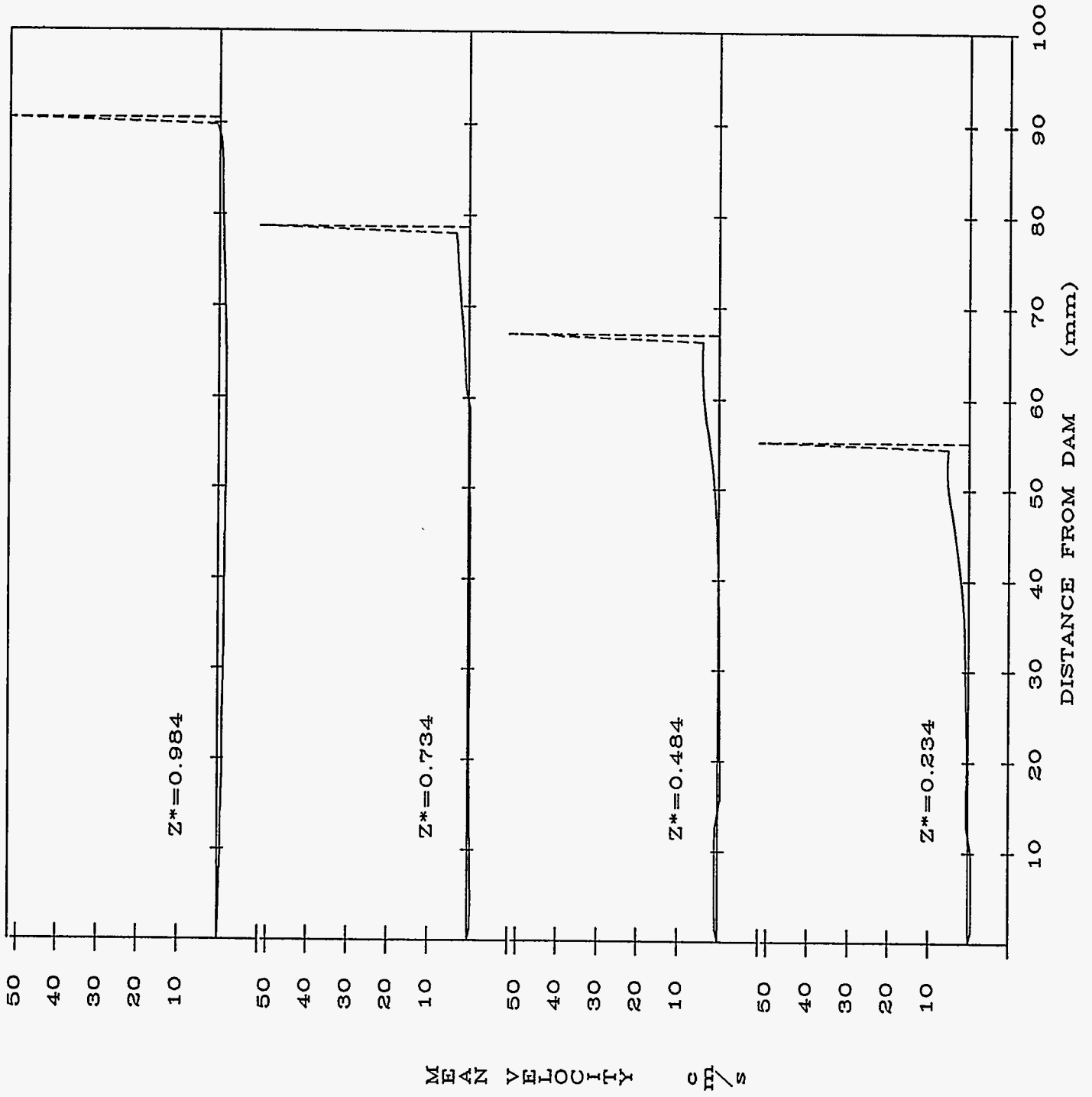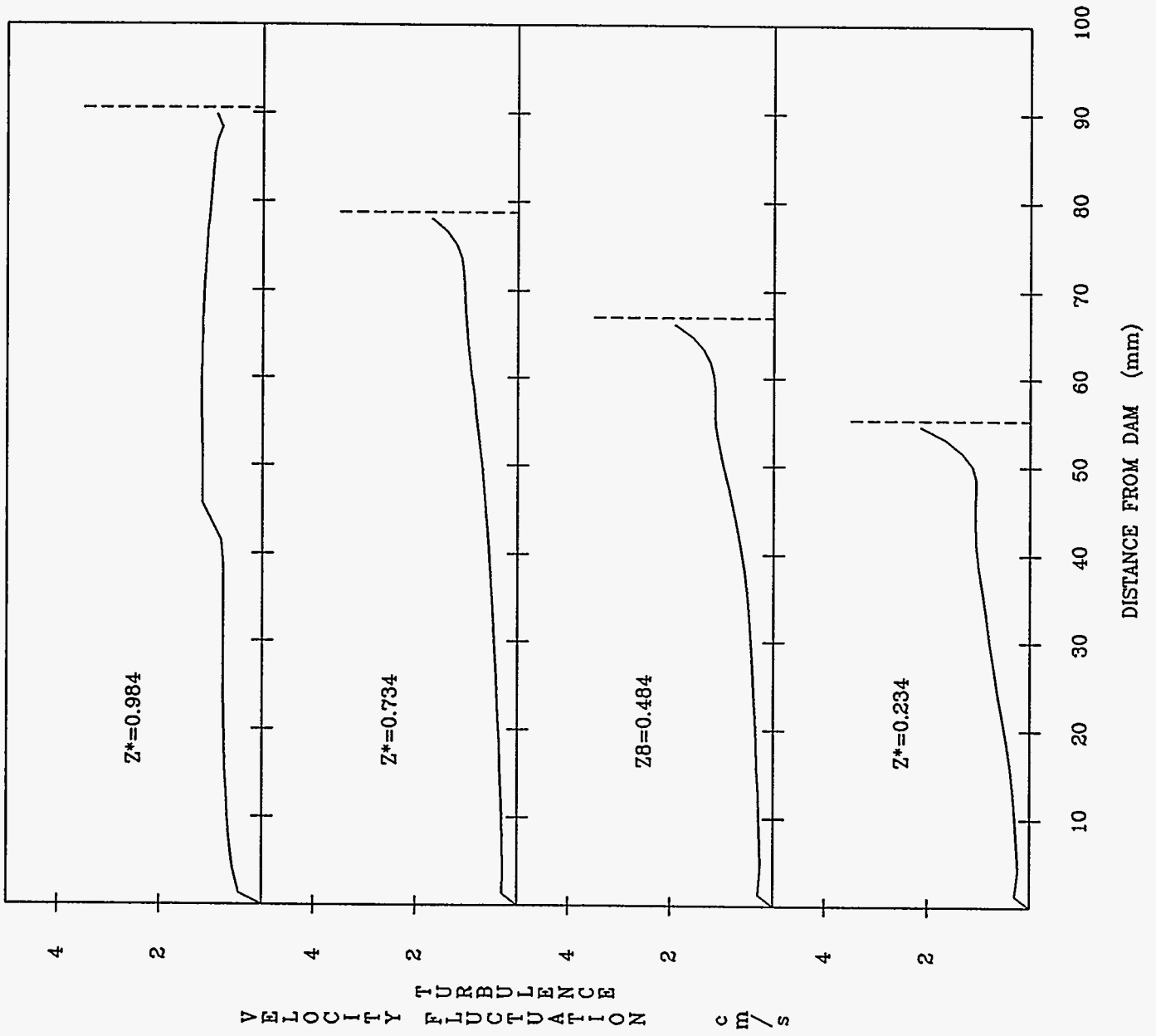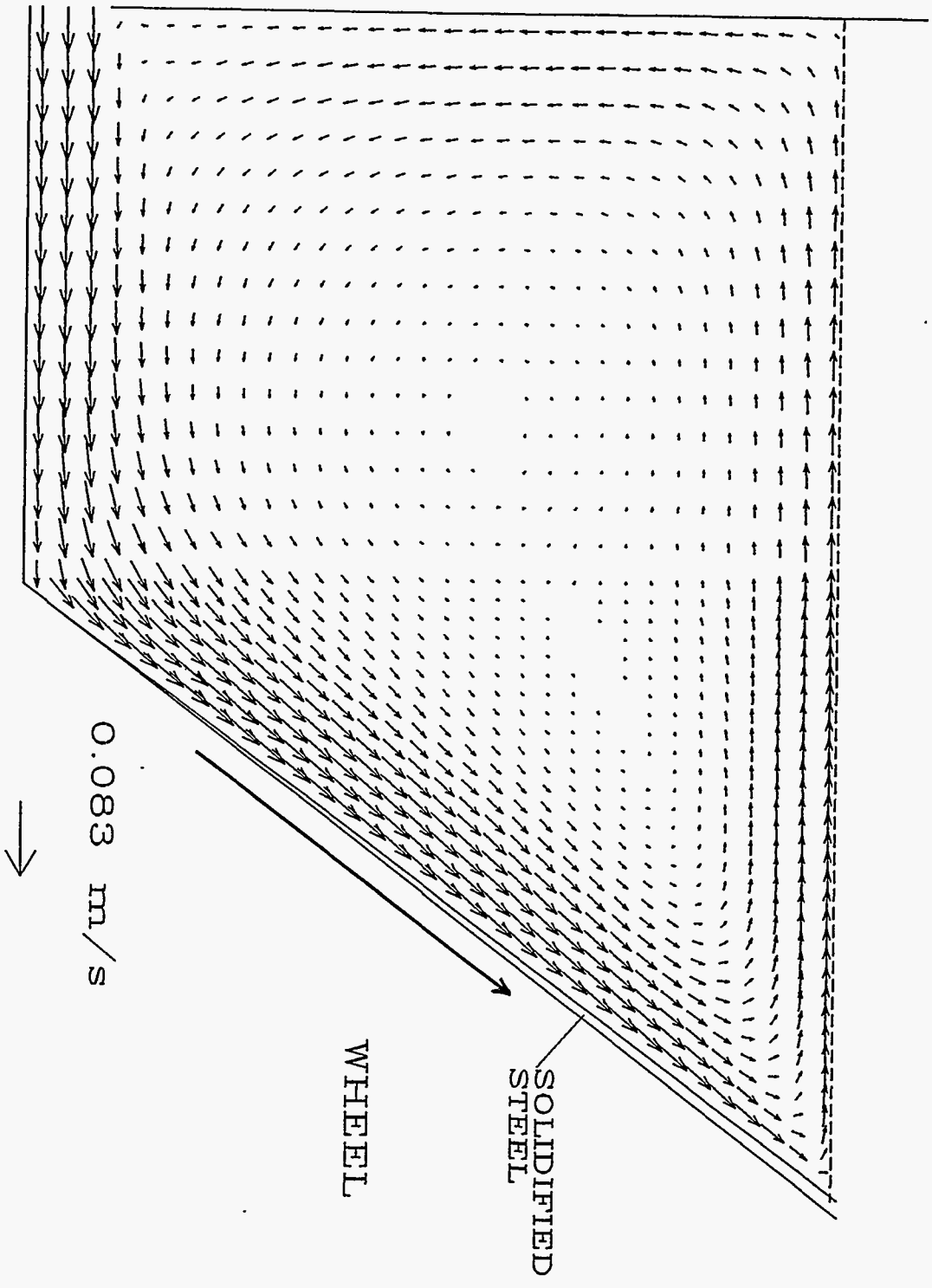
Figure 22

Figure 23

Figure 24

DISTANCE FROM DAM (mm)

Z*=0.984

Z*=0.734

Z*=0.484

Z*=0.234

VELOCITY FLUCTUATION TURBULENCE cm/s

0.05 M/S
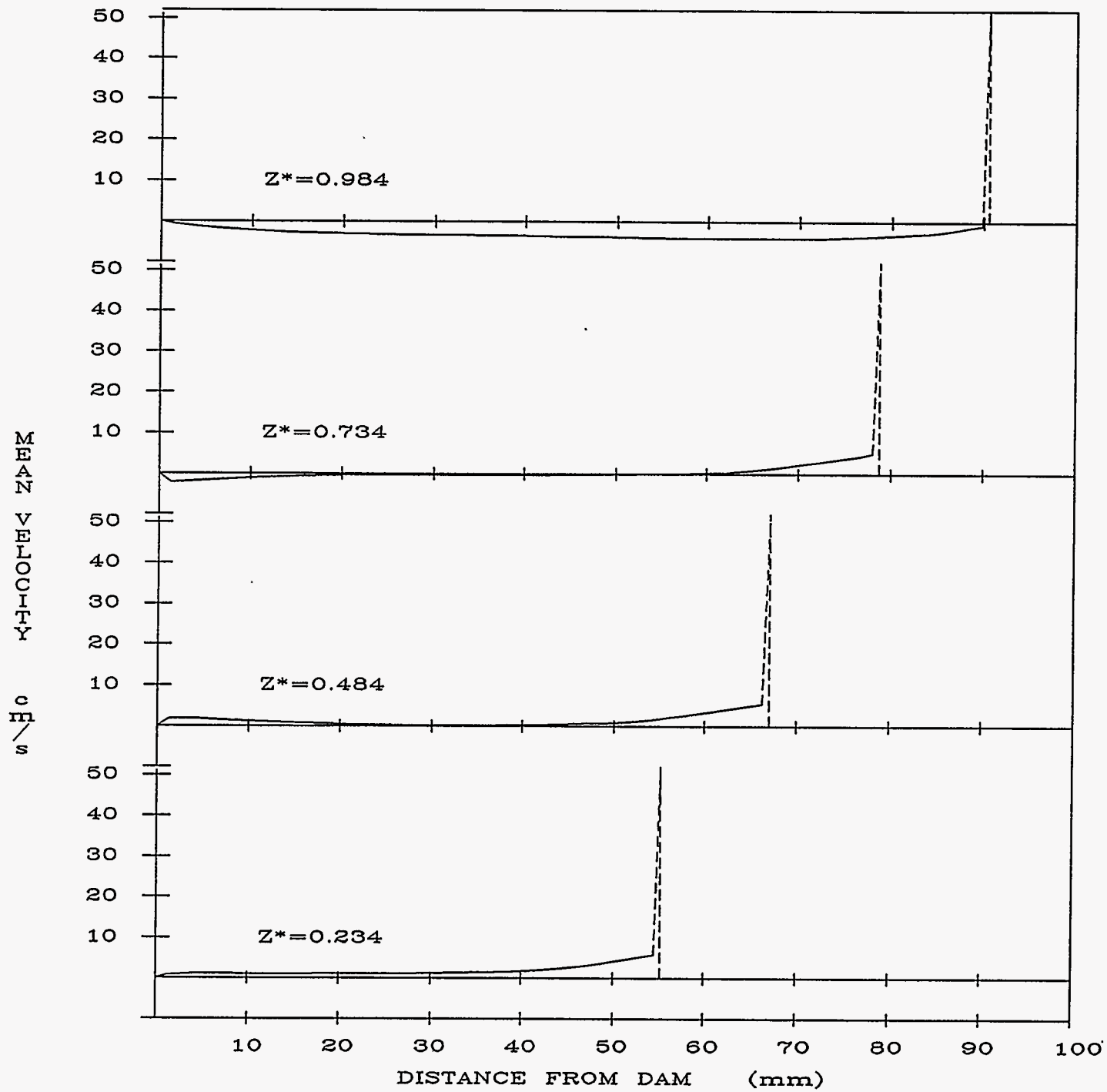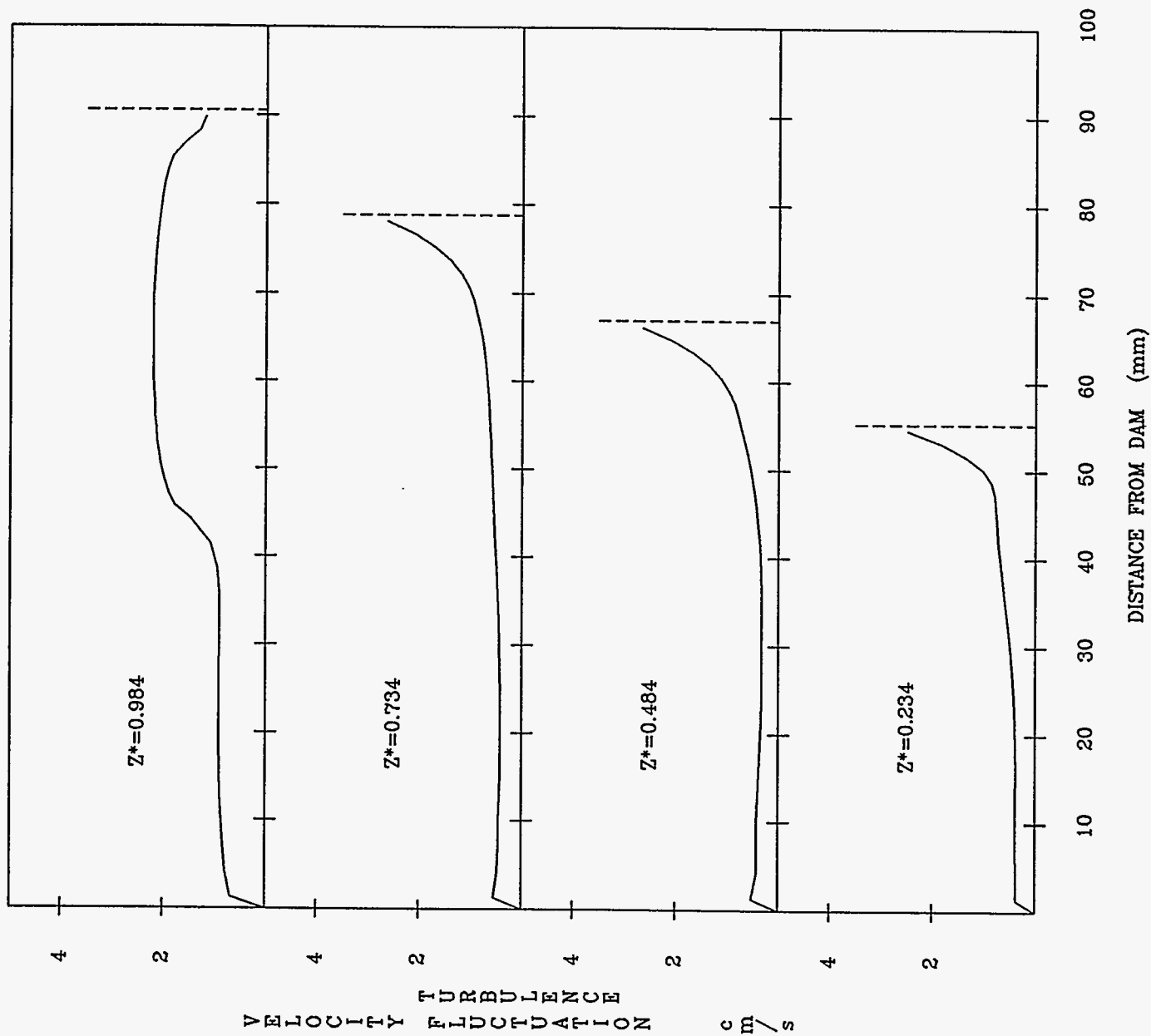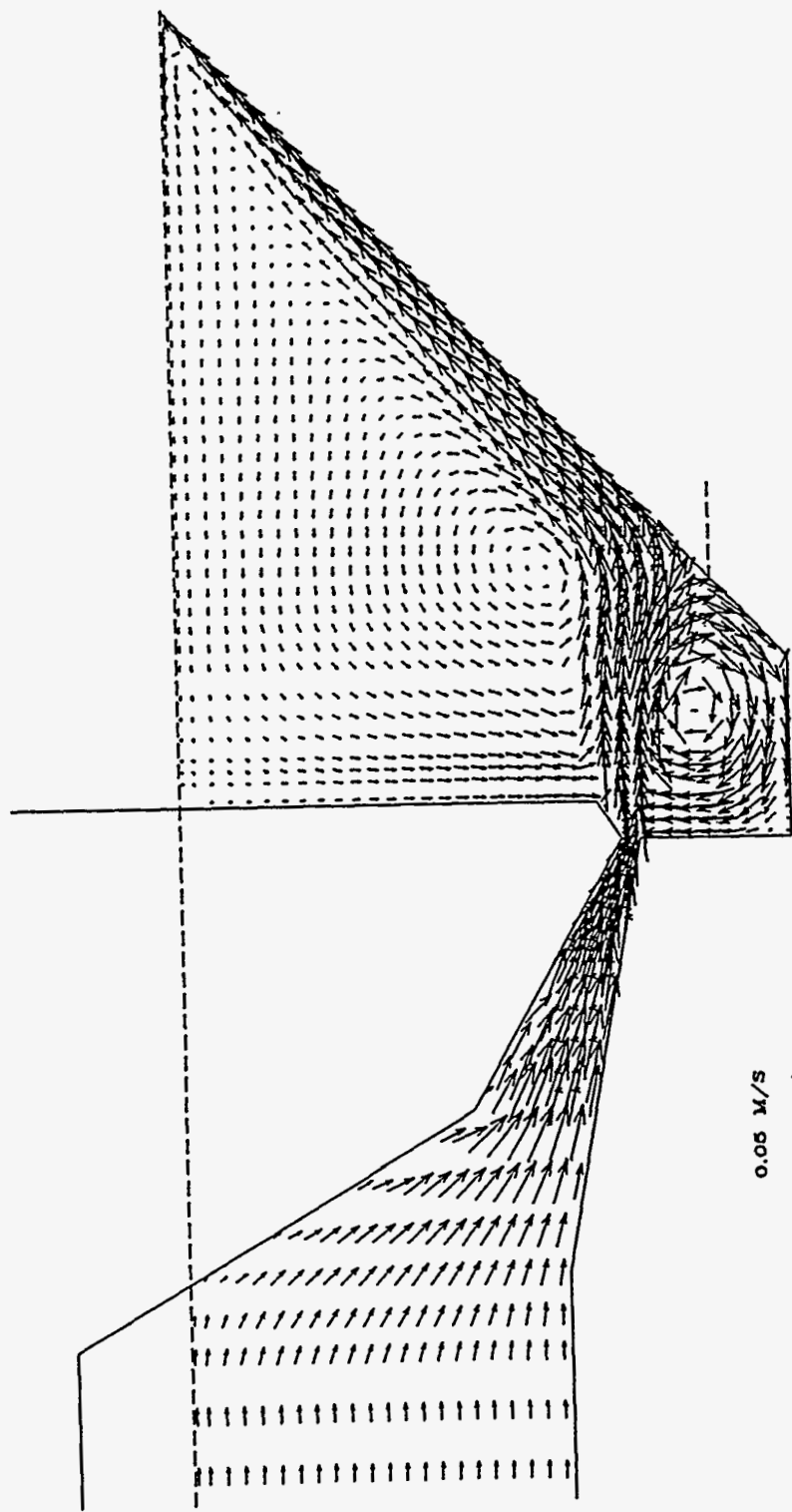
Weir Location - 0 mm

Figure 25

0.05 m/s
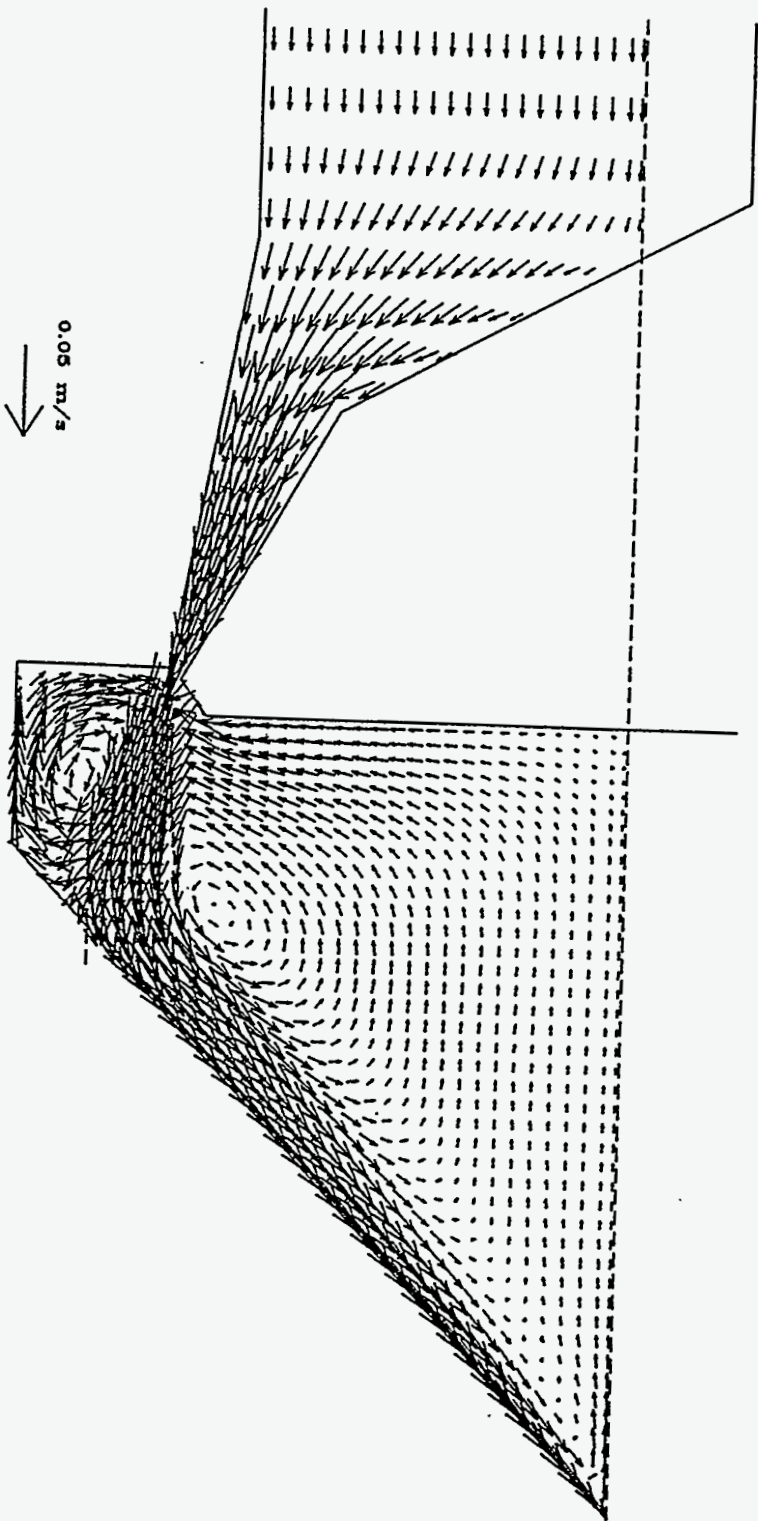
Weir Location - 1.75 mm

Figure 26

0.05 m/s
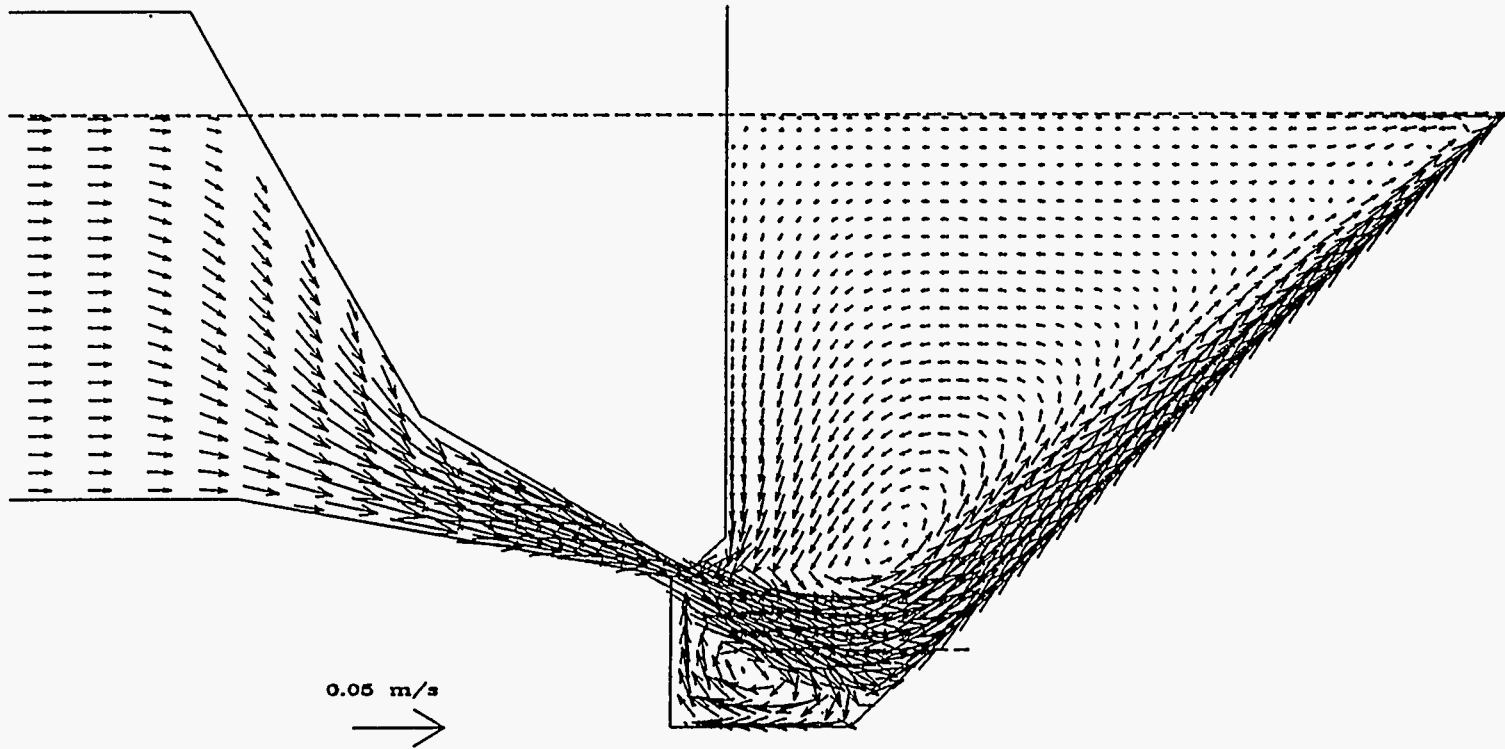
Weir Location - 3 mm

Figure 27

Strip Casting Of Plain Carbon Steel;

STREAMLINE;
CONTOUR PLOT;

LEGEND;
A - 0.2400E-02;
B - 0.9000E-02;
C - 0.1500E-01;
D - 0.2200E-01;
E - 0.2800E-01;

MINIMUM;
    -0.33081E-01;
MAXIMUM;
    0.31590E-01;
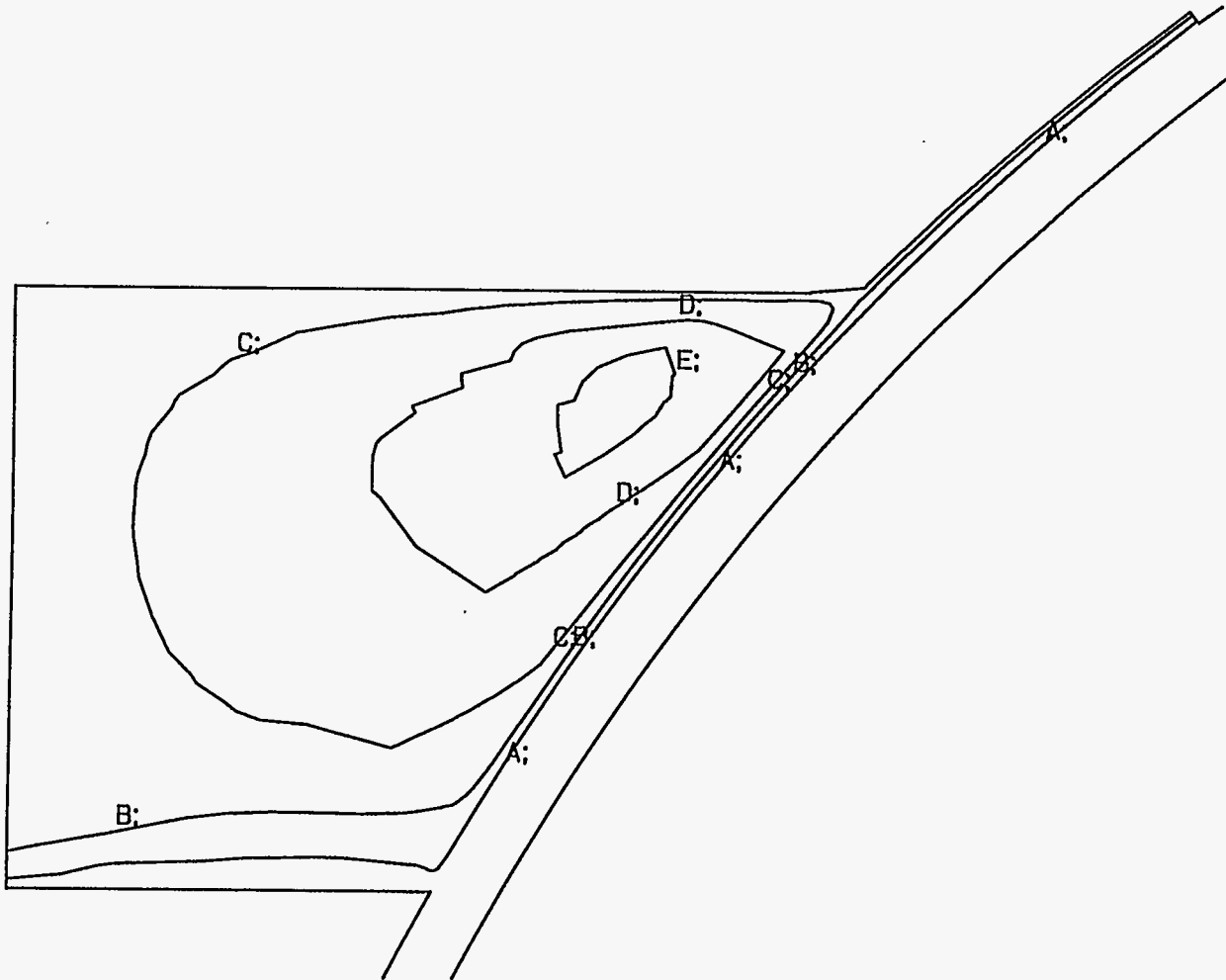
SCREEN LIMITS;
XMIN -.349E+00;
XMAX 0.199E+01;
YMIN -.140E+00;
YMAX 0.148E+01;

FIDAP 6.02;
08/05/93;
22: 57: 19;

Figure 30

Strip Casting Of Plain Carbon Steel;

TEMPERATURE;
CONTOUR PLOT;

LEGEND;
A - 0.8500E+00;
B - 0.9000E+00;
C - 0.9400E+00;
D - 0.9500E+00;

MINIMUM;
0.84421E-02;
MAXIMUM;
0.10011E+01;

D;
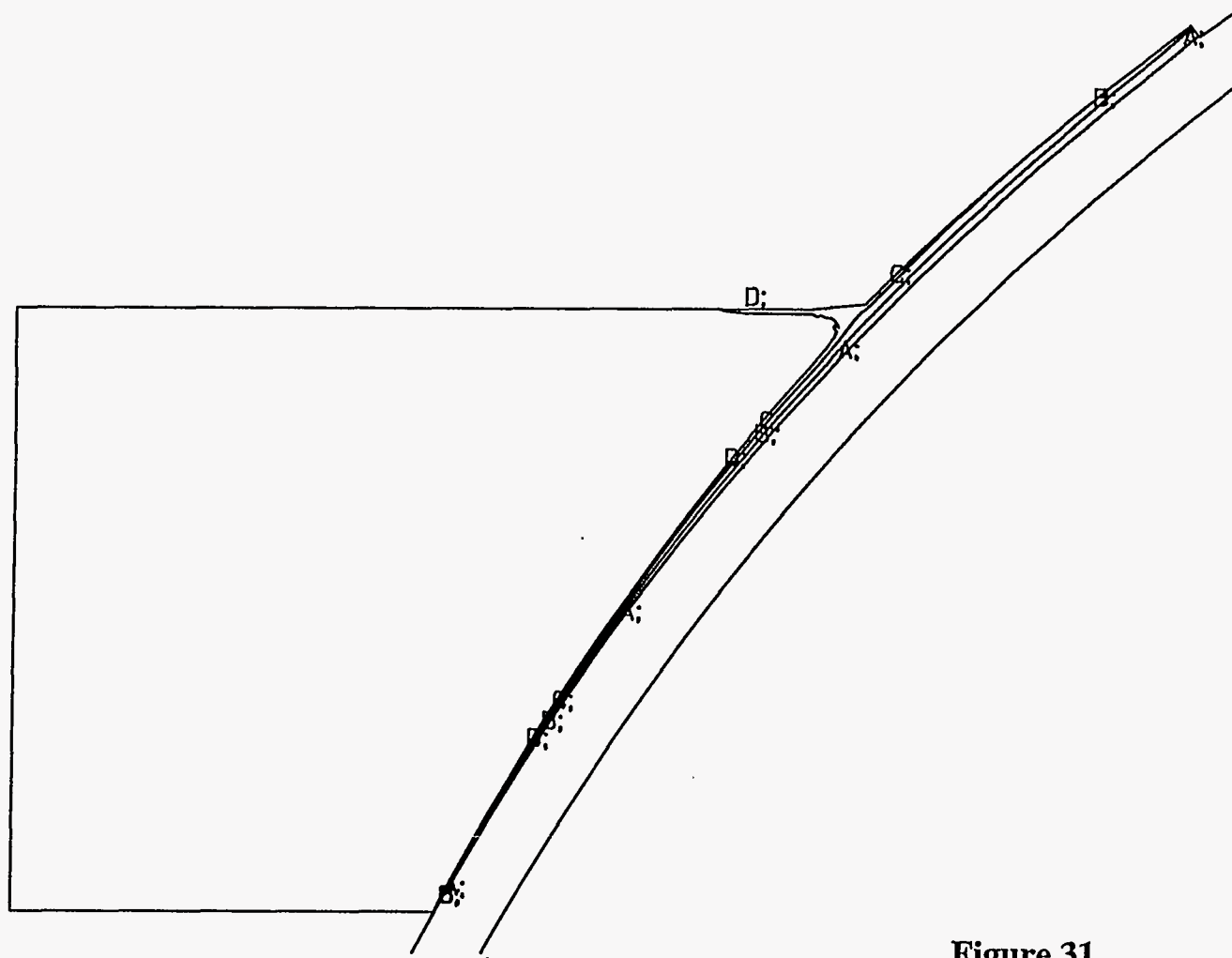
SCREEN LIMITS;
XMIN -.220E+00;
XMAX 0.199E+01;
YMIN -.642E-01;
YMAX 0.157E+01;

FIDAP 6.02;
08/05/93;
22: 47: 58;

Figure 31

Appendix II

Modeling of Strip Casting

- *Freeze-up Prediction for Single-Roll Strip Casting*

- *Transient Thermal Model of the Continuous Single-Wheel*

- *Thin-Strip Casting Process*

- *STRIP1D User Manual*

Metal Process Simulation Laboratory
Department of Mechanical and Industrial Engineering
University of Illinois at Urbana-Champaign
Urbana, IL 61801

Modeling of Strip Casting

Guowei Li
Brian G. Thomas

Final Report
1993

Submitted to

ARMCO Inc., Middletown, OH

August 10, 1993

This report covers work completed from June 1, 1991 to summer, 1993, completing Phase I of modeling of strip casting.

The report is presented in three sections.

I. Freeze-up Prediction for Single-Roll Strip Casting.

II. Transient Thermal Model of the Continuous Single-Wheel Thin-Strip Casting Process.

III. STRIP1D User Manual, input and output data files.

The FORTRAN program, STRIP1D, for IBM-PC and UNIX workstation, accompanies this report.

Freezing Danger in Liquid Pool of Continuous Strip Casting

Department of Mechanical and Industrial Engineering
University of Illinois at Urbana-Champaign
1206 West Green Street
Urbana, IL 61801

Guowei Li and Brian G. Thomas

I. INTRODUCTION

In the light of the numerous advantages that direct strip casting offers, attempts are being made all over the world to develop this processes in steel industries. Freeze up is one problem that plagues process, particularly at startup. Freeze up is caused by: (1) metal not sticking to wheel; (2) metal leaking to gap between wheel and nozzle; (3) superheat not high enough to overcome heat demand of nozzle. Once non moving solid metal comes between liquid and wheel, total freeze-up/breakouts can be rapid, so it is necessary to predict start of freeze-up problems.

The present investigation deals with freeze-up in single-roll strip casting process. The main objective of this study is to develop a fluid flow and heat transfer numerical model in liquid pool and a heat transfer model in the mold, to predict steel freezing danger of molten steel pool in direct strip casting processes. Also an effort has been made to examine the effect of processing parameters, including casting speed, caster temperature in melted steel pool, and the mold thermal properties on the performance of strip casting process.

The physical phenomena occurring in the strip casting process are illustrated in Figure 1. Liquid steel at caster temperature flows from tundish into the liquid pool. As soon as the rotating caster roll, with substantially lower temperature, comes into contact with the molten steel, a solidified shell is formed. Due to the large radius of the caster roll (12 inch), the solid / liquid interface along the roll was assumed to be a slope flat plane (2.1-inch-long). The superheat contained in liquid steel must be removed before it can solidify. In order to investigate how mold properties, and process parameters affect the heat removed by the

turbulent kinetic energy and dissipation were employed, setting (input velocity * inlet height) equal to (strip thickness * casting speed). Temperature across the inlet plane is simply fixed to the casting temperature, T_0, given in Table IV.

2. Outlet and Top surface

For top surface, v_x and normal gradients ($\partial/\partial x$) of all other variables, including v_y, v_z, K, ε, and p are set to zero. To account for the heat loss due to the top free surface radiation from liquid steel to ambient , the equivalent heat transfer coefficient, h, and ambient temperature, T_∞, given in Table I, were used. The small variations in the liquid level due to motion of the free surface are neglected. Across the outlet plane, similarly, normal gradients ($\partial/\partial x$) of all variables, including v_x, v_y, v_z, K, ε, and p are set to zero also.

3. Pool bottom, back wall and side wall

To account for the steep gradients that exist near the pool bottom, back wall and side wall, Non-slip velocity boundary condition and empirical "wall law" functions, given in Appendix I, are employed to define the tangential velocities, K, ε at the near-wall grid nodes. The thermal boundary conditions for the pool bottom, back wall and side wall are different. For the back wall, a simple adiabatic condition is used, while the pool bottom and side wall are treated as two kinds of boundary conditions in this study, i.e. in some cases assuming bottom and side wall temperature equal to liquidus temperature; and in other cases using heat flux profiles obtained from mold heat transfer simulations.

4. moving slope wall against the roll

To simulate velocity, temperature distribution in liquid pool where one boundary of the solution domain does not lie along a coordinate line, by using the finite difference program designed for orthogonal coordinate system, the real boundary along the roll was approximated as a serious of steps, utilizing the block-off solution method, shown in Figure 2. The moving boundary condition was imposed to these steps. The mesh was carefully designed to let both of the values and directions of the combined velocity of Vxri and Vyri equal to tangential velocity of rotating roll.

To avoid the computational difficulties associated with modeling latent heat evolution at the solidification front, fluid flow is modeled up to, but not including, the mushy zone. The boundaries of the mesh along the roll then correspond to the dendrite tips forming the

3

$$\rho C_p \frac{\partial T}{\partial t} = \frac{\partial}{\partial x}\left(k\frac{\partial T}{\partial x}\right) + \frac{\partial}{\partial y}\left(k\frac{\partial T}{\partial y}\right) + \frac{\partial}{\partial z}\left(k\frac{\partial T}{\partial z}\right)$$ [2]

To compare the results with fluid flow simulation in liquid pool, the roll / liquid steel interface was approximated as a flat plate just as what has been done in fluid flow simulation. By assuming no heat transfer (big contact resistance) between side wall and bottom of the mold, the boundary conditions for mold bottom are independent of the mold width direction, so a 2-D solution was actually obtained in the mold bottom.

Figure 3 shows the boundary conditions used in mold heat transfer simulations. As initial conditions for the mold heat transfer simulation, hot faces (which contact with liquid steel) were assumed to have an even preheat temperature T_i. Furthermore, adiabatic condition was employed to mold back (interior) surfaces and symmetry plane in the center of the mold. Free convection condition was applied to other mold surfaces which open to ambient.

In transient simulation, because the liquid pool is set just beside the roll, both radiation and forced convection were taken into account for the roll / liquid interface. Forced convection was also taken into account for mold hot faces, and the surface against the roll on the first step on side wall.

As initial conditions for the mold heat transfer simulation, hot faces (which contact with liquid steel) were assumed to have an even preheat temperature T_i. Furthermore, same as the transient simulation, adiabatic condition was employed to mold back (interior) surfaces and symmetry plane in the center of the mold. Free convection condition was applied to other mold surfaces which open to ambient.

The commercial finite element program FIDAP was chosen to model this complex geometry problem. The standard mesh of half of the mold (the center plane of the mold is a symmetry plane), shown in Figure 4, consists of a 37 by 23 by 15 grid of eight-node, linear, brick elements. Due to the big gradient of temperature in the region near the roll, the mesh was refined in this region.

Metal Process Simulation Laboratory
Department of Mechanical and Industrial Engineering
University of Illinois at Urbana-Champaign
Urbana, IL 61801

Modeling of Strip Casting

Guowei Li
Brian G. Thomas

Final Report
1993

Submitted to

ARMCO Inc., Middletown, OH

August 10, 1993

This report covers work completed from June 1, 1991 to summer, 1993, completing Phase I of modeling of strip casting.

The report is presented in three sections.

I.   Freeze-up Prediction for Single-Roll Strip Casting.

II.   Transient Thermal Model of the Continuous Single-Wheel Thin-Strip Casting Process.

III. STRIP1D User Manual, input and output data files.

The FORTRAN program, STRIP1D, for IBM-PC and UNIX workstation, accompanies this report.

Metal Process Simulation Laboratory
Department of Mechanical and Industrial Engineering
University of Illinois at Urbana-Champaign
Urbana, IL 61801

Freeze-up Prediction for Single-Roll Strip Casting

Guowei Li
Brian G. Thomas

Freezing Danger in Liquid Pool of Continuous Strip Casting

Department of Mechanical and Industrial Engineering
University of Illinois at Urbana-Champaign
1206 West Green Street
Urbana, IL 61801

Guowei Li and Brian G. Thomas

I. INTRODUCTION

In the light of the numerous advantages that direct strip casting offers, attempts are being made all over the world to develop this processes in steel industries. Freeze up is one problem that plagues process, particularly at startup. Freeze up is caused by: (1) metal not sticking to wheel; (2) metal leaking to gap between wheel and nozzle; (3) superheat not high enough to overcome heat demand of nozzle. Once non moving solid metal comes between liquid and wheel, total freeze-up/breakouts can be rapid, so it is necessary to predict start of freeze-up problems.

The present investigation deals with freeze-up in single-roll strip casting process. The main objective of this study is to develop a fluid flow and heat transfer numerical model in liquid pool and a heat transfer model in the mold, to predict steel freezing danger of molten steel pool in direct strip casting processes. Also an effort has been made to examine the effect of processing parameters, including casting speed, caster temperature in melted steel pool, and the mold thermal properties on the performance of strip casting process.

The physical phenomena occurring in the strip casting process are illustrated in Figure 1. Liquid steel at caster temperature flows from tundish into the liquid pool. As soon as the rotating caster roll, with substantially lower temperature, comes into contact with the molten steel, a solidified shell is formed. Due to the large radius of the caster roll (12 inch), the solid / liquid interface along the roll was assumed to be a slope flat plane (2.1-inch-long). The superheat contained in liquid steel must be removed before it can solidify. In order to investigate how mold properties, and process parameters affect the heat removed by the

mold, a 3-D finite element model has been developed. A number of additional assumptions were made in the numerical treatment, namely:

1. the molten metal behaves as a Newtonian fluid, and the viscosity is determined by k-ε model;

2. the free surface is waveless;

3. the flow at the inlet is already fully turbulent.

II. FLUID FLOW AND HEAT TRANSFER MODEL IN LIQUID POOL

To understand superheat removal in direct strip casting, to further understand freezing danger in liquid pool, a numerical model based on the finite-volume method has been developed to calculate the fluid flow and heat transfer within the molten steel pool of a continuous strip caster. The heat transfer model calculates temperatures in this domain by solving a 3D energy conservation equation:

$$\rho C_p \left(v_x \frac{\partial T}{\partial x} + v_y \frac{\partial T}{\partial y} + v_z \frac{\partial T}{\partial z} \right) = \frac{\partial}{\partial x} \left(k_{eff} \frac{\partial T}{\partial x} \right) + \frac{\partial}{\partial y} \left(k_{eff} \frac{\partial T}{\partial y} \right) + \frac{\partial}{\partial z} \left(k_{eff} \frac{\partial T}{\partial z} \right) \qquad [1]$$

Although the Reynolds number in the liquid pool, based on the hydraulic diameter, is relatively low with the value about 2000 , the flow is still treated as turbulence anywhere in liquid pool due to the separation in inlet region. The K-ε turbulence model is used in calculating velocities and temperatures.

The 3D governing equations and solution methods of fluid flow model used to calculate the velocities v_x, v_y and v_z needed in equation [1], is expressed elsewhere

Figure 2 shows the 60 x 40x 20 grid of nodes used to model the liquid pool in the present work and the corresponding boundary conditions, descried as follows.

Boundary conditions

1. Inlet:

The liquid steel from a tundish with a constant liquid depth enters the pool through a weir with an adjustable opening height. The weir's opening height has obvious influence on the flow pattern and heat transfer. To account for this, even input profiles of velocity,

turbulent kinetic energy and dissipation were employed, setting (input velocity * inlet height) equal to (strip thickness * casting speed). Temperature across the inlet plane is simply fixed to the casting temperature, T_0, given in Table IV.

2. Outlet and Top surface

For top surface, v_x and normal gradients ($\partial/\partial x$) of all other variables, including v_y, v_z, K, ε, and p are set to zero. To account for the heat loss due to the top free surface radiation from liquid steel to ambient, the equivalent heat transfer coefficient, h, and ambient temperature, T_∞, given in Table I, were used. The small variations in the liquid level due to motion of the free surface are neglected. Across the outlet plane, similarly, normal gradients ($\partial/\partial x$) of all variables, including v_x, v_y, v_z, K, ε, and p are set to zero also.

3. Pool bottom, back wall and side wall

To account for the steep gradients that exist near the pool bottom, back wall and side wall, Non-slip velocity boundary condition and empirical "wall law" functions, given in Appendix I, are employed to define the tangential velocities, K, ε at the near-wall grid nodes. The thermal boundary conditions for the pool bottom, back wall and side wall are different. For the back wall, a simple adiabatic condition is used, while the pool bottom and side wall are treated as two kinds of boundary conditions in this study, i.e. in some cases assuming bottom and side wall temperature equal to liquidus temperature; and in other cases using heat flux profiles obtained from mold heat transfer simulations.

4. moving slope wall against the roll

To simulate velocity, temperature distribution in liquid pool where one boundary of the solution domain does not lie along a coordinate line, by using the finite difference program designed for orthogonal coordinate system, the real boundary along the roll was approximated as a serious of steps, utilizing the block-off solution method, shown in Figure 2. The moving boundary condition was imposed to these steps. The mesh was carefully designed to let both of the values and directions of the combined velocity of Vxri and Vyri equal to tangential velocity of rotating roll.

To avoid the computational difficulties associated with modeling latent heat evolution at the solidification front, fluid flow is modeled up to, but not including, the mushy zone. The boundaries of the mesh along the roll then correspond to the dendrite tips forming the

outer limit of the mushy zone. Consequently, a fixed-temperature, nominally equal to the liquidus, T_{liq}, is imposed along roll, which should behave like a rough solid wall.

Again, empirical "wall law" functions are employed to define the tangential velocities, K, ε, and T at the near-wall grid nodes. The thermal wall function was used to calculate the heat flux due to superheat dissipation, q_{sh}, which is presented graphically in the following section

Solution method

A computer program based on finite difference calculations, MUPFA, was chosen for this complex problem. The steady-state (elliptic) system of differential equations and boundary conditions are discretized into finite difference equations using a staggered grid and seven-point stencil of control volumes. To aid convergence, an upwinding scheme is employed for the advection terms. In addition, the source terms are linearized to increase diagonal dominance of the coefficient matrix. The equations are solved with the Semi-Implicit Method of Pressure-Linked Equations algorithm, whose Alternating-Direction-semi-Implicit iteration scheme consists of 3 successive Tri-Diagonal-Matrix-Algorithm solutions (one for each coordinate direction) followed by a pressure-velocity-modification to satisfy the mass conservation equation.

Obtaining reasonably-converged velocity and turbulence fields for this problem is difficult, owing to the moving slope boundary condition. The current strategy employed is successive iteration using an under-relaxation factor of 0.2 or 0.3 until the maximum relative residual error and maximum relative error between successive solutions falls below 0.1 pct. Over 2500 iterations are required to achieve this, starting from an initial guess of zero velocity, which takes about 20 CPU hours on a Silicon Graphics 4D/35 workstation. For subsequent processing conditions, convergence from a previously-obtained solution is much faster. Solving the energy equation is much easier, because it needs fewer iterations with just one unknown, and requires only 0.5 hour of CPU time.

III. HEAT TRANSFER MODEL IN CERAMIC MOLD

The energy equation used to calculate temperature distribution in the mold and heat flux across the mold hot faces is:

4

$$\rho C_p \frac{\partial T}{\partial t} = \frac{\partial}{\partial x}\left(k\frac{\partial T}{\partial x}\right) + \frac{\partial}{\partial y}\left(k\frac{\partial T}{\partial y}\right) + \frac{\partial}{\partial z}\left(k\frac{\partial T}{\partial z}\right)$$ [2]

To compare the results with fluid flow simulation in liquid pool, the roll / liquid steel interface was approximated as a flat plate just as what has been done in fluid flow simulation. By assuming no heat transfer (big contact resistance) between side wall and bottom of the mold, the boundary conditions for mold bottom are independent of the mold width direction, so a 2-D solution was actually obtained in the mold bottom.

Figure 3 shows the boundary conditions used in mold heat transfer simulations. As initial conditions for the mold heat transfer simulation, hot faces (which contact with liquid steel) were assumed to have an even preheat temperature T_i. Furthermore, adiabatic condition was employed to mold back (interior) surfaces and symmetry plane in the center of the mold. Free convection condition was applied to other mold surfaces which open to ambient.

In transient simulation, because the liquid pool is set just beside the roll, both radiation and forced convection were taken into account for the roll / liquid interface. Forced convection was also taken into account for mold hot faces, and the surface against the roll on the first step on side wall.

As initial conditions for the mold heat transfer simulation, hot faces (which contact with liquid steel) were assumed to have an even preheat temperature T_i. Furthermore, same as the transient simulation, adiabatic condition was employed to mold back (interior) surfaces and symmetry plane in the center of the mold. Free convection condition was applied to other mold surfaces which open to ambient.

The commercial finite element program FIDAP was chosen to model this complex geometry problem. The standard mesh of half of the mold (the center plane of the mold is a symmetry plane), shown in Figure 4, consists of a 37 by 23 by 15 grid of eight-node, linear, brick elements. Due to the big gradient of temperature in the region near the roll, the mesh was refined in this region.

IV. MODEL RESULTS AND DISCUSSION

MOLD HEAT TRANSFER RESULTS

Figure 5 to 10 show the heat transfer results for a typical case with the simulation condition in Table IV. Comparing temperature distribution in the mold at initial and final steady state conditions in Figure 5, It can be found that the temperature gradients in mold thickness direction are greater at final steady state than at initial steady state. This is because the hot face reference temperature (liquid steel) is higher than the preheat temperature so that more heat needs to be removed. The mold heat flux results into mold hot faces in the corner of mold bottom and side wall versus the distance from roll at different time steps are plotted in Figure 6 to 9. The heat fluxes are nearly constant at every time step except a small region near the roll. The heat flux into the mold side wall is bigger than the heat flux into mold bottom at the same time step, and the longer the physical time, the bigger the difference between the heat fluxes into mold side wall and bottom. At the final steady state, the heat flux into the mold side wall is about 10 times of the heat flux into mold bottom. It can be attributed to the better convection condition of the mold side wall. The heat fluxes into the mold side wall and bottom versus time in the region far from roll, shown in Figure 10, drop very rapidly in the first 40-50 seconds, and the decrease still cannot be ignored after about 2000 seconds.

Effect of mold properties and processing parameters:

To understand the effect of mold properties and processing parameter on the heat transfer results, six cases with different processing parameters and mold properties, varying preheat temperature, insulation of side wall, mold material, reference temperature and heat transfer coefficient on hot face, are listed in Table II.

Figure 11 and Figure 12 give the heat fluxes into hot face of mold bottom in case 1 to case 6. According to these two figures, the reference temperature and heat transfer coefficient on hot faces have very little effect on the simulation results, which confirms that those parameters used in this study are reasonable. On the other hand, the preheat temperature shows a big effect on heat flux, the lower the mold preheat temperature, the longer the time to reach steady state. Another conclusion reached from these two figures is that the insulation of side wall had no large effect on masking the heat fluxes difference between side wall and bottom. The time for mold heat flow or temperature to reach steady state were listed in Table III.

6

FLUID FLOW AND HEAT TRANSFER IN LIQUID POOL

3-D velocity and temperature results are shown in Figure 13 to Figure 14 under standard casting conditions, designated as Base Case in Table IV. It was found that in strip width direction temperature shows 3-d effect only in 1/2" wide region, so the symmetry plane was set at 1/2" away from side wall. The post processor FIPOST of the commercial finite element program FIDAP was used to visualize and plot the results.

Two frames viewing the symmetry plane and side wall plane show how flow enters the opening weir and goes to the outlet on top surface driven by the fast rotating roll. In the most area except for near the roll wall, velocity is nearly ten times smaller than the casting speed. A recirculation zone can be found in the middle of the pool. Both frames show the flow pattern almost two-dimensional in most of the domain. Only near the top back corner, a very weak vortex is formed.

The temperature distribution inside the pool is further revealed viewing the symmetry plane and side wall plane. The isotherms in the first frame of Figure 14 show the temperature distribution in the symmetry plane. Except for a very thin layer against the roll, liquid steel at high temperature loses very little superheat on the mold bottom, as soon as it comes close to the rotating caster roll, with substantially lower temperature, it becomes colder and colder along the roll, till it reaches the top surface, the liquid steel has lost nearly 25% of superheat. Then the liquid steel continually loses heat while it goes to the back top corner due to the free surface radiation. The region which has the most danger of freezing is in the front bottom corner against the roll. Comparing two frames in this figure, it is found that the side wall is colder, and the difference between the symmetry plane and side wall plane in the middle region is about 6 °C.

Typical predictions of heat flux leaving the liquid pool across the liquid/solid shell boundary are presented in Figure 15 as a function of distance from the mold bottom. These results show that heat flux, the rate of extraction by shell, reaches the maximum just above the pool bottom and then decreases slightly in the most part along the roll. Increasing heat flux near the outlet because the velocity near the outlet is bigger than the real casting condition, duo to without modeling the solidified shell. The heat flux into shell near the side wall plane is negligible, compared with the value in symmetry plane. Other data of heat balance on strip caster were included in Table V.

Effect of surface radiation

The temperature contours presented in Figure 16 have the same input data as Base Case in Table IV except for neglecting the radiation form liquid steel to ambient on the free surface. This Figure shows the hotter temperature in the upper of the pool compared with Figure 14. The biggest temperature difference in the top back corner against the side wall in both cases is about 10 °C. In the lower part of the pool, the temperature results are qualitatively similar in both cases and the differences can be ignored.

Effect of inlet temperature and casting speed

According to the results in Figure 13 and 14, because the width of strip is much bigger than other simulation geometry sizes, two dimension approximation can be reasonably made in most part of the pool except for the two end layers against the side walls. So a quantity of simulation results were obtained using 2-D model in this study, to further understand the effect of casting speed, inlet temperature and weir opening height on the freezing possibilities in the most dangerous zone of front bottom corner. Figure 17 and Figure 18 show the heat fluxes into mold bottom at different casting speeds, inlet temperatures respectively, by setting a constant temperature (liquidus) boundary condition on the bottom of the pool. Both the casting speed and inlet temperature increase the heat flux extracted by mold bottom directly, and the function between casting speed or inlet temperature and heat flux is approximately linear. This has been conformed by theory analysis and simulation results. The heat flux almost remains the constant versus the distance from the roll, which agrees with the previous conclusion that along the bottom only little heat is lost and the steel temperature remains the same.

Effect of weir opening height

Increasing the weir opening height will decrease the inlet velocity, kinetic energy and turbulence dissipation if casting speed remains the same. Figure 19 shows the heat fluxes into mold bottom in two cases whose only difference is weir opening height (3/4" and 3/8" high respectively). From this figure, the weir opening has obvious effect on heat transfer in the liquid pool. Same cases are simulated repeatedly using heat flux boundary condition on mold bottom, and the temperature differences of these two cases is about 20 °C.

8

To further understand the possibilities of steel freezing in the liquid pool, the heat fluxes into mold hot faces calculated by mold heat transfer model are used as the boundary conditions for liquid steel pool model simulations. By using the heat fluxes into the mold side wall and bottom at different time steps as the boundary conditions of the liquid pool, a series of temperature contours can be obtained using the fluid flow and heat transfer model for liquid steel pool in this study. The bigger the values of heat fluxes into the mold side wall and bottom, the colder the temperature in the pool. By set the criterion heat flux as the value used in pool simulations which makes temperature in the liquid pool barely hotter than liquidus, the criterion time corresponding to reach this heat flux in mold simulation also can be decided. Table VI shows the time to reach no freezing in liquid pool at different casting speeds and inlet temperatures. The columns "no freezing in center of mold" give the results obtained in the way descried above, by neglecting the heat flux into the mold side wall. The columns "no freezing in front corner" are the results by adding the heat flux into mold side to the mold bottom, ignoring the freezing potential at center of side wall. This table again conforms that the higher casting speed and inlet temperature will cause less freezing danger in the front bottom corner of the liquid pool.

V. CONCLUSIONS

A 3-D heat transfer model for mold and A 3-D turbulent fluid flow and heat transfer model of liquid pool in directly strip casting processes have been developed to understand the freezing danger. The following conclusion can be reached:

1. The mold heat transfer results are not sensitive to the reference temperature and heat transfer coefficient on hot face.

2. The preheat temperature shows a big effect on heat flux, the lower the mold preheat temperature, the longer the time to reach steady state.

3. The insulation of side wall does not efficiently reduce the heat fluxes difference between side wall and bottom.

4. Calculations using 2-D model in liquid pool can get reasonable results for many cases.

5. Surface radiation has small local effect on temperature in copper pool.

9

6. Increasing casting speed and inlet temperature both directly increase the temperature in the liquid pool, therefore decrease the freezing danger.

7. Larger weir opening height decreases velocity and temperature in the lower part of the liquid, and increases danger of freeze-up.

8. There is no freeze-up at steady state.

APPENDIX A

Volume Conservation Equation:

$$\frac{\partial v_x}{\partial x} + \frac{\partial v_y}{\partial y} + \frac{\partial v_z}{\partial z} = 0 \qquad\qquad [A1]$$

Momentum Conservation Equations:

$$\rho\left(v_x\frac{\partial v_x}{\partial x} + v_y\frac{\partial v_x}{\partial y} + v_z\frac{\partial v_x}{\partial z}\right)$$

$$= -\frac{\partial p}{\partial x} + \frac{\partial}{\partial x}\left(2\mu_{eff}\frac{\partial v_x}{\partial x}\right) + \frac{\partial}{\partial y}\left(\mu_{eff}\left[\frac{\partial v_x}{\partial y} + \frac{\partial v_y}{\partial x}\right]\right) + \frac{\partial}{\partial z}\left(\mu_{eff}\left[\frac{\partial v_x}{\partial z} + \frac{\partial v_z}{\partial x}\right]\right) \qquad [A2]$$

$$\rho\left(v_x\frac{\partial v_y}{\partial x} + v_y\frac{\partial v_y}{\partial y} + v_z\frac{\partial v_y}{\partial z}\right)$$

$$= -\frac{\partial p}{\partial y} + \frac{\partial}{\partial x}\left(\mu_{eff}\left[\frac{\partial v_y}{\partial x} + \frac{\partial v_x}{\partial y}\right]\right) + \frac{\partial}{\partial y}\left(2\mu_{eff}\frac{\partial v_y}{\partial y}\right) + \frac{\partial}{\partial z}\left(\mu_{eff}\left[\frac{\partial v_y}{\partial z} + \frac{\partial v_z}{\partial y}\right]\right) \qquad [A3]$$

$$\rho\left(v_x\frac{\partial v_z}{\partial x} + v_y\frac{\partial v_z}{\partial y} + v_z\frac{\partial v_z}{\partial z}\right)$$

$$= -\frac{\partial p}{\partial z} + \frac{\partial}{\partial x}\left(\mu_{eff}\left[\frac{\partial v_z}{\partial x} + \frac{\partial v_x}{\partial z}\right]\right) + \frac{\partial}{\partial y}\left(\mu_{eff}\left[\frac{\partial v_z}{\partial y} + \frac{\partial v_y}{\partial z}\right]\right) + \frac{\partial}{\partial z}\left(2\mu_{eff}\frac{\partial v_z}{\partial z}\right) + \rho \qquad [A4]$$

Turbulence Equations

$$\rho\left(v_x\frac{\partial K}{\partial x} + v_y\frac{\partial K}{\partial y} + v_z\frac{\partial K}{\partial z}\right)$$

$$= \frac{\partial}{\partial x}\left(\frac{\mu_{eff}}{\sigma_K}\frac{\partial K}{\partial x}\right) + \frac{\partial}{\partial y}\left(\frac{\mu_{eff}}{\sigma_K}\frac{\partial K}{\partial y}\right) + \frac{\partial}{\partial z}\left(\frac{\mu_{eff}}{\sigma_K}\frac{\partial K}{\partial z}\right) + \rho G_K - \rho\varepsilon \qquad [A5]$$

$$\rho\left(v_x\frac{\partial\varepsilon}{\partial x} + v_y\frac{\partial\varepsilon}{\partial y} + v_z\frac{\partial\varepsilon}{\partial z}\right)$$

$$= \frac{\partial}{\partial x}\left(\frac{\mu_{eff}}{\sigma_\varepsilon}\frac{\partial\varepsilon}{\partial x}\right) + \frac{\partial}{\partial y}\left(\frac{\mu_{eff}}{\sigma_\varepsilon}\frac{\partial\varepsilon}{\partial y}\right) + \frac{\partial}{\partial z}\left(\frac{\mu_{eff}}{\sigma_\varepsilon}\frac{\partial\varepsilon}{\partial z}\right) + c_1\frac{\varepsilon}{K}\rho G_K - c_2\frac{\varepsilon}{K}\rho\varepsilon \qquad [A6]$$

where

11

$\mu_{eff} = \mu_o + \mu_t$ = effective viscosity (kg m^{-1} s^{-1})

$\mu_t = c_\mu \rho \dfrac{K^2}{\varepsilon}$ = turbulent viscosity (kg m^{-1} s^{-1})

$$G_K = \frac{\mu_t}{\rho}\left[\ 2\left(\frac{\partial v_x}{\partial x}\right)^2 + 2\left(\frac{\partial v_y}{\partial y}\right)^2 + 2\left(\frac{\partial v_z}{\partial z}\right)^2 + \left(\frac{\partial v_x}{\partial y} + \frac{\partial v_y}{\partial x}\right)^2 + \left(\frac{\partial v_x}{\partial z} + \frac{\partial v_z}{\partial x}\right)^2 + \left(\frac{\partial v_z}{\partial y} + \frac{\partial v_y}{\partial z}\right)^2\ \right]$$

= turbulence generation rate (m^2 s^{-3})

$c_1 = 1.44,$ $c_2 = 1.92,$ $c_\mu = 0.09,$ $\sigma_K = 1.0,$ $\sigma_\varepsilon = 1.3$

APPENDIX B   PROPERTY CALCULATION

For the liquid steel at 1638 °C:

$\rho = 7000$ kg/m^3, $C_p = 680$ J /kg°K, $K = 30$ W/m°K, $\mu = 5.8$ e -3 Pa-s.

The process parameters:

Casting speed $V_c = 1.0$ m/s,

Strip thickness $t = 1.6$ mm $= 0.0016$ m,

Weir opening height $\Delta X_i = 18$ mm $= 0.018$ m,

Strip width $\Delta W = 0.3048$ m,

Liquid steel depth $H_1 = 0.054$ m

So: Equivalent hydraulic diameter at liquid pool inlet:

$$L_{D1} = \frac{4A_1}{P_1} = \frac{4\Delta X_i \Delta W}{2(\Delta X_i + \Delta W)} = \frac{4 \times 0.018 \times 0.3048}{2 \times (0.018 + 0.3048)} = 0.034 \text{ m}$$

Equivalent hydraulic diameter in center of liquid pool:

$$L_{D2} = \frac{4A_2}{P_2} = \frac{4H_1 \Delta W}{2(H_1 + \Delta W)} = \frac{4 \times 0.054 \times 0.3048}{2 \times (0.054 + 0.3048)} = 0.092 \text{ m}$$

Reynolds number: $Re = \dfrac{\rho V_c t}{\mu} = \dfrac{7000 \times 1.0 \times 0.0016}{5.8 \text{ e -3}} = 1317.7$

Prandt number: $Pr = \dfrac{\mu C_p}{K} = \dfrac{5.8 \text{ e-3} \times 680}{30} = 0.13$

Nussel number: $Nu = 4.8 + 0.0156 \, (Re)^{0.85} \, (Pr)^{0.93} = 5.88$

At pool inlet, the heat transfer coefficient from liquid steel to nozzle:

$$h_{31} = \frac{Nu \, K}{L_{D1}} = \frac{5.88 \times 30}{0.034} = 4809 \text{ W/m}^2 \text{ °K}$$

In the center of pool, the heat transfer coefficient from liquid steel to nozzle:

$$h_{32} = \frac{Nu \, K}{L_{D2}} = \frac{5.88 \times 30}{0.092} = 1782 \text{ W/m}^2 \text{ °K}$$

TABLE I MOLD SIMULATION CONDITIONS (BASE CASE)

Symbol	Variable	Value
Mold properties:		
C_p	Mold specific heat	1088 J kg^{-1} K^{-1}
ρ	Mold density	3200 kg m^{-3}
K	Mold thermal conductivity	0.865 W m^{-1}K^{-1}(NA33)
Mold geometry:		
t_m	thickness of mold bottom and side wall	3"
H	Pool depth	3"
W	Strip width	12"
R	Roll radius	12"
Simulation parameter:		
T_o	Casting temperature	1638 °C (2980 °F)
T_{liq}	Liquidus temperature	1515 °C (2760 °F)
ΔT_s	Superheat temperature ($T_o - T_{liq}$)	123 °C (220 °F)
T_∞	Ambient temperature	30 °C
T_i	Preheat temperature	1037 °C
T_r	Roll temperature	500 °C
h_1	(free convection)	10 W m^{-2}K^{-1}
h_2	(forced convection)	50 W m^{-2}K^{-1}
h_3	(liquid/ceramic surface)	2000 W m^{-2}K^{-1}
h_4	Equivalent heat transfer coefficient in gap	$h_4 = K_a/\Delta x + \varepsilon\sigma(T+T_r)*(T^2+T_r^2)$
ε	Emissivity of ceramic	0.91
σ	Stefan-Boltzmann constant	5.67e-8 W m^{-2}K^4
K_a	Thermal conductivity of air	0.4 W m^{-1}K^{-1}
Δx	Mold/roll gap width	3.175 mm

TABLE II CONDITIONS FOR MOLD SIMULATIONS

Cases	Reference temperature on hot face (°C)	Heat transfer coefficient on hot face (W m^{-2}K^{-1})	Heat transfer coefficient for free convection (W m^{-2}K^{-1})	preheat temperature (°C)
1 base case	1638	2000	10	1037
2	1515	4800	10	1037
3	1515	2000	10	1037
4 low preheat	1638	2000	10	610
5 insulation	1638	2000	1.3	1037
6* zirconia	1638	2000	10	1037

* In case 6: mold conductivity = 1.514, specific heat = 711.4 J /kg-K;
  In case 1-5: mold conductivity = 0.865, specific heat = 1088.0 J /kg-K.

TABLE III TIME FOR MOLD HEAT FLOW OR TEMPERATURE

TO REACH STEADY STATE

Criterion	Base case	Case 4	Case 5
$(Q_{in}-Q) / (Q_{in}-Q_f)$ $> 75\%$	27 s	24 s	32 s
$(Q-Q_{in}) / (Q_{in}-Q_f)$ $> 85\%$	56 s	40 s	70 s
$(Q_{in}-Q) / (Q_{in}-Q_f)$ $> 95\%$	395 s	> 4000 s	690 s
$(T-T_{in}) / (T_{in}-T_f)$ $> 75\%$	32 s	15 s	30 s
$(T-T_{in}) / (T_{in}-T_f)$ $> 85\%$	120 s	80 s	70 s
$(T-T_{in}) / (T_{in}-T_f)$ $> 95\%$	500 s	560 s	210 s

* Q_{in}, T_{in} are the heat and temperature at initial steady state.

Q_f, T_f are the heat and temperature at final steady state.

TABLE IV FLUID FLOW MODEL SIMULATION CONDITIONS (BASE CASE)

Symbol	Variable	Value
Metal properties:		
C_p	Specific heat	$680 \text{ J kg}^{-1}\text{ K}^{-1}$
μ_o	Laminar (molecular) viscosity	$0.00385 \text{ kg m}^{-1}\text{ s}^{-1}$
k_o	Laminar thermal conductivity	$26 \text{ W m}^{-1}\text{K}^{-1}$
T_{liq}	Liquidus temperature (at wall)	$1515 \,°C$ $(2860 \,°F)$
ρ	Liquid density	7020 kg m^{-3}
Geometry:		
ΔX_i	Weir opening height	3/4" (0.018 m)
ΔW	Strip width	12" (0.3048 m)
R	Radius of the roll	12" (0.3048 m)
L	Pool bottom length	1.6" (0.0408 m)
t	Shell thickness at exit	1.6mm
Operating conditions:		
h	Free surface heat transfer coefficient	$360 \text{ W m}^{-2}\text{ K}^{-1}$
T_o	Casting temperature (at inlet)	$1590 \,°C$ $(3017 \,°F)$
ΔT_s	Superheat temperature $(T_o - T_{liq})$	$75 \,°C$ $(157 \,°F)$
T_∞	Ambient temperature	$30 \,°C$
V_c	Casting speed	1.5 m s^{-1} (90 m/min.)
Hl	Liquid steel depth	2(1/8)" (0.054 m)
M_i	Mass into domain	0.0421 kg s^{-1}
Simulation Parameters:		
κ	Von Karman constant	0.4
Pr_o	Laminar Prandtl Number, $C_p\,\mu_o^{-1}\,k_o^{-1}$	0.1
Pr_t	Turbulent Prandtl Number	0.9
V_i	Average velocity at inlet	0.104 m s^{-1}
K	Average turbulent kinetic energy: (inlet and initial)	$4.06e\text{-}5 \text{ m}^2\text{ s}^{-2}$
ε	Average dissipation: inlet and initial values	$2.23e\text{-}5 \text{ m}^2\text{ s}^{-3}$
E	Calculation error in mass balance	3.7 %
H_b	Heat flux out of pool bottom	10 kW m^{-2}
H_s	Heat flux out of pool side wall	100 kW m^{-2}

TABLE V HEAT BALANCE ON STRIP CASTER(BASE CASE)

(V_C=1.5 M/S, WITH FREE SURFACE RADIATION)

Variable	Value	%
Heat in	9092.7 W	
Heat out of outlet	5537.9 W	60.9 %
Heat go to the shell	2373.4 W	26.1 %
Heat out of pool bottom	9.6 W	0.1 %
Heat out of pool side wall	365.6 W	4.0 %
Radiation on top free surface	567.3 W	6.2 %
Heat out of domain	8853.8	2.6 %

TABLE VI TIME TO REACH NO FREEZING IN DIFFERENT FLUID CONDITIONS

(USE Q--BOUNDARY CONDITIONS) *

(UNIT: SECOND)

Super heat (C)	V_c (m/s)	Case 1		Case 4		Case 5	
		no freezing in center of mold	no freezing in front corner	no freezing in center of mold	no freezing in front corner	no freezing in center of mold	no freezing in front corner
123	1.5	0	0	0	0	0	0
	1.0	0	5	3	10	0	5
	0.83	0	9	5	15	0	9
	0.5	9	30	15	40	8	22
75	2.0	0	3	0	9	0	3
	1.5	0	9	5	18	0	9
	1.0	4	15	10	24	4	15
	0.83	9	30	15	40	8	22
50	2.5	0	5	3	9	0	5
	2.0	0	9	5	18	0	9
	1.5	4	15	10	24	4	15
	1.0	9	30	15	40	8	22
20	5.0	0	9	5	18	0	9
	3.5	4	15	10	24	4	15
	2.5	11	30	17	40	10	22
	2.0	17	70	24	290	17	70

* Ignores freezing potential at center of side wall
  and assuming shell thickness = 1.6 (mm)
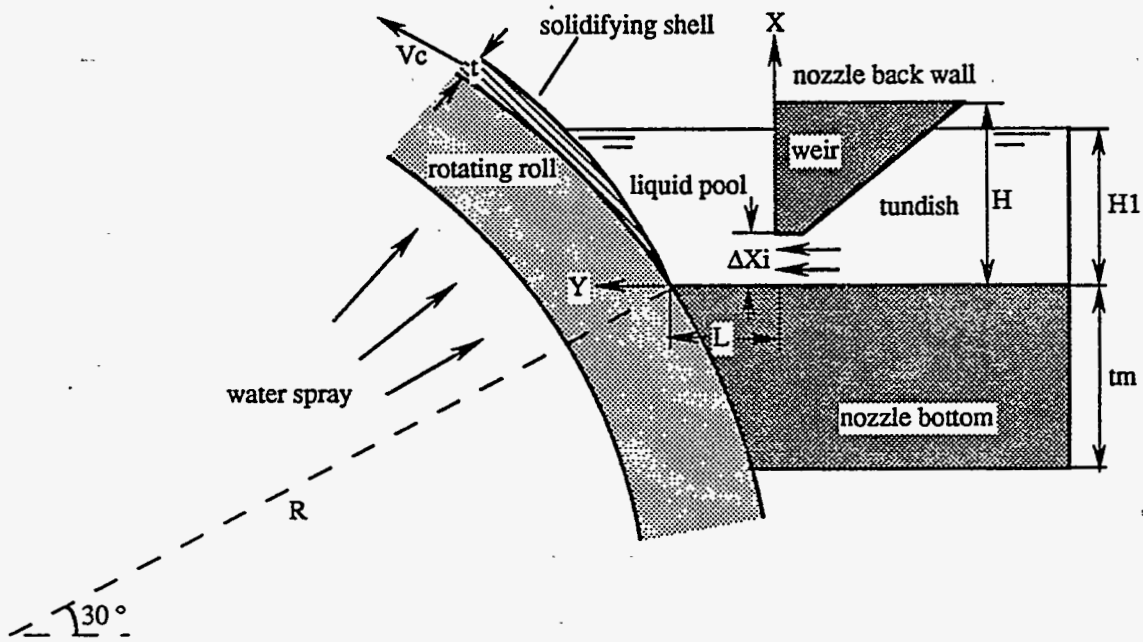
Fig . 1 Schematic of continuous strip casting process.

$\ell' = 2 \times 0.9 \div 48 \cdot \sin^{-1} 5° = \ldots$

$\ell = \frac{15}{360} \times 2\pi \cdot 0.3 \times 48 = \ldots$
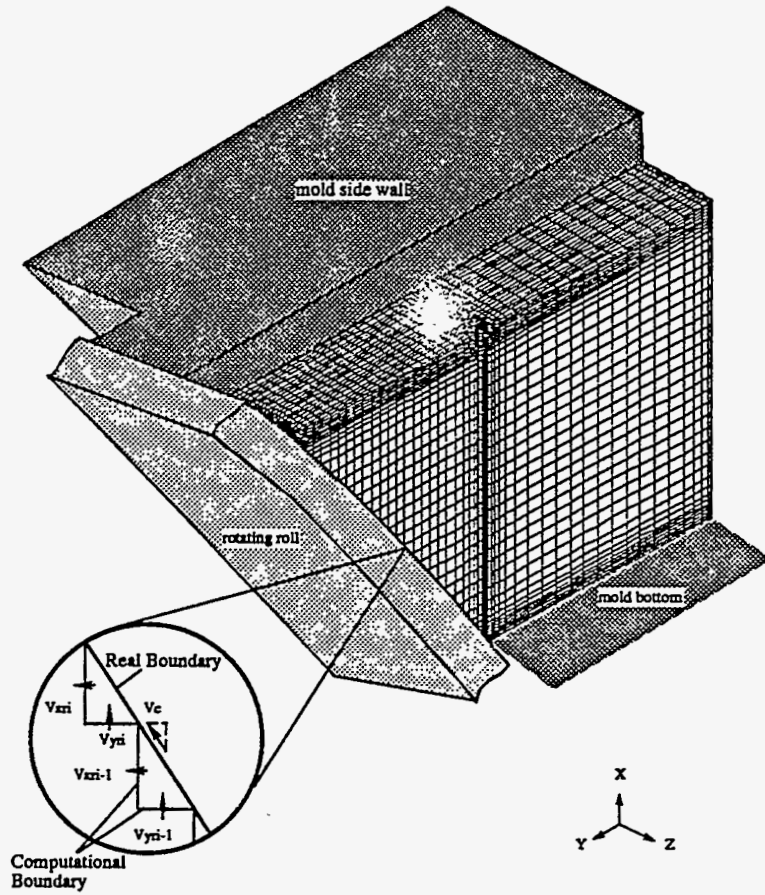
Fig. 2 Simulation domain and typical mesh used in the 3-D fluid flow
and heat transfer model.
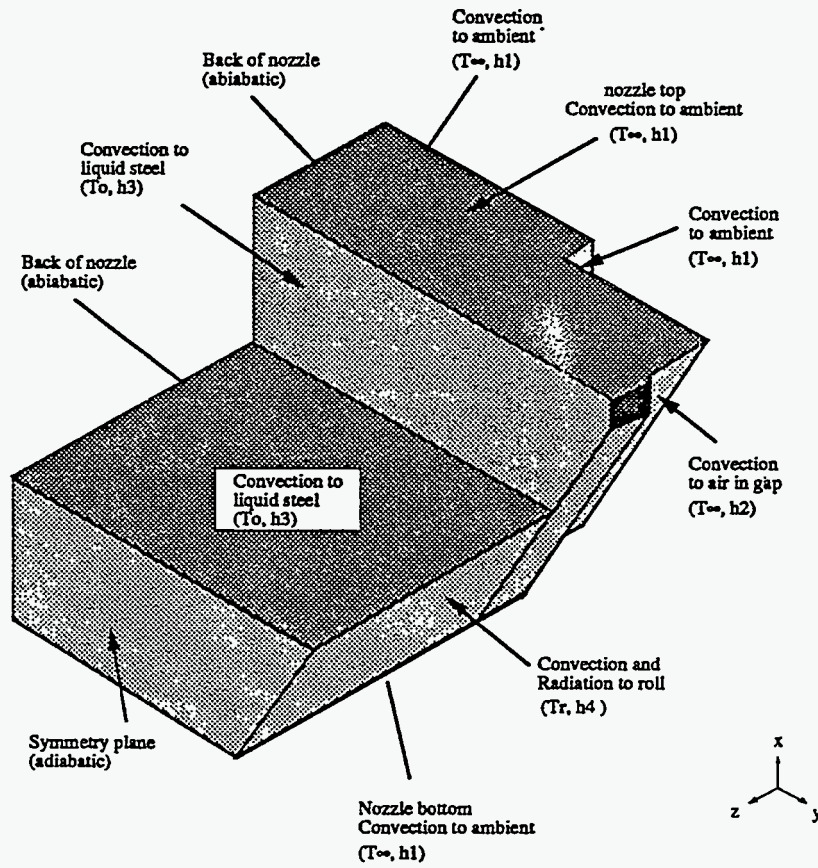
Fig. 3a   Transient simulation boundary conditions of the nozzle
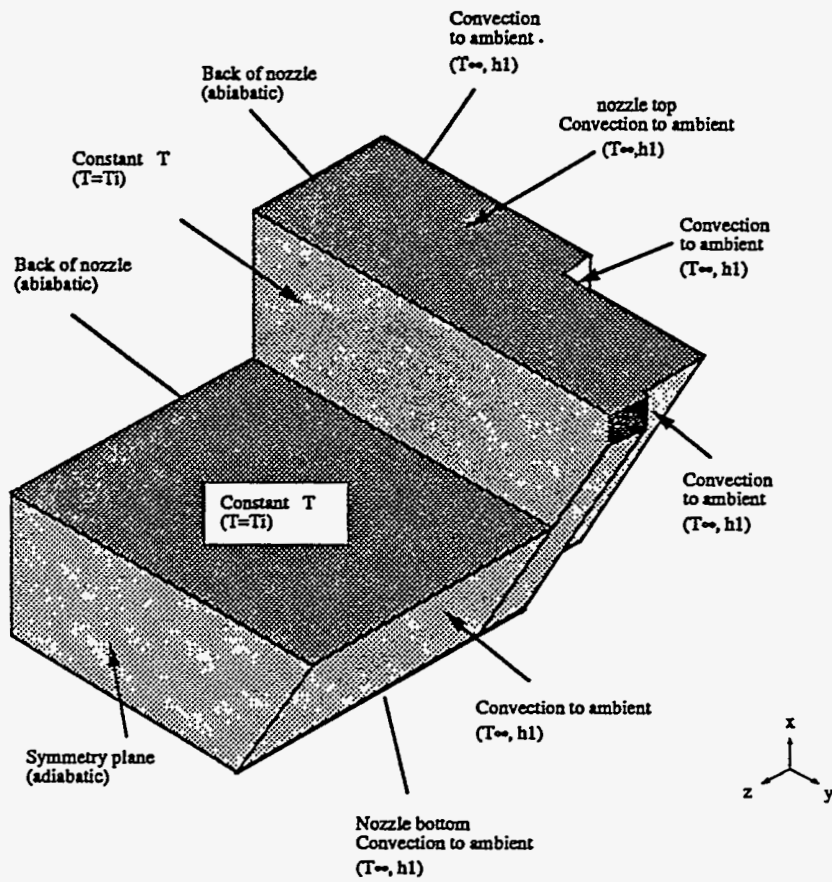
Fig. 3b   Initial condition in the nozzle heat transfer simulation
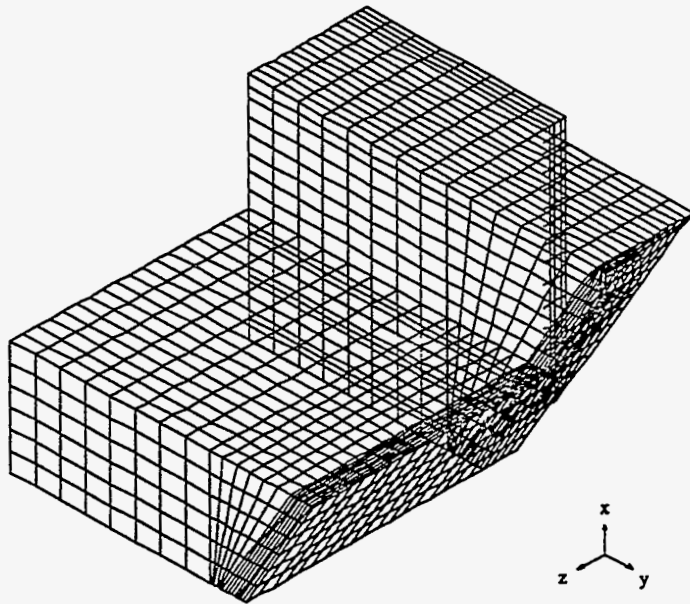
Fig. 4 simulation mesh for nozzle heat transer model
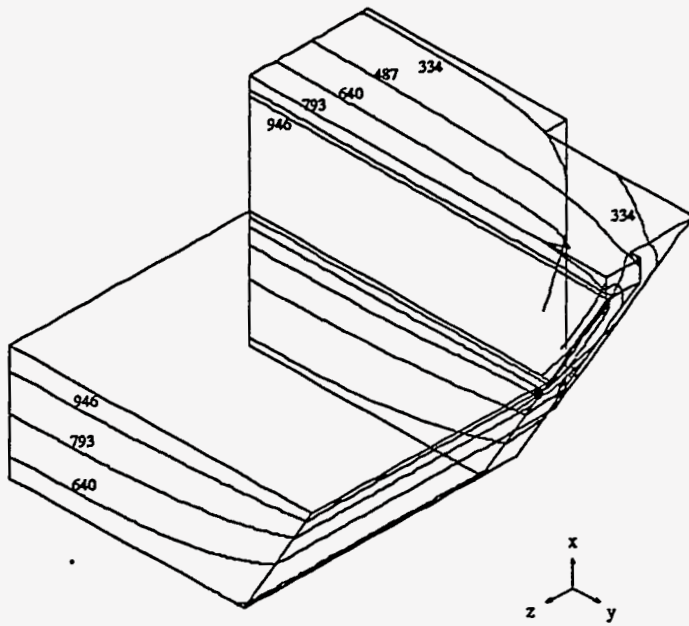
Fig 5a Temperature distribution in nozzle
(initial steady state)
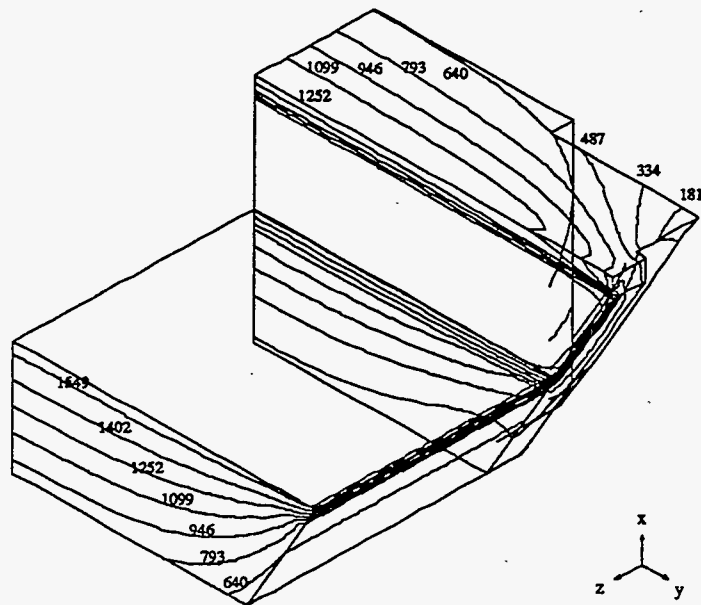
Fig 5b Temperature distribution in nozzle
(final steady state)
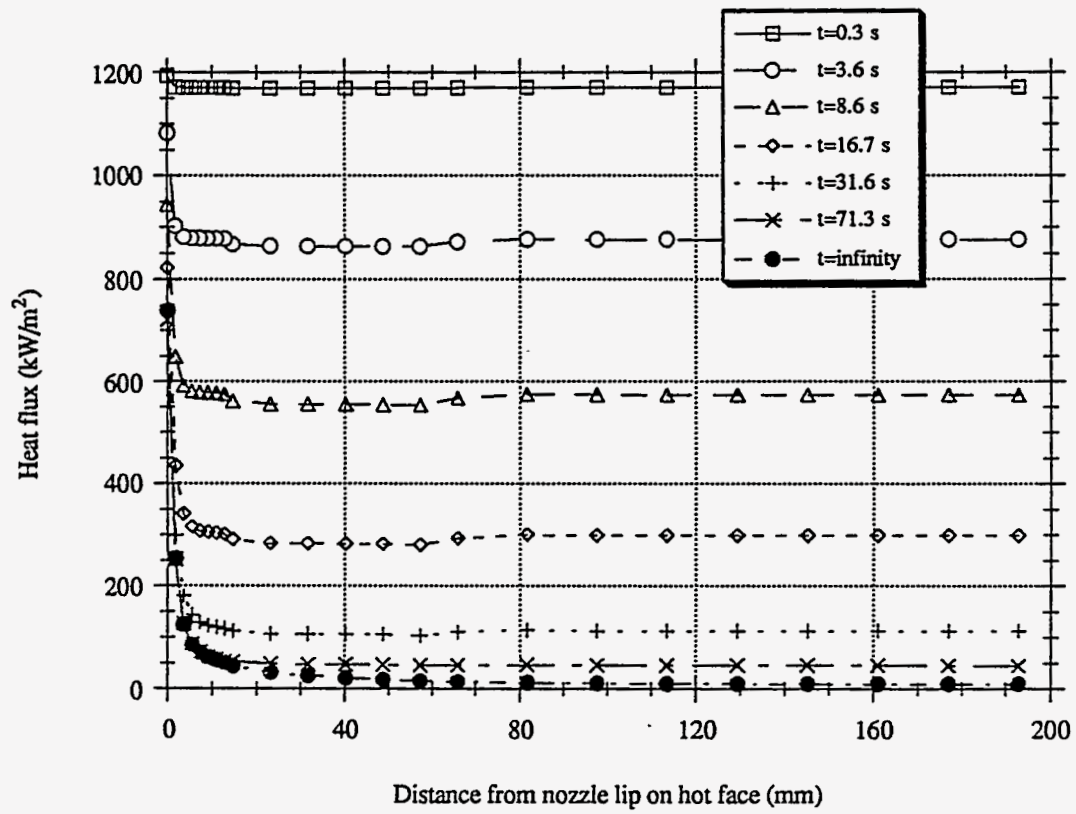
Fig. 6 Heat flux on hot face of nozzle bottom at different time
(short term) (Base case)
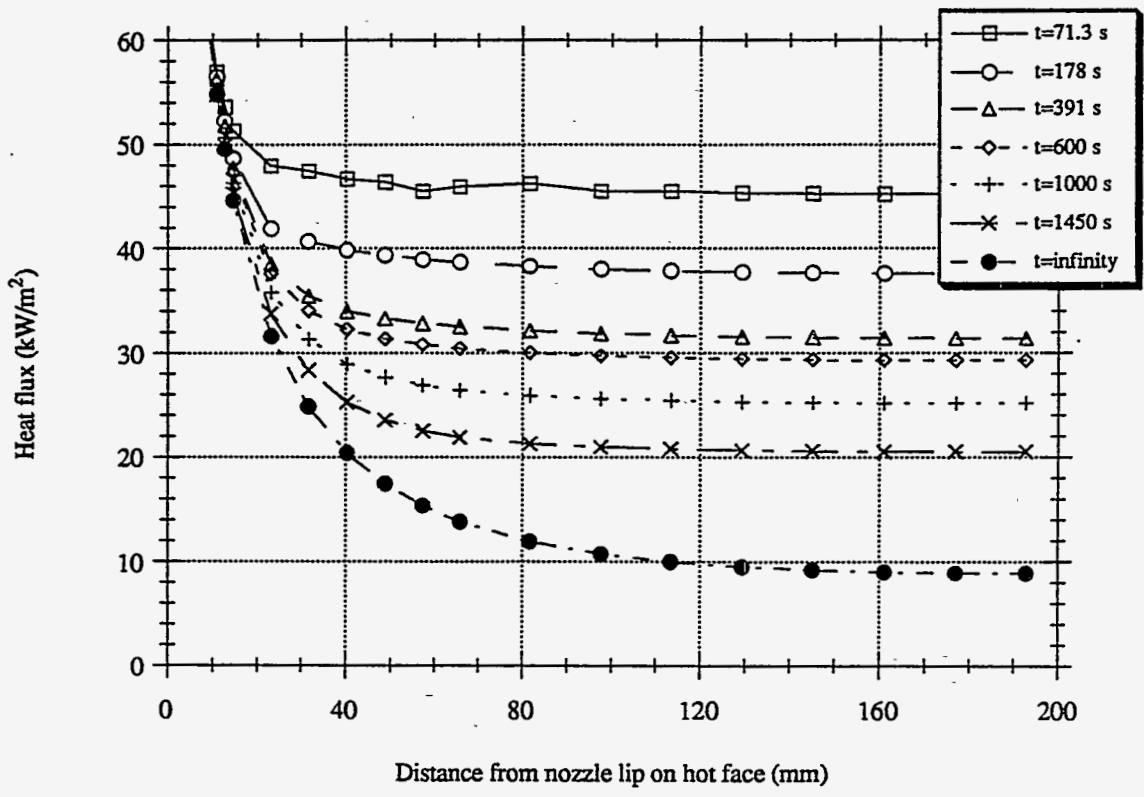
Fig. 7 Heat flux on hot face of nozzle bottom at different time
(long term)(base case)
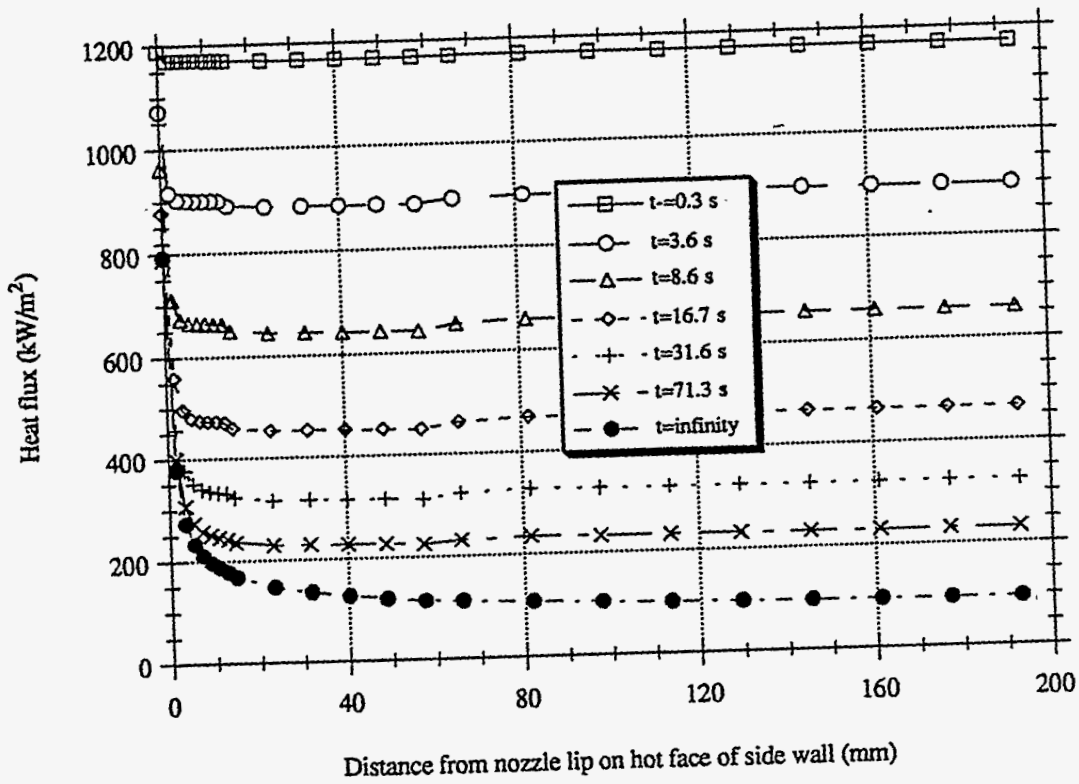
Fig. 8 Heat flux on hot face of nozzle side wall
(short term)
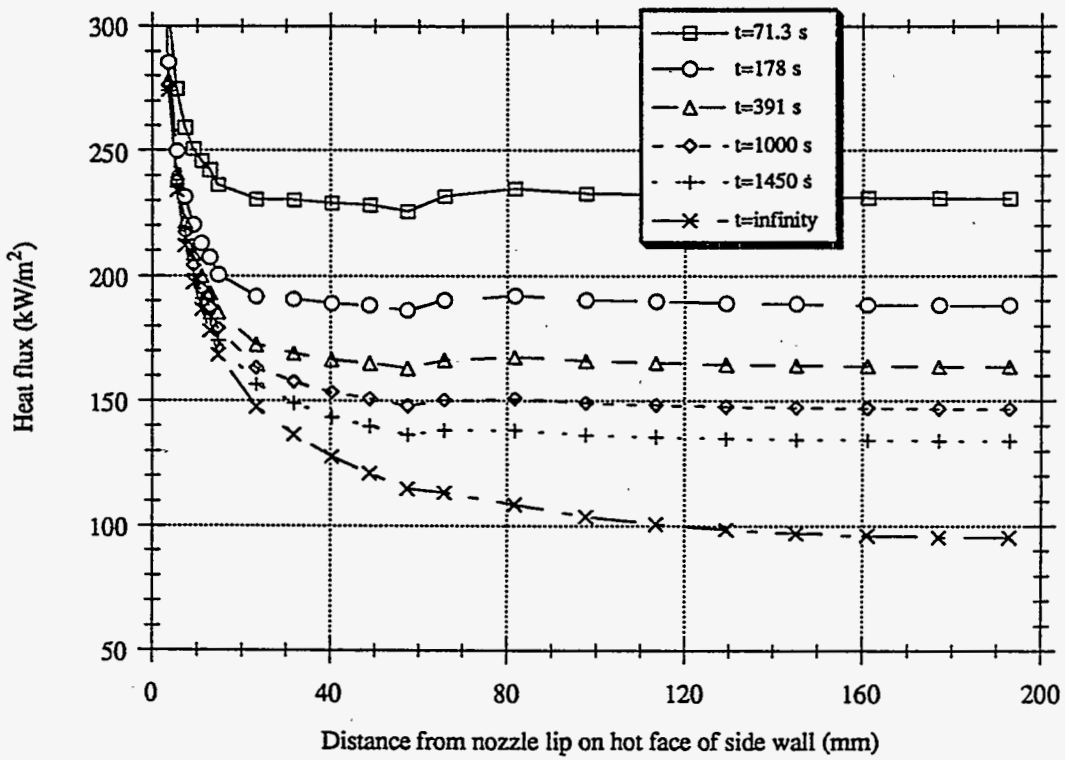
Fig. 9 Heat flux on hot face of nozzle side wall
(long term)(base case)
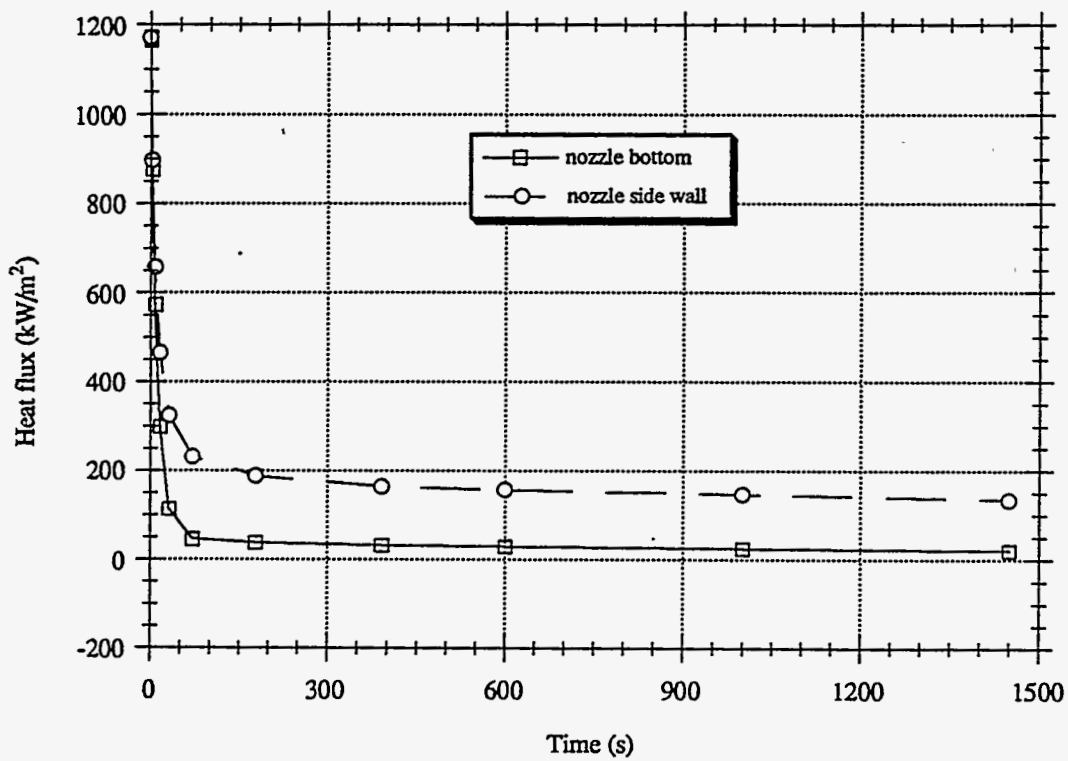
Fig. 10 Heat flux on hot face of nozzle bottom versus time
(Base case)

$\mathcal{L}_b \sim t$
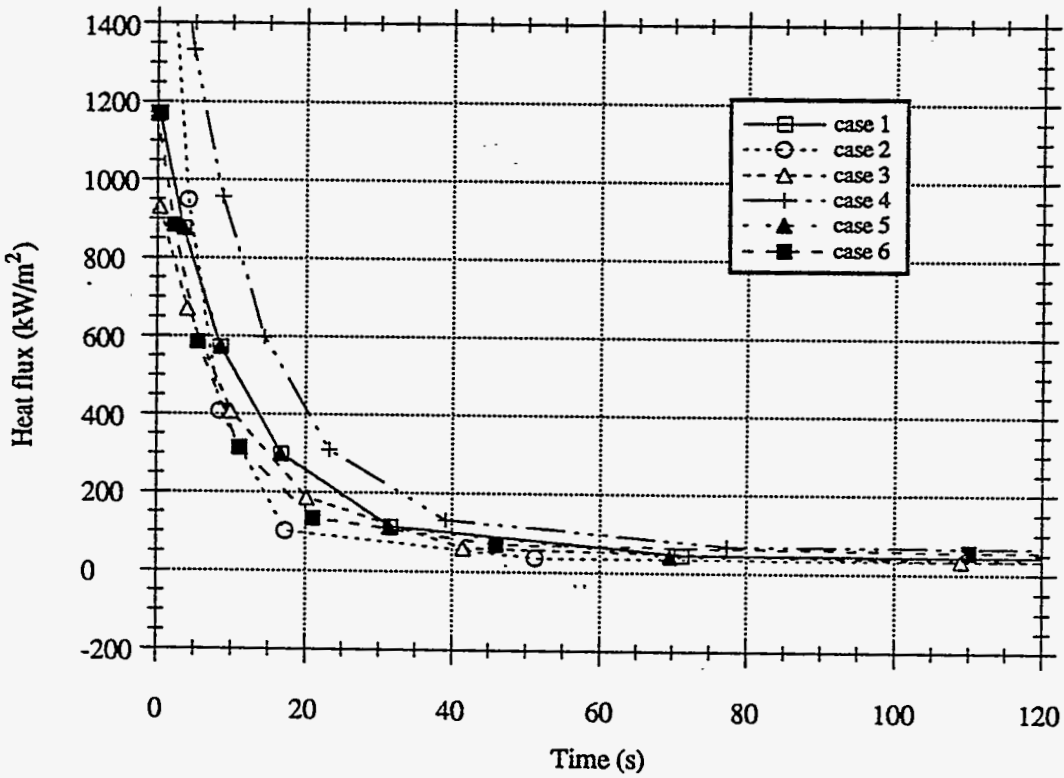
Fig. 11(a) Heat flux on hot face of nozzle bottom versus time
(short term)

$$\acute{t}_s \sim t$$
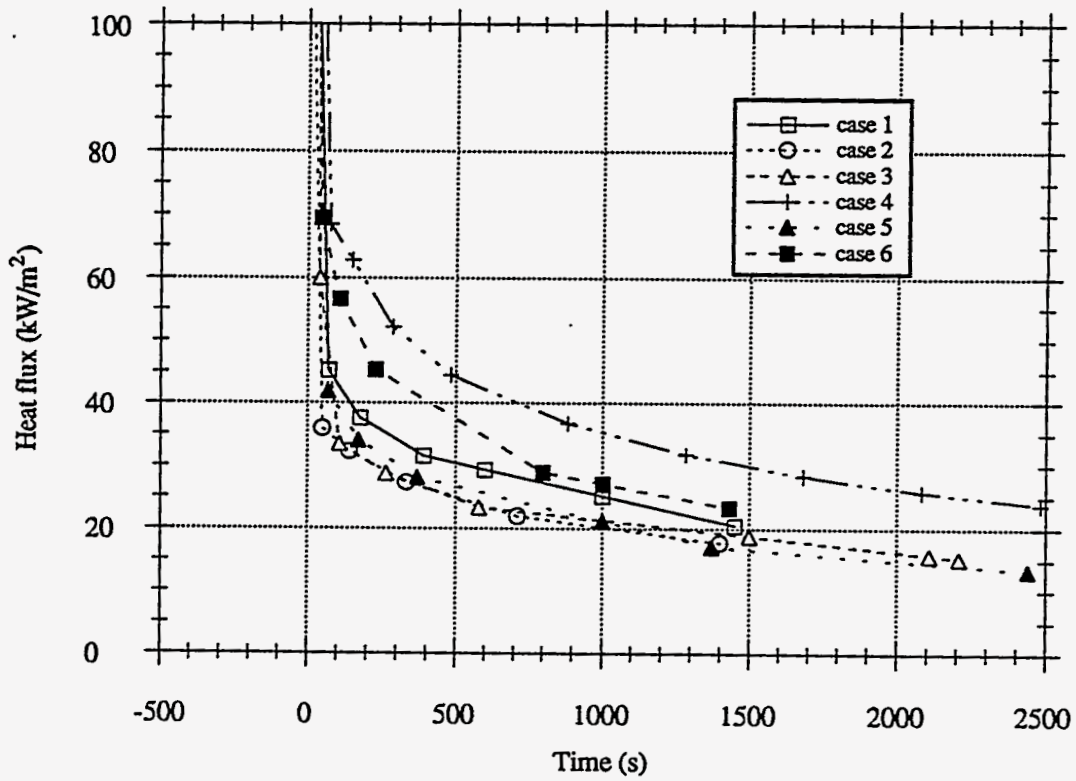
Fig. 11(b)   Heat flux on hot face of nozzle bottom versus time
(long term)
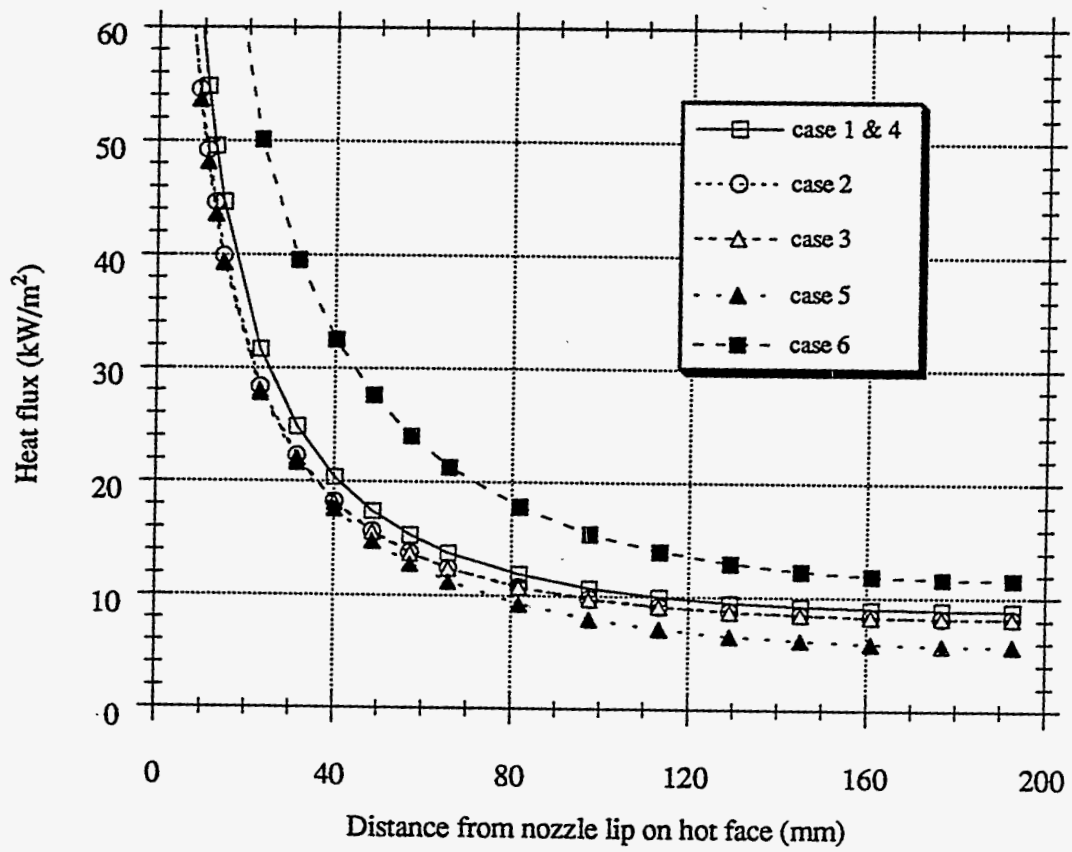
Fig. 12 Heat flux on nozzle hot face at steady state
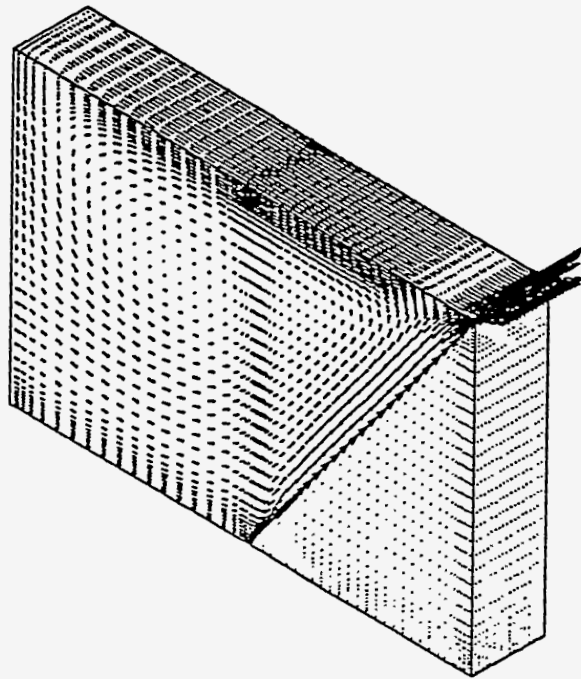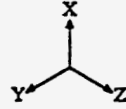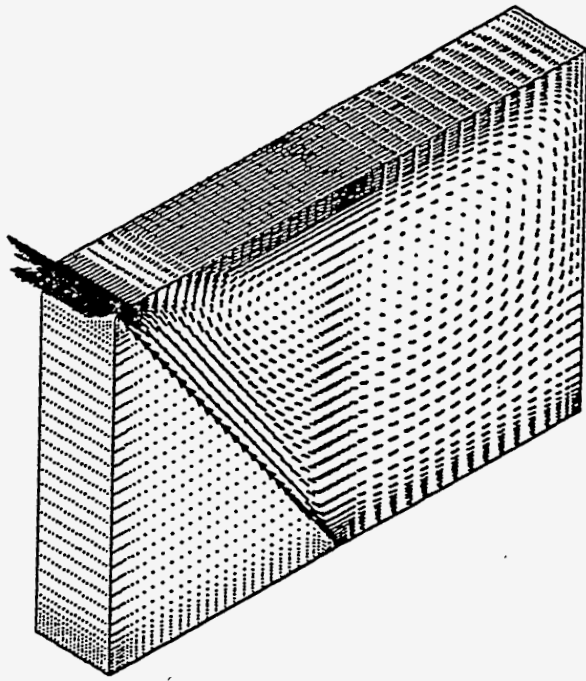
Fig. 13 Velocity distribution in liquid pool
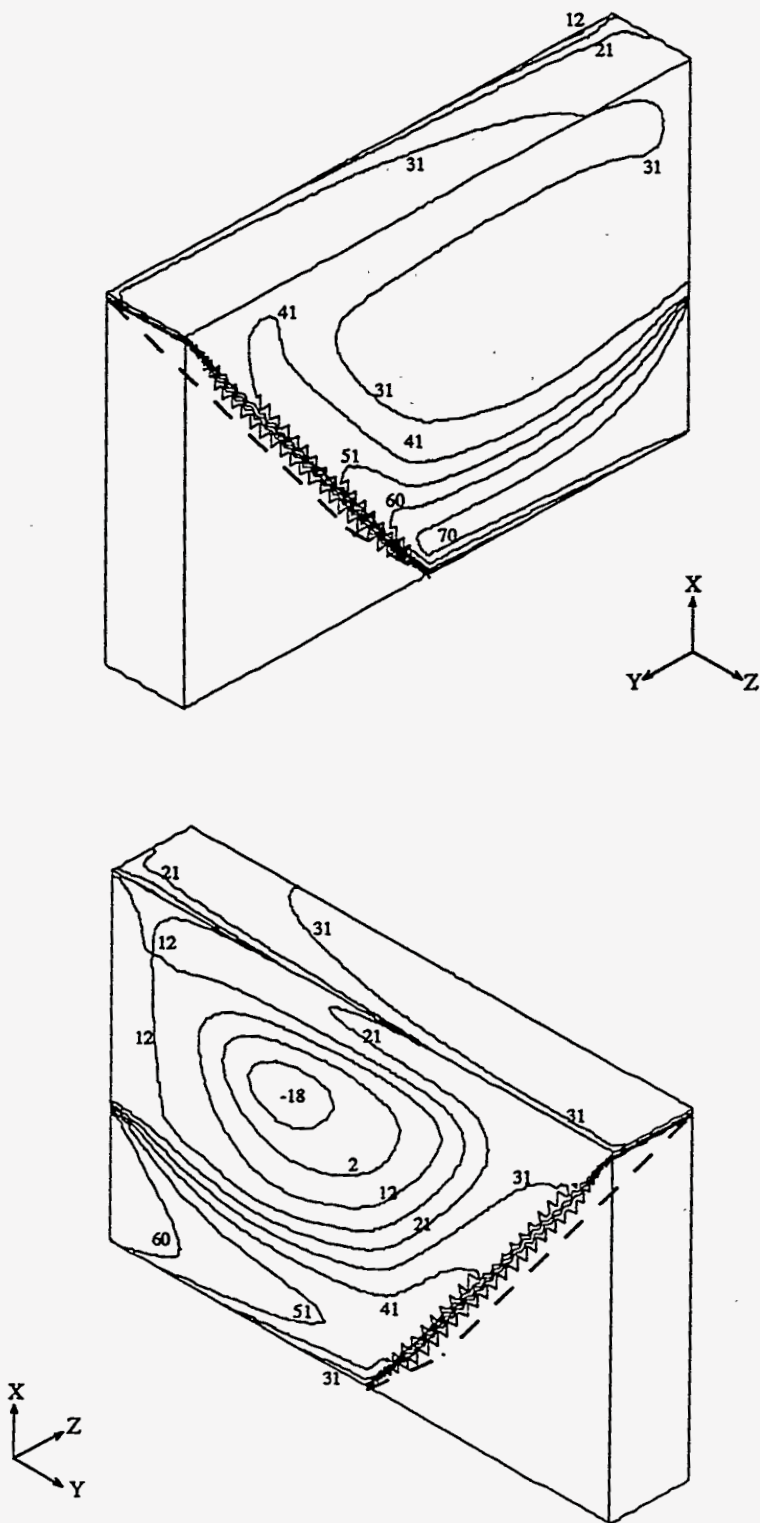
Fig. 14(a) Super heat temperature distribution in liquid pool (10s)
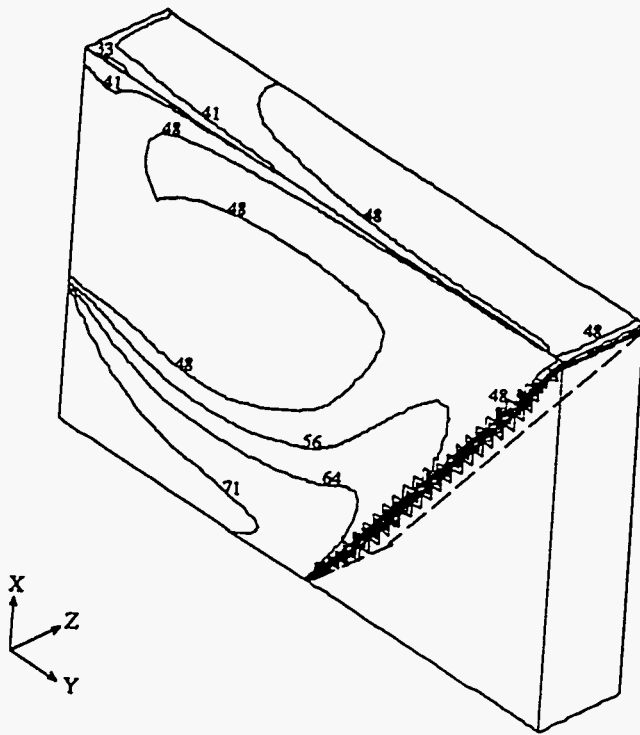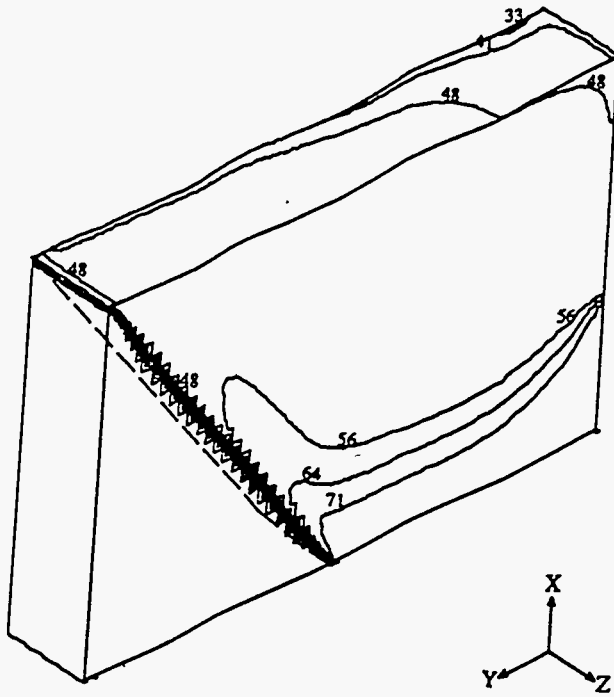
Fig. 14(b) Steady state superheat temperature distribution in liquid pool

Therefore, heat flux to wheel in center and at edge
is small (< 2%)
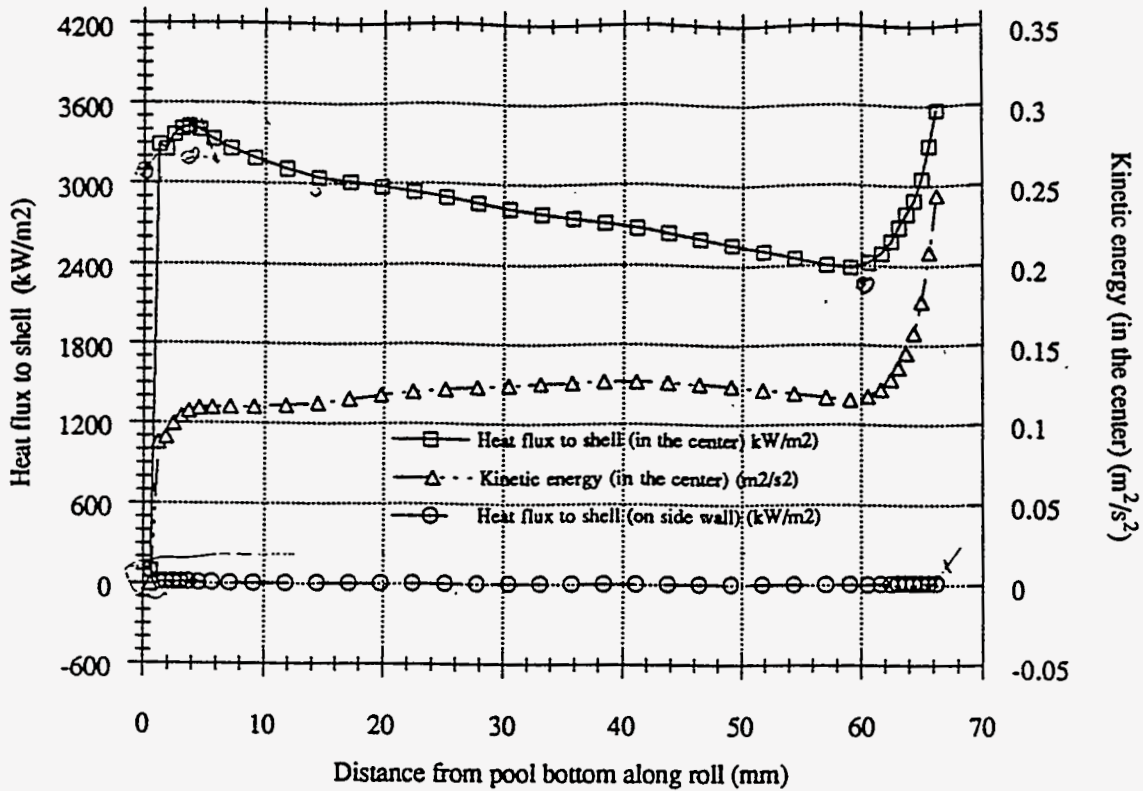
Fig. 15 Heat flux to shell along the roll with steady state nozzle heat loss
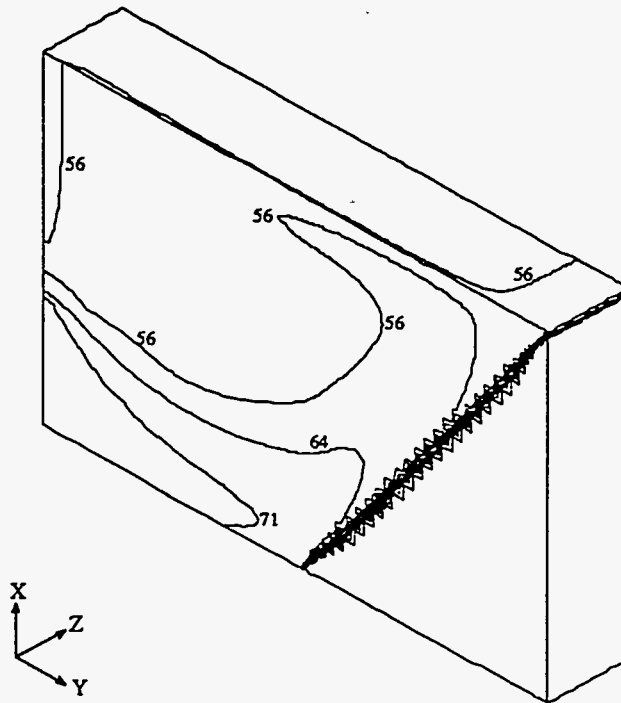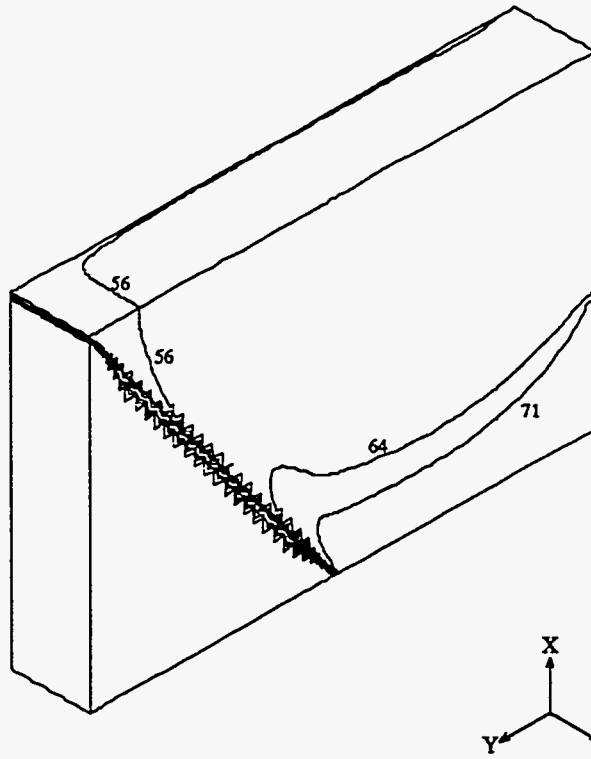
Fig . 16 Steady state superheat temperature distribution in liquid pool
(without free surface radiation)
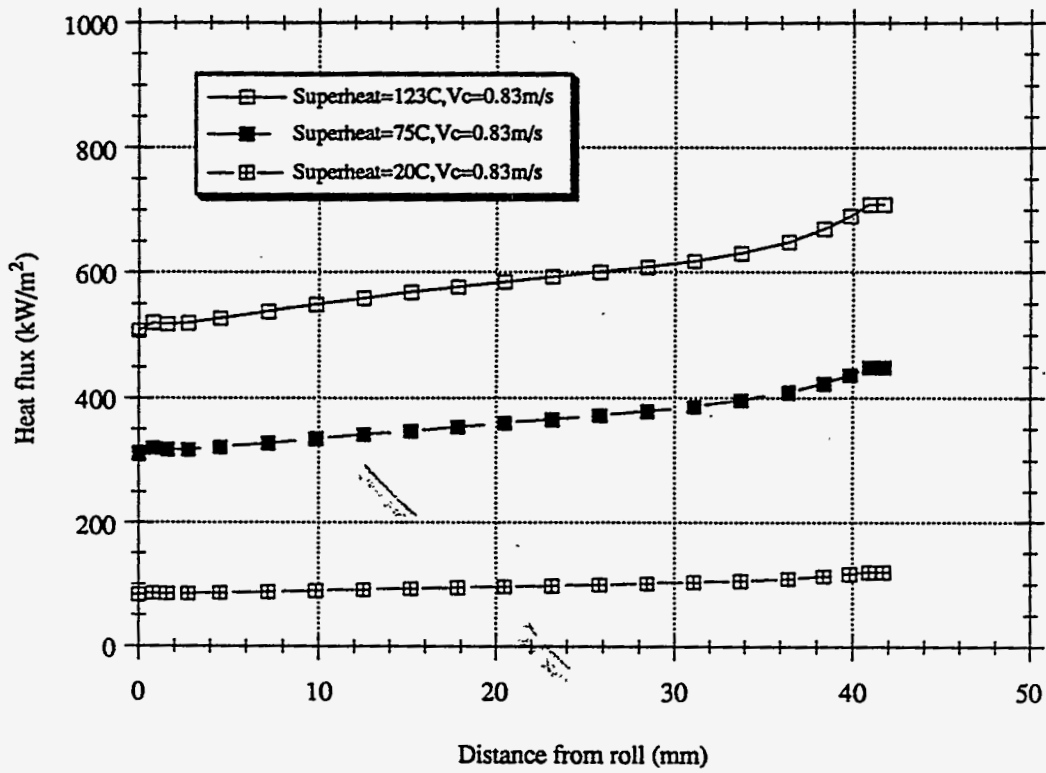
Fig 17 Heat flux out of pool at different superheat temperature
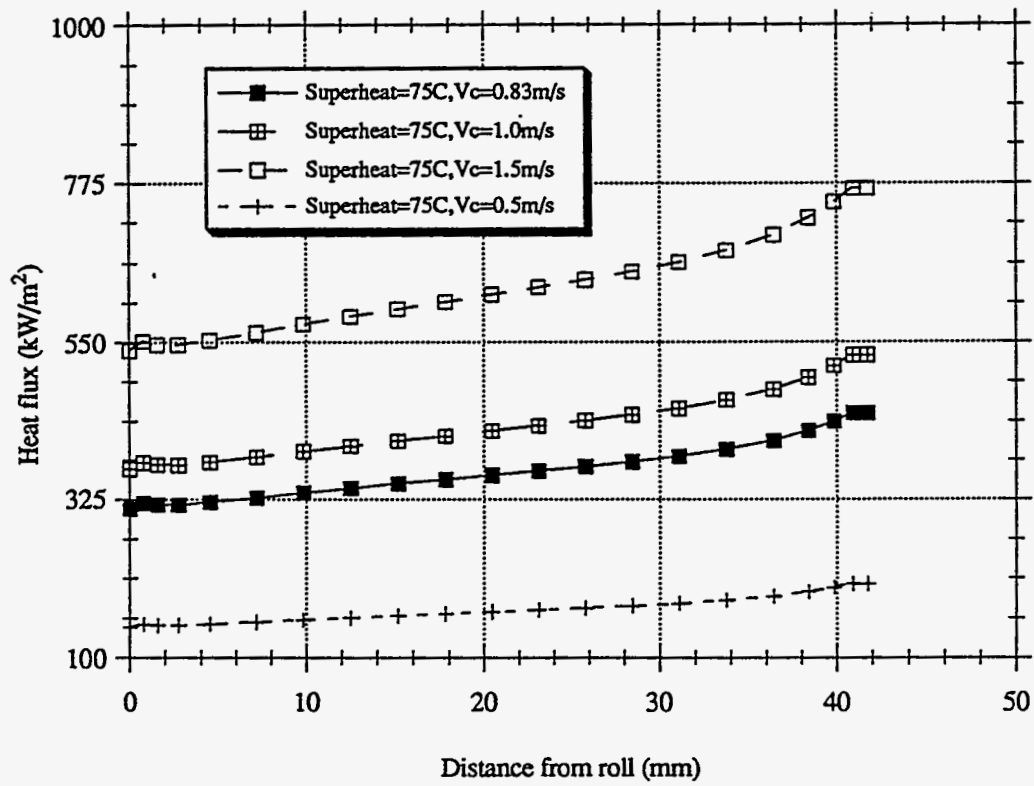
Fig. 18 Heat flux out of pool at different casting speed
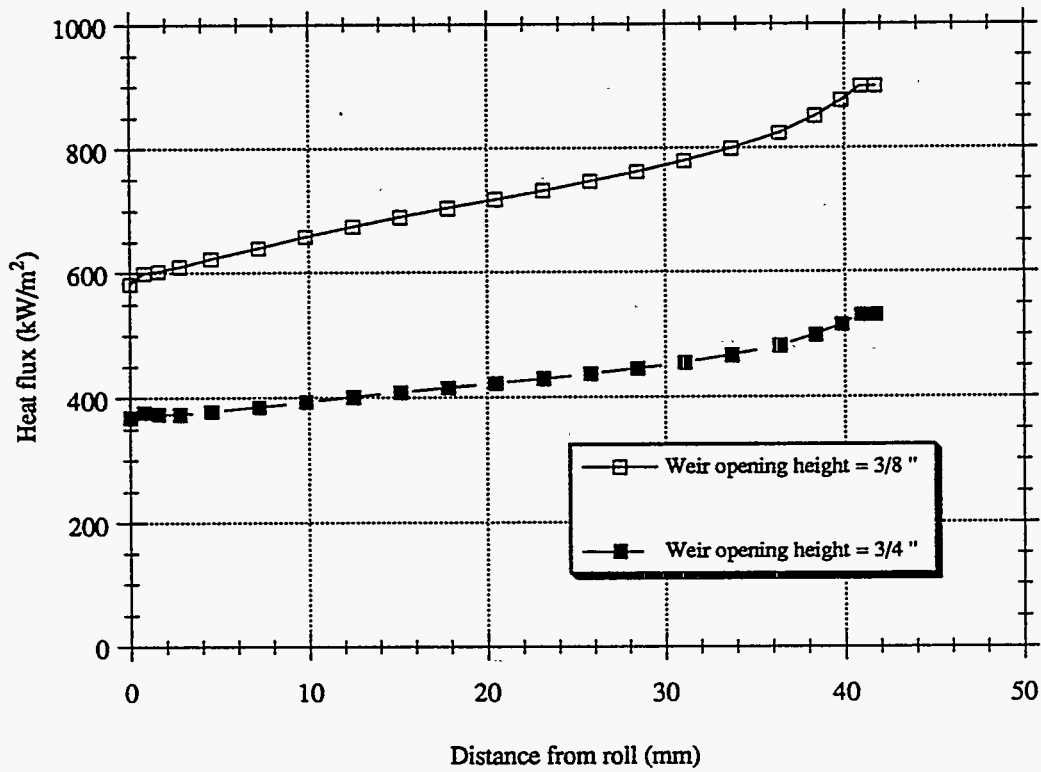
Fig. 19 Heat flux out of pool at different weir opening height

Metal Process Simulation Laboratory
Department of Mechanical and Industrial Engineering
University of Illinois at Urbana-Champaign
Urbana, IL 61801

Transient Thermal Model of the Continuous Single-Wheel Thin-Strip Casting Process

Guowei Li
Brian G. Thomas

Report

Submitted to

ARMCO Inc., Middletown, OH
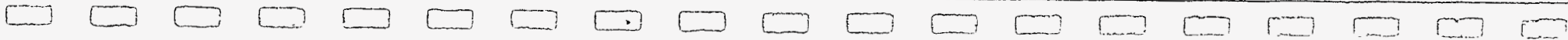
August 10, 1993

Transient Thermal Model of the Continuous Single-Wheel Thin-Strip Casting Process

Guowei Li and Brian G. Thomas

Department of Mechanical and Industrial Engineering
University of Illinois at Urbana-Champaign
1206 West Green Street
Urbana, IL 61801

ABSTRACT

A transient heat transfer model (STRIP1D) has been developed to simulate the single-roll continuous strip-casting process. The model predicts temperature in the solidifying strip coupled with heat transfer in the rotating wheel, using an explicit finite difference procedure. The model has been calibrated using strip thickness data from a test caster at ARMCO Inc. and verified with a range of other available measurements. The strip/wheel interface contact resistance and heat transfer was investigated in particular, and an empirical formula to calculate this heat transfer coefficient as a function of contact time was obtained. Wheel temperature and final strip thickness are investigated as a function of casting speed, liquid steel pool depth, coatings on wheel hot surface, strip detachment point, and wheel wall thickness and material.

I. INTRODUCTION

Despite the simple concept proposed by Bessemer in 1846[1], the continuous casting of thin strip has been difficult to commercialize, in part because the process involves complex interactions between fluid flow, solidification, shrinkage and stress. The direct casting of strip and sheet for some aluminum and other low-melting alloys has been established practice in the last few decades[2]. However for high-melting alloys such as steel, the process is still not commercial. During the last decade, a great deal of effort has been invested to develop strip casting of steel[3-6]. Among the several techniques under study, single-roll continuous strip casting appears promising for economic production of steel sheet.

Although much effort has been made on the single roll strip casting process, many problems still exist. These include surface cracks, tears, folds, excessive scale,[7] and internal voids or cracks, which have to be minimized, since hot-rolling is not able to correct these flaws. Thickness and quality of the strip is affected by the thermal properties of the strip, wheel cooling conditions, wheel geometry, and other process parameters. To understand how these parameters affect strip formation, mathematical models have been developed to characterize heat transfer in the process, including the prediction the strip thickness and temperature distribution in the wheel.

II. MODEL DESCRIPTION

A simplified schematic of the single roll continuous strip caster, such as used in ARMCO, is shown in Figure 1. Liquid steel flows through a ceramic nozzle, which develops a shallow pool of liquid steel against the rotating copper wheel. While in the pool, the steel solidifies against this water-cooled wheel, which rapidly withdraws the solid steel strip.

A one-dimensional transient finite-difference model, called STRIP1D, was developed to follow temperature evolution in a slice through both the wheel and the shell. It is a Lagrangian model so there is no relative motion between either the wheel, the strip or the domain. The model is transient in both the strip and wheel because the wheel heats up with time. The model follows temperature development in the wheel continuously and reinitializes the steel nodes to simulate casting of a new piece of strip once every revolution.

The following assumptions greatly simplify this model:
(1) heat losses along the width direction of strip are negligible;
(2) heat conduction along the perimeter of wheel and strip is negligible:

This is justified because the Peclet number, Pe based on a typical final strip thickness of 0.7 mm, is very large;

(3) there is no slipping between the wheel and strip;

(4) the strip thickness does not change after it gets out of the liquid pool.

Temperature in the strip and wheel is governed by the 1D transient heat conduction equation in cylindrical coordinates:

$$\rho C_p^* \frac{\partial T}{\partial t} = k \frac{\partial^2 T}{\partial r^2} + k \frac{1 \partial T}{r \partial r} + \frac{\partial k}{\partial T} \left(\frac{\partial T}{\partial r}\right)^2 \qquad [1]$$

where C_p^* is effective specific heat. For the solidifying steel, C_p^* is defined as:

$$C_p^* = \frac{dH}{dT} = C_p - \Delta H_L \frac{df_s}{dT} \qquad [2]$$

The solid fraction, f_s, is assumed to vary linearly between the solidus and liquidus temperatures, so:

$$C_p^* = C_p + \frac{\Delta H_L}{T_{liq} - T_{sol}} \qquad [3]$$

Details regarding the solution methodology are presented in Appendix I. Since this model is explicit, no iteration is required. There is, however, a well-known theoretical restriction on the time step and mesh size combinations possible to achieve stable solution for this problem:

$$\frac{\Delta t}{\Delta r^2} \frac{k}{\rho C_p^*} < 0.5 \qquad [4]$$

The time step size mainly depends on the number of cells and thermal diffusivity of the steel strip because the mesh size in the steel is much smaller than that in wheel. A fine spacing (less than 0.05 mm) is used between the nodes in the steel, requiring a small time step (less than 10^{-5} s). To accelerate the program, the time step size is increased to 10^{-3} s when the simulation domain includes only the wheel. Typically it takes 10 minutes CPU time on a IRIS4D workstation to simulate 250 seconds physical time (about 100 cycles) using this numerical model. The model has also been implemented into a user-friendly package that runs quickly on an IBM-PC. This program is currently being used by researchers at ARMCO to further develop the strip casting process.

3

A. *Boundary Conditions:*

The simulation domain containing the wheel and the strip is divided into five zones according to the different heat transfer conditions. They are: (I) shell growth zone, (II) strip cooling zone, (III) non-contact zone, (IV) no spray zone (V) non-contact zone. The strip solidifies in the pool in zone I, contacts the wheel in zones I and II, and is exposed to the environment in zones III to V. Cooling water is sprayed uniformly onto the wheel inner surface except in zone IV.

1. *Zone I (shell growth zone):*

The simulation domain is a slice through the liquid steel, strip, interface and wheel, presented in Figure 2. It includes about 4 mm of solid and/or liquid steel, and about 40 mm of copper from the cold inner surface (wheel/water interface) to the outer hot surface (strip/wheel interface) of the wheel.

In this zone, the shell thickness, x_{shl} is determined by linear interpolation:

$$x_{shl} = (1 - f_s) * x_{liq} + f_s * x_{sol}$$

Here x_{liq} and x_{sol} are the thickness corresponding to T_{liq} and T_{sol} respectively, each found by linear interpolating between the thickness of the adjacent nodes[8]. After leaving the liquid pool, the shell thickness is fixed to the position of the closest node to the solidification front. This avoids the complexity of adjusting the simulation mesh after each revolution. In the liquid steel, the strip temperature is set initially to T_{liq}, and the temperature distribution in the solid shell is obtained by solving Equations [1] to [3], imposing a "superheat flux", q_{sh} to the solid/liquid interface. Figure 3 shows the predicted superheat flux to the shell for typical conditions (casting speed $V_c = 1.5$ ms^{-1}, superheat temperature = 75 °C), obtained from a turbulent fluid flow and heat transfer model of the liquid steel in the nozzle[9, 10].

The superheat flux delivered to the shell increases in direct proportion to superheat temperature (the difference between the liquidus and pouring temperature) and casting speed[9, 10]. Therefore, the superheat flux for other casting speeds and superheat temperatures can be found from q_{sh} for standard conditions by:

$$q_{suph} = (\frac{V_c}{V_{c0}}) (\frac{\Delta T}{\Delta T_0}) q_{sh} \qquad [5]$$

4

The superheat flux to the shell has only a small effect on the simulation results in the range of this work, and it is relatively constant across the pool.

Thermal convection boundary conditions are employed at the wheel/water interface ($q_{w1} = q_{spray}$) and the strip/wheel interface:

$$q_{sn} = -q_{wn} = h_{gap1}(T_{s1} - T_{wn})$$

The values of the heat transfer coefficient h_{gap1} and heat flux q_{spray} are described in detail in the next section.

2. *Zone II (strip cooling zone)*:

The simulation domain for the steel is only the solid strip in this zone. Because the upper surface of the strip is exposed to the ambient, forced convection and radiation boundary conditions are used on this surface. To match experimental measurements, it has been found that the heat transfer coefficient across the strip/wheel interface must decrease from h_{gap1} to a much lower value h_{gap2}. This reduction implies to a sharp decrease in contact between the shell and wheel, possibly related to thermal contraction induced by temperature changes in the strip.

3. *Zones III and V (non-contact zone)*:

After leaving zone II, the domain representing the solid steel strip is mathematically separated from the wheel. Both sides of the strip are exposed to air, so forced convection together with the radiation boundary conditions are applied to both upper and lower surfaces of the strip:

$$q_{s1} = (h_{air} + h_{rad,s1}) * (T_{s1} - T_{air}) ; \text{ where, } h_{rad,s1} = \varepsilon \sigma (T_{s1}^2 + T_{air}^2) (T_{s1} + T_{air})$$

$$q_{sf} = (h_{air} + h_{rad,sf}) * (T_{sf} - T_{air}) ; \text{ where, } h_{rad,sf} = \varepsilon \sigma (T_{sf}^2 + T_{air}^2) (T_{sf} + T_{air})$$

The forced convection boundary condition is also employed on the wheel hot face:

$$q_{wn} = h_{conv} (T_{wn} - T_{air})$$

The wheel/water interface boundary conditions are the same as those in the previous zones.

4. *Zone IV (no spray zone)*:

Boundary conditions for this zone are the same as those in zones III and V, except that heat transfer at the wheel/water boundary is changed to convection:

$$q_{w1} = h_{no\text{-}spray} (T_{w1} - T_{air})$$

Because there is a pool of cooling water in the bottom of the rotating wheel, the heat transfer coefficient in this "no spray zone" is still much bigger than that for forced convection with air, h_{conv}.

B. *Interface Heat Transfer* :

1. *Heat Transfer Coefficient at Strip/Wheel Interface:*

The heat transfer coefficient at the strip/wheel interface h_{gap1} governs heat conduction in the entire process. It depends on the microgeometry and materials of both of the surfaces of the strip and the wheel and other process conditions. Despite the many pertinent theoretical and experimental investigations[11-13], the heat transfer mechanisms across these intermittently contacting surfaces and their dependencies upon applied conditions are still not fully understood or quantified. Thus, experimental measurements were needed to calibrate the model. These measurements were obtained from pilot strip casting trails on plain carbon steel, conducted at ARMCO[14]. A single constant value for h_{gap1} was found to be inadequate to predict shell thickness for all cases. At first, different constants were simply fit for each set of experimental conditions at ARMCO[14].

Next, a more fundamental relationship was sought. It has been postulated that the best parameter to characterize the heat transfer coefficient between the strip and wheel should be the contact time[2]. When the liquid steel first contacts the clear cold wheel surface, the heat transfer coefficient is known to have an extremely high value, and the bond is accepted to be very strong[15]. As the time elapses, the solidifying shell gains in strength and its thermal shrinkage due to the rapid cooling generates important shear stresses. These soon break the intimate bond, and a tiny gap is created between the two surfaces. The heat transfer coefficient drops accordingly with increasing time, as the shell continues to thicken and bend, further increasing the gap and lowering the heat transfer coefficient. To take this into account, the following empirical formula to calculate heat transfer coefficient between strip/wheel interface was adopted:

6

$$h_{gap1} = \begin{cases} h_0 & \text{when } 0 < t < t_0 \\ h_0 * \left(\frac{t_0}{t}\right) m & \text{when } t_0 < t < t_I \end{cases} \qquad [6]$$

The three adjustable model parameters h_0, t_0 and m in equation [6] were calibrated using numerical trial-and-error for the same series of casting experiments, according to the contact time. Figure 4 shows that Equation [6] adequately reproduces the experimental data[14]. The average coefficient, found by integrating Equation [6], decreases with time as follows:

$$h_{gap1, avg.} = \frac{1}{t_I} \int_0^{t_I} h_{gap1} \, dt = \frac{h_0 \, t_0}{t_I} + \frac{h_0 \, t_0}{t_I} \frac{1}{1-m} \left[\left(\frac{t_0}{t_I}\right) 1-m - 1 \right] \qquad [7]$$

Note that the average heat transfer coefficient $h_{gap1, avg}$ based on the fitted values decreases from (28 kWm^{-2}) at high casting speed (1.5 ms^{-1}) to (16 kWm^{-2}) at lower casting speed (0.5 ms^{-1}). This shows how the strip/wheel interface heat transfer coefficient decreases as the contact time increases. It is also interesting to note that the fitted value for the exponent m of 0.55 is very similar to the square root time relationship expected for shell growth. This appears to demonstrate a probable link between shell deformation and heat transfer. The fitted value of t_0 0.01 s shows that loss of perfect contact must occur very quickly.

2. *Heat Flux at Spray Water/Wheel Interface*:

Heat flux extracted by the spray cooling water at the wheel inner surface is based on the following empirical formula[16] relating water flux and surface temperature:

$$q_{spray} = B * \exp(A) \qquad [8]$$

$$A = a_0 + a_1*V_w^2 + a_2*V_w^3 + a_3/V_w + a_4/V_w^2 + a_5*V_w*T + a_6*T + a_7*T^2$$

$$+ a_8*T^3 + a_9*T^4 + a_{10}*V_w*T^4 \qquad [9]$$

$$\text{where } V_w \text{ (l/m}^2\text{-min.)} = \frac{60000w}{(L_1 + L_2 + L_3 + L_5)(R_i/R_o) W}$$

Here T (°C) is the surface temperature and V_w (l/m^2-min.) is the water flux. Besides the eleven empirical constants given by Chen[16], an extra constant, B, was introduced according to Jeschar et al to account for the effect of different materials[17]. This formula was then linearly extrapolated between the heat flux at 150 °C and 0 (at 30 °C) to determine values for the wheel inner surface temperature in this work.

III. MODEL VERIFICATION

To verify the model using equation [6] with the three empirical constants given in Table I, the model was applied to simulate other available experimental continuous casting data, including experiments on continuous casting, compiled by Birat[4], tin strip casting[3], and "hot dip" test measurements performed at ARMCO[14, 18].

The heat flux extracted across the strip/wheel interface was calculated to decrease with inversely the square root of contact time, matching the Birat experimental data as shown in Figure 5. In continuous strip casting, the contact time is very short, typically about 0.1 second. Thus, the heat flux to the cooling wheel, typically 10 MW m^{-2}, is much bigger than that in continuous slab casting processes. The higher the casting speed, the shorter the contact time, so the average heat flux increases. Figure 6 reveals that the model using Equation [6] predicts strip thicknesses at pool exit almost proportional to 0.55 power of the contact time.

The model was next used to simulate the tin strip casting, and the predictions are compared with experimental data from Birat[3]. In the first run, the pool depth, which was not reported, was chosen to reproduce the measured tin strip thickness. It is significant that all of the other simulations with different casting speeds match the measurements, despite the different contact times in those runs. Figure 7 shows that good agreement has been obtained between predicted and measured tin strip thicknesses.

To further confirm the model using the Equation [6], a series of "hot dip" experiments were undertaken in ARMCO Inc.[18]. In this test, a 4" x 4" x 1.5" copper block at a uniform preheat temperature is submerged into a liquid steel pool, and the temperatures of five thermocouples installed at different depths from the block hot face are recorded. Because the submerged depth of the copper block is small compared with the dimensions of the copper block, the assumption inherent in STRIP1D is reasonable. A comparison between the model predictions and temperature measurements for a typical dip test is shown in Figure 8. The trends are the same. The difference in quantitative matching might be due to differences of conditions between the simulation and the test and the inaccuracy of the thermocouples. It is interesting that the model with Equation [6] also appears to apply to this case with a stationary copper block and match the measured temperatures. Based on the large range of contact times and conditions in the experimental data, and the accuracy of the model predictions, it appears that Equation [6] with the three fixed empirical constants may be universal for casting processes.

IV. TYPICAL MODEL RESULTS

The mathematical model has been tested for the casting of carbon steel in the strip thickness range of 0.6-1.0 mm. The predicted results, including strip final thickness, strip and wheel temperature, are now presented and compared with available measurements. The results presented here were obtained by running the model under the standard casting conditions in Table I, except as otherwise indicated.

Figure 9 compares the predicted temperature histories of the wheel cold face and the cooling water leaving the wheel with experimental thermocouple measurements. The wheel cold face temperature increases in about the first 70 seconds, to reach a quasi-steady-state condition, or steady periodic function of time. The roughly 7 °C fluctuations of the wheel cold face temperature are caused by the alterations of the cooling water heat transfer conditions between the spray zones and non spray zone. The amplitude of the variations depend greatly on the heat flux values in the spray and no spray zones and the period is determined by the casting speed and wheel outer radius. The wheel cold face temperature increases in the no spray zone IV, because the heat transfer coefficient is smaller in this region.

Figure 10 shows the strip thickness as a function of casting time for Standard conditions. The strip thickness increases while liquid pool fills. Then, thickness decreases slightly with time due to the slightly smaller heat flux associated with the hotter wheel at later times. In addition, for the first few seconds, the strip thickness is slightly larger, due to the absence of superheat. After about 70 seconds, the strip thickness has reduced about 10%, and the conditions have reached quasi-steady state. The time to reach the quasi-steady state depends on wheel and strip properties, wheel geometry, the definition of quasi-steady state and other process parameters, but it is generally in the range of 50 to 80 seconds. Of greater importance is the larger relatively random fluctuation in shell thickness with time. This is undoubtedly related to local variations in heat transfer across the interface. Thus, Eq. [6] is valid only in a time-averaged sense.

The predicted quasi-steady state temperatures of the hot and cold surfaces of the wheel are given in Figure 11. The hot surface temperature increases in zone I. This is because the heat flow from the wheel cold surface to the cooling water is bigger than that from the strip to the wheel hot surface in zone I. After zone I, the surface temperature decreases continuously, due to thermal equilibration in the wheel. Note that temperature in the wheel at no time is steady state.

The typical temperature distribution in the strip at quasi-steady state with standard conditions is presented in Figure 12. It is found that the temperatures of both sides of the strip decrease very fast as soon as the strip leaves the liquid pool of zone I. Further loss of contact

between the strip and wheel is believed to cause a rapid drop in interfacial heat transfer between zones I and II. This causes the inner surface of the strip to quickly reheat to equal the outer temperature, which could generate detrimental thermal stresses. Temperature within the strip soon becomes almost uniform across its thickness, because the strip is so thin.

To demonstrate that the numerical model works properly, heat balances in the strip and wheel can be calculated at any desired time. For standard conditions, (see Table II), the heat balance on the strip while in the liquid pool indicates that most of the heat extracted to the wheel comes from latent heat of solidification (69%), with cooling of the strip accounting for 24% and superheat extraction only 10%. Heat enters the wheel mainly in Zone I, due to contact with the hot strip (76%), with 25% more heat entering in Zone II. Heat losses from the wheel exterior due to convection and radiation cooling in zone III-V are negligible (less than 1% of the total heat lost). Heat loss to the cooling water is almost uniformly distributed per unity length around the wheel interior perimeter, and almost equals the total heat extracted from the strip for these quasi-steady state conditions. Numerical errors are always less than 5%.

The casting speed, liquid steel pool depth, coatings on the wheel hot surface, strip detachment point and wheel wall thickness all affect the casting process. To understand and compare the effects of these casting parameters, a set of cases were studied whose conditions are given in Table III.

A. *Effect of Casting Speed:*

The speed of the rotating wheel, or casting speed is, perhaps, the most important parameter that affects the operation of the caster. Figure 13 shows how strip thickness varies with casting speed. To cast thicker strip requires longer residence time of the solidifying strip in the liquid steel pool. One way to achieve this is by lowering the casting speed. As shown in Figure 13 and discussed previously, the numerical prediction of the final strip thickness matches the experimental data used to calibrate the model.

The temperature histories predicted on the wheel hot face and cold face are given in Figure 14 for a "sliding thermocouple" located at the initial pool/wheel junction. The wheel hot face temperature increases with casting speed, while the wheel cold face temperature is much less sensitive. Because the average heat transfer coefficient across the strip/wheel interfacial gap is large at higher casting speed, due to the smaller contact time.

B. *Effect of Liquid Steel Pool Depth:*

The contact time of the solidifying strip with the liquid steel in the pool increases in direction proportion with the contact length. The contact distance between the solidifying strip and the liquid steel is determined by the liquid pool depth and the angular position α_1 of the liquid pool in zone I. Thus the final strip thickness increases with increasing pool depth. Variations in pool depth produce changes in strip thickness. It is significant to note that a variation in pool depth of 10 mm (12.5%), such as likely due to surface waves, only produces a thickness variation of 0.05 mm (7%). Thus, variations in liquid level are clearly unable to account for the observed variation in strip thickness.

C. *Effect of Coatings on Wheel Hot Face:*

Coating the wheel outer surface with a thin plate of Ni or Cr has a significant effect on the wheel temperature. Figure 15 presents the quasi-steady state wheel temperatures on the cold and hot surfaces with a 2 mm Ni coating layer (Case 7) compared with a pure copper wheel. Property data were taken from the handbook[19]. The total wheel thicknesses in these two cases are the same. Owing to the smaller conductivity and specific heat of the coating materials, these layers, act as heat insulators, to decrease the average heat flux to the copper wheel. This lowers the wheel surface temperature outside zone I, and lowers the copper temperature everywhere. The temperature in the Ni layer is much higher than that in the corresponding copper layer with no coating in zone I due to the small conductivity of Ni. This is predicted to decrease the final strip thickness, but the effect is extremely small. The same conclusions can be obtained from the results of the other cases with coatings in Table IV. It should be noted that changing wheel material and temperature might influence the heat transfer across the strip/wheel gap, which was ignored here.

D. *Effect of Strip Detachment Point:*

The strip is totally detached from the wheel between zones II and III. The effect of this strip detachment point on the strip thickness and temperature distribution in wheel is almost negligible. Increasing the contact distance 100 mm (20%), caused the final strip thickness to decrease less than 0.01 mm (less than 1%). The detachment point has little effect on other parameters such as wheel temperature also (3% drop in surface temperature of wheel). This is because the most dramatic drop in heat transfer coefficient occurs much earlier (moving from zone I to II) due to loss of contact on the micro-scale.

11

E. *Effect of Wheel Wall Thickness:*

The wheel wall thickness is an important design parameter of the caster. Firstly, it determines the thermal resistance to heat flow from the strip to the spray water. Naturally, the wheel surface temperature increases in almost direct proportion to wheel thickness. However, the rate of heat withdrawal does not change much with wall thickness, so the final strip thicknesses for different wheel wall thickness are almost the same (only 1.5% difference). Any direct effect of wheel surface temperature on the interface heat transfer coefficient was thought to be small and ignored. The time needed to reach quasi-steady-state temperature also increases with the wheel thickness. Finally, the hotter, thicker wheel is more likely to produce thermal distortion, which could interfere with the wheel roundness and good uniform sealing between the wheel and the nozzle.

F. *Effect of Wheel Wall Material:*

The wheel thermal properties (thermal conductivity, specific heat and density) have a big effect on the wheel temperature (the steel wheel temperature is about 220% higher than copper wheel temperature). A comparison between a steel wheel and a copper wheel with the same geometry was made, and the results are presented in Table IV. A steel wheel has a much higher hot face temperature due to the poor thermal conduction of steel. This lowers the heat transfer rate, and produces 30% thinner strip, for a given set of casting conditions. It also delays the time needed to reach quasi-steady state.

V. CONCLUSIONS

In the present study a simple but realistic mathematical model of strip solidification coupled with wheel heat transfer has been developed to describe the single-roll strip casting processes. The simulation results have been calibrated with available measurements, and good agreement has been obtained between calculations and a wide range of experimental data.

The model has been implemented into a user friendly program for the IBM-PC and is serving as an active research tool. In addition, the following conclusions are predicted by this model:

1. Heat transfer in the strip casting process is controlled mainly by the heat transfer coefficient between the solidifying strip and copper wheel. This coefficient decreases with contact time, according to a function that appears valid over a wide range of casting processes. $h = (28 \frac{kW}{m^{2}{}^{\circ}K}) (\frac{0.01}{t(s)})^{0.55}$ for $t > 0.01$ s.

2. Casting speed is the most influential parameter on the final strip thickness. Higher casting speed produces thinner strip with the same exponential dependency of 0.55 that governs the interfacial heat transfer coefficient.

3. Strip thickness is almost directly proportional to the liquid steel pool depth. Non uniformity of strip thickness is not significantly influenced by small pool depth variations.

4. Coatings on the wheel hot surface have a significant effect on wheel temperature in the liquid pool zone.

5. Transient heat up of the wheel takes 50 to 70 seconds. This may have a significant influence on pilot-plant experiments with short run times. There is even a slight influence on strip thickness.

6. A thinner wheel reaches quasi-steady state faster than thicker wheel.

7. Superheat has very little effect on the final strip thickness and wheel temperature.

13

ACKNOWLEDGMENT

APPENDIX I. SOLUTION METHODOLOGY

Equation [1] is solved at each time step using a 1-D finite difference discretization. The simulation domain, a slice through the liquid steel, solid shell, interface and wheel, was presented in Figure 2.

The specific heat is treated as a function of temperature in strip and wheel, the conductivity is assumed to be linear to the temperature in steel and a constant in wheel. Using the central difference scheme, the following equations are derived from Eq. [1] to [3].

A. *Liquid Nodes*:

$$T_{si} = T_{liq} \qquad\qquad (si > sf \text{ i.e. in liquid}, t < t_I) \quad [A1]$$

B. *Solid/liquid Interface Node:*

$$T_{sf}{}^{new} = T_{sf} + \frac{\Delta t}{\Delta r^2} \frac{k}{\rho\, C_p{}^*} (T_{sf-1} - 2\, T_{sf} + T_{sf+1}) + \frac{\Delta t}{2\, r_{sf}\, \Delta r} \frac{k}{\rho\, C_p{}^*} (T_{sf+1} - T_{sf-1})$$

$$+ \frac{\Delta t}{4\, \Delta r^2\, \rho\, C_p{}^*} \frac{\partial k}{\partial T} (T_{sf+1} - T_{sf-1})^2 + \frac{\Delta t\, q_{sf}}{\rho\, C_p} \left(\frac{1}{r_{sf}} + \frac{2}{\Delta r}\right) \qquad [A2]$$

$$\text{where } q_{sl} = \begin{cases} q_{suph} & (t < t_I) \\ = -q_{air} = -h_{air}{}^* (T_{sf} - T_{air}) & (t_I < t < t_{II}) \end{cases} \qquad [A3]$$

To ensure latent heat is not missed, a post-iterative correction is performed after each time step. Whenever a solidifying node cools below the solidus, or a liquid node cools below the liquidus, its temperature is adjusted to account for any incorrect change in enthalpy that occurred during that time step[8]

C. *Interior Strip Nodes:*

$$T_{si}{}^{new} = T_{si} + \frac{\Delta t}{\Delta r^2} \frac{k}{\rho\, C_p{}^*} (T_{si-1} - 2\, T_{si} + T_{si+1}) + \frac{\Delta t}{2\, r_{si}\, \Delta r} \frac{k}{\rho\, C_p{}^*} (T_{si+1} - T_{si-1})$$

15

$$+ \frac{\Delta t}{4 \, \Delta r^2 \, \rho \, C_p^*} \frac{\partial k}{\partial T} (T_{si+1} - T_{si-1})^2 \qquad (si < sf, \, t < t_{II}) \qquad [A4]$$

D. *Strip Surface Node:*

$$T_{s1}^{new} = T_{s1} + \frac{\Delta t}{\Delta r^2 \, \rho \, C_p^*} \frac{k}{} (2 \, T_{s2} - 2 \, T_{s1}) - \frac{\Delta t \, k}{\rho \, C_p^*} \left(\frac{1}{r_{s1}} + \frac{2}{\Delta r} \right)$$

$$+ \frac{\Delta t}{\rho \, C_p^*} \frac{\partial k}{\partial T} \left(\frac{q_{s1}}{k} \right)^2 \qquad [A5]$$

where: $q_{s1} = h_{gap1} * (T_{s1} - T_{wn})$, and h_{gap1} is given in Eq. [5].

The model can deal with up to four different materials in the wheel. For example, equations are presented here for a wheel of two different materials A and B, representing a copper wheel with a coating. The interface node between A and B corresponds to node number wc. For nodes in wheel material A (number $wi < wc$), properties k_{wA}, ρ_{wA}, C_{pwA} and cell spacing Δr_{wA} are used. For nodes in wheel material B (number $wi > wc$), properties k_{wB}, ρ_{wB}, C_{pwB} and cell spacing Δr_{wB} are used.

E. *Wheel Hot Surface Node:*

$$T_{wn}^{new} = T_{wn} + \frac{\Delta t \, k_w}{\Delta r_w^2 \, \rho_w \, C_{pw}} (2 \, T_{wn-1} - 2 \, T_{wn}) - \frac{\Delta t \, k_w}{\rho_w \, C_{pw}} \left(\frac{1}{r_{wn}} + \frac{2}{\Delta r_w} \right)$$

$$[A6]$$

where: $q_{wn} = h_{gap1} * (T_{s1} - T_{wn})$

F. *Interior Wheel Nodes:*

$$T_{wi}^{new} = T_{wi} + \frac{\Delta t \, k_w}{\Delta r_w^2 \, \rho_w \, C_{pw}} (T_{wi-1} - 2 \, T_{wi} + T_{wi+1})$$

$$+ \frac{\Delta t \, k_w}{2 \, r_{wi} \, \Delta r_w \, \rho_w \, C_{pw}} (T_{wi+1} - T_{wi-1}) \qquad [A7]$$

16

G. *Interface Node Between Different Wheel Materials:*

Eq. [A6] with

$$q_{wc} = \frac{\dfrac{\alpha_{wB}}{\Delta r_{wB}^2} * (T_{wc+1} - T_{wc}) - \dfrac{\alpha_{wA}}{\Delta r_{wA}^2} * (T_{wc-1} - T_{wc})}{\dfrac{\alpha_{wB}}{\Delta r_{wB} \, k_{wB}} + \dfrac{\alpha_{wA}}{\Delta r_{wA} \, k_{wA}} + \dfrac{\alpha_{wB}}{2 r_{wc} \, k_{wB}} + \dfrac{\alpha_{wA}}{2 r_{wc} \, k_{wA}}} \qquad [A8]$$

H. *Wheel Cold Surface Node:*

$$T_{w1}^{new} = T_{w1} + \frac{\Delta t \quad k_w}{\Delta r_w^2 \, \rho_w \, C_{pw}} (2 T_{w2} - 2 T_{w1}) - \frac{\Delta t \quad k_w}{r_{w1} \, \rho_w \, C_{pw}} \left(\frac{1}{r_{w1}} + \frac{2}{\Delta r_w}\right)$$

$$[A9]$$

$$\text{where } q_{w1} = \begin{cases} q_{spray} & \text{see Eq. [8] and [9]} & \text{in zone I-III and V} \\ h_{no\text{-}spray} * (T_{w1} - T_{water}) & & \text{in zone IV} \end{cases} \qquad [A10]$$

To ensure latent heat is not missed, a post-iterative correction is performed after each time step. Whenever a solidifying node cools below the solidus, or a liquid node cools below the liquidus, its temperature is adjusted to account for any incorrect change in enthalpy that occurred during that time step[8].

17

Table I. Standard Simulation Conditions and Nomenclature

Symbol	Variable	Value	Unit
C_p	strip specific heat (steel)	690	$J\ kg^{-1}\ °K^{-1}$
C_{pw}	wheel specific heat (copper)	866	$J\ kg^{-1}\ °K^{-1}$
C_{pwater}	water specific heat	4179	$J\ kg^{-1}\ °K^{-1}$
$C_p{}^*$	effective specific heat	see Eq. [3]	$J\ kg^{-1}\ °K^{-1}$
f_s	solid fraction at solid/liquid interface	0.7	
h_{air}	forced convection coefficient	50	$W\ m^{-2}\ °K^{-1}$
h_0	empirical constant in h_{gap1}, see Eq. [6]	28	$kW\ m^{-2}\ °K^{-1}$
h_{gap1}	strip/wheel interface heat transfer coefficient in zone I	see Eq. [6]	
h_{gap2}	strip/wheel interface heat transfer coefficient in zone II	200	$W\ m^{-2}\ °K^{-1}$
$h_{no\text{-}spray}$	wheel/water heat transfer coefficient in zone IV	12,000	$W\ m^{-2}\ °K^{-1}$
ΔH_L	strip latent heat fusion of steel	271.96	$kJ\ kg^{-1}$
k	strip conductivity (steel)	29	$W\ m^{-1}\ °K^{-1}$
k_w	wheel conductivity (copper)	380.16	$W\ m^{-1}\ °K^{-1}$
$L_1, L_2, L_3,$		80, 372, 585,	mm
L_4, L_5	length along wheel outer perimeter of zone I -- V	479, 399	mm
L_{pool}	pool depth in nozzle		mm
ΔL	final strip thickness		mm
m	empirical exponent in h_{gap1}, see Eq. [6]	0.55	
Pe	Peclet number $= \dfrac{V_c \Delta L}{\alpha}$		
q_{spray}	heat flux extracted by spray water in zone I,II,III,V		Wm^{-2}
q_{sh}	superheat flux added at shell/liquid interface		Wm^{-2}
r	distance from wheel center		m
Δr	cell spacing		m
R_i	wheel inner radius	0.2667	m
R_0	wheel outer radius	0.3048	m

t	time from start of casting		sec
t_0	empirical reference time in h_{gap1} see Eq. [6]	0.01	sec
t_I	contact time in zone I		
Δt	time increment		
T	temperature		°K
T_{air}	ambient temperature	30	°C
T_{init}	wheel initial temperature	50	°C
T_{liq}	steel liquidus temperature	1530 (2786)	°C (°F)
T_{pour}	pour temperature	1600 (2919)	°C (°F)
T_{sol}	steel solidus temperature	1520 (2768)	°C (°F)
T_{water0}	initial water temperature into spray zone	50	°C
V_c	casting speed	0.766 (150)	ms^{-1} (ft min^{-1})
w	total flowrate of spray water	0.00615 (98)	$m^3 s^{-1}$ (GPM)
W	width of strip	0.3048 (12)	m (inch)
α	thermal diffusivity of strip $= \dfrac{k}{\rho C_p}$		
α_c	thermal diffusivity of coating $= \dfrac{k_c}{\rho_c C_{pc}}$		
α_w	thermal diffusivity of wheel $= \dfrac{k_w}{\rho_w C_{pw}}$		
ε	strip emissivity (steel)	0.8	
ε_w	wheel emissivity (copper)	0.5	
ρ	strip density (steel)	7400	kg m^{-3}
ρ_w	wheel density (copper)	8950	kg m^{-3}
ρ_{water}	water density	995	kg m^{-3}
σ	Stefan-Boltzmann constant	5.678e-8	W m^{-2} °K^{-4}

Subscripts:

s	strip
w	wheel

Table II Heat Balance at Steady State (Standard Conditions)

A. Heat balance of strip		(kJ/s)	(%)
1. Region I:	1) Heat loss from strip to wheel:	1196	
	2) Heat input to shell inside (superheat):	123	10
	3) Latent heat:	826	69
	4) Sensible heat from cooling strip:	292	24
Error in heat balance:[2) +3) +4) - 1)]/ 1) * 100%			**3.79**
2. Region II:	1) Heat loss from strip to ambient:	118	25
	2) Heat loss from shell to wheel:	387	82
	3) Sensible heat from cooling strip:	474	
Error in heat balance:[1) +2) - 3)]		**31.33**	
Error of heat balance on Strip:			**0.89**

B. Heat balance of wheel			
1. Region I:	1) Heat loss from wheel inside to water:	71	5
	2) Heat into wheel from strip or ambient:	1196	76
	3) Heat to increase wheel temperature:	1130	72
Heat balance error in region 1:[1) +3) - 2)]		**5**	
2. Region II:	1) Heat loss from wheel inside to water:	328	21
	2) Heat into wheel from strip or ambient:	387	25
	3) Heat to increase wheel temperature:	75	5
Heat balance error in region 2:[1) +3) - 2)]		**16**	
3. Region III:	1) Heat loss from wheel inside to water:	510	32
	2) Heat into wheel from strip or ambient:	-4	0
	3) Heat to increase wheel temperature:	-523	-33
Heat balance error in region 3:[1) +3) - 2)]		**-8**	
4. Region IV	1) Heat loss from wheel inside to water:	300	19
	2) Heat into wheel from strip or ambient:	-3	0
	3) Heat to increase wheel temperature:	-300	-19
Heat balance error in region 4:[1) +3) - 2)]		**3**	
5. Region V:	1) Heat loss from wheel inside to water:	363	23
	2) Heat into wheel from strip or ambient:	-3	0
	3) Heat to increase wheel temperature:	-382	-24
Heat balance error in region 5: [1) +3) - 2)]		**-20.**	
Error of heat balance on wheel:			**0.06**

Table III Simulation Conditions

Cases	Casting speed (m/s)	Liquid steel pool depth ( )	Coatings (mm)	Strip detachment point ( )	Wheel wall thickness (mm)
1 standard	0.766	15.1	no	85	38
2	1.5	15.1	no	85	38
3	1.0	15.1	no	85	38
4	0.5	15.1	no	85	38
5 pool depth	0.766	20.05	no	85	38
6 pool depth	0.766	30.0	no	85	38
7 coating	0.766	15.1	2mm Ni	85	36+2
8 coating	0.766	15.1	10mm Ni 10mm Cr	85	38+20
9 detachment point	0.766	15.1	no	105	38
10 wheel thickness	0.766	15.1	no	85	20
11 steel wheel	0.766	15.1	no	85	38

21

Table IV.   Simulation Results at Steady State

Cases	Final strip thickness (mm)	Water ΔT(°C)	Temperature on wheel inner and outer surface (°C)			
			Inner Surface		Outer Surface	
			Max	Min	Max	Min
1 Standard	0.66	18	95	89	249	162
2	0.47	23	103	98	277	196
3	0.60	20	96	92	259	174
4	0.95	14	84	80	222	132
5	0.78	20	98	92	260	173
6	0.97	23	105	98	277	191
7	0.61	17	91	87	385	156
8	0.59	16	86	83	533	294
9	0.65	19	95	90	256	168
10	0.67	18	94	88	210	119
11	0.46	12	80	75	805	624

22

REFERENCES

1. H. Bessemer: U. S. Patent, Report No. 49053, 1865.

2. S. Caron, E. Essadiqi, F.G. Hamel and J. Masounave: "Numerical Modelling of Heat Transfer in High Productivity Rate Twin-Roll Casting Process", *Light Metals*, C.M. Bickert, eds., The Minerals, Metals & Materials Society, 1990, pp. 967-973.

3. J.P. Birat, P. Blin, J.L. Jacquot, P. Riboud and B. Thomas: "Near Net Shape Continuous Casting of Flat Products at IRSID", *Revue Met.,* 1989, vol. 86, pp. 920-930.

4. J. Birat, M. Larrecq, J. Lamant and J. Petegnief: "The Continuous Casting Mold: A Basic Tool for Surface Quality and Strand Produtivity", in *Mold Operation for Quality and Productivity,* Iron and Steel Society, Warrendale, PA, 1991, pp. 3-14.

5. A. Kumar and S.P. Mehrotra: "A Methematical Model of Single Roll Strip Caster Based on Macroscopic Enthalpy Balances", *Steel Research,* 1991, vol. 62, pp. 164-170.

6. A.C.M. Sousa, X. Liu and J.G. Lenard: "Modelling of Single-Roll Continuous Strip Casting", *Heat Transfer,* 1991, ,

7. J.F. Grubb, D.B. Love, A. Murthy and J.D. Nauman: "Casting Specialty Steel Strip", in *Near Net Shape Casting*, ISS, Warrendale, 1987, pp. 51-57.

8. B.G. Thomas and B. Ho.: "Spread Sheet Model for Continuous Casting", *Materials Processing in Computer Age*, TMS-AIME, 1991.

9. G. Li and B.G. Thomas: *Freeze-up Prediction for Single-Roll Strip Casting*, University of Illinois at Urbana-Champaign, Report, 1992.

10. X. Huang, B.G. Thomas and F.M. Najjar: "Modeling Superheat Removal during Continuous Casting of Steel Slabs", *Metall. Trans.,* 1992, vol. 23B, pp. 339-356.

11. L.S. Fletcher: "Recent Developments in Contact Conductance Heat Transfer", *Journal of Heat Transfer,* 1988, vol. 110, pp. 1059-1070.

12. B. Snaith, S.D. Probert and P.W. O'Callaghan: "Thermal Resistances of Pressed Contacts", *Applied Energy,* 1986, vol. 22, pp. 31-84.

13. B. Snaith, P.W. O'Callaghan and S.D. Probert: "Use of Interstitial Materials for Thermal Contact Conductance Control", *AIAA Paper,* 1984, vol. No. 84-0145,

14. R. Williams: Armco Inc., private communication, 1993.

15. R.M. Maringer: "The Role of Surface in Continuous Casting", in *Casting of Near Net Shape Product*, 1988, pp. 351-362.

16. J. Chen, J.Q. Zhu, C.-M. Rogall and R. Kopp: "Untersuchungen zur Warmeubertragung bei der Spritzwasserkuhlung", *Steel Research,* 1989, vol. 60, pp. 550-560.

17. R. Jeschar, U. Reiners and R. Scholz: "Heat Transfer during Water and Water-Air Spray Cooling in the Secondary Cooling Zone of Continuous casting Plants", *Steelmaking Proceedings of Fifth International Iron and Steel Congress*, Iron and Steel Society, 1986, Vol. 69, pp. 511-521.

18. R. Williams: Armco Inc., private communication, 1993.

19. E.A. Avallone and T.B. III: *Marks' Standard Handbook for Mechanical Engineers*, McGRAW-HILL book Company, 1978, pp. 4-64.

LIST OF FIGURES

Figure 1   Schematic of Single-wheel Thin Strip Casting process
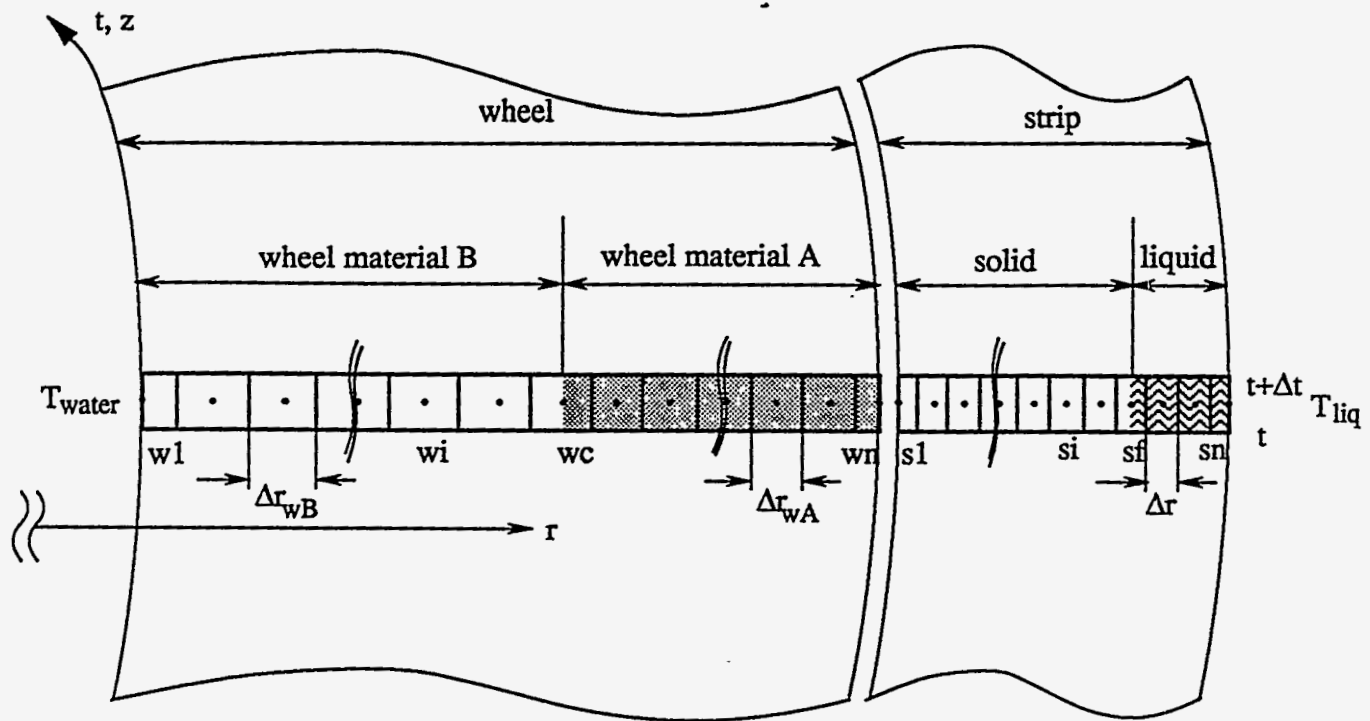
Figure 2   Simulation Domain for Strip and Wheel Heat Transfer Model
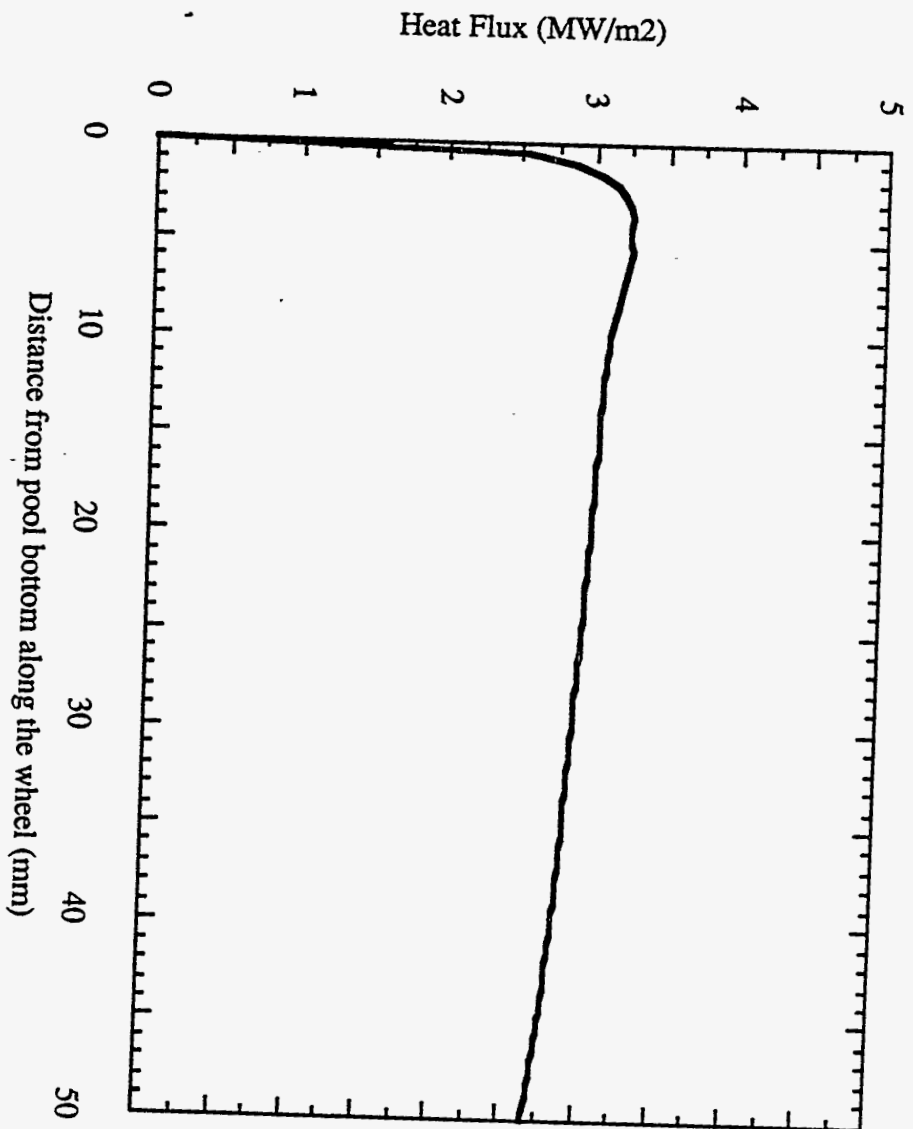
Figure 3 Predicted Superheat Flux to Shell at Quasi-steady-state [9]
(Vc = 1.5 m/s, Superheat ∆T = 75 C)
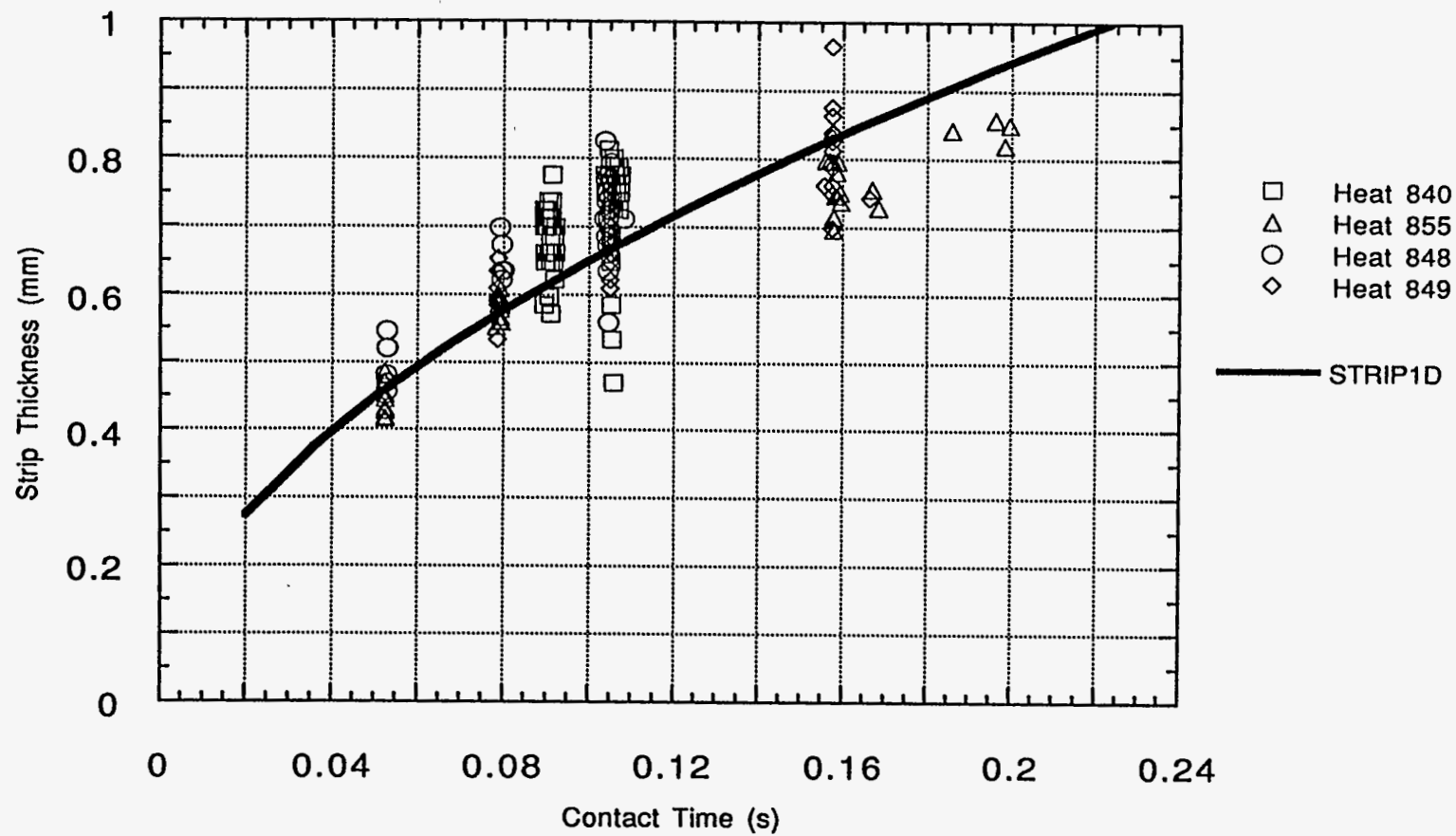
Figure 4   Effect of Contact Time on Final Strip Thickness
             (STRIP1D Compared with ARMCO Experimental Data[14])
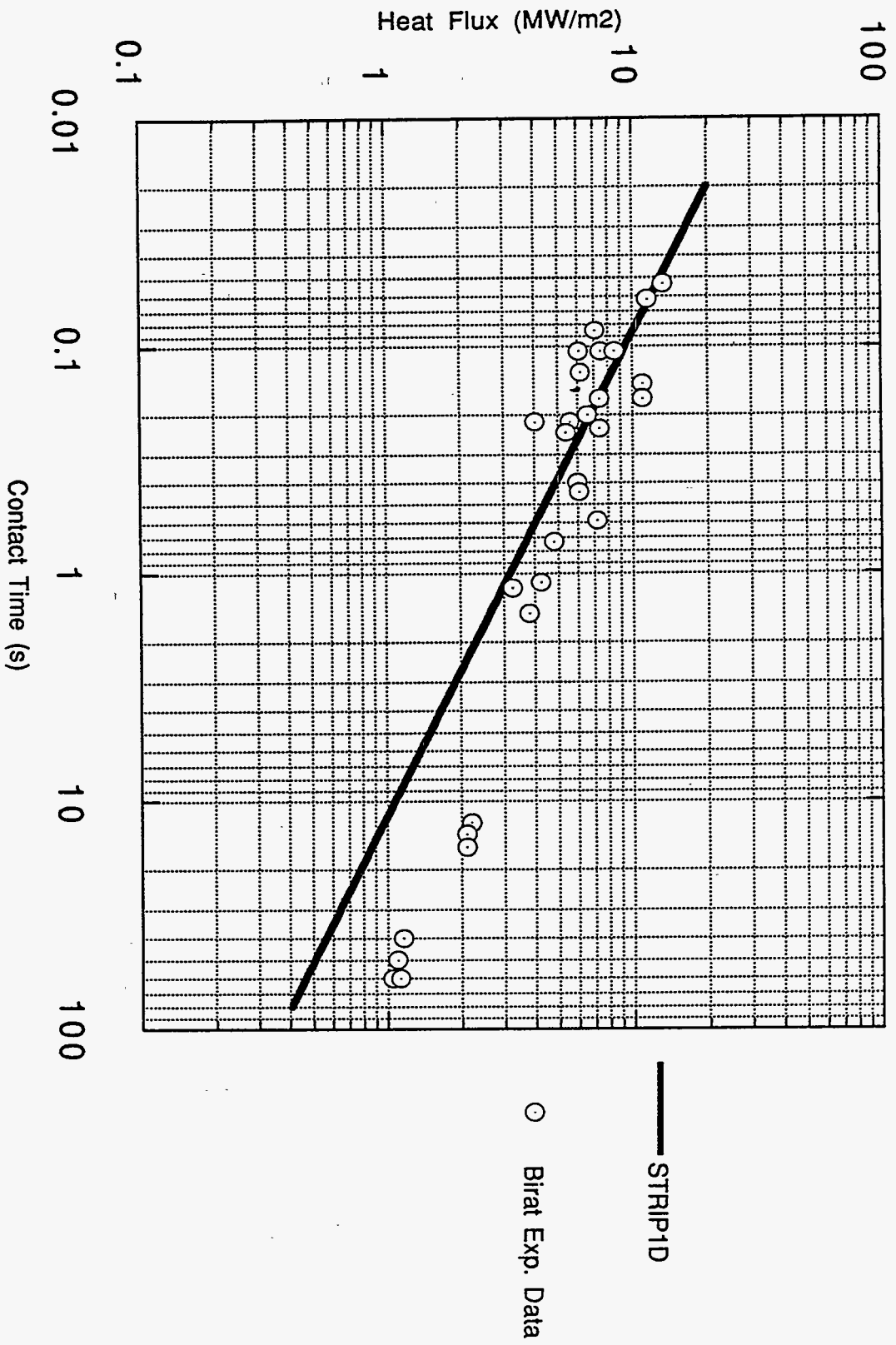
Figure 5   Effect of Contact Time on Heat Flux
(STRIP1D Compared with Birat Experimental Data[4])
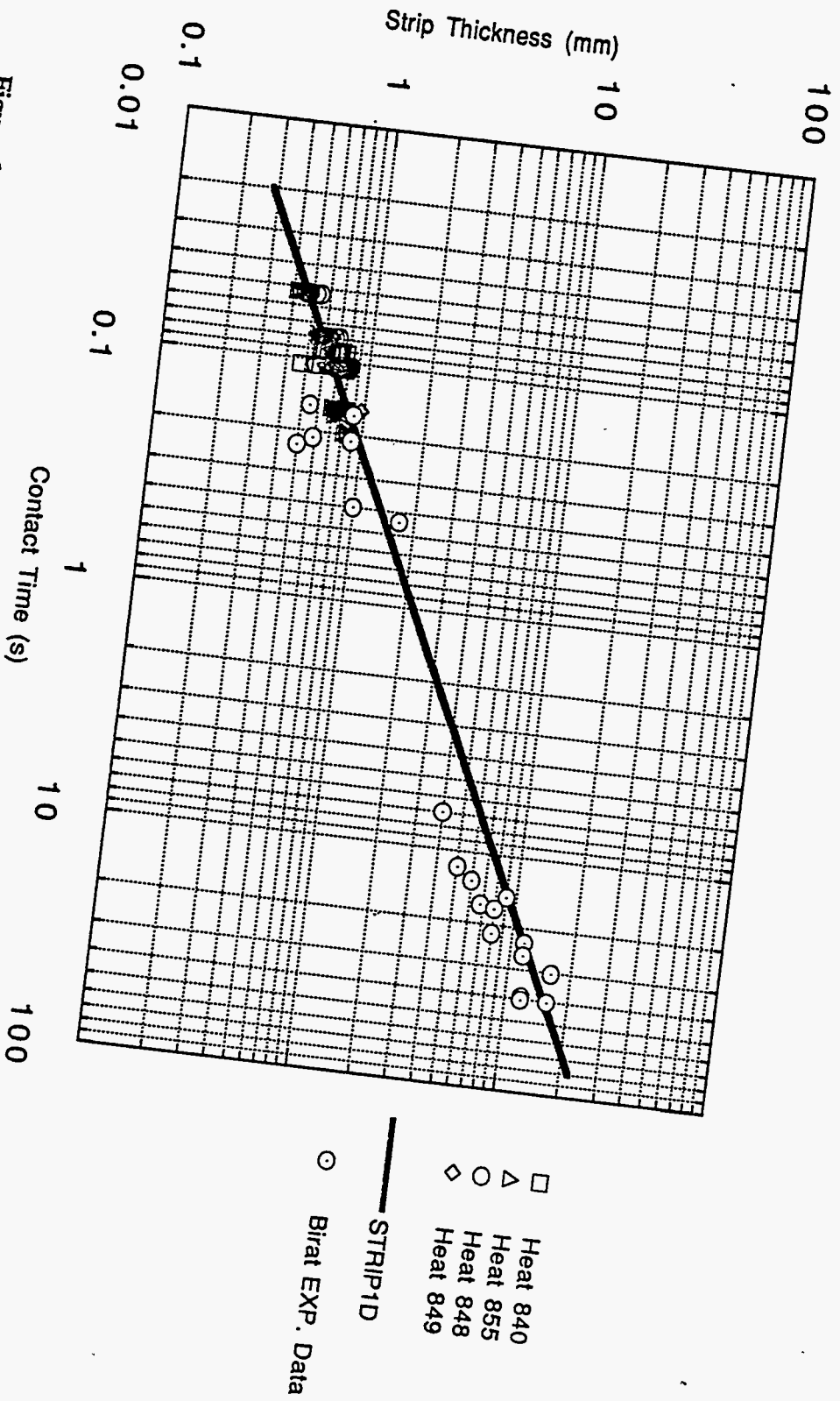
Figure 6

Effect of Contact Time on Final Strip Thickness
(STRIP1D Compared with ARMCO and Birat Experimental Data[4][14])
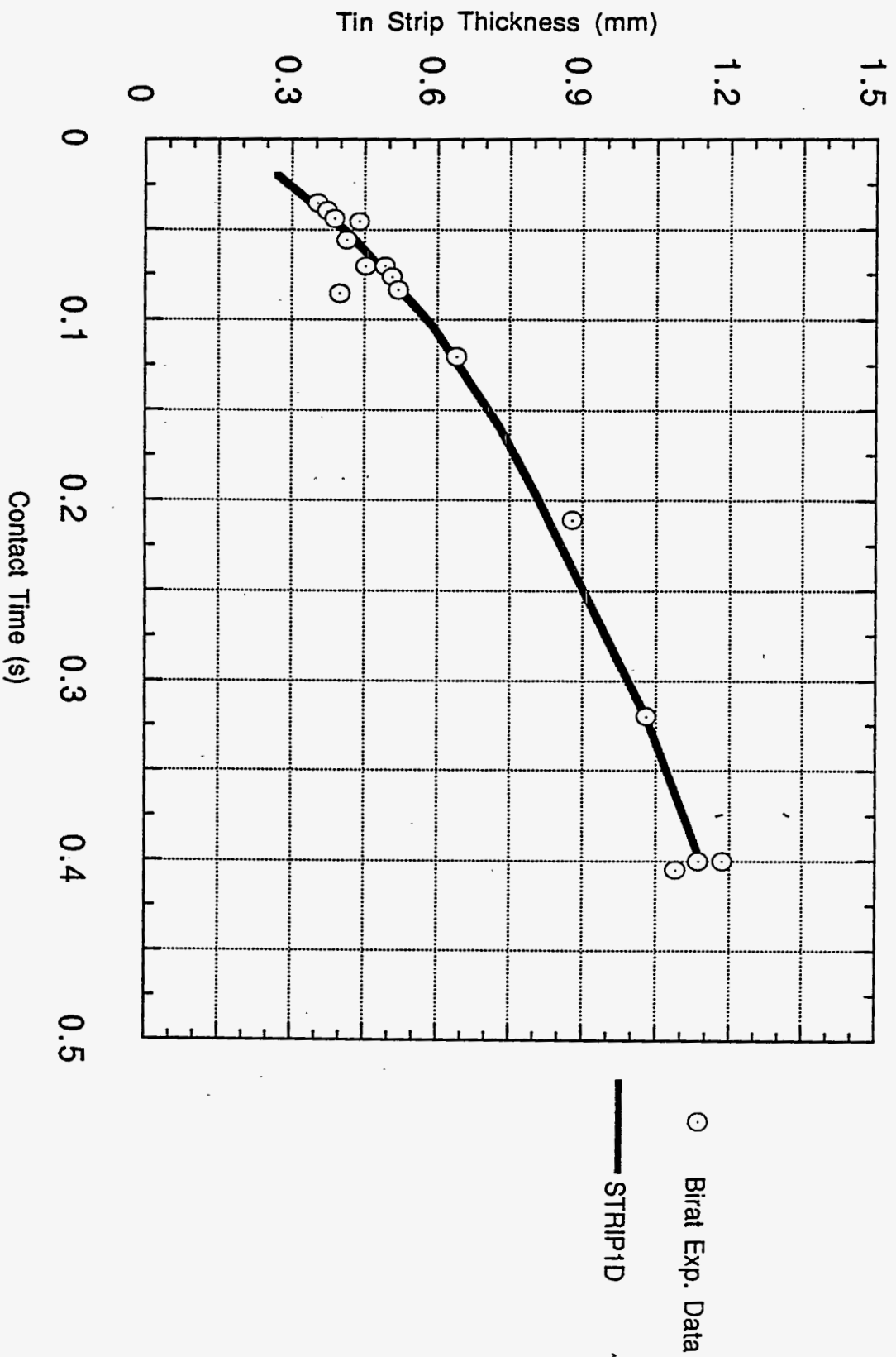
Figure 7   Comparison between Predicted and Measured
Strip Thickness for Tin Casting Process[7]
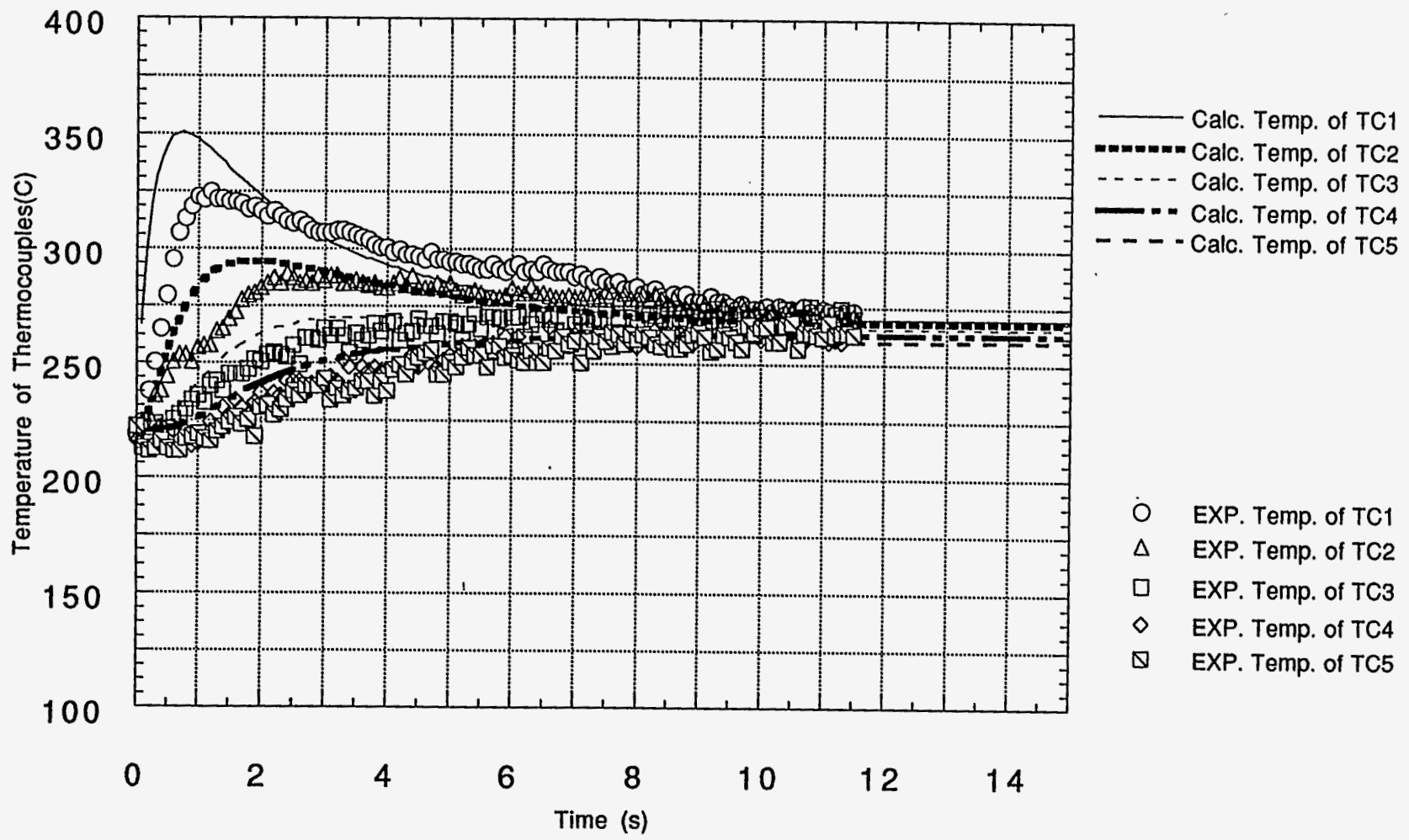
Figure 8   Comparison between Predicted and Measured
            Thermocouple Temperatures for Dip Experiment[18]
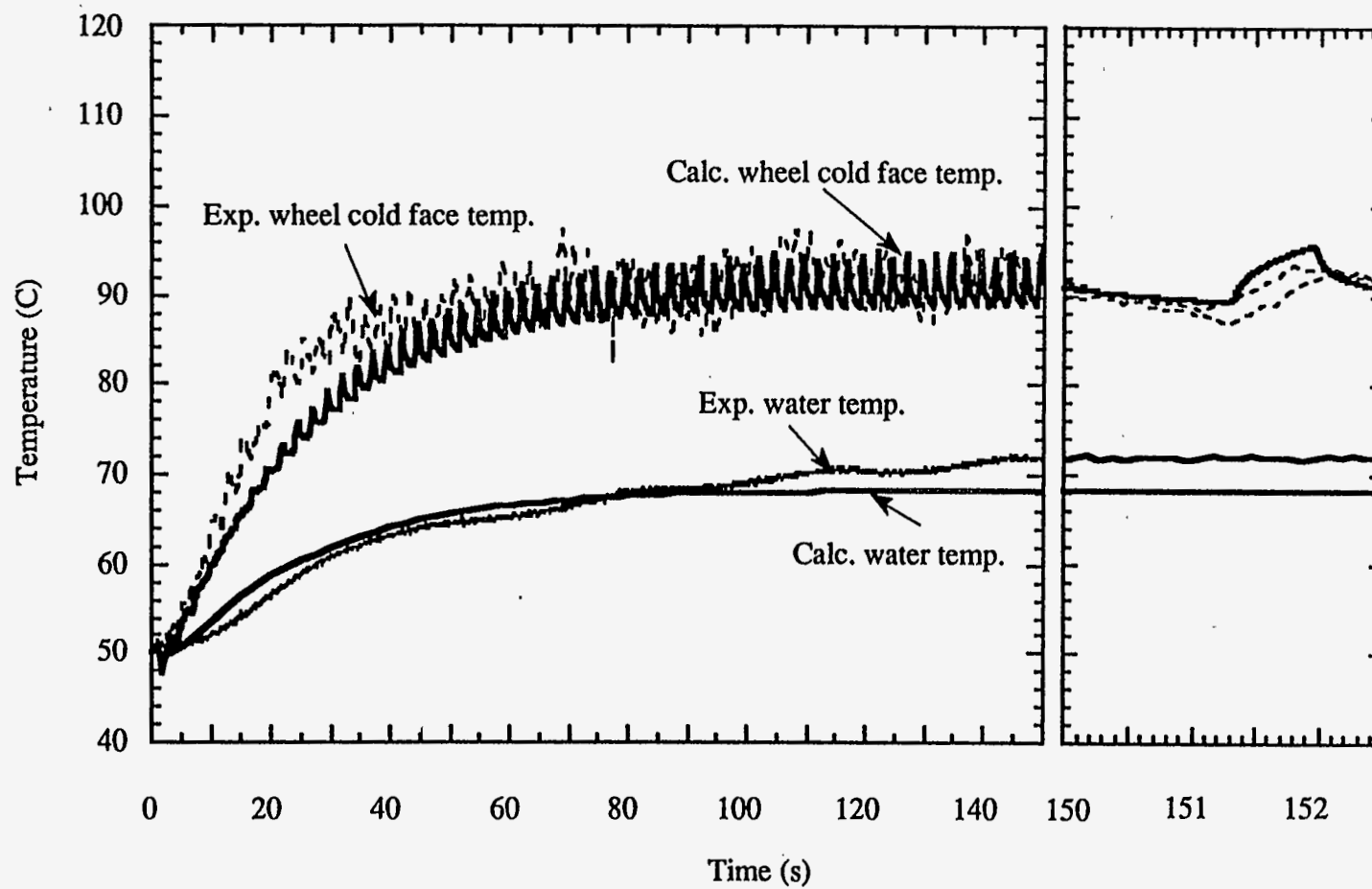
Figure 9 Wheel Cold Face Temperature and Water Temperature
(Standard Conditions)
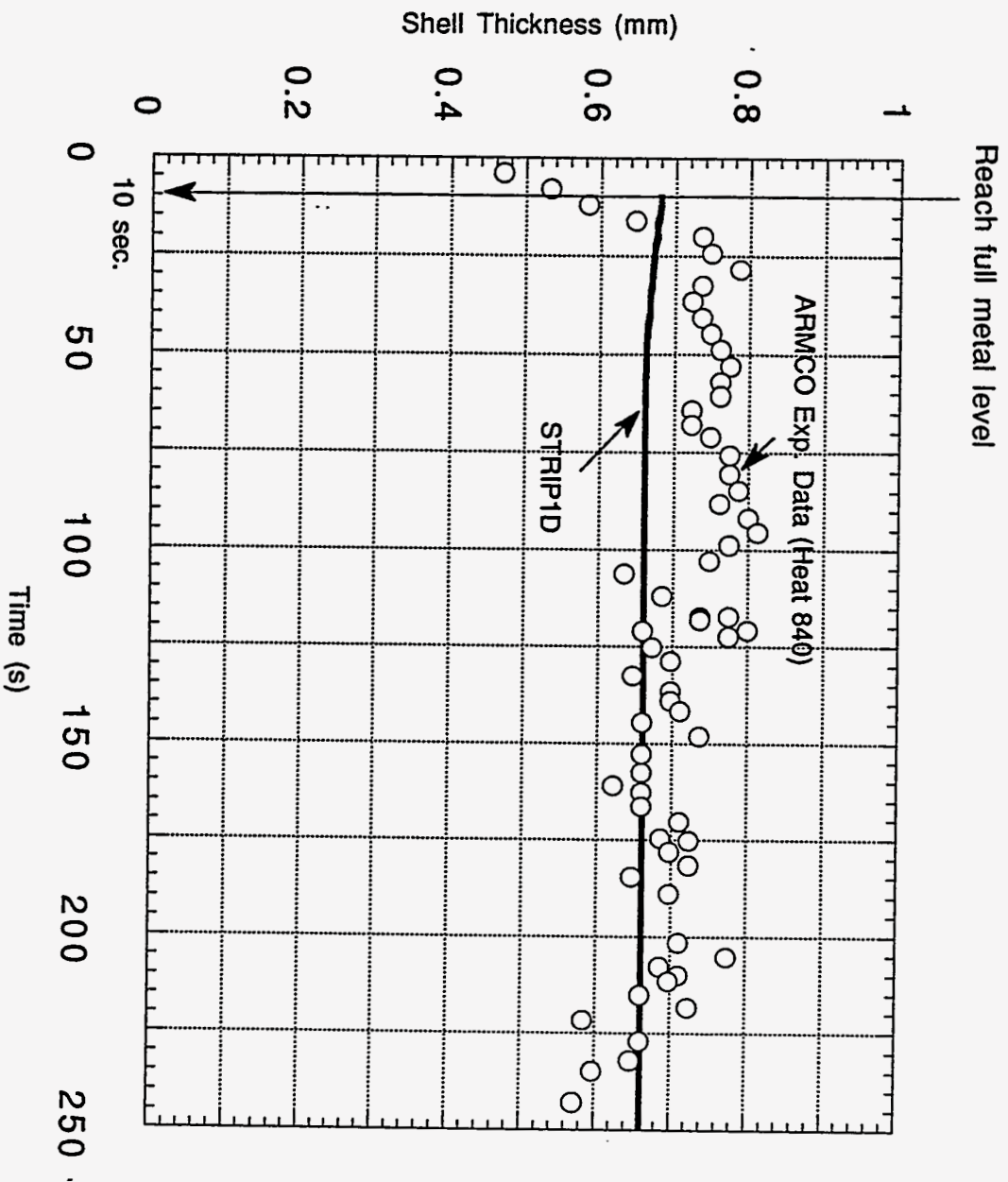
Figure 10   Comparison between Predicted and Measured Strip Thickness
(Standard Conditions)
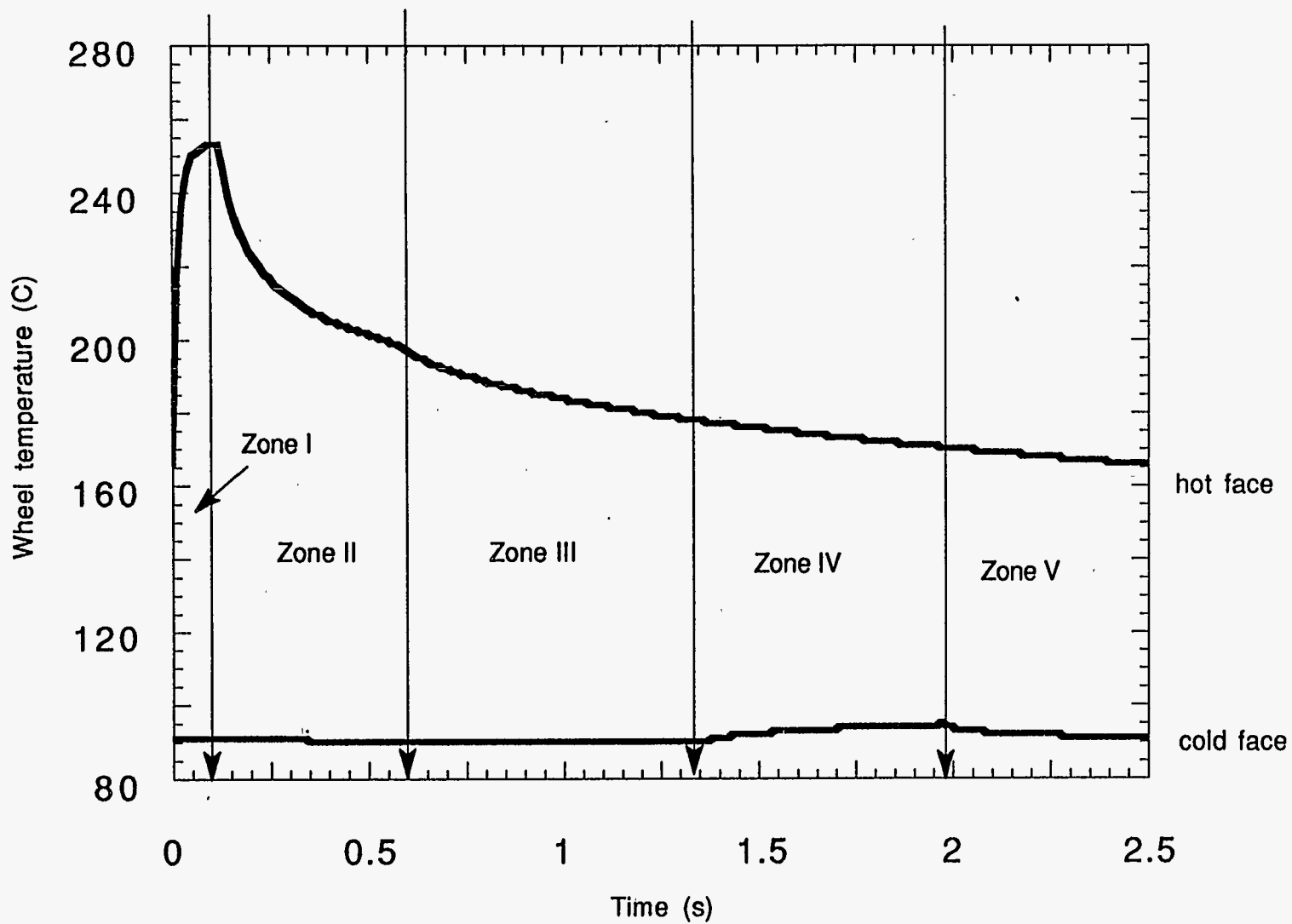
Figure 11   Predicted Wheel Temperature at Steady State
(Standard Conditions)
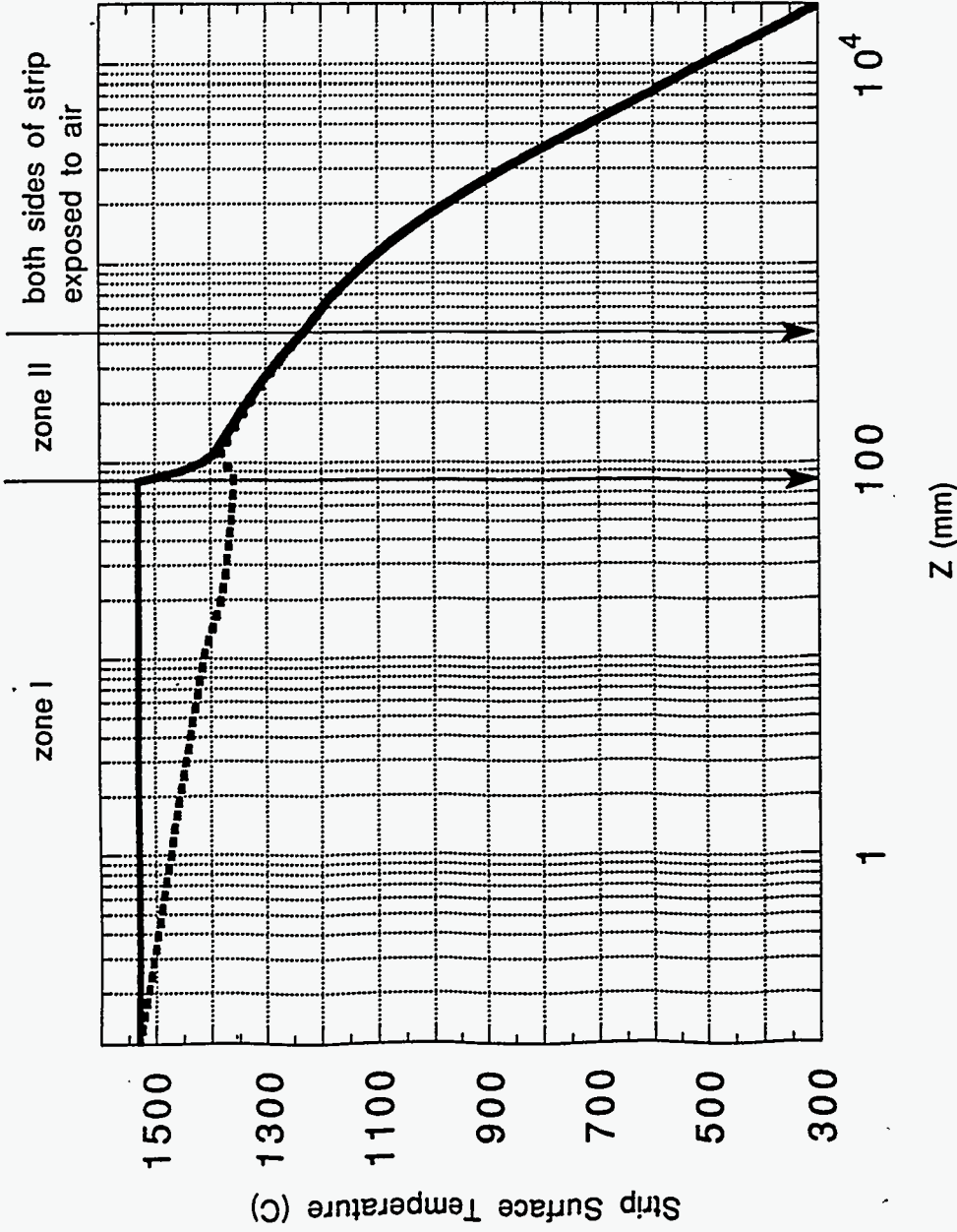
Figure 12   Steady State Strip Hot and Cold Face Temperatures
(Standard Conditions)
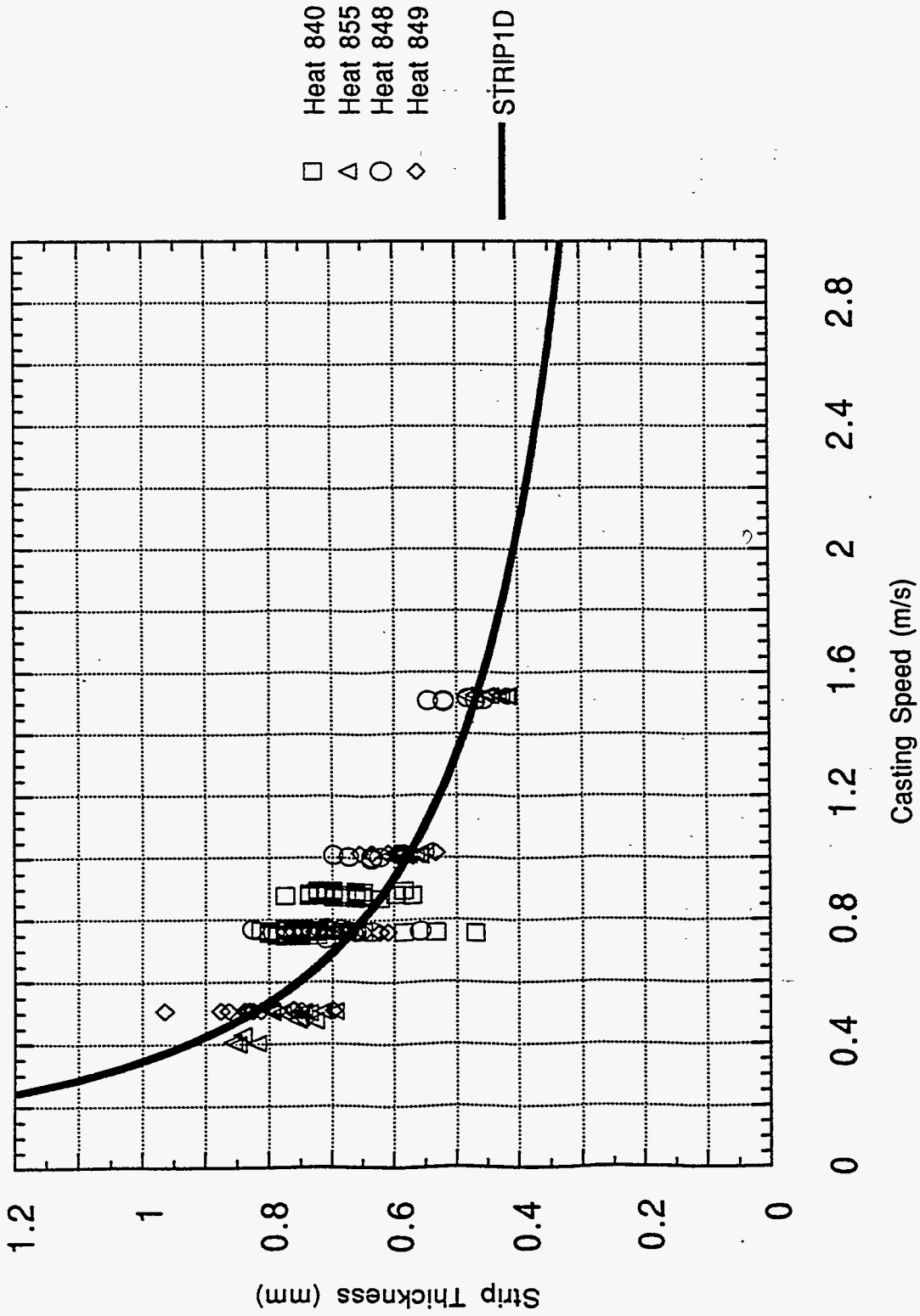
Figure 13   Effect of Casting Speed on Predicted and Measured
Final Strip Thickness[15]

Wheel Temperature (C)

Time (s)

Vc = 1.5 m/s

Vc = 1.0 m/s

Vc = 0.4 m/s

Vc = 1.5 m/s

Vc = 1.0 m/s

Vc = 0.4 m/s
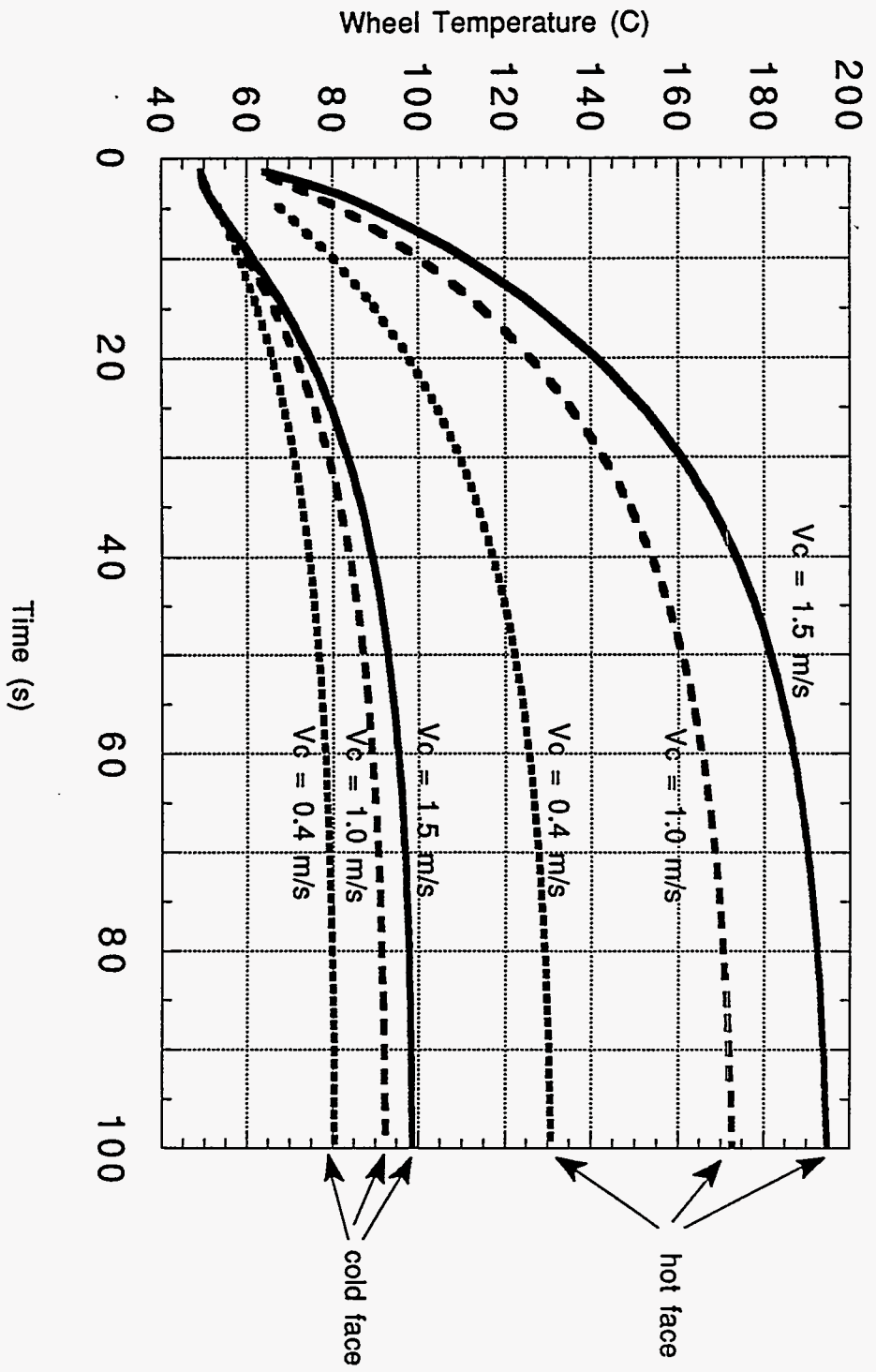
cold face

hot face

Figure 14 Effect of Casting Speed on Predicted Wheel Temperature
on Cold and Hot Faces at z=0
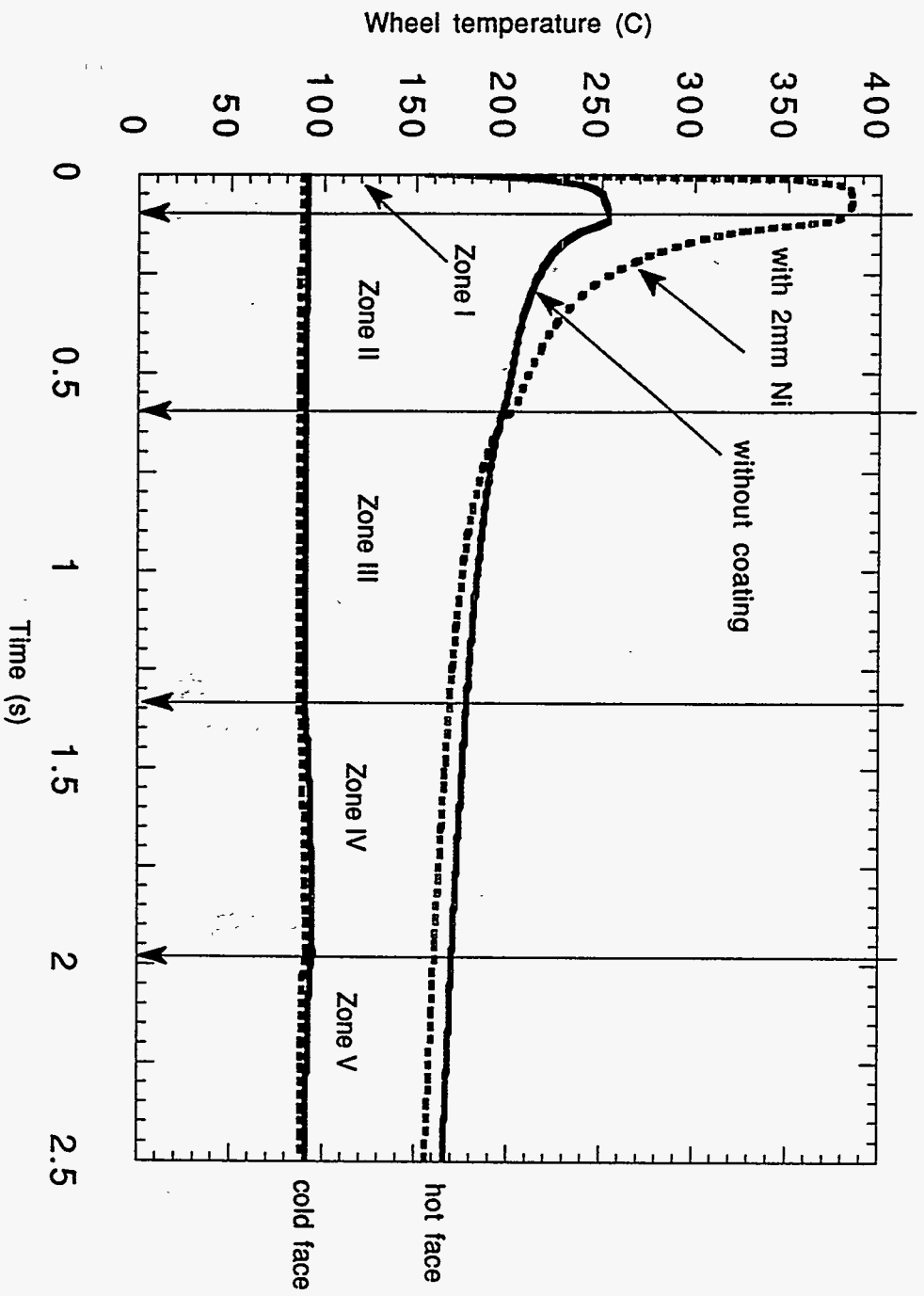
Figure 15   Effect of Wheel Coatings on Steady State
Wheel Hot and Cold Face Temperatures

Metal Process Simulation Laboratory
Department of Mechanical and Industrial Engineering
University of Illinois at Urbana-Champaign
Urbana, IL 61801

STRIP1D
USER MANUAL

Guowei Li
Brian G. Thomas

Submitted to
ARMCO Inc., Middletown, OH

August 10, 1993

STRIP1D User's Manual

Part I   Introduction

Welcome to STRIP1D! STRIP1D is a program which predicts temperature in the solidifying strip coupled with heat transfer in the rotating wheel, using one-dimensional explicit finite difference procedure. A large quantity of information can be obtained using STRIP1D in about ten minutes on IRIS4D workstation. The results include the following valuables (as a function of time):

(1) Temperatures:

        (a) temperature on of wheel hot face, cold face, strip surface

        (b) temperature of wheel and shell sliding thermocouple positions which are supplied by user

        (c) temperature in coating layers on wheel outer surface

        (d) water temperature

(2) Strip thickness;

(3) Heat fluxes at strip/wheel interface and wheel/water interface;

(4) Heat balance calculation.

Part II   How to run STRIP1D

1. How to run STRIP1D:

        a) Edit input data file 'xxxx.inp' (begin with 4-user specified characters)
           Change data as desired (See Part III)

        b) Type "strip1d"

        c) Examine output data contained in following output files:

           xxxx.whl   (summary of wheel temperature and heat fluxes)

           xxxx.shl   (shell temperature and thickness)

           xxxx.ext   (summary of selected results)

           xxxx.tmp (temperature at wheel/pool junction and shell thickness)

           xxxx.prf   (heat balance calculation)

           xxxx.cnt   (temperature in the wheel for the heat balance calculation cycle)

xxxx.stc	(adjustable sliding thermocouple temperature)
xxxx.sst	(strip surface temperature at after reach quasi-steady-state)
xxxx.ttc	(temperature of thermocouples in the wheel)
xxxx.ech	(echo file containing input data)

2. STRIP1D Subprograms

a)	strip1d.for.	main program
		initialize variables, handle input and output files,
		control simulation
b)	input.for	input and write echo file with SI unit system
c)	simuls.for	generate strip temperature at next time step
d)	simulw.for	wheel (including coating layers) temperature calculation
e)	heat.for	convert input superheat flux to inside of shell
f)	heatd.for	defining default superheat flux to inside of shell
g)	k.for	define thermal conductivity of steel
h)	cp.for	define specific heat of steel
i)	print.for	interpolate between nodal temperatures to locate solidus
		and liquidus, and shell thickness calculation
j)	hbal.for	perform approximate heat balance on shell, whole wheel and
		each zone, output temperature distribution and heat balance
		output temperature distribution and heat balance
		compare heat loss from shell surface with heat content in shell:
		1) superheat or heat flux to shell inside
		2) latent heat
		3) sensible heat

These *.for files are compiled into *.obj files and linked using Microsoft 8087
FORTRAN compiler on IBM-PC or standard FORTRAN-77 on UNIX workstations.

Part III   Input data:

The input file should be put in a file 'xxxx.inp'. The data included in this file can be written in free format. Units are metric in input data file. FORTRAN variables in the program are referred to in italic's and their locations in the input file are listed in the last column.

Section (1) Casting conditions:

Variables in program	Comments	Line No. in file
nvel	the number casting speeds data points The casting speed is found by linearly interpolating between casting speed values at specified cycles (or wheel revolution) in the following table (line 9-10)	7
cyclev	the cycle numbers	9
vel	(= V_c) casting speeds It is used (1) to calculate the time step (2) to calculate increment in casting direction	10
tinit	(= T_{pour}) pour temperature	11
swidth	(= W) strip width It is used to find the spray area on wheel cold face	12

3

Section (2) Simulation parameters:

Variables in program	Comments	Line No. in file
fflux	flag for treatment of superheat	15

    =0   for calculating temperature in liquid steel via conduction to
indirectly get the superheat flux added to shell surface
In this case the superheat flux input data (in lines 19-20) are inactive

    =-1   for taking default superheat flux data (q_{suph} and q_{sh} see heatd.for)
It means that the program will create superheat flux data according
to superheat temperature ΔT (pour temperature - liquidus temperature)
.and the casting speed.

$$q_{suph} = (\frac{V_c}{V_{c0}})(\frac{\Delta T}{\Delta T_0}) q_{sh}$$

Where V_c, ΔT_0 and $q_{\tilde{s}h}$ are parameters in a special case
In this case the superheat flux input data (in lines 19-20) are inactive

    =1   for entering superheat flux data
It means the program will use the user input superheat flux data
in lines 19-20.

nflux	number of input superheat flux data points (< 20) (see *fflux*)	17
zqdata	z data (distance from liquid steel nozzle bottom) (see *fflux*)	19
qdata	q data (superheat flux) (see *fflux*)	20
istrpc	flag to calculate and output extra strip temperature results	21

    = 1   calculate and output temperature of the strip for further 20 meters
of air cooling after the last cycle (both sides of the strip are exposed
to air)

    = 0   no further calculation

Variables in program	Comments	Line No. in file
dtime1	time step size in zone I and II	22
	The program adopts explicit solution scheme, so a large time increment will cause solution to be more unstable. It should satisfy criterion:	
	$dtime1 < 0.5 * dr * dr * dense * Cp / k$	
	dtime1 depends on distance increment *dr* (see *nstep*). The bigger the distance increment, the bigger the time increment can be.	
dtime2	time step size in zone III, IV and V	23
	Usually, it could be much bigger than *dtime1*, because the wheel is much thicker than the strip	
nstep	number of "elements" (subdivisions between nodes) in steel	24
	It is used to determine the increment of distance in the steel ($dr = thmax / nstep$) (<300)	
	The increment of distance *dr* is related to the *dtime1* by the stable criterion (see *dtime1*)	
nstepw	number of "elements" (subdivisions between nodes) in wheel	25
	It is used to determine the increment of distance in the wheel ($drw = (radwo-radwi)/nstepw$) (<300)	
	The increment of distance *drw* is related to the *dtime2* by the stable criterion (see *dtime2*)	
freqz	long printout interval for wheel temperature history	26
	It is used in	
	(1) output wheel temperature history in xxxx.SHL file	
	(2) output extra strip temperature calculation (except for zone I, II) in xxxx.SST	
freqzs	short printout interval	27
	It is used in	
	(1) output extra results in shell thickness in xxxx.SHL file	
	(2) output extra strip temperature in zone I, II in xxxx.SST	

5

Variables in program	Comments	Line No. in file
zpmin	the start point of output at casting (z) direction	28
	(z = 0 is at liquid steel nozzle bottom)	
izmax	number of simulation cycles	29
ihbal	cycle number for extended calculations, which includes:	30
	(1) heat balance calculation	
	(2) wheel temperature at each node for making contour plot	
	(3) max. and min. temperatures on wheel hot and cold faces	
thmax	maximum simulation thickness in the steel	31
	To save CPU time, it is usually set as 4--5 times thick as the final strip, because adiabatic boundary condition is applied to the liquid side edge of the domain	
itmax	maximum number of simulation time steps	32
xshlt	sliding shell thermocouple position below shell hot face (only for output shell thermocouple temperature in xxxx.SHL)	33
fsolid	($= f_s$) fraction solid for shell thickness location	34
	It is employed to calculate shell thickness:	
	$xshell = (1-fsolid)*xliq + fsolid* xsol$	

Section (3) steel properties:

Variables in program	*Comments*	*Line No. in file*
	The compositions of the steel in lines 37-39 are used to get steel default liquidus and default solidus temperatures.	
pc pmn ps	%C %Mn %S	37
pp psi	%P %Si	
pcr pni	%Cr %Ni	38
pcu pmo pti	%Cu %Mo %Ti	
pal pv	%Al %V	39
dense	(= ρ) steel density	40
delh	(= ΔH_L) heat fusion of steel	41
esteel	(= ε) steel emissivity	42
icp	flag of steel properties	43

=0   for using default temperature dependent properties
The program will use 304 steel specific heat and thermal
conductivity as functions of temperature in the simulation
In this case the user input steel properties in lines 45-48 are inactive

=1   entering constant properties
The program will use constant properties inputted in lines 45-48
in the simulation.

tsol -	constant steel solidus temperature (see *icp*)	45
tliq	constant steel liquidus temperature (see *icp*)	46
cpcte	constant steel specific heat (see *icp*)	47
kcte	constant steel thermal conductivity (see *icp*)	48

7

Section (4) wheel properties and geometry:

Variables in program	Comments	Line No. in file
densew	(= ρ_w)wheel density	51
ecopper	wheel emissivity	52
cpw	wheel specific heat	53
rkw	wheel thermal conductivity	54
radwo	(= R_o) wheel outer radius	55
radwi	(= R_i) wheel inner radius	56
twinit	wheel initial temperature	57
twater	water inlet temperature in spray zone	58
tair	ambient temperature	59
regn1	angle subtended by zone I	60

It is related to liquid steel pool depth L_{pool} by:

$$L_{pool} = R_o [\sin (regn1 - \alpha_0) - \sin (\alpha_0)]$$

where α_0 is the angle between the horizon and axial segment through the center of the wheel and the junction of wheel/liquid pool bottom

regn2	angle subtended by zone II	61
regn3	angle subtended by zone III	62
regn4	angle subtended by zone IV	63
aslitc	(= α) angle of defining the position of the adjustable sliding	64

thermocouple measured with respect to the axial segment through the center of the wheel and the junction of wheel/liquid pool bottom

8

<u>Section (5) heat transfer coefficients:</u>

Variables in program	*Comments*	*Line No. in file*
hcontact	$(= h_0)$ initial strip/wheel interface heat transfer coefficient It is used to find the local heat transfer coefficient in zone I ($h_{gap1} = h_0 \; (\frac{t_0}{t})^m$, see *nhtc* and *thtc*, the next two variables)	67
nhtc	$(= m)$ time exponent in formula $h_{gap1} = h_0 \; (\frac{t_0}{t})^m$	68 .
	$m=0$ means that the program will use constant heat transfer coefficient $h_{gap1} = h_0$	
nhtc	$(= t_0)$ reference time in formula $h_{gap1} = h_0 \; (\frac{t_0}{t})^m$	69
nhgap2	the number of data points of the heat transfer coefficient in zone II (*hgap2*). It is found by interpolating between the given values in following table in lines 72-73.	70
zhgap2	the distance from liquid steel nozzle bottom in zone II	72
hgap2	the strip/wheel interface heat transfer coefficients in zone II	73
ispray	flag of spray heat transfer coefficient calculation in zone I, II, III, V	74
=0	for using default water flux and temperature dependent spray heat calculation built in program In this case, the *fsmat* and *qspray* in lines 77-78 are active	
=1	using constant spray heat transfer coefficient provided by user (see *hspray*, the next variable)	
hspray	constant spray heat transfer coefficient in zone I, II, III, V	75
fsmat	$(= B)$ factor of spray heat transfer coefficient calculation for different materials (see *ispray*)	77
qspray	$(= w)$ total flowrate of spray water (see *ispray*)	78
hpool	$(= h_{no\text{-}spray})$ wheel inner surface heat transfer coefficient in no spray zone in zone IV	79
cpwat	specific heat of water	80
rhowat	density of water	81

9

<u>Section (6) property table for wheel coatings:</u>

Variables in program	*Comments*	*Line No. in file*
	The complete wheel is composed of at most four layers of materials, whose thicknesses and compositions are arbitrary. Properties for each of three "coating layers" are provided in the column under the corresponding material. The left most column is closest to the "wheel". The first layer closest to cooling water (usually copper) is defined under <u>Section (4) wheel properties</u>	
	coating materials	84
dni, dcr, dpoly	coating thicknesses	85
nstepni *nstepcr* } *nsteppo*	number of "elements" (subdivisions between nodes) in each coating layer	86
tkni, tkcr, tkpoly	conductivity of coating layers	87
tcpni,cpcr,cppoly	specific heat of coating layers	88
denseni *densecr* } *densepo*	density of coating layers	89

<u>Section (7) thermocouple locations in wheel:</u>

Variables in program	*Comments*	*Line No. in file*
nwthc	the number of thermocouples (< 100)	92
dwthc	the distances between wheel cold face and thermocouple positions (enter *dwthc* in a single row below each corresponding thermocouple number)	95

INPUT   Input Data   INP

  (1)   casting conditions:
      4   number of cycle and Vc data points
               next 2 lines contain (cycle #) and Vc(m/s)
   0.0   59.9   60.0   200.
   0.766   0.766   0.766   0.766
   1600.000   pour temperature (C)
    0.3048   strip width (m) (for water spray flowrate calculation)

  (2)   simulation parameters:
   -1.000000E+00   Is superheat treated as heatflux?
               0=no; -1=yes (take default); 1=yes (enter data)
        10   If =1, enter number of z and qsh data points
               (next 2 lines contain z(mm) and qsh(kW/m2) data)
   0.   6.   10.   20.   30.   40.   50.   60.   70.   80.
   1.5   2.4   2.5   2.4   2.3   2.2   2.1   2.0   1.9   1.8
            0   Do you want to extend strip temp calc. time? (0=No, 1=Yes)
   1.0000000E-05   time increment in region I and II (s)
   4.0000000e-04   time increment in region III,IV and V (s)
        40   number of elements in steel (=nodes-1)
        20   number of elements in wheel (=nodes-1)
   200.00000E+00   long printout interval (multiple cycle output) (mm)
    10.00000E+00   short printout interval (single cycle and Zone I,II) (mm)
   0.0000000E+00   start output at (mm)
       102   number of simulation cycles
       100   cycle number for extended calculations (& heat balance)
   2.0000000   max. simulation thickness of steel (mm)
   1.000E+09   max. number of iterations
   2.0000000   shell thermocouple position below hot face (mm)
   0.7000000   fraction solid for shell thicknesss location (-)

  (3)   steel properties:
  0.0400 0.2300 0.0150 0.0100 0.0300   %C,%Mn,%S,%P,%Si
  0.0000 0.0000 0.0000 0.0000 0.0000   %Cr,%Ni,%Cu,%Mo,%Ti
  0.0550 0.0000   %Al, %V
   7400.000   steel density (kg/m^3)
   271.9600   heat fusion of steel (kJ/kg)
   0.8000000   steel emissivity (-)
         1   User special subroutine to define Tsol,Tliq,Cp,K; (=0)
               or enter constant Tsol,Tliq,Cp,K below (=1)
   1520.000   steel solidus temperature (C)
   1530.000   steel liquidus temperature (C)
   690.3600   steel specific heat (J/kg deg K)
     29.0   steel thermal conductivity (W/mK)

  (4) wheel properties and geometry:
   8950.000   wheel density (kg/m^3)
   0.5000000   wheel emissivity (-)
   866.0000   wheel specific heat (J/kg deg K)
   380.1600   wheel thermal conductivity (W/mK)
   0.3048000   wheel outer radius (m)
   0.2667000   wheel inner radius (m)
   50.00000   wheel initial temperature (C)
   50.00000   water inlet temperature in spray zone (C)
   30.00000   ambient temperature (C)
   15.10000   angle of zone I of wheel (Deg)
   69.90000   angle of zone II of wheel (Deg)
   110.00000   angle of zone III of wheel (Deg)
   90.00000   angle of zone IV of wheel (Deg)
   14.00000   angle of sliding thermocouple (Deg)

  (5) heat transfer coefficients (HTC):

```
2.8000000E+04    Zone I: ho = initial strip/wheel HTC for hgap1 (W/m2K)
 0.55                    m  = time exponent for hgap1 (m=0 means hgap1=ho)
 0.01                    to = reference time for shl/whl HTC for hgap1 (s)
 4               Zone II: Enter number of z and hgap2 HTC data points
                         next 2 lines contain z(mm) and hgap2(W/m2K) data
 79.    100.    200.    455.
10000.  1000.   500.    200.
        0       constant wheel/spray water HTC (=1) or default (=0)?
2.6000000E+04    If=1, Enter HTC for spray cooling (hspray) (W/m2K)
                 If=0, Enter factor & flowrate for default HTC below:
1.5000000E+00       factor for spray HTC for different wheel materials
0.0062000E+00       total flowrate of spray water (m^3/s)
1.2000000E+04    Zone IV: HTC on water side of wheel (hnospray) (W/m2K)
4179.000         water heat capacity(J/kgK)
 995.6000        water density(kg/m3)

(6) property table for wheel coatings
     Ni         Cr        others      (left column is closest to wheel)
   0.000      0.000      0.000        coating thickness (mm)
     1          1          1          number of elements in coating layer
  80.000     72.000      4.200        conductivity (W/mK)
 490.000    501.000    500.000        specific heat (J/kgK)
8860.000   7120.000   8000.000        density (kg/m3)

(7) thermocouple locations in wheel:
        0       number of thermocouples (TCs): next 2 lines contain:
                TC ID # and distance below cold face (dwthc) (mm) data
     1     2     3     4     5
   2.95  9.30 15.65 22.00 28.35
```

Carbon content:		0.04	(%)
Carbon equivalent:		0.0783	(%)
Liquidus Temp:		1530.00	Deg C
Solidus Temp:		1520.00	Deg C
Zone 1 length:	0.10(s)	80.	(mm)
Zone 2 length:	0.49(s)	372.	(mm)
Zone 3 length:	0.76(s)	585.	(mm)
Zone 4 length:	0.63(s)	479.	(mm)
Zone 5 length:	0.52(s)	399.	(mm)
Length of a cycle:	2.50(s)	1915.	(mm)
Strip thickness:		0.66	(mm)
Max wheel hot face temperature:		246.	(C)
Min wheel hot face temperature:		158.	(C)
Max wheel cold face temperature:		91.	(C)
Min wheel cold face temperature:		87.	(C)
Water temperature increase in spray zone:		17.	(C)

STRIP1D-1.2 Strip Casting Heat Transfer Analysis
University of Illinois, Brian G. Thomas, 1993

PROFILE   Temperature Distribution at   178.6m   PRF
                         — and Heat Balance at   100 to 101 cyc

Temperature Deg C	Super Heat kJ/s	Sensible Heat kJ/s	Latent Heat kJ/s
1530.1	0.0	0.0	0.0
1530.1	0.0	0.0	0.0
1530.1	0.0	0.0	0.0
1530.1	0.0	0.0	0.0
1530.1	0.0	0.0	0.0
1530.1	0.0	0.0	0.0
1530.1	0.0	0.0	0.0
1530.1	0.0	0.0	0.0
1530.1	0.0	0.0	0.0
1530.1	0.0	0.0	0.0
1530.1	0.0	0.0	0.0
1530.1	0.0	0.0	0.0
1530.1	0.0	0.0	0.0
1530.1	0.0	0.0	0.0
1530.1	0.0	0.0	0.0
1530.1	0.0	0.0	0.0
1530.1	0.0	0.0	0.0
1530.1	0.0	0.0	0.0
1530.1	0.0	0.0	0.0
1530.1	0.0	0.0	0.0
1530.1	0.0	0.0	0.0
1530.1	0.0	0.0	0.0
1530.1	0.0	0.0	0.0.
1530.0	0.0	0.0	0.0
1530.0	0.0	0.0	0.0
1530.0	0.0	0.0	0.0
1529.8	0.0	0.0	1.7
1526.2	0.0	0.7	29.3
1514.3	0.0	3.1	77.1
1501.9	0.0	5.5	77.1
1489.1	0.0	8.0	77.1
1475.6	0.0	10.6	77.1
1461.7	0.0	13.4	77.1
1447.4	0.0	16.2	77.1
1432.7	0.0	19.0	77.1
1417.9	0.0	21.9	77.1
1402.9	0.0	24.9	77.1
1387.8	0.0	27.8	77.1
1372.7	0.0	30.8	77.1
1357.5	0.0	33.8	77.1
1342.3	0.0	18.4	38.5

(1) Heat balance of strip in region I :
    1) Heat loss from strip to wheel: 1299.   (kJ/s)
    2a) Heat input to shell inside: 123.   (kJ/s)
    2b) Super heat: 0.   (kJ/s)
    3) Latent heat: 994.   (kJ/s)
    4) Sensible heat from cooling strip: 234.   (kJ/s)
    Error In Heat Balance:
    [2) +3) +4) − 1)]/ 1) * 100%   4.09   (%)

(2) Heat balance of strip in region II :
    1) Heat loss from strip to ambient: 137.   (kJ/s)
    2) Heat loss from shell to wheel: 299.   (kJ/s)
    3) Sensible heat from cooling strip: 410.   (kJ/s)

```
              Error In Heat Balance:
              [ 1) +2) - 3) ]                               25.64     (kJ/s)

(3) Heat balance of wheel in region 1
     1) Heat loss from wheel inside to water:        72.     (kJ/s)
     2) Heat into wheel from strip or ambient:     1299.     (kJ/s)
     3) Heat to increase wheel temperature:        1233.     (kJ/s)
     Heat balance error in region 1:
     [ 1)  +3) - 2) ]                                 6.      (kJ/s)

(4) Heat balance of wheel in region 2
     1) Heat loss from wheel inside to water:       331.     (kJ/s)
     2) Heat into wheel from strip or ambient:      299.     (kJ/s)
     3) Heat to increase wheel temperature:         -16.     (kJ/s)
     Heat balance error in region 2:
     [ 1)  +3) - 2) ]                                17.      (kJ/s)

(5) Heat balance of wheel in region 3
     1) Heat loss from wheel inside to water:       515.     (kJ/s)
     2) Heat into wheel from strip or ambient:       -4.     (kJ/s)
     3) Heat to increase wheel temperature:        -528.     (kJ/s)
     Heat balance error in region 3:
     [ 1)  +3) - 2) ]                                -9.      (kJ/s)

(6) Heat balance of wheel in region 4
     1) Heat loss from wheel inside to water:       302.     (kJ/s)
     2) Heat into wheel from strip or ambient:       -3.     (kJ/s)
     3) Heat to increase wheel temperature:        -302.     (kJ/s)
     Heat balance error in region 4:
     [ 1)  +3) - 2) ]                                 3.      (kJ/s)

(7) Heat balance of wheel in region 5
     1) Heat loss from wheel inside to water:       366.     (kJ/s)
     2) Heat into wheel from strip or ambient:       -3.     (kJ/s)
     3) Heat to increase wheel temperature:        -386.     (kJ/s)
     Heat balance error in region 5:
     [ 1)  +3) - 2) ]                                -17.     (kJ/s)

     Error of Heat Balance on wheel:                0.03     (%)
     Error of Heat Balance on strip:                1.72     (%)
```

TEMPERATURE   Temperature Output   TMP

Z (mm)	Time (s)	Tcold Deg C	Thot Deg C	Tcoat. Deg C	Shell (mm)	Twater Deg C
1915.2	2.5	50.1	65.4	65.4	0.69	49.92
3827.1	5.0	52.8	76.1	76.1	0.69	50.59
5743.9	7.5	56.0	84.8	84.8	0.69	51.93
7669.3	10.0	59.1	92.3	92.3	0.69	53.37
9594.7	12.5	62.0	99.0	99.0	0.68	54.75
11520.1	15.0	64.7	104.9	104.9	0.68	56.06
13445.5	17.6	67.0	110.3	110.3	0.68	57.21
15370.9	20.1	69.1	115.1	115.1	0.68	58.17
17296.3	22.6	71.1	119.3	119.3	0.67	59.04
19221.6	25.1	72.8	123.2	123.2	0.67	60.02
21147.0	27.6	74.3	126.7	126.7	0.67	60.76
23072.4	30.1	75.7	129.8	129.8	0.67	61.42
24997.8	32.6	76.9	132.5	132.5	0.67	61.83
26923.2	35.1	78.1	135.0	135.0	0.67	62.43
28848.6	37.7	79.1	137.3	137.3	0.66	63.00
30774.0	40.2	80.0	139.4	139.4	0.67	63.53
32699.4	42.7	80.8	141.2	141.2	0.66	63.80
34615.5	45.2	81.6	142.9	142.9	0.66	64.24
36531.6	47.7	82.2	144.3	144.3	0.66	64.44
38447.6	50.2	82.7	145.6	145.6	0.66	64.65
40363.7	52.7	83.2	146.8	146.8	0.66	65.01
42279.8	55.2	83.7	147.9	147.9	0.66	65.16
44195.8	57.7	84.2	148.8	148.8	0.66	65.33
46111.9	60.2	84.5	149.7	149.7	0.66	65.66
48028.0	62.7	84.9	150.5	150.5	0.66	65.77
49944.1	65.2	85.2	151.2	151.2	0.66	65.88
51860.1	67.7	85.5	151.8	151.8	0.66	65.97
53776.2	70.2	85.8	152.4	152.4	0.66	66.19
55692.3	72.7	86.0	152.9	152.9	0.66	66.37
57608.3	75.2	86.2	153.4	153.4	0.66	66.44
59524.4	77.7	86.4	153.8	153.8	0.66	66.50
61440.5	80.2	86.6	154.2	154.2	0.66	66.56
63356.5	82.7	86.8	154.5	154.5	0.66	66.61
65272.6	85.2	86.9	154.9	154.9	0.66	66.66
67188.7	87.7	87.0	155.1	155.1	0.66	66.73
69104.8	90.2	87.2	155.4	155.4	0.66	66.83
71020.8	92.7	87.3	155.6	155.6	0.66	66.92
72936.9	95.2	87.4	155.9	155.9	0.66	67.00
74853.0	97.7	87.4	156.0	156.0	0.66	67.06
76769.0	100.2	87.5	156.2	156.2	0.66	67.08
78685.1	102.7	87.6	156.4	156.4	0.66	67.11
80601.2	105.2	87.7	156.5	156.5	0.66	67.13
82517.3	107.7	87.7	156.6	156.6	0.66	67.14
84433.3	110.2	87.8	156.7	156.7	0.66	67.16
86349.4	112.7	87.8	156.9	156.9	0.66	67.18
88265.5	115.2	87.8	156.9	156.9	0.66	67.19
90181.5	117.7	87.9	157.0	157.0	0.66	67.20
92097.6	120.2	87.9	157.1	157.1	0.66	67.21
94013.7	122.7	88.0	157.2	157.2	0.66	67.22
95929.7	125.2	88.0	157.2	157.2	0.66	67.23
97845.8	127.7	88.0	157.3	157.3	0.66	67.24
99761.9	130.2	88.0	157.3	157.3	0.66	67.25
101678.0	132.7	88.0	157.4	157.4	0.66	67.25
103594.0	135.2	88.1	157.4	157.4	0.66	67.26
105510.1	137.7	88.1	157.5	157.5	0.66	67.26
107426.2	140.2	88.1	157.5	157.5	0.66	67.27
109342.2	142.7	88.1	157.5	157.5	0.66	67.27
111258.3	145.2	88.1	157.6	157.6	0.66	67.28

113174.4	147.7	88.1	157.6	157.6	0.66	67.28
115090.4	150.2	88.1	157.6	157.6	0.66	67.28
117006.5	152.8	88.1	157.6	157.6	0.66	67.29
118922.6	155.3	88.2	157.6	157.6	0.66	67.29
120838.7	157.8	88.2	157.7	157.7	0.66	67.29
122754.7	160.3	88.2	157.7	157.7	0.66	67.29
124670.8	162.8	88.2	157.7	157.7	0.66	67.29
126586.9	165.3	88.2	157.7	157.7	0.66	67.30
128502.9	167.8	88.2	157.7	157.7	0.66	67.30
130419.0	170.3	88.2	157.7	157.7	0.66	67.30
132367.5	172.8	88.2	157.7	157.7	0.66	67.30
133859.7	174.8	88.2	157.7	157.7	0.66	67.30
135351.8	176.7	88.2	157.7	157.7	0.66	67.30
136844.0	178.6	88.2	157.7	157.7	0.66	67.30
138336.2	180.6	88.2	157.7	157.7	0.66	67.30
139828.4	182.5	88.2	157.7	157.7	0.66	67.30
141320.6	184.5	88.2	157.7	157.7	0.66	67.30
142812.8	186.4	88.2	157.8	157.8	0.66	67.30
144305.0	188.4	88.2	157.8	157.8	0.66	67.30
145797.2	190.3	88.2	157.8	157.8	0.66	67.31
147289.3	192.3	88.2	157.8	157.8	0.66	67.31
148781.5	194.2	88.2	157.8	157.8	0.66	67.31
150273.7	196.2	88.2	157.8	157.8	0.66	67.31
151765.9	198.1	88.2	157.8	157.8	0.66	67.31
153258.1	200.1	88.2	157.8	157.8	0.66	67.31
154750.3	202.0	88.2	157.8	157.8	0.66	67.31
156242.5	204.0	88.2	157.8	157.8	0.66	67.31
157734.7	205.9	88.2	157.8	157.8	0.66	67.31
159226.8	207.9	88.2	157.8	157.8	0.66	67.31
160719.0	209.8	88.2	157.8	157.8	0.66	67.31
162211.2	211.8	88.2	157.8	157.8	0.66	67.31
163703.4	213.7	88.2	157.8	157.8	0.66	67.31
165195.6	215.7	88.2	157.8	157.8	0.66	67.31
166687.8	217.6	88.2	157.8	157.8	0.66	67.31
168180.0	219.6	88.2	157.8	157.8	0.66	67.31
169672.2	221.5	88.2	157.8	157.8	0.66	67.31
171164.3	223.5	88.2	157.8	157.8	0.66	67.31
172656.5	225.4	88.2	157.8	157.8	0.66	67.31
174148.7	227.3	88.2	157.8	157.8	0.66	67.31
175640.9	229.3	88.2	157.8	157.8	0.66	67.31
177133.1	231.2	88.2	157.8	157.8	0.66	67.31
178625.3	233.2	88.2	157.8	157.8	0.66	67.31
180117.5	235.1	88.2	157.8	157.8	0.66	67.31
181609.7	237.1	88.2	157.8	157.8	0.66	67.31

STRIP1D-1.2 Strip Casting Heat Transfer Analysis
University of Illinois, Brian G. Thomas, 1993

SLIDING TC   Adjustable Sliding Thermocouple Temperatures   STC

Z (mm)	Time (s)	Tcold Deg C	Thot Deg C	Tcoat. Deg C	Ts cold Deg C	Ts hot Deg C	Shell mm
74.5	0.1	50.0	144.7	144.7	1320.3	1530.1	0.00
1990.0	2.6	50.3	158.9	158.9	1323.6	1530.1	0.69
3900.7	5.1	53.0	168.9	168.9	1325.5	1530.1	0.69
5819.8	7.6	56.2	177.1	177.1	1327.5	1530.1	0.69
7745.2	10.1	59.3	184.1	184.1	1329.0	1530.1	0.69
9670.6	12.6	62.2	190.4	190.4	1330.2	1530.1	0.68
11596.0	15.1	64.8	196.0	196.0	1331.4	1530.1	0.68
13521.4	17.7	67.1	201.0	201.0	1332.5	1530.1	0.68
15446.8	20.2	69.2	205.5	205.5	1333.3	1530.1	0.68
17372.2	22.7	71.1	209.5	209.5	1334.3	1530.1	0.67
19297.6	25.2	72.9	213.2	213.2	1335.1	1530.1	0.67
21223.0	27.7	74.3	216.4	216.4	1335.7	1530.1	0.67
23148.4	30.2	75.7	219.3	219.3	1336.3	1530.1	0.67
25073.8	32.7	76.9	221.9	221.9	1336.9	1530.1	0.67
26999.2	35.2	78.1	224.3	224.3	1337.5	1530.1	0.67
28924.6	37.8	79.1	226.4	226.4	1337.8	1530.1	0.66
30850.0	40.3	80.0	228.3	228.3	1338.4	1530.1	0.67
32775.4	42.8	80.8	230.1	230.1	1338.7	1530.1	0.66
34691.5	45.3	81.5	231.6	231.6	1339.2	1530.1	0.66
36607.5	47.8	82.1	233.0	233.0	1339.5	1530.1	0.66
38523.6	50.3	82.7	234.2	234.2	1339.7	1530.1	0.66
40439.7	52.8	83.2	235.3	235.3	1339.9	1530.1	0.66
42355.7	55.3	83.6	236.3	236.3	1340.2	1530.1	0.66
44271.8	57.8	84.1	237.2	237.2	1340.3	1530.1	0.66
46187.9	60.3	84.5	238.0	238.0	1340.6	1530.1	0.66
48103.9	62.8	84.8	238.8	238.8	1340.6	1530.1	0.66
50020.0	65.3	85.1	239.4	239.4	1340.7	1530.1	0.66
51936.1	67.8	85.4	240.0	240.0	1341.0	1530.1	0.66
53852.2	70.3	85.7	240.6	240.6	1340.9	1530.1	0.66
55768.2	72.8	85.9	241.1	241.1	1341.2	1530.1	0.66
57684.3	75.3	86.1	241.5	241.5	1341.3	1530.1	0.66
59600.4	77.8	86.3	241.9	241.9	1341.3	1530.1	0.66
61516.4	80.3	86.5	242.3	242.3	1341.2	1530.1	0.66
63432.5	82.8	86.6	242.6	242.6	1341.4	1530.1	0.66
65348.6	85.3	86.8	242.9	242.9	1341.6	1530.1	0.66
67264.6	87.8	86.9	243.2	243.2	1341.6	1530.1	0.66
69180.7	90.3	87.0	243.4	243.4	1341.6	1530.1	0.66
71096.8	92.8	87.1	243.6	243.6	1341.7	1530.1	0.66
73012.9	95.3	87.2	243.8	243.8	1341.7	1530.1	0.66
74928.9	97.8	87.3	244.0	244.0	1341.7	1530.1	0.66
76845.0	100.3	87.4	244.2	244.2	1341.8	1530.1	0.66
78761.1	102.8	87.5	244.3	244.3	1341.7	1530.1	0.66
80677.1	105.3	87.5	244.4	244.4	1341.9	1530.1	0.66
82593.2	107.8	87.6	244.6	244.6	1341.8	1530.1	0.66
84509.3	110.3	87.6	244.7	244.7	1341.9	1530.1	0.66
86425.4	112.8	87.7	244.8	244.8	1341.9	1530.1	0.66
88341.4	115.3	87.7	244.9	244.9	1341.9	1530.1	0.66
90257.5	117.8	87.7	244.9	244.9	1342.1	1530.1	0.66
92173.6	120.3	87.8	245.0	245.0	1342.0	1530.1	0.66
94089.6	122.8	87.8	245.1	245.1	1341.9	1530.1	0.66
96005.7	125.3	87.8	245.1	245.1	1342.1	1530.1	0.66
97921.8	127.8	87.9	245.2	245.2	1341.9	1530.1	0.66
99837.8	130.3	87.9	245.2	245.2	1342.1	1530.1	0.66
101753.9	132.8	87.9	245.3	245.3	1341.9	1530.1	0.66
103670.0	135.3	87.9	245.3	245.3	1342.0	1530.1	0.66
105586.1	137.8	87.9	245.3	245.3	1342.1	1530.1	0.66
107502.1	140.3	88.0	245.4	245.4	1342.0	1530.1	0.66
109418.2	142.8	88.0	245.4	245.4	1342.0	1530.1	0.66

111334.3	145.3	88.0	245.4	245.4	1342.1	1530.1	0.66
113250.3	147.8	88.0	245.5	245.5	1342.1	1530.1	0.66
115166.4	150.3	88.0	245.5	245.5	1342.2	1530.1	0.66
117082.5	152.8	88.0	245.5	245.5	1342.2	1530.1	0.66
118998.5	155.4	88.0	245.5	245.5	1342.2	1530.1	0.66
120914.6	157.9	88.0	245.5	245.5	1342.2	1530.1	0.66
122830.7	160.4	88.0	245.5	245.5	1342.2	1530.1	0.66
124746.8	162.9	88.0	245.6	245.6	1342.2	1530.1	0.66
126662.8	165.4	88.0	245.6	245.6	1342.2	1530.1	0.66
128578.9	167.9	88.0	245.6	245.6	1342.2	1530.1	0.66
130495.0	170.4	88.0	245.6	245.6	1342.2	1530.1	0.66
132367.5	172.8	88.0	245.6	245.6	1342.2	1530.1	0.66
133859.7	174.8	88.0	245.6	245.6	1342.2	1530.1	0.66
135351.8	176.7	88.1	245.6	245.6	1342.2	1530.1	0.66
136844.0	178.6	88.1	245.6	245.6	1342.2	1530.1	0.66
138336.2	180.6	88.1	245.6	245.6	1342.2	1530.1	0.66
139828.4	182.5	88.1	245.6	245.6	1342.2	1530.1	0.66
141320.6	184.5	88.1	245.6	245.6	1342.2	1530.1	0.66
142812.8	186.4	88.1	245.6	245.6	1342.2	1530.1	0.66
144305.0	188.4	88.1	245.6	245.6	1342.2	1530.1	0.66
145797.2	190.3	88.1	245.6	245.6	1342.2	1530.1	0.66
147289.3	192.3	88.1	245.6	245.6	1342.2	1530.1	0.66
148781.5	194.2	88.1	245.6	245.6	1342.2	1530.1	0.66
150273.7	196.2	88.1	245.6	245.6	1342.2	1530.1	0.66
151765.9	198.1	88.1	245.6	245.6	1342.2	1530.1	0.66
153258.1	200.1	88.1	245.6	245.6	1342.2	1530.1	0.66
154750.3	202.0	88.1	245.6	245.6	1342.2	1530.1	0.66
156242.5	204.0	88.1	245.6	245.6	1342.2	1530.1	0.66
157734.7	205.9	88.1	245.6	245.6	1342.2	1530.1	0.66
159226.8	207.9	88.1	245.6	245.6	1342.2	1530.1	0.66
160719.0	209.8	88.1	245.6	245.6	1342.2	1530.1	0.66
162211.2	211.8	88.1	245.6	245.6	1342.2	1530.1	0.66
163703.4	213.7	88.1	245.6	245.6	1342.2	1530.1	0.66
165195.6	215.7	88.1	245.6	245.6	1342.2	1530.1	0.66
166687.8	217.6	88.1	245.6	245.6	1342.2	1530.1	0.66
168180.0	219.6	88.1	245.6	245.6	1342.2	1530.1	0.66
169672.2	221.5	88.1	245.6	245.6	1342.2	1530.1	0.66
171164.3	223.5	88.1	245.6	245.6	1342.2	1530.1	0.66
172656.5	225.4	88.1	245.6	245.6	1342.2	1530.1	0.66
174148.7	227.3	88.1	245.6	245.6	1342.2	1530.1	0.66
175640.9	229.3	88.1	245.6	245.6	1342.2	1530.1	0.66
177133.1	231.2	88.1	245.6	245.6	1342.2	1530.1	0.66
178625.3	233.2	88.1	245.6	245.6	1342.2	1530.1	0.61
180117.5	235.1	88.1	245.6	245.6	1342.2	1530.1	0.66
181609.7	237.1	88.1	245.6	245.6	1342.2	1530.1	0.66

SHELL   Output Shell Temperature, Taper Histories   SHL

Position mm	Liquidus Loc. mm	Solidus Loc. mm	shell mm	Thermo-couple T	Surface Temp.(C)	Outer q MW/m2
80.3	0.80	0.65	0.69	1530.1	1320.2	9.40
1995.9	0.80	0.64	0.69	1530.1	1323.5	9.32
3906.5	0.80	0.64	0.69	1530.1	1325.5	9.26
5825.8	0.80	0.64	0.69	1530.1	1327.6	9.21
7751.2	0.80	0.63	0.68	1530.1	1329.1	9.17
9676.6	0.78	0.63	0.68	1530.1	1330.4	9.14
11602.0	0.78	0.63	0.68	1530.1	1331.6	9.10
13527.4	0.79	0.63	0.68	1530.1	1332.7	9.07
15452.8	0.78	0.63	0.67	1530.1	1333.6	9.05
17378.2	0.77	0.63	0.67	1530.1	1334.6	9.02
19303.6	0.77	0.63	0.67	1530.1	1335.3	9.00
21229.0	0.77	0.62	0.67	1530.1	1336.0	8.98
23154.4	0.77	0.62	0.67	1530.1	1336.6	8.97
25079.8	0.77	0.62	0.67	1530.1	1337.1	8.95
27005.2	0.76	0.62	0.66	1530.1	1337.7	8.94
28930.6	0.77	0.62	0.67	1530.1	1338.0	8.92
30856.0	0.76	0.62	0.66	1530.1	1338.6	8.91
32781.4	0.76	0.62	0.66	1530.1	1338.9	8.90
34697.4	0.75	0.62	0.66	1530.1	1339.3	8.89
36613.5	0.77	0.62	0.66	1530.1	1339.6	8.89
38529.6	0.75	0.62	0.66	1530.1	1339.9	8.88
40445.6	0.76	0.62	0.66	1530.1	1340.1	8.87
42361.7	0.76	0.62	0.66	1530.1	1340.3	8.87
44277.8	0.76	0.62	0.66	1530.1	1340.4	8.86
46193.8	0.75	0.62	0.66	1530.1	1340.7	8.86
48109.9	0.76	0.62	0.66	1530.1	1340.7	8.85
50026.0	0.76	0.62	0.66	1530.1	1340.8	8.85
51942.1	0.76	0.62	0.66	1530.1	1341.1	8.84
53858.1	0.76	0.62	0.66	1530.1	1341.0	8.84
55774.2	0.76	0.62	0.66	1530.1	1341.3	8.84
57690.3	0.76	0.62	0.66	1530.1	1341.4	8.84
59606.3	0.75	0.62	0.66	1530.1	1341.4	8.83
61522.4	0.75	0.62	0.66	1530.1	1341.3	8.83
63438.5	0.75	0.62	0.66	1530.1	1341.5	8.83
65354.5	0.76	0.62	0.66	1530.1	1341.6	8.83
67270.6	0.76	0.62	0.66	1530.1	1341.6	8.83
69186.7	0.76	0.62	0.66	1530.1	1341.7	8.82
71102.8	0.76	0.62	0.66	1530.1	1341.8	8.82
73018.8	0.75	0.62	0.66	1530.1	1341.8	8.82
74934.9	0.75	0.62	0.66	1530.1	1341.8	8.82
76851.0	0.76	0.62	0.66	1530.1	1341.8	8.82
78767.0	0.76	0.62	0.66	1530.1	1341.8	8.82
80683.1	0.75	0.62	0.66	1530.1	1341.9	8.82
82599.2	0.76	0.62	0.66	1530.1	1341.9	8.82
84515.3	0.75	0.62	0.66	1530.1	1341.9	8.82
86431.3	0.76	0.62	0.66	1530.1	1341.9	8.82
88347.4	0.76	0.62	0.66	1530.1	1342.0	8.82
90263.5	0.76	0.62	0.66	1530.1	1342.1	8.82
92179.5	0.75	0.62	0.66	1530.1	1342.0	8.81
94095.6	0.76	0.62	0.66	1530.1	1342.0	8.81
96011.7	0.75	0.62	0.66	1530.1	1342.1	8.81
97927.7	0.76	0.62	0.66	1530.1	1342.0	8.81
99843.8	0.76	0.62	0.66	1530.1	1342.2	8.81
101759.9	0.76	0.62	0.66	1530.1	1342.0	8.81
103676.0	0.76	0.62	0.66	1530.1	1342.1	8.81
105592.0	0.76	0.62	0.66	1530.1	1342.1	8.81
107508.1	0.76	0.62	0.66	1530.1	1342.1	8.81
109424.2	0.75	0.62	0.66	1530.1	1342.0	8.81

111340.2	0.75	0.62	0.66	1530.1	1342.2	8.81
113256.3	0.76	0.62	0.66	1530.1	1342.2	8.81
115172.4	0.76	0.62	0.66	1530.1	1342.2	8.81
117088.4	0.76	0.62	0.66	1530.1	1342.2	8.81
119004.5	0.76	0.62	0.66	1530.1	1342.2	8.81
120920.6	0.76	0.62	0.66	1530.1	1342.2	8.81
122836.7	0.75	0.62	0.66	1530.1	1342.3	8.81
124752.7	0.76	0.62	0.66	1530.1	1342.2	8.81
126668.8	0.76	0.62	0.66	1530.1	1342.2	8.81
128584.9	0.75	0.62	0.66	1530.1	1342.2	8.81
130500.9	0.76	0.62	0.66	1530.1	1342.2	8.81
132367.5	0.76	0.62	0.66	1530.1	1342.2	8.81
133859.7	0.76	0.62	0.66	1530.1	1342.2	8.81
135351.8	0.76	0.62	0.66	1530.1	1342.2	8.81
136844.0	0.76	0.62	0.66	1530.1	1342.2	8.81
138336.2	0.75	0.62	0.66	1530.1	1342.3	8.81
139828.4	0.75	0.62	0.66	1530.1	1342.3	8.81
141320.6	0.75	0.62	0.66	1530.1	1342.3	8.81
142812.8	0.76	0.62	0.66	1530.1	1342.3	8.81
144305.0	0.76	0.62	0.66	1530.1	1342.3	8.81
145797.2	0.76	0.62	0.66	1530.1	1342.3	8.81
147289.3	0.76	0.62	0.66	1530.1	1342.3	8.81
148781.5	0.75	0.62	0.66	1530.1	1342.3	8.81
150273.7	0.75	0.62	0.66	1530.1	1342.3	8.81
151765.9	0.75	0.62	0.66	1530.1	1342.3	8.81
153258.1	0.75	0.62	0.66	1530.1	1342.3	8.81
154750.3	0.75	0.62	0.66	1530.1	1342.3	8.81
156242.5	0.75	0.62	0.66	1530.1	1342.3	8.81
157734.7	0.75	0.62	0.66	1530.1	1342.3	8.81
159226.8	0.75	0.62	0.66	1530.1	1342.3	8.81
160719.0	0.75	0.62	0.66	1530.1	1342.3	8.81
162211.2	0.75	0.62	0.66	1530.1	1342.3	8.81
163703.4	0.75	0.62	0.66	1530.1	1342.3	8.81
165195.6	0.75	0.62	0.66	1530.1	1342.3	8.81
166687.8	0.75	0.62	0.66	1530.1	1342.3	8.81
168180.0	0.75	0.62	0.66	1530.1	1342.3	8.81
169672.2	0.75	0.62	0.66	1530.1	1342.3	8.81
171164.3	0.75	0.62	0.66	1530.1	1342.3	8.81
172656.5	0.75	0.62	0.66	1530.1	1342.3	8.81
174148.7	0.75	0.62	0.66	1530.1	1342.3	8.81
175640.9	0.75	0.62	0.66	1530.1	1342.3	8.81
177133.1	0.75	0.62	0.66	1530.1	1342.3	8.81
178625.3	0.05	0.00	0.00	1530.1	1527.6	31.64
178625.3	0.29	0.18	0.21	1530.1	1365.2	28.35
178625.3	0.40	0.28	0.32	1530.1	1348.6	18.86
178625.3	0.49	0.35	0.39	1530.1	1344.3	15.00
178625.3	0.55	0.42	0.46	1530.1	1343.6	12.81
178625.3	0.60	0.48	0.51	1530.1	1342.8	11.35
178625.3	0.66	0.53	0.57	1530.1	1342.5	10.29
178625.3	0.70	0.57	0.61	1530.1	1342.4	9.48
178625.3	0.75	0.62	0.66	1530.1	1342.2	8.83
178625.3	0.75	0.62	0.66	1530.1	1342.3	8.81
180117.5	0.75	0.62	0.66	1530.1	1342.3	8.81
181609.7	0.75	0.62	0.66	1530.1	1342.3	8.81

STRIP   Quasi-Steady-State Strip Surface Temp (at   100 cycle)   SST

z (mm)	Time (s)	Tcold Deg C	Thot Deg C
0.00	0.00	1530.10	1530.10
10.00	0.01	1530.10	1412.72
20.00	0.03	1530.10	1380.82
30.00	0.04	1530.10	1370.21
40.00	0.05	1530.10	1365.64
50.00	0.07	1530.10	1362.34
60.00	0.08	1530.10	1360.22
70.00	0.09	1530.10	1358.72
80.00	0.10	1530.10	1357.48
90.00	0.12	1453.21	1362.14
100.00	0.13	1413.55	1379.97
110.00	0.14	1396.76	1385.94
120.00	0.16	1388.78	1382.32
130.00	0.17	1382.67	1377.39
140.00	0.18	1377.10	1372.46
150.00	0.20	1371.82	1367.72
160.00	0.21	1366.80	1363.22
170.00	0.22	1362.04	1358.96
180.00	0.23	1357.51	1354.96
190.00	0.25	1353.24	1351.20
200.00	0.26	1349.19	1347.68
210.00	0.27	1345.38	1344.16
220.00	0.29	1341.72	1340.63
230.00	0.30	1338.13	1337.15
240.00	0.31	1334.63	1333.76
250.00	0.33	1331.16	1330.41
260.00	0.34	1327.81	1327.14
270.00	0.35	1324.47	1323.94
280.00	0.37	1321.25	1320.79
290.00	0.38	1318.07	1317.73
300.00	0.39	1314.94	1314.72
310.00	0.40	1311.91	1311.78
320.00	0.42	1308.89	1308.90
330.00	0.43	1306.00	1306.08
340.00	0.44	1303.14	1303.34
350.00	0.46	1300.32	1300.64
360.00	0.47	1297.62	1298.02
370.00	0.48	1294.91	1295.45
380.00	0.50	1292.32	1292.94
390.00	0.51	1289.77	1290.51
400.00	0.52	1287.25	1288.12
410.00	0.54	1284.86	1285.79
420.00	0.55	1282.47	1283.54
430.00	0.56	1280.15	1281.32
440.00	0.57	1277.92	1279.18
450.00	0.59	1275.69	1277.10

STRIP1D-1.2 Strip Casting Heat Transfer Analysis
University of Illinois, Brian G. Thomas, 1993

WHEEL | Wheel Output | WHL

Z (mm)	Time (s) (s)	Inner T Deg C	Outer T Deg C	Shell T Deg C	Inner q kW/m2	Outer q MW/m2	S/A q KW/m2
0.0	0.00	50.00	50.06	1530.10	0.00	42.04	0.00
200.0	0.26	50.00	102.38	1346.94	0.00	0.62	378.28
400.0	0.52	50.00	87.18	1286.49	0.00	0.32	331.11
600.2	0.78	50.00	78.60	1274.81	0.07	0.00	322.57
800.2	1.04	50.03	74.29	1274.81	0.76	0.00	322.57
1000.0	1.31	50.10	71.53	1274.81	2.79	0.00	322.57
1200.1	1.57	48.19	69.56	1274.81	218.34	0.00	322.57
1400.2	1.83	47.50	68.06	1274.81	210.04	0.00	322.57
1600.2	2.09	48.80	66.86	1274.81	-32.33	0.00	322.57
1800.0	2.35	49.78	65.88	1274.81	-6.03	0.00	322.57
1915.2	2.50	50.12	65.44	1530.10	3.21	34.21	0.00
2115.2	2.76	50.58	116.54	1351.95	15.51	0.62	382.42
2315.2	3.02	50.95	100.73	1290.93	25.62	0.31	334.41
2515.5	3.28	51.27	91.68	1279.87	34.27	0.00	326.25
2715.2	3.54	51.58	86.93	1279.87	42.56	0.00	326.25
2915.3	3.81	51.90	83.75	1279.87	51.16	0.00	326.25
3115.4	4.07	50.44	81.39	1279.87	245.23	0.00	326.25
3315.5	4.33	50.07	79.52	1279.87	240.81	0.00	326.25
3515.2	4.59	51.41	78.00	1279.87	37.90	0.00	326.25
3715.3	4.85	52.41	76.72	1279.87	64.76	0.00	326.25
3827.1	5.00	52.78	76.13	1530.10	74.76	34.06	0.00
4027.2	5.26	53.31	126.31	1353.94	89.21	0.61	384.07
4227.2	5.52	53.74	110.77	1294.26	100.71	0.31	336.89
4427.2	5.78	54.13	101.57	1282.71	111.16	0.00	328.33
4627.4	6.04	54.49	96.58	1282.71	120.77	0.00	328.33
4827.3	6.30	54.85	93.21	1282.71	130.37	0.00	328.33
5027.3	6.56	53.81	90.66	1282.71	285.73	0.00	328.33
5227.2	6.82	53.63	88.63	1282.71	283.53	0.00	328.33
5427.4	7.09	54.75	86.94	1282.71	127.78	0.00	328.33
5627.4	7.35	55.63	85.51	1282.71	151.59	0.00	328.33
5743.9	7.50	55.99	84.82	1530.10	161.11	33.90	0.00
5943.9	7.76	56.47	135.56	1359.66	174.14	0.63	388.86
6143.9	8.02	56.87	119.44	1299.53	184.92	0.32	340.86
6344.0	8.28	57.23	110.01	1285.93	194.63	0.00	330.70
6543.9	8.54	57.57	104.82	1285.93	203.60	0.00	330.70
6744.1	8.80	57.90	101.30	1285.93	212.57	0.00	330.70
6944.1	9.07	57.26	98.63	1285.93	327.09	0.00	330.70
7144.0	9.33	57.21	96.48	1285.93	326.51	0.00	330.70
7343.9	9.59	58.06	94.69	1285.93	216.86	0.00	330.70
7544.2	9.85	58.80	93.15	1285.93	236.83	0.00	330.70
7669.3	10.01	59.13	92.34	1530.10	245.57	33.78	0.00
7869.3	10.27	59.54	142.76	1362.08	256.67	0.63	390.89
8069.3	10.53	59.88	126.62	1301.95	265.79	0.32	342.70
8269.4	10.80	60.19	117.14	1288.33	274.20	0.00	332.47
8469.3	11.06	60.48	111.89	1288.33	282.14	0.00	332.47
8669.5	11.32	60.78	108.30	1288.33	290.12	0.00	332.47
8869.5	11.58	60.46	105.56	1288.33	365.53	0.00	332.47
9069.4	11.84	60.54	103.34	1288.33	366.49	0.00	332.47
9269.3	12.10	61.19	101.47	1288.33	300.99	0.00	332.47
9469.6	12.36	61.75	99.86	1288.33	316.31	0.00	332.47
9594.7	12.53	62.02	99.01	1530.10	323.45	33.67	0.00
9794.7	12.79	62.37	149.15	1363.92	332.79	0.63	392.45
9994.7	13.05	62.68	133.01	1303.82	341.14	0.32	344.12
10194.8	13.31	62.96	123.49	1290.20	348.74	0.00	333.86
10394.7	13.57	63.20	118.19	1290.20	355.32	0.00	333.86
10594.9	13.83	63.45	114.54	1290.20	362.03	0.00	333.86
10794.9	14.09	63.42	111.74	1290.20	401.04	0.00	333.86
10994.8	14.35	63.61	109.46	1290.20	403.31	0.00	333.86

11194.7	14.61	64.06	107.54	1290.20	378.28	0.00	333.86
11395.0	14.88	64.46	105.86	1290.20	389.17	0.00	333.86
11520.1	15.04	64.67	104.97	1530.10	394.76	33.56	0.00
11720.1	15.30	64.98	154.87	1365.67	403.16	0.63	393.93
11920.1	15.56	65.18	138.73	1305.57	408.40	0.32	345.46
12120.2	15.82	65.36	129.18	1291.94	413.46	0.00	335.16
12320.1	16.08	65.57	123.84	1291.94	419.09	0.00	335.16
12520.3	16.35	65.79	120.14	1291.94	424.97	0.00	335.16
12720.3	16.61	66.02	117.29	1291.94	432.22	0.00	335.16
12920.2	16.87	66.31	114.96	1291.94	435.73	0.00	335.16
13120.1	17.13	66.59	112.98	1291.94	446.49	0.00	335.16
13320.3	17.39	66.85	111.25	1291.94	453.56	0.00	335.16
13445.5	17.55	67.01	110.32	1530.10	457.84	33.46	0.00
13645.5	17.81	67.20	160.00	1367.32	462.97	0.63	395.33
13845.5	18.08	67.38	143.86	1307.23	467.60	0.32	346.73
14045.6	18.34	67.54	134.29	1293.59	472.00	-0.01	336.39
14245.5	18.60	67.72	128.91	1293.59	476.82	0.00	336.39
14445.7	18.86	67.91	125.16	1293.59	481.94	0.00	336.39
14645.7	19.12	68.37	122.26	1293.59	460.43	0.00	336.39
14845.6	19.38	68.75	119.89	1293.59	465.03	0.00	336.39
15045.5	19.64	68.88	117.86	1293.59	508.08	0.00	336.39
15245.7	19.90	69.02	116.08	1293.59	511.70	0.00	336.39
15370.9	20.07	69.13	115.13	1530.10	514.79	33.37	0.00
15570.9	20.33	69.31	164.45	1339.44	519.70	0.61	372.15
15770.9	20.59	69.48	148.30	1277.67	524.25	0.31	324.65
15971.0	20.85	69.61	138.76	1263.68	527.67	-0.01	314.59
16170.9	21.11	69.74	133.37	1263.68	531.18	-0.01	314.59
16371.1	21.37	69.89	129.59	1263.68	535.13	0.00	314.59
16571.0	21.63	70.55	126.66	1263.68	486.62	0.00	314.59
16771.0	21.89	71.01	124.25	1263.68	492.12	0.00	314.59
16970.9	22.16	70.99	122.19	1263.68	564.83	0.00	314.59
17171.1	22.42	71.00	120.37	1263.68	565.09	0.00	314.59
17296.3	22.58	71.07	119.39	1530.10	567.00	32.38	0.00
17496.3	22.84	71.24	168.55	1340.70	571.55	0.61	373.17
17696.3	23.10	71.39	152.39	1278.94	575.53	0.31	325.57
17896.3	23.36	71.49	142.84	1264.94	578.32	-0.01	315.49
18096.3	23.62	71.58	137.41	1264.94	580.61	-0.01	315.49
18296.5	23.89	71.68	133.61	1264.94	583.44	-0.01	315.49
18496.4	24.15	72.53	130.65	1264.94	510.38	-0.01	315.49
18696.4	24.41	73.06	128.20	1264.94	516.67	0.00	315.49
18896.3	24.67	72.90	126.10	1264.94	616.24	0.00	315.49
19096.5	24.93	72.80	124.25	1264.94	613.44	0.00	315.49
19221.6	25.09	72.83	123.25	1530.10	614.25	32.31	0.00
19421.6	25.35	72.89	172.26	1341.67	616.09	0.61	373.96
19621.6	25.62	72.89	156.09	1279.94	616.09	0.31	326.30
19821.7	25.88	72.98	146.52	1265.94	618.40	-0.01	316.20
20021.7	26.14	73.06	141.08	1265.94	620.57	-0.01	316.20
20221.9	26.40	73.16	137.24	1265.94	623.17	-0.01	316.20
20421.8	26.66	74.18	134.25	1265.94	530.16	-0.01	316.20
20621.8	26.92	74.78	131.76	1265.94	537.30	-0.01	316.20
20821.7	27.18	74.52	129.63	1265.94	659.75	0.00	316.20
21021.9	27.44	74.33	127.74	1265.94	654.60	0.00	316.20
21147.0	27.61	74.33	126.72	1530.10	654.62	32.24	0.00
21347.0	27.87	74.33	175.58	1342.45	654.62	0.60	374.60
21547.0	28.13	74.33	159.41	1280.76	654.62	0.31	326.89
21747.1	28.39	74.36	149.82	1266.76	655.45	-0.01	316.78
21947.1	28.65	74.42	144.35	1266.76	657.07	-0.01	316.78
22147.3	28.91	74.50	140.48	1266.76	659.22	-0.01	316.78
22347.2	29.17	75.67	137.46	1266.76	548.04	-0.01	316.78
22547.2	29.43	76.33	134.94	1266.76	555.90	-0.01	316.78
22747.1	29.70	75.97	132.78	1266.76	698.90	-0.01	316.78
22947.3	29.96	75.70	130.86	1266.76	691.59	-0.01	316.78
23072.4	30.12	75.67	129.81	1530.10	690.87	32.18	0.00
23272.4	30.38	75.67	178.55	1343.27	690.87	0.60	375.27
23472.4	30.64	75.67	162.37	1281.59	690.87	0.31	327.51
23672.5	30.90	75.68	152.77	1267.59	690.97	-0.01	317.38

23872.5	31.17	75.70	147.27	1267.59	691.73	-0.01	317.38
24072.7	31.43	75.76	143.38	1267.59	693.17	-0.01	317.38
24272.6	31.69	77.07	140.33	1267.59	564.77	-0.01	317.38
24472.6	31.95	77.77	137.79	1267.59	573.22	-0.01	317.38
24672.5	32.21	77.32	135.60	1267.59	735.22	-0.01	317.38
24872.7	32.47	76.97	133.65	1267.59	725.79	-0.01	317.38
24997.8	32.63	76.92	132.59	1530.10	724.33	32.13	0.00
25197.8	32.90	76.92	181.20	1343.84	724.32	0.60	375.74
25397.8	33.16	76.92	165.03	1282.19	724.32	0.31	327.95
25597.9	33.42	76.90	155.42	1268.20	723.78	-0.01	317.81
25797.9	33.68	76.89	149.90	1268.20	723.72	-0.01	317.81
25998.1	33.94	76.92	145.99	1268.20	724.47	-0.01	317.81
26198.0	34.20	78.35	142.92	1268.20	580.17	-0.01	317.81
26398.0	34.46	79.10	140.36	1268.20	589.15	-0.01	317.81
26597.9	34.72	78.56	138.14	1268.20	768.57	-0.01	317.81
26798.1	34.98	78.14	136.17	1268.20	757.17	-0.01	317.81
26923.2	35.15	78.06	135.09	1530.10	755.00	32.08	0.00
27123.2	35.41	78.06	183.61	1344.67	754.99	0.60	376.41
27323.2	35.67	78.06	167.44	1283.02	754.99	0.31	328.55
27523.3	35.93	78.01	157.82	1269.02	753.82	-0.01	318.40
27723.3	36.19	77.98	152.28	1269.02	752.98	-0.01	318.40
27923.5	36.45	77.98	148.35	1269.02	753.05	-0.01	318.40
28123.4	36.71	79.52	145.26	1269.02	594.22	-0.01	318.40
28323.4	36.98	80.31	142.68	1269.02	603.66	-0.01	318.40
28523.3	37.24	79.69	140.44	1269.02	798.96	-0.01	318.40
28723.5	37.50	79.20	138.46	1269.02	785.73	-0.01	318.40
28848.6	37.66	79.09	137.36	1530.10	782.91	32.04	0.00
29048.6	37.92	79.08	185.79	1345.01	782.50	0.60	376.69
29248.6	38.18	79.08	169.61	1283.40	782.50	0.31	328.83
29448.7	38.44	79.02	159.98	1269.40	780.97	-0.01	318.67
29648.7	38.71	78.96	154.43	1269.40	779.46	-0.01	318.67
29848.9	38.97	78.94	150.48	1269.40	778.90	-0.01	318.67
30048.8	39.23	80.58	147.37	1269.40	606.92	-0.01	318.67
30248.8	39.49	81.40	144.77	1269.40	616.77	-0.01	318.67
30448.7	39.75	80.71	142.52	1269.40	826.38	-0.01	318.67
30648.9	40.01	80.16	140.51	1269.40	811.51	-0.01	318.67
30774.0	40.17	80.03	139.41	1530.10	808.10	31.99	0.00
30974.0	40.44	79.97	187.75	1345.92	806.56	0.60	377.44
31174.0	40.70	79.93	171.58	1284.29	805.40	0.30	329.49
31374.1	40.96	79.87	161.94	1270.28	803.80	-0.01	319.30
31574.1	41.22	79.80	156.37	1270.28	801.98	-0.01	319.30
31774.3	41.48	79.77	152.41	1270.28	801.08	-0.01	319.30
31974.2	41.74	81.49	149.28	1270.28	617.88	-0.01	319.30
32174.1	42.00	82.35	146.66	1270.28	628.15	-0.01	319.30
32374.1	42.26	81.59	144.39	1270.28	850.27	-0.01	319.30
32574.3	42.53	80.99	142.37	1270.28	834.03	-0.01	319.30
32699.4	42.69	80.85	141.25	1530.10	830.14	31.96	0.00
32899.4	42.95	80.69	189.52	1346.34	825.88	0.60	377.79
33099.4	43.21	80.62	173.35	1284.73	824.12	0.30	329.81
33299.5	43.47	80.56	163.66	1270.72	822.51	-0.01	319.62
33499.4	43.73	80.50	158.07	1270.72	820.65	-0.01	319.62
33699.6	43.99	80.46	154.08	1270.72	819.69	-0.01	319.62
33899.5	44.26	82.29	150.93	1270.72	627.48	-0.01	319.62
34099.7	44.52	83.18	148.29	1270.72	638.11	-0.01	319.62
34299.5	44.78	82.31	145.99	1270.72	869.45	-0.01	319.62
34499.7	45.04	81.70	143.95	1270.72	853.05	-0.01	319.62
34615.5	45.19	81.56	142.90	1530.10	849.17	31.93	0.00
34815.5	45.45	81.37	191.11	1346.75	844.22	0.60	378.12
35015.5	45.71	81.24	174.94	1285.15	840.57	0.30	330.12
35215.6	45.97	81.18	165.24	1271.14	838.95	-0.01	319.92
35415.5	46.23	81.11	159.63	1271.14	837.08	-0.01	319.92
35615.7	46.50	81.07	155.63	1271.14	836.06	-0.01	319.92
35815.5	46.76	82.97	152.47	1271.14	635.66	-0.01	319.92
36015.7	47.02	83.89	149.80	1271.14	646.66	-0.01	319.92
36215.6	47.28	82.98	147.49	1271.14	887.44	-0.01	319.92
36415.8	47.54	82.33	145.43	1271.14	870.13	-0.01	319.92

36531.6	47.69	82.18	144.38	1530.10	865.96	31.90	0.00
36731.6	47.95	81.99	192.52	1347.26	860.95	0.60	378.54
36931.6	48.21	81.82	176.35	1285.65	856.32	0.30	330.49
37131.7	48.47	81.72	166.64	1271.64	853.67	-0.01	320.28
37331.6	48.74	81.65	161.02	1271.64	851.77	-0.01	320.28
37531.7	49.00	81.61	157.01	1271.64	850.69	-0.01	320.28
37731.6	49.26	83.58	153.83	1271.64	642.97	-0.01	320.28
37931.8	49.52	84.53	151.15	1271.64	654.29	-0.01	320.28
38131.7	49.78	83.57	148.83	1271.64	903.49	-0.01	320.28
38331.9	50.04	82.90	146.75	1271.64	885.36	-0.01	320.28
38447.6	50.19	82.74	145.69	1530.10	880.94	31.88	0.00
38647.6	50.45	82.55	193.77	1347.45	875.88	0.60	378.69
38847.6	50.71	82.38	177.60	1285.86	871.25	0.30	330.64
39047.8	50.98	82.26	167.88	1271.85	868.02	-0.01	320.43
39247.6	51.24	82.17	162.26	1271.85	865.85	-0.01	320.43
39447.8	51.50	82.13	158.23	1271.85	864.53	-0.01	320.43
39647.7	51.76	84.15	155.04	1271.85	649.83	-0.01	320.43
39847.9	52.02	85.12	152.35	1271.85	661.41	-0.01	320.43
40047.7	52.28	84.13	150.02	1271.85	918.38	-0.01	320.43
40247.9	52.54	83.42	147.92	1271.85	899.44	-0.01	320.43
40363.7	52.69	83.25	146.86	1530.10	894.75	31.85	0.00
40563.7	52.96	83.06	194.89	1347.77	889.64	0.60	378.96
40763.7	53.22	82.89	178.72	1286.19	885.01	0.30	330.89
40963.8	53.48	82.76	169.00	1272.18	881.50	-0.01	320.67
41163.7	53.74	82.66	163.36	1272.18	878.95	-0.01	320.67
41363.9	54.00	82.60	159.33	1272.18	877.36	-0.01	320.67
41563.8	54.26	84.68	156.13	1272.18	656.16	-0.01	320.67
41763.9	54.52	85.67	153.43	1272.18	667.97	-0.01	320.67
41963.8	54.78	84.63	151.08	1272.18	932.08	-0.01	320.67
42164.0	55.04	83.90	148.98	1272.18	912.38	-0.01	320.67
42279.8	55.20	83.72	147.91	1530.10	907.43	31.83	0.00
42479.8	55.46	83.53	195.90	1348.10	902.27	0.60	379.23
42679.8	55.72	83.36	179.73	1286.52	897.64	0.30	331.14
42879.9	55.98	83.22	170.00	1272.52	893.87	-0.01	320.91
43079.8	56.24	83.11	164.36	1272.52	891.00	-0.01	320.91
43280.0	56.50	83.04	160.32	1272.52	889.16	-0.01	320.91
43479.8	56.76	85.17	157.11	1272.52	661.98	-0.01	320.91
43680.0	57.02	86.17	154.41	1272.52	673.98	-0.01	320.91
43879.9	57.28	85.10	152.05	1272.52	944.64	-0.01	320.91
44080.1	57.55	84.34	149.94	1272.52	924.22	-0.01	320.91
44195.8	57.70	84.15	148.86	1530.10	919.03	31.82	0.00
44395.8	57.96	83.96	196.81	1348.19	913.83	0.60	379.31
44595.8	58.22	83.79	180.65	1286.63	909.20	0.30	331.21
44796.0	58.48	83.64	170.91	1272.62	905.21	-0.01	320.99
44995.8	58.74	83.52	165.27	1272.62	902.02	-0.01	320.99
45196.0	59.00	83.44	161.22	1272.62	899.92	-0.01	320.99
45395.9	59.26	85.61	158.00	1272.62	667.28	-0.01	320.99
45596.1	59.52	86.62	155.29	1272.62	679.46	-0.01	320.99
45796.0	59.79	85.52	152.92	1272.62	956.05	-0.01	320.99
45996.1	60.05	84.74	150.81	1272.62	934.97	-0.01	320.99
46111.9	60.20	84.54	149.72	1530.10	929.56	31.79	0.00
46311.9	60.46	84.35	197.64	1348.60	924.31	0.60	379.64
46511.9	60.72	84.18	181.48	1287.02	919.68	0.30	331.51
46712.0	60.98	84.02	171.74	1273.02	915.50	-0.01	321.27
46911.9	61.24	83.89	166.08	1273.02	912.00	-0.01	321.27
47112.1	61.50	83.80	162.03	1273.02	909.66	-0.01	321.27
47312.0	61.76	86.01	158.81	1273.02	672.07	-0.01	321.27
47512.1	62.03	87.04	156.09	1273.02	684.41	-0.01	321.27
47712.0	62.29	85.91	153.71	1273.02	966.37	-0.01	321.27
47912.2	62.55	85.10	151.59	1273.02	944.69	-0.01	321.27
48028.0	62.70	84.90	150.50	1530.10	939.08	31.78	0.00
48228.0	62.96	84.70	198.38	1348.47	933.79	0.60	379.54
48428.0	63.22	84.53	182.22	1286.93	929.11	0.30	331.44
48628.1	63.48	84.37	172.48	1272.93	924.79	-0.01	321.21
48828.0	63.74	84.23	166.82	1272.93	921.05	-0.01	321.21
49028.2	64.01	84.13	162.76	1272.93	918.49	-0.01	321.21

49228.0	64.27	86.37	159.53	1272.93	676.42	-0.01	321.21
49428.2	64.53	87.41	156.80	1272.93	688.89	-0.01	321.21
49628.1	64.79	86.26	154.43	1272.93	975.71	-0.01	321.21
49828.3	65.05	85.43	152.29	1272.93	953.49	-0.01	321.21
49944.1	65.20	85.22	151.20	1530.10	947.69	31.76	0.00
50144.1	65.46	85.01	199.06	1348.65	942.25	0.60	379.69
50344.1	65.72	84.84	182.89	1287.12	937.55	0.30	331.57
50544.2	65.98	84.68	173.15	1273.11	933.14	-0.01	321.34
50744.1	66.25	84.53	167.49	1273.11	929.22	-0.01	321.34
50944.2	66.51	84.43	163.42	1273.11	926.49	-0.01	321.34
51144.1	66.77	86.70	160.19	1273.11	680.37	-0.01	321.34
51344.3	67.03	87.75	157.46	1273.11	692.98	-0.01	321.34
51544.2	67.29	86.57	155.07	1273.11	984.23	-0.01	321.34
51744.3	67.55	85.73	152.94	1273.11	961.52	-0.01	321.34
51860.1	67.70	85.51	151.84	1530.10	955.55	31.75	0.00
52060.1	67.96	85.30	199.68	1349.06	949.92	0.60	380.03
52260.1	68.22	85.12	183.51	1287.51	945.20	0.30	331.87
52460.3	68.49	84.96	173.77	1273.50	940.73	-0.01	321.62
52660.1	68.75	84.81	168.10	1273.50	936.66	-0.01	321.62
52860.3	69.01	84.70	164.03	1273.50	933.78	-0.01	321.62
53060.2	69.27	87.00	160.79	1273.50	683.96	-0.01	321.62
53260.4	69.53	88.06	158.05	1273.50	696.69	-0.01	321.62
53460.2	69.79	86.86	155.66	1273.50	991.97	-0.01	321.62
53660.4	70.05	86.00	153.52	1273.50	968.82	-0.01	321.62
53776.2	70.20	85.77	152.42	1530.10	962.70	31.74	0.00
53976.2	70.47	85.56	200.23	1348.80	956.91	0.60	379.81
54176.2	70.73	85.38	184.07	1287.29	952.16	0.30	331.70
54376.3	70.99	85.21	174.32	1273.29	947.65	-0.01	321.47
54576.2	71.25	85.06	168.65	1273.29	943.43	-0.01	321.47
54776.4	71.51	84.95	164.57	1273.29	940.40	-0.01	321.47
54976.3	71.77	87.27	161.33	1273.29	687.22	-0.01	321.47
55176.4	72.03	88.34	158.59	1273.29	700.06	-0.01	321.47
55376.3	72.29	87.12	156.20	1273.29	999.00	-0.01	321.47
55576.5	72.55	86.25	154.05	1273.29	975.44	-0.01	321.47
55692.3	72.71	86.01	152.95	1530.10	969.18	31.72	0.00
55892.3	72.97	85.79	200.74	1349.36	963.18	0.60	380.27
56092.3	73.23	85.61	184.58	1287.81	958.41	0.30	332.09
56292.4	73.49	85.44	174.82	1273.80	953.85	-0.01	321.84
56492.3	73.75	85.28	169.15	1273.80	949.52	-0.01	321.84
56692.4	74.01	85.17	165.07	1273.80	946.37	-0.01	321.84
56892.3	74.27	87.52	161.82	1273.80	690.17	-0.01	321.84
57092.5	74.53	88.59	159.08	1273.80	703.10	-0.01	321.84
57292.4	74.79	87.36	156.68	1273.80	1005.33	-0.01	321.84
57492.6	75.06	86.47	154.53	1273.80	981.40	-0.01	321.84
57608.3	75.21	86.23	153.42	1530.10	975.02	31.73	0.00
57808.3	75.47	86.00	201.19	1349.42	968.82	0.60	380.32
58008.3	75.73	85.82	185.03	1287.88	964.02	0.30	332.14
58208.5	75.99	85.65	175.28	1273.87	959.43	-0.01	321.89
58408.3	76.25	85.49	169.60	1273.87	955.00	-0.01	321.89
58608.5	76.51	85.37	165.52	1273.87	951.75	-0.01	321.89
58808.4	76.77	87.74	162.27	1273.87	692.82	-0.01	321.89
59008.6	77.03	88.82	159.52	1273.87	705.85	-0.01	321.89
59208.4	77.30	87.57	157.12	1273.87	1011.06	-0.01	321.89
59408.6	77.56	86.67	154.96	1273.87	986.80	-0.01	321.89
59524.4	77.71	86.43	153.85	1530.10	980.30	31.72	0.00
59724.4	77.97	86.19	201.60	1349.46	973.92	0.59	380.35
59924.4	78.23	86.01	185.44	1287.93	969.09	0.30	332.18
60124.5	78.49	85.84	175.69	1273.92	964.46	-0.01	321.93
60324.4	78.75	85.67	170.01	1273.92	959.95	-0.01	321.93
60524.6	79.01	85.55	165.92	1273.92	956.61	-0.01	321.93
60724.5	79.27	87.94	162.67	1273.92	695.22	-0.01	321.93
60924.6	79.54	89.03	159.91	1273.92	708.32	-0.01	321.93
61124.5	79.80	87.76	157.51	1273.92	1016.23	-0.01	321.93
61324.7	80.06	86.85	155.35	1273.92	991.67	-0.01	321.93
61440.5	80.21	86.61	154.24	1530.10	985.07	31.71	0.00
61640.5	80.47	86.36	201.97	1349.21	978.52	0.59	380.15

61840.5	80.73	86.18	185.81	1287.71	973.67	0.30	332.02
62040.6	80.99	86.01	176.06	1273.72	969.02	-0.01	321.78
62240.5	81.25	85.84	170.37	1273.72	964.43	-0.01	321.78
62440.7	81.52	85.71	166.28	1273.72	961.00	-0.01	321.78
62640.5	81.78	88.12	163.03	1273.72	697.38	-0.01	321.78
62840.7	82.04	89.21	160.27	1273.72	710.56	-0.01	321.78
63040.6	82.30	87.93	157.86	1273.72	1020.89	-0.01	321.78
63240.8	82.56	87.01	155.70	1273.72	996.07	-0.01	321.78
63356.5	82.71	86.77	154.59	1530.10	989.38	31.69	0.00
63556.5	82.97	86.52	202.31	1349.54	982.67	0.59	380.42
63756.5	83.23	86.34	186.15	1288.02	977.80	0.30	332.24
63956.7	83.49	86.16	176.39	1274.02	973.12	-0.01	321.99
64156.5	83.76	85.99	170.71	1274.02	968.47	-0.01	321.99
64356.7	84.02	85.86	166.62	1274.02	964.96	-0.01	321.99
64556.6	84.28	88.28	163.36	1274.02	699.34	-0.01	321.99
64756.8	84.54	89.38	160.60	1274.02	712.58	-0.01	321.99
64956.7	84.80	88.09	158.19	1274.02	1025.10	-0.01	321.99
65156.8	85.06	87.16	156.02	1274.02	1000.03	-0.01	321.99
65272.6	85.21	86.91	154.91	1530.10	993.26	31.69	0.00
65472.6	85.47	86.66	202.62	1349.86	986.42	0.59	380.68
65672.6	85.73	86.47	186.46	1288.32	981.53	0.30	332.47
65872.7	86.00	86.30	176.70	1274.32	976.82	-0.01	322.21
66072.6	86.26	86.12	171.01	1274.32	972.11	-0.01	322.21
66272.8	86.52	85.99	166.92	1274.32	968.54	-0.01	322.21
66472.7	86.78	88.43	163.65	1274.32	701.10	-0.01	322.21
66672.9	87.04	89.54	160.89	1274.32	714.41	-0.01	322.21
66872.7	87.30	88.23	158.48	1274.32	1028.91	-0.01	322.21
67072.9	87.56	87.29	156.31	1274.32	1003.62	-0.01	322.21
67188.7	87.71	87.04	155.20	1530.10	996.78	31.69	0.00
67388.7	87.97	86.78	202.89	1349.74	989.81	0.59	380.59
67588.7	88.24	86.60	186.73	1288.22	984.90	0.30	332.40
67788.8	88.50	86.42	176.97	1274.22	980.18	-0.01	322.14
67988.7	88.76	86.25	171.28	1274.22	975.41	-0.01	322.14
68188.9	89.02	86.11	167.19	1274.22	971.78	-0.01	322.14
68388.7	89.28	88.56	163.92	1274.22	702.70	-0.01	322.14
68588.9	89.54	89.67	161.16	1274.22	716.06	-0.01	322.14
68788.8	89.80	88.36	158.74	1274.22	1032.36	-0.01	322.14
68989.0	90.06	87.41	156.57	1274.22	1006.87	-0.01	322.14
69104.8	90.22	87.16	155.46	1530.10	999.96	31.68	0.00
69304.8	90.48	86.89	203.14	1349.89	992.84	0.59	380.71
69504.8	90.74	86.71	186.98	1288.37	987.91	0.30	332.50
69704.9	91.00	86.53	177.22	1274.36	983.17	-0.01	322.24
69904.8	91.26	86.36	171.53	1274.36	978.37	-0.01	322.24
70104.9	91.52	86.22	167.43	1274.36	974.68	-0.01	322.24
70304.8	91.78	88.68	164.16	1274.36	704.13	-0.01	322.24
70505.0	92.04	89.80	161.40	1274.36	717.55	-0.01	322.24
70704.9	92.30	88.48	158.98	1274.36	1035.46	-0.01	322.24
70905.0	92.57	87.52	156.81	1274.36	1009.80	-0.01	322.24
71020.8	92.72	87.27	155.69	1530.10	1002.83	31.68	0.00
71220.8	92.98	87.00	203.37	1350.02	995.58	0.59	380.82
71420.8	93.24	86.81	187.21	1288.50	990.63	0.30	332.60
71621.0	93.50	86.63	177.45	1274.49	985.86	-0.01	322.33
71820.8	93.76	86.46	171.75	1274.49	981.03	-0.01	322.33
72021.0	94.02	86.32	167.65	1274.49	977.30	-0.01	322.33
72220.9	94.28	88.79	164.38	1274.49	705.43	-0.01	322.33
72421.1	94.54	89.91	161.62	1274.49	718.88	-0.01	322.33
72620.9	94.81	88.58	159.20	1274.49	1038.25	-0.01	322.33
72821.1	95.07	87.62	157.02	1274.49	1012.43	-0.01	322.33
72936.9	95.22	87.36	155.91	1530.10	1005.41	31.68	0.00
73136.9	95.48	87.09	203.57	1349.95	998.04	0.59	380.76
73336.9	95.74	86.90	187.41	1288.43	993.07	0.30	332.55
73537.0	96.00	86.72	177.65	1274.43	988.29	-0.01	322.29
73736.9	96.26	86.54	171.95	1274.43	983.42	-0.01	322.29
73937.1	96.52	86.40	167.85	1274.43	979.65	-0.01	322.29
74137.0	96.78	88.88	164.58	1274.43	706.59	-0.01	322.29
74337.1	97.05	90.01	161.81	1274.43	720.09	-0.01	322.29

74537.0	97.31	88.67	159.39	1274.43	1040.77	-0.01	322.29
74737.2	97.57	87.71	157.22	1274.43	1014.81	-0.01	322.29
74853.0	97.72	87.45	156.10	1530.10	1007.74	31.67	0.00
75053.0	97.98	87.17	203.75	1350.02	1000.26	0.59	380.81
75253.0	98.24	86.98	—187.60	1288.50	995.28	0.30	332.60
75453.1	98.50	86.81	177.83	1274.50	990.48	-0.01	322.34
75653.0	98.76	86.62	172.13	1274.50	985.57	-0.01	322.34
75853.1	99.03	86.48	168.03	1274.50	981.75	-0.01	322.34
76053.0	99.29	88.97	164.76	1274.50	707.62	-0.01	322.34
76253.2	99.55	90.10	161.99	1274.50	721.16	-0.01	322.34
76453.1	99.81	88.76	159.56	1274.50	1042.99	-0.01	322.34
76653.3	100.07	87.79	157.39	1274.50	1016.90	-0.01	322.34
76769.0	100.22	87.52	156.27	1530.10	1009.79	31.67	0.00
76969.0	100.48	87.24	203.91	1350.10	1002.22	0.59	380.88
77169.0	100.74	87.06	187.76	1288.58	997.22	0.30	332.66
77369.2	101.00	86.88	177.99	1274.58	992.42	-0.01	322.40
77569.0	101.27	86.69	172.30	1274.58	987.46	-0.01	322.40
77769.2	101.53	86.55	168.19	1274.58	983.61	-0.01	322.40
77969.1	101.79	89.05	164.92	1274.58	708.54	-0.01	322.40
78169.3	102.05	90.18	162.14	1274.58	722.10	-0.01	322.40
78369.1	102.31	88.83	159.72	1274.58	1044.97	-0.01	322.40
78569.3	102.57	87.86	157.54	1274.58	1018.77	-0.01	322.40
78685.1	102.72	87.59	156.42	1530.10	1011.62	31.66	0.00
78885.1	102.98	87.31	204.06	1350.01	1003.96	0.59	380.81
79085.1	103.24	87.12	187.91	1288.51	998.96	0.30	332.60
79285.2	103.51	86.94	178.14	1274.51	994.14	-0.01	322.35
79485.1	103.77	86.76	172.44	1274.51	989.17	-0.01	322.35
79685.3	104.03	86.61	168.34	1274.51	985.28	-0.01	322.35
79885.2	104.29	89.12	165.06	1274.51	709.37	-0.01	322.35
80085.3	104.55	90.25	162.29	1274.51	722.96	-0.01	322.35
80285.2	104.81	88.90	159.86	1274.51	1046.77	-0.01	322.35
80485.4	105.07	87.92	157.68	1274.51	1020.47	-0.01	322.35
80601.2	105.22	87.65	156.56	1530.10	1013.28	. 31.66	0.00
80801.2	105.48	87.37	204.20	1350.25	1005.55	0.59	381.00
81001.2	105.75	87.18	188.04	1288.72	1000.54	0.30	332.77
81201.3	106.01	87.00	178.28	1274.72	995.71	-0.01	322.50
81401.2	106.27	86.82	172.57	1274.72	990.72	-0.01	322.50
81601.4	106.53	86.67	168.47	1274.72	986.81	-0.01	322.50
81801.2	106.79	89.18	165.19	1274.72	710.12	-0.01	322.50
82001.4	107.05	90.31	162.42	1274.72	723.74	-0.01	322.50
82201.3	107.31	88.96	159.99	1274.72	1048.40	-0.01	322.50
82401.5	107.57	87.98	157.81	1274.72	1022.01	-0.01	322.50
82517.3	107.72	87.71	156.68	1530.10	1014.79	31.66	0.00
82717.3	107.99	87.42	204.31	1350.15	1006.99	0.59	380.92
82917.3	108.25	87.23	188.16	1288.64	1001.97	0.30	332.70
83117.4	108.51	87.05	178.39	1274.64	997.13	-0.01	322.44
83317.3	108.77	86.87	172.69	1274.64	992.12	-0.01	322.44
83517.4	109.03	86.72	168.58	1274.64	988.19	-0.01	322.44
83717.3	109.29	89.24	165.31	1274.64	710.81	-0.01	322.44
83917.5	109.55	90.37	162.53	1274.64	724.45	-0.01	322.44
84117.4	109.81	89.01	160.10	1274.64	1049.88	-0.01	322.44
84317.5	110.08	88.03	157.92	1274.64	1023.40	-0.01	322.44
84433.3	110.23	87.76	156.80	1530.10	1016.16	31.66	0.00
84633.3	110.49	87.47	204.43	1350.21	1008.30	0.59	380.97
84833.3	110.75	87.28	188.27	1288.70	1003.26	0.30	332.74
85033.4	111.01	87.10	178.50	1274.69	998.41	-0.01	322.48
85233.3	111.27	86.91	172.80	1274.69	993.39	-0.01	322.48
85433.5	111.53	86.77	168.69	1274.69	989.44	-0.01	322.48
85633.4	111.79	89.29	165.41	1274.69	711.42	-0.01	322.48
85833.6	112.05	90.43	162.64	1274.69	725.09	-0.01	322.48
86033.4	112.32	89.06	160.21	1274.69	1051.21	-0.01	322.48
86233.6	112.58	88.08	158.02	1274.69	1024.66	-0.01	322.48
86349.4	112.73	87.81	156.90	1530.10	1017.40	31.65	0.00
86549.4	112.99	87.51	204.52	1350.21	1009.48	0.59	380.98
86749.4	113.25	87.33	188.37	1288.70	1004.44	0.30	332.75
86949.5	113.51	87.14	178.60	1274.70	999.58	-0.01	322.48

87149.4	113.77	86.96	172.90	1274.70	994.54	-0.01	322.48
87349.6	114.03	86.81	168.79	1274.70	990.57	-0.01	322.48
87549.4	114.29	89.33	165.51	1274.70	711.98	-0.01	322.48
87749.6	114.56	90.47	162.73	1274.70	725.67	-0.01	322.48
87949.5	114.82	89.11	160.30	1274.70	1052.43	-0.01	322.48
88149.7	115.08	88.12	158.12	1274.70	1025.81	-0.01	322.48
88265.5	115.23	87.85	156.99	1530.10	1018.52	31.65	0.00
88465.5	115.49	87.55	204.61	1350.22	1010.55	0.59	380.98
88665.5	115.75	87.36	188.46	1288.71	1005.50	0.30	332.76
88865.6	116.01	87.18	178.69	1274.71	1000.63	-0.01	322.49
89065.5	116.27	87.00	172.99	1274.71	995.58	-0.01	322.49
89265.6	116.53	86.85	168.88	1274.71	991.59	-0.01	322.49
89465.5	116.80	89.38	165.60	1274.71	712.49	-0.01	322.49
89665.7	117.06	90.52	162.82	1274.71	726.20	-0.01	322.49
89865.6	117.32	89.15	160.39	1274.71	1053.52	-0.01	322.49
90065.8	117.58	88.16	158.20	1274.71	1026.84	-0.01	322.49
90181.5	117.73	87.89	157.08	1530.10	1019.53	31.65	0.00
90381.5	117.99	87.59	204.70	1350.49	1011.52	0.59	381.21
90581.5	118.25	87.40	188.54	1288.97	1006.46	0.30	332.95
90781.7	118.51	87.22	178.77	1274.96	1001.58	-0.01	322.67
90981.5	118.77	87.03	173.07	1274.96	996.52	-0.01	322.67
91181.7	119.04	86.88	168.96	1274.96	992.52	-0.01	322.67
91381.6	119.30	89.41	165.67	1274.96	712.95	-0.01	322.67
91581.8	119.56	90.56	162.90	1274.96	726.67	-0.01	322.67
91781.6	119.82	89.18	160.46	1274.96	1054.51	-0.01	322.67
91981.8	120.08	88.19	158.28	1274.96	1027.78	-0.01	322.67
92097.6	120.23	87.92	157.15	1530.10	1020.45	31.65	0.00
92297.6	120.49	87.62	204.77	1350.26	1012.39	0.59	381.02
92497.6	120.75	87.43	188.61	1288.76	1007.33	0.30	332.79
92697.7	121.02	87.25	178.84	1274.75	1002.45	-0.01	322.52
92897.6	121.28	87.06	173.14	1274.75	997.37	-0.01	322.52
93097.8	121.54	86.91	169.03	1274.75	993.36	-0.01	322.52
93297.7	121.80	89.45	165.74	1274.75	713.36	-0.01	322.52
93497.8	122.06	90.59	162.96	1274.75	727.10	-0.01	322.52
93697.7	122.32	89.22	160.53	1274.75	1055.41	-0.01	322.52
93897.9	122.58	88.22	158.34	1274.75	1028.63	-0.01	322.52
94013.7	122.73	87.95	157.22	1530.10	1021.28	31.65	0.00
94213.7	122.99	87.65	204.83	1350.21	1013.19	0.59	380.98
94413.7	123.26	87.46	188.68	1288.71	1008.12	0.30	332.76
94613.8	123.52	87.28	178.91	1274.71	1003.24	-0.01	322.49
94813.7	123.78	87.09	173.20	1274.71	998.14	-0.01	322.49
95013.9	124.04	86.94	169.09	1274.71	994.12	-0.01	322.49
95213.7	124.30	89.48	165.81	1274.71	713.74	-0.01	322.49
95413.9	124.56	90.63	163.03	1274.71	727.49	-0.01	322.49
95613.8	124.82	89.25	160.60	1274.71	1056.22	-0.01	322.49
95814.0	125.08	88.25	158.41	1274.71	1029.39	-0.01	322.49
95929.7	125.23	87.98	157.28	1530.10	1022.03	31.64	0.00
96129.7	125.50	87.68	204.90	1350.52	1013.90	0.59	381.23
96329.7	125.76	87.49	188.74	1289.00	1008.83	0.30	332.97
96529.9	126.02	87.31	178.97	1274.99	1003.95	-0.01	322.70
96729.7	126.28	87.12	173.26	1274.99	998.84	-0.01	322.70
96929.9	126.54	86.97	169.15	1274.99	994.81	-0.01	322.70
97129.8	126.80	89.51	165.87	1274.99	714.08	-0.01	322.70
97330.0	127.06	90.65	163.09	1274.99	727.84	-0.01	322.70
97529.9	127.32	89.27	160.65	1274.99	1056.96	-0.01	322.70
97730.0	127.58	88.28	158.46	1274.99	1030.08	-0.01	322.70
97845.8	127.74	88.00	157.34	1530.10	1022.71	31.65	0.00
98045.8	128.00	87.70	204.94	1350.23	1014.55	0.59	380.99
98245.8	128.26	87.51	188.79	1288.73	1009.47	0.30	332.77
98445.9	128.52	87.33	179.02	1274.73	1004.59	-0.01	322.51
98645.8	128.78	87.14	173.32	1274.73	999.48	-0.01	322.51
98846.0	129.04	86.99	169.20	1274.73	995.43	-0.01	322.51
99045.9	129.30	89.53	165.92	1274.73	714.39	-0.01	322.51
99246.0	129.56	90.68	163.14	1274.73	728.16	-0.01	322.51
99445.9	129.82	89.30	160.70	1274.73	1057.63	-0.01	322.51
99646.1	130.09	88.30	158.51	1274.73	1030.72	-0.01	322.51

99761.9	130.24	88.03	157.39	1530.10	1023.32	31.64	0.00
99961.9	130.50	87.72	205.00	1350.54	1015.14	0.59	381.25
100161.9	130.76	87.53	188.84	1289.02	1010.05	0.30	332.99
100362.0	131.02	87.35	179.07	1275.01	1005.15	-0.01	322.71
100561.9	131.28	87.16	173.37	1275.01	1000.03	-0.01	322.71
100762.1	131.54	87.01	169.25	1275.01	995.97	-0.01	322.71
100961.9	131.80	89.56	165.97	1275.01	714.66	-0.01	322.71
101162.1	132.07	90.70	163.19	1275.01	728.44	-0.01	322.71
101362.0	132.33	89.32	160.75	1275.01	1058.21	-0.01	322.71
101562.2	132.59	88.32	158.56	1275.01	1031.27	-0.01	322.71
101678.0	132.74	88.05	157.44	1530.10	1023.87	31.65	0.00
101878.0	133.00	87.74	205.04	1350.27	1015.66	0.59	381.02
102078.0	133.26	87.55	188.88	1288.77	1010.56	0.30	332.80
102278.1	133.52	87.37	179.11	1274.76	1005.66	-0.01	322.53
102478.0	133.78	87.18	173.41	1274.76	1000.52	-0.01	322.53
102678.1	134.04	87.03	169.29	1274.76	996.46	-0.01	322.53
102878.0	134.31	89.58	166.01	1274.76	714.90	-0.01	322.53
103078.2	134.57	90.73	163.23	1274.76	728.69	-0.01	322.53
103278.1	134.83	89.34	160.79	1274.76	1058.73	-0.01	322.53
103478.2	135.09	88.34	158.60	1274.76	1031.76	-0.01	322.53
103594.0	135.24	88.06	157.48	1530.10	1024.35	31.64	0.00
103794.0	135.50	87.76	205.08	1350.37	1016.12	0.59	381.10
103994.0	135.76	87.57	188.93	1288.86	1011.01	0.30	332.87
104194.1	136.02	87.39	179.15	1274.85	1006.10	-0.01	322.60
104394.0	136.28	87.20	173.45	1274.85	1000.95	-0.01	322.60
104594.2	136.55	87.04	169.33	1274.85	996.88	-0.01	322.60
104794.1	136.81	89.59	166.05	1274.85	715.11	-0.01	322.60
104994.3	137.07	90.74	163.27	1274.85	728.91	-0.01	322.60
105194.1	137.33	89.36	160.83	1274.85	1059.19	-0.01	322.60
105394.3	137.59	88.36	158.64	1274.85	1032.20	-0.01	322.60
105510.1	137.74	88.08	157.51	1530.10	1024.78	31.64	0.00
105710.1	138.00	87.77	205.12	1350.50	1016.53	0.59	381.21
105910.1	138.26	87.58	188.96	1288.98	1011.41	0.30	332.95
106110.2	138.53	87.40	179.19	1274.97	1006.49	-0.01	322.68
106310.1	138.79	87.21	173.48	1274.97	1001.34	-0.01	322.68
106510.3	139.05	87.06	169.37	1274.97	997.27	-0.01	322.68
106710.1	139.31	89.61	166.08	1274.97	715.30	-0.01	322.68
106910.3	139.57	90.76	163.30	1274.97	729.11	-0.01	322.68
107110.2	139.83	89.37	160.86	1274.97	1059.61	-0.01	322.68
107310.4	140.09	88.37	158.67	1274.97	1032.59	-0.01	322.68
107426.2	140.24	88.10	157.55	1530.10	1025.16	31.64	0.00
107626.2	140.50	87.79	205.15	1350.40	1016.90	0.59	381.13
107826.2	140.77	87.60	188.99	1288.89	1011.77	0.30	332.89
108026.3	141.03	87.41	179.22	1274.89	1006.84	-0.01	322.62
108226.2	141.29	87.22	173.51	1274.89	1001.69	-0.01	322.62
108426.3	141.55	87.07	169.40	1274.89	997.61	-0.01	322.62
108626.2	141.81	89.62	166.11	1274.89	715.47	-0.01	322.62
108826.4	142.07	90.78	163.33	1274.89	729.28	-0.01	322.62
109026.3	142.33	89.39	160.89	1274.89	1059.98	-0.01	322.62
109226.5	142.59	88.38	158.70	1274.89	1032.94	-0.01	322.62
109342.2	142.74	88.11	157.58	1530.10	1025.51	31.64	0.00
109542.2	143.01	87.80	205.17	1350.27	1017.23	0.59	381.03
109742.2	143.27	87.61	189.02	1288.78	1012.09	0.30	332.81
109942.4	143.53	87.43	179.25	1274.78	1007.15	-0.01	322.54
110142.2	143.79	87.23	173.54	1274.78	1002.00	-0.01	322.54
110342.4	144.05	87.08	169.42	1274.78	997.91	-0.01	322.54
110542.3	144.31	89.64	166.14	1274.78	715.62	-0.01	322.54
110742.5	144.57	90.79	163.36	1274.78	729.44	-0.01	322.54
110942.3	144.83	89.40	160.92	1274.78	1060.31	-0.01	322.54
111142.5	145.09	88.40	158.73	1274.78	1033.25	-0.01	322.54
111258.3	145.25	88.12	157.60	1530.10	1025.81	31.64	0.00
111458.3	145.51	87.81	205.20	1350.49	1017.53	0.59	381.20
111658.3	145.77	87.62	189.05	1288.97	1012.38	0.30	332.95
111858.4	146.03	87.44	179.27	1274.97	1007.43	-0.01	322.68
112058.3	146.29	87.24	173.57	1274.97	1002.27	-0.01	322.68
112258.5	146.55	87.09	169.45	1274.97	998.18	-0.01	322.68

112458.4	146.81	89.65	166.17	1274.97	715.75	-0.01	322.68
112658.5	147.07	90.80	163.38	1274.97	729.58	-0.01	322.68
112858.4	147.33	89.41	160.94	1274.97	1060.60	-0.01	322.68
113058.6	147.60	88.41	158.75	1274.97	1033.53	-0.01	322.68
113174.4	147.75	88.13	157.63	1530.10	1026.09	31.64	0.00
113374.4	148.01	87.82	205.22	1350.56	1017.79	0.59	381.26
113574.4	148.27	87.63	189.07	1289.04	1012.64	0.30	333.00
113774.5	148.53	87.45	179.30	1275.03	1007.68	-0.01	322.73
113974.4	148.79	87.25	173.59	1275.03	1002.52	-0.01	322.73
114174.6	149.05	87.10	169.47	1275.03	998.43	-0.01	322.73
114374.4	149.31	89.66	166.19	1275.03	715.88	-0.01	322.73
114574.6	149.58	90.81	163.40	1275.03	729.71	-0.01	322.73
114774.5	149.84	89.42	160.97	1275.03	1060.87	-0.01	322.73
114974.7	150.10	88.41	158.77	1275.03	1033.78	-0.01	322.73
115090.4	150.25	88.14	157.65	1530.10	1026.34	31.64	0.00
115290.4	150.51	87.83	205.25	1350.63	1018.03	0.59	381.32
115490.4	150.77	87.64	189.09	1289.11	1012.87	0.30	333.05
115690.6	151.03	87.45	179.32	1275.10	1007.91	-0.01	322.78
115890.4	151.29	87.26	173.61	1275.10	1002.74	-0.01	322.78
116090.6	151.55	87.11	169.49	1275.10	998.65	-0.01	322.78
116290.5	151.82	89.67	166.21	1275.10	715.99	-0.01	322.78
116490.7	152.08	90.82	163.42	1275.10	729.82	-0.01	322.78
116690.6	152.34	89.43	160.99	1275.10	1061.11	-0.01	322.78
116890.7	152.60	88.42	158.79	1275.10	1034.01	-0.01	322.78
117006.5	152.75	88.15	157.67	1530.10	1026.56	31.64	0.00
117206.5	153.01	87.84	205.26	1350.63	1018.24	0.59	381.32
117406.5	153.27	87.65	189.11	1289.11	1013.08	0.30	333.05
117606.6	153.53	87.46	179.34	1275.10	1008.12	-0.01	322.78
117806.5	153.79	87.27	173.63	1275.10	1002.95	-0.01	322.78
118006.7	154.06	87.12	169.51	1275.10	998.85	-0.01	322.78
118206.6	154.32	89.68	166.23	1275.10	716.09	-0.01	322.78
118406.8	154.58	90.83	163.44	1275.10	729.93	-0.01	322.78
118606.6	154.84	89.44	161.00	1275.10	1061.32	-0.01	322.78
118806.8	155.10	88.43	158.81	1275.10	1034.22	-0.01	322.78
118922.6	155.25	88.15	157.68	1530.10	1026.76	31.64	0.00
119122.6	155.51	87.85	205.28	1350.64	1018.43	0.59	381.33
119322.6	155.77	87.65	189.13	1289.11	1013.27	0.30	333.05
119522.7	156.03	87.47	179.35	1275.10	1008.30	-0.01	322.78
119722.6	156.30	87.28	173.64	1275.10	1003.13	-0.01	322.78
119922.8	156.56	87.12	169.53	1275.10	999.03	-0.01	322.78
120122.6	156.82	89.68	166.24	1275.10	716.17	-0.01	322.78
120322.8	157.08	90.84	163.46	1275.10	730.02	-0.01	322.78
120522.7	157.34	89.44	161.02	1275.10	1061.51	-0.01	322.78
120722.9	157.60	88.44	158.83	1275.10	1034.40	-0.01	322.78
120838.7	157.75	88.16	157.70	1530.10	1026.94	31.64	0.00
121038.7	158.01	87.85	205.30	1350.64	1018.60	0.59	381.33
121238.7	158.28	87.66	189.14	1289.11	1013.43	0.30	333.05
121438.8	158.54	87.47	179.37	1275.10	1008.47	-0.01	322.78
121638.7	158.80	87.28	173.66	1275.10	1003.29	-0.01	322.78
121838.8	159.06	87.13	169.54	1275.10	999.19	-0.01	322.78
122038.7	159.32	89.69	166.26	1275.10	716.25	-0.01	322.78
122238.9	159.58	90.84	163.47	1275.10	730.10	-0.01	322.78
122438.8	159.84	89.45	161.03	1275.10	1061.69	-0.01	322.78
122638.9	160.10	88.44	158.84	1275.10	1034.56	-0.01	322.78
122754.7	160.25	88.17	157.71	1530.10	1027.10	31.64	0.00
122954.7	160.52	87.86	205.31	1350.74	1018.76	0.59	381.41
123154.7	160.78	87.67	189.16	1289.21	1013.58	0.30	333.13
123354.9	161.04	87.48	179.38	1275.20	1008.61	-0.01	322.85
123554.7	161.30	87.29	173.67	1275.20	1003.44	-0.01	322.85
123754.9	161.56	87.14	169.56	1275.20	999.33	-0.01	322.85
123954.8	161.82	89.70	166.27	1275.20	716.32	-0.01	322.85
124155.0	162.08	90.85	163.48	1275.20	730.17	-0.01	322.85
124354.8	162.34	89.46	161.05	1275.20	1061.84	-0.01	322.85
124555.0	162.60	88.45	158.85	1275.20	1034.71	-0.01	322.85
124670.8	162.76	88.17	157.73	1530.10	1027.24	31.65	0.00
124870.8	163.02	87.86	205.32	1350.70	1018.90	0.59	381.38

125070.8	163.28	87.67	189.17	1289.17	1013.72	0.30	333.10
125270.9	163.54	87.49	179.39	1275.16	1008.75	-0.01	322.82
125470.8	163.80	87.29	173.68	1275.16	1003.57	-0.01	322.82
125671.0	164.06	87.14	169.57	1275.16	999.46	-0.01	322.82
125870.9	164.32	89.70	166.28	1275.16	716.39	-0.01	322.82
126071.0	164.58	90.85	163.50	1275.16	730.24	-0.01	322.82
126270.9	164.84	89.46	161.06	1275.16	1061.98	-0.01	322.82
126471.1	165.11	88.45	158.86	1275.16	1034.84	-0.01	322.82
126586.9	165.26	88.18	157.74	1530.10	1027.37	31.64	0.00
126786.9	165.52	87.87	205.33	1350.70	1019.02	0.59	381.38
126986.9	165.78	87.67	189.18	1289.17	1013.84	0.30	333.10
127187.0	166.04	87.49	179.40	1275.16	1008.87	-0.01	322.82
127386.9	166.30	87.30	173.69	1275.16	1003.68	-0.01	322.82
127587.0	166.56	87.14	169.58	1275.16	999.58	-0.01	322.82
127786.9	166.82	89.71	166.29	1275.16	716.45	-0.01	322.82
127987.1	167.08	90.86	163.51	1275.16	730.30	-0.01	322.82
128187.0	167.35	89.47	161.07	1275.16	1062.10	-0.01	322.82
128387.2	167.61	88.46	158.87	1275.16	1034.96	-0.01	322.82
128502.9	167.76	88.18	157.75	1530.10	1027.49	31.64	0:00
128702.9	168.02	87.87	205.34	1350.66	1019.13	0.59	381.35
128902.9	168.28	87.68	189.19	1289.14	1013.95	0.30	333.07
129103.1	168.54	87.49	179.41	1275.13	1008.98	-0.01	322.80
129302.9	168.80	87.30	173.70	1275.13	1003.79	-0.01	322.80
129503.1	169.06	87.15	169.59	1275.13	999.68	-0.01	322.80
129703.0	169.33	89.71	166.30	1275.13	716.50	-0.01	322.80
129903.2	169.59	90.86	163.51	1275.13	730.35	-0.01	322.80
130103.0	169.85	89.47	161.08	1275.13	1062.21	-0.01	322.80
130303.2	170.11	88.46	158.88	1275.13	1035.06	-0.01	322.80
130419.0	170.26	88.19	157.76	1530.10	1027.59	31.64	0.00
130619.0	170.52	87.87	205.35	1350.59	1019.23	0.59	381.29
130819.0	170.78	87.68	189.20	1289.07	1014.04	0.30	333.02
131019.1	171.04	87.50	179.42	1275.06	1009.07	-0.01	322.75
131219.0	171.30	87.31	173.80	1275.06	1003.97	-0.01	322.75
131419.0	171.57	87.16	169.76	1275.06	999.92	-0.01	322.75
131619.0	171.83	89.61	166.51	1275.06	715.24	-0.01	322.75
131819.0	172.09	90.78	163.77	1275.06	729.35	-0.01	322.75
132019.0	172.35	89.74	161.36	1275.06	1069.54	-0.01	322.75
132219.0	172.61	88.55	159.20	1275.06	1037.53	-0.01	322.75
132367.5	172.80	88.19	157.76	1530.10	1027.68	31.64	0.00
132567.5	173.06	87.44	177.58	1275.07	1007.63	-0.01	322.75
132767.5	173.33	87.26	172.56	1275.07	1002.79	-0.01	322.75
132967.5	173.59	87.30	168.79	1275.07	687.47	-0.01	322.75
133167.5	173.85	90.01	165.71	1275.07	720.09	-0.01	322.75
133367.5	174.11	91.03	163.07	1275.07	732.35	-0.01	322.75
133567.5	174.37	89.22	160.74	1275.07	1055.45	-0.01	322.75
133767.5	174.63	88.40	158.63	1275.07	1033.31	-0.01	322.75
133859.7	174.75	88.19	157.77	1530.10	1027.76	31.64	0.00
134059.7	175.01	87.45	177.58	1275.07	1007.70	-0.01	322.75
134259.7	175.27	87.27	172.57	1275.07	1002.86	-0.01	322.75
134459.7	175.53	87.31	168.79	1275.07	687.50	-0.01	322.75
134659.7	175.80	90.01	165.71	1275.07	720.13	-0.01	322.75
134859.7	176.06	91.03	163.08	1275.07	732.39	-0.01	322.75
135059.7	176.32	89.22	160.74	1275.07	1055.53	-0.01	322.75
135259.7	176.58	88.40	158.64	1275.07	1033.39	-0.01	322.75
135351.8	176.70	88.19	157.78	1530.10	1027.84	31.64	0.00
135551.8	176.96	87.45	177.59	1275.07	1007.77	-0.01	322.75
135751.8	177.22	87.27	172.57	1275.07	1002.93	-0.01	322.75
135951.8	177.48	87.31	168.80	1275.07	687.53	-0.01	322.75
136151.8	177.74	90.02	165.72	1275.07	720.16	-0.01	322.75
136351.8	178.01	91.04	163.08	1275.07	732.42	-0.01	322.75
136551.8	178.27	89.22	160.75	1275.07	1055.60	-0.01	322.75
136751.8	178.53	88.40	158.64	1275.07	1033.46	-0.01	322.75
136844.0	178.65	88.20	157.78	1530.10	1027.90	31.64	0.00
137044.0	178.91	87.45	177.60	1275.07	1007.83	-0.01	322.75
137244.0	179.17	87.27	172.58	1275.07	1002.99	-0.01	322.75
137444.0	179.43	87.31	168.81	1275.07	687.56	-0.01	322.75

137644.0	179.69	90.02	165.73	1275.07	720.19	-0.01	322.75
137844.0	179.95	91.04	163.09	1275.07	732.45	-0.01	322.75
138044.0	180.21	89.23	160.75	1275.07	1055.66	-0.01	322.75
138244.0	180.48	88.40	158.65	1275.07	1033.52	-0.01	322.75
138336.2	180.60	88.20	157.79	1530.10	1027.96	31.64	0.00
138536.2	180.86	87.45	177.60	1275.15	1007.89	-0.01	322.81
138736.2	181.12	87.27	172.58	1275.15	1003.04	-0.01	322.81
138936.2	181.38	87.31	168.81	1275.15	687.58	-0.01	322.81
139136.2	181.64	90.02	165.73	1275.15	720.22	-0.01	322.81
139336.2	181.90	91.04	163.09	1275.15	732.48	-0.01	322.81
139536.2	182.16	89.23	160.76	1275.15	1055.72	-0.01	322.81
139736.2	182.42	88.41	158.65	1275.15	1033.57	-0.01	322.81
139828.4	182.54	88.20	157.79	1530.10	1028.01	31.64	0.00
140028.4	182.80	87.45	177.60	1275.15	1007.93	-0.01	322.81
140228.4	183.07	87.27	172.59	1275.15	1003.09	-0.01	322.81
140428.4	183.33	87.32	168.81	1275.15	687.60	-0.01	322.81
140628.4	183.59	90.02	165.73	1275.15	720.24	-0.01	322.81
140828.4	183.85	91.04	163.10	1275.15	732.50	-0.01	322.81
141028.4	184.11	89.23	160.76	1275.15	1055.77	-0.01	322.81
141228.4	184.37	88.41	158.66	1275.15	1033.62	-0.01	322.81
141320.6	184.49	88.20	157.80	1530.10	1028.06	31.64	0.00
141520.6	184.75	87.46	177.61	1275.15	1007.98	-0.01	322.81
141720.6	185.01	87.28	172.59	1275.15	1003.13	-0.01	322.81
141920.6	185.27	87.32	168.82	1275.15	687.62	-0.01	322.81
142120.6	185.54	90.02	165.74	1275.15	720.26	-0.01	322.81
142320.6	185.80	91.05	163.10	1275.15	732.52	-0.01	322.81
142520.6	186.06	89.23	160.77	1275.15	1055.81	-0.01	322.81
142720.6	186.32	88.41	158.66	1275.15	1033.66	-0.01	322.81
142812.8	186.44	88.20	157.80	1530.10	1028.10	31.64	0.00
143012.8	186.70	87.46	177.61	1275.20	1008.01	-0.01	322.85
143212.8	186.96	87.28	172.59	1275.20	1003.17	-0.01	322.85
143412.8	187.22	87.32	168.82	1275.20	687.64	-0.01	322.85
143612.8	187.48	90.03	165.74	1275.20	720.28	-0.01	322.85
143812.8	187.75	91.05	163.10	1275.20	732.54	-0.01	322.85
144012.8	188.01	89.23	160.77	1275.20	1055.85	-0.01	322.85
144212.8	188.27	88.41	158.66	1275.20	1033.70	-0.01	322.85
144305.0	188.39	88.21	157.80	1530.10	1028.14	31.64	0.00
144505.0	188.65	87.46	177.62	1275.20	1008.05	-0.01	322.85
144705.0	188.91	87.28	172.60	1275.20	1003.20	-0.01	322.85
144905.0	189.17	87.32	168.83	1275.20	687.65	-0.01	322.85
145105.0	189.43	90.03	165.75	1275.20	720.30	-0.01	322.85
145305.0	189.69	91.05	163.11	1275.20	732.56	-0.01	322.85
145505.0	189.95	89.23	160.77	1275.20	1055.89	-0.01	322.85
145705.0	190.22	88.41	158.67	1275.20	1033.73	-0.01	322.85
145797.2	190.34	88.21	157.81	1530.10	1028.17	31.64	0.00
145997.2	190.60	87.46	177.62	1275.20	1008.08	-0.01	322.85
146197.2	190.86	87.28	172.60	1275.20	1003.23	-0.01	322.85
146397.2	191.12	87.32	168.83	1275.20	687.67	-0.01	322.85
146597.2	191.38	90.03	165.75	1275.20	720.31	-0.01	322.85
146797.2	191.64	91.05	163.11	1275.20	732.58	-0.01	322.85
146997.2	191.90	89.24	160.78	1275.20	1055.92	-0.01	322.85
147197.2	192.16	88.41	158.67	1275.20	1033.76	-0.01	322.85
147289.3	192.28	88.21	157.81	1530.10	1028.20	31.64	0.00
147489.3	192.54	87.46	177.62	1275.20	1008.11	-0.01	322.85
147689.3	192.81	87.28	172.60	1275.20	1003.26	-0.01	322.85
147889.3	193.07	87.32	168.83	1275.20	687.68	-0.01	322.85
148089.3	193.33	90.03	165.75	1275.20	720.32	-0.01	322.85
148289.3	193.59	91.05	163.11	1275.20	732.59	-0.01	322.85
148489.3	193.85	89.24	160.78	1275.20	1055.95	-0.01	322.85
148689.3	194.11	88.42	158.67	1275.20	1033.79	-0.01	322.85
148781.5	194.23	88.21	157.81	1530.10	1028.23	31.64	0.00
148981.5	194.49	87.46	177.62	1275.20	1008.13	-0.01	322.85
149181.5	194.75	87.28	172.60	1275.20	1003.28	-0.01	322.85
149381.5	195.02	87.32	168.83	1275.20	687.69	-0.01	322.85
149581.5	195.28	90.03	165.75	1275.20	720.34	-0.01	322.85
149781.5	195.54	91.05	163.11	1275.20	732.60	-0.01	322.85

149981.5	195.80	89.24	160.78	1275.20	1055.98	-0.01	322.85
150181.5	196.06	88.42	158.67	1275.20	1033.81	-0.01	322.85
150273.7	196.18	88.21	157.81	1530.10	1028.25	31.64	0.00
150473.7	196.44	87.46	177.62	1275.21	1008.16	-0.01	322.85
150673.7	196.70	87.28	172.61	1275.21	1003.31	-0.01	322.85
150873.7	196.96	87.32	168.83	1275.21	687.70	-0.01	322.85
151073.7	197.22	90.03	165.75	1275.21	720.35	-0.01	322.85
151273.7	197.49	91.05	163.11	1275.21	732.61	-0.01	322.85
151473.7	197.75	89.24	160.78	1275.21	1056.00	-0.01	322.85
151673.7	198.01	88.42	158.67	1275.21	1033.84	-0.01	322.85
151765.9	198.13	88.21	157.82	1530.10	1028.28	31.64	0.00
151965.9	198.39	87.46	177.63	1275.21	1008.17	-0.01	322.85
152165.9	198.65	87.28	172.61	1275.21	1003.33	-0.01	322.85
152365.9	198.91	87.32	168.84	1275.21	687.71	-0.01	322.85
152565.9	199.17	90.03	165.76	1275.21	720.36	-0.01	322.85
152765.9	199.43	91.05	163.12	1275.21	732.62	-0.01	322.85
152965.9	199.69	89.24	160.78	1275.21	1056.02	-0.01	322.85
153165.9	199.96	88.42	158.68	1275.21	1033.86	-0.01	322.85
153258.1	200.08	88.21	157.82	1530.10	1028.30	31.64	0.00
153458.1	200.34	87.46	177.63	1275.21	1008.19	-0.01	322.85
153658.1	200.60	87.28	172.61	1275.21	1003.34	-0.01	322.85
153858.1	200.86	87.32	168.84	1275.21	687.71	-0.01	322.85
154058.1	201.12	90.03	165.76	1275.21	720.37	-0.01	322.85
154258.1	201.38	91.05	163.12	1275.21	732.63	-0.01	322.85
154458.1	201.64	89.24	160.78	1275.21	1056.04	-0.01	322.85
154658.1	201.90	88.42	158.68	1275.21	1033.87	-0.01	322.85
154750.3	202.02	88.21	157.82	1530.10	1028.31	31.64	0.00
154950.3	202.28	87.47	177.63	1275.21	1008.21	-0.01	322.85
155150.3	202.55	87.28	172.61	1275.21	1003.36	-0.01	322.85
155350.3	202.81	87.33	168.84	1275.21	687.72	-0.01	322.85
155550.3	203.07	90.03	165.76	1275.21	720.37	-0.01	322.85
155750.3	203.33	91.05	163.12	1275.21	732.64	-0.01	322.85
155950.3	203.59	89.24	160.79	1275.21	1056.05	-0.01	322.85
156150.3	203.85	88.42	158.68	1275.21	1033.89	-0.01	322.85
156242.5	203.97	88.21	157.82	1530.10	1028.33	31.64	0.00
156442.5	204.23	87.47	177.63	1275.21	1008.22	-0.01	322.85
156642.5	204.49	87.29	172.61	1275.21	1003.37	-0.01	322.85
156842.5	204.76	87.33	168.84	1275.21	687.73	-0.01	322.85
157042.5	205.02	90.03	165.76	1275.21	720.38	-0.01	322.85
157242.5	205.28	91.06	163.12	1275.21	732.65	-0.01	322.85
157442.5	205.54	89.24	160.79	1275.21	1056.07	-0.01	322.85
157642.5	205.80	88.42	158.68	1275.21	1033.90	-0.01	322.85
157734.7	205.92	88.21	157.82	1530.10	1028.34	31.64	0.00
157934.7	206.18	87.47	177.63	1275.21	1008.23	-0.01	322.85
158134.7	206.44	87.29	172.61	1275.21	1003.39	-0.01	322.85
158334.7	206.70	87.33	168.84	1275.21	687.73	-0.01	322.85
158534.7	206.96	90.03	165.76	1275.21	720.39	-0.01	322.85
158734.7	207.23	91.06	163.12	1275.21	732.65	-0.01	322.85
158934.7	207.49	89.24	160.79	1275.21	1056.08	-0..01	322.85
159134.7	207.75	88.42	158.68	1275.21	1033.91	-0.01	322.85
159226.8	207.87	88.21	157.82	1530.10	1028.35	31.64	0.00
159426.8	208.13	87.47	177.63	1275.21	1008.25	-0.01	322.85
159626.8	208.39	87.29	172.61	1275.21	1003.40	-0.01	322.85
159826.8	208.65	87.33	168.84	1275.21	687.74	-0.01	322.85
160026.8	208.91	90.03	165.76	1275.21	720.39	-0.01	322.85
160226.8	209.17	91.06	163.12	1275.21	732.66	-0.01	322.85
160426.8	209.43	89.24	160.79	1275.21	1056.09	-0.01	322.85
160626.8	209.70	88.42	158.68	1275.21	1033.93	-0.01	322.85
160719.0	209.82	88.21	157.82	1530.10	1028.36	31.64	0.00
160919.0	210.08	87.47	177.63	1275.21	1008.26	-0.01	322.85
161119.0	210.34	87.29	172.61	1275.21	1003.41	-0.01	322.85
161319.0	210.60	87.33	168.84	1275.21	687.74	-0.01	322.85
161519.0	210.86	90.04	165.76	1275.21	720.40	-0.01	322.85
161719.0	211.12	91.06	163.12	1275.21	732.67	-0.01	322.85
161919.0	211.38	89.24	160.79	1275.21	1056.10	-0.01	322.85
162119.0	211.64	88.42	158.68	1275.21	1033.94	-0.01	322.85

162211.2	211.76	88.21	157.82	1530.10	1028.37	31.64	0.00
162411.2	212.03	87.47	177.63	1275.21	1008.26	-0.01	322.85
162611.2	212.29	87.29	172.62	1275.21	1003.41	-0.01	322.85
162811.2	212.55	87.33	168.84	1275.21	687.75	-0.01	322.85
163011.2	212.81	90.04	165.76	1275.21	720.40	-0.01	322.85
163211.2	213.07	91.06	163.12	1275.21	732.67	-0.01	322.85
163411.2	213.33	89.24	160.79	1275.21	1056.11	-0.01	322.85
163611.2	213.59	88.42	158.68	1275.21	1033.94	-0.01	322.85
163703.4	213.71	88.21	157.82	1530.10	1028.38	31.64	0.00
163903.4	213.97	87.47	177.63	1275.21	1008.27	-0.01	322.85
164103.4	214.23	87.29	172.62	1275.21	1003.42	-0.01	322.85
164303.4	214.50	87.33	168.84	1275.21	687.75	-0.01	322.85
164503.4	214.76	90.04	165.76	1275.21	720.41	-0.01	322.85
164703.4	215.02	91.06	163.13	1275.21	732.67	-0.01	322.85
164903.4	215.28	89.24	160.79	1275.21	1056.12	-0.01	322.85
165103.4	215.54	88.42	158.68	1275.21	1033.95	-0.01	322.85
165195.6	215.66	88.22	157.82	1530.10	1028.39	31.64	0.00
165395.6	215.92	87.47	177.64	1275.21	1008.28	-0.01	322.85
165595.6	216.18	87.29	172.62	1275.21	1003.43	-0.01	322.85
165795.6	216.44	87.33	168.85	1275.21	687.75	-0.01	322.85
165995.6	216.70	90.04	165.76	1275.21	720.41	-0.01	322.85
166195.6	216.97	91.06	163.13	1275.21	732.68	-0.01	322.85
166395.6	217.23	89.24	160.79	1275.21	1056.13	-0.01	322.85
166595.6	217.49	88.42	158.68	1275.21	1033.96	-0.01	322.85
166687.8	217.61	88.22	157.83	1530.10	1028.40	31.64	0.00
166887.8	217.87	87.47	177.64	1275.21	1008.29	-0.01	322.85
167087.8	218.13	87.29	172.62	1275.21	1003.44	-0.01	322.85
167287.8	218.39	87.33	168.85	1275.21	687.75	-0.01	322.85
167487.8	218.65	90.04	165.77	1275.21	720.41	-0.01	322.85
167687.8	218.91	91.06	163.13	1275.21	732.68	-0.01	322.85
167887.8	219.17	89.24	160.79	1275.21	1056.13	-0.01	322.85
168087.8	219.44	88.42	158.69	1275.21	1033.96	-0.01	322.85
168180.0	219.56	88.22	157.83	1530.10	1028.40	31.64	0.00
168380.0	219.82	87.47	177.64	1275.21	1008.29	-0.01	322.85
168580.0	220.08	87.29	172.62	1275.21	1003.44	-0.01	322.85
168780.0	220.34	87.33	168.85	1275.21	687.76	-0.01	322.85
168980.0	220.60	90.04	165.77	1275.21	720.41	-0.01	322.85
169180.0	220.86	91.06	163.13	1275.21	732.68	-0.01	322.85
169380.0	221.12	89.24	160.79	1275.21	1056.14	-0.01	322.85
169580.0	221.38	88.42	158.69	1275.21	1033.97	-0.01	322.85
169672.2	221.50	88.22	157.83	1530.10	1028.41	31.64	0.00
169872.2	221.77	87.47	177.64	1275.21	1008.30	-0.01	322.85
170072.2	222.03	87.29	172.62	1275.21	1003.45	-0.01	322.85
170272.2	222.29	87.33	168.85	1275.21	687.76	-0.01	322.85
170472.2	222.55	90.04	165.77	1275.21	720.42	-0.01	322.85
170672.2	222.81	91.06	163.13	1275.21	732.69	-0.01	322.85
170872.2	223.07	89.24	160.79	1275.21	1056.15	-0.01	322.85
171072.2	223.33	88.42	158.69	1275.21	1033.98	-0.01	322.85
171164.3	223.45	88.22	157.83	1530.10	1028.41	31.64	0.00
171364.3	223.71	87.47	177.64	1275.21	1008.30	-0.01	322.85
171564.3	223.97	87.29	172.62	1275.21	1003.45	-0.01	322.85
171764.3	224.24	87.33	168.85	1275.21	687.76	-0.01	322.85
171964.3	224.50	90.04	165.77	1275.21	720.42	-0.01	322.85
172164.3	224.76	91.06	163.13	1275.21	732.69	-0.01	322.85
172364.3	225.02	89.24	160.79	1275.21	1056.15	-0.01	322.85
172564.3	225.28	88.42	158.69	1275.21	1033.98	-0.01	322.85
172656.5	225.40	88.22	157.83	1530.10	1028.42	31.64	0.00
172856.5	225.66	87.47	177.64	1275.21	1008.31	-0.01	322.85
173056.5	225.92	87.29	172.62	1275.21	1003.45	-0.01	322.85
173256.5	226.18	87.33	168.85	1275.21	687.76	-0.01	322.85
173456.5	226.44	90.04	165.77	1275.21	720.42	-0.01	322.85
173656.5	226.71	91.06	163.13	1275.21	732.69	-0.01	322.85
173856.5	226.97	89.24	160.79	1275.21	1056.15	-0.01	322.85
174056.5	227.23	88.42	158.69	1275.21	1033.98	-0.01	322.85
174148.7	227.35	88.22	157.83	1530.10	1028.42	31.64	0.00
174348.7	227.61	87.47	177.64	1275.21	1008.31	-0.01	322.85

|							
174548.7	227.87	87.29	172.62	1275.21	1003.46	-0.01	322.85
174748.7	228.13	87.33	168.85	1275.21	687.76	-0.01	322.85
174948.7	228.39	90.04	165.77	1275.21	720.42	-0.01	322.85
175148.7	228.65	91.06	163.13	1275.21	732.69	-0.01	322.85
175348.7	228.91	89.24	160.79	1275.21	1056.16	-0.01	322.85
175548.7	229.18	88.42	158.69	1275.21	1033.99	-0.01	322.85
175640.9	229.30	88.22	157.83	1530.10	1028.43	31.64	0.00
175840.9	229.56	87.47	177.64	1275.21	1008.31	-0.01	322.85
176040.9	229.82	87.29	172.62	1275.21	1003.46	-0.01	322.85
176240.9	230.08	87.33	168.85	1275.21	687.77	-0.01	322.85
176440.9	230.34	90.04	165.77	1275.21	720.42	-0.01	322.85
176640.9	230.60	91.06	163.13	1275.21	732.69	-0.01	322.85
176840.9	230.86	89.25	160.80	1275.21	1056.16	-0.01	322.85
177040.9	231.12	88.42	158.69	1275.21	1033.99	-0.01	322.85
177133.1	231.24	88.22	157.83	1530.10	1028.43	31.64	0.00
177333.1	231.51	87.47	177.64	1275.21	1008.31	-0.01	322.85
177533.1	231.77	87.29	172.62	1275.21	1003.46	-0.01	322.85
177733.1	232.03	87.33	168.85	1275.21	687.77	-0.01	322.85
177933.1	232.29	90.04	165.77	1275.21	720.43	-0.01	322.85
178133.1	232.55	91.06	163.13	1275.21	732.70	-0.01	322.85
178333.1	232.81	89.25	160.80	1275.21	1056.16	-0.01	322.85
178533.1	233.07	88.42	158.69	1275.21	1033.99	-0.01	322.85
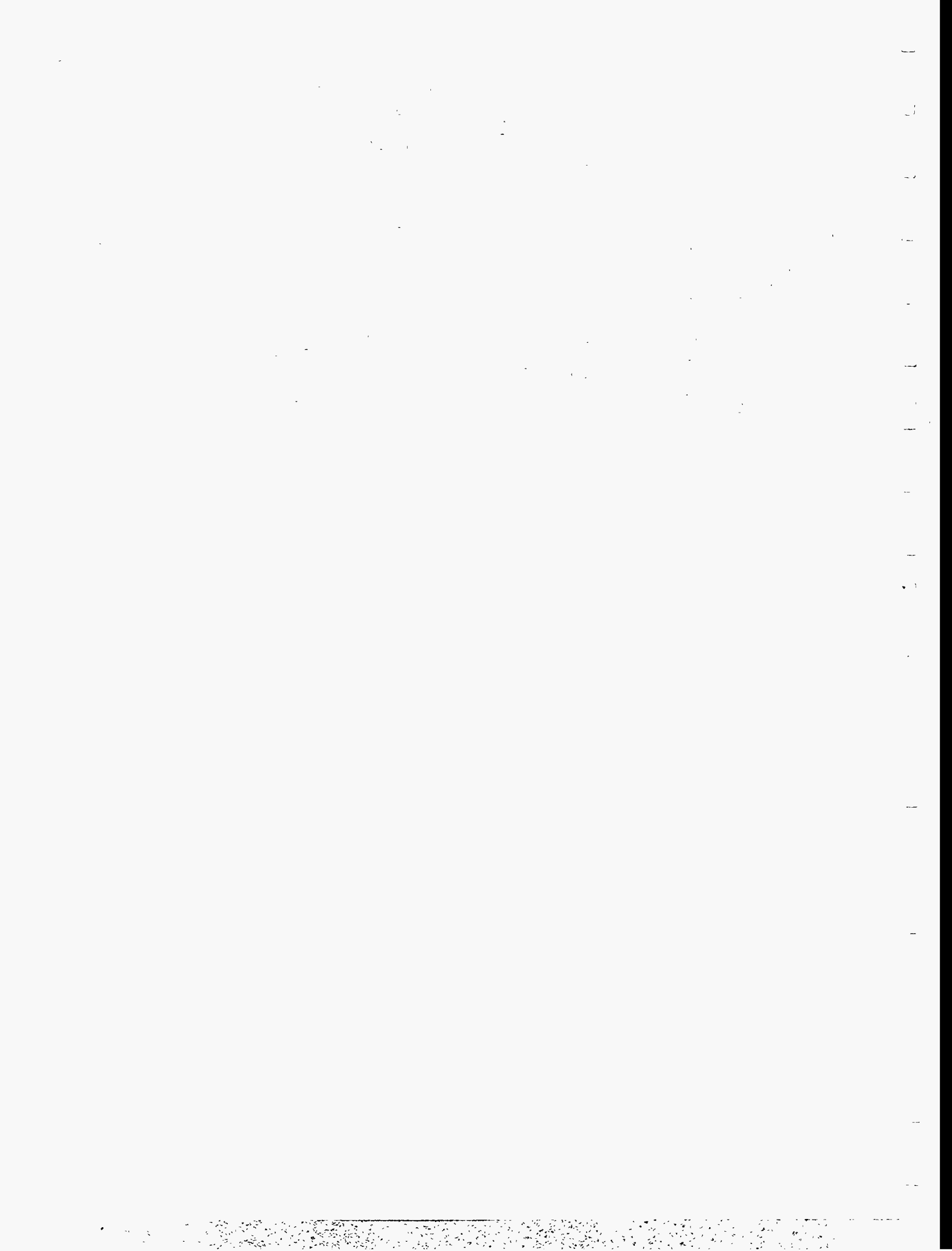
Appendix III

Experimental Plan for 12-Inch Casting
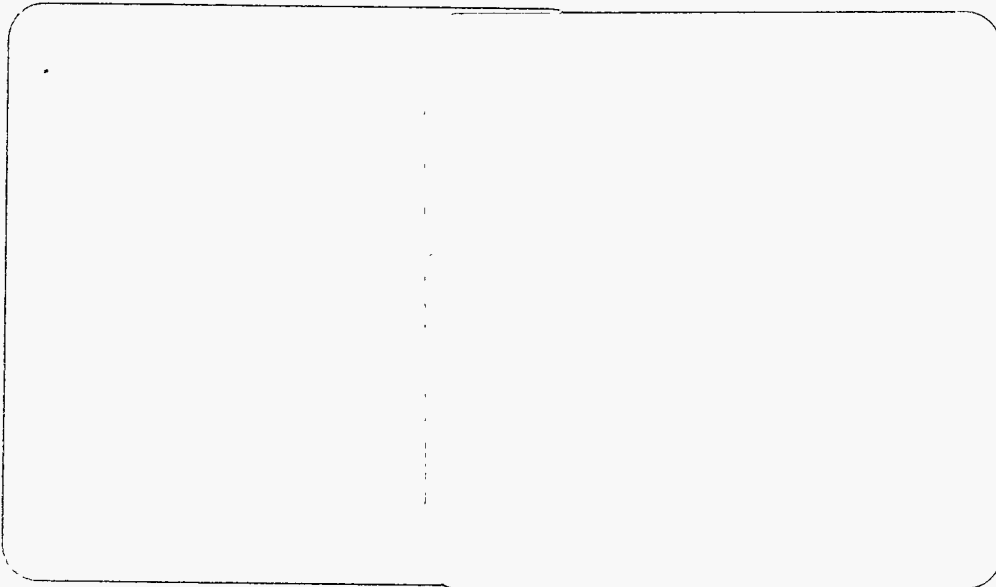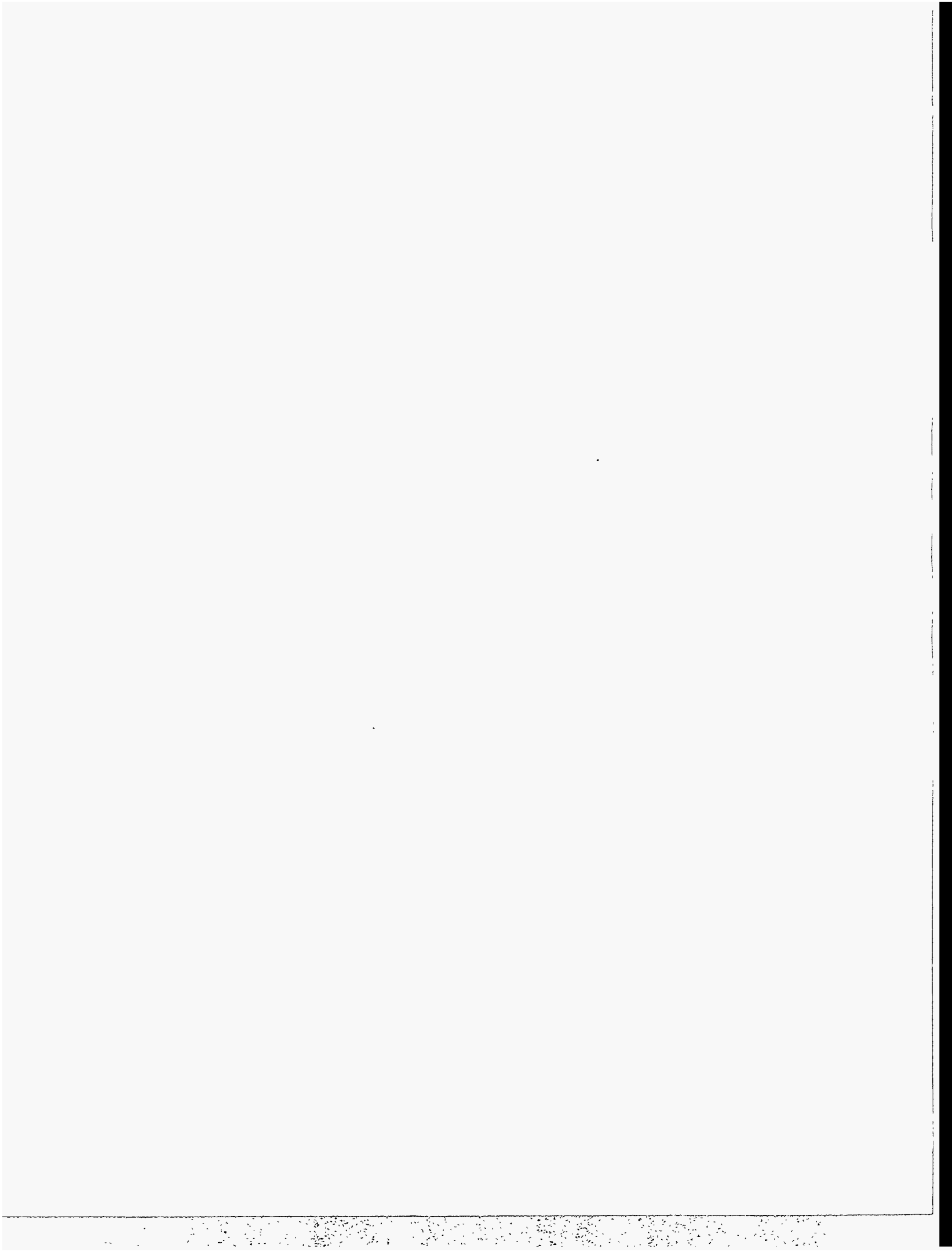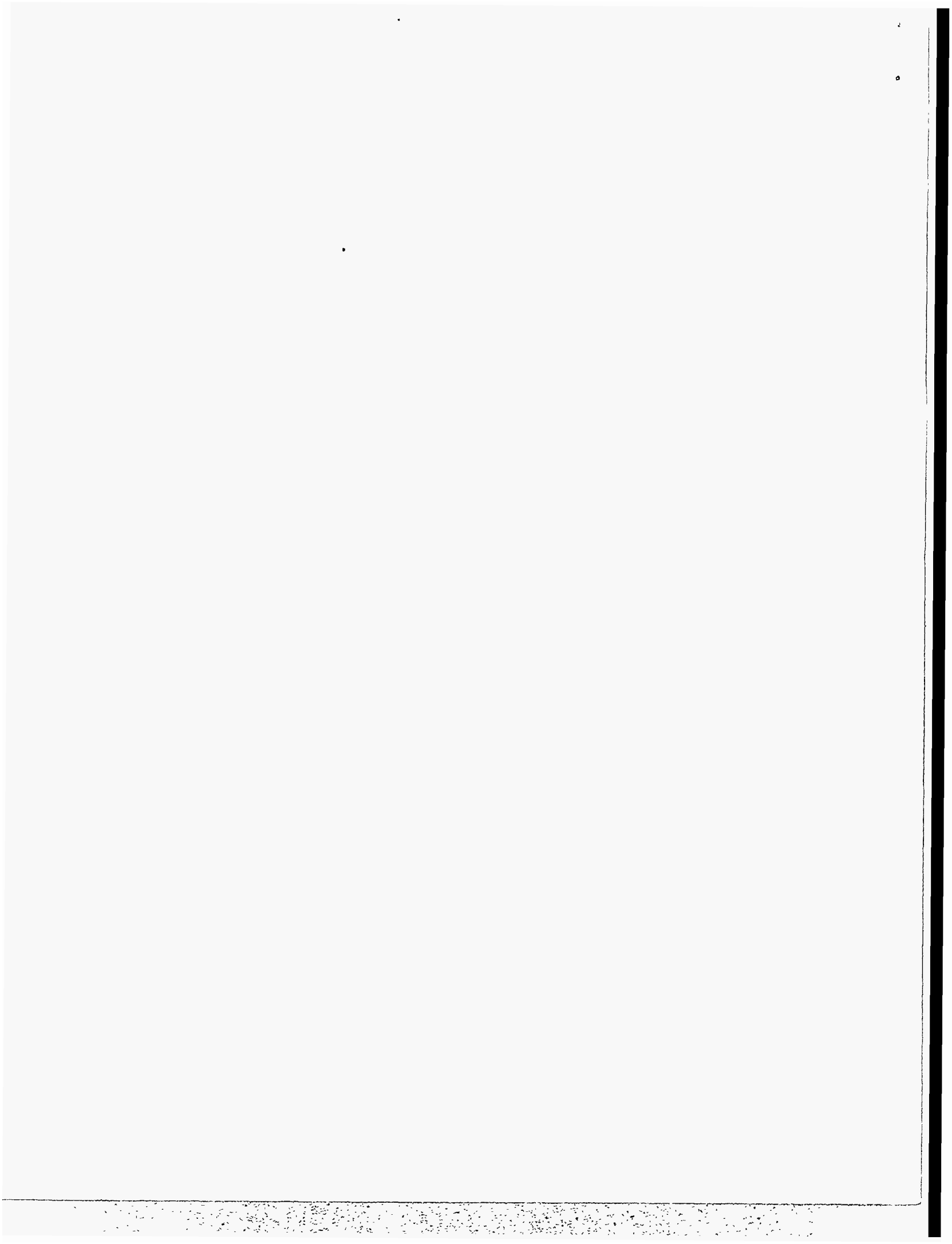
A R M C O

Research and Technology
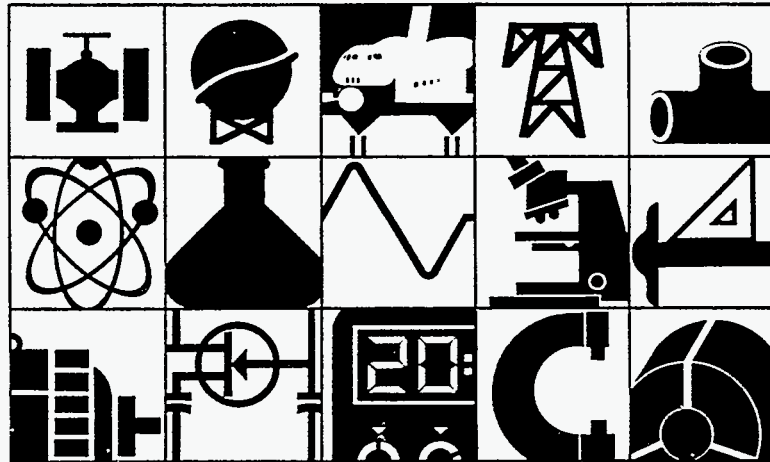
**EXPERIMENTAL PLAN
FOR 12-INCH CASTING**

April 22, 1992

R. C. Sussman, Program Manager
R. S. Willliams, Principal Investigator

Prepared for the
U.S. Department of Energy
Idaho Operation's Office
Under Federal Assistance Award
DE-FC07-92ID13086

△ ARMCO

Experimental Plan For 12 inch Casting

I.   Introduction

This report describes the experimental plan of Task 2.2 for casting twelve-inch-wide strip. The underlying experimental philosophy will first be discussed in order to establish the foundation of the plan. The goals and techniques of the main phases of the resulting program are given. Finally, the detailed plans of each phase are described in a separate section.

Process development does not generally proceed in a linear fashion, particularly in leapfrog efforts such as direct casting of steel strip. Rather, it is expected that the development will proceed in relatively abrupt steps. We see three levels of competence required for our twelve-inch casting development, which result in three separate phases for the experimental plan. These stages correspond to our experience in developing the three-inch casting capability, as well as to other major advances in steelmaking processes.

Phase I: The goal of this phase is to establish control over the basic parameters of Open Channel Casting (OCC): melt temperature and chemistry, cooling substrate, casting speed, and nozzle geometry (Fig. 1). Much of this has been accomplished in the early trial heats on the new caster but, as anticipated, refractory performance for wide nozzle designs has been a major problem. Many of our trials have been aborted due to cracking or distortion of the nozzle during preheat. Some casts have terminated early due to cracking of the nozzle. In short, we cannot maintain the desired nozzle geometry for the full trial. Achieving this capability is the objective of Phase I.

Experiments to achieve this objective will require discrete changes in nozzle geometry and refractory joint design, or more radical changes such as the use of refractory board liners. These experimental parameters are not continuous and the results (cracked or not cracked) are also of a qualitative nature which dictates a different experimental methodology from the response surface technique employed for optimization of well-established processes. The appropriate method utilizes a multiple decision tree approach in order to provide for flexibility and boldness in

design. Formal tools for this exist[*] but the direction is provided by the skillful interpretation of the results by the experimenter. The primary requirement is a means of determining the most important areas to seek improvement in order to make the next step in proficiency. Also, sufficient boldness in proposing new approaches and competence of execution are essential so that no branch of the tree is eliminated due to faulty data.

Phase II: The purpose of this phase is to establish casting parameters which consistently yield acceptable product for a full trial heat. This was the state of development for three-inch casting at the end of the last program. Qualitative changes are still required, but there are fewer branches of the decision tree, and each branch can lead to a fully statistically designed set of trials for the OCC controlling variables of speed, temperature, and melt pool depth.

Phase III: In this phase, the casting parameters which were established to produce complete casts in Phase II will be optimized using the techniques of statistically designed experiments. Experience from Phase II on the selection of viable operating parameters, will also be useful in constructing an aggressive and efficient plan of experimental trials. While the plan will constitute a systematic exploration of the controlling variables, flexibility must be maintained so that new approaches to parts of the problem, such as MFD devices in the nozzle, can be tried. It is here that many of the other tasks such as Instrumentation and Control and Mathematical Modeling are expected to be incorporated into the casting developmental trials.

---

[*]R.J. Quinlan, "Learning Efficient Classification Procedures", Chapter 15, *Machine Learning*, R.S. Michaliski, J.G. Carbonell, and T.M. Mitchell, eds., Tioga Publishing Company: Palo Alto, 1983

PLAN DETAILS

The nature of process development requires a high degree of flexibility, particularly in the early phases. The following sections will give the experimental plans for the aforementioned three phases in as much detail as is reasonable at this time. Experimental plans for work to be performed two years from now may need some modification at that time. A brief description of the current status of casting is given below.

- Good control over nozzle to substrate gap
- Good procedures to achieve desired melt chemistry, melt temperature, substrate condition and speed
- Lack of consistent nozzle geometry due to nozzle cracking and deformation during heating
- All casts terminated by early freeze-up in nozzle, apparently due to freezing started at cracks or gaps in nozzle

Our early nozzles where constructed from insulating fire brick. This material is easily formed into the desired shapes and offers superior insulating qualities. Unfortunately, the high temperature strength is low and thermal expansion during pre-heating has most often caused serious cracking and opening of joints between the nozzle segments. Improved mounting techniques and nozzle designs have reduced some of the joint opening problems, but it is clear that fire brick does not possess adequate strength to be useful for the entire nozzle design. One design using zirconia plates from fully stabilized, slide gate material, with a castable back-up lining also resulted in a major crack in the nozzle. One subsequent trial using zirconia felt glued to the face of the cracked zirconia nozzle as a gasket was very promising.

Table I gives brief results of the casting trials on the twelve inch caster to date. Problems associated with the furnace and the human errors associated with wheel positioning have been solved, so only those trials affected by nozzle performance are listed. The problems we must still overcome to achieve our first goal of reproducible trials are the effects of thermal expansion on the geometry of the nozzle refractory; specifically, the loss of fit between nozzle components to each other, and to the wheel. Also, the cracking in the inside face of the refractory in the nozzle and especially on the lip of the nozzle must be eliminated.

The results of the early casting trials are analyzed below in order to establish a Phase I experimental plan which is directed at the best candidate solutions for the most critical problems with the nozzle. Each trial ending in nozzle failure is put into one of three failure modes, Metal Leakage, Loss of Close Fit, Opening of Nozzle Joints. Possible causes for each of these failure modes have been determined. Table II relates the nozzle failures to possible causes for the twelve inch trials. In some cases, the cause was apparent, in which case the trial is listed in the appropriate row for that cause. Where more than one cause can explain the

observed mode of failure, the cast is included in the row for each candidate cause. A sum of trials is then taken for each cause, reduced by the number of multiple listings. (i.e., Trial 6 contributes one to the sum of Cracking of Nozzle Material, whereas Trial 3 contributes only one third.) This provides a means of selecting the most important factors in our failures to date, and thus some guidance as to possible areas for improvement. Table III lists these potential areas for improvement versus the causes of failure. Each improvement is given a subjective factor of 0 to 10 to estimate the impact the improvement will have on the cause of failure. The factors used are the averages given by three metal technologists who have worked most closely on the project. A figure of merit for each area is then computed by the sum of each impact, weighted by the importance of the corresponding failure mode as computed on Table II. The figure of merit of a given area for improvement is then proportional to the likelihood of improvement and to the importance of the problems addressed. This yields a ranked list to be used in planning the future experimental work of Phase I. The top four candidates: Reduce Thermal Gradient, Improved Mounting to Minimize Constraints, Abradable Refractory on Nozzle Face, and Improved Thermal Shock Resistance of Material, and Design of Joints for Strains, are all of near equal importance. Therefore, our initial plan is to develop these areas simultaneously.

A near and far term plan, based on this list, is given below. The timing is determined by the availability of materials. Note that the resulting experimental plan represents several radically different approaches to the problem all proceeding in parallel. This is the essential characteristic of Phase I.

PHASE I: Control of Casting Parameters

Near Term: (5 weeks, 5 to 8 casting trials)

- Switch to NARCO zirconia brick
- Trial using horizontal joint design with improved mounting
- Trial using zirconia felt as face gasket on nozzle
- Redesign nozzle to reduce machining requirements
- Test zirconia board for wear in molten steel
- Test zirconia felt with rigidizer as liner for firebrick and castable nozzles, use in trial if results positive

Long Term: (duration up to 18 weeks, 24 trials)
- Continue trials with pressed zirconia using larger brick as they become available
- Try shaped vacuum cast zirconia fiber parts
- Explore use of zirconia foam materials
- Continue trials with gaskets
- Employ improved preheating as available from Task 3.1
- Verify nozzle heat transfer experimentally and use as guide in setting material dimensions, joint design, preheating, and casting gap

Tools available from the other tasks include mathematical modeling of the heat transfer of the nozzle (Task 1), improved preheating of the nozzle to reduce thermal gradients (Task 3), and improved nozzle materials, including specially formulated, hot-pressed zirconia brick from NARCO (Task 4). Figure 1 gives a timeline which shows the interaction between Task 2.2 and the other parts of the strip casting program.

PHASE II: Reliable Casting Parameters

Phase II will establish a set of conditions for Open Channel Casting which will consistently yield strip for an entire cast heat. Problems with OCC casting that can prevent a full cast include freeze-off in the nozzle, tearing of strip, and loss of desired superheat. Available tools include mathematical modeling of heat transfer to substrate (Task 1.2), improved metal temperature control (Task 1.1, 3.1), modifications of nozzle geometry guided by flow visualization in nozzle (Task 1.1), improved wetting and insulating refractory properties (Task 4.0), improved gap and metal level control (Task 3.3), modifications to the substrate guided by measurements of strip and substrate temperature (Task 3.3), changes in control parameters of speed, melt temperature, metal pool height. The exact order in which the various modifications will be tried will be determined by material availability and the current analysis of the causes for failure to completely cast the heat. Improved refractories will be adopted immediately. Primary variables will be nozzle design and substrate condition.

Nozzle design parameters are:
- Weir design
- Nozzle material
- Nozzle lining and/or gasket
- Angle of attack on wheel

Substrate parameters are:
- Roughness
- Longitudinal grooving
- Transverse grooving
- In-situ dressing
- Flux Agents
- Temperature

For each basic approach (e.g., grooving of substrate, use of flux, etc.) a set of OCC parameters will be selected based on experience of previous heats, the results of the mathematical and physical modeling, and the judgment of the experimenters. A screening experiment, designed to establish confounding effects, will be performed for each approach, and will provide the results needed to determine the likelihood of success. The most promising approaches will be pursued until reliable sets of casting conditions have been established.

PHASE III: Statistically Designed Experiment to Improve Cast Thickness, and Properties

At the appropriate time the basic approach to OCC will be fixed, and a statistically designed experiment will be executed to optimize cast thickness, gauge uniformity, and cleanliness by adjustments to the primary cast variables. Primary cast parameters and likely ranges are:

Speed:	50 to 300 fpm
Superheat:	100 to 200 F
Metal Level:	1 to 6 inches
Substrate Temperature:	100 to 600 F
Substrate Condition:	(dependent on Phase II results)
Metal Chemistry:	(dependent on Task 6)

Also as part of Phase III, the steel making and handling practices will be modified to produce clean steel in order to satisfy the mechanical properties requirements of commercial quality steel strip. These changes should have no confounding effects with the casting parameters being varied above, assuming we have adequate control of melt temperature at the pouring box. The modifications will be directed at reducing the formation of oxides in the molten steel, and allowing for separation of the oxides that do form. A list of possible techniques is given below:

- Increase floatation time in the ladle
- Addition of flow controllers in the pouring box
- Improved steelmaking:
  Ladle metallurgy
  Slag practice in the furnace and ladle
- Cover molten pool in nozzle
- Shrouding of melt pool and pouring box
- Basic flux addition to pouring box
- Ceramic filters

Additionally, the use of electromagnetic devices for improved melt pool control will be explored in this phase if the results of the experimental study in Task 3.2 are promising.

WEIR DESIGN

MELT POOL HEIGHT

WEIR GAP

NOZZLE GAP

CLEAN STEEL PRACTICE

POURING BOX HEATING

MELT – CHEMISTRY
– TEMPERTURE
– SLAG CONDITIONING

NOZZLE PREHEATING-SHIELDING

WHEEL SPEED

SUBSTRATE COOLING

ANGLE OF ATTACK

NOZZLE REFRACTORY CONSTRUCTION

SUBSTRATE CONDITIONING
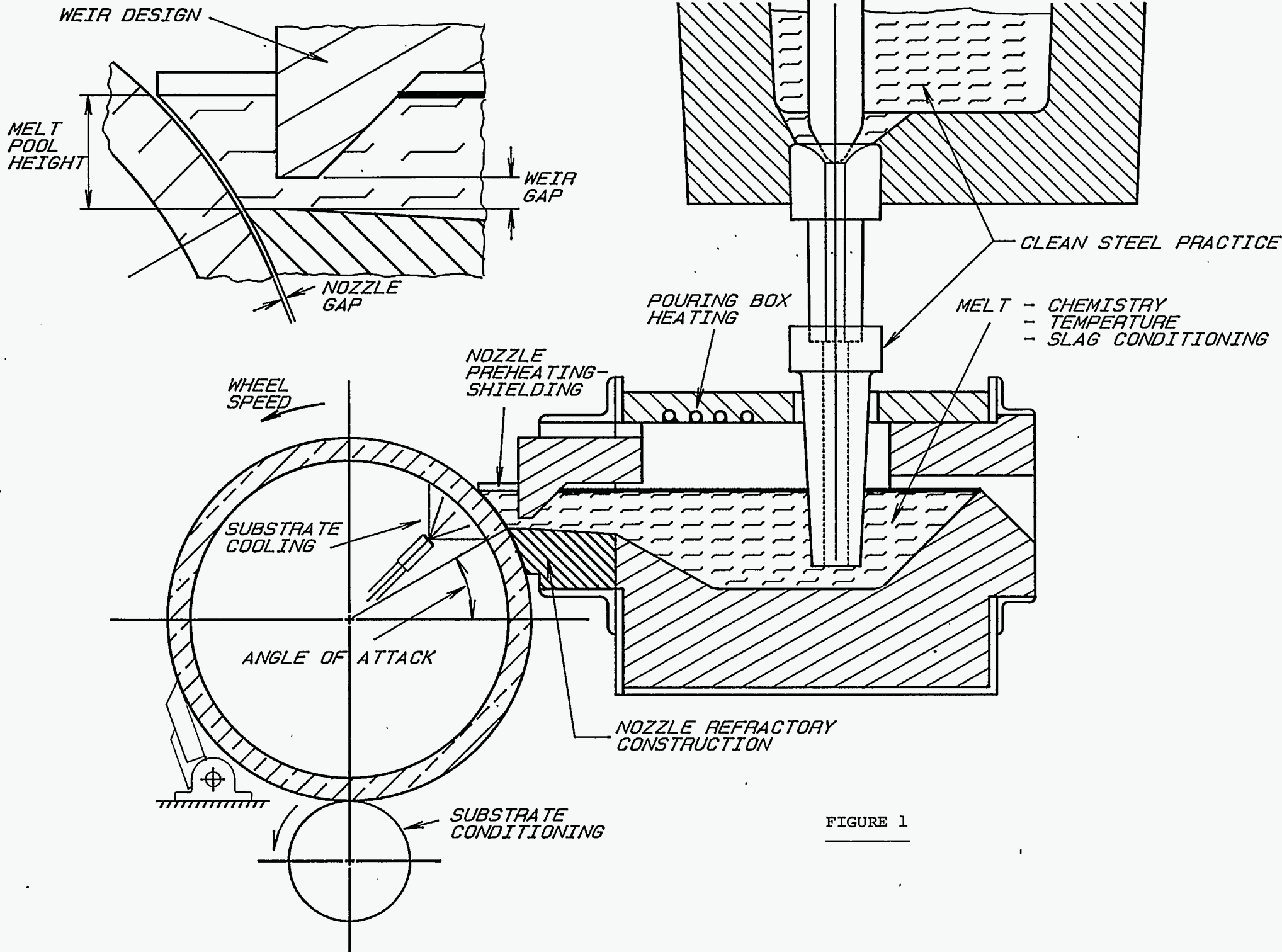
FIGURE 1

	Table I			
	Nozzle Performance on 12-Inch-Wide Casting Trials			
No.	**DATE**	**NOZZLE MATERIAL**	**RESULTS**	**CAUSES**
1	7/11/91	INSULATING FIRE BRICK	Freeze-up	joints opened
2	8/1/91	INSULATING FIRE BRICK	Freeze-up	joints opened
3	8/21/91	INSULATING FIRE BRICK	Rubbing	loss of fit
6	9/13/91	INSULATING FIRE BRICK	Abort	cracks
14	11/21/91	INSULATING FIRE BRICK	Breakout	wear
15	12/5/91	INSULATING FIRE BRICK	Abort	joints opened
16	1/13/92	INSULATING FIRE BRICK	Abort	joints opened, loss of fit
17	1/30/92	Zirconia	Abort	loss of fit
18	2/11/92	Zirconia/Felt	Freeze-up	cracks

Talbe II Number of Casting Trial Recorded by Observed Failure and Suspected Cause Nozzle Performance for Early 12-Inch-Wide Trials			
	Metal Leakage at Chips in	Loss of Close Fit to Wheel	Opening of Nozzle Joints	Weighted Totals
Cracking of Nozzle Material	6, 14, 18	3	1, 2, 15, 17	5
Uneven Thermal Expansion of Backup Material		3	2, 15	1
Unequal Thermal Expansion of Nozzle Components				
Thermal Warping of Component Surfaces		3	2, 15, 16, 17	2.5
Wear of Nozzle Surfaces by Metal	14			0.5

Talbe III

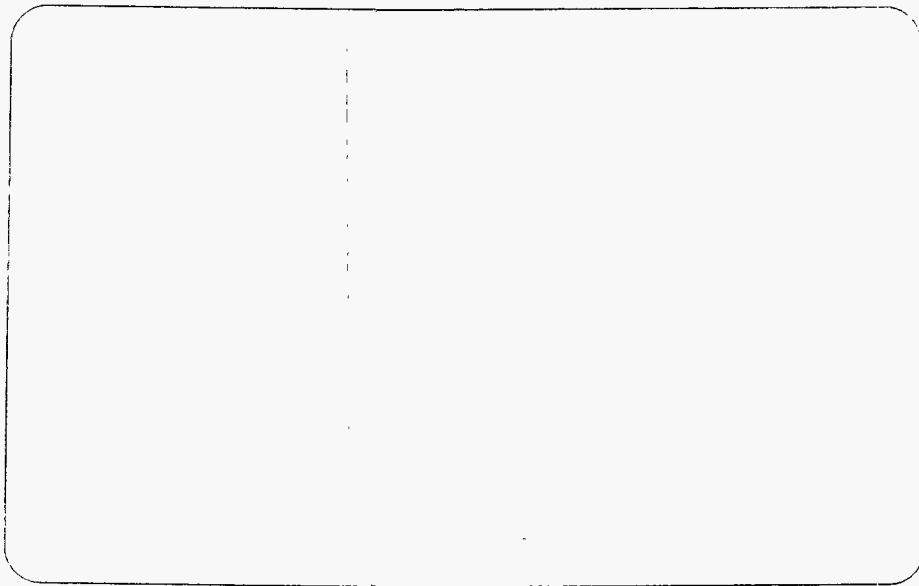### Possible Areas for Improvement of Nozzle

Number in table represents expected impact on problem.
Figure of merit weighted sum of impacts

Average RSW, RCS, DWF	Cracking	Warping	Backup Expansion	Wear	Unequal Expansion	Merit
WEIGHT	5	2.5	1	0.5	0.1	
Reduce Thermal Gradient	7.67	8.33	1.67	0.00	9.33	62
Improved Mounting to Minimize Constraints	8.00	4.33	7.67	0.00	0.67	59
Abradable Refractory on Nozzle Face	5.67	7.67	5.67	6.00	10.00	57
Improved Thermal Shock Resistance of Material	9.67	1.67	0.00	2.00	3.00	54
Design Joints for Strains	6.00	6.67	4.33	0.67	5.67	52
Reduce Expansion of Backup Material	4.33	4.33	10.00	0.33	3.67	43
Use Zirconia Material to Line Inner Surfaces	3.00	2.33	1.33	8.33	2.67	27

Appendix IV

Heat Casting Log

MELT OVERFLOW STRIP CASTING LOG

CAST NUMBER:	821	DATE:	3/11/92	TIME:	1:30 PM
HEAT WEIGHT:	1000 Lbs.	AMOUNT CAST:	¯100'	GRADE:	Si-Killed

HEAT ANALYSIS

	C	MN	SI	AL	N2	O2	S	Cu
AIM:	0.05	0.3	0.17	<.004	<.005	<.03	<.008	<.025
FINAL:	N/A	N/A	N/A	N/A	N/A	N/A	N/A	N/A

CASTING PARAMETERS

SUBSTRATE:	Normal Cu	POOL DEPTH:	2-1/2" max
SUBSTRATE FINISH:	250 u in	DAM GAP:	1"
NOZZLE POS. WRT WHEEL:	60 deg BTDC	NOZZLE WIDTH:	8.00 "
NOZZLE GAP:	0.015"	NOZZLE BRICK:	Zirconia
AUTO GAP ADJUST:	0.003	MANUFACTURE:	Narco
LADLE PREHEAT TEMP.:	1745 deg F	LOT #:	3006A
POUR BOX PREHEAT TEMP.:	2400 deg F	INITIAL CAST SPEED:	200 FPM
FURNACE TAP TEMP.:	3107 deg F	WATER IN TEMP.:	105 F
STEEL TRANS. TEMP.:	2957 deg F	WATER FLOW:	¯83 GPM
AIM CASTING TEMPERATURE:	2930 deg F	TEMP DIFFERENTIAL:	F
CAST TEMPERATURE:	2892 deg F	DEW POINT:	N/A
		SHROUD GAS:	Argon

PURPOSE OF TRIAL: Trial used a modified Ziconia nozzle brick. Bottom of nozzle was made thinner (1") to overcome problems with the brick buckling due to thermal gradients. Slightly different bottom plate to side plate joint was also used in an attempt to limit gaps openning up in the nozzle. Nozzle was backed-up with K-brick in an attempt to allow the K-brick to crush (making more room for the nozzle itself). Wheel thermocouples were reinstalled and nozzle thermocouples eliminated for this run.

RESULTS OF TRIAL: The nozzle looked excellent after preheat and the hot test obtained all four bumpers very quickly. During the cast, metal penetrated beyond the wings of the nozzle almost instantly. This metal penetration shorted the gap sensors driving the wheel away from the nozzle. The cast was aborted after only a few feet of strip were produced.

FILES: C:\DATA\03112 C:\DATA\821.XLS Heat Log 4545

MELT OVERFLOW STRIP CASTING LOG

CAST NUMBER:	823	**DATE:**	3/20/92	**TIME:**	1:15 PM
HEAT WEIGHT:	1000 Lbs.	**AMOUNT CAST:**	¯20'	**GRADE:**	Si-Killed

HEAT ANALYSIS

	C	MN	SI	AL	N2	O2	S	Cu
AIM:	0.05	0.3	0.17	<.004	<.005	<.03	<.008	<.025
FINAL:	N/A	N/A	N/A	N/A	N/A	N/A	N/A	N/A

CASTING PARAMETERS

SUBSTRATE:	Normal Cu	**POOL DEPTH:**	2-1/2" max
SUBSTRATE FINISH:	246 u in	**DAM GAP:**	1"
NOZZLE POS. WRT WHEEL:	60 deg BTDC	**NOZZLE WIDTH:**	8.00"
NOZZLE GAP:	0	**NOZZLE BRICK:**	Zirconia
AUTO GAP ADJUST:	N/A	**MANUFACTURE:**	Narco
LADLE PREHEAT TEMP.:	1780 deg F	**LOT #:**	3006B
POUR BOX PREHEAT TEMP.:	2300 deg F	**INITIAL CAST SPEED:**	200 FPM
FURNACE TAP TEMP.:	3109 deg F	**WATER IN TEMP.:**	160 F
STEEL TRANS. TEMP.:	2696 deg F	**WATER FLOW:**	¯83 GPM
AIM CASTING TEMPERATURE:	2930 deg F	**TEMP DIFFERENTIAL:**	N/A
CAST TEMPERATURE:	2570 deg F	**DEW POINT:**	N/A
		SHROUD GAS:	Argon

PURPOSE OF TRIAL: Trial was run to evaluate the zirconia brick nozzle material and to establish the ability of Krojok to work as a seal in the nozzle joints. The gap sensors were ground too close to the wheel

RESULTS OF TRIAL: Both top bumpers sounded the instant the wheel touched the nozzle. The wheel did not stay in contact with the nozzle and a steel leak developed at the wings and also at the bottom of the nozzle. The cast was aborted with only minimal amount of strip cast.

FILES: C:\DATA\CAST823.XLS   C:\DATA\HT823.XLS
Heat Log 4545

MELT OVERFLOW STRIP CASTING LOG

CAST NUMBER:	824	DATE:	3/27/92	TIME:	1:15 PM

HEAT WEIGHT:	1000 Lbs.	AMOUNT CAST:	40'	GRADE:	Si-Killed

HEAT ANALYSIS

	C	MN	SI	AL	N2	O2	S	Cu
AIM:	0.05	0.3	0.17	<.004	<.005	<.03	<.008	<.025
FINAL:	N/A	N/A	N/A	N/A	N/A	N/A	N/A	N/A

CASTING PARAMETERS

SUBSTRATE:	Normal Cu	POOL DEPTH:	2-1/2" max
SUBSTRATE FINISH:	246 u in	DAM GAP:	1"
NOZZLE POS. WRT WHEEL:	60 deg BTDC	NOZZLE WIDTH:	8.00"
NOZZLE GAP:	0	NOZZLE BRICK:	Zirconia
AUTO GAP ADJUST:	N/A	MANUFACTURE:	Narco
LADLE PREHEAT TEMP.:	1749 deg F	LOT #:	3006A
POUR BOX PREHEAT TEMP.:	2222 deg F	INITIAL CAST SPEED:	200 FPM
FURNACE TAP TEMP.:	3100 deg F	WATER IN TEMP.:	65 F
STEEL TRANS. TEMP.:	2930 deg F	WATER FLOW:	~83 GPM
AIM CASTING TEMPERATURE:	2930 deg F	TEMP DIFFERENTIAL:	N/A
CAST TEMPERATURE:	2897 deg F	DEW POINT:	N/A
		SHROUD GAS:	Argon

PURPOSE OF TRIAL: To attempt to reuse a nozzle _____ _____ _____ _____ Other data to be obtained from trial included conductance of zirconia at cast temperatures and heat losses in the pouring box.

RESULTS OF TRIAL: One bumper sounded prior to casting and wheel positioning. A thermoucouple was found shorting the sensor to the pouring box through the zirconia. This established the suspected problem with previous bumper failures (Zirconia is conducting at these temperatures). The pouring box thermocouples exceeded their maximum range prior to casting so only the temperature of the top of the pouring box was measured. A small defect in the nozzle bottom was noted during the hot test. The cast itself only lasted a few seconds before a breakout occured at the bottom of the nozzle. The sides of the nozzle held up very well.

FILES: C:\DATA\CAST824.XLS   C:\DATA\HT824.XLS
Heat Log 4545

MELT OVERFLOW STRIP CASTING LOG

CAST NUMBER:	827	DATE:	4/30/92	TIME:	4:15 PM

HEAT WEIGHT:	1000 Lbs.	AMOUNT CAST:	¯90'	GRADE:	Si-Killed

HEAT ANALYSIS

	C	MN	SI	AL	N2	O2	S	Cu
AIM:	0.05	0.3	0.17	<.004	<.005	<.03	<.008	<.025
FINAL:	N/A	N/A	N/A	N/A	N/A	N/A	N/A	N/A

CASTING PARAMETERS

SUBSTRATE:	Normal Cu	POOL DEPTH:	2-1/2" max .
SUBSTRATE FINISH:	242 u in	WEIR GAP:	0.25"
NOZZLE POS. WRT WHEEL:	60 deg BTDC	NOZZLE WIDTH:	8.00"
NOZZLE GAP:	.015"	NOZZLE BRICK:	Zirconia
AUTO GAP ADJUST:	N/A	MANUFACTURE:	Narco
LADLE PREHEAT TEMP.:	1746 deg F	LOT #:	3006A
POUR BOX PREHEAT TEMP.:	2267 deg F	INITIAL CAST SPEED:	200 FPM
FURNACE TAP TEMP.:	3150 deg F	WATER IN TEMP.:	117 F
STEEL TRANS. TEMP.:	2956 deg F	WATER FLOW:	83 GPM
AIM CASTING TEMPERATURE:	2950 deg F	TEMP DIFFERENTIAL:	N/A
CAST TEMPERATURE:	2966 deg F	DEW POINT:	34 F
		SHROUD GAS:	Argon

PURPOSE OF TRIAL: To determine if a new procedure for mounting gap sensors in zirconia brick would eliminate the problem of the sensors when the zirconia brick becomes conductive (at high temperatures). Sensor wires were glued into boron nitride sleves using Autocrete cement. Also looked at the effect of increasing superheat to prevent early freeze off.

RESULTS OF TRIAL: Problems with nozzle alignment delayed casting slightly. Steel temperatures indicated that there was about 20 degrees more superheat. The cast began to show signs of freeze-off shortly afte the casting began. Liquid steel also was observed leaking from the bottom of the nozzle. Only one bumper was heard or seen during the cast. Upon disassembly, the joint between the nozzle and k-brick w found to be the culprit for some of the steel leakage below the noz Examining the stepper log revealed an outward movement of the wheel shortly after the cast started. This most probably contributed to problem.

FILES:	C:\DATA\CAST827.XLS	C:\DATA\HT827.XLS
	Heat Log 4545	C:\DATA\CUT827
	C :\DATA\HTT827	C:\DATA\HEAT827

MELT OVERFLOW STRIP CASTING LOG

CAST NUMBER:	828	DATE:	5/7/92	TIME:	4:30 PM

HEAT WEIGHT:	1000 Lbs.	AMOUNT CAST:	0	GRADE:	Si-Killed

HEAT ANALYSIS

	C	MN	SI	AL	N2	O2	S	Cu
AIM:	0.05	0.3	0.17	<.004	<.005	<.03	<.008	<.025
FINAL:	N/A	N/A	N/A	N/A	N/A	N/A	N/A	N/A

CASTING PARAMETERS

SUBSTRATE:	Normal Cu	POOL DEPTH:	2-1/2" max
SUBSTRATE FINISH:	242 u in	WEIR GAP:	0.25"
NOZZLE POS. WRT WHEEL:	60 deg BTDC	NOZZLE WIDTH:	6.00"
NOZZLE GAP:		NOZZLE BRICK:	Zirconia*
AUTO GAP ADJUST:	N/A	MANUFACTURE:	Narco
LADLE PREHEAT TEMP.:	N/A	LOT #:	3006A
POUR BOX PREHEAT TEMP.:	N/A	INITIAL CAST SPEED:	200 FPM
FURNACE TAP TEMP.:	3140 deg F	WATER IN TEMP.:	117 F
STEEL TRANS. TEMP.:	N/A	WATER FLOW:	83 GPM
AIM CASTING TEMPERATURE:	2950 deg F	TEMP DIFFERENTIAL:	N/A
CAST TEMPERATURE:	N/A	DEW POINT:	34 F
		SHROUD GAS:	Argon

PURPOSE OF TRIAL:

RESULTS OF TRIAL: The nozzle was assembled, mounted, and cut to form with little problem. A soft preheat was given to the front of the nozzle. Just prior to the hot test, the kaowool was removed from the face of the nozzle. The autostick failed _____ The test was aborted at this point.

FILES: C:\DATA\CUT828

MELT OVERFLOW STRIP CASTING LOG

CAST NUMBER:	829	DATE:	5/14/92	TIME:	14:00:00

HEAT WEIGHT:	1000 Lbs.	AMOUNT CAST:	85'	GRADE:	Si-Killed

HEAT ANALYSIS

	C	MN	SI	AL	N2	O2	S	CU
AIM:	0.05	0.3	0.17	<.004	<.005	<.03	<.008	<.025
FINAL:	0.032	0.28	0.14	0.001	0.0064	0.026	0.009	0.026

CASTING PARAMETERS

SUBSTRATE:	Normal Cu	POOL DEPTH:	2-1/2" max
SUBSTRATE FINISH:	242 u in	WEIR GAP:	0.50"
NOZZLE POS. WRT WHEEL:	60 deg BTDC	NOZZLE WIDTH:	11.00"
NOZZLE GAP:		NOZZLE BRICK:	Tund. Brd*
AUTO GAP ADJUST:	0.3 u in	MANUFACTURE:	Comat
LADLE PREHEAT TEMP.:	1766 deg F	LOT #:	N/A
POUR BOX PREHEAT TEMP.:	2267 deg F	INITIAL CAST SPEED:	200 FPM
FURNACE TAP TEMP.:	3150 deg F	WATER IN TEMP.:	117 F
STEEL TRANS. TEMP.:	2974 deg F	WATER FLOW:	83 GPM
AIM CASTING TEMPERATURE:	2950 deg F	TEMP DIFFERENTIAL:	N/A
CAST TEMPERATURE:	2913 deg F	DEW POINT:	49 F
		SHROUD GAS:	Argon

PURPOSE OF TRIAL:

To evaluate the potential of using tundish liner board as a nozzle material

RESULTS OF TRIAL:

The shinkage of the material caused some initial mating problems with the wheel. In addition to this, the heating and cooling of the tundish board due to preheating the box and nozzle, and hot testing the nozzle fit caused numerous cracks to develop. At the start of testing, steel pool height was limited to ~1". As the cast proceded, failure of the wings (due to cracks caused by thermal cycling) made it necessary to abort the run. Despite the problems, 85' of strip was cast with no signs of freeze-off and without any break-outs. The Krojok joints held very well, the concept was proven, and the tundish liner board proved acceptable. Future tests will focus on eliminating the termal cycling.

FILES:

C:\DATA\CUT829   C:\DATA\HOT829   C:\DATA\CAST829
C:\DATA\HEAT829   C:\DATA\HT829.XLS

MELT OVERFLOW STRIP CASTING LOG

CAST NUMBER:	830	DATE:	5/21/92	TIME:	13:00:00

HEAT WEIGHT:	1000 Lbs.	AMOUNT CAST:	¯50'	GRADE:	Si-Killed

HEAT ANALYSIS

	C	MN	SI	AL	N2	O2	S	Cu
AIM:	0.05	0.3	0.17	<.004	<.005	<.03	<.008	<.025
FINAL:	0.044	0.36	0.17	0.002	0.0061	0.027	0.007	0.02

CASTING PARAMETERS

SUBSTRATE:	Normal Cu	POOL DEPTH:	2-1/2" max
SUBSTRATE FINISH:	242 u in	WEIR GAP:	0.50"
NOZZLE POS. WRT WHEEL:	60 deg BTDC	NOZZLE WIDTH:	11.00"
NOZZLE GAP:	- ·	NOZZLE BRICK:	Tund. Brd*
AUTO GAP ADJUST:	0.1 mil	MANUFACTURE:	Comat
LADLE PREHEAT TEMP.:	1600 deg F	LOT #:	N/A
POUR BOX PREHEAT TEMP.:	2046 deg F	INITIAL CAST SPEED:	150 FPM
FURNACE TAP TEMP.:	3099 deg F	WATER IN TEMP.:	117 F
STEEL TRANS. TEMP.:	2973 deg F	WATER FLOW:	81 GPM
AIM CASTING TEMPERATURE:	2930 deg F	TEMP DIFFERENTIAL:	N/A
CAST TEMPERATURE:	2929 deg F	DEW POINT:	59 F
		SHROUD GAS:	Argon

PURPOSE OF TRIAL:

To evaluate the potential of using tundish liner board as a nozzle material. This was the second test with this material. A softer preheat was attempted to eliminate cracking problems encountered previously. Also, this material was thinner than the original material (1" versus 1-1/2").

RESULTS OF TRIAL:

The plug used to keep heat off the nozzle came loose after the hot test. This in turn heated the nozzle too hot prior to casting and may have been responsible for some of the cracking and refractory failure. Stepper system did not engage auto-creep and a manual wheel move to eliminate a breakout may have led to additional nozzle damage. The nozzle was completely destroyed showing severe refractory failure in the floor area. It is not clear how much of the damage was due to the wheel movement or the preheat. The worn material from the nozzle was very prevelent in the strip that was made. Only a minimal amount of strip was produced prior to aborting the cast.

FILES:

C:\DATA\CUT830   C:\DATA\CAST830

C:\DATA\HEAT830   C:\DATA\HT830.XLS

MELT OVERFLOW STRIP CASTING LOG

CAST NUMBER:	831	DATE:	5/27/92	TIME:	1:15 PM

HEAT WEIGHT:	1000 Lbs.	AMOUNT CAST:	⁻400'	GRADE:	Si-Killed

HEAT ANALYSIS

	C	MN	SI	AL	N2	O2	S	Cu
AIM:	0.05	0.3	0.17	<.004	<.005	<.03	<.008	<.025
FINAL:	0.044	0.36	0.16	0.002	0.0049	0.023	0.007	0.019

CASTING PARAMETERS

SUBSTRATE:	Normal Cu	POOL DEPTH:	2-1/2" max
SUBSTRATE FINISH:	242 u in	WEIR GAP:	0.50"
NOZZLE POS. WRT WHEEL:	60 deg BTDC	NOZZLE WIDTH:	6.50"
NOZZLE GAP:		NOZZLE BRICK:	Zirconia*
AUTO GAP ADJUST:	0.1 u	MANUFACTURE:	Narco
LADLE PREHEAT TEMP.:	N/A	LOT #:	3006A
POUR BOX PREHEAT TEMP.:	2210 deg F	INITIAL CAST SPEED:	150 FPM
FURNACE TAP TEMP.:	3150 deg F	WATER IN TEMP.:	117 F
STEEL TRANS. TEMP.:	2970 deg F	WATER FLOW:	83 GPM
AIM CASTING TEMPERATURE:	2950 deg F	TEMP DIFFERENTIAL:	N/A
CAST TEMPERATURE:	2860 deg F	DEW POINT:	46 F
		SHROUD GAS:	Argon

PURPOSE OF TRIAL:
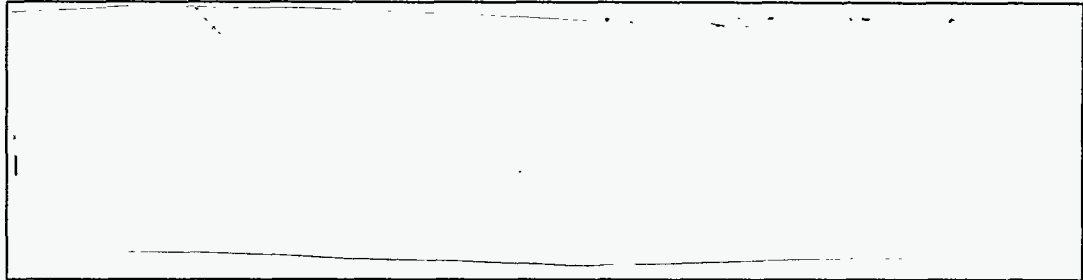
RESULTS OF TRIAL:

The cast went very well. Cast speed was reduced to 100 ft/min and thicker (>30 mils) strip was produced. The thicker strip exhibited defiate transverse cracking and some longitudinal cracking. The transverse cracks are assumed to be due to shrinkage. After several seconds at the lower speed a dam started to form on the north side. Three times the wheel was sped up to dislodge the dam. Each time the dam was dislodged. Finally (at maximum speed) a dam formed that could not be dislodged and froze off the cast. One small leak in the pouring box was present during most of the cast. It originated in the corner where the zirconia and k-brick meet on the north side. This was a Krojoc joint.

FILES:	C:\DATA\CUT831	C:\DATA\HOT831	C:\DATA\HEAT831
	C:\DATA\CAST831	C:\DATA\HT831.XLS	

MELT OVERFLOW STRIP CASTING LOG

CAST NUMBER:	832	DATE:	6/9/92	TIME:	11:15 AM

HEAT WEIGHT:	1000 Lbs.	AMOUNT CAST:	0	GRADE:	Si-Killed

HEAT ANALYSIS

	C	MN	SI	AL	N2	O2	S	Cu
AIM:	0.05	0.3	0.17	<.004	<.005	<.03	<.008	<.025
FINAL:	N/A	N/A	N/A	N/A	N/A	N/A	N/A	N/A

CASTING PARAMETERS

SUBSTRATE:	Normal Cu	POOL DEPTH:	2-1/2" max
SUBSTRATE FINISH:	242 u in	WEIR GAP:	0.75"
NOZZLE POS. WRT WHEEL:	60 deg BTDC	NOZZLE WIDTH:	12.00"
NOZZLE GAP:		NOZZLE BRICK:	Tundish Spray
AUTO GAP ADJUST:	0.3 u	MANUFACTURE:	Comat
LADLE PREHEAT TEMP.:	1841 deg F	LOT #:	N/A
POUR BOX PREHEAT TEMP.:	1079 deg F	INITIAL CAST SPEED:	150 FPM
FURNACE TAP TEMP.:	3150 deg F	WATER IN TEMP.:	N/A
STEEL TRANS. TEMP.:	N/A	WATER FLOW:	N/A
AIM CASTING TEMPERATURE:	2930 deg F	TEMP DIFFERENTIAL:	N/A
CAST TEMPERATURE:	N/A	DEW POINT:	N/A
		SHROUD GAS:	Argon

PURPOSE OF TRIAL:

To evaluate the effectiveness of tundish spray material as a nozzle material. The nozzle and interior of the entire box were coated to ~1" thick with the spray material. The material was "pumped" between the box walls and a form. The box sat for > 7 days prior to use. Preheat was kept below 1200 degrees F at the surface. A three hour preheat was used.

RESULTS OF TRIAL:

The trial was aborted when the overhead crane failed to respond in the north direction during attempts to remove the ladle from in front of the furnace right after tap.
Further testing of the wheel and nozzle fit showed that a maximum creep rate of 0.3 microns is acceptable with 0.1 microns being very good.
Cracking of the spray material was noted on disassembly. This seems primarily associated with constraints to the front of the nozzle not allowing the nozzle to shrink back into the box.

FILES: C:\DATA\CUT832   C:\DATA\HOT832

MELT OVERFLOW STRIP CASTING LOG

CAST NUMBER:	833	**DATE:**	6/11/92	**TIME:** 11:00 AM
HEAT WEIGHT:	1000 Lbs.	**AMOUNT CAST:**	80'	**GRADE:** Si-Killed

HEAT ANALYSIS

	C	MN	SI	AL	N2	O2	S	Cu
AIM:	0.05	0.3	0.17	<.004	<.005	<.03	<.008	<.025
FINAL:	0.044	0.37	0.17	0.002	0.0047	0.024	0.007	0.018

CASTING PARAMETERS

SUBSTRATE:	Normal Cu	**POOL DEPTH:**	2-1/2" max
SUBSTRATE FINISH:	242 u in	**WEIR GAP:**	0.25"
NOZZLE POS. WRT WHEEL:	60 deg BTDC	**NOZZLE WIDTH:**	12.06"
NOZZLE GAP:		**NOZZLE BRICK:**	Tundish Brd.
AUTO GAP ADJUST:	0.1 mils	**MANUFACTURE:**	Comat
LADLE PREHEAT TEMP.:	1510 deg F	**LOT #:**	NonPreheat
POUR BOX PREHEAT TEMP.:	2132 deg F	**INITIAL CAST SPEED:**	150 FPM
FURNACE TAP TEMP.:	3150 deg F	**WATER IN TEMP.:**	114 F
STEEL TRANS. TEMP.:	3020 deg F	**WATER FLOW:**	99 GPM
AIM CASTING TEMPERATURE:	2930 deg F	**TEMP DIFFERENTIAL:**	N/A
CAST TEMPERATURE:	2967 deg F	**DEW POINT:**	47 F
		SHROUD GAS:	Argon

PURPOSE OF TRIAL:

This trial was conducted to evaluate the use of tundish liner board (non preheatable - 1" thick) as a candidate nozzle material.

RESULTS OF TRIAL:

The nozzle was kept below 1200 F during the preheat of the pouring box. Despite this, some cracking was observed in the wings. Shortly after the start of casting there was a breakout under the north wing. This wing eventually failed causing the cast to be aborted. The strip produced contained many defects associated with the incorporation of the nozzle material into the strip.

The tundish liner board material used for this trial was the 1" thick material.

FILES:

C:\DATA\CUT833 C:\DATA\HOT833 C:\DATA\HEAT833
C:\DATA\CAST833 C:\DATA\HT833.XLS

MELT OVERFLOW STRIP CASTING LOG

CAST NUMBER: 834   **DATE:** 6/16/92   **TIME:** 1:00 PM

HEAT WEIGHT: 1000 Lbs.   **AMOUNT CAST:** 0   **GRADE:** Si-Killed

HEAT ANALYSIS

	C	MN	SI	AL	N2	O2	S	Cu
AIM:	0.05	0.3	0.17	<.004	<.005	<.03	<.008	<.025
FINAL:	N/A	N/A	N/A	N/A	N/A	N/A	N/A	N/A

CASTING PARAMETERS

SUBSTRATE:	Normal Cu	POOL DEPTH:	2-1/2" max
SUBSTRATE FINISH:	242 m	WEIR GAP:	0.50"
NOZZLE POS. WRT WHEEL:	60 deg BTDC	NOZZLE WIDTH:	12.0"
NOZZLE GAP:		NOZZLE BRICK:	Tun. Broad
AUTO GAP ADJUST:	N/A	MANUFACTURE:	Comat
LADLE PREHEAT TEMP.:	1749 deg F	LOT #:	NonPreheat
POUR BOX PREHEAT TEMP.:	N/A	INITIAL CAST SPEED:	150 FPM
FURNACE TAP TEMP.:	2967 deg F	WATER IN TEMP.:	N/A
STEEL TRANS. TEMP.:	N/A	WATER FLOW:	N/A
AIM CASTING TEMPERATURE:	2950 deg F	TEMP DIFFERENTIAL:	N/A
CAST TEMPERATURE:	N/A	DEW POINT:	N/A
		SHROUD GAS:	Argon

PURPOSE OF TRIAL:

To evaluate the potential of using tundish liner board (non preheatable - 1" thick) as a nozzle material.

RESULTS OF TRIAL:

The material did not survive the hot test and no cast was made.

FILES: C:\DATA\CUT834   C:\DATA\HOT834

MELT OVERFLOW STRIP CASTING LOG

CAST NUMBER:	836	DATE:	6/23/92	TIME:	9:00 AM

HEAT WEIGHT:	1000 Lbs.	AMOUNT CAST:	0 ft.	GRADE:	Si-Killed

HEAT ANALYSIS

	C	MN	SI	AL	N2	O2	S	Cu
AIM:	0.05	0.3	0.17	<.004	<.005	<.03	<.008	<.025
FINAL:	N/A	N/A	N/A	N/A	N/A	N/A	N/A	N/A

CASTING PARAMETERS

SUBSTRATE:	Normal Cu	POOL DEPTH:	2.0" max
SUBSTRATE FINISH:	242 m	WEIR GAP:	0.50"
NOZZLE POS. WRT WHEEL:	60 deg BTDC	NOZZLE WIDTH:	12.0"
NOZZLE GAP:		NOZZLE BRICK:	Tun. Spray
AUTO GAP ADJUST:	.3 mils	MANUFACTURE:	Comat
LADLE PREHEAT TEMP.:	1538 deg F	LOT #:	
POUR BOX PREHEAT TEMP.:	1110 deg F	INITIAL CAST SPEED:	150 FPM
FURNACE TAP TEMP.:	3152 deg F	WATER IN TEMP.:	104 F
STEEL TRANS. TEMP.:	3000 deg F	WATER FLOW:	99 GPM
AIM CASTING TEMPERATURE:	2950 deg F	TEMP DIFFERENTIAL:	N/A
CAST TEMPERATURE:	N/A deg F	DEW POINT:	50 F
		SHROUD GAS:	Argon

PURPOSE OF TRIAL:

To evaluate the potential of using tundish spray material as a nozzle material. The box and nozzle were sprayed in and cured (~300 F). The box was not preheated prior to casting in order to avoid cracking due to thermal cycling.

RESULTS OF TRIAL:

A large amount of gas was seen evolving from the box as the cast started. A small amount of material formed up the wheel, but would not cast over the wheel. Head height in the nozzle appeared very low. Material then began to flow out of the overflow in the back of the box. Since material was not casting from the wheel the cast was aborted. It is beleived that the gasses escaping from the spray material in the back of the box along with the cold box causing restrictions in the dam and increasing the height of the dam, caused the steel to preferentially flow out of the overflow in the back of the box.

FILES:

C:\DATA\CUT836	C:\DATA\HOT836	C:\DATA\HEAT836
C:\DATA\CAST836	C:\DATA\HT836.XLS	

MELT OVERFLOW STRIP CASTING LOG

CAST NUMBER: 837 **DATE:** 6/26/92 **TIME:** 4:30 PM

HEAT WEIGHT: 1000 Lbs. **AMOUNT CAST:** 190' **GRADE:** Si-Killed

HEAT ANALYSIS

	C	MN	SI	AL	N2	O2	S	Cu
AIM:	0.05	0.3	0.17	<.004	<.005	<.03	<.008	<.025
FINAL:	0.45	0.36	0.16	0.003	0.0053	0.027	0.007	0.02

CASTING PARAMETERS

SUBSTRATE:	Normal Cu	POOL DEPTH:	2-1/2" max
SUBSTRATE FINISH:	242 m	WEIR GAP:	0.50"
NOZZLE POS. WRT WHEEL:	60 deg BTDC	NOZZLE WIDTH:	11.00"
NOZZLE GAP:		NOZZLE BRICK:	96% Al
AUTO GAP ADJUST:	0.5 mils	MANUFACTURE:	_
LADLE PREHEAT TEMP.:	1740 deg F	LOT #:	"AA"
POUR BOX PREHEAT TEMP.:	2230 deg F	INITIAL CAST SPEED:	150 FPM
FURNACE TAP TEMP.:	3156 deg F	WATER IN TEMP.:	113 F
STEEL TRANS. TEMP.:	3010 deg F	WATER FLOW:	99 GPM
AIM CASTING TEMPERATURE:	2930 deg F	TEMP DIFFERENTIAL:	N/A
CAST TEMPERATURE:	2940 deg F	DEW POINT:	61 F
		SHROUD GAS:	Argon

PURPOSE OF TRIAL:

To evaluate the potential of using an alumina material for construction of the nozzle.

RESULTS OF TRIAL:

The nozzle runner showed signs of cracking after the hot test (due to cooling). Some failure of the material ,due to spalling, was noted at the start of cast (south wing). Cast speed was reduced to 100 FPM for part of the cast. A strip break caused the emerging strip to kick back into the steel pool. After the kickback, a breakout occured at the south wing and the run was aborted. Upon cooling some metal penetration was noted in the Krojoc joints at the front of the nozzle wings. Also, some bowing of the nozzle runner was noted. The alumina material held up very well to the steel, but, showed severe errosion at the slag line.

FILES:

C:\DATA\CUT837 C:\DATA\HOT837 C:\DATA\HEAT837
C:\DATA\CAST837 C:\DATA\HT837.XLS

MELT OVERFLOW STRIP CASTING LOG

CAST NUMBER: 838   **DATE:** 6/30/92   **TIME:** 4:00 PM

HEAT WEIGHT: 1000 Lbs.   **AMOUNT CAST:** 295'   **GRADE:** Si-Killed

HEAT ANALYSIS

	C	MN	SI	AL	N2	O2	S	Cu
AIM:	0.05	0.3	0.17	<.004	<.005	<.03	<.008	<.025
FINAL:	0.043	0.37	0.17	0.003	0.0046	0.027	0.006	0.021

CASTING PARAMETERS

SUBSTRATE:	Normal Cu	POOL DEPTH:	2-1/2" max
SUBSTRATE FINISH:	242 m	WEIR GAP:	0.50"
NOZZLE POS. WRT WHEEL:	60 deg BTDC	NOZZLE WIDTH:	11.00"
NOZZLE GAP:	.	NOZZLE BRICK:	96% Al
AUTO GAP ADJUST:	0.5 mils	MANUFACTURE:	
LADLE PREHEAT TEMP.:	1630 deg F	LOT #:	"AA"
POUR BOX PREHEAT TEMP.:	2125 deg F	INITIAL CAST SPEED:	150 FPM
FURNACE TAP TEMP.:	3150 deg F	WATER IN TEMP.:	118 F
STEEL TRANS. TEMP.:	2990 deg F	WATER FLOW:	98 GPM
AIM CASTING TEMPERATURE:	2930 deg F	TEMP DIFFERENTIAL:	N/A
CAST TEMPERATURE:	2980 deg F	DEW POINT:	60 F
		SHROUD GAS:	Argon

PURPOSE OF TRIAL:

To evaluate the potential of using an alumina ~~~~~~~~ material for construction of the nozzle. Specifically to evaluate the ability of a coating of Ruby mortar to stop the erosion at the slag line.

RESULTS OF TRIAL:

The nozzle runner showed signs of cracking after the hot test (due to cooling). Shortly after the start of cast a small breakout was noted at the south bottom of the nozzle. This proceeded under the south wing and led to a spalling of the inside of the wing. Metal level was reduced to 2" with freeze offs occuring on the north and south sides. A large breakout on the south side resulted in an abort of the cast. The Ruby mortar material did not retard the slag attack to any significant extent.

FILES: C:\DATA\CUT838   C:\DATA\HOT838   C:\DATA\HEAT838
    C:\DATA\CAST838   C:\DATA\HT838.XLS

MELT OVERFLOW STRIP CASTING LOG

CAST NUMBER:	839	**DATE:**	7/7/92	**TIME:**	12:00 PM

HEAT WEIGHT: 1000 Lbs.   **AMOUNT CAST:** 360'   **GRADE:** Si-Killed

HEAT ANALYSIS

	C	MN	SI	AL	N2	O2	S	Cu
AIM:	0.05	0.3	0.17	<.004	<.005	<.03	<.008	<.025
FINAL:	0.045	0.33	0.14	0.001	0.0046	0.025	0.007	0.019

CASTING PARAMETERS

SUBSTRATE:	Normal Cu	POOL DEPTH:	2-1/2" max
SUBSTRATE FINISH:	242 m	WEIR GAP:	0.50"
NOZZLE POS. WRT WHEEL:	60 deg BTDC	NOZZLE WIDTH:	11.00"
NOZZLE GAP:		NOZZLE BRICK:	96% Al
AUTO GAP ADJUST:	0.5 mils	MANUFACTURE:	
LADLE PREHEAT TEMP.:	1740 deg F	LOT #:	"AA"
POUR BOX PREHEAT TEMP.:	2110 deg F	INITIAL CAST SPEED:	150 FPM
FURNACE TAP TEMP.:	3151 deg F	WATER IN TEMP.:	118 F
STEEL TRANS. TEMP.:	3025 deg F	WATER FLOW:	97 GPM
AIM CASTING TEMPERATURE:	2930 deg F	TEMP DIFFERENTIAL:	N/A
CAST TEMPERATURE:	2927 deg F	DEW POINT:	60 F
		SHROUD GAS:	Argon

PURPOSE OF TRIAL:

To evaluate the potential of using an alumina material for construction of the nozzle. Specifically to evaluate the ability of a coating of zirconia to stop the erosion at the slag line.

RESULTS OF TRIAL:

The nozzle runner showed signs of cracking after the hot test (due to cooling). Also, there were signs of a spalled area on the top of the south wing. This spall area fell off a the start of cast. a dam started to form on the north side and the wheel speed was increased to 200 FPM. The steel level was increased to >2.5" to attempt to flush the dam. A breakout at the south bottom which made its way up the south wing resulted in the remainder of the heat being aborted.

FILES:

C:\DATA\CUT839   C:\DATA\HOT839   C:\DATA\HEAT839
C:\DATA\CAST839   C:\DATA\HT839.XLS

HT840.XLS

MELT OVERFLOW STRIP CASTING LOG

CAST NUMBER:	840	DATE:	7/10/92	TIME:	1:00 PM

HEAT WEIGHT:	1000 Lbs.	AMOUNT CAST:	700'	GRADE:	Si-Killed

HEAT ANALYSIS

	C	MN	SI	AL	N2	O2	S	Cu
AIM:	0.05	0.3	0.17	<.004	<.005	<.03	<.008	<.025
FINAL:	0.045	0.34	0.15	0.002	0.0047	0.027	0.008	0.019

CASTING PARAMETERS

SUBSTRATE:	Normal Cu	POOL DEPTH:	2-1/2" max
SUBSTRATE FINISH:	242 m	WEIR GAP:	0.50"
NOZZLE POS. WRT WHEEL:	60 deg BTDC	NOZZLE WIDTH:	12.00"
NOZZLE GAP:		NOZZLE BRICK:	
AUTO GAP ADJUST:	0.5 mils	MANUFACTURE:	Nar./Zir.
LADLE PREHEAT TEMP.:	N/A	LOT #:	3006
POUR BOX PREHEAT TEMP.:	2080 deg F	INITIAL CAST SPEED:	150 FPM
FURNACE TAP TEMP.:	3150 deg F	WATER IN TEMP.:	120 F
STEEL TRANS. TEMP.:	3018 deg F	WATER FLOW:	97 GPM
AIM CASTING TEMPERATURE:	2930 deg F	TEMP DIFFERENTIAL:	42 F
CAST TEMPERATURE:	2926 deg F	DEW POINT:	56 F
		SHROUD GAS:	Argon

PURPOSE OF TRIAL:
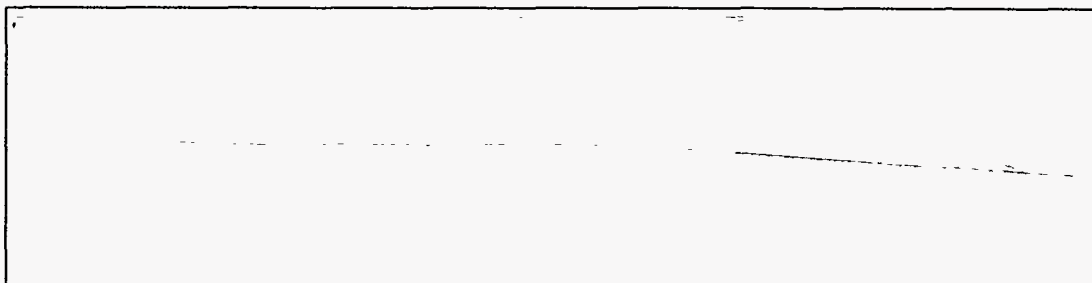
RESULTS OF TRIAL:

The nozzle looked good after the hot test, showing only moderate signs of cracking and bowing. At cast, there was some penetration of steel under the south wing and a dam formed on the north side. Wheel was sped up to dislodge dam (175 FPM). The north wing tip broke off about 1/2 way through the cast. Steel was emptied from the ladle prior to serious dam formation. Dam started at south side and continued across wheel as metal level dropped. Complete cast sequence was achieved.

FILES:

C:\DATA\CUT840   C:\DATA\HOT840   C:\DATA\HEAT840
C:\DATA\CAST840   C:\DATA\HT840.XLS

MELT OVERFLOW STRIP CASTING LOG

CAST NUMBER: 841 **DATE:** 7/15/92 **TIME:** 1:00 PM

HEAT WEIGHT: 1000 Lbs. **AMOUNT CAST:** 0 **GRADE:** Si-Killed

HEAT ANALYSIS

	C	MN	SI	AL	N2	O2	S	Cu
AIM:	0.05	0.3	0.17	<.004	<.005	<.03	<.008	<.025
FINAL:	N/A	N/A	N/A	N/A	N/A	N/A	N/A	N/A

CASTING PARAMETERS

SUBSTRATE:	Normal Cu	POOL DEPTH:	2-1/2" max
SUBSTRATE FINISH:	242 m	WEIR GAP:	0.5"
NOZZLE POS. WRT WHEEL:	60 deg BTDC	NOZZLE WIDTH:	10.125"
NOZZLE GAP:		NOZZLE BRICK:	3 Piece
AUTO GAP ADJUST:	0.3 mils	MANUFACTURE:	See
LADLE PREHEAT TEMP.:	1835 deg F	LOT #:	Below
POUR BOX PREHEAT TEMP.:	2148 deg F	INITIAL CAST SPEED:	150 FPM
FURNACE TAP TEMP.:	3150 deg F	WATER IN TEMP.:	117 F
STEEL TRANS. TEMP.:	3012 deg F	WATER FLOW:	97 GPM
AIM CASTING TEMPERATURE:	2950 deg F	TEMP DIFFERENTIAL:	3 F
CAST TEMPERATURE:	N\A	DEW POINT:	69 F
		SHROUD GAS:	Argon

PURPOSE OF TRIAL:

RESULTS OF TRIAL:

Also, a few spider web cracks were in existance and one larger crack just north of center was noted. There was no cracks evident in the zirconia. During the wheel in procedure prior to cast the wheel was ramed into the nozzle several times as the result of a positioning error after the hot test. This caused a failure of the Ruby joint on the north wing and the cast was aborted.

FILES:

C:\DATA\CUT841   C:\DATA\HOT841   C:\DATA\HEAT841

C:\DATA\CAST841   C:\DATA\HT841.XLS   C:\DATA\PRE841

MELT OVERFLOW STRIP CASTING LOG

CAST NUMBER:	842	DATE:	7/17/92	TIME:	1:00 PM

HEAT WEIGHT:	1000 Lbs.	AMOUNT CAST:	200'	GRADE:	Si-Killed

HEAT ANALYSIS

	C	MN	SI	AL	N2	O2	S	Cu
AIM:	0.05	0.3	0.17	<.004	<.005	<.03	<.008	<.025
FINAL:	0.044	0.34	0.16	0.002	0.004	0.036	0.007	0.018

CASTING PARAMETERS

SUBSTRATE:	Normal Cu	POOL DEPTH:	2-1/2" max
SUBSTRATE FINISH:	242 m	WEIR GAP:	0.25"
NOZZLE POS. WRT WHEEL:	60 deg BTDC	NOZZLE WIDTH:	12.00"
NOZZLE GAP:		NOZZLE BRICK:	
AUTO GAP ADJUST:	0.3 mils	MANUFACTURE:	
LADLE PREHEAT TEMP.:	1885	LOT #:	N/A
POUR BOX PREHEAT TEMP.:	2202 deg F	INITIAL CAST SPEED:	300 FPM
FURNACE TAP TEMP.:	3150 deg F	WATER IN TEMP.:	119 F
STEEL TRANS. TEMP.:	3021 deg F	WATER FLOW:	34 GPM
AIM CASTING TEMPERATURE:	2930 deg F	TEMP DIFFERENTIAL:	79 F
CAST TEMPERATURE:	2990 deg F	DEW POINT:	68 F
		SHROUD GAS:	Argon

PURPOSE OF TRIAL:

A 3/4" high opening was added to the corners of the weir (dogbones) to attempt to eliminate freezeoffs.

RESULTS OF TRIAL:

Post analysis showed some continuation of the failure into the Kbrick backing up the south wing.

FILES:

C:\DATA\CUT842	C:\DATA\HOT842	C:\DATA\HEAT842
C:\DATA\CAST842	C:\DATA\HT842.XLS	C:\DATA\PRE842

MELT OVERFLOW STRIP CASTING LOG

CAST NUMBER:	843	DATE:	7/21/92	TIME:	1:00 PM

WEIGH:	1000 Lb.	AMOUNT CAST:	~	GRADE:	Si-Killed

HEAT ANALYSIS

	C	MN	SI	AL	N2	O2	S
AIM:							
FINAL:							

CASTING PARAMETERS

SUBSTRATE:	Normal Cu	POOL DEPTH:	2-1/2" max
SUBSTRATE FINISH:	242 m	WEIR GAP:	0.25"
NOZZLE POS. WRT WHEEL:	60 deg BTDC	NOZZLE WIDTH:	12.00"
NOZZLE GAP:		NOZZLE BRICK:	
AUTO GAP ADJUST:	0.3 mils	MANUFACTURE:	
LADLE PREHEAT TEMP.:	N/A	LOT #:	N/A
POUR BOX PREHEAT TEMP.:	N/A	INITIAL CAST SPEED:	300 FPM
FURNACE TAP TEMP.:	N/A	WATER IN TEMP.:	N/A
STEEL TRANS. TEMP.:	N/A	WATER FLOW:	N/A
AIM CASTING TEMPERATURE:	2930 deg F	TEMP DIFFERENTIAL:	N/A
CAST TEMPERATURE:	N/A	DEW POINT:	N/A
		SHROUD GAS:	Argon

FILES: C:\DATA\CUT843   C:\DATA\HOT843   C:\DATA\PRE843

MELT OVERFLOW STRIP CASTING LOG

CAST NUMBER:	844	DATE:	8/13/92	TIME:	4:00 PM

HEAT WEIGHT:	1200 Lbs.	AMOUNT CAST:	190'	GRADE:	Si-Killed

HEAT ANALYSIS

	C	MN	SI	AL	N2	O2	S	Cu
AIM:	0.05	0.3	0.17	<.004	<.005	<.03	<.008	<.025
FINAL:	0.054	0.44	0.25	0.003	0.009	0.043	0.007	0.025

CASTING PARAMETERS

SUBSTRATE:	Normal Cu	POOL DEPTH:	2-1/2" max
SUBSTRATE FINISH:	Threaded**	WEIR GAP:	0.25"*
NOZZLE POS. WRT WHEEL:	60 deg BTDC	NOZZLE WIDTH:	12.06"
NOZZLE GAP:		NOZZLE BRICK:	Zirconia***
AUTO GAP ADJUST:	0.2 mils	MANUFACTURE:	Narco
LADLE PREHEAT TEMP.:	1890 deg F	LOT #:	3006A
POUR BOX PREHEAT TEMP.:	2090 deg F	INITIAL CAST SPEED:	300 FPM
FURNACE TAP TEMP.:	3150 deg F	WATER IN TEMP.:	116.8 F
STEEL TRANS. TEMP.:	2994 deg F	WATER FLOW:	32.9 GPM
AIM CASTING TEMPERATURE:	2950 deg F	TEMP DIFFERENTIAL:	64.8 F
CAST TEMPERATURE:	2953 deg F	DEW POINT:	60 F
		SHROUD GAS:	Argon

PURPOSE OF TRIAL:

To evaluate the use of a threaded wheel* (* - 5.9 mils deep/21pitch/10 mil flats), an embedded thermocouple in the nozzle, enlarged overflow holes, the use of dogbones in the weir** (** - 3/4" notches cut out of the corners).

RESULTS OF TRIAL:

One small gap did open up in Krojoc joint under the south wing, prior to cast. Also, a crack in the nozzle bottom just south of center was noticed. No hot test was conducted. Cast started normally, shortly after casting started pieces of the nozzle bottom were seen floating to the top of the steel. A breakout in the center of the nozzle bottom caused the cast to be aborted. A fuse blew and shut the wheel off seconds later. After cooling the Ruby joint had failed. The Phoxbond joint, while weak, was still intact. The material had horizontal cracks (north & south) where the zirconia cracked.

FILES:

C:\DATA\CUT844	C:\DATA\HEAT844	
C:\DATA\CAST844	C:\DATA\HT844.XLS	C:\DATA\PRE844

MELT OVERFLOW STRIP CASTING LOG

CAST NUMBER:	845	DATE:	8/20/92	TIME:	2:00 PM
HEAT WEIGHT:	1000 Lbs.	AMOUNT CAST:	0	GRADE:	Si-Killed

HEAT ANALYSIS

	C	MN	SI	AL	N2	O2	S	Cu
AIM:	0.05	0.3	0.17	<.004	<.005	<.03	<.008	<.025
FINAL:	N/A	N/A	N/A	N/A	N/A	N/A	N/A	N/A

CASTING PARAMETERS

SUBSTRATE:	Normal Cu	POOL DEPTH:	2-1/2" max
SUBSTRATE FINISH:	4/17/5 Thread	WEIR GAP:	0.25" w/bones
NOZZLE POS. WRT WHEEL:	60 deg BTDC	NOZZLE WIDTH:	12.00"
NOZZLE GAP:	· ··	NOZZLE BRICK:	
AUTO GAP ADJUST:	0.2 mils	MANUFACTURE:	—
LADLE PREHEAT TEMP.:	1832 deg F	LOT #:	
POUR BOX PREHEAT TEMP.:	2163 deg F	INITIAL CAST SPEED:	300 FPM
FURNACE TAP TEMP.:	3156 deg F	WATER IN TEMP.:	N/A
STEEL TRANS. TEMP.:	2954 deg F	WATER FLOW:	N/A
AIM CASTING TEMPERATURE:	2950 deg F	TEMP DIFFERENTIAL:	N/A
CAST TEMPERATURE:	N/A	DEW POINT:	52 F
		SHROUD GAS:	Argon

PURPOSE OF TRIAL:

To evaluate ⸱ ⸱⸱⸱⸱ the use of an expansion joint in the nozzle K-brick, to evaluate the use of a board material between the box and nozzle assembly, to evaluate a threaded copper wheel and new one piece dresser, and to evaluate the use of a type B thermocouple mortared into the nozzle with Phoxbond.
⸱⸱⸱⸱ simple joints; joints sealed with Kronoc; spring or sponge type hold downs.

RESULTS OF TRIAL:

After preheating the wings showed significant deformation (bowed inward by 1/2" or better). The cast was aborted at this time. The expansion joint in the K-brick along with the board material behind the nozzle assembly eliminated all cracking in the nozzle bottom. No evaluation could be performed on the one piece dresser. The type B thermocouple worked adequately, however, no evaluation of mortar attack due to the steel could be done.

FILES:	C:\DATA\CUT845		C:\DATA\HEAT845
	C:\DATA\CAST845	C:\DATA\HT845.XLS	C:\DATA\PRE845

HT846.XLS

MELT OVERFLOW STRIP CASTING LOG

CAST NUMBER:	846	DATE:	8/25/92	TIME:	2:00 PM

HEAT WEIGHT:	1000 Lbs.	AMOUNT CAST:	360'	GRADE:	Si-Killed

HEAT ANALYSIS

	C	MN	SI	AL	N2	O2	S	Cu
AIM:	0.05	0.3	0.17	<.004	<.005	<.03	<.008	<.025
FINAL:								

CASTING PARAMETERS

SUBSTRATE:	Normal Cu	POOL DEPTH:	2-1/2" max
SUBSTRATE FINISH:	Threaded *	WEIR GAP:	0.25" w/bones
NOZZLE POS. WRT WHEEL:	60 deg BTDC	NOZZLE WIDTH:	12.00"
NOZZLE GAP:	-	NOZZLE BRICK:	Zirconia**
AUTO GAP ADJUST:	0.2 mils	MANUFACTURE:	Narco
LADLE PREHEAT TEMP.:	1800 deg F	LOT #:	3006A
POUR BOX PREHEAT TEMP.:	2193 deg F	INITIAL CAST SPEED:	300 FPM
FURNACE TAP TEMP.:	3150 deg F	WATER IN TEMP.:	118.5 F
STEEL TRANS. TEMP.:	3011 deg F	WATER FLOW:	32.7 GPM
AIM CASTING TEMPERATURE:	2950 deg F	TEMP DIFFERENTIAL:	88 F
CAST TEMPERATURE:	2973 deg F	DEW POINT:	68 F
		SHROUD GAS:	Argon

PURPOSE OF TRIAL:

To reevaluate the use   Zirconia brick.
Materials were bonded together and heated in an oven to 600 deg F prior to nozzle assembly. This trial also used a *threaded wheel with 5 mil deep threads, 17 pitch, and 3 mil flats. Wheel was heated a start of cast by using only 1 cooling zone and running at high wheel speeds (300 FPM) at the start. The dresser was turned off shortly after start of cast.

RESULTS OF TRIAL:

Prior to casting the North and South wings showed hairline cracks in the Phoxbond joints. Cracks were also noted to originate in the relieved areas
During the cast,
Metal eventually penetrated through the opening on the South wing and the cast was aborted. After the cast the Krojoc under the front of the wings and the Phoxbond joints in the wings and bottom all showed signs of failure.

FILES:

C:\DATA\CUT846		C:\DATA\HEAT846
C:\DATA\CAST846	C:\DATA\HT846.XLS	C:\DATA\PREA846

MELT OVERFLOW STRIP CASTING LOG

CAST NUMBER:	847	DATE:	8/28/92	TIME:	2:00 PM
HEAT WEIGHT:	1000 Lbs.	AMOUNT CAST:	100'	GRADE:	Si-Killed

HEAT ANALYSIS

	C	MN	SI	AL	N2	O2	S	Cu
AIM:	0.05	0.3	0.17	<.004	<.005	<.03	<.008	<.025
FINAL:	N/A	N/A	N/A	N/A	N/A	N/A	N/A	N/A

CASTING PARAMETERS

SUBSTRATE:	Normal Cu	POOL DEPTH:	2-1/2" max
SUBSTRATE FINISH:	Threaded •	WEIR GAP:	0.25" w/bones
NOZZLE POS. WRT WHEEL:	60 deg BTDC	NOZZLE WIDTH:	12.00"
NOZZLE GAP:		NOZZLE BRICK:	Zirconia**
AUTO GAP ADJUST:	0.3 mils	MANUFACTURE:	Narco
LADLE PREHEAT TEMP.:	1840 deg F	LOT #:	3006A
POUR BOX PREHEAT TEMP.:	N/A	INITIAL CAST SPEED:	300 FPM
FURNACE TAP TEMP.:	3150 deg F	WATER IN TEMP.:	N/A
STEEL TRANS. TEMP.:	3152 deg F	WATER FLOW:	N/A
AIM CASTING TEMPERATURE:	2950 deg F	TEMP DIFFERENTIAL:	N/A
CAST TEMPERATURE:	N/A	DEW POINT:	55 deg F
		SHROUD GAS:	Argon

PURPOSE OF TRIAL:

To evaluate the use of Phoxbond to attach   materials and to determine the ability to use a multiple section   nozzle bottom. The nozzle was constructed of zirconia 3006   The bottom of the nozzle consited of 3 pieces with shiplap joints between the pieces.

RESULTS OF TRIAL:

After preheat small hairline cracks were noted in the Phoxbond joints in both the north and south wings. Small gaps were also noted in the Krojoc joint under the north wing. Shortly after the start of the cast the center section of the nozzle footprint broke away, causing a large breakout. The cast was aborted at this time. All strip cast was at 300 FPM.

FILES:	C:\DATA\CUT847		C:\DATA\HEAT847
	C:\DATA\CAST847	C:\DATA\HT847.XLS	C:\DATA\PREA847

MELT OVERFLOW STRIP CASTING LOG

CAST NUMBER:	848	**DATE:**	9/3/92	**TIME:**	12:00 PM
HEAT WEIGHT:	1000 Lbs.	**AMOUNT CAST:**	580'	**GRADE:**	Si-Killed

HEAT ANALYSIS

	C	MN	SI	AL	N2	O2	S	Cu
AIM:	0.05	0.3	0.17	<.004	<.005	<.03	<.008	<.025
FINAL:	0.04	0.18	0.052	0.003	0.004	0.065	0.007	0.021

CASTING PARAMETERS

SUBSTRATE:	Normal Cu	**POOL DEPTH:**	2-1/2" max
SUBSTRATE FINISH:	Threaded *	**WEIR GAP:**	0.25" w/bones
NOZZLE POS. WRT WHEEL:	60 deg BTDC	**NOZZLE WIDTH:**	12.00"
NOZZLE GAP:		**NOZZLE BRICK:**	Zirconia**
AUTO GAP ADJUST:	0.5 mils	**MANUFACTURE:**	Narco
LADLE PREHEAT TEMP.:	1765 deg F	**LOT #:**	3006A
POUR BOX PREHEAT TEMP.:	2105 deg F	**INITIAL CAST SPEED:**	300 FPM
FURNACE TAP TEMP.:	3150 deg F	**WATER IN TEMP.:**	113.1 F
STEEL TRANS. TEMP.:	2993 deg F	**WATER FLOW:**	95.5 GPM
AIM CASTING TEMPERATURE:	2950 deg F	**TEMP DIFFERENTIAL:**	40.9 deg F
CAST TEMPERATURE:	2953 deg F	**DEW POINT:**	66 deg F
		SHROUD GAS:	Argon

PURPOSE OF TRIAL:

Trial was to evaluate the effects of a threaded wheel (* - 4.5 mil deep threads with a 17 pitch and 3 mil flats), and to evaluate the effects of using zirconia foot print wings. 3/4" dogbones were cut into the weir to increase flow along the wings and retard dam formation. **The bottom was of one piece and the wings were zirconia 3006 attached with Phoxbond.

RESULTS OF TRIAL:

The zirconia was cut with an overhang
During heatup of the box, openings occured under the wings in the Krojoc joint between the wings and bottom. Cracks were also seen in close proximity to the area where the zirconia overhung. All but ~100 pounds of the heat were cast. The cast was aborted due to a breakout on the south wing. The breakout was attributed to a opening at the top of the nozzle, due to moving the wheel in and not up during the cast.

FILES:

C:\DATA\CUT848	C:\DATA\HEAT848
C:\DATA\CAST848	C:\DATA\HT848.XLS

MELT OVERFLOW STRIP CASTING LOG

CAST NUMBER: **849**   DATE: 9/8/92   TIME: 15:00:00 P

HEAT WEIGHT: 1000 Lbs.   AMOUNT CAST: 660'   GRADE: Si-Killed

HEAT ANALYSIS

	C	MN	SI	AL	N2	O2	S	Cu
AIM:	0.05	0.3	0.17	<.004	<.005	<.03	<.008	<.025
FINAL:	0.047	0.21	0.059	0.001	0.004	0.049	0.006	0.016

CASTING PARAMETERS

SUBSTRATE:	Normal Cu	POOL DEPTH:	2-1/2" max
SUBSTRATE FINISH:	Threaded *	WEIR GAP:	0.25" w/bones
NOZZLE POS. WRT WHEEL:	60 deg BTDC	NOZZLE WIDTH:	12.00"
NOZZLE GAP:		NOZZLE BRICK:	Zirconia**
AUTO GAP ADJUST:	0.5 mils	MANUFACTURE:	Narco
LADLE PREHEAT TEMP.:	1910 deg F	LOT #:	3006A
POUR BOX PREHEAT TEMP.:	2199 deg F	INITIAL CAST SPEED:	300 FPM
FURNACE TAP TEMP.:	3151 deg F	WATER IN TEMP.:	125 F
STEEL TRANS. TEMP.:	>3000 deg F	WATER FLOW:	95.8 GPM
AIM CASTING TEMPERATURE:	2950 deg F	TEMP DIFFERENTIAL:	N/A
CAST TEMPERATURE:	N/A	DEW POINT:	66 deg F
		SHROUD GAS:	Argon

PURPOSE OF TRIAL: to evaluate the effects of a threaded wheel (* - 4.5 mil deep threads with a 17 pitch and 3 mil flats), and to evaluate the effects of using zirconia foot print wings. 3/4" dogbones were cut into the weir to increase flow along the wings and retard dam formation. **The bottom was one piece and the wings were zirconia 3006 This was also an attempt to duplicate previous results (CAST 848).

RESULTS OF TRIAL: The zirconia was cut with an overhang
During heatup of the box openings occured under the wings in the Krojoc joint between the wings and bottom. Cracks were also seen in close proximity to the area where the zirconia overhung. The entire heat was cast. The only failure was the breaking of the top of the north wing ≥3/4 of the way through the cast. This resulted in having to complete the cast at less than full metal height.

FILES:
C:\DATA\CUT849   C:\DATA\HEAT849
C:\DATA\CAST849   C:\DATA\HT849.XLS

MELT OVERFLOW STRIP CASTING LOG

CAST NUMBER:	850	DATE:	9/11/92	TIME:	1:00 PM

HEAT WEIGHT:	1000 Lbs.	AMOUNT CAST:	0 '	GRADE:	Si-Killed

HEAT ANALYSIS

	C	MN	SI	AL	N2	O2	S	Cu
AIM:	0.05	0.3	0.17	<.004	<.005	<.03	<.008	<.025
FINAL:	N/A	N/A	N/A	N/A	N/A	N/A	N/A	N/A

CASTING PARAMETERS

SUBSTRATE:	Normal Cu	POOL DEPTH:	2-1/2" max
SUBSTRATE FINISH:	Threaded •	WEIR GAP:	0.25" w/bones
NOZZLE POS. WRT WHEEL:	60 deg BTDC	NOZZLE WIDTH:	12.00"
NOZZLE GAP:		NOZZLE BRICK:	
AUTO GAP ADJUST:	0.3 mils	MANUFACTURE:	
LADLE PREHEAT TEMP.:	N/A	LOT #:	
POUR BOX PREHEAT TEMP.:	N/A	INITIAL CAST SPEED:	300 FPM
FURNACE TAP TEMP.:	N/A	WATER IN TEMP.:	N/A
STEEL TRANS. TEMP.:	N/A	WATER FLOW:	N/A
AIM CASTING TEMPERATURE:	2950 deg F	TEMP DIFFERENTIAL:	N/A
CAST TEMPERATURE:	N/A	DEW POINT:	N/A
		SHROUD GAS:	Argon

PURPOSE OF TRIAL:

To evaluate the use of 1" material for use as nozzle wings. The joint between the two materials was a straight joint with Krojoc used as a seal.

RESULTS OF TRIAL:

The wings did not survive to the hot test. There were large openings between the wings and floor in the Krojoc joint. The wings were bowed inward towards the runner. Due to the severity of the bowing the cast was aborted.

FILES:

C:\DATA\CUT850   C:\DATA\HEAT850
C:\DATA\HT850.XLS

HT851.XLS

MELT OVERFLOW STRIP CASTING LOG

CAST NUMBER:	851	DATE:	9/15/92	TIME:	2:00 PM

HEAT WEIGHT:	1000 Lbs.	AMOUNT CAST:	0 '	GRADE:	Si-Killed

HEAT ANALYSIS

	C	MN	SI	AL	N2	O2	S	Cu
AIM:	0.05	0.3	0.17	<.004	<.005	<.03	<.008	<.025
FINAL:	N/A	N/A	N/A	N/A	N/A	N/A	N/A	N/A

CASTING PARAMETERS

SUBSTRATE:	Normal Cu	POOL DEPTH:	2-1/2" max
SUBSTRATE FINISH:	Threaded *	WEIR GAP:	0.25" w/bones
NOZZLE POS. WRT WHEEL:	60 deg BTDC	NOZZLE WIDTH:	12.00"
NOZZLE GAP:		NOZZLE BRICK:	Zirconia
AUTO GAP ADJUST:	0.3 mils	MANUFACTURE:	Narco
LADLE PREHEAT TEMP.:	N/A	LOT #:	3006
POUR BOX PREHEAT TEMP.:	N/A	INITIAL CAST SPEED:	300 FPM
FURNACE TAP TEMP.:	N/A	WATER IN TEMP.:	N/A
STEEL TRANS. TEMP.:	N/A	WATER FLOW:	N/A
AIM CASTING TEMPERATURE:	2950 deg F	TEMP DIFFERENTIAL:	N/A
CAST TEMPERATURE:	N/A	DEW POINT:	N/A
		SHROUD GAS:	Argon

PURPOSE OF TRIAL:

To evaluate the use of Phoxbond to attach ⸱⸱⸱ ⸱⸱⸱ material to ziconia brick and to evaluate the use of ⸱⸱⸱ a nozzle bottom with zirconia wings. The ziconia brick had simple cut fronts ⸱⸱⸱ ⸱⸱⸱ The joints between the bottom and wings were simple joints sealed with Krojoc.

RESULTS OF TRIAL:

The joint between the wings and bottom opened up early in the preheat. A hot repair with Krojoc was attemped with minor success. The ⸱⸱⸱ material cracked along the Phoxbond joints on both wings. The crack on the south wing was long enough to cause the heat to be aborted. The south wing was also noted to have a horizontal crack about half way up ⸱⸱⸱

FILES:	C:\DATA\CUT851	C:\DATA\HEAT851
	C:\DATA\HT851.XLS	

MELT OVERFLOW STRIP CASTING LOG

CAST NUMBER:	852	**DATE:**	9/18/92	**TIME:**	1:00 PM
HEAT WEIGHT:	1000 Lbs.	**AMOUNT CAST:**	600'	**GRADE:**	Si-Killed

HEAT ANALYSIS

	C	MN	SI	AL	N2	O2	S	Cu
AIM:	0.05	0.3	0.17	<.004	<.005	<.03	<.008	<.025
FINAL:	0.047	0.26	0.1	0.003	0.004	0.051	0.007	0.02

CASTING PARAMETERS

SUBSTRATE:	Normal Cu	**POOL DEPTH:**	2-1/2" max
SUBSTRATE FINISH:	Threaded *	**WEIR GAP:**	0.25" w/bones
NOZZLE POS. WRT WHEEL:	60 deg BTDC	**NOZZLE WIDTH:**	12.00"
NOZZLE GAP:		**NOZZLE BRICK:**	Zirconia**
AUTO GAP ADJUST:	0.3 mils	**MANUFACTURE:**	Narco
LADLE PREHEAT TEMP.:	1710 deg F	**LOT #:**	3006A
POUR BOX PREHEAT TEMP.:	2019 deg F	**INITIAL CAST SPEED:**	300 FPM
FURNACE TAP TEMP.:	3150 deg F	**WATER IN TEMP.:**	118.4 F
STEEL TRANS. TEMP.:	3041 deg F	**WATER FLOW:**	99 GPM
AIM CASTING TEMPERATURE:	2950 deg F	**TEMP DIFFERENTIAL:**	34.3 deg F
CAST TEMPERATURE:	3046 deg F	**DEW POINT:**	66 deg F
		SHROUD GAS:	Argon

PURPOSE OF TRIAL:

Trial was to evaluate a threaded wheel (* - 4 mils deep/17 mil pitch/with 3 mil flats), and the use of zirconia materials

RESULTS OF TRIAL:

There were no problems prior to or during the cast. The entire heat was cast. After the cast some slag attack was noted on the material and on the Phoxbond joint.

FILES:

C:\DATA\CUT852   C:\DATA\HEAT852

C:\DATA\CAST852   C:\DATA\HT852.XLS

MELT OVERFLOW STRIP CASTING LOG

'AST NUMBER:	853	DATE:	9/22/92	TIME:	4:00 PM
HEAT WEIGHT:	1200 Lbs.	AMOUNT CAST:	0	GRADE:	Si-Killed

HEAT ANALYSIS

	C	MN	SI	AL	N2	O2	S	Cu
AIM:	0.05	0.3	0.17	<.004	<.005	<.03	<.008	<.025
FINAL:	N/A	N/A	N/A	N/A	N/A	N/A	N/A	N/A

CASTING PARAMETERS

SUBSTRATE:	Normal Cu	POOL DEPTH:	N/A
SUBSTRATE FINISH:	242 u in.	WEIR GAP:	0.25" w/bones
NOZZLE POS. WRT WHEEL:	60 deg BTDC	NOZZLE WIDTH:	12.00"
NOZZLE GAP:	.	NOZZLE BRICK:	Zirconia**
AUTO GAP ADJUST:	0.3 mils	MANUFACTURE:	Narco
LADLE PREHEAT TEMP.:	N/A	LOT #:	3006A
POUR BOX PREHEAT TEMP.:	N/A	INITIAL CAST SPEED:	N/A
FURNACE TAP TEMP.:	N/A	WATER IN TEMP.:	N/A
STEEL TRANS. TEMP.:	N/A	WATER FLOW:	N/A
AIM CASTING TEMPERATURE:	2950 deg F	TEMP DIFFERENTIAL:	N/A
CAST TEMPERATURE:	N/A	DEW POINT:	N/A
		SHROUD GAS:	N/A

PURPOSE OF TRIAL: This trial was being run to evaluate the effects of wheel speed changes on strip thickness, to attempt to determine if a dam is always present in the steel pool next to the wheel, and to reevaluate the effects of a nonthreaded wheel.

RESULTS OF TRIAL: During furnace tap the laddle began to leak from the nozzle. The ladle stopper rod did not seat properly and the ladle could not be shut off. The entire heat was aborted directly to the mold. The nozzle looked very good after preheating. An attempt was made to cool the box to see if the nozzle could be saved. The Phoxbond joints on the wings did not survive the cool down. Maximum cooldown rate was 3 degrees F/minute.

FILES: C:\DATA\CUT853   C:\DATA\HT853.XLS

MELT OVERFLOW STRIP CASTING LOG

CAST NUMBER:	854	DATE:	9/25/92	TIME:	1:00 PM

HEAT WEIGHT:	1200 Lbs.	AMOUNT CAST:	800'	GRADE:	Si-Killed

HEAT ANALYSIS

	C	MN	SI	AL	N2	O2	S	Cu
AIM:	0.05	0.3	0.17	<.004	<.005	<.03	<.008	<.025
FINAL:	0.052	0.31	0.13	0.003	0.004	0.047	0.007	0.02

CASTING PARAMETERS

SUBSTRATE:	Normal Cu	POOL DEPTH:	2-1/2" max
SUBSTRATE FINISH:	240 u inches	WEIR GAP:	0.25" w/bones
NOZZLE POS. WRT WHEEL:	60 deg BTDC	NOZZLE WIDTH:	12.00"
NOZZLE GAP:		NOZZLE BRICK:	Spinel**
AUTO GAP ADJUST:	0.3 mils	MANUFACTURE:	
LADLE PREHEAT TEMP.:	1630 deg F	LOT #:	
POUR BOX PREHEAT TEMP.:	2138 deg F	INITIAL CAST SPEED:	300 FPM
FURNACE TAP TEMP.:	3150 deg F	WATER IN TEMP.:	116.2 F
STEEL TRANS. TEMP.:	3036 deg F	WATER FLOW:	99.1 GPM
AIM CASTING TEMPERATURE:	2950 deg F	TEMP DIFFERENTIAL:	41.0 deg F
CAST TEMPERATURE:	3041 deg F	DEW POINT:	49 deg F
		SHROUD GAS:	Argon

PURPOSE OF TRIAL:

Trial was to evaluate the use of Mg-Al-Spinel** as a backup brick _____ The Spinel materials were cast at Research. During the cast the wheel speed was varied up and down to look for dams and to evaluate the strip quality at various wheel speeds.

RESULTS OF TRIAL:

There was a slight bow in the floor and small openings in the Krojoc joints (under the wings) prior to casting. During the cast the bottom Spinel _____ cracked in three fairly evenly spaced locations. The most severe crack was on the South side where numerous dams were formed during casting. After the cast, some metal penetration was noted under the wings and slag attack _____ was significant. _____ Testing of the Mg-Al-Spinel material showed that it was not fully stabilized (not cured at high enough temperature). The next batch will be cured at 3000 F versus the 2700 F used for the bricks in this run.

FILES:

C:\DATA\CUT854   C:\DATA\HEAT854

C:\DATA\CAST854   C:\DATA\HT854.XLS

MELT OVERFLOW STRIP CASTING LOG

CAST NUMBER:	855	DATE:	9/29/92	TIME:	1:00 PM

HEAT WEIGHT:	1000 Lbs.	AMOUNT CAST:	450	GRADE:	Si-Killed

HEAT ANALYSIS

	C	MN	SI	AL	N2	O2	S	Cu
AIM:	0.05	0.3	0.17	<.004	<.005	<.03	<.008	<.025
FINAL:								

CASTING PARAMETERS

SUBSTRATE:	Normal Cu	POOL DEPTH:	2-1/2" max
SUBSTRATE FINISH:	240 u inches	WEIR GAP:	0.25" w/bones
NOZZLE POS. WRT WHEEL:	60 deg BTDC	NOZZLE WIDTH:	12.00"
NOZZLE GAP:		NOZZLE BRICK:	Zirconia**
AUTO GAP ADJUST:	0.3 mils	MANUFACTURE:	Narco
LADLE PREHEAT TEMP.:	1960 deg F	LOT #:	3006A
POUR BOX PREHEAT TEMP.:	2154 deg F	INITIAL CAST SPEED:	300 FPM
FURNACE TAP TEMP.:	3151 deg F	WATER IN TEMP.:	116.0 F
STEEL TRANS. TEMP.:	3030 deg F	WATER FLOW:	34.1 GPM
AIM CASTING TEMPERATURE:	2950 deg F	TEMP DIFFERENTIAL:	64.0 deg F
CAST TEMPERATURE:	3021 deg F	DEW POINT:	43 deg F
		SHROUD GAS:	Argon

PURPOSE OF TRIAL:

Trial was to evaluate casting with the weir moved closer to the wheel (31/32" weir to wheel prior to cast) and to evaluate casting without the dam in the back of the pouring box. The nozzle design used   a TC installed .15/32" from the wheel and   wings attached to zirconia 3006 with Phoxbond.

RESULTS OF TRIAL:

After preheat the Krojoc joints under the wings had opened slightly and several hairline cracks where in the south Phoxbond joint. During the cast a dam formed in the center of the strip and on the south side of the nozzle. eventually the south side opened up   . An apparent flat (low) spot on the wheel was noted. When the high side of the wheel came   in contact with the nozzle a portion of the wing was broken off and also a substantial portion of the bottom of the nozzle. The cast was aborted at this time. While the TC in the nozzle indicated dam formation it's location may have precipitated the dam, as a large crack in the nozzle floor in the vicinity of the TC was noted after the cast.

FILES:

C:\DATA\CUT848   C:\DATA\HEAT848

C:\DATA\CAST848   C:\DATA\HT848.XLS

HT856.XLS

MELT OVERFLOW STRIP CASTING LOG

CAST NUMBER:	856	DATE:	10/2/92	TIME:	1:00 PM
HEAT WEIGHT:	1000 Lbs.	AMOUNT CAST:	510'	GRADE:	Si-Killed

HEAT ANALYSIS

	C	MN	SI	AL	N2	O2	S	Cu
AIM:	0.05	0.3	0.17	<.004	<.005	<.03	<.008	<.025
FINAL:	0.043	0.31	0.13	0.01	0.004	0.051	0.007	0.022

CASTING PARAMETERS

SUBSTRATE:	Normal Cu	POOL DEPTH:	2-1/2" max
SUBSTRATE FINISH:	240 u inches	WEIR GAP:	0.25" w/bones
NOZZLE POS. WRT WHEEL:	60 deg BTDC	NOZZLE WIDTH:	12.00"
NOZZLE GAP:		NOZZLE BRICK:	Zirconia**
AUTO GAP ADJUST:	0.3 mils	MANUFACTURE:	Narco
LADLE PREHEAT TEMP.:	1692 deg F	LOT #:	3006A
POUR BOX PREHEAT TEMP.:	2140 deg F	INITIAL CAST SPEED:	300 FPM
FURNACE TAP TEMP.:	3154 deg F	WATER IN TEMP.:	117.4 F
STEEL TRANS. TEMP.:	2993 deg F	WATER FLOW:	33.7 GPM
AIM CASTING TEMPERATURE:	2950 deg F	TEMP DIFFERENTIAL:	92.7 deg F
CAST TEMPERATURE:	2951 deg F	DEW POINT:	47 deg F
		SHROUD GAS:	Argon

PURPOSE OF TRIAL:

Trial was to evaluate running a hot wheel with an oxide layer on the wheel, and to evaluate changes in wheel speed on strip thickness.

RESULTS OF TRIAL:

Small opennings were noted in the Krojoc joints between the wings and nozzle floor. A crack also developed in the northern 1/3 of the nozzle bottom. The bottom was warped enough that there was significant missfit between the wheel and nozzle. During casting erratic fluctuations were noted in the wheel speed. A leak developed in the nozzle bottom (south side). Cast was aborted due to leak and restarted after leak froze off. Wheel then stopped suddenly causing cast to be aborted.

FILES:

C:\DATA\CUT856   C:\DATA\HEAT856
C:\DATA\CAST856   C:\DATA\HT856.XLS

Page 1

MELT OVERFLOW STRIP CASTING LOG

CAST NUMBER:	857	DATE:	10/16/92	TIME:	1:00 PM

HEAT WEIGHT:	1000 Lbs.	AMOUNT CAST:	330	GRADE:	Si-Killed

HEAT ANALYSIS

	C	MN	SI	AL	N2	O2	S	Cu
AIM:	0.05	0.3	0.17	<.004	<.005	<.03	<.008	<.025
FINAL:								

CASTING PARAMETERS

SUBSTRATE:	Normal Cu	POOL DEPTH:	2-1/2" max
SUBSTRATE FINISH:	240 u inch	WEIR GAP:	0.375" w/bones
NOZZLE POS. WRT WHEEL:	60 deg BTDC	NOZZLE WIDTH:	11.94"
NOZZLE GAP:		NOZZLE BRICK:	Spinel**
AUTO GAP ADJUST:	0.3 mils	MANUFACTURE:	
LADLE PREHEAT TEMP.:	1991 deg F	LOT #:	
POUR BOX PREHEAT TEMP.:	2165 deg F	INITIAL CAST SPEED:	300 FPM
FURNACE TAP TEMP.:	3160 deg F	WATER IN TEMP.:	115.8 F
STEEL TRANS. TEMP.:	3028 deg F	WATER FLOW:	33.6 GPM
AIM CASTING TEMPERATURE:	2950 deg F	TEMP DIFFERENTIAL:	79.9 deg F
CAST TEMPERATURE:	N/A	DEW POINT:	55 deg F
		SHROUD GAS:	Argon

PURPOSE OF TRIAL:

Trial was to evaluate ___ . Spinel backup brick. ___ For this cast, a new copper wheel was used and wheel growth sensors were installed. No inner wheel temperatures were recorded. Dresser pressure was reduced and Titanium was added to the heat to see if it would reduce strip cracking.

RESULTS OF TRIAL:

Cracks were seen in the ___ nozzle bottom prior to nozzle assembly. The ___ material was suspect prior to assembly. The spinel held up quite well. The cast was aborted when the nozzle bottom ___ failed. There appeared to be metal penetration in the joints ___ (used 3 pieces to make the bottom ___). The wheel growth indicators showed a growth of >45 mils on the south side of the wheel and ~ 30 mils on the north side. The laser level gauge was run during this cast, but, partially due to positioning problems with the head no good data was collected.

FILES:

C:\DATA\CUT857	C:\DATA\HEAT857
C:\DATA\CAST857	C:\DATA\HT857.XLS

MELT OVERFLOW STRIP CASTING LOG

CAST NUMBER:	858	DATE:	10/21/92	TIME:	2:00 PM

HEAT WEIGHT:	1000 Lbs.	AMOUNT CAST:	600'	GRADE:	Si-Killed

HEAT ANALYSIS

	C	MN	SI	AL	N2	O2	S	Cu
AIM:	0.05	0.3	0.17	<.004	<.005	<.03	<.008	<.025
FINAL:								

CASTING PARAMETERS

SUBSTRATE:	Normal Cu	POOL DEPTH:	2-1/2" max
SUBSTRATE FINISH:	283 u in.	WEIR GAP:	0.25" w/bones
NOZZLE POS. WRT WHEEL:	60 deg BTDC	NOZZLE WIDTH:	12.00"
NOZZLE GAP:		NOZZLE BRICK:	Zirconia**
AUTO GAP ADJUST:	0.3 mils	MANUFACTURE:	Narco
LADLE PREHEAT TEMP.:	1810 deg F	LOT #:	3006A
POUR BOX PREHEAT TEMP.:	2111 deg F	INITIAL CAST SPEED:	280 FPM
FURNACE TAP TEMP.:	3154 deg F	WATER IN TEMP.:	117.6 F
STEEL TRANS. TEMP.:	3040 deg F	WATER FLOW:	98.7 GPM
AIM CASTING TEMPERATURE:	2950 deg F	TEMP DIFFERENTIAL:	41.3 deg F
CAST TEMPERATURE:	2946 deg F	DEW POINT:	48 deg F
		SHROUD GAS:	Argon

PURPOSE OF TRIAL:

Trial was to evaluate the use of Titanium and Columbium to reduce the cracking in the strip. The heat was run with a nozzle constructed with zirconia backup brick . The wings were 1 1/2" thick and the floor was 1" thick The materials were attached with Phoxbond. Wheel growth sensors were used on this run which was conducted on a new copper wheel. This heat was used for the DOE review meeting.

RESULTS OF TRIAL:

There were no problems noted with the nozzle prior to casting. During the cast no refractory problems were noted. After the cast small vertical cracks in the nozzle bottom were noted. They were ~2-1/2" apart. One horizontal crack was also noted (~3/16" from the top of the floor). On the wings, a horizontal crack was noted half way up the material and extending the entire perimiter of the material. Also, vertical cracks were noted in the machined corners of the wing material.

FILES:

C:\DATA\CUT858   C:\DATA\HEAT858
C:\DATA\CAST858   C:\DATA\HT858.XLS

MELT OVERFLOW STRIP CASTING LOG

CAST NUMBER:	859	DATE:	10/28/92	TIME:	12:30 PM
HEAT WEIGHT:	1000 Lbs.	AMOUNT CAST:	425'	GRADE:	Si-Killed

HEAT ANALYSIS

	C	MN	SI	AL	N2	O2	S	Cu
AIM:	0.05	0.3	0.17	<.004	<.005	<.03	<.008	<.025
FINAL:								

CASTING PARAMETERS

SUBSTRATE:	Normal Cu	POOL DEPTH:	2-1/2" max
SUBSTRATE FINISH:	220 u in.	WEIR GAP:	0.25" w/bones
NOZZLE POS. WRT WHEEL:	60 deg BTDC	NOZZLE WIDTH:	12.00"
NOZZLE GAP:		NOZZLE BRICK:	Zirconia***
AUTO GAP ADJUST:	0.3 mils	MANUFACTURE:	Narco
LADLE PREHEAT TEMP.:	1935 deg F	LOT #:	3006A
POUR BOX PREHEAT TEMP.:	2195 deg F	INITIAL CAST SPEED:	280 FPM
FURNACE TAP TEMP.:	3152 deg F	WATER IN TEMP.:	114.6 F
STEEL TRANS. TEMP.:	2947 deg F	WATER FLOW:	33.9 GPM
AIM CASTING TEMPERATURE:	2950 deg F	TEMP DIFFERENTIAL:	84.4 deg F
CAST TEMPERATURE:	2907 deg F	DEW POINT:	46 deg F
		SHROUD GAS:	Argon

PURPOSE OF TRIAL:

Trial was to evaluate the use of Titanium and Columbium to reduce the cracking in the strip. The heat was run with a nozzle constructed with zirconia backup brick   The wings were 1-1/2" thick and the floor was 1" thick The   materials were attached with Phoxbond. A 1/4" plate of SiC was used under the nozzle floor to prevent bowing. Wheel growth sensors were used on this run which was conducted on a new copper wheel. This heat was used for the   demonstration.

RESULTS OF TRIAL:

Three and a half hours into the preheat the   material had numerous cracks (both sides). The typical "after cast" horizontal crack at the mid-line was present as were vertical cracks in the machined corners of the footprint material. The Krojoc joints opened marginally. During casting the center of the wheel did not mate up to the wheel due to the floor bowing. Oscillation of the wheel was also noted during the cast. The cast was aborted due to a dam formed in the center of the nozzle and lack of metal due to abort hole errosion. After the cast it could be seen that steel ran down between the wheel and nozzle at the center of the nozzle and then penetrated under the refractory floor through a horizontal crack.

FILES:

C:\DATA\CUT859   C:\DATA\HEAT859
C:\DATA\CAST859   C:\DATA\HT859.XLS

MELT OVERFLOW STRIP CASTING LOG

CAST NUMBER:	860	DATE:	11/3/92	TIME:	1:00 PM

HEAT WEIGHT:	1000 Lbs.	AMOUNT CAST:	0	GRADE:	Si-Killed

HEAT ANALYSIS

	C	MN	SI	AL	N2	O2	S	Cu
AIM:	0.05	0.3	0.17	<.004	<.005	<.03	<.008	<.025
FINAL:	N/A	N/A	N/A	N/A	N/A	N/A	N/A	N/A

CASTING PARAMETERS

SUBSTRATE:	Normal Cu	POOL DEPTH:	2-1/2" max
SUBSTRATE FINISH:	164 u inch	WEIR GAP:	0.25" w/bones
NOZZLE POS. WRT WHEEL:	60 deg BTDC	NOZZLE WIDTH:	12.00"
NOZZLE GAP:		NOZZLE BRICK:	
AUTO GAP ADJUST:	0.3 mils	MANUFACTURE:	Foseco
LADLE PREHEAT TEMP.:	N/A	LOT #:	
POUR BOX PREHEAT TEMP.:	N/A	INITIAL CAST SPEED:	280 FPM
FURNACE TAP TEMP.:	N/A	WATER IN TEMP.:	N/A
STEEL TRANS. TEMP.:	N/A	WATER FLOW:	N/A
AIM CASTING TEMPERATURE:	2950 deg F	TEMP DIFFERENTIAL:	N/A
CAST TEMPERATURE:	N/A	DEW POINT:	46 deg F
		SHROUD GAS:	Argon

PURPOSE OF TRIAL:

Trial was to evaluate the use of .... a nozzle material and the use of a refractory ring inside the pouring box to deflect splash at the start of casting. The weir was positioned 2 - 2/32" from the wheel (minimum distance) and the weir contained 3/4" dogbone cuts in each corner.

RESULTS OF TRIAL:

The south wing had a gouge .... (apparently from a grain pulling loose). A crack developed in the nozzle bottom in conjuction with a stray saw cut. The Krojoc joints under both wings showed significant seperation at temperature. Also, cracks running both parallel and perpendicular to the cast direction were noted in the nozzle bottom (seen on the bottom side only). JUST PRIOR TO CAST the ground fault breaker tripped and could not be reset. This prevented the wheel from being brought into cast position and the cast was aborted. THE NOZZLE WAS SAVED FOR THE NEXT RUN.

FILES:	C:\DATA\CUT860		C:\DATA\HEAT860
	C:\DATA\CAST860	C:\DATA\HT860.XLS	

HT861.XLS

MELT OVERFLOW STRIP CASTING LOG

CAST NUMBER: 861   **DATE:** 11/4/92   **TIME:** 1:00 PM

HEAT WEIGHT: 1000 Lbs.   **AMOUNT CAST:** 450'   **GRADE:** Si-Killed

HEAT ANALYSIS

	C	MN	SI	AL	N2	O2	S	Cu
AIM:	0.05	0.3	0.17	<.004	<.005	<.03	<.008	<.025
FINAL:								

CASTING PARAMETERS

SUBSTRATE:	Normal Cu	POOL DEPTH:	2-1/2" max
SUBSTRATE FINISH:	164 u inch	WEIR GAP:	0.25" w/bones
NOZZLE POS. WRT WHEEL:	60 deg BTDC	NOZZLE WIDTH:	12.00"
NOZZLE GAP:		NOZZLE BRICK:	
AUTO GAP ADJUST:	0.3 mils	MANUFACTURE:	Foseco
LADLE PREHEAT TEMP.:	1805 Deg. F	LOT #:	
POUR BOX PREHEAT TEMP.:	2122 Deg. F	INITIAL CAST SPEED:	280 FPM
FURNACE TAP TEMP.:	3153 Deg. F	WATER IN TEMP.:	116.1 Deg. F
STEEL TRANS. TEMP.:	2992 Deg. F	WATER FLOW:	34.3 GPM
AIM CASTING TEMPERATURE:	2950 deg F	TEMP DIFFERENTIAL:	95.0 Deg. F
CAST TEMPERATURE:	2913 Deg. F	DEW POINT:	45 deg F
		SHROUD GAS:	Argon

PURPOSE OF TRIAL:

Trial was to evaluate the use of   a nozzle material and the use of a refractory ring inside the pouring box to deflect splash at the start of casting. The weir was positioned 2 - 2/32" from the wheel (minimum distance) and the weir contained 3/4" dogbone cuts in each corner. THIS IS THE SAME NOZZLE AS USED FOR THE ABORTED CAST FROM HEAT 860.

RESULTS OF TRIAL:

The south wing had a gouge   (apparently from a grain pulling loose). A crack developed in the nozzle bottom in conjuction with a stray saw cut. The Krojoc joints under both wings showed significant seperation at temperature. Also, cracks running both parallel and perpendicular to the cast direction were noted in the nozzle bottom (seen on the bottom side only). Steel erroded under both wings (mainly south). Some freeze-up was noted on both the north and south sides. Errosion under the south wing eventually lead to a south wing breakout and cast abort.

FILES: C:\DATA\CUT861   C:\DATA\HEAT861

            C:\DATA\CAST861   C:\DATA\HT861.XLS

HT862.XLS

MELT OVERFLOW STRIP CASTING LOG

CAST NUMBER: 862 **DATE:** 11/6/92 **TIME:** 2:00 PM

HEAT WEIGHT: 1000 Lbs. **AMOUNT CAST:** 595' **GRADE:** Si-Killed

HEAT ANALYSIS

	C	MN	SI	AL	N2	O2	S	Cu
AIM:	0.05	0.3	0.17	<.004	<.005	<.03	<.008	<.025
FINAL:								

CASTING PARAMETERS

SUBSTRATE:	Normal Cu	POOL DEPTH:	2-1/2" max
SUBSTRATE FINISH:	164 u inch	WEIR GAP:	0.4
NOZZLE POS. WRT WHEEL:	60 deg BTDC	NOZZLE WIDTH:	12.00"
NOZZLE GAP:		NOZZLE BRICK:	Spinel
AUTO GAP ADJUST:	0.3 mils	MANUFACTURE:	
LADLE PREHEAT TEMP.:	1841 Deg. F	LOT #:	
POUR BOX PREHEAT TEMP.:	2033 Deg. F	INITIAL CAST SPEED:	295 FPM
FURNACE TAP TEMP.:	3103 Deg. F	WATER IN TEMP.:	115.3 Deg. F
STEEL TRANS. TEMP.:	2985 Deg. F	WATER FLOW:	97.8 GPM
AIM CASTING TEMPERATURE:	2900 deg F	TEMP DIFFERENTIAL:	56.2 Deg. F
CAST TEMPERATURE:	2884 Deg. F	DEW POINT:	42 deg F
		SHROUD GAS:	Argon

PURPOSE OF TRIAL:

Trial was to evaluate the use of Alumina Spinel refractories as an alternative backup material and to attempt to provide data to confirm freeze-off data generated by Brian Thomas. The nozzle bottom was 1" thick _____ attached with Phoxbond. The wings were 1.5" thick _____ attached with Phoxbond. The weir was a strait weir and measured 1 - 20/32" from the wheel at minimum distance. A thermocouple was inserted into the nozzle from the north side (1-3/8" from the wheel just off the nozzle bottom.

RESULTS OF TRIAL:

Prior to cast only a small separation in the Krojoc joint under the south wing was noted. During the cast, small dams were noted to form on the north side and center. The longer the cast lasted the fewer number of dams formed. The wheel speed was lowered and dams began to form again. A large dam started and froze off the north side. Casting continued on the south side until the full heat was cast.

FILES:

C:\DATA\CUT862 C:\DATA\HEAT862

C:\DATA\CAST862 C:\DATA\HT862.XLS

MELT OVERFLOW STRIP CASTING LOG

CAST NUMBER:	863	DATE:	11/10/92	TIME:	2:45 PM

HEAT WEIGHT:	1000 Lbs.	AMOUNT CAST:	0'	GRADE:	Si-Killed

HEAT ANALYSIS

	C	MN	SI	AL	N2	O2	S	Cu
AIM:	0.05	0.3	0.17	<.004	<.005	<.03	<.008	<.025
FINAL:	N/A	N/A	N/A	N/A	N/A	N/A	N/A	N/A

CASTING PARAMETERS

SUBSTRATE:	Normal Cu	POOL DEPTH:	2-1/2" max
SUBSTRATE FINISH:	162 u inch	WEIR GAP:	0.25" w/bones
NOZZLE POS. WRT WHEEL:	60 deg BTDC	NOZZLE WIDTH:	12.00"
NOZZLE GAP:		NOZZLE BRICK:	
AUTO GAP ADJUST:	0.3 mils	MANUFACTURE:	Foseco
LADLE PREHEAT TEMP.:	1648 Deg. F	LOT #:	
POUR BOX PREHEAT TEMP.:	2145 Deg. F	INITIAL CAST SPEED:	295 FPM
FURNACE TAP TEMP.:	3102 Deg. F	WATER IN TEMP.:	N/A
STEEL TRANS. TEMP.:	2958 Deg. F	WATER FLOW:	N/A
AIM CASTING TEMPERATURE:	2900 deg F	TEMP DIFFERENTIAL:	N/A
CAST TEMPERATURE:	2860 Deg. F	DEW POINT:	49 deg F
		SHROUD GAS:	Argon

PURPOSE OF TRIAL:

Trial was to evaluate ⸻ a nozzle material, a new shroud disign, and casting with lower initial steel temperatures. ⸻ The bottom was 1" thick and the wings were 1.5" thick. The weir was set 1-2/32" back from the wheel (minimum distance).

RESULTS OF TRIAL:

Prior to casting a small opening was noted in the Krojoc joint between the wing and floor on the north side. At start of cast it was discovered that the splash board did not fit with the new shroud system. In addition, no splash ring had been placed into the box. Therefore, the cast was started slow to avoid splash. A dam formed across the nozzle immediately and no steel was cast onto the wheel.

FILES:

C:\DATA\CUT863	C:\DATA\HEAT863
C:\DATA\CAST863	C:\DATA\HT863.XLS

MELT OVERFLOW STRIP CASTING LOG

CAST NUMBER:	864	**DATE:** 11/13/92	**TIME:** 1:00 PM
HEAT WEIGHT:	1000 Lbs.	**AMOUNT CAST:** 37'	**GRADE:** Si-Killed

HEAT ANALYSIS

	C	MN	SI	AL	N2	O2	S	Cu
AIM:	0.05	0.3	0.17	<.004	<.005	<.03	<.008	<.025
FINAL:	N/A	N/A	N/A	N/A	N/A	N/A	N/A	N/A

CASTING PARAMETERS

SUBSTRATE:	Normal Cu	**POOL DEPTH:**	2-1/2" max
SUBSTRATE FINISH:	165 u inch	**WEIR GAP:**	0.25" w/bones
NOZZLE POS. WRT WHEEL:	60 deg BTDC	**NOZZLE WIDTH:**	12.00"
NOZZLE GAP:		**NOZZLE BRICK:**	
AUTO GAP ADJUST:	0.3 mils	**MANUFACTURE:**	
LADLE PREHEAT TEMP.:	1954 Deg. F	**LOT #:**	
POUR BOX PREHEAT TEMP.:	2134 Deg. F	**INITIAL CAST SPEED:**	295 FPM
FURNACE TAP TEMP.:	3157 Deg. F	**WATER IN TEMP.:**	N/A
STEEL TRANS. TEMP.:	2997 Deg. F	**WATER FLOW:**	N/A
AIM CASTING TEMPERATURE:	2900 deg F	**TEMP DIFFERENTIAL:**	N/A
CAST TEMPERATURE:	N/A	**DEW POINT:**	41 deg F
		SHROUD GAS:	Argon

PURPOSE OF TRIAL:

Trial was to evaluate the use of   an alternative backup material. *The nozzle bottom was 1" thick   attached with a postmixed Phoxbond. The wings were 1.5" thick   attached with a postmixed Phoxbond. (Postmixed - the Phoxbond material as delivered was dry and according to manufactures recommendations phosphoric acid was mixed into the mortar to make it the correct consistency). Weir contained 3/4" dogbones and was placed 25/32" back from the running lip.

RESULTS OF TRIAL:

Prior to cast the only flaw was a minute opening in the Krojoc joint on the north side. Just prior to casting a large crack was noted in the nozzle bottom (just south of nozzle center). Shortly after the start of cast the bottom   material broke loose from the backup material. The failure extended from the south wing to almost 3/4 the way across the nozzle. The mortar joint showed no signs of bonding to the   material.

FILES:

C:\DATA\CUT864   C:\DATA\HEAT864

C:\DATA\CAST864   C:\DATA\HT864.XLS

MELT OVERFLOW STRIP CASTING LOG

CAST NUMBER:	865	DATE:	11/17/92	TIME:	2:00 PM
HEAT WEIGHT:	1000 Lbs.	AMOUNT CAST:	285'	GRADE:	Si-Killed

HEAT ANALYSIS

	C	MN	SI	AL	N2	O2	S	Cu
AIM:	0.05	0.3	0.17	<.004	<.005	<.03	<.008	<.025
FINAL:								

CASTING PARAMETERS

SUBSTRATE:	Normal Cu	POOL DEPTH:	2-1/2" max
SUBSTRATE FINISH:	165 u inch	WEIR GAP:	0.25" w/bones
NOZZLE POS. WRT WHEEL:	60 deg BTDC	NOZZLE WIDTH:	12.00"
NOZZLE GAP:		NOZZLE BRICK:	
AUTO GAP ADJUST:	0.3 mils	MANUFACTURE:	Foseco
LADLE PREHEAT TEMP.:	16105 Deg. F	LOT #:	
POUR BOX PREHEAT TEMP.:	2172 Deg. F	INITIAL CAST SPEED:	295 FPM
FURNACE TAP TEMP.:	3150 Deg. F	WATER IN TEMP.:	117.5 Deg. F
STEEL TRANS. TEMP.:	3012 Deg. F	WATER FLOW:	34.1 GPM
AIM CASTING TEMPERATURE:	2950 deg F	TEMP DIFFERENTIAL:	74.7 Deg. F
CAST TEMPERATURE:	3146 Deg. F	DEW POINT:	47 deg F
		SHROUD GAS:	Argon

PURPOSE OF TRIAL:

Trial was to evaluate the use of a nozzle material . *The nozzle bottom was made of 1" . material and the wings were of 1.5" thick material. The weir was set back 1-7/32 from the running lip and contained 3/4" dogbones.

RESULTS OF TRIAL:

Prior to casting a large separation was noted in the Krojoc joint between the floor and wings (both sides). This was sealed from the outside with Krojoc. During the cast a large section If the south wing spalled into the pool. shortly after that the floor spalled and the cast was aborted. After the cast it could be seen that the steel had penetrated under the wings neat the front of the nozzle and that dams were starting to form here.

FILES:

C:\DATA\CUT865   C:\DATA\HEAT865
C:\DATA\CAST865   C:\DATA\HT865.XLS

MELT OVERFLOW STRIP CASTING LOG

CAST NUMBER:	866	**DATE:** 11/23/92	**TIME:**	1:00 PM
HEAT WEIGHT:	1000 Lbs.	**AMOUNT CAST:** 345'	**GRADE:**	Si-Killed

HEAT ANALYSIS

	C	MN	SI	AL	N2	O2	S	Cu
AIM:	0.05	0.3	0.17	<.004	<.005	<.03	<.008	<.025
FINAL:								

CASTING PARAMETERS

SUBSTRATE:	Normal Cu	**POOL DEPTH:**	2-1/2" max
SUBSTRATE FINISH:	53 u inch	**WEIR GAP:**	0.25" w/bones
NOZZLE POS. WRT WHEEL:	60 deg BTDC	**NOZZLE WIDTH:**	12.00"
NOZZLE GAP:		**NOZZLE BRICK:**	
AUTO GAP ADJUST:	0.3 mils	**MANUFACTURE:**	Foseco
LADLE PREHEAT TEMP.:	1640 Deg. F	**LOT #:**	
POUR BOX PREHEAT TEMP.:	2070 Deg. F	**INITIAL CAST SPEED:**	295 FPM
FURNACE TAP TEMP.:	3153 Deg. F	**WATER IN TEMP.:**	104.1 Deg. F
STEEL TRANS. TEMP.:	2931 Deg. F	**WATER FLOW:**	78 GPM
AIM CASTING TEMPERATURE:	2950 deg F	**TEMP DIFFERENTIAL:**	69.6 Deg. F
CAST TEMPERATURE:	2818 Deg. F	**DEW POINT:**	47 deg F
		SHROUD GAS:	Argon

PURPOSE OF TRIAL:

Trial was to evaluate _____ a nozzle material and the use of a very smooth wheel finish.
The wheel had been turned on the lathe just prior to this cast, to eliminate several imperfections in the surface.

RESULTS OF TRIAL:

Prior to casting small openings were noted in the Krojoc joint between the wing and floor. Also two cracks were observed in the floor just prior to casting. The furnace tap took a long time leading to cooler steel at the wheel. In conjunction with the smooth wheel numerous dams formed in the center and at both corners. A breakout occured in the floor just as the dams appeared to be deminishing. The cast was aborted to keep the breakout from scratching the wheel. After the cast a gouge could be seen _____ _____ where the breakout occured. This was in the vicinity of one of the cracks in the floor noted prior to casting. All material cast was at 290 feet/minute.

FILES:

C:\DATA\CUT866   C:\DATA\HEAT866
C:\DATA\CAST866   C:\DATA\HT866.XLS

HT872.XLS

MELT OVERFLOW STRIP CASTING LOG

CAST NUMBER:	872	DATE:	1/19/93	TIME:	1:00 PM

HEAT WEIGHT:	1000 Lbs.	AMOUNT CAST:	550'	GRADE:	Si-Killed

HEAT ANALYSIS

	C	MN	SI	AL	N2	O2	S	Cu
AIM:	0.05	0.3	0.17	<.004	<.005	<.03	<.008	<.025
FINAL:								

CASTING PARAMETERS

SUBSTRATE:	Normal Cu	POOL DEPTH:	2-1/2" max
SUBSTRATE FINISH:	102 u inch	WEIR GAP:	0.25" w/bones
NOZZLE POS. WRT WHEEL:	60 deg BTDC	NOZZLE WIDTH:	12.00"
NOZZLE GAP:		NOZZLE BRICK:	
AUTO GAP ADJUST:	0.3 mils	MANUFACTURE:	
LADLE PREHEAT TEMP.:	1607 Deg. F	LOT #:	
POUR BOX PREHEAT TEMP.:	2202 Deg. F	INITIAL CAST SPEED:	295 FPM
FURNACE TAP TEMP.:	3155 Deg. F	WATER IN TEMP.:	116.7 Deg. F
STEEL TRANS. TEMP.:	N/A	WATER FLOW:	66.7 GPM
AIM CASTING TEMPERATURE:	2950 deg F	TEMP DIFFERENTIAL:	47.5 Deg. F
CAST TEMPERATURE:	2959 Deg. F	DEW POINT:	37 deg F
		SHROUD GAS:	Argon

PURPOSE OF TRIAL:

Trial was to evaluate _____ a nozzle material, to evaluate the use of the one piece dresser design, to evaluate the operation of the pinch rolls and coiler, and to evaluate a new method of nozzle thermocouple placement. The nozzle was constructed with 1.5" thick _____, and using 1" thick _____ for the bottom. The thermocouple was placed in the joint between the _____ material. The dresser was turned off half way through the cast.

RESULTS OF TRIAL:

A very small openning was noted in the north side Krojoc joint just prior to casting. Also, three cracks were noted in the _____ north, center, and south _____ The one on the south was fairly large. _____ During the cast several dams formed on the soutn side and near center. The full heat was cast. After the cast steel could be found in the center and south cracks and in cracks along the joint between the _____ material. The nozzle thermocouple did not perform well during the cast and may have been partially responsible for the center crack and steel penetration.

FILES:

C:\DATA\CUT872   C:\DATA\HEAT872
C:\DATA\CAST872   C:\DATA\HT872.XLS

MELT OVERFLOW STRIP CASTING LOG

CAST NUMBER:	873	DATE:	1/22/93	TIME:	1:00 PM

HEAT WEIGHT:	1000 Lbs.	AMOUNT CAST:	163'	GRADE:	Si-Killed

HEAT ANALYSIS

	C	MN	SI	AL	N2	O2	S	Cu
AIM:	0.05	0.3	0.17	<.004	<.005	<.03	<.008	<.025
FINAL:								

CASTING PARAMETERS

SUBSTRATE:	Normal Cu	POOL DEPTH:	2-1/2" max
SUBSTRATE FINISH:	105 u inch	WEIR GAP:	0.25" w/bones
NOZZLE POS. WRT WHEEL:	60 deg BTDC	NOZZLE WIDTH:	12.125"
NOZZLE GAP:		NOZZLE BRICK:	
AUTO GAP ADJUST:	0.3 mils	MANUFACTURE:	
LADLE PREHEAT TEMP.:	1864 Deg. F	LOT #:	
POUR BOX PREHEAT TEMP.:	2204 Deg. F	INITIAL CAST SPEED:	295 FPM
FURNACE TAP TEMP.:	3161 Deg. F	WATER IN TEMP.:	115.9 Deg. F
STEEL TRANS. TEMP.:	3007	WATER FLOW:	34.3 GPM
AIM CASTING TEMPERATURE:	2950 deg F	TEMP DIFFERENTIAL:	70.0 Deg. F
CAST TEMPERATURE:	N/A	DEW POINT:	45 deg F
		SHROUD GAS:	Argon

PURPOSE OF TRIAL:

Trial was to evaluate the use of 93Z3 ....material as nozzle materials and to evaluate the use of a dual nozzle burner (heating the corners) as a means of reducing nozzle bottom warpage. Wings were constructed of 1-1/2" wide 93Z3 . Nozzle bottom was of 1 piece 1" thick. Weir to wheel distance prior to cast was 1-7/32" and after cast was 1-1/32".

RESULTS OF TRIAL:

A very small openning was noted in the north side Krojc joint just prior to casting. Both K-brick wing sections were cracked at the top, just in front of the metal framework. Just prior to starting the cast it was noted that the bottom of the nozzle was bowed. Duing the first part of the cast an attempt was made to intentionally break the strip by running the pinch rolls faster than the wheel. The strip did break, but caused the wheel to crash into the nozzle stopping the wheel. The cast had to be aborted due to failure to get the wheel to restart.

FILES:

C:\DATA\CUT873	C:\DATA\HEAT873
C:\DATA\CAST873	C:\DATA\HT873.XLS

MELT OVERFLOW STRIP CASTING LOG

CAST NUMBER:	███████	DATE:	1/29/93	TIME:	1:00 PM

HEAT WEIGHT:	1000 Lbs.	AMOUNT CAST:	550'	GRADE:	Si-Killed

HEAT ANALYSIS

	C	MN	SI	AL	N2	O2	S	Cu
AIM:	0.05	0.3	0.17	<.004	<.005	<.03	<.008	<.025
FINAL:								

CASTING PARAMETERS

SUBSTRATE:	Normal Cu	POOL DEPTH:	2-1/2" max
SUBSTRATE FINISH:	116 u inch	WEIR GAP:	0.25" w/bones
NOZZLE POS. WRT WHEEL:	60 deg BTDC	NOZZLE WIDTH:	11.875"
NOZZLE GAP:		NOZZLE BRICK:	
AUTO GAP ADJUST:	0.3 mils	MANUFACTURE:	
LADLE PREHEAT TEMP.:	1918 Deg. F	LOT #:	
POUR BOX PREHEAT TEMP.:	2156 Deg. F	INITIAL CAST SPEED:	295 FPM
FURNACE TAP TEMP.:	3161 Deg. F	WATER IN TEMP.:	118.0 Deg. F
STEEL TRANS. TEMP.:	3022 deg. F	WATER FLOW:	61.6 GPM
AIM CASTING TEMPERATURE:	2950 deg F	TEMP DIFFERENTIAL:	53.3 Deg. F
CAST TEMPERATURE:	N/A	DEW POINT:	39 deg F
		SHROUD GAS:	Argon

PURPOSE OF TRIAL: Trial was to evaluate the use of 93Z3 as a nozzle material. The nozzle was constructed with 1.5" thick 93Z3 backup brick for the wings ⸱ ⸱ ⸱ ⸱ ⸱ ⸱ ⸱ ⸱ ⸱ ⸱ ⸱ The bottom was 1" thick, one piece, ⸱ ⸱ ⸱

RESULTS OF TRIAL: A very small openning was noted in the north side Krojc joint just prior to casting. Some bowing was noted in the floor at the start of cast. The entire heat was cast without problem.

FILES:

C:\DATA\CUT874   C:\DATA\HEAT874

C:\DATA\CAST874   C:\DATA\HT874.XLS

MELT OVERFLOW STRIP CASTING LOG

CAST NUMBER: 875	**DATE:** 2/9/93		**TIME:** 1:00 PM
HEAT WEIGHT: 1000 Lbs.	**AMOUNT CAST:** 0'		**GRADE:** Si-Killed

HEAT ANALYSIS

	C	MN	SI	AL	N2	O2	S	Cu
AIM:	0.05	0.3	0.17	<.004	<.005	<.03	<.008	<.025
FINAL:	N/A	N/A	N/A	N/A	N/A	N/A	N/A	N/A

CASTING PARAMETERS

SUBSTRATE:	Normal Cu	**POOL DEPTH:**	2-1/2" max
SUBSTRATE FINISH:	113 u inch	**WEIR GAP:**	0.25" w/bones
NOZZLE POS. WRT WHEEL:	45 deg BTDC	**NOZZLE WIDTH:**	11.75"
NOZZLE GAP:	--	**NOZZLE BRICK:**	
AUTO GAP ADJUST:	0.3 mils	**MANUFACTURE:**	
LADLE PREHEAT TEMP.:	1902 Deg. F	**LOT #:**	
POUR BOX PREHEAT TEMP.:	N/A	**INITIAL CAST SPEED:**	295 FPM
FURNACE TAP TEMP.:	3152 Deg. F	**WATER IN TEMP.:**	N/A
STEEL TRANS. TEMP.:	N/A	**WATER FLOW:**	N/A
AIM CASTING TEMPERATURE:	2950 deg F	**TEMP DIFFERENTIAL:**	N/A
CAST TEMPERATURE:	N/A	**DEW POINT:**	N/A
		SHROUD GAS:	Argon

PURPOSE OF TRIAL:

Trial was to evaluate the use of 93Z3 as a nozzle material and to evaluate the use of an extended nozzle   The nozzle was constructed with 1.5" thick 93Z3 backup brick for the wings   The bottom was 1" thick, one piece.

RESULTS OF TRIAL:

A moderate sized openning was noted in the north side Krojc joint, and a small openning in the south side joint, just prior to casting. Some bowing was noted in the floor during the hot cut in.   The cast was aborted before any steel was cast.

FILES:

C:\DATA\CUT875   C:\DATA\HEAT875

C:\DATA\CAST875   C:\DATA\HT875.XLS

MELT OVERFLOW STRIP CASTING LOG

CAST NUMBER: ▮▮▮▮▮ **DATE:** 2/12/93 **TIME:** 2:00 PM

HEAT WEIGHT: 1000 Lbs. **AMOUNT CAST:** 485' **GRADE:** Si-Killed

HEAT ANALYSIS

	C	MN	SI	AL	N2	O2	S	Cu
AIM:	0.05	0.3	0.17	<.004	<.005	<.03	<.008	<.025
FINAL:								

CASTING PARAMETERS

SUBSTRATE:	Normal Cu	**POOL DEPTH:**	2-1/2" max
SUBSTRATE FINISH:	110 u inch	**WEIR GAP:**	0.3125" *
NOZZLE POS. WRT WHEEL:	45 deg BTDC	**NOZZLE WIDTH:**	11.75"
NOZZLE GAP:		**NOZZLE BRICK:**	
AUTO GAP ADJUST:	0.3 mils	**MANUFACTURE:**	
LADLE PREHEAT TEMP.:	1601 Deg. F	**LOT #:**	
POUR BOX PREHEAT TEMP.:	2185 Deg. F	**INITIAL CAST SPEED:**	295 FPM
FURNACE TAP TEMP.:	3152 Deg. F	**WATER IN TEMP.:**	120.0 Deg. F
STEEL TRANS. TEMP.:	3034 deg. F	**WATER FLOW:**	59.6 GPM
AIM CASTING TEMPERATURE:	2950 deg F	**TEMP DIFFERENTIAL:**	49.3 Deg. F
CAST TEMPERATURE:	2927 deg. F	**DEW POINT:**	49 deg F
		SHROUD GAS:	Argon

PURPOSE OF TRIAL: Trial was to evaluate the use of an extended nozzle and the use of teeth on the weir to reduce the bow in the nozzle bottom. The nozzle wings were of 1.5" thick 93Z3 ___ . The floor was a one piece ___ 1" thick. The wier was cut with .75" dogbones and two "teeth" were added (extentions of the wier to the nozzle floor).

RESULTS OF TRIAL: Wing holddowns were only finger tight and large gaps openned in the Krojoc joints. At 1100 F the joints were resealed with Krojoc and the wing holddowns were tightened. Prior to cast the south side had reopenned and both footprints exhibited a horizontal crack about half way up. The bottom bowed despite the teeth (nozzle burners were not used, but, holes were left in the Kaowool cover). Weir to wheel distance before cast was 1-3/16". A thermocouple was inserted in the nozzle bottom ~ 1" from the wier and 3/8" deep into the floor.

FILES: C:\DATA\CUT876   C:\DATA\HEAT876
C:\DATA\CAST876   C:\DATA\HT876.XLS

MELT OVERFLOW STRIP CASTING LOG

CAST NUMBER:	███████	DATE:	2/19/93	TIME:	1:00 PM
HEAT WEIGHT:	1000 Lbs.	AMOUNT CAST:	360'	GRADE:	Si-Killed

HEAT ANALYSIS

	C	MN	SI	AL	N2	O2	S	Cu
AIM:	0.05	0.3	0.17	<.004	<.005	<.03	<.008	<.025
FINAL:	N/A	N/A	N/A	N/A	N/A	N/A	N/A	N/A

CASTING PARAMETERS

SUBSTRATE:	Normal Cu	POOL DEPTH:	2-1/2" max
SUBSTRATE FINISH:	112 u inch	WEIR GAP:	0.25" w/bones
NOZZLE POS. WRT WHEEL:	60 deg BTDC	NOZZLE WIDTH:	11.75"
NOZZLE GAP:		NOZZLE BRICK:	
AUTO GAP ADJUST:	0.3 mils	MANUFACTURE:	
LADLE PREHEAT TEMP.:	1697 Deg. F	LOT #:	
POUR BOX PREHEAT TEMP.:	2224 Deg. F	INITIAL CAST SPEED:	295 FPM
FURNACE TAP TEMP.:	3150 Deg. F	WATER IN TEMP.:	114.4 Deg. F
STEEL TRANS. TEMP.:	N/A	WATER FLOW:	N/A
AIM CASTING TEMPERATURE:	2950 deg F	TEMP DIFFERENTIAL:	N/A
CAST TEMPERATURE:	N/A	DEW POINT:	37 deg F
		SHROUD GAS:	Argon

PURPOSE OF TRIAL: Trial was to evaluate the use of the joystick to control metal level. Nozzle was constructed of 1.5" thick 93Z3 backup material for the wings _____ The nozzle bottom was constructed of 1 piece,

RESULTS OF TRIAL: The Krojoc joints were allowed to open in an attempt to reduce the nozzle bottom warpage. At 1500 F Krojoc was used to reseal the joints. Just prior to casting the north side wing _____ exhibited a horizontal crack 1/2 way up _____ During the cast the metal level overflowed the wings and damaged the North side wing. The overflow was due to drift in the joystick control. The cast was aborted. Wheel speed did not get below 275 FPM so no evaluation was done on the strip.

FILES: C:\DATA\CUT877   C:\DATA\HEAT877
C:\DATA\CAST877   C:\DATA\HT877.XLS

MELT OVERFLOW STRIP CASTING LOG

CAST NUMBER:	███████	DATE:	2/25/93	TIME:	1:15 PM

HEAT WEIGHT:	1000 Lbs.	AMOUNT CAST:	0'	GRADE:	Si-Killed

HEAT ANALYSIS

	C	MN	SI	AL	N2	O2	S	Cu
AIM:	0.05	0.3	0.17	<.004	<.005	<.03	<.008	<.025
FINAL:	N/A	N/A	N/A	N/A	N/A	N/A	N/A	N/A

CASTING PARAMETERS

SUBSTRATE:	Normal Cu	POOL DEPTH:	0
SUBSTRATE FINISH:	112 u inch	WEIR GAP:	0" •
NOZZLE POS. WRT WHEEL:	45 deg BTDC	NOZZLE WIDTH:	11.75"
NOZZLE GAP:		NOZZLE BRICK:	
AUTO GAP ADJUST:	0.3 mils	MANUFACTURE:	
LADLE PREHEAT TEMP.:	N/A	LOT #:	
POUR BOX PREHEAT TEMP.:	2186 Deg. F	INITIAL CAST SPEED:	295 FPM
FURNACE TAP TEMP.:	N/A	WATER IN TEMP.:	N/A
STEEL TRANS. TEMP.:	N/A	WATER FLOW:	N/A
AIM CASTING TEMPERATURE:	2950 deg F	TEMP DIFFERENTIAL:	N/A
CAST TEMPERATURE:	N/A	DEW POINT:	36 deg F
		SHROUD GAS:	Argon

PURPOSE OF TRIAL:

Trial was to evaluate the use of an elongated nozzle and the use of a zero gap weir to hold down the nozzle floor. The nozzle was constructed of 1.5" thick 93Z3 backup material for the wings ....
.... The nozzle bottom was constructed of 1 piece ....
The wier contained 3/4" dogbone cuts in each corner and two 1" wide by 1/2" tall semicircular cut outs equally spaced across the weir.

RESULTS OF TRIAL:

The wing holdowns were kept snug, but, the Krojoc joints openned up significantly during preheat. At 1200 F the joints were resealed. The south joint still opened up significantly
nozzle bottom broke in 2 places (cracked in center of holes in the weir). The top of the south wing ... spalled and a large crack developed in the upper 1/3 of the north wing.

FILES:

C:\DATA\CUT878   C:\DATA\HEAT878
C:\DATA\CAST878   C:\DATA\HT878.XLS

MELT OVERFLOW STRIP CASTING LOG

CAST NUMBER:	▓▓▓▓	DATE:	3/2/93		TIME:	1:13 PM
HEAT WEIGHT:	1000 Lbs.	AMOUNT CAST:	0'		GRADE:	Si-Kill

HEAT ANALYSIS

	C	MN	SI	AL	N2	O2	S	Cu
AIM:	0.05	0.3	0.17	<.004	<.005	<.03	<.008	<.025
FINAL:	N/A	N/A	N/A	N/A	N/A	N/A	N/A	N/A

CASTING PARAMETERS

SUBSTRATE:	Normal Cu	POOL DEPTH:	2-1/2" max
SUBSTRATE FINISH:	112 u inch	WEIR GAP:	0" *
NOZZLE POS. WRT WHEEL:	60 deg BTDC	NOZZLE WIDTH:	11.75"
NOZZLE GAP:		NOZZLE BRICK:	
AUTO GAP ADJUST:	0.3 mils	MANUFACTURE:	
LADLE PREHEAT TEMP.:	1745 Deg. F	LOT #:	
POUR BOX PREHEAT TEMP.:	2107 Deg. F	INITIAL CAST SPEED:	295 FPM
FURNACE TAP TEMP.:	3157 Deg. F	WATER IN TEMP.:	120.2 Deg. F
STEEL TRANS. TEMP.:	3024 Deg. F	WATER FLOW:	87.8 GPM
AIM CASTING TEMPERATURE:	2950 deg F	TEMP DIFFERENTIAL:	55.4 Deg. F
CAST TEMPERATURE:	3128 Deg. F	DEW POINT:	.43 deg F
		SHROUD GAS:	Argon

PURPOSE OF TRIAL:

Trial was to evaluate the use of the Selcom unit for metal level control, the use of an extended nozzle, and the use of the thermal vision system. The nozzle was constructed of 1.5" thick 93Z3 material for the wings
The bottom was of a 1 piece 1" thick material. The wier had a gap of 1/32 of an inch with 3/4" dogbones cut in each corner and two 1" X 0.5" semicircular ports equally space across the face.

RESULTS OF TRIAL:

Even with aggressive holdown the Krojoc joints openned up during preheat. The north side moderately and the south side significantly. During the process of bringing the wheel in
the ladle opened. The metal quickly penetrated the gap between the wheel and the nozzle and the cast was aborted.

FILES:

C:\DATA\CUT879 C:\DATA\HEAT879
C:\DATA\CAST879.XLS   C:\DATA\HT879.XLS

MELT OVERFLOW STRIP CASTING HEAT LOG

FINAL

CAST NUMBER: 880	DATE: 4/16/93	TIME: 2:02:00 PM
HEAT WEIGHT: 1200	AMTCST: 174	GRADE: SI-KILLED

HEAT ANALYSIS

	C	Mn	Si	Al	N2	O2	S	Cu
AIM:	0.05	0.30	0.17	<0.004	<0.005	<0.03	<0.008	<0.025
FINAL:	0.04	0.13	0.061	0.011	0.0068	0.027	0.0072	0.021

CASTING PARAMETERS

SUBSTRATE:	COPPER2	AIM METAL LEVEL:	2.5
FINISH:	136	WEIR GAP:	0
NOZZLE POSITION:	60	NOZZLE WIDTH:	11.75
NOZZLE GAP:		NOZZLE FLOOR :	
AUTO GAP ADJUST:	99	NOZZLE WING :	93Z3
LADLE PREHEAT:	1727		
POUR BOX PREHEAT:	2134	AVG.WATER IN:	122.7
FURNACE TAP TEMP:	3163	AVG.WATER OUT:	169.7
STEEL TRANS. TEMP:	99	AVG.WATER FLOW:	34.2
CAST TEMPERATURE:	99	SHROUD GAS:	80
RELATIVE HUMIDITY:	25	AMBIENT TEMP:	ARGON

PURPOSE OF TRIAL:

RUNOUT TABLE	IR CAMERA
SELCOM	

RESULTS OF TRIAL:

DELAY 1:	NOZZLE ALIGNMENT	FAILURE 1:	RUNOUT TABLE
DELAY 2:	NONE	FAILURE 2:	NONE
DELAY 3:	NONE	FAILURE 3:	NONE

MELT OVERFLOW STRIP CASTING HEAT LOG

FINAL

CAST NUMBER: 881   DATE: 4/22/93   TIME: 3:00:00 PM

HEAT WEIGHT: 1000   AMTCST: 228   GRADE: SI-KILLED

HEAT ANALYSIS

	C	Mn	Si	Al	N2	O2	S	Cu
AIM:	0.05	0.30	0.17	<0.004	<0.005	<0.03	<0.008	<0.025
FINAL:	0.04	0.27	0.12	0.012	0.0072	0.04	0.0077	0.015

CASTING PARAMETERS

SUBSTRATE:	COPPER2	AIM METAL LEVEL:	2.5
FINISH:	81	WEIR GAP:	0
NOZZLE POSITION:	60	NOZZLE WIDTH:	11.75
NOZZLE GAP:		NOZZLE FLOOR :	
AUTO GAP ADJUST:	99	NOZZLE WING :	93Z3
LADLE PREHEAT:	1685		
POUR BOX PREHEAT:	2235	AVG.WATER IN:	120.7
FURNACE TAP TEMP:	3156	AVG.WATER OUT:	167.9
STEEL TRANS. TEMP:	3007	AVG.WATER FLOW:	67.2
CAST TEMPERATURE:	99	SHROUD GAS:	79
RELATIVE HUMIDITY:	18	AMBIENT TEMP:	ARGON

PURPOSE OF TRIAL:

RUNOUT TABLE UP   SELCOM

NONE   ZERO GAP WEIR

RESULTS OF TRIAL:

DELAY 1:	NOZZLE ALIGNMENT	FAILURE 1:	RUNOUT TABLE
DELAY 2:	NONE	FAILURE 2:	NONE
DELAY 3:	NONE	FAILURE 3:	NONE

MELT OVERFLOW STRIP CASTING HEAT LOG

FINAL

CAST NUMBER: 882   DATE: 4/27/93   TIME: 1:30:00 PM

HEAT WEIGHT: 1000   AMTCST: 400   GRADE: SI-KILLED

HEAT ANALYSIS

	C	Mn	Si	Al	N2	O2	S	Cu
AIM:	0.05	0.30	0.17	<0.004	<0.005	<0.03	<0.008	<0.025
FINAL:	0.04	0.23	0.071	0.006	0.005	0.023	0.006	0.021

CASTING PARAMETERS

SUBSTRATE:	COPPER2	AIM METAL LEVEL:	2.5
FINISH:	67	WEIR GAP:	0
NOZZLE POSITION:	60	NOZZLE WIDTH:	11.75
NOZZLE GAP:		NOZZLE FLOOR :	
AUTO GAP ADJUST:	99	NOZZLE WING :	93Z3
LADLE PREHEAT:	1760		
POUR BOX PREHEAT:	2141	AVG.WATER IN:	108.8
FURNACE TAP TEMP:	3130	AVG.WATER OUT:	199.5
STEEL TRANS. TEMP:	2985	AVG.WATER FLOW:	33.6
CAST TEMPERATURE:	2957	SHROUD GAS:	76
RELATIVE HUMIDITY:	26	AMBIENT TEMP:	ARGON

PURPOSE OF TRIAL:

SELCOM   WEIR SLANT

                  NONE

RESULTS OF TRIAL:

DELAY 1:	NONE	FAILURE 1:	GAP CONTROL
DELAY 2:	NONE	FAILURE 2:	BOTTOM BREAKAGE
DELAY 3:	NONE	FAILURE 3:	NONE

MELT OVERFLOW STRIP CASTING HEAT LOG

FINAL

CAST NUMBER: 883   DATE: 5/3/93   TIME: 6:00:00 PM

HEAT WEIGHT: 1000   AMTCST: 0   GRADE: Si-Killed

HEAT ANALYSIS

	C	Mn	Si	Al	N2	O2	S	Cu
AIM:	0.05	0.30	0.17	<0.004	<0.005	<0.03	<0.008	<0.025
FINAL:	99	99	99	99	99	99	99	99

CASTING PARAMETERS

SUBSTRATE:	N/A	AIM METAL LEVEL:	99
FINISH:	99	WEIR GAP:	99
NOZZLE POSITION:	99	NOZZLE WIDTH:	99
NOZZLE GAP:	99	NOZZLE FLOOR :	NONE
AUTO GAP ADJUST:	99	NOZZLE WING :	NONE
LADLE PREHEAT:	0	FOOTPRINT:	NONE
POUR BOX PREHEAT:	99	AVG.WATER IN:	99
FURNACE TAP TEMP:	2950	AVG.WATER OUT:	99
STEEL TRANS. TEMP:	99	AVG.WATER FLOW:	99
CAST TEMPERATURE:	99	SHROUD GAS:	99
RELATIVE HUMIDITY:	99	AMBIENT TEMP:	99

PURPOSE OF TRIAL:

AJAX SERVICE   NONE

NONE   NONE

RESULTS OF TRIAL:

DELAY 1:	NONE	FAILURE 1:	NONE
DELAY 2:	NONE	FAILURE 2:	NONE
DELAY 3:	NONE	FAILURE 3:	NONE

MELT OVERFLOW STRIP CASTING LOG

CAST NUMBER:	████████	DATE:	5/4/93	TIME:	1:00 PM

HEAT WEIGHT:	1000 Lbs.	AMOUNT CAST:	0'	GRADE:	Si-Killed

HEAT ANALYSIS

	C	MN	SI	AL	N2	O2	S	Cu
AIM:	0.05	0.3	0.17	<.004	<.005	<.03	<.008	<.025
FINAL:	N/A	N/A	N/A	N/A	N/A	N/A	N/A	N/A

CASTING PARAMETERS

SUBSTRATE:	Normal Cu	POOL DEPTH:	2-1/2" max
SUBSTRATE FINISH:	56 u inch	WEIR GAP:	Bones & Ports
NOZZLE POS. WRT WHEEL:	60 deg BTDC	NOZZLE WIDTH:	11.75"
NOZZLE GAP:		NOZZLE BRICK:	
AUTO GAP ADJUST:	N/A	MANUFACTURE:	
LADLE PREHEAT TEMP.:	N/A	LOT #:	
POUR BOX PREHEAT TEMP.:	N/A	INITIAL CAST SPEED:	150 FPM
FURNACE TAP TEMP.:	N/A	WATER IN TEMP.:	N/A
STEEL TRANS. TEMP.:	N/A	WATER FLOW:	N/A
AIM CASTING TEMPERATURE:	2925 Deg F	TEMP DIFFERENTIAL:	N/A
CAST TEMPERATURE:	N/A	DEW POINT:	N/A
		SHROUD GAS:	N/A

PURPOSE OF TRIAL: Trial was to evaluate the use of a modified weir design using two 3/4" dogbones in the corners and two 1/2" tall semicircles cut at the 1/3 and 2/3 distance across the weir. Also to be tested was a 15 degree slant on the weir for the Selcom, Selcom multi level control, wheel dusting, and the new "Wheel In" preheat procedure. The nozzle was constructed with 1.5" thick 93Z3 as the backup material

RESULTS OF TRIAL: There were no gaps in the Krojoc joints during preheat, however, the wheel was left too far in and the expansion of the refractory was fast enough that when it reached the wheel it caused the bottom to break. The cast was aborted 4.8 hours into the preheat.

FILES:

C:\DATA\HT884.XLS

MELT OVERFLOW STRIP CASTING HEAT LOG

FINAL

CAST NUMBER: 885   DATE: 5/7/93   TIME: 1:00:00 PM

HEAT WEIGHT: 1000   AMTCST: 505   GRADE: SI-KILLED

HEAT ANALYSIS

	C	Mn	Si	Al	N2	O2	S	Cu
AIM:	0.05	0.30	0.17	<0.004	<0.005	<0.03	<0.008	<0.025
FINAL:	0.06	0.27	0.12	0.01	0.0062	0.056	0.0082	0.016

CASTING PARAMETERS

SUBSTRATE:	COPPER2	AIM METAL LEVEL:	2.25
FINISH:	56	WEIR GAP:	0
NOZZLE POSITION:	60	NOZZLE WIDTH:	11.75
NOZZLE GAP:		NOZZLE FLOOR :	
AUTO GAP ADJUST:	99	NOZZLE WING :	93Z3
LADLE PREHEAT:	1694		
POUR BOX PREHEAT:	2148	AVG.WATER IN:	115.8
FURNACE TAP TEMP:	3127	AVG.WATER OUT:	174
STEEL TRANS. TEMP:	2970	AVG.WATER FLOW:	46.8
CAST TEMPERATURE:	2897	SHROUD GAS:	81
RELATIVE HUMIDITY:	27	AMBIENT TEMP:	ARGON

PURPOSE OF TRIAL:

SELCOM

RESULTS OF TRIAL:

DELAY 1:	NONE	FAILURE 1:	SELCOM UNDERFILL
DELAY 2:	NONE	FAILURE 2:	NOZZLE OVERFLOW
DELAY 3:	NONE	FAILURE 3:	NONE

MELT OVERFLOW STRIP CASTING LOG

CAST NUMBER:	███████	DATE:	5/14/93	TIME:	1:00 PM
HEAT WEIGHT:	1000 Lbs.	AMOUNT CAST:	220'	GRADE:	Si-Killed

HEAT ANALYSIS

	C	MN	SI	AL	N2	O2	S	Cu
AIM:	0.05	0.3	0.17	<.004	<.005	<.03	<.008	<.025
FINAL:								

CASTING PARAMETERS

SUBSTRATE:	Steel	POOL DEPTH:	2-1/2" max
SUBSTRATE FINISH:	29 u inch	WEIR GAP:	bones & ports
NOZZLE POS. WRT WHEEL:	60 deg BTDC	NOZZLE WIDTH:	11.75"
NOZZLE GAP:		NOZZLE BRICK:	Za193Z3
AUTO GAP ADJUST:	N/A	MANUFACTURE:	
LADLE PREHEAT TEMP.:	1600 Deg. F	LOT #:	
POUR BOX PREHEAT TEMP.:	2320 Deg. F	INITIAL CAST SPEED:	2005 FPM
FURNACE TAP TEMP.:	3133 Deg. F	WATER IN TEMP.:	121.0 Deg. F
STEEL TRANS. TEMP.:	2966 Deg. F	WATER FLOW:	54.2 GPM
AIM CASTING TEMPERATURE:	2925 deg F	TEMP DIFFERENTIAL:	50.4 Deg. F
CAST TEMPERATURE:	2893 Deg. F	DEW POINT:	45 Deg F
		SHROUD GAS:	Argon

PURPOSE OF TRIAL: Trial was to evaluate the use of a steel wheel, ⸺ ⸺ ⸺ automatic water temperature control. This was the first run with the steel wheel so standard 1.5" thick 93Z3 nozzle wings ⸺ ⸺ and a 1" thick 1 piece ⸺ bottom were used.

RESULTS OF TRIAL: A small opening was noted in the Krojoc joint on the south side prior to casting. The cast started very good. Some dams were noted to form on both the north and south wings. ⸺ one of the north dams broke off the top of the nozzle wing. A south side dam then did the same thing to the south wing. The cast was aborted at this time. All the strip produced was in one piece and all of the material was coiled. The scratches in the steel wheel did show through on the strip, but, were not as prone to forming cracks as the ones on the copper wheel.

FILES:

C:\DATA\CAST886   C:\DATA\HT886.XLS

MELT OVERFLOW STRIP CASTING HEAT LOG

FINAL

CAST NUMBER: 886   DATE: 5/14/93   TIME: 1:00:00 PM

HEAT WEIGHT: 1000   AMTCST: 220   GRADE: SI-KILLED

HEAT ANALYSIS

	C	Mn	Si	Al	N2	O2	S	Cu
AIM:	0.05	0.30	0.17	<0.004	<0.005	<0.03	<0.008	<0.025
FINAL:	0.05	0.27	0.11	0.024	0.0064	0.028	0.0088	0.02

CASTING PARAMETERS

SUBSTRATE: STEEL 1	AIM METAL LEVEL: 2.5
FINISH: 29	WEIR GAP: 0
NOZZLE POSITION: 60	NOZZLE WIDTH: 11.75
NOZZLE GAP:	NOZZLE FLOOR :
AUTO GAP ADJUST: 99	NOZZLE WING : 93Z3
LADLE PREHEAT: 1600	
POUR BOX PREHEAT: 2320	AVG.WATER IN: 121
FURNACE TAP TEMP: 3133	AVG.WATER OUT: 171.4
STEEL TRANS. TEMP: 2966	AVG.WATER FLOW: 54.2
CAST TEMPERATURE: 2893	SHROUD GAS: 70
RELATIVE HUMIDITY: 38	AMBIENT TEMP: ARGON

PURPOSE OF TRIAL:

STEEL WHEEL

AUTO WATER

RESULTS OF TRIAL:

DELAY 1: NONE	FAILURE 1: DAM FORMATION
DELAY 2: NONE	FAILURE 2: WING BREAKAGE
DELAY 3: NONE	FAILURE 3: PIN HOLES

MELT OVERFLOW STRIP CASTING LOG

CAST NUMBER:	███████	DATE:	5/18/93	TIME:	1:00 PM

HEAT WEIGHT:	1000 Lbs.	AMOUNT CAST:	500'	GRADE:	Si-Killed

HEAT ANALYSIS

	C	MN	SI	AL	N2	O2	S	Cu
AIM:	0.05	0.3	0.17	<.004	<.005	<.03	<.008	<.025
FINAL:								

CASTING PARAMETERS

SUBSTRATE:	Steel	POOL DEPTH:	2-1/2" max
SUBSTRATE FINISH:	15 u inch	WEIR GAP:	bones & ports
NOZZLE POS. WRT WHEEL:	60 deg BTDC	NOZZLE WIDTH:	11.75"
NOZZLE GAP:	~	NOZZLE BRICK:	
AUTO GAP ADJUST:	N/A	MANUFACTURE:	
LADLE PREHEAT TEMP.:	1614 Deg. F	LOT #:	
POUR BOX PREHEAT TEMP.:	2150 Deg. F	INITIAL CAST SPEED:	200 FPM
FURNACE TAP TEMP.:	3125 Deg. F	WATER IN TEMP.:	117.8 Deg. F
STEEL TRANS. TEMP.:	3028 Deg. F	WATER FLOW:	67.6 GPM
AIM CASTING TEMPERATURE:	2925 deg F	TEMP DIFFERENTIAL:	47.4 Deg. F
CAST TEMPERATURE:	2895 Deg. F	DEW POINT:	51 deg F
		SHROUD GAS:	Argon

PURPOSE OF TRIAL: Trial was to evaluate the use of a steel wheel with a smooth finish ⸮⸮⸮⸮⸮ ⸮⸮ ⸮⸮⸮⸮⸮⸮⸮ ⸮⸮⸮ ⸮⸮⸮⸮⸮⸮⸮⸮ The nozzle was constructed of 1" thick Zal-45AA one piece bottom with 1.5" thick 93Z3 wings. Zal-45AA HA was used for the footprint material, for the wings only, and were attached using Phoxbond.

RESULTS OF TRIAL: A small opening was noted in the South side Krojc joint just prior to casting. During the opening of the ladle a leak developed in the nozzle/sen assembly. The fill was slow and the first material cast was very slow coming out of the caster. Metal level was reduced due to erosion of the footprint material and the freezing off of the nozzle, due to the leak. Eventually, the nozzle froze off and the cast was stopped.

FILES:

C:\DATA\CAST887   C:\DATA\HT887.XLS

MELT OVERFLOW STRIP CASTING HEAT LOG

FINAL

CAST NUMBER: 887   DATE: 5/18/93   TIME: 1:00:00 PM

HEAT WEIGHT: 1000   AMTCST: 500   GRADE: SI-KILLED

HEAT ANALYSIS

	C	Mn	Si	Al	N2	O2	S	Cu
AIM:	0.05	0.30	0.17	<0.004	<0.005	<0.03	<0.008	<0.025
FINAL:	0.04	0.097	0.055	0.0088	0.0056	0.044	0.0088	0.022

CASTING PARAMETERS

SUBSTRATE:	STEEL 1	AIM METAL LEVEL:	2.5
FINISH:	15	WEIR GAP:	0
NOZZLE POSITION:	60	NOZZLE WIDTH:	11.75
NOZZLE GAP:		NOZZLE FLOOR :	
AUTO GAP ADJUST:	99	NOZZLE WING :	93Z3
LADLE PREHEAT:	1614		
POUR BOX PREHEAT:	2150	AVG.WATER IN:	117.8
FURNACE TAP TEMP:	3125	AVG.WATER OUT:	165.2
STEEL TRANS. TEMP:	3028	AVG.WATER FLOW:	67.6
CAST TEMPERATURE:	2895	SHROUD GAS:	67
RELATIVE HUMIDITY:	63	AMBIENT TEMP:	ARGON

PURPOSE OF TRIAL:

STEEL WHEEL

SMOOTH WHEEL

RESULTS OF TRIAL:

DELAY 1: LADLE ALIGNMENT   FAILURE 1: LADLE/SEN LEAK

DELAY 2: NONE   FAILURE 2: DAM FORMATION

DELAY 3: NONE   FAILURE 3: WING EROSION

MELT OVERFLOW STRIP CASTING LOG

CAST NUMBER: ███████ **DATE:** 5/21/93 **TIME:** 2:30 PM

HEAT WEIGHT: 1200 Lbs. **AMOUNT CAST:** 935' **GRADE:** Si-Killed

HEAT ANALYSIS

	C	MN	SI	AL	N2	O2	S	Cu
AIM:	0.05	0.3	0.17	<.004	<.005	<.03	<.008	<.025
FINAL:								

CASTING PARAMETERS

SUBSTRATE:	Steel	POOL DEPTH:	2-1/2" max
SUBSTRATE FINISH:	19.5 u inch	WEIR GAP:	bones & Ports
NOZZLE POS. WRT WHEEL:	60 deg BTDC	NOZZLE WIDTH:	11.75"
NOZZLE GAP:	.	NOZZLE BRICK:	
AUTO GAP ADJUST:	N/A	MANUFACTURE:	
LADLE PREHEAT TEMP.:	1875 Deg. F	LOT #:	
POUR BOX PREHEAT TEMP.:	2167 Deg. F	INITIAL CAST SPEED:	200 FPM
FURNACE TAP TEMP.:	3125 Deg. F	WATER IN TEMP.:	120.3
STEEL TRANS. TEMP.:	2999 Deg. F	WATER FLOW:	64.1
AIM CASTING TEMPERATURE:	2925 deg F	TEMP DIFFERENTIAL:	64.1
CAST TEMPERATURE:	N/A	DEW POINT:	46 Deg F
		SHROUD GAS:	Argon

PURPOSE OF TRIAL: Trial was to evaluate the use of a steel wheel, higher wheel temperatures. The nozzle was constructed with 1.5" thick 93Z3 and using 1" thick nozzle bottom.

RESULTS OF TRIAL: No defects were noted in the nozzle prior to starting the cast. During the first part of the cast the SEN appeared to be clogged and it was difficult to maintain level. Many dams were noted to form on both the north and south sides. Many more transverse cracks were also noted. The full heat was cast. After the cast the ___ materials were seen to be significantly erroded.

FILES:

C:\DATA\CAST888 C:\DATA\HT888.XLS

MELT OVERFLOW STRIP CASTING HEAT LOG

FINAL

CAST NUMBER: 888   DATE: 5/21/93   TIME: 2:30:00 PM

HEAT WEIGHT: 1200   AMTCST: 935   GRADE: SI-KILLED

HEAT ANALYSIS

	C	Mn	Si	Al	N2	O2	S	Cu
AIM:	0.05	0.30	0.17	<0.004	<0.005	<0.03	<0.008	<0.025
FINAL:	0.04	0.18	0.081	0.01	0.0055	0.021	0.0086	0.015

CASTING PARAMETERS

SUBSTRATE:	STEEL 1	AIM METAL LEVEL:	2.5
FINISH:	19.5	WEIR GAP:	0
NOZZLE POSITION:	60	NOZZLE WIDTH:	11.75
NOZZLE GAP:	—	NOZZLE FLOOR :	
AUTO GAP ADJUST:	99	NOZZLE WING :	93Z3
LADLE PREHEAT:	1875		
POUR BOX PREHEAT:	2167	AVG.WATER IN:	120.3
FURNACE TAP TEMP:	3125	AVG.WATER OUT:	184.4
STEEL TRANS. TEMP:	2999	AVG.WATER FLOW:	67.5
CAST TEMPERATURE:	99	SHROUD GAS:	70
RELATIVE HUMIDITY:	44	AMBIENT TEMP:	ARGON

PURPOSE OF TRIAL:

STEEL WHEEL   HIGH WHEEL TEMP

RESULTS OF TRIAL:

DELAY 1:	LADLE ALIGNMENT	FAILURE 1:	SEN CLOG
DELAY 2:	NONE	FAILURE 2:	DAM FORMATION
DELAY 3:	NONE	FAILURE 3:	TRANSVERSE CRKS

MELT OVERFLOW STRIP CASTING HEAT LOG

FINAL

CAST NUMBER: 889   DATE: 5/25/93   TIME: 3:00:00 PM

HEAT WEIGHT: 1200   AMTCST: 460   GRADE: SI-KILLED

HEAT ANALYSIS

	C	Mn	Si	Al	N2	O2	S	Cu
AIM:	0.05	0.30	0.17	<0.004	<0.005	<0.03	<0.008	<0.025
FINAL:	0.03	0.233	0.13	0.01	0.0047	0.014	0.0095	0.016

CASTING PARAMETERS

SUBSTRATE:	STEEL 1	AIM METAL LEVEL:	2.5
FINISH:	18	WEIR GAP:	0.25
NOZZLE POSITION:	60	NOZZLE WIDTH:	11.75
NOZZLE GAP:		NOZZLE FLOOR :	
AUTO GAP ADJUST:	99	NOZZLE WING :	93Z3
LADLE PREHEAT:	1565		
POUR BOX PREHEAT:	2170	AVG.WATER IN:	111.7
FURNACE TAP TEMP:	3127	AVG.WATER OUT:	173.3
STEEL TRANS. TEMP:	3076	AVG.WATER FLOW:	67.2
CAST TEMPERATURE:	2929	SHROUD GAS:	76
RELATIVE HUMIDITY:	43	AMBIENT TEMP:	ARGON

PURPOSE OF TRIAL:

STEEL WHEEL   LOW WATER TEMP

RUNOUT TABLE

RESULTS OF TRIAL:

DELAY 1:	LADLE ALIGNMENT	FAILURE 1:	SLOW START
DELAY 2:	NONE	FAILURE 2:	SLOW TABLE ROLLS
DELAY 3:	NONE	FAILURE 3:	TRANSVERSE CRKS

STRIP CASTING HEAT LOG - PRELIMINARY

CAST #: 890   DATE: 6/1/93   TIME: 1:00:00 PM

HEATWT: 1200   AMTCST: 700   GRADE: SI-KILLED

HEAT ANALYSIS

	C	Mn	Si	Al	N2	O2	S	Cu
AIM:	0.05	0.30	0.17	<0.004	<0.005	<0.03	<0.008	<0.025
FINAL:								

CASTING PARAMETERS

SUBSTRATE:	STEEL 1	AIM METAL LEVEL:	2.5
FINISH:	88	WEIRGAP:	0.25
NOZZLE POSITION:	60	NOZZLEWDTH:	11.75
NOZZLE GAP:		FLOOR MTRL.:	
AUTO GAP ADJ:	99	WING MTRL.:	93Z3
LADLE PREHEAT:	1788		
POUR BOX PREHEAT:	2230	AVG. WATER-IN:	112.1
FURNACE TAP TEMP.:	3140	AVG. WATER-OUT:	158.8
STEEL TRANS.TEMP.:	3101	AVG. WATER FLOW:	58.6
CAST TEMPERATURE:	2959	SHROUD GAS:	ARGON
RELATIVE HUMIDITY:	31	AMBIENT:	71

PURPOSE OF TRIAL:

STEEL WHEEL   LOW WATER TEMP

RUNOUT TABLE

RESULTS OF TRIAL:

AMOUNT CAST (FEET):   700

DELAY 1:	NONE	FAILURE 1:	WING BREAKAGE
DELAY 2:	NONE	FAILURE 2:	NOZZLE RESTRICTION
DELAY 3:	NONE	FAILURE 3:	RING FAILURE

MELT OVERFLOW STRIP CASTING HEAT LOG

FINAL

CAST NUMBER: 891   DATE: 8/3/93   TIME: 2:00:00 PM

HEAT WEIGHT: 1000   AMTCST: 0   GRADE: Si-Killed

HEAT ANALYSIS

	C	Mn	Si	Al	N2	O2	S	Cu
AIM:	0.05	0.30	0.17	<0.004	<0.005	<0.03	<0.008	<0.025
FINAL:	99	99	99	99	99	99	99	99

CASTING PARAMETERS

SUBSTRATE:	N/A	AIM METAL LEVEL:	99
FINISH:	99	WEIR GAP:	99
NOZZLE POSITION:	99	NOZZLE WIDTH:	99
NOZZLE GAP:	99	NOZZLE FLOOR :	NONE
AUTO GAP ADJUST:	99	NOZZLE WING :	NONE
LADLE PREHEAT:	0	FOOTPRINT:	NONE
POUR BOX PREHEAT:	99	AVG.WATER IN:	99
FURNACE TAP TEMP:	3125	AVG.WATER OUT:	99
STEEL TRANS. TEMP:	99	AVG.WATER FLOW:	99
CAST TEMPERATURE:	99	SHROUD GAS:	99
RELATIVE HUMIDITY:	99	AMBIENT TEMP:	ARGON

PURPOSE OF TRIAL:

AJAX SERVICE   NONE

NONE   NONE

RESULTS OF TRIAL:

DELAY 1: NONE   FAILURE 1: PIN HOLES

DELAY 2: NONE   FAILURE 2: NONE

DELAY 3: NONE   FAILURE 3: NONE

MELT OVERFLOW STRIP CASTING HEAT LOG

FINAL

CAST NUMBER: 892   DATE: 6/4/93   TIME: 1:00:00 PM

HEAT WEIGHT: 1000   AMTCST: 40   GRADE: SI-KILLED

HEAT ANALYSIS

	C	Mn	Si	Al	N2	O2	S	Cu
AIM:	0.05	0.30	0.17	<0.004	<0.005	<0.03	<0.008	<0.025
FINAL:	99	99	99	99	99	99	99	99

CASTING PARAMETERS

SUBSTRATE:	STEEL 1	AIM METAL LEVEL:	2.5
FINISH:	18	WEIR GAP:	0.25
NOZZLE POSITION:	60	NOZZLE WIDTH:	11.75
NOZZLE GAP:		NOZZLE FLOOR :	
AUTO GAP ADJUST:	99	NOZZLE WING :	93S
LADLE PREHEAT:	1645		
POUR BOX PREHEAT:	2138	AVG.WATER IN:	99
FURNACE TAP TEMP:	3125	AVG.WATER OUT:	99
STEEL TRANS. TEMP:	3022	AVG.WATER FLOW:	99
CAST TEMPERATURE:	2981	SHROUD GAS:	71
RELATIVE HUMIDITY:	65	AMBIENT TEMP:	ARGON

PURPOSE OF TRIAL:

STEEL WHEEL   LOW WATER TEMP

RUNOUT TABLE

RESULTS OF TRIAL:

DELAY 1:	LADLE ALIGNMENT	FAILURE 1:	TRANSVERSE CRKS
DELAY 2:	NONE	FAILURE 2:	RUNOUT TABLE
DELAY 3:	NONE	FAILURE 3:	PIN HOLES

MELT OVERFLOW STRIP CASTING HEAT LOG

FINAL

CAST NUMBER: 893   DATE: 6/16/93   TIME: 2:18:00 PM

HEAT WEIGHT: 1000   AMTCST: 808   GRADE: SI-KILLED

HEAT ANALYSIS

	C	Mn	Si	Al	N2	O2	S	Cu
AIM:	0.05	0.30	0.17	<0.004	<0.005	<0.03	<0.008	<0.025
FINAL:	0.02	0.24	0.13	99	0.0051	0.023	0.0068	0.016

CASTING PARAMETERS

SUBSTRATE:	STEEL 1	AIM METAL LEVEL:	2.5
FINISH:	120	WEIR GAP:	0.25
NOZZLE POSITION:	60	NOZZLE WIDTH:	11.75
NOZZLE GAP:		NOZZLE FLOOR :	
AUTO GAP ADJUST:	99	NOZZLE WING :	93Z3
LADLE PREHEAT:	1873		
POUR BOX PREHEAT:	2265	AVG.WATER IN:	121.8
FURNACE TAP TEMP:	3128	AVG.WATER OUT:	173
STEEL TRANS. TEMP:	99	AVG.WATER FLOW:	66.3
CAST TEMPERATURE:	2973	SHROUD GAS:	86
RELATIVE HUMIDITY:	38	AMBIENT TEMP:	ARGON

PURPOSE OF TRIAL:

STEEL WHEEL

RUNOUT TABLE   NONE

RESULTS OF TRIAL:

DELAY 1:	NONE	FAILURE 1:	RUNOUT TABLE
DELAY 2:	NONE	FAILURE 2:	PIN HOLES
DELAY 3:	NONE	FAILURE 3:	NONE

MELT OVERFLOW STRIP CASTING HEAT LOG

FINAL

CAST NUMBER: 894   DATE: 7/9/93   TIME: 12:00:00 PM

HEAT WEIGHT: 1000   AMTCST: 150   GRADE: SI-KILLED

HEAT ANALYSIS

	C	Mn	Si	Al	N2	O2	S	Cu
AIM:	0.05	0.30	0.17	<0.004	<0.005	<0.03	<0.008	<0.025
FINAL:	99	99	99	99	99	99	99	99

CASTING PARAMETERS

SUBSTRATE:	STEEL 1	AIM METAL LEVEL:	2.5
FINISH:	120	WEIR GAP:	0.25
NOZZLE POSITION:	48	NOZZLE WIDTH:	11.75
NOZZLE GAP:	~	NOZZLE FLOOR :	
AUTO GAP ADJUST:	99	NOZZLE WING :	93Z3
LADLE PREHEAT:	1630		
POUR BOX PREHEAT:	2258	AVG.WATER IN:	124.5
FURNACE TAP TEMP:	3131	AVG.WATER OUT:	179.6
STEEL TRANS. TEMP:	2949	AVG.WATER FLOW:	67.1
CAST TEMPERATURE:	3033	SHROUD GAS:	91
RELATIVE HUMIDITY:	58	AMBIENT TEMP:	ARGON

PURPOSE OF TRIAL:

STEEL WHEEL

RUNOUT TABLE   EXTENDED NOZ

RESULTS OF TRIAL:

DELAY 1:	SELCOM	FAILURE 1:	SELCOM
DELAY 2:	NONE	FAILURE 2:	RUNOUT TABLE
DELAY 3:	NONE	FAILURE 3:	PIN HOLES

MELT OVERFLOW STRIP CASTING HEAT LOG

FINAL

CAST NUMBER: 895   DATE: 7/14/93   TIME: 1:00:00 PM

HEAT WEIGHT: 1000   AMTCST: 0   GRADE: SI-KILLED

HEAT ANALYSIS

	C	Mn	Si	Al	N2	O2	S	Cu
AIM:	0.05	0.30	0.17	<0.004	<0.005	<0.03	<0.008	<0.025
FINAL:	99	99	99	99	99	99	99	99

CASTING PARAMETERS

SUBSTRATE:	STEEL 1	AIM METAL LEVEL:	99
FINISH:	120	WEIR GAP:	0.25
NOZZLE POSITION:	48	NOZZLE WIDTH:	11.75
NOZZLE GAP:		NOZZLE FLOOR :	
AUTO GAP ADJUST:	99	NOZZLE WING :	93Z3
LADLE PREHEAT:	99		
POUR BOX PREHEAT:	99	AVG.WATER IN:	99
FURNACE TAP TEMP:	99	AVG.WATER OUT:	99
STEEL TRANS. TEMP:	99	AVG.WATER FLOW:	99
CAST TEMPERATURE:	99	SHROUD GAS:	99
RELATIVE HUMIDITY:	99	AMBIENT TEMP:	ARGON

PURPOSE OF TRIAL:

STEEL WHEEL

RUNOUT TABLE   EXTENDED NOZ

RESULTS OF TRIAL:

DELAY 1:		FAILURE 1:	NOZZLE BROKE
DELAY 2:	NONE	FAILURE 2:	NONE
DELAY 3:	NONE	FAILURE 3:	NONE

MELT OVERFLOW STRIP CASTING HEAT LOG

FINAL

CAST NUMBER: 896   DATE: 7/20/93   TIME: 12:00:00 PM

HEAT WEIGHT: 1000   AMTCST: 0   GRADE: SI-KILLED

HEAT ANALYSIS

	C	Mn	Si	Al	N2	O2	S	Cu
AIM:	0.05	0.30	0.17	<0.004	<0.005	<0.03	<0.008	<0.025
FINAL:	99	99	99	99	99	99	99	99

CASTING PARAMETERS

SUBSTRATE:	STEEL 1	AIM METAL LEVEL:	99
FINISH:	120	WEIR GAP:	99
NOZZLE POSITION:	48	NOZZLE WIDTH:	99
NOZZLE GAP:	-	NOZZLE FLOOR :	
AUTO GAP ADJUST:	99	NOZZLE WING :	93Z3
LADLE PREHEAT:	99		
POUR BOX PREHEAT:	99	AVG.WATER IN:	99
FURNACE TAP TEMP:	99	AVG.WATER OUT:	99
STEEL TRANS. TEMP:	99	AVG.WATER FLOW:	99
CAST TEMPERATURE:	99	SHROUD GAS:	99
RELATIVE HUMIDITY:	99	AMBIENT TEMP:	ARGON

PURPOSE OF TRIAL:

STEEL WHEEL

RUNOUT TABLE   EXTENDED NOZ

RESULTS OF TRIAL:

DELAY 1:	AJAX FURNACE	FAILURE 1:	AJAX FURNACE
DELAY 2:	NONE	FAILURE 2:	NONE
DELAY 3:	NONE	FAILURE 3:	NONE

MELT OVERFLOW STRIP CASTING HEAT LOG

FINAL

CAST NUMBER: 897   DATE: 7/20/93   TIME: 1:00:00 PM

HEAT WEIGHT: 1000   AMTCST: 850   GRADE: SI-KILLED

HEAT ANALYSIS

	C	Mn	Si	Al	N2	O2	S	Cu
AIM:	0.05	0.30	0.17	<0.004	<0.005	<0.03	<0.008	<0.025
FINAL:	0.02	0.26	0.18	99	0.0056	0.03	0.008	0.016

CASTING PARAMETERS

SUBSTRATE:	STEEL 1	AIM METAL LEVEL:	2.5
FINISH:	120	WEIR GAP:	0.25
NOZZLE POSITION:	48	NOZZLE WIDTH:	11.75
NOZZLE GAP:		NOZZLE FLOOR :	
AUTO GAP ADJUST:	99	NOZZLE WING :	93Z3
LADLE PREHEAT:	1877		
POUR BOX PREHEAT:	2323	AVG.WATER IN:	125.4
FURNACE TAP TEMP:	3129	AVG.WATER OUT:	175.9
STEEL TRANS. TEMP:	2942	AVG.WATER FLOW:	67.7
CAST TEMPERATURE:	2972	SHROUD GAS:	88
RELATIVE HUMIDITY:	51	AMBIENT TEMP:	ARGON

PURPOSE OF TRIAL:

STEEL WHEEL

RUNOUT TABLE   EXTENDED NOZ

RESULTS OF TRIAL:

DELAY 1:	NONE	FAILURE 1:	RUNOUT TABLE
DELAY 2:	NONE	FAILURE 2:	NONE
DELAY 3:	NONE	FAILURE 3:	NONE

STRIP CASTING HEAT LOG - PRELIMINARY

CAST #: 899   **DATE:** 7/28/93   **TIME:** 12:30:00 PM

HEATWT: 1000   **AMTCST:** 600   **GRADE:** SI-KILLED

HEAT ANALYSIS

	C	Mn	Si	Al	N2	O2	S	Cu
AIM:	0.05	0.30	0.17	<0.004	<0.005	<0.03	<0.008	<0.025
FINAL:								

CASTING PARAMETERS

SUBSTRATE:	STEEL 1	AIM METAL LEVEL:	3.7
FINISH:	120	WEIRGAP:	0.375
NOZZLE POSITION:	57	NOZZLEWDTH:	11.75
NOZZLE GAP:		FLOOR MTRL.:	
AUTO GAP ADJ:	99	WING MTRL.:	93Z3
LADLE PREHEAT:	1521		
POUR BOX PREHEAT:	2238	AVG. WATER-IN:	125
FURNACE TAP TEMP.:	3125	AVG. WATER-OUT:	174.5
STEEL TRANS.TEMP.:	99	AVG. WATER FLOW:	98.8
CAST TEMPERATURE:	2964	SHROUD GAS:	ARGON
RELATIVE HUMIDITY:	56	AMBIENT:	92

PURPOSE OF TRIAL:

STEEL WHEEL

RUNOUT TABLE

RESULTS OF TRIAL:

AMOUNT CAST (FEET):   600

DELAY 1:	INDUCTOTHERM	FAILURE 1:	PIN HOLES
DELAY 2:	NONE	FAILURE 2:	DIMPLED SURFACE
DELAY 3:	NONE	FAILURE 3:	DATA ACQUISITION

STRIP CASTING HEAT LOG - PRELIMINARY

CAST #: **900**   DATE: 7/30/93   TIME: 12:30:00 PM

HEATWT: 1000   AMTCST: 300   GRADE: SI-KILLED

HEAT ANALYSIS

	C	Mn	Si	Al	N2	O2	S	Cu
AIM:	0.05	0.30	0.17	<0.004	<0.005	<0.03	<0.008	<0.025
FINAL:								

CASTING PARAMETERS

SUBSTRATE:	STEEL 1	AIM METAL LEVEL:	3.7
FINISH:	120	WEIRGAP:	0.125
NOZZLE POSITION:	57	NOZZLEWDTH:	11.75
NOZZLE GAP:		FLOOR MTRL.:	
AUTO GAP ADJ:	99	WING MTRL.:	93Z3
LADLE PREHEAT:	1607		
POUR BOX PREHEAT:	2045	AVG. WATER-IN:	124.1
FURNACE TAP TEMP.:	3127	AVG. WATER-OUT:	194.2
STEEL TRANS.TEMP.:	2983	AVG. WATER FLOW:	73.6
CAST TEMPERATURE:	2945	SHROUD GAS:	ARGON
RELATIVE HUMIDITY:	39	AMBIENT:	84

PURPOSE OF TRIAL:

STEEL WHEEL

RUNOUT TABLE

RESULTS OF TRIAL:

AMOUNT CAST (FEET):   300

DELAY 1:	NONE	FAILURE 1:	RUNOUT TABLE
DELAY 2:	NONE	FAILURE 2:	DIMPLED SURFACE
DELAY 3:	NONE	FAILURE 3:	PIN HOLES

STRIP CASTING HEAT LOG - PRELIMINARY

CAST #: 901   DATE: 8/20/93   TIME: 12:01:00 PM

HEATWT: 1000   AMTCST: 20   GRADE: 304-26

HEAT ANALYSIS

	C	Mn	Si	Al	N2	O2	S	Cu
AIM:	0.05	0.30	0.17	<0.004	<0.005	<0.03	<0.008	<0.025
FINAL:								

CASTING PARAMETERS

SUBSTRATE:	STEEL 2	AIM METAL LEVEL:	4
FINISH:	102	WEIRGAP:	0.125
NOZZLE POSITION:	57	NOZZLEWDTH:	12
NOZZLE GAP:		FLOOR MTRL.:	
AUTO GAP ADJ:	99	WING MTRL.:	93Z3
LADLE PREHEAT:	1802		
POUR BOX PREHEAT:	2174	AVG. WATER-IN:	123.6
FURNACE TAP TEMP.:	3030	AVG. WATER-OUT:	132.1
STEEL TRANS.TEMP.:	2949	AVG. WATER FLOW:	32.4
CAST TEMPERATURE:	2907	SHROUD GAS:	ARGON
RELATIVE HUMIDITY:	68	AMBIENT:	84

PURPOSE OF TRIAL:

STEEL WHEEL - Ni

RUNOUT TABLE

RESULTS OF TRIAL:

AMOUNT CAST (FEET): 20

DELAY 1:	NONE	FAILURE 1:	STRIPPER BAR
DELAY 2:	NONE	FAILURE 2:	WHEEL WRAP
DELAY 3:	NONE	FAILURE 3:	PIN HOLES

STRIP CASTING HEAT LOG - PRELIMINARY

CAST #: 902   **DATE:** 8/27/93   **TIME:** 12:01:00 PM

HEATWT: 1000   **AMTCST:** 150   **GRADE:** 304-26

HEAT ANALYSIS

	C	Mn	Si	Al	N2	O2	S	Cu
AIM:	0.05	0.30	0.17	<0.004	<0.005	<0.03	<0.008	<0.025
FINAL:								

CASTING PARAMETERS

SUBSTRATE:	STEEL 2	AIM METAL LEVEL:	4
FINISH:	105	WEIRGAP:	0.125
NOZZLE POSITION:	57	NOZZLEWDTH:	12
NOZZLE GAP:		FLOOR MTRL.:	
AUTO GAP ADJ:	99	WING MTRL.:	93Z3
LADLE PREHEAT:	1895		
POUR BOX PREHEAT:	2074	AVG. WATER-IN:	123.4
FURNACE TAP TEMP.:	3028	AVG. WATER-OUT:	176.3
STEEL TRANS.TEMP.:	2924	AVG. WATER FLOW:	60.9
CAST TEMPERATURE:	99	SHROUD GAS:	ARGON
RELATIVE HUMIDITY:	64	AMBIENT:	89

PURPOSE OF TRIAL:

STEEL WHEEL

RUNOUT TABLE

RESULTS OF TRIAL:

AMOUNT CAST (FEET): 150

DELAY 1:	NONE	FAILURE 1:	NOZZLE BROKE
DELAY 2:	NONE	FAILURE 2:	RUNOUT TABLE
DELAY 3:	NONE	FAILURE 3:	WHEEL STOP

STRIP CASTING HEAT LOG - PRELIMINARY

CAST #: 903   **DATE:** 9/3/93   **TIME:** 1:04:00 PM

HEATWT: 1000   **AMTCST:** 450   **GRADE:** 304-26

HEAT ANALYSIS

	C	Mn	Si	Al	N2	O2	S	Cu
AIM:	0.05	0.30	0.17	<0.004	<0.005	<0.03	<0.008	<0.025
FINAL:								

CASTING PARAMETERS

SUBSTRATE:	STEEL 2	**AIM METAL LEVEL:**	4
FINISH:	103	**WEIRGAP:**	0.1875
NOZZLE POSITION:	57	**NOZZLEWDTH:**	12
NOZZLE GAP:		**FLOOR MTRL.:**	
AUTO GAP ADJ:	99	**WING MTRL.:**	93Z3
LADLE PREHEAT:	1811		
POUR BOX PREHEAT:	2296	**AVG. WATER-IN:**	123.3
FURNACE TAP TEMP.:	3025	**AVG. WATER-OUT:**	187.7
STEEL TRANS.TEMP.:	2913	**AVG. WATER FLOW:**	39.9
CAST TEMPERATURE:	2933	**SHROUD GAS:**	ARGON
RELATIVE HUMIDITY:	76	**AMBIENT:**	81

PURPOSE OF TRIAL:

STEEL WHEEL

LOW SPEED

RESULTS OF TRIAL:

AMOUNT CAST (FEET): 450

DELAY 1:	NONE	**FAILURE 1:**	NOZZLE BROKE
DELAY 2:	NONE	**FAILURE 2:**	DAM FORMATION
DELAY 3:	NONE	**FAILURE 3:**	NONE

STRIP CASTING HEAT LOG - PRELIMINARY

CAST #: 904   DATE: 9/10/93   TIME: 1:06:00 PM

HEATWT: 1000   AMTCST: 300   GRADE: 304-26

HEAT ANALYSIS

	C	Mn	Si	Al	N2	O2	S	Cu
AIM:	0.05	0.30	0.17	<0.004	<0.005	<0.03	<0.008	<0.025
FINAL:								

CASTING PARAMETERS

SUBSTRATE:	STEEL 2	AIM METAL LEVEL:	4
FINISH:	108	WEIRGAP:	0.125
NOZZLE POSITION:	57	NOZZLEWDTH:	11
NOZZLE GAP:		FLOOR MTRL.:	
AUTO GAP ADJ:	99	WING MTRL.:	93Z3
LADLE PREHEAT:	1718		
POUR BOX PREHEAT:	2265	AVG. WATER-IN:	122.4
FURNACE TAP TEMP.:	3028	AVG. WATER-OUT:	218.3
STEEL TRANS.TEMP.:	2923	AVG. WATER FLOW:	24
CAST TEMPERATURE:	2945	SHROUD GAS:	ARGON
RELATIVE HUMIDITY:	39	AMBIENT:	76

PURPOSE OF TRIAL:

HOT WHEEL

RUNOUT TABLE

RESULTS OF TRIAL:

AMOUNT CAST (FEET):   300

DELAY 1:	NONE	FAILURE 1:	STRIPPER BAR
DELAY 2:	NONE	FAILURE 2:	WHEEL STOPED
DELAY 3:	NONE	FAILURE 3:	NONE
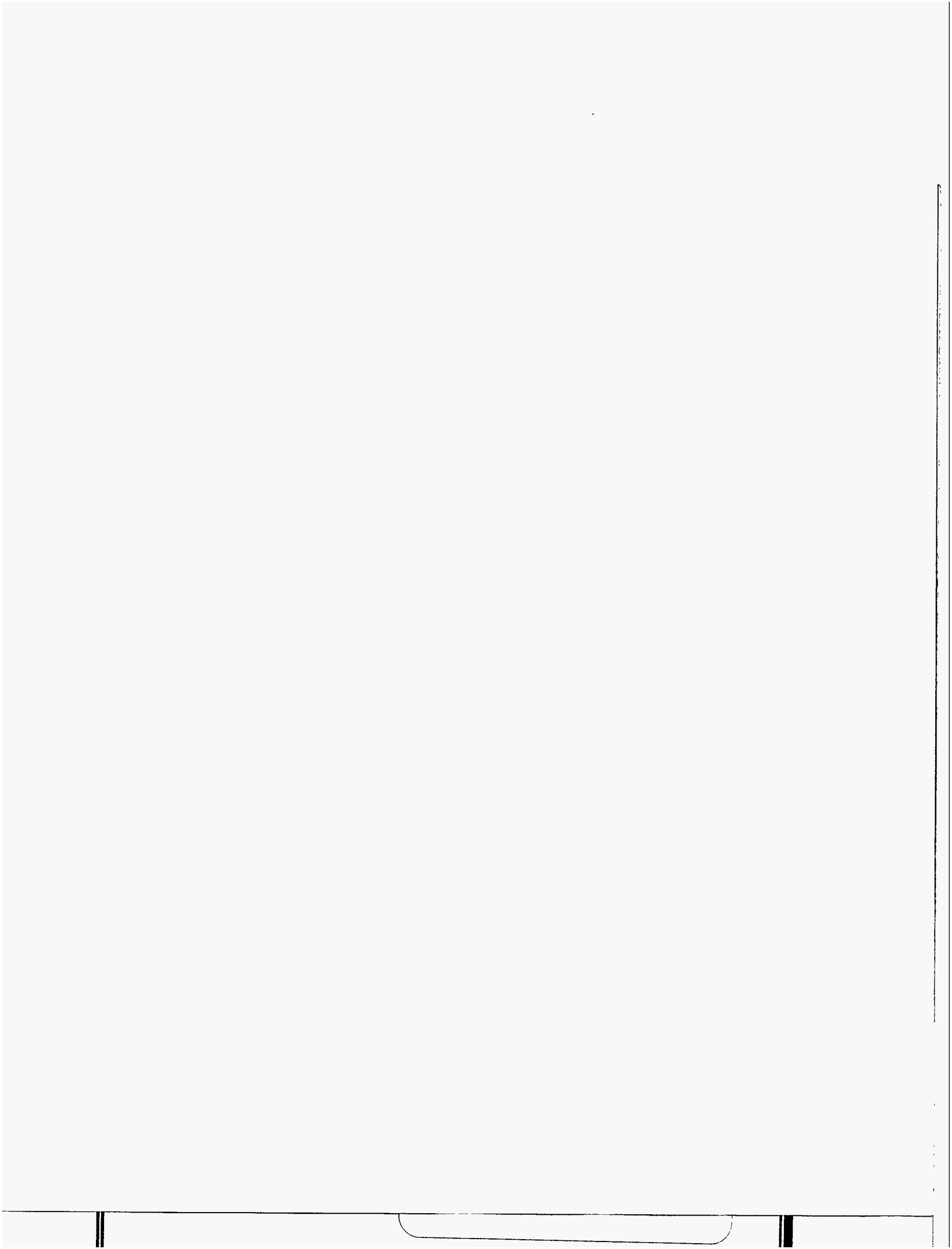
June 24, 1992

To: Mr. R. S. Williams
              Senior Research Engineer
              Casting
              Research & Technology

From: J. R. Sauer

Subject: Selection of Pouring Box Heating Technology

INTRODUCTION

Pursuant to the DOE contract Section 3, Task 3.1 (pouring box heating), the following report is submitted. Listed below are the companies contacted regarding this application and their responses. In total, 24 different companies representing five (5) different technologies were contacted. In addition, one (1) non-commercial approach was also pursued.

EXECUTIVE SUMMARY

Induction heating was chosen as the most promising technology for the purpose of heating the pouring box. In particular, Inductotherm was chosen as the company best suited to provide the needed equipment. The reasons for these selections are described in the results and discussion section of the report.

RESULTS AND DISCUSSION

An initial list of twenty-four (24) companies were contacted regarding the pouring box heating application. Names of the companies contacted were obtained from trade journals, personal contacts, and referrals from some of the companies contacted. The

companies contacted represent five (5) distinctly different technologies for heating the
pouring box. Those five (5) technologies include the following:

1)   Radiant Tube Heaters;
2)   Radiant Electric Heaters;
3)   Other Gas and Electric Heaters;
4)   Induction Heaters; and
5)   Plasma Arc Torches.

In addition to these options, one non-commercial approach was investigated. The
non-commercial approach involved forcing preheated air through pre-cast channels in the
pouring box.

Initial phone contacts with the selected companies resulted in twelve (12) of the
companies expressing no interest in pursuing our request. The remaining twelve (12)
companies were all sent sketches of the pouring box with a request to submit a budgetary
price and general information on their proposed heating system(s). Of the twelve that
were requested to submit prices and information, only eight (8) responded.

Given below is a general response by category. This is followed by a description of the
non-commercial unit. Finally, a detailed description of the responses received from the
eight (8) companies that did reply is given. Table I contains a brief synopsis of the
following information.

Radiant Tube Heaters

Radiant tube heaters use natural gas, oil, or some other gas as the heat source. The
combustible material (usually natural gas) is fed into a tube where it is combust under
controlled conditions to obtain maximum efficiency. The combustion gas is routed
through the tube for better heat transfer efficiencies. The tubes themselves are capable of
sustaining temperatures of 2700 degrees Fahrenheit, but burner manufactures suggested
that operating temperatures were limited to about 2200 degrees Fahrenheit. Based on
these temperature limits, these units would only marginally suffice for preheating the box
and would not be capable of superheating the steel. In fact, the tubes may not be capable
of surviving the temperatures generated in the box during casting.

Radiant Electric Heaters

Several element manufacturers and furnace manufacturers were contacted regarding preheating the box and superheating the steel. The response from all of them was very similar. First, they explained the difficulty of obtaining the watt density necessary to obtain the temperatures required for superheating. Second, they explained the fragile nature of the elements at the temperatures that we wished to obtain. Third, they explained the high cost of the elements required to withstand these temperatures (usually platinum). Finally, they explained the problems that would be associated with heating and cooling these elements (they are usually designed to go to a temperature and maintain that temperature). Only one company (Watlow/Tapco) expressed any interest in pursuing our application.

Other Natural Gas and Electric

There were three (3) companies which supplied natural gas and/or electric heaters (primarily for ladle preheating) that were contacted. Two (2) of the companies responded with suggestions for an automated natural gas burner system. These systems would only provide preheat for the pouring box. These companies were requested to submit bids in the likelihood that no single system would be capable of both preheating the box and maintaining the superheat in the steel. The two (2) companies were Heat Equipment and Technology, and Hot Works.

Plasma Arc Torches

Two firms were contacted regarding plasma arc torches. Two other firms in Europe were discovered later, but not contacted, because of the high prices quoted by the other two firms.

Plasma arcs are available in several configurations. The primary difference depends on if the units operate off of AC or DC current. DC current offers several advantages in that the power supply can be located further away, and the systems allow for more turn-down capability. The DC plasma arcs can be operated in transferred or untransferred mode. In untransferred mode, the arc exits the torch and returns back to the torch to complete the circuit. In transferred mode, the arc leaves the torch and couples itself to an external ground (the melt pool). By switching between untransferred and transferred operation, the torch can be used for box preheating and metal superheating.

The torch offers several unique advantages and disadvantages. The real advantages are that it can be easily moved from one pouring box to the next and it has the capability to put a lot of heat in very fast. The disadvantages include refractory wear rate, the need to have good agitation in the bath for heat transfer, and the cost.

The two companies that were contacted were Plasma Energy Corporation, and Mannesmann-DeMag (through Air Products Inc.).

Induction Heating

By far the most prolific technology in metal heating is induction heating. Both ferrous and non-ferrous companies were contacted to attempt to obtain a broad perspective on the variety of induction units available. A total of eleven (11) companies were initially contacted. Several of the companies only produced smaller units that were not capable of the needed temperatures. Other companies only sold standard units or much larger units and were not interested in special applications. Of all the companies contacted, four (4) expressed significant interest in the project to submit budgetary estimates. Each of the four (Pillar Industries, Asea Brown Boveri, Inductotherm Corp., and Lepel Corporation) presented very unique ways of superheating the steel with induction. In some cases, they stated that they were also capable of providing preheat to the box.

Non-Commercial Gas Heater

One non-commercial application was investigated. This process involved the use of an external gas burner firing a stove with oxygen enrichment (similar to a blast furnace stove). The heated gas would then be piped into the bottom of the pouring box. In the pouring box would be a series of channels that were cast in during construction of the box. The gas would flow through the channels and then exit the box. This system was eventually dropped due to the size of the furnace and the maximum temperature that it could achieve (~2700-2800 degrees Fahrenheit).

Alternatives By Company

Watlow/Tapco

The proposed system uses sixteen (16) electric heating elements backed by a fiber board to heat the pouring box. The elements can be inserted into notches located along the bottom, both sides, and back of the box. The elements would be placed so as to be

sandwiched between the current two layers of refractory material in the box. Diagrams depicting the proposed setup are in Appendix I.

The system would be capable of both preheating and adding superheat to the pouring box. As designed, the system would provide 27.8 kilowatts of power and would be capable of temperatures approaching 3000 degrees Fahrenheit. Element life is projected to be a minimum of three months under current operating conditions (heating the box in 6 to 10 hours, holding temperature for 1 to 2 hours, cooling to room temperature, moving the box, and repeating the cycle again 2 to 3 days later).

The control provided by electric heating, along with the low noise and air pollution levels are definite benefits. However, it is not clear that 27.8 kilowatts is sufficient power to provide superheat to the steel. Higher watt densities would increase the ability of the system, but may not be practical (especially in a larger commercial system).

The system price was quoted as $40,000. The price included heating elements for one box, the control instrumentation, and the necessary transformer(s). Each additional box would cost roughly $27,000 (price of elements only). To operate three boxes would then cost $94,000 or $3381 per kilowatt. Delivery of a system would require 14 weeks.

Plasma Energy Corporation

The system proposed by PEC consists of a 24" long plasma torch 2-½" in diameter, gas and water supplies to the torch, and the electrical supply. The system is rated at 96 kilowatts and would be capable of operating under transferred or untransferred mode (it would take ~5 minutes to switch between the two modes). This would provide the flexibility needed to use the torch for preheating as well as superheating. Plasma torches are capable of providing a lot of heat very fast, as the flame temperature ranges from 7000 to 14000 degrees Fahrenheit. Also, the torch could easily be moved from one box to the next (would only need one system).

The torch does have a few drawbacks, namely that because of the extreme temperatures generated they do tend to be hard on refractories. Secondly, there needs to be vigorous stirring taking place in the bath in order to get the heat into the metal. Finally, it is not entirely clear as to whether the system would be capable of a controlled preheat of the box when slow heating rates are required. Further information can be found in Appendix II.

The price of the system was quoted as $155,000, which included setup and training. The system itself would cost $140,000 or $1458 per kilowatt for all three boxes. Delivery was stated as being 26 weeks.

Mannesmann-DeMag

This proposal incorporated the use of a plasma arc torch for superheating the steel (preheating is not possible with their configuration). The unit was rated at 400 KW and the quote included cost for all items (including training) except for wiring and plumbing requirements. The unit would be usable with multiple boxes, but would be too large for our current configuration (see Appendix III). Based on the quoted price of 1,750,000 DM ($1,030,000) the cost in U.S. dollars, per kilowatt, would be $2575 for a system capable of handling three boxes. Delivery of a system would require 36 weeks.

Pillar Industries

This system is a uniquely designed induction heater. The system incorporates a vacuum pump to raise the liquid steel up into a tube where it enters an induction coil. The liquid steel is then heated and released into the main bath in a controlled manner to maintain metal level and temperature. The unit is designed such that only one unit would be need for three pouring boxes and would be easily incorporated into the current box design.

Two drawbacks exist with this system. First, the system is not capable of preheating the box, and second, the level control is rather crude considering the control that may be necessary.

The quoted price for the system is $78,000 for a 50 kilowatt system or $1560 per kilowatt for three boxes. Appendix IV contains further information on the system and price quote. Delivery of a system was not included in the quote.

ABB Asea Brown Boveri

The system proposed by ABB would utilize a coreless inductor. The unit would mount on the side of the box and require about 10" of clearance on both sides. The unit would be capable of superheating the steel, but, not preheating the box. The price of the system was based on 75 KW of power and conversations with ABB revealed that the price was the same for all their systems in the 50 to 200 KW range.

While they could possibly use one of our existing power supplies, they would prefer to use theirs (to avoid confusion if something should go wrong). The price of their unit was quoted as $35,000 for the coil only and $95,000 for the entire system. Delivery of a system would be 12 weeks. Based upon ABB providing the power supply for a 200 KW unit, the cost of equipping three boxes would be $825 per Kilowatt. Appendix V contains the response from ABB regarding their system and quote.

Inductotherm

Inductotherm offered four potential solutions to our problems with preheating and superheating the pouring box. They felt that one particular solution offered the most advantage and only quoted prices for that system. The induction unit proposed would replace our existing pouring box. The price of the unit does not include retuning or a control loop. Prices for tuning the power supply were quoted verbally as $2,000 to $4,000, and the price of an isolated control unit was estimated at $800. The Inductotherm unit would be powered off of the existing Inductotherm Mark IV system in the laboratory (rated at 250 KW). The price to equip a single box was quoted as $9,860. The price for three boxes (including controls and tuning) would then be $34,380 or $137 per KW. Further details can be found in Appendix VI. Delivery was quoted as 8 weeks.

A distinct advantage of going with Inductotherm (other than the ability to utilize the existing power unit) is that they did offer several unique solutions. It is felt that this provides more opportunity to explore other options if the initial proposal proves to be unsatisfactory.

James R. Sauer
Research Engineer
Casting
Research & Technology

JRS/2410/k
Attachments

Mr. R. S. Williams
June 24, 1992
Page 8

cc: <u>Research</u>
J. W. Allen
C. Bennett
S. L. Campbell
R. Engel
D. W. Follstaedt
K. C. Schneider
R. C. Sussman

TABLE I

Company							
Type	Company Name	Phone #	Contact	Power (KiloWatts)	Capability	System Price	Delivery (Weeks)
Radiant Tube							
	Coors Ceramics Co	(303)277-4438	Gil Gilbert	...	N/A	...	...
	Eclipse	(815)877-3035	Dave Sorenson	...	N/A	...	...
	Pyronics	(216) 662-8800	Tom Garvis	...	N/A	...	...
Radiant Electric							
	Kanthal Corp.	(203)744-2703		...	N/A	...	...
	Watlow/Tapco	(314)878-4600	Scott Jordahl	27.8	Pre/Superheat	$40,000	14
	Custom Electric Manufacturing Co	(313)261-2300	John Edwards	...	N/A	...	...
	Thermcraft	(919)784-4800	Will	...	N/A	$300,000	...
	Zircar	(914)651-4481	Phil Hamlin	...	N/A	...	...
Plasma							
	Plasma Energy Corp	(919)787-2237	Tom Gahagan	96	Pre/Superheat	$140,000	26
	Air Products/Manisman-Demag	(215)481-7316	Otto Metalmann		Pre/Superheat		
Induction							
	Pillar Industries Inc	(414)255-6470	Jack Theilke	50	Superheat	$78,000	...
	Ajax Magnethermic Corp	(216)372-8511	Tim Keenan		N/A	...	...
	Tocco	(216)-441-1141	Ed Fitzgerald	...	N/A	...	...
	Bradley Induction	(416)666-2262			N/A		
	ABB Asea Brown Boveri	(908)932-6134	Viren Goyal	150	Superheat	$60-95000	12
	Hi T E Q Inc	(513)847-8051	Tim Via	...	N/A	...	...
	InductoTherm (Consarc)	(609)267-9000	Joe Belsh	up to 250	Pre/Superheat	$9,860	8
Fuel/Electric							
	Heat Equipment and Technology	(513)591-3000	Mike Wilkens	2500000 Btu/Hr	Preheat	$10,150	6
	Lindberg	(414)261-7000	Jerry Naveraty	...	N/A	...	...
	Hot Works	(606)276-1570	Ben Griffen	2 MBtu	Preheat	$48,000	6 to 10
Non-Ferrous Melting							
	Leybold Durferrit GmbH	(6181)59-2636		...	N/A	...	...
	Aichelin-Stahl	(916)597-3616	Don Bilois	...	N/A	...	...
	Lepel	(516)586-3300	Vlad Pilic	...	N/A	...	...
	Seco/Warwick Corp	(814)724-1400	Scott Hamilton	...	N/A	...	...

TABLE I

Company		
Type	Company Name	Comments
Radiant Tube		
	Coors Ceramics Co	Only manufactures tubes (not burners)
	Eclipse	Not interested
	Pyronics	Can not attain needed temperatures
Radiant Electric		
	Kanthal Corp.	Provide elements only
	Watlow/Tapco	System good to 3000 F. Minimum 3 month element life.
	Custom Electric Manufacturing Co	Not interested
	ThermCraft	Provide elements only
	Zircar	Failed to respond to several requests
Plasma		
	Plasma Energy Corp	24" long by 2.5" diameter unit
	Air Products/Manisman-Demag	
Induction		
	Pillar Industries Inc	Vacumn system with induction coil
	Ajax Magnethermic Corp	Failed to respond to request for quote
	Tocco	Not interested
	Bradley Induction	Not contacted
	ABB Asea Brown Boveri	Side mounted coreless inductor (same price for 50 to 200 KW)
	Hi T E Q Inc	Did not respond to inquiry for prices
	InductoTherm (Consarc)	Replaces Pour Box. Uses existing Mark IV power supply
Fuel\Electric		
	Heat Equipment and Technology	Gas fired flat burners with flame and temperature control
	Lindberg	Not interested
	Hot Works	2700 F with controls (12 programs). Rental available ($8,000)
Non-Ferrous Melting		
	Leybold Durferrit GmbH	Not contacted due to responses recieved by others
	Aichelin-Stahl	Beyond their range (temperature)
	Lepel	Not interested - does not fit with their products
	Seco/Warwick Corp	Temperatures are way too high for their process

APPENDIX I

WATLOW/TAPPCO PRICE QUOTE
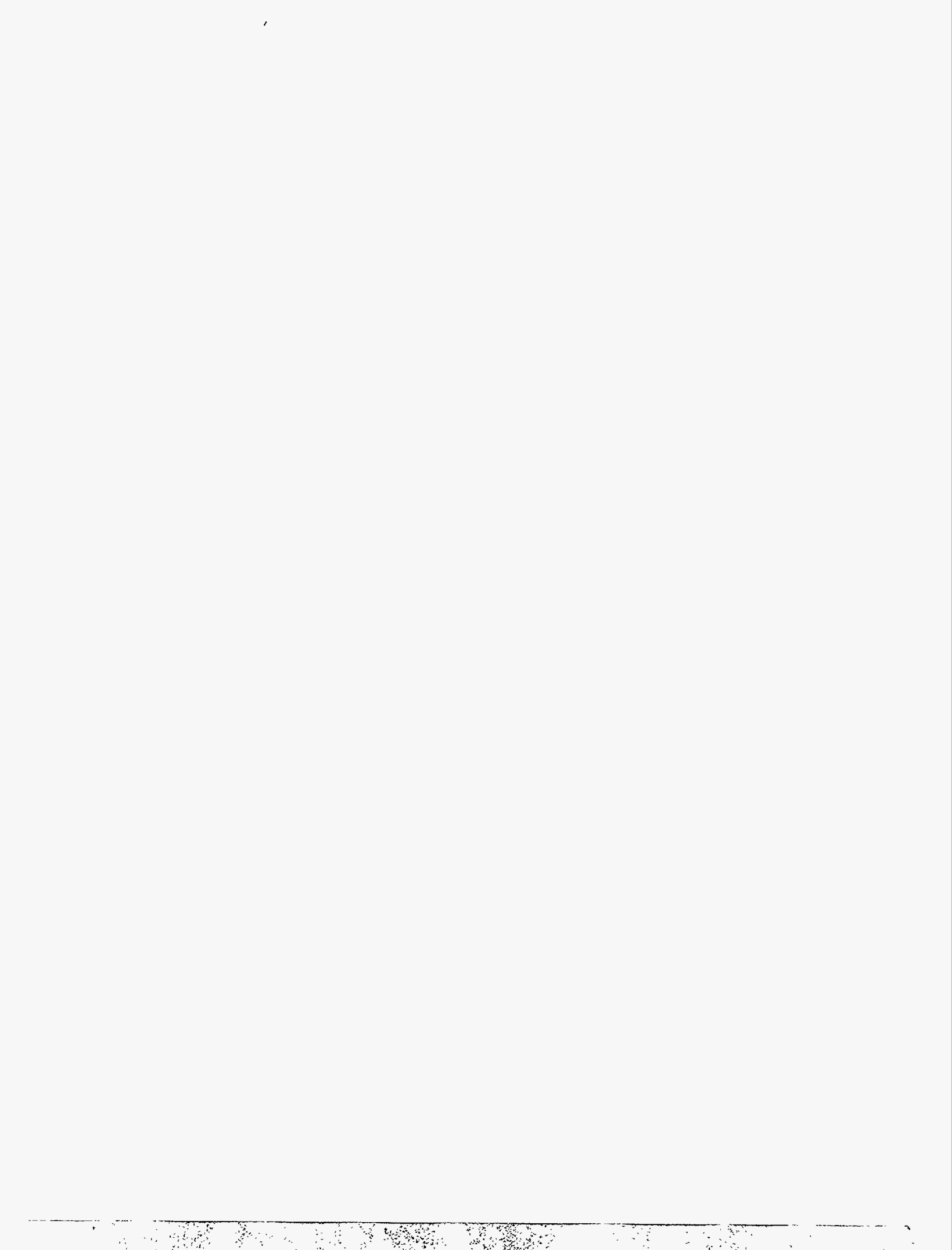
TAPCO PRODUCTS, INC.

P.O.BOX 42395 • CINCINNATI, OHIO 45242
1-800-242-4481   FAX 513-683-7675

CINCINNATI	LOUISVILLE	DAYTON	FT WAYNE
(513) 683-4481	(502) 581-9693	(513) 268-8287	(219) 447-4036
INDIANAPOLIS	COLUMBUS	CLEVELAND	EVANSVILLE
(317) 263-0042	(614) 464-2292	(216) 566-5442	(812) 464-2939

MAY 28, 1992

ARMCO RESEARCH & TECHNOLOGY
705 CURTIS ST.
MIDDLETOWN, OHIO 45043

ATTN:MR. JIM SAUER

DEAR JIM:

TAPCO IS PLEASED TO QUOTE THE FOLLOWING:
              POURING BOX
ESTIMATED PRICE.............................$27,000.00
PRICE INCLUDES:1.HEATING ELEMENTS
               2.BACK UP INSULATION
               3.BUSSING STRAPS;NO WIRING OR CONTROL CIRCUIT
THE POWER REQUIREMENTS ARE AS FOLLOWS:
               1.150 AMPS
               2.185 VOLTS
               3.27,810 WATTS
               4.1.236 HOT(1500 DEGREES C) RESISTANCE

WATLOW IS LOOKING FORWARD TO A WATLOW/ARMCO PARTNERSHIP ON
THIS PROJECT. PLEASE LET ME KNOW IF I CAN BE OF ANY
ASSISTANCE.

THANK YOU,

SCOTT M. JORDAHL
TAPCO PRODUCTS

D-CAST 85T

CERAMIC FIBER
HEATER MODULE

BUBBLED ALUMINA

SECTION A-A

BACK

FRONT

3.25"

1.0"

3.5"

26"

25"

A

A

B

B
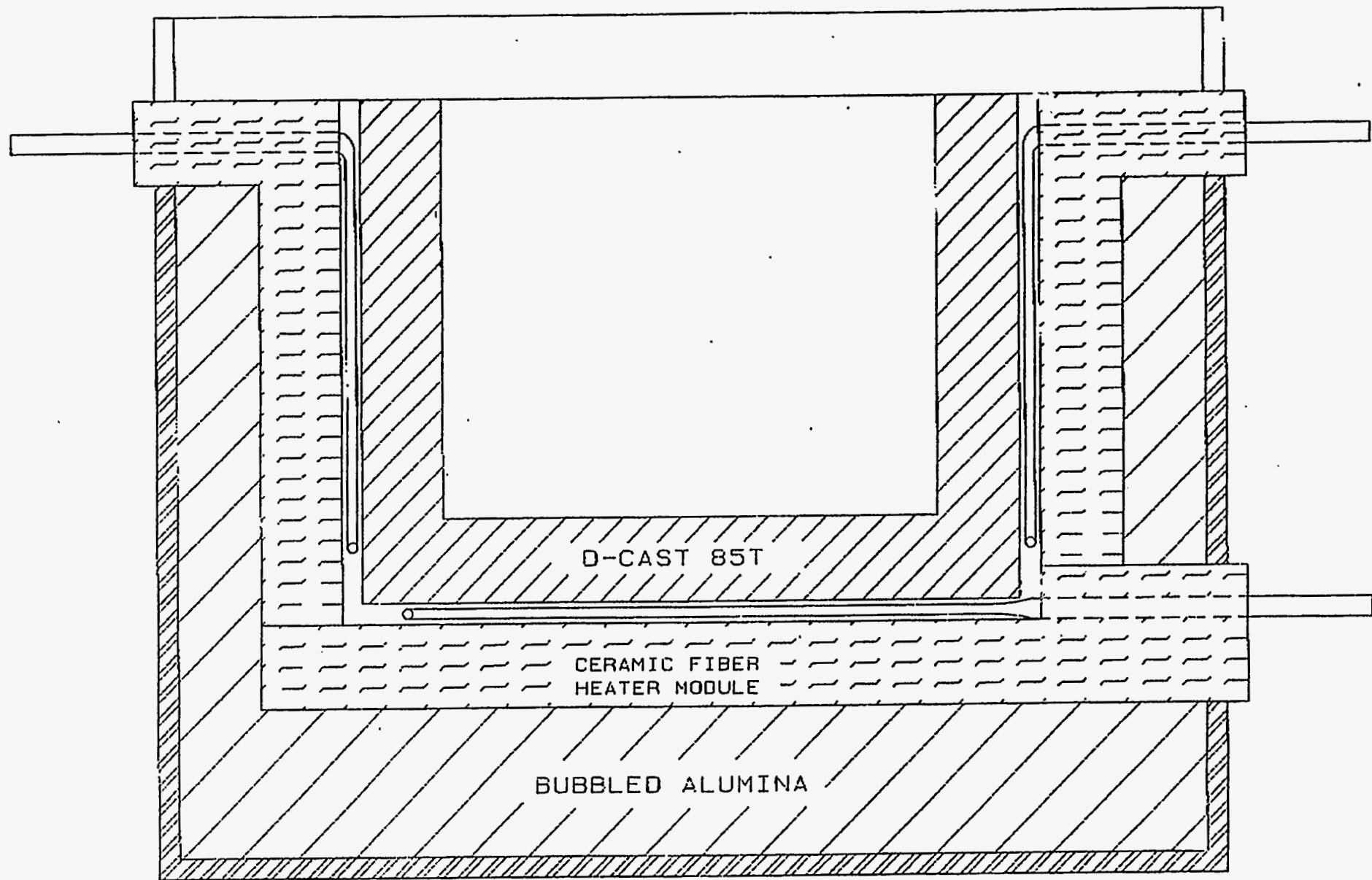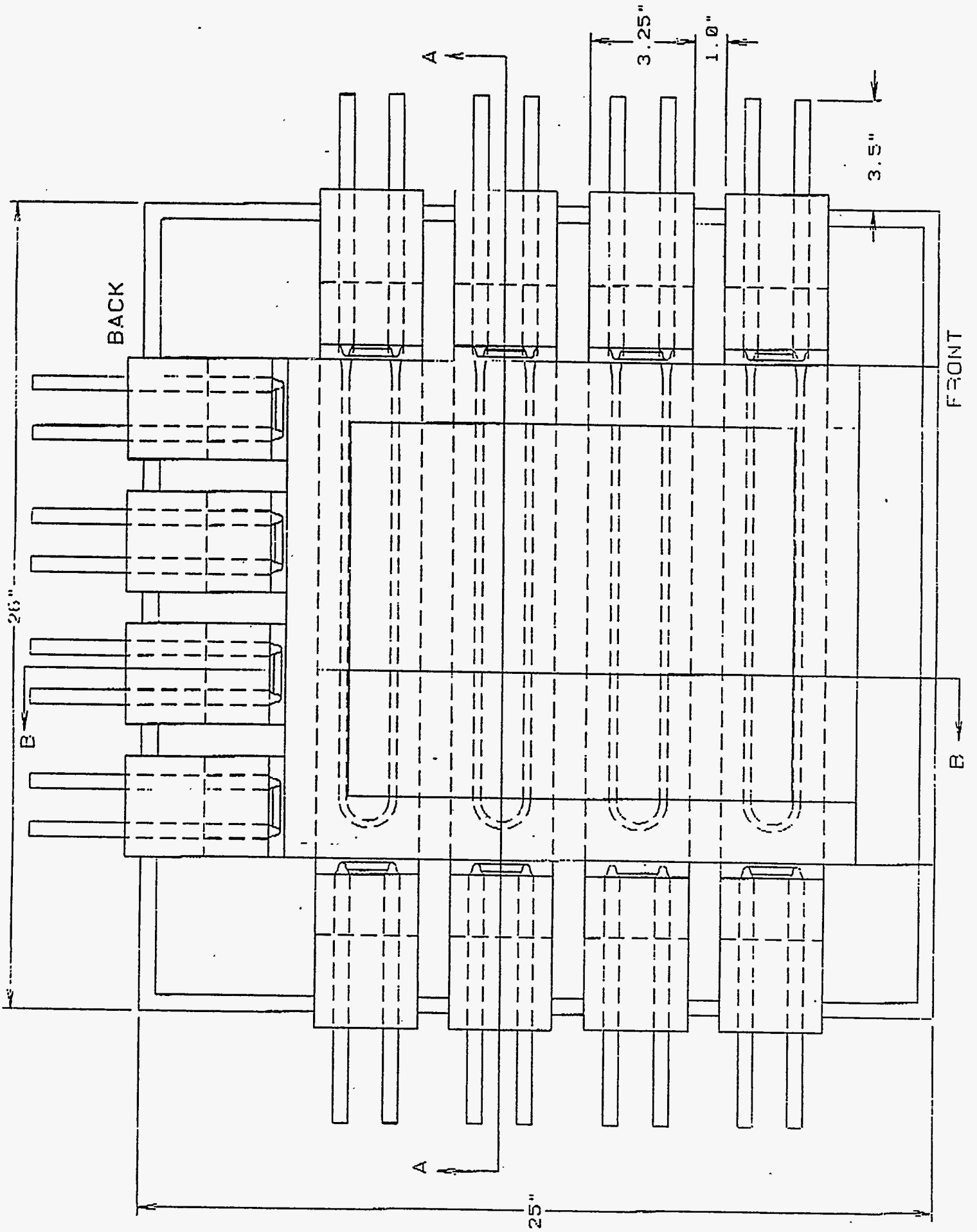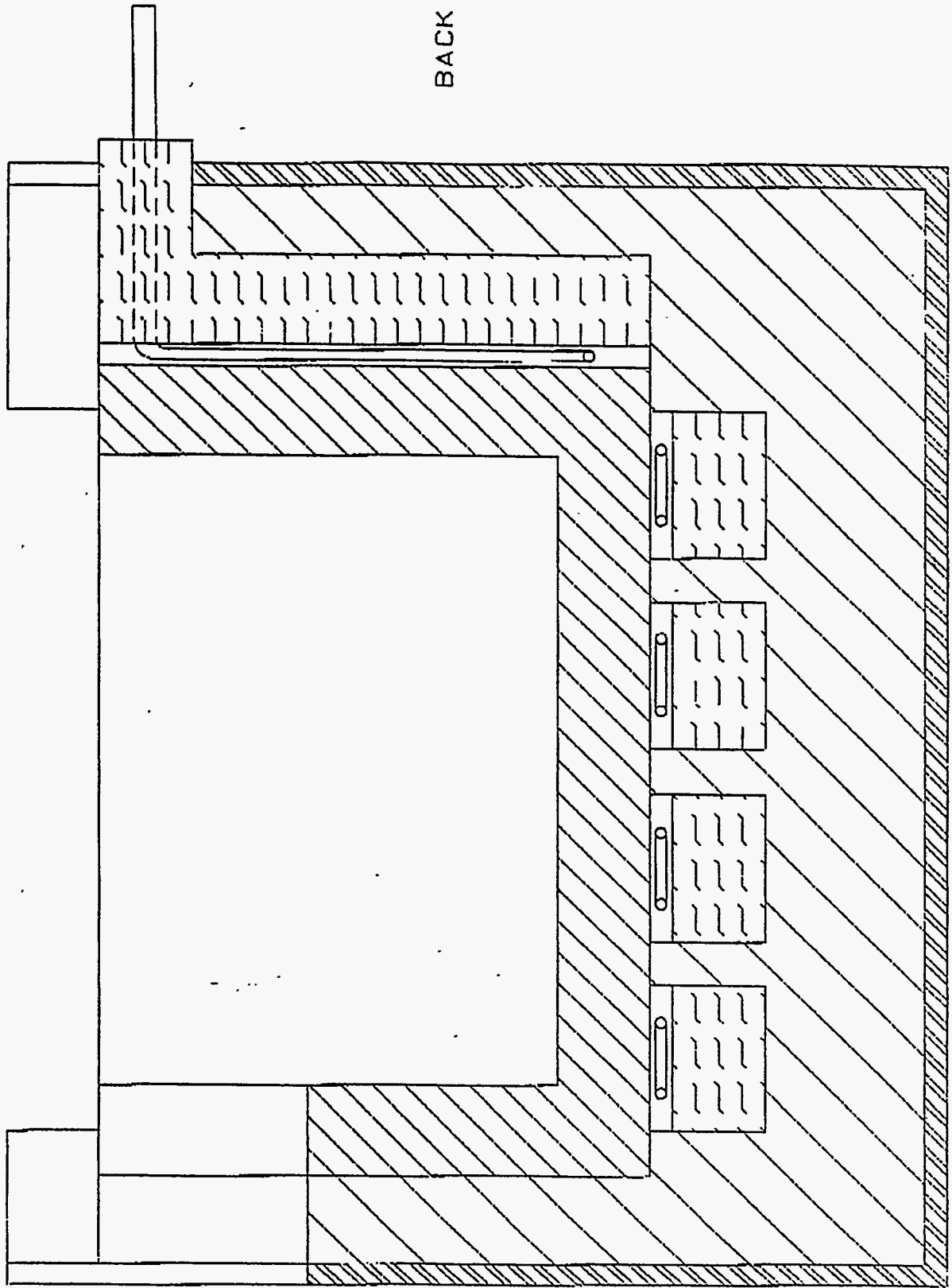
BACK

FRONT

SECTION B-B

APPENDIX II

PLASMA ENERGY CORPORATION PRICE QUOTE
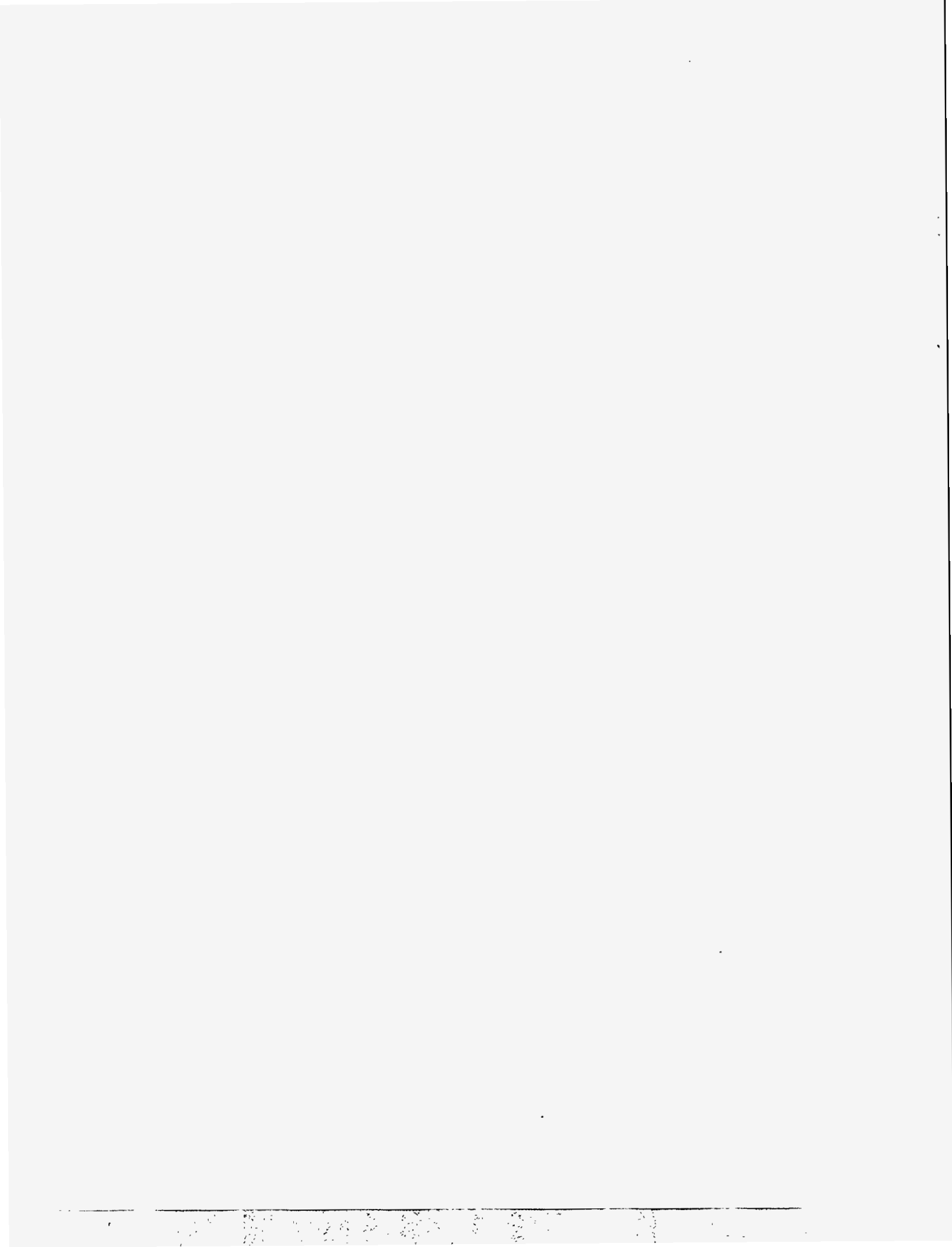
May 27, 1992

Mr. James R. Sauer
Armco Inc.
Research & Technology
705 Curtis Street
Middletown, Ohio 45043
Subject: PEC proposal: 92-056

Dear Jim,

Attached please find our quotation for a 96KW Plasma Heating
System. This system will be able to preheat your tundish
vessel and maintain superheat of the molten steel bath during
casting.

I.   Scope of Supply

This 96KW Plasma Heating System is convertible meaning that
it can be operated in either the transferred or non-
transferred mode by changing certain torch parts. It can
also be operated with a variety of arc gases. The plasma
system interacts electrical energy from the plasma power
supply with a small amount of gas to produce a plasma flame
with temperatures approaching 6000 degrees C. The plasma
flame transfers its energy by radiation, convection, and
molecular recombination. This PEC proposal includes system
hardware, startup assistance and operator training.

    A. Plasma Arc Torch - PEC's PT50C convertable plasma
arc torch operable on a variety of arc gases. The plasma
torch is made up of a stainless steel shroud, electrical
insulators, and copper alloy electrodes. The PT50C is
approximately 24 inches long and 2.5 inches in diameter.

    B. Plasma Power Supply - This is a current-regulated DC
power supply with an output rating of 96KW. Customer
supplied power input requirements are 480 VAC, 3-phase, 60
Hz. A three pole circuit breaker is provided to switch the
3-phase primary high voltage AC supply on and off. The power
supply is housed in a NEMA 12 enclosure and includes all
relevant interlocks and alarms for safe operation.

    C. LEP Arc Starter - The arc starter circuit generates
a high voltage Low Energy Plasma (LEP) that initiates the
plasma arc in the torch.

D. Water/Power Junction Box - The Water/Power Junction Box is installed near the plasma arc torch. The dry DC cables from the LEP arc starter enter this unit along with torch cooling water hoses. The DC power and torch cooling water are combined and exit via water/power conductors to the plasma arc torch. The unit is housed in a NEMA 12 enclosure.

E. Water-Gas Manifold - This unit includes instrumentation necessary to monitor and control the plasma arc torch gas flow and cooling water flow. The Water-Gas Manifold is mounted on the power supply enclosure.

F. Cooling System - Not included. PEC will provide water cooling specifications at customer's request.

G. Control System - PEC will supply a control panel for operation of the PTH system. The control panel is mounted on the front of the power supply and includes all necessary pushbuttons, key switches and indicators required for safe and efficient operation.

I. Water/Power Junction Box Isolation Water Hoses - These 3/4 inch diameter 15 foot long hoses supply torch cooling water from the water cooling system to the W/P junction box. They are non-conductive and provide electrical isolation for the water/power junction box. Two are supplied. Hose fittings are JIC.

J. Torch Arc Gas Hose - This hose supplies gas to the plasma torch and is 3/8 inch diameter and 25 ft. long. It is non-conductive and provides electrical isolation for the plasma torch. Hose fittings are JIC.

K. Water Power Conductors - These conductors are copper core, full flow head design and provide DC power and cooling water from the W/P junction box to the plasma arc torch. They are 3/4 inch diameter, 25 ft. long, and rated for 1000 amps. Two are supplied. Hose fittings are JIC.

L. Operators Manuals - PEC will provide two (2) copies of operators manuals in English language. These manuals include operating instructions, troubleshooting guidelines, drawings and parts lists.

II.   Installation & Startup Assistance

PEC will provide a Plasma System Engineering Specialist or Product Support Engineer in a supervisory capacity to assist in the installation of the Plasma System according to the attached Field Service Rate Schedule. Customer will be responsible for supplying the required utilities and interconnections to the PEC supplied receptors including power wiring, control and instrument wiring, water piping, and gas piping. Customer will supply labor for installation of the Plasma System.

III.   Training

PEC will provide hands-on and classroom instruction on the Plasma System upon completion of installation. The training course is conducted for one week at the Product Support Engineer level on the attached field service rate schedule.

IV.   Price and Delivery

The price for this PTH system is $155,000.00 US. Typically $10,000.00 is budgeted for startup and installation assistance and $5,000.00 for operator training. Recommended spare parts for the PTH system can be provided as part of the contract at a budgetary cost of $10,000.00. Shipment of the system is twenty-six weeks after acceptance of order, F.O.B. Raleigh, N.C.

PEC is excited about the possibility of providing a Plasma Heating system to Armco Inc. We would be happy to meet with you in the near future to discuss this proposal in detail and to answer any questions you may have. In the meantime please don't hesitate to contact us if you require any additional information. We look forward to talking with you soon.

Sincerely,

Tom Gahagan
Sales Engineer

PLASMA ENERGY CORPORATION
6016 TRIANGLE DRIVE
RALEIGH, NC 27613 USA

FAX: 919-571-6218
PHONE: 919-787-2237

FAX NO: 513-425-6459

DATE: 06/05/92   **FROM:** TOM GAHAGAN
REF #: 0605-4TG   **TOTAL PAGES: 4**

TO: ARMCO RESEARCH
ATTN: JIM SAUER
RE: 96 KW Plasma System

Dear Jim,

As a result of our conversation the other day, I am sending you the
attached information. The torch parts circled in the drawings are
switched to change from transferred to non-transferred mode.
Probably a 5 minute maximum process.

A switch on the power supply is used to change operating modes for
the electrics. I hope this helps you to understand the convertible
system better.

Regards,

Tom Gahagan
Tom Gahagan
Sales Engineer

01 PLASMA ARC TORCH ASSEMBLY
02 SHROUD ASSEMBLY
03 OUTER SHROUD EXTENSION-TRANS
04 TORCH BOOT
05 REAR SLEEVE
06 GAP INSULATOR
07 REAR ELECTRODE HOLDER ASSEMBLY
08 WATER GUIDE-REAR ELECTRODE
09 VORTEX GENERATOR
10 INSULATOR
11 REAR INSULATOR
12 INSULATOR ASSEMBLY
13 SOCKET-HEAD CAP SCREW
14 WOODRUFF KEYS
15 LOCKING BUSHING
16 REAR ELECTRODE
17 COLLIMATOR ASSEMBLY
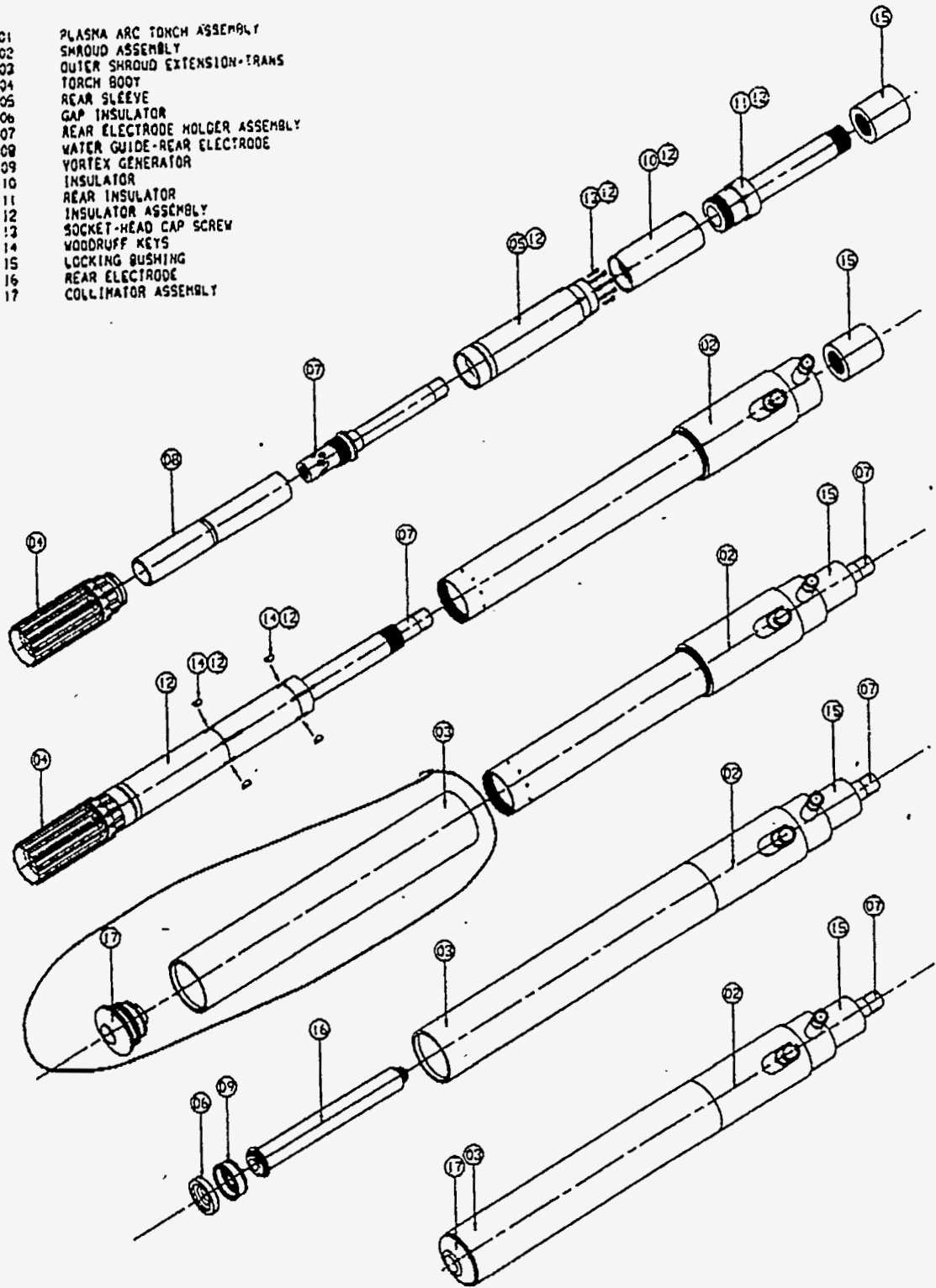
Figure 4002-01.1 Torch Assembly-
Transferred Arc Mode

01   PLASMA ARC TORCH ASSEMBLY
02   SHROUD ASSEMBLY
03   OUTER SHROUD EXTENSION-NITRANS
04   TORCH BODY
05   REAR SLEEVE
06   GAP INSULATOR
07   REAR ELECTRODE HOLDER ASSEMBLY
08   WATER GUIDE-REAR ELECTRODE
09   VORTEX GENERATOR
10   INSULATOR
11   REAR INSULATOR
12   INSULATOR ASSEMBLY
13   SOCKET-HEAD CAP SCREW
14   WOODRUFF KEYS
15   LOCKING BUSHING
16   REAR ELECTRODE
17   WATER GUIDE-FRONT ELECTRODE
18   FRONT ELECTRODE
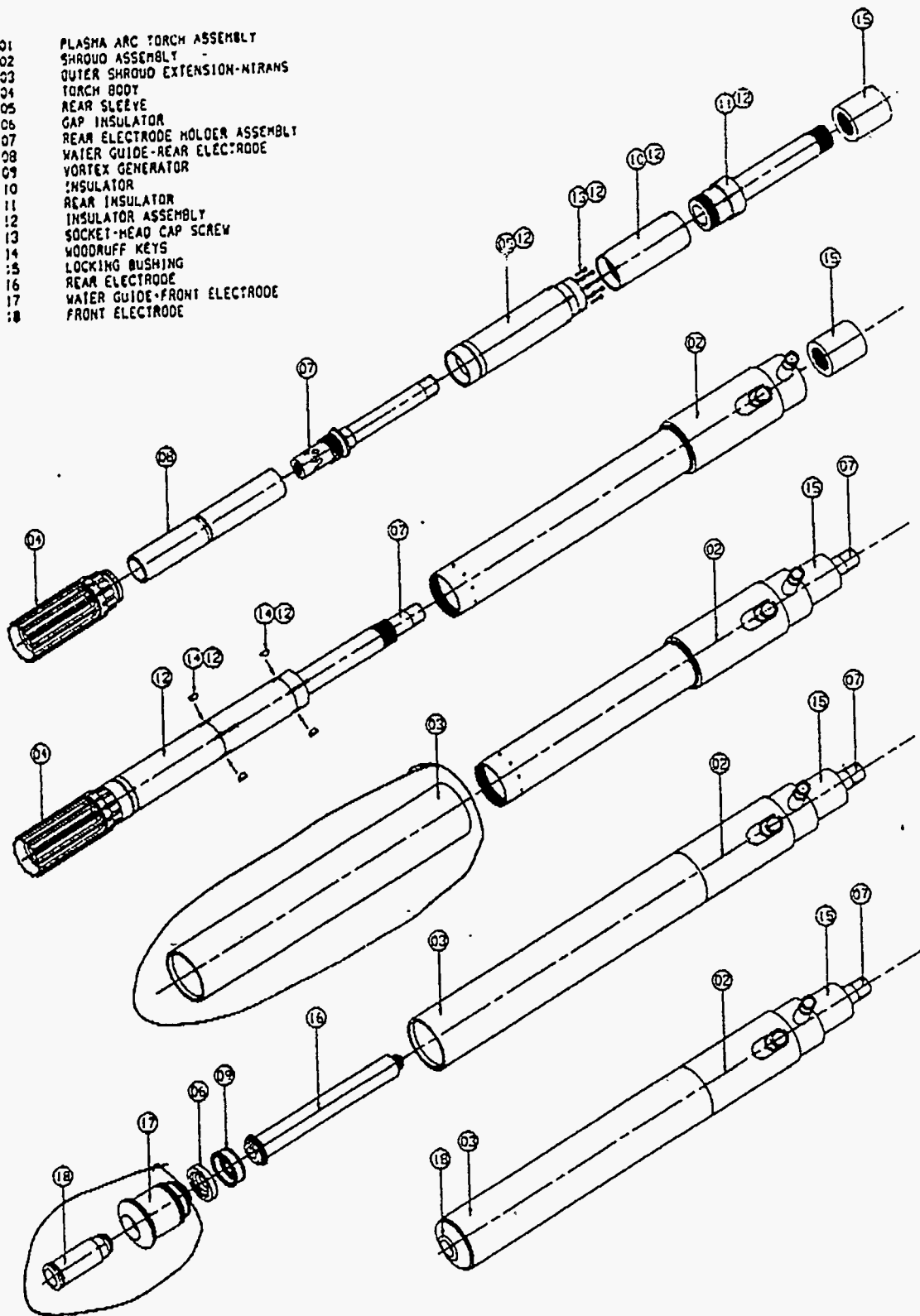
Figure 4002-01.5 Torch Assembly-
Non-transferred Arc Mode
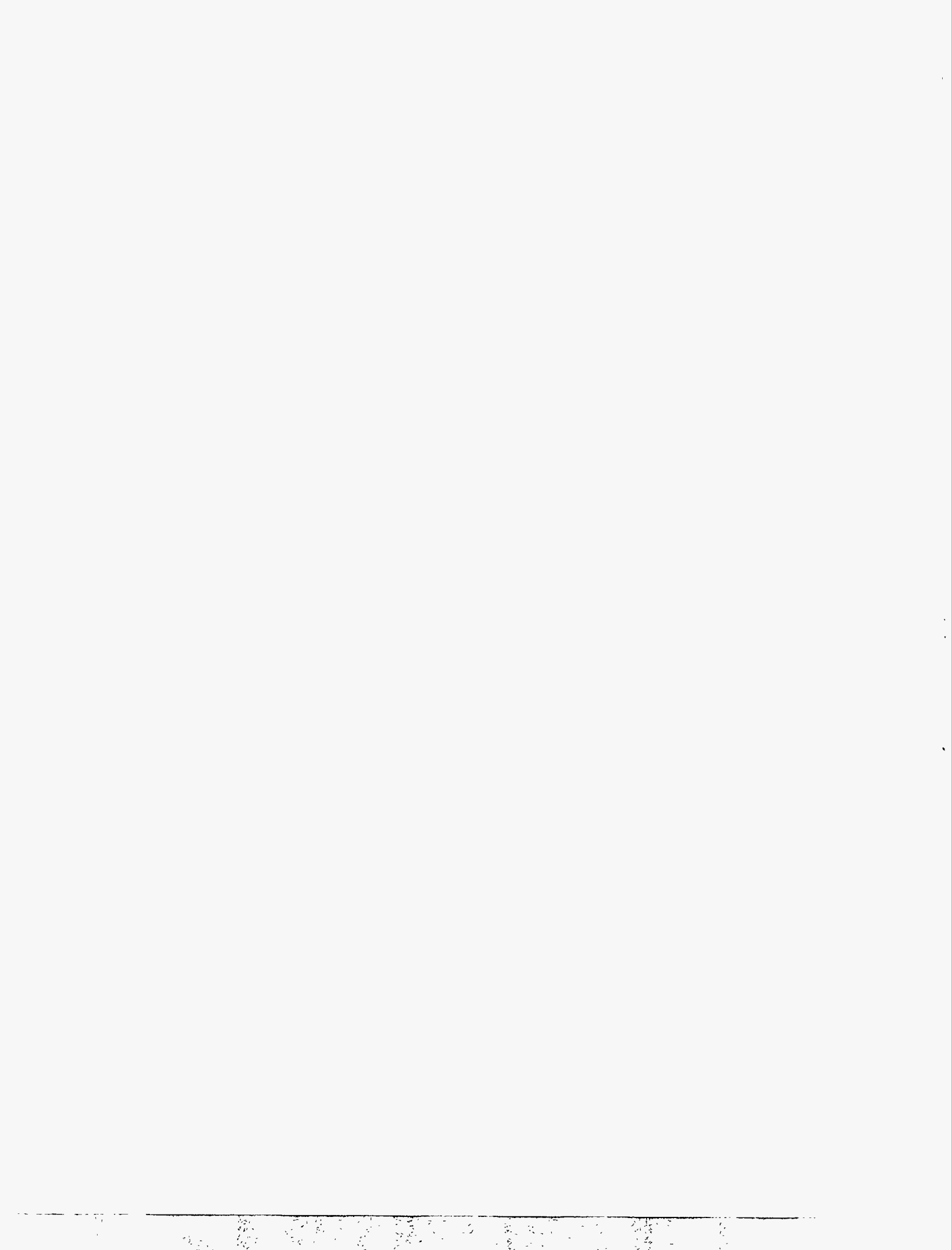
APPENDIX III

MANNESMANN DEMAG PRICE QUOTE

Armco Inc. Reasearch Center	**MANNESMANN DEMAG HÜTTENTECHNIK**
Mr. James R. Sauer	**ABT. 6405 - PLASMATECHNIK**
	Wolfgang-Reuter-Platz
	W-4100 Duisburg
Fax No.: 001 513 425 6459	**From** Dr. Bebber/cs
	Doc. 2518
	Date 04.06.92
cc: O. Metelmann, MDC Pittsburgh	**Telephone** 0203 - 605 2150
B. Best, Air Products	**Telefax** 0203 - 605 333?
	Telex 85585512 mD D
CONCERN: Plasma Tundish Heater	Page 1 / 10

Dear Mr. Sauer,

attached we send you the budgetary quotation for a 400 kW plasma heater. We are aware that its capacity may be a little to big for the tundish size which you have in mind now. But it provides you a lot of savety and flexibility and moreover our understanding is that the tundish size is not fixed yet. Thus the quotation should be used as a frame to work in.

If you have any question to ask please don't hesitate to call us.

With best regards

MANNESMANN DEMAG HÜTTENTECHNIK
Abt. 6405 - Plasmatechnik

- Dr. Bebber -
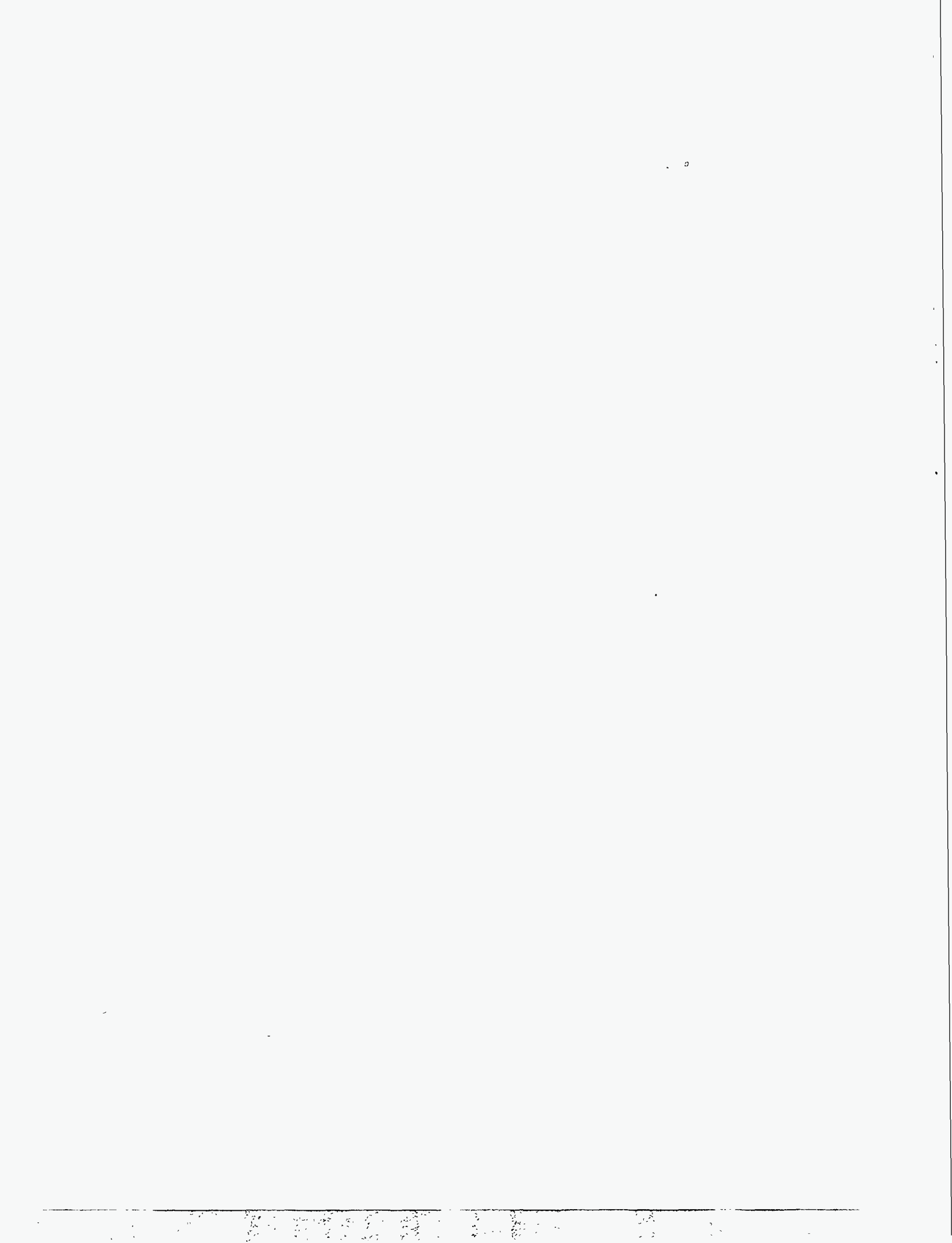
BUDGETARY QUOTATION

for

DC PLASMA TUNDISH HEATER

for

ARMCO INC. RESEARCH CENTER
U S A

DUISBURG, JUNE 1992
MDH-Project-No. 10.0119
Status 06/92
2517

3110

1.   INTRODUCTION

The application of the Mannesmann Demag plasma heating system offers
the possibility to have nearly constant parameters in the casting
process with all associated advantages. The specific input of heat,
in particular, makes the start of the casting process much safer and
the continual compensation of the temperature drop by the end of the
cast allows the production to be shortened and more effective.

As a result consistent quality can be observed in particular in
regards to equiaxed structure and segregation. Besides the
improvements in quality the plasma system leads to an increase in
productivity. In particular it provides:

- **Near liquidus casting**   The rise in casting speed especially in the
                               beginning of casting improves caster
                               productivity,

- **Energy savings**   The tapping temperature in the primary
                               steel-making facilities can be lowered. The
                               refractory material consumption is reduced
                               accordingly.

- **Sequence casting**   Heating of the tundish offers optimum
                               conditions for multi-ladle casting. The
                               temperature loss is compensated and the
                               waiting time for the ladle change-over is
                               savely bridged,

- **Higher yield**   Formation of skulls in the tundish can be
                               largely avoided by use of the heating system
                               until end of casting,

2517

- **Homogeneous temperature** The appropriate torch position and
individual power control lead to uniform
temperature in the mould.

References

Direct current plasma torches feature stability and low noise
operation. In addition, thyristor control of the power supply ensures
good controllability and excellent efficiency. The Mannesmann Demag
plasma torch is compactly designed and has short connections to the
media supply lines.

In 1991, Mannesmann Demag delivered a direct current controlled
plasma heating system for the single strand horizontal caster of
Boschgotthardshütte (BGH Edelstahl) in Siegen, FRG. A first report is
enclosed.

2517

ARMCO INC. RESEARCH CENTER
DC Plasma Tundish Heater
MDH-Project-No. 10.0119
Status 06/92   - 4 -

2.   **PLASMA TUNDISH HEATING CONCEPT**

          The following technical and process data were submitted or are
          estimated as well:

          ladle capacity   0.5 - 1.5 t
          tundish capacity   0.2 t

          It is proposed to install a plasma heating system of 400 kW power
          capacity. This is by far sufficient to recover all temperature losses
          taking into account the efficiency of the plasma system and a safety
          rate.

          Plasma Tundish Heating System (design figures)

          torch current   2,000 A
          torch voltage   100 - 200 V

          ignition distance   150 - 250 mm
          gas consumption   ~ 150 Nl/min Argon
          cooling water consumption   ~ 10 m³/h

          main power supply   400 kW
          auxiliary power supply   about 80 kVA

2517

ARMCO INC. RESEARCH CENTER
DC Plasma Tundish Heater
MDH-Project-No. 10.0119
Status 06/92   - 5 -

3.   **PRELIMINARY SUPPLY LIST FOR THE PLASMA SYSTEM**

Item	Title	Hardware*	Supply Engineering Basic	Detail	Remarks
3.1	**MECHANICAL EQUIPMENT**				
3.1.1	**Plasma Torch System**				
	- DC plasma torch	M (1)	M	M	
	- torch fixing device	M (1)	M	M	
3.1.2	**Torch Movement**				
	- torch lifting and swivelling device	M (1)	M	M	
	- hydraulic valve unit	M (1)	M	M	
3.1.3	**Counter Electrode System**				
	- counter electrode	M (1)	M	M	
3.1.4	**Auxiliary Equipment**				
	- temperature measurement equipment	C (1)	M	M	
	- steel level sensor	C (1)	M	M	

C = Client,   M = Mannesmann Demag,

* No. in brackets indicates No. of required pieces.

2517

Item	Title	Hardware*	Supply Engineering Basic	Detail	Remarks
3.2	**ELECTRICAL EQUIPMENT**				
3.2.1	**Main Power Supply**				
	- transformer	M (1)	M	M	
	- thyristor power supply	M (1)	M	M	
	- operator switch	M (1)	M	M	
3.2.2	**Ignition Power Unit**				
	- ignition power supply	M (1)	M	M	
	- HF starting unit	M (1)	M	M	
3.2.3	**Visualization and Process Control**				
	- visualization incl. software	M (1)	M	M	
	- programmable logic control incl. software	M (1)	M	M	
	- main control panel	M (1)	M	M	
3.2.4	**Auxiliary Devices**				
	- LV-subdistribution	M (1)	M	M	
	- local control devices	M (1)	M	M	

C = Client,   M = Mannesmann Demag,

* No. in brackets indicates No. of required pieces.

2517

ARMCO INC. RESEARCH CENTER
DC Plasma Tundish Heater
MDH-Project-No. 10.0119
Status 06/92   - 7 -

Item	Title	Hardware*	Supply Engineering Basic	Detail	Remarks
3.3	**MEDIA SUPPLIES/PLASMA SYSTEM**				
3.3.1	**Media Units Plasma System**				
	- cooling water station	M (1)	M	M	
	- gas distribution unit	M (1)	M	M	
3.3.2	**Media Supplies**				
	- plasma torch	M (1)	M	M	
	- counter electrode	M (1)	M	M	
	- pipes and installation material	C (1)	M	C	

C = Client,   M = Mannesmann Demag,

* No. in brackets indicates No. of required persons.

ARMCO INC. RESEARCH CENTER
DC Plasma Tundish Heater
MDH-Project-No. 10.0119
Status 06/92

- 8 -

Item	Title	Personnel dispatch	Expected period
3.4	**ENGINEERING SERVICES**		
3.4.1	**Assembly supervision**		
	- mechanics and media supplies	M (1)	1 week, 1 person
	- electric	M (1)	1 week, 1 person
3.4.2	**Commissioning supervision**		
	- plasma system	M (1)	1 week, 1 person
3.4.3	**Services**		
	- operator's training	M (1)	2 weeks, 1 person

C = Client,   M = Mannesmann Demag,

* No. in brackets indicates No. of required persons.

2517

ARMCO INC. RESEARCH CENTER
DC Plasma Tundish Heater
MDH-Project-No. 10.0119
Status 06/92   - 9 -

4. BUDGET PRICE OF THE MANNESMANN DEMAG PLASMA SYSTEM

This budgetary quotation comprises the equipment, additional basic and
detail engineering as well as the engineering services for an
installation of the D.C. Plasma System.

The budgetary price according the "Preliminary supply list for the Plasma
System", item 3, is estimated to:

<div align="center">

DM   1,750,000.--

</div>

COMMERCIAL CONDITIONS

Our price is a budgetary price.
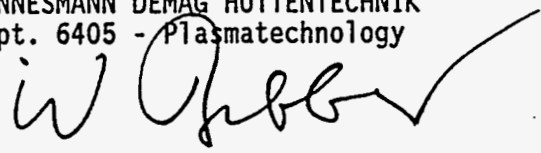
Moreover, our price is based on present-day material and labour costs and
is calculated for delivery of Germany supply free North Sea Port.

Payment terms including a down payment and otherwise in step with actual
expenditures are requested.

The delivery period is about 9 months ex works, reckoned from the final
clarification of all technical and commercial details.

Our detailed conditions will be the basis of our later final quotation.

MANNESMANN DEMAG HÜTTENTECHNIK
Dept. 6405 - Plasmatechnology

2517

OPERATIONAL RESULTS IN HORIZONTAL CASTING WITH PLASMA

by

P. Stadler, BGH Edelstahl GmbH and

H. Bebber, Mannesmann Demag Hüttentechnik, Germany

Plasma 2000, April 26-29, 1992, Charleston, SC, USA

ABSTRACT

Since 1991, a direct-current plasma system has been in operation at BGH Edelstahl GmbH. The purpose of this system is to heat the tundish of a horizontal continuous casting machine. The system has an output of 400 kW and its improved temperature control results in a more efficient mode of operation of the plant, with improved energy utilisation and higher yield.

INTRODUCTION

The production program of BGH Edelstahl GmbH covers the entire range of products, from unalloyed grades to high alloy heat-resisting Ni-based grades. A 27 tonne UHP furnace with eccentric bottom tapping serves as the melting unit, providing an annual output of approx. 90 000 t liquid steel. The tap-to-tap time is approx. 100 minutes. High-alloy grades of low carbon content are produced in an AOD converter with a capacity of 27 tonnes. The metallurgical treatment of low- and medium-alloy steels takes place in a ladle furnace and in a vacuum degassing station. Where required, additional treatment with Ca is carried out by feeding in CaSi wire.

The steel is cast in ingots of 2 to 27 tonnes or by the horizontal continuous casting machine in the dimensions 150 mm rd. to 360 mm rd. A diagram of the units and the process sequence is given in Fig. 1. The cast strand is, wherever possible, subjected to further rolling in hot charging from the casting heat of the continuous caster. For this further treatment, a semi-finished product rolling mill for square dimensions and a planetary high reduction mill for round dimensions are available.

The tundish of the single-strand horizontal continous caster (Fig. 2) has approx. 6.5 t capacity. It is connected rigidly to the 1300 mm-long mould. In the area of the inlet, the mould comprises a short copper mould which is joined to a graphite cooler of length 1100 mm. No extra spray cooling is required due to the good cooling of this mould. An essential component of the mould is the break ring made from boron nitride which, in the inlet to the mould, takes the form of an artificial meniscus to prevent any solidification from reaching the tundish. Use can be made of two stirring coils for improvement of the strand solidification structure. The strand is withdrawn in a discontinuous manner according to the pattern: pull - push-back - pause. This operation is carried out by a withdrawal machine with two clamping shoes which move the strand alternatingly. The system is completed by a torch cutter and a cooling bed. With a height of approx. 3 m and a length of 43 m, the system is very compact.

The single-strand horizontal continuous caster has a casting rate of 15 to 24 t/h, depending on the strand dimensions. The casting times per ladle are accordingly 70 to 100 minutes. In order to ensure that a ladle is fully emptied when casting, temperatures of 110 to 130 K above liquidus in the ladle are required. This is around 50 K above ingot casting. In addition to the increased refractory wear, these high temperatures lead to problems with the ladle furnace because of the considerably longer holding time. Furthermore, consideration must also be given to influences on quality through the high degree of superheat in the tundish at the start of casting.

Therefore, in order to allow better control of the low-level temperature in the tundish, it was decided that the liquid steel should be heated in the tundish. Another alternative considered was to heat the ladle during casting. This, however, was seen to be impractical owing to the substantially higher costs and the space considerations.

Various electrical systems are feasible for heating the liquid steel in the tundish:

> Besides inductive heating,
> heating with graphite rods (ladle heating furnace) or
> heating with plasma torches could be chosen.

In the inductive heating systems familiar up to now, either the whole tundish is constructed as an induction furnace or a partial quantity is heated by means of a smaller, flanged-on vessel and mixed with the remaining content.

At BGH, 12 tundishes are in use and these are operated as cold tundishes. The costs of converting these vessels and purchasing the 4 to 6 induction furnaces necessary for trouble-free operation would not have permitted profitable utilisation. In addition, operation of the flanged-on inductors has also proved troublesome because of the high superheating of partial quantities. This system was therefore rejected.

Heating of the liquid steel with graphite electrodes is current practice for electric-arc furnaces and ladle furnaces. However, as it is also necessary to cast high-alloy grades of very low carbon content, consideration has also had to be given to the danger of carbon pick-up. This danger is greater than it is in ladle heating furnaces because the tundish is not covered with slag.

This risk is avoided by the inert argon atmosphere and the fairly long electric arc of a plasma torch. Preference was accordingly given to this system. It also required very little conversion work as regards adapting the existing plant. Plasma torches can be operated both with direct current under utilisation of a counter electrode and with alternating current using two or three torches.

The noise generated by an alternating current torch is comparable with that of a ladle furnace and it may be uncomfortable for the operating personnel working in the immediate vicinity on the ladle and continuous caster if no sound proofing is applied. Since the tundish geometry also prevented the use of two torches, the decision was made in favour of one direct current torch.

IMPLEMENTATION OF THE HEATING SYSTEM

The primary objective was to lower the ladle temperature to a level comparable with that for ingot casting in order to attain a uniform sequence in the steel plant and above all at the ladle furnace. Furthermore, it was also important to control the temperature of the liquid steel in the tundish since casting problems would occasionally occur as a result of too low a temperature in combination with the long casting times. In such cases, it was difficult to empty the tundish at the end of casting, the result being a poorer yield.

pla2000

STRUCTURE OF THE TUNDISH HEATING SYSTEM

The BGH plasma system for tundish heating consists of a direct-current plasma
torch and the auxiliary units required for positioning and operating the
torch. As shown in Fig. 3, the torch is secured to a torch fixing device.
This device can be moved upwards and downwards with the aid of a torch
carrying device. The torch can thus be positioned in a vertical direction.
The torch carrying device is supported on a rotating bearing to allow the
torch to be swivelled into the maintenance and parking position from its
operating position above the tundish. This ensures that no obstructions occur
during work on the continuous caster and that tundish changes can be carried
out without problems.

All of the media required for operation of the torch, such as electricity,
cooling water and gas, are conveyed to the heating unit in a media connecting
box. All of the hoses and cables are laid inside the supporting arm
underneath the appropriated protective covers in order to comply with the
technical requirements relating to high-temperature operation in a casting
plant and also to guarantee the highest possible degree of safety and freedom
from problems during operation.

A heating chamber has been integrated into the tundish cover.   In this area,
the clearance above the steel bath is around 500 mm. The average diameter of
the cone-shaped heating chamber is about 450 mm. The tundish cover, heating
chamber and torch are sealed against one another in as gas-tight a manner as
possible in order to retain a clean and argon-rich atmosphere in the tundish.

pla2000

The photograph Fig. 4, shows an overall view of the plasma system for tundish heating, with the tundish and the mould in the foreground. This is supplemented in Fig. 5 by an illustration of the plasma torch with the traversing system. The ceramic ring suspended from the torch shell serves as a seal between the torch and the heating chamber. As is clearly visible in both illustrations, the attachment of the torch to the supporting arm is extremely compact and does not involve any exposed cables or hoses.

Fig. 6 provides a detailed view of how this interface between the torch and the fixing device is constructed. As can be seen, the connections for cooling water, torch gas and electricity are provided automatically via the mechanical torch securing system. This not only allows safer operation but also, as is required, more rapid and easier changing of torches.

On Fig. 6 it is also recognisable that the torch possesses only one cooling water circuit. This is designed in such a manner that first the electrode and then the torch shell are cooled in direction of flow. The cooling water is deionised in order to insulate the electrode and the torch shell electrically from one another. The torch shell is shaped in the form of a nozzle pointing downwards. The argon plasma gas issues from the annular gap between this nozzle and the centrally positioned main electrode. The argon serves to stabilise the electric arc and to provide chemical protection for the main electrode. The electric arc itself burns between the main electrode and the steel bath. A further component of the plasma torch is a starting electrode, which for the sake of simplicity is not illustrated on the diagram. This starting electrode enables the arc to be started in a contactless manner. It is integrated into the main electrode unit. Starting takes place by means of a non-transmitted direct-current electric arc which burns between the point of ignition and the main electrode and which is switched off during operation of the main electric arc.

COUNTER ELECTRODE

A particular feature of the BGH plasma system is the design of the counter electrode contact. In the majority of cases, conventional DC systems have a current contact which is integrated into the tundish lining and which must, accordingly, be fitted in every tundish. This might require additional space and, furthermore, makes tundish changing more difficult. In addition, this type of contact design requires pains-taking maintenance. It should also be mentioned that it is virtually impossible to check the reliability of their functioning.

For the first time, therefore, a mould contact has been implemented for the BGH plasma heating system. This contact utilises the very close proximity between the strand and the mould wall. As is shown in Fig. 7, the current flows from the torch via the electric arc and the steel and then via the strand shell into the mould. From the mould, the current is conducted back to the power supply via cables. The mould is anodically polarised.

The table in Fig. 8 indicates the technical specifications of the BGH plasma system by way of a summary.

pla2000

FLOW CONDITIONS AND TEMPERATURE UNIFORMITY

The tundish was originally equipped with a weir and a dam in order to improve
the flow conditions.   This made the separation of non-metallic inclusions a
great deal more efficient. However, when the plasma torch was put into use,
temperature layers began to occur, with the uppermost layer being heated the
most. The deeper layer, on the other hand, were influenced to an inadequate
degree.   Therefore, in order to improve temperature uniformity, the dam and
the weir were combined to provide a continuous, closed wall as shown in
Fig. 9.   Inserted into this intermediate wall is a runner brick which
generates a directed flow underneath the torch and allows improved mixing of
the entire tundish volume.   Measurements have confirmed that the temperature
distribution has been much more uniform since this step was introduced.   The
forced flow has not proved detrimental to the separation behaviour.

TEMPERATURE DEVELOPMENT

The temperature development in a non-heated tundish is characterised by a
steep decline at the beginning of casting and by a weaker fall in temperature
during stationary casting.   The high degree of ladle superheating provides
temperatures of up to 80 K above liquidus which decline rapidly during the
first half hour. - Owing to the long mould and the favourable cooling effect,
the casting does not suffer any detriment through this superheating.   After
the tundish has been balanced, the temperature remains stable until shortly
before end of casting.   The fairly high temperature losses of the ladle
shortly before end of casting lead to a higher temperature drop in the
tundish. During ladle changing, the tundish loses up to 2 K/min. The
following ladle again heats up the tundish contents. The temperatures are
virtually constant even though they are at a high level.

Problems often arise with ladle changing and with emptying the tundish when casting because the temperature declines more rapidly then it does when casting. This has a damaging effect on the strand surface and may cause rejects. The use of the torch allows lower ladle temperatures and accordingly lower temperatures in the tundish at a largely constant level. The heating capacity of the torch is necessary here on the one hand for compensating the heat conduction losses from the tundish, while on the other hand it may be necessary to heat up to the desired temperature level the steel flowing into the tundish.

Whereas the heat conduction losses from the tundish reach a constant value of around 90 kW relatively quickly after start of casting, the power requirement for increasing the temperature of the steel flowing out of the ladle and into the torch area rises at an increasing rate owing to the continuous decline in ladle temperature as soon as the temperature falls below the desired temperature in the pouring area. Fig. 10 shows an example of the measured temperature development in the tundish with and without plasma heating for comparable casting situations. In both cases the casting rate was typically 260 kg/min. According to the diagram it was possible to control the steel temperature very precisely to 1570 °C although the heating power was kept nearly constant.

To improve the power control and thus the temperature development still further, model calculations for this system are in progress. Fig. 11 shows some first results. The model considers the detailed tundish geometry as well as all refractory parameters. The power losses consider the radiation and conductivity contributions, the heating power curve indicates the power necessary to increase the falling ladle temperature to the set-temperature of the tundish. To get the necessary heating power in addition the torch efficiency has to be taken into account.

EFFICIENCY

As illustrated in Fig. 9, the energy of the plasma arc is conducted to the steel through thermal conduction and also through direct and reflected radiation. On the other hand, the system efficiency is reduced by the cooling of the torch P_{cw}, exhaust gas losses and tundish losses P_1 as a result of radiation, thermal conduction and convection.

The initial efficiency measurement results, Fig. 12, show that every possibility for optimisation has not yet been fully exploited. The surface area of the torch shell which is exposed to radiation ought therefore to be reduced further and, in addition, insulated with refractory material. It is also intended that the heat transfer to the bath should be improved by installing an argon stirring facility in the tundish.

It would, in principle, also be possible to reduce the radiation losses of the electric arc yet further by shortening the arc length and accordingly improve the efficiency to a further degree. In practice, however, this would increase the risk of the electrode becoming contaminated by steel splashes and thus cause the service life of the electrode to be diminished.

POWER CONTROL

The BGH plasma system is equipped with an automatic torch position and power control system which ensures that the values preset by the operator for power and arc length are maintained within the range of the specified operational boundary conditions. The plasma system control then automatically ensures that the torch is able to recognise fluctuations in the bath level and to change its position in accordance with these fluctuations. This is particularly important towards the end of the casting process in order to ensure that a liquid crater is maintained in the tundish until it is certain that the end of the strand has fully solidified.

FURTHER IMPROVEMENTS

A series of further improvements are feasible for the system control which is in use at present. Upon closer consideration, however, such improvements will make it necessary to retrofit a metal level indicator as well as a continuous temperature measurement facility. Such systems would pose some prob'ems with a relatively small tundish. The practical utilisation of these is nevertheless being tested.
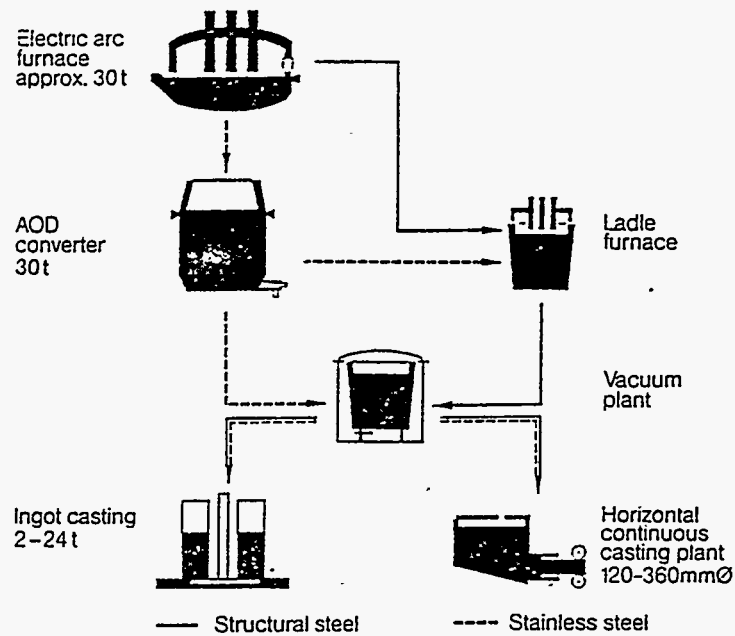
<u>Fig. 1</u>   Process in the steel mill of BGH Edelstahl GmbH
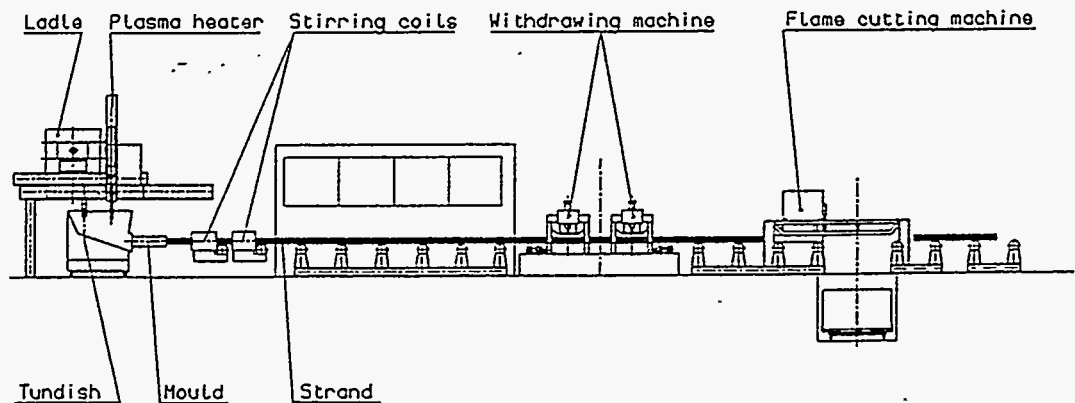
<u>Fig. 2</u>   Single   strand   horizontal   continuous   caster   of
BGH Edelstahl GmbH
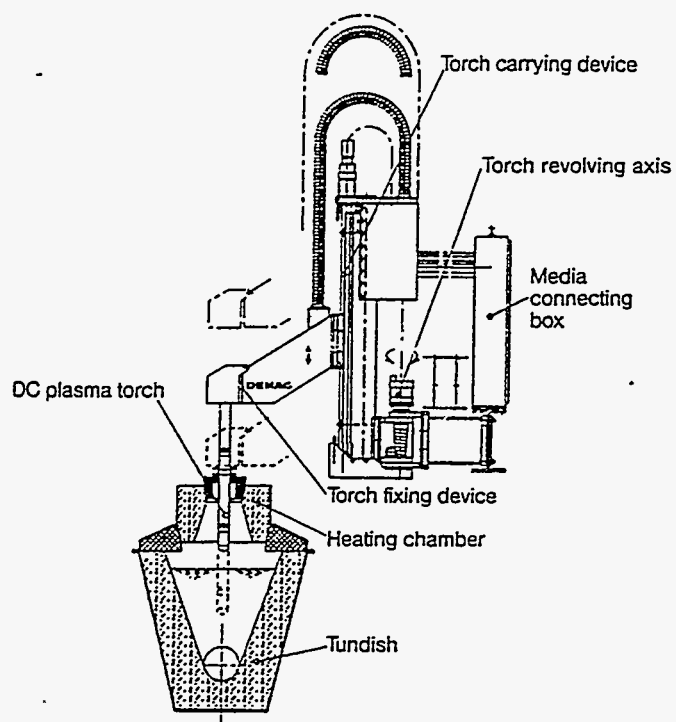
__Fig. 3__   Layout of the DC plasma heating system at BGH Edelstahl GmbH
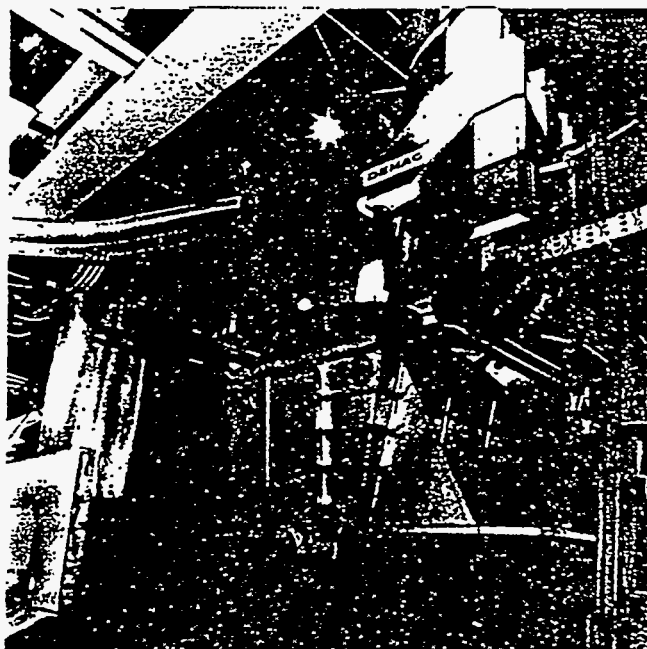
__Fig. 4__   DC plasma heating system at the horizontal continuous caster of BGH Edelstahl GmbH

Fig. 5   DC plasma torch and torch lifting and tilting device
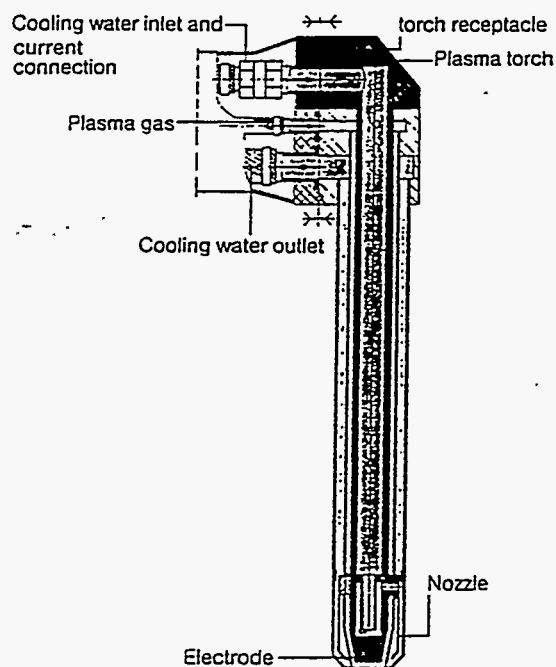
Fig. 6   Sectional view of a plasma torch

pla2000
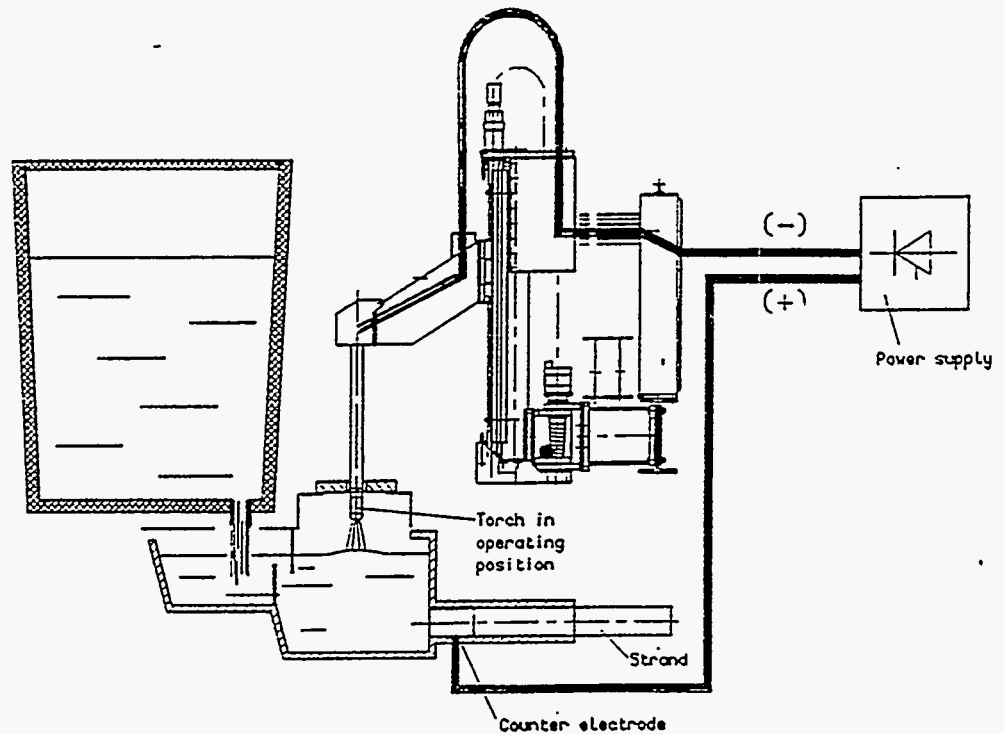
Fig. 7   Main current flow sheet of the BGH plasma system

Heating capacity	max. 400 kW
Current-carrying capacity	max. 3000 ADC
Torch length	1400 mm
Torch diameter	90 mm
Plasma gas	Argon
Gas consumption	150 Nl/min
Electrode	Tungsten
Operation mode	Transferred arc
Ignition	Non-transferred pilot arc

Fig. 8   Technical data of the BGH plasma system
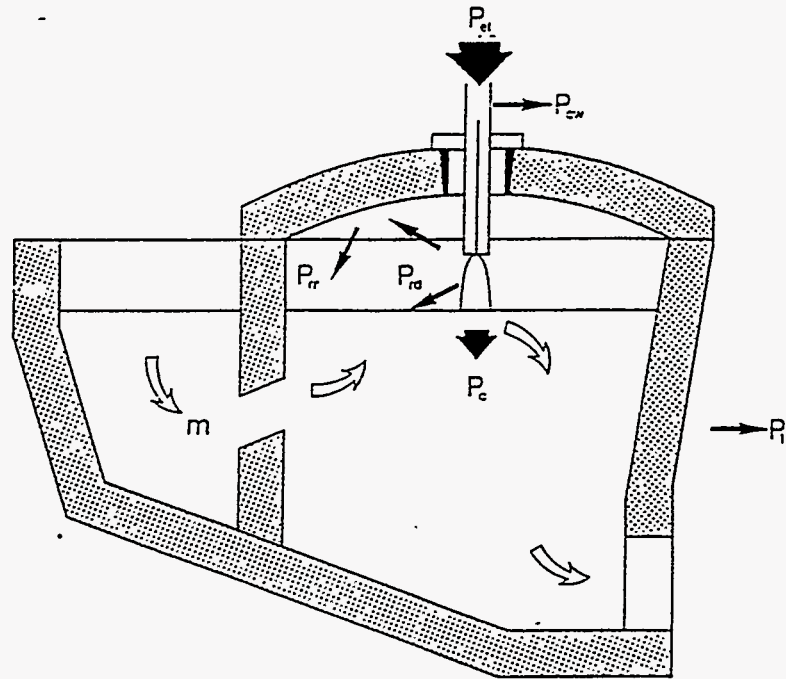
Fig. 9   Tundish design showing the flow pattern and the power
          distribution
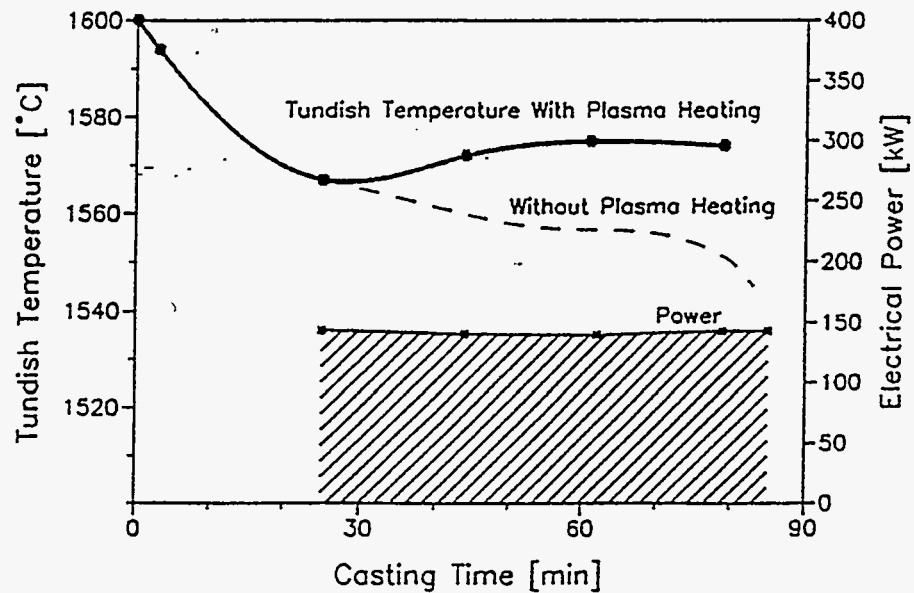
Fig. 10   Measurement results of the temperature development with and
          without plasma heating
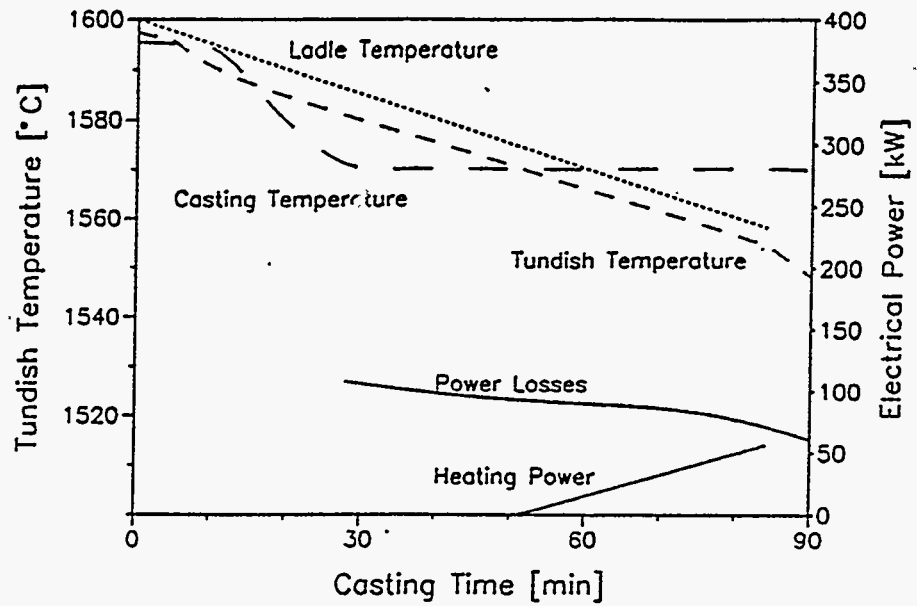
Fig. 11   Model calculation results of BGH plasma tundish heating
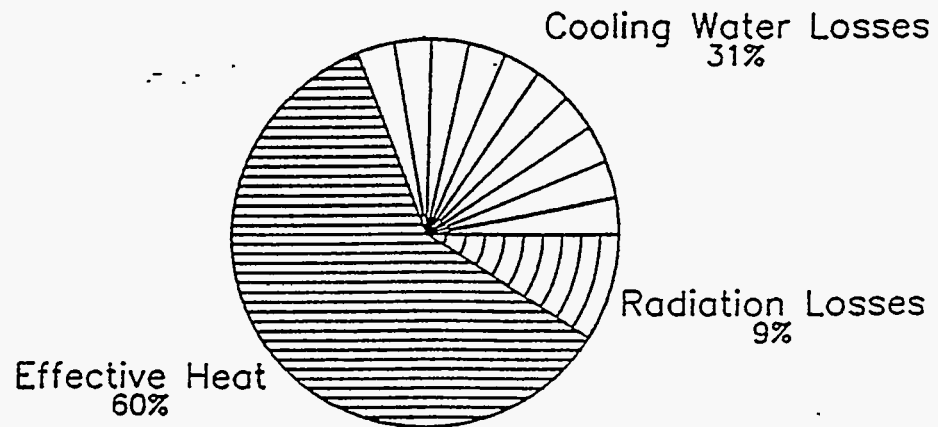
Fig. 12   Heat efficiency of the BGH plasma system

APPENDIX IV

PILLAR INDUSTRIES PRICE QUOTE
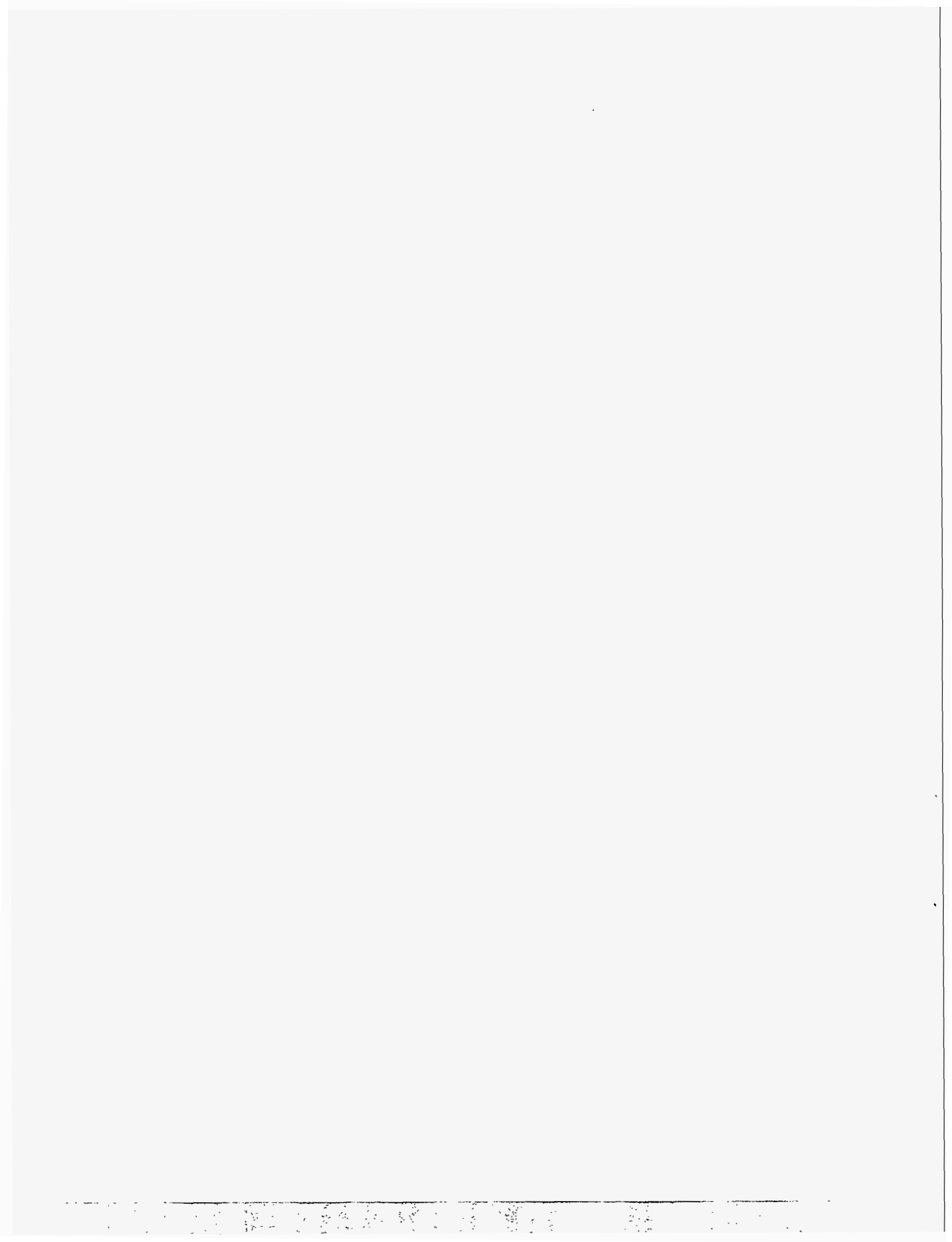
May 26, 1992

Armco Inc.
Research Center
705 Curtis Street
Middletown, OH 45043

Attention: Mr. James R. Sauer

Subject: VLH Autoheat System

Dear Mr. Sauer:

In accordance with your request, we are pleased to submit
this budgetary quotation for your consideration.

The Pillar equipment proposed utilizes an inverted
coreless induction furnace and crucible assembly in
conjunction with a vacuum system to lift and heat metal
within a refractory tube.   The tube is constructed of
the same type of refractory materials as metal transfer
shroud tubes.   The use of an air gap between the lift
tube and the water cooled coil provides an extremely safe
system.

Attached is a sketch of the tube and coil assembly
mounted to the top of your tundish.

The following is a budgetary price for the scaled down
version of the VLH Autoheat System.

ITEM	QTY	DESCRIPTION
1.	–	**INDUCTION POWER SYSTEM**
1.1	1	50 Kw 3 KHz Power Supply
1.2	1 Set	Water Cooled Power Leads
2.	–	**25 Lb. VLH LIFT TUBE AND COIL ASSEMBLY**
2.1	1	VLH Autopour Induction Coil Assembly
3.	–	**VACUUM SYSTEM**
4.1	1	Packaged Vacuum Pump Assembly
3.2	1	Vacuum Reservoir
3.3	1	Flexable Vacuum Hose Assembly
4.	–	**VLH AUTOPOUR SYSTEM CONTROLS**
4.1	1	Vacuum Control Panel
4.2	1	VLH Electrical Control Panel
4.3	1	Remote Operators' Panel
5.	–	**COOLING SYSTEM**
5.1	1	Internal Pumping Station
5.2	1	Closed Circuit Dry Type Cooler
6.	2 Sets	**OPERATING AND INSTRUCTION MANUALS**

BUDGETARY PRICE FOR ABOVE ITEMS................$ 78,000

Pillar Industries thanks you for the opportunity to submit this proposal for your consideration and for your interest in our products.

If there are any items in this proposal that are not clear or if you have any questions, please feel free to contact us.

Sincerely,

PILLAR INDUSTRIES LTD. PARTNERSHIP,

Jack Thielke
Senior Product Manager
Induction Melting Systems

Enclosures

PILLAR VLH AUTOHEAT
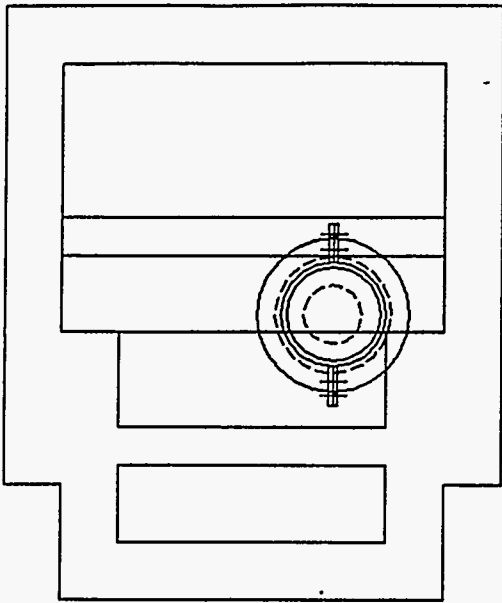
ARMCO INC.

VACUUM LIFT AND HEAT APPROX.

25 LBS. OF STEEL PER LIFT/HEAT CYCLE

2 CYCLES PER MINUTE

120 CYCLES PER HOUR

KW INPUT = 50 KW AT 3 KHZ

VESSEL MAXIMUM HEAT LOSS = 25 KW

= 85,000 BTU
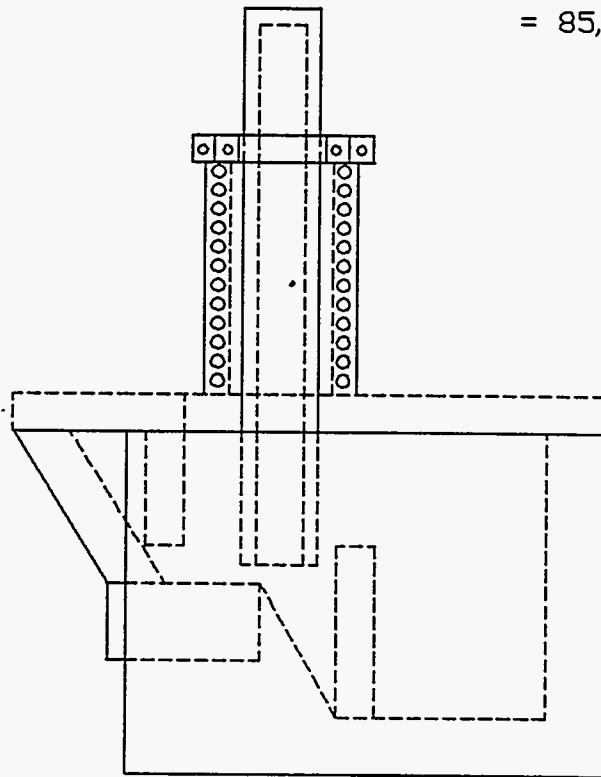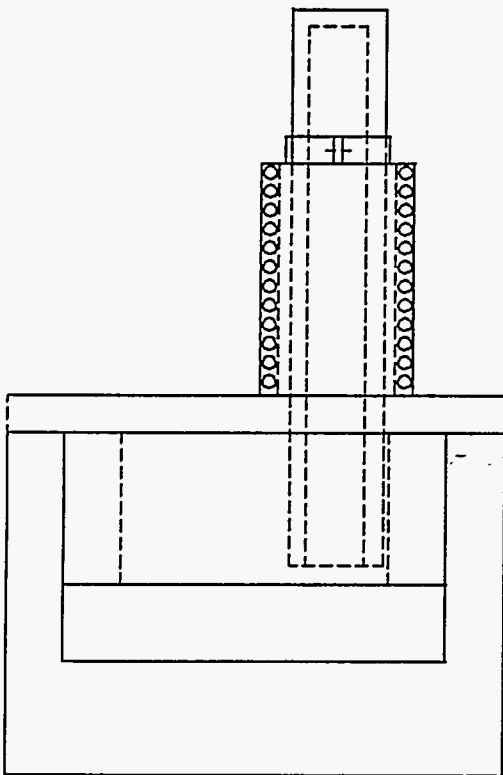
APPENDIX V

ABB ASEA BROWN BOVERI PRICE QUOTE

ABB
ASEA BROWN BOVERI
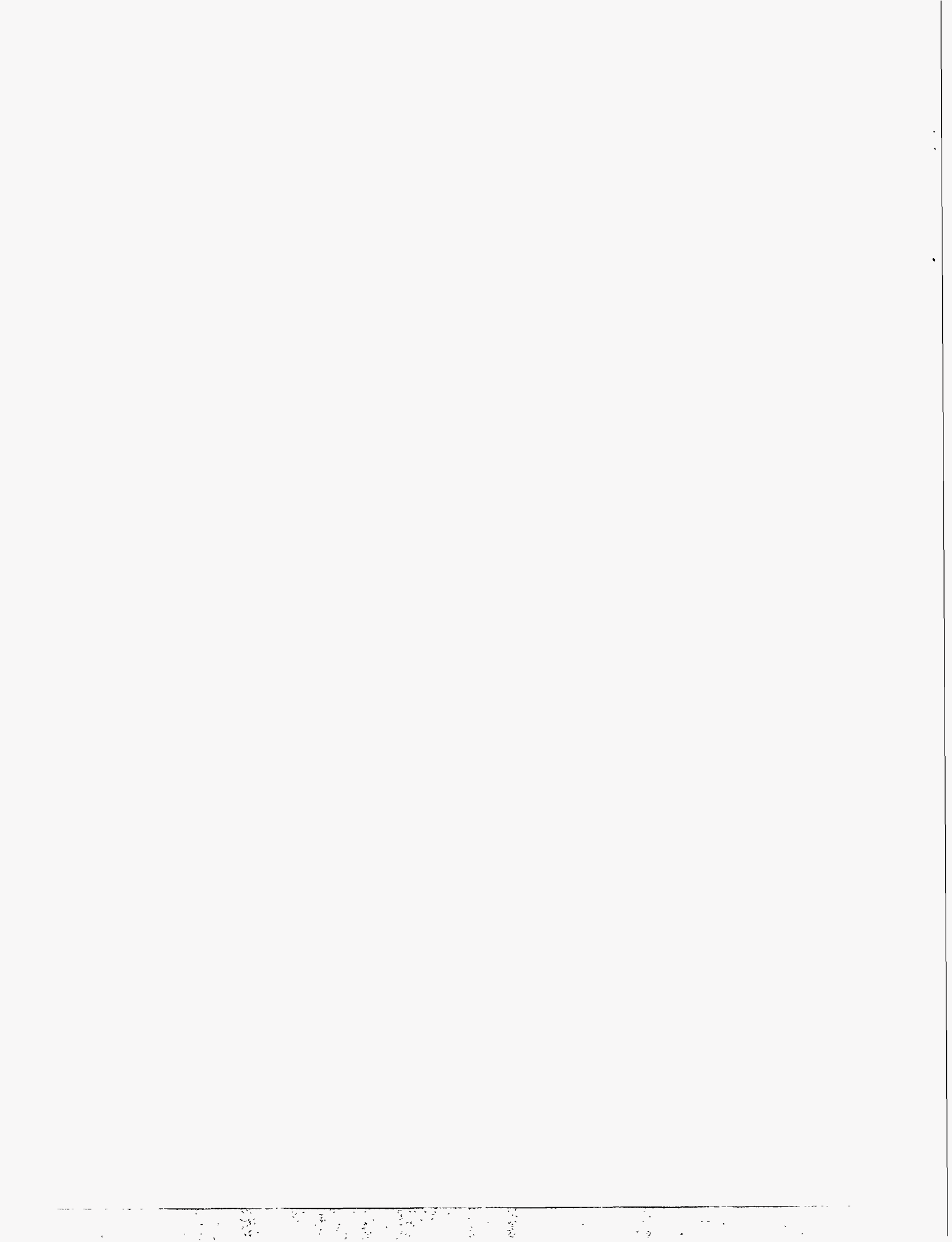
ABB METALLURGY, INC.

DATE: 5/21/92

1460 LIVINGSTON AVENUE

TOTAL # PAGES: 1

NORTH BRUNSWICK, NJ 08902

A/VG

FAX TRANSMISSION COVER SHEET

If you do not receive fax complete, please call (908) 932-6134

TO	FAX #	COMPANY	LOCATION
James Sauer	(513) 425-6459	ARMCO, INC.	

FROM	FAX #	COMPANY	LOCATION
Viren Goyal	(908) 828-7274	ABB Metallurgy, Inc. No. Brunswick, N.J.	

SUBJECT: TUNDISH HEATER

Dear Mr. Sauer:

Please refer to your fax inquiry for a budgetary proposal.

Item 1. - One coreless inductor of 150 lbs. capacity, complete with magnetic yokes, open cage all steel construction and suitable flange for mounting on your pouring device. A matching flange to be installed on the pouring device not included.

Item 2. - One 150 KW - 1000 Hz free standing power supply ABB MICROMTIC with solid state stepless controls designed for ABB coreless inductor.

TOTAL PRICE FOR ITEMS 1 AND 2............$ 95,000.

Water cooling system and bus/cables to connect the coreless inductor to the power supply are not included in the budgetary prices. These items can be quoted after the layout details are known. The proposed coreless inductor would have to be side mounted and requires minor tundish modifications.

We hope this will serve your immediate needs. If we can be of any further assistance at this time, please let us know.

Best regards: Viren Goyal

APPENDIX VI

INDUCTOTHERM CORP. PRICE QUOTE

INDUCTOTHERM CORP.

A SUBSIDIARY OF INDUCTOTHERM INDUSTRIES. INC

10 INDEL AVENUE RANCOCAS, NEW JERSEY, USA 08073-0157 (609) 267-9000 FAX (609) 267-3537 TELEX 685-1048
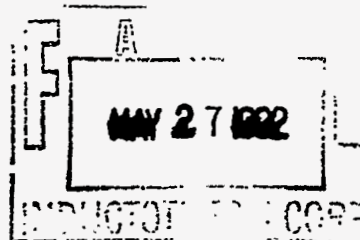
May 27, 1992

FAX and MAIL: 513-425-6459 or 2587

Mr. James R. Sauer
Armco Inc.
Research Center
705 Curtis Street
Middletown, OH 45043

Jim,

My apologies for the delay in getting back to you on methods using coreless induction power to heat molten steel in your tundish. I have reviewed this with our application group and we can report/comment on the following methods proposed of heating your existing tundish configuration. We discussed the following possibilities for your application:

A. Heating your present tundish with new stainless steel skin and proper separation joints utilizing a low frequency power supply.

B. Using the same tundish and installing a 100 to 200 pound coreless furnace on the bottom side of the tundish in the pour area.

C. Using the same tundish, we looked at top coil heating-- basically, this coil would need to be located directly/near top molten steel.

D. This last option we feel has the most favorable application for Armco. This option would consist of a special coil which can operate from the existing 250 KW Mark IV. This coil configuration would be such that it would replace the existing tundish (see enclosed sketch). The price on this special coil is $9,860. The price includes coil and base plate--power leads and any re-tuning requirements of Mark IV will be priced separately. Delivery on this coil will be approximately eight weeks from order date. This system permits itself to be scaled up to large volume tundish and you can accomplish both preheat and superheat.

Jim, the above outline covers our thoughts for your project requirements--my recommendation would be to go with Item D as it fills your requirements and maintains your R&D investment minimal and you can utilize the existing Mark IV power supply. We would size the coil for maximum power and we estimate approximately 150-200°F superheat at thru-put rate of 12,000 pounds/hour.

INDUCTION MELTING & HEATING EQUIPMENT

I will follow up with you to review your thoughts on the above mentioned areas. In the meantime, should you have any questions, please do not hesitate to call us.

Best regards,

Joseph T. Belsh
District Manager

JTB/dmd

Enc.   Above Mentioned Sketch

October 1, 1993

To: Mr. R. S. Williams
        Senior Staff Engineer
        Casting
        Research & Technology

From: J. R. Sauer

Subject: Selection of Pouring Box Heating Technology - Final Report

INTRODUCTION

In February, 1993 a preliminary report was issued on pouring box heating. Since that time, a pouring box has been designed and constructed by Inductotherm and tested at the Armco strip casting facility. This final report deals with the results of using induction pouring box heating and the extrapolation of the data to larger heat sizes.

Pursuant to the DOE contract Section 3, Task 3.1 (pouring box heating), the following report is submitted. Below is listed the information on using induction heating for the pouring box. The reader is referred to the initial report[1] for information on the selection of this technology.

EXECUTIVE SUMMARY

Induction heating was chosen as the most promising technology for the purpose of preheating the pouring box and supplying temperature to the melt during the cast. In particular, Inductotherm was chosen as the company best suited to provide the needed

---

[1] Sauer, J. R., letter to Mr. R. S. Williams, "Selection of Pouring Box Heating Technology", dated June 24, 1992.

equipment. The reasons for these selections are described in the preliminary report[1]. Due to the nature of the design of the pouring box heater (the heater replaces the existing pouring box) it was estimated that the expense of running an off-line test of the design was far inferior to actually incorporating the technology into the current caster. While the expenses were very similar (off-line testing versus on-line testing) the time required to incorporate the heater into the caster has lead to several delays in the schedule, which were necessary to assure that the delivered product would fit into the current caster design. The decision to incorporate the box into the existing caster has been very valuable in terms of assessing the feasibility of this type of induction heating process.

Trials of the induction heated box were promising, but, with the current caster and box design, stray induction fields over heated surrounding structures before the steel in the box could be melted. Due to project termination, sufficient time to resolve these problems did not exist. However, based on limited data, it is projected that a 4640 KW unit would be required for a production size facility.

RESULTS AND DISCUSSION

Analysis Of Available Technologies

The analysis of the available technologies for heating and maintaining heat in the pouring box were covered in the initial report[1].

Results Of Using The Induction Heated Box

The induction heated pouring box (tundish) was designed and installed by Inductotherm. Initial attempts to tune the box (match the capacitance of the power supply to the resistance of the coils in the box) resulted in substantial heating of the exterior framework of the box (see Figure I). An engineer from Inductotherm visited the site to examine the stray heating and recommended the box be modified before further work on tuning was completed. Observations made during the initial attempts included the following:

1)	No single run was sustainable for longer than 10 minutes before some part of the pouring box enclosure or support structure became red hot.

2)	During the longest run (10 minutes) the temperature of the steel charge in the pouring box reached 760 degrees Celsius (1400 F).

3)   The hottest spot was originally directly beneath the center of the box, on the
        pouring box support ("T bar").

4)   The addition of an isolated aluminum sheet under the pouring box took care of the
        hot spot under the center of the box.

5)   Additional hot spots then occurred at eight distinct locations. The hottest spots
        were the center of the south lower cross member (>315 C), the center of the north
        lower cross member (>250 C), the center of the rear lower cross member, to either
        side of the break, (>149 C), the bottom center of the front plate (121 C), and the
        four corners (>93 C).

6)   The thermal gradients in the pouring box enclosure caused the arms (created by
        the break in the lower rear cross member) of the lower rear cross member to bow
        downward 0.635 to 0.952 centimeters (1/4 to 3/8 inch). This in turn raised the
        back of the box and lowered the front of the box (see Figure 2).

The box was slightly redesigned, tested at Inductotherm at rated power (175 KW) with no
load, and shipped back to Armco for a second attempt at tuning. The modifications to the
box are listed below and shown in Figure 3:

1)   Straitening of the frame;

2)   Addition of copper plates to the lower side and lower rear cross members;

3)   Replacement of the transite top;

4)   Addition of mica washers for isolation of the frame; and

5)   Movement of the "break" in the back of the box from the center of the lower rear
        cross member to the two sides (corners) of the lower rear cross member.

Testing of the box at Inductotherm involved running the coil at full power (175 KW) for
an extended period of time. During the run, the temperature of the steel enclosure was
monitored. The test was continued until the temperatures of the steel enclosure began to
level off. Temperatures of the steel enclosure were roughly 111 degrees Celsius (230 F)
when they began to level off[2]. There were no signs of metal discoloration or of phenolic
insulation material deterioration. A large aluminum plate was used under the box during
testing at Inductotherm. This plate was supposed to ship with the box, but, was forgotten.

To tune the box to the power supply at Armco the second time, the box was left empty. The power was turned up to 100% for very brief periods of time. The capacitors were switched in and out until the correct combination was found. During this time, it was noticed that a portion of the support structure ("T bar") under the caster was getting warm.

After initial tuning, the box to the was allowed to cool overnight and charged with 83.043 kilograms (183.04 pounds) of carbon steel. The charge was in the form of six , approximately 8.25 X 8.25 X 24.13 cm (3-1/4" X 3-1/4" X 9-1/2") ingots with some loose 6.35 X 67.35 X 0.63 cm (2-1/2" X 2-1/2" X 1/4") pieces making up the remainder of the charge. The plan for the final tuning involved a typical 6 hour heat up and cast. Table I shows the sequence of events. After almost two hours, it became obvious that the "T bar" and the front of the box were getting too hot to continue with the trial. An aluminum plate was installed, as had been done previously, under the box between the "'T' bar" and the pouring box. At this time neither the Inductotherm technician nor any of the Armco personnel were aware of the missing aluminum plate used by Inductotherm at their facility. The furnace was again turned on and the temperatures monitored. The front of the box continued to get too hot for the phenolic material, which was used to electrically isolate portions of the box.

Inductotherm was contacted regarding the outcome of the trial. At their direction, the box was heated again with disregard to the burning phenolic in the front of the box. Inductotherm was unaware that the aluminum plate being used was not the one used by them and supposedly shipped with the box. This trial lasted approximately 20 minutes at a power setting of 145 KW (83% full power). During this time, the charge reached a temperature of 1432 degrees Celsius (2609 F). At the same time, the corners of the box heated to 204 Celsius and several locations on the box and around the box became red hot (>425 degrees Celsius). The phenolic material around the bolts, used to isolate portions of the box, then began to fail. At this time the power was switched off for the final time.

In checking around the box, some of the main support structures for the caster 68 centimeters (27 inches) from the coil were being heated. Most of these objects were only being heated slightly. Others, that were closer, were heated beyond the point were they could be touched.

Inductotherm was again contacted regarding the stray heat. Their only solution to the problem at this time was to install water cooling jackets in the areas where the heating was significant (i.e., the front lower portion of the box, along the bottom cross members of both sides, and along the lower cross member at the back of the box). Also, it is suggested that redesign of the "T bar" and of the SEN support bracket may be necessary.

As a final option, breakpoints may be required in the I beam support structure and the railing near the box.

The addition of cooling jackets will not diminish the stray fields, only the temperatures which they cause. The losses due to these stray fields is obviously significant as it required 20 minutes at 145 KW to raise the temperature of the 83.043 kilograms (183.04 pounds) of steel from 815 C to 1427 C. This calculates out to less than 13.5% of the total energy input going into heating the steel inside the pouring box (see Appendix I). Typical efficiencies for an induction furnace would be 95%. Losses in the case of the pouring box are due to water circulating to keep the coil cool, losses to air and surrounding surfaces by conduction and radiation, and losses due to stray fields. The data from the trial was insufficient to quantitatively separate the losses.

Based solely on bench top testing at Inductotherm, this process should be feasible, however, testing on site indicates that stray fields need to be addressed. If stray fields can be controlled, induction heating using a coil design as used for these trials could be beneficial to the overall process. However, as the system (caster structure and box) exists now, there are some concerns as will be discussed below.

An average temperature loss for a 454 kg (1000 pound) heat would be 100 degrees Celsius (180 F) over a 4.4 minute cast. Based upon a metal flow rate of 61.9 kg/minute (136 lbs./min.), the temperature of the last metal leaving the ladle and entering the pouring box being 1529 degrees Celsius (2770 F), and an aim pouring box metal temperature of 1621 degrees Celsius (2950 F), 47.3 KW would be required to maintain the temperature of the steel in the pouring box. This calculation assumes no temperature losses in the box (it only accounts for the energy needed to heat the steel). At an efficiency of only 13.5% (includes temperature losses of the box) the power supply would have to be capable of 350 KW at full power or 2.0 times the power capability of the current unit (i.e., with all losses considered, to supply 47.3 KW to the steel in the pouring box would require 350 KW of total power to the box). The stray fields at this power level (350 KW) would significantly increase the temperature of the pouring box enclosure and surrounding structures beyond acceptable limits. In addition, the costs for such an excessively large unit would make other methods much more plausible.

The attempted melting of the original heal in the pouring box was to demonstrate that the unit had the capability of supplying sufficient heat to the process to both maintain temperature during a cast and also to provide for holding steel in the pouring box during ladle changes (required for long casting sequences). The results from the trial indicate that with sufficient cooling of the pouring box enclosure and support structures that the current system is capable of melting a heal in the box over a six hour period and that it

should also be capable of maintaining a molten heal in the box for extended periods of time, provided that adequate cooling of the steel enclosure is available.

Had the pouring box isolation system not failed, to further demonstrate the capability of the unit, the furnace <u>was</u> to be tapped 28 degrees Celsius colder than cast 899, to which it <u>was</u> to be compared. The purpose being that while melting the heal proved the unit had the heating capacity, it did not prove that the heat could be supplied within the required time constraints of the process, once casting began. By tapping the furnace colder, the theory of providing sufficient heat quickly could be proven, if the unit responded quickly in order to recover and eventually catch up to the temperatures recorded during cast 899.

Due to the stray fields overheating certain portions of the box enclosure, which eventually caused failures in the box isolation system, no data were obtained on the capability of the system during casting. Calculations described previously do indicate that the system is not capable of performing adequately without either a significant increase in the power supply capability and the addition of water cooling jackets, or the redesign of the pouring box enclosure, support stand and surrounding ironworks to reduce the tendencies for stray fields.

Current Status Of Pouring Box Heating Project

After the attempted cast (heat 905), the 175 KW power supply was returned to Inductotherm (the unit was under a lease to buy arrangement and due to the program being terminated it was decided not to pursue purchasing the unit). The test did show the potential problems associated with using this technology to maintain heat in a pouring box during long cast sequences (i.e., special attention must be paid to the construction of surrounding areas). However, it is felt that this process or some other method of adding heat to the pouring box during casting is a necessity in order to maintain control over the process. Provided that the shortcomings discussed above can be overcome, this method of pouring box heating does have a substantial economical advantage over the other processes investigated.

<u>EXTRAPOLATION TO LARGER HEAT SIZES</u>

The 1361 kilogram (3000 Pound) Heat

Based on the information gathered from the 454 kilogram heat, an extrapolation was made for a 1361 kilogram heat. Indications are that the heat losses from the larger heat would be less (on a weight per weight basis), since the surface area of material exposed to colder heat conducting surfaces is smaller for larger (by weight) bodies of material (contained in

similarly shaped vessels). Heat losses during the 454 kg test above were calculated to be 100 degrees Celsius over 4.4 minutes (heat 899). Based upon ladle interior surface area, heat losses for the 1361 kilogram ladle would be 2.18 times the heat losses for the smaller 454 kilogram heat (see Appendix II). Based on the information presented above on the 454 kilogram heat, the 1361 kilogram heat would require 103 KW. This would only be valid for a pouring box and wheel equivalent to the current non induction pouring box system, only accounts for the energy to heat the steel (not losses due to stray fields or conduction/radiation to other surfaces), and 100% efficiency in heating the charge. Based upon information from Inductotherm, one would expect an efficiency of 95 to 97% from an induction furnace coil[2]. If it is assumed that the induction pouring box can be constructed such that it is only slightly less efficient (say 75%), then the power requirements for the 1361 kilogram heat would be:

103 KW / 0.75 = 137 KW

Production Size Facility Heat

The information presented below is estimated based upon the following assumptions:

1) The production of carbon steel;

2) The use of a 204,300 kilogram ladle;

3) The use of a 36,320 kilogram tundish feeding four pouring boxes;

4) The use of pouring boxes capable of holding a 3280 kilogram heal and 6563 kilograms of metal at full run height;

5) Production of 2.032 meter (80 inch) wide strip 3.062 millimeters (0.125 inches) thick;

6) Operating at a rate of 272,400 kilograms per hour (300 tons per hour) total production or 68,100 kilograms per hour (75 tons per hour) per pouring box;

7) Initial metal temperature of 1621 degrees Celsius (2950 F) and final metal temperature of 1521 degrees Celsius (2770 F), and

8) 75 % efficient in the heating of the charge.

---

[2] Inductotherm Safety Video.
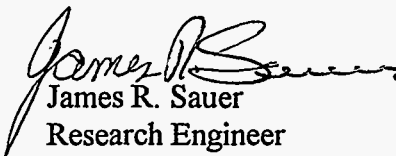
The following calculations are different than those used to determine the power requirements for a 1361 kg (3000 lb.) heat. This is necessary due to the different configurations and metal flow rates. The scale factor being applied is quite large and, therefore, there may be significant error in the calculation. Also, consideration should be given to the fact that the data on which the calculations are based are minimal and may not reflect true operating conditions (i.e., the addition of a tundish between the ladle and pouring box adds to the temperature losses of the steel). Further consideration should also be given to the feasibility of designing a workable coil, since the upper coils will be required to span a distance of 203.2 centimeters (80 inches). The weir will be required to play a crucial role in the support of the coil in this area.

Two conditions are calculated to determine the required induction power unit size. The first calculation determines the power requirement to melt the heal in the tundish during tundish heat up (6 hours required). The second calculation determines how much power is required to assure that the last metal entering the pouring box can be heated to the same temperature as the first metal that left the pouring box. The greater of these two values determines the required size of the power unit.

Both of these calculations appear in Appendix III. From the calculations it is obvious that the heating of the steel coming into the pouring box during casting is a much more rigorous task than the preheating of the box. 1160 KW are required to heat the last minute of steel entering the box at the end of a cast versus only 100 KW for preheating the box. Based upon 1160 KW per box, for four boxes, a total power requirement of 4640 KW would be needed. Again, the data are very limited and the size estimated here is only a ball park figure.

FUTURE WORK

No future work is planned as a result of the termination of the project.

James R. Sauer
Research Engineer
Casting
Research & Technology

JRS2/jh

Mr. R. S. Williams
October 1, 1993
Page 9

cc: <u>Research</u>
   J. W. Allen
   R. Birch
   S. L. Campbell
   S. F. Cox
   R. Engel
   D. W. Follstaedt*
   K. C. Schneider
   R. C. Sussman*
   R. S. Williams* - X3

   * - color figures

TABLE I

Sequence Of Events During Second Pouring Box Trial

TIME	FREQ	KW	KWMR	TEMPERATURES REFRACTORY	T BAR
7:15	2050	20	1.64	75	80
7:30	2150	40	2.03	86	136
7:45	2150	50	2.74	219	200
8:00	2250	50	2.97	373	250
8:15	2300	50	2.84	525	330
8:30	2300	50	3.26	644	600
8:45	2300	50	3.29	762	700
9:00	2400	70	3.87	826	700
9:07	0	0	0	863	>750
Aluminum plate added between box and "T bar"					
9:38	2400	70	3.73	751	350
9:48	0	0	0	n/a	270

REFRACTORY = temperature of refractory 1" away from inside of box.
T BAR = temperature of hottest spot on "T bar" support structure
under the box.

JRS2

FIGURE 1
Hot Spots On First Pouring Box Enclosure Design

rear

front

Breaks In Induction
Loops
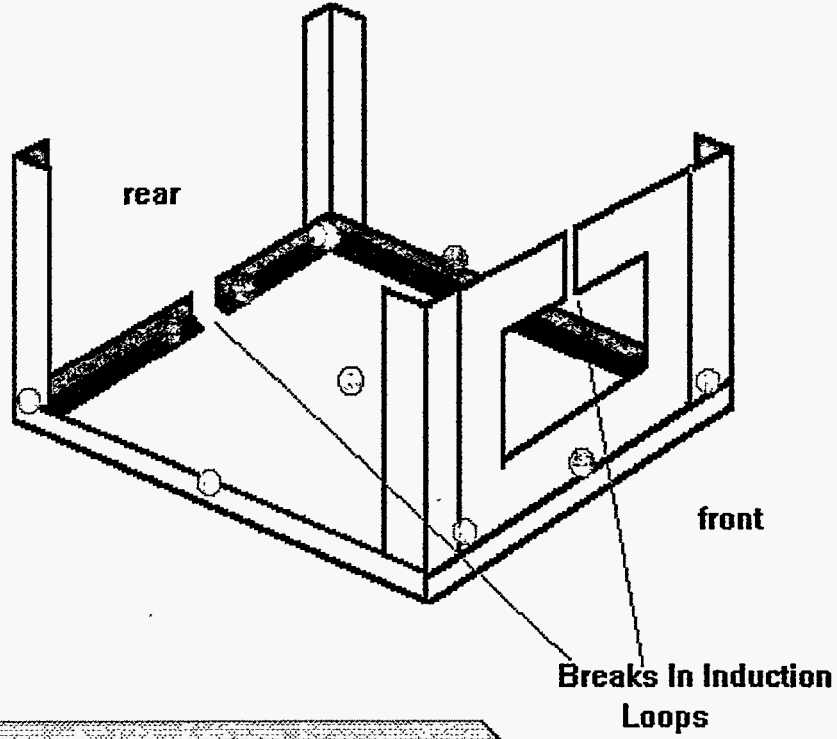
○ - Spots of intense structure heating

○ - Spots of moderate structure heating

FIGURE 2

Rear View Showing Nature of 1/4 - 3/8" Deflection

View From Back
of Box

Induction Unit

vertical
frame of
induction box

Original Position

horizontal
crossmembers

Deflected Position
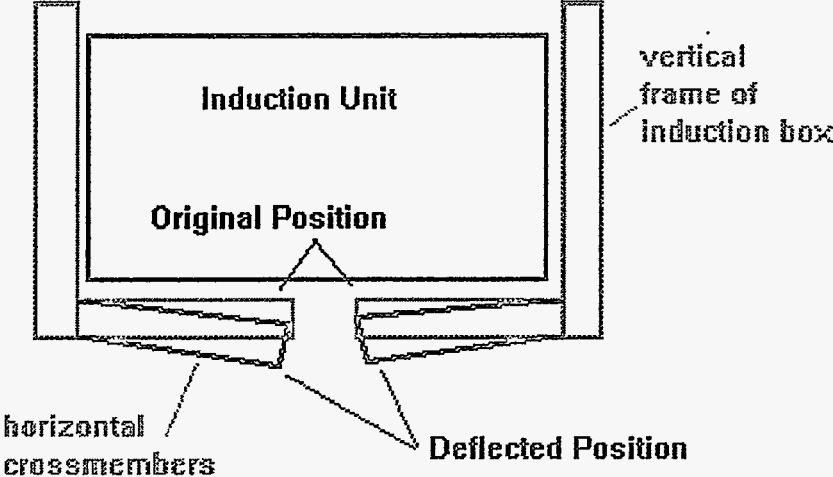
FIGURE 3

Pouring Box Modifications

This original section removed

Old Break

New Break

TOP VIEW

Original Construction

Modifications

Copper plate

Mica Washers

FRONT VIEW

SIDE VIEW
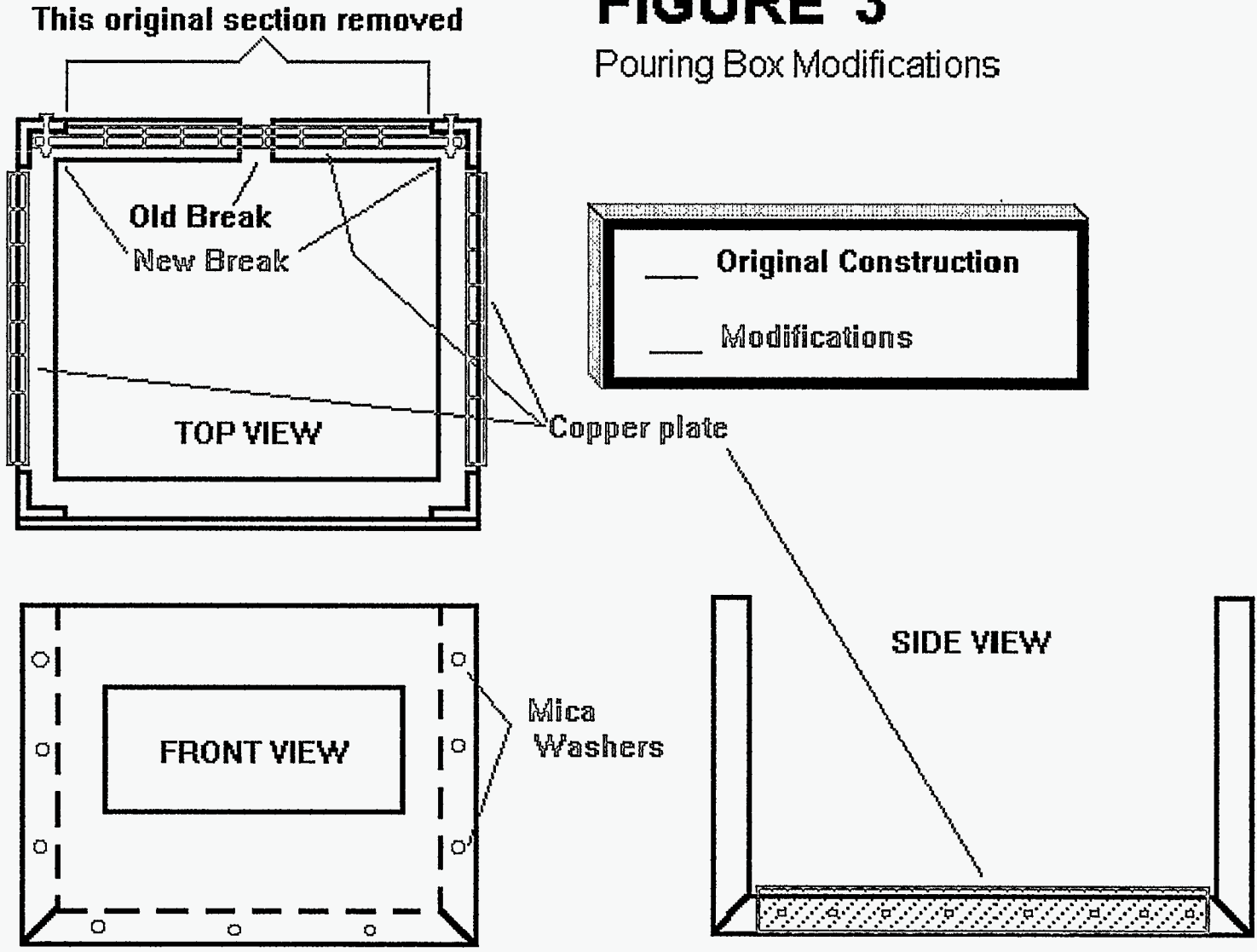
APPENDIX I

Calculation Of Energy Input Efficiency To Steel Charge[*]

Temperature of steel charge just
prior to turning on power(T_1)..................... 1500 F

Temperature of steel charge just
before turning off power(T_2)..................... 2600 F

Elapsed time from power on to power off(ET).... 20 min.

Heat capacity of steel(H_s)..................................... 0.11 BTU/lb.

Weight of steel charge(Wt_s)................................. 183.04 lbs

Power setting on power supply(KW_p)................... 145 KW

KW_s = Kilowatts required to heat steel

$$\text{Efficiency} = \frac{KW_s}{KW_p}$$

KW_s = (((T2 - T1) * Wts * Hs)/ET)/56.92 =
((1100 * 183.04 * 0.11)/20)/56.92 =
19.5 KW

KW_p = 145 KW

Efficiency = 19.5/145 = 0.134

Efficiency = 13.4%

* - Assumes that entire charge is heated uniformly.

APPENDIX II

Heat Loss Calculation For 1362 Kilogram Heat

T_s = Temperature in pour box at start (2950 F).

T_e = Temperature in pour box at end (2770 F).

ET = Elapsed time (1 minute).

Wts = Weight of steel cast (136 lbs.)

Hs = Heat capacity of steel (0.11 BTU/lb.)

B_{1000} = Radius at bottom (inside) of 1000 lb. ladle.

T_{1000} = Radius at top (line of full metal level) of 1000 lb. ladle (inside).

H_{1000} = Height of 1000 lb. ladle from bottom to line of full metal level (inside).

SA_{1000} = Surface area (inside) of 1000 lb. ladle.

B_{3000} = Radius at bottom (inside) of 3000 lb. ladle.

T_{3000} = Radius at top (line of full metal level) of 3000 lb. ladle (inside).

H_{3000} = Height of 3000 lb. ladle from bottom to line of full metal level (inside).

SA_{3000} = Surface area (inside) of 3000 lb. ladle.

R = Ratio of 1000 lb. ladle surface area times 3 to 3000 lb. ladle surface area.

L_{1000} = Heat lost from steel during a 1000 lb. cast.

$L_{1000} = (((T_e - T_s) * Wt_s * H_s)/ET)/56.92$

$L_{1000} = (((2950 - 2770) * 136 * 0.11)/1)/56.92 = 47.3$ KW

$SA_{1000} = (\pi * (B_{1000})^2)/4 + (\pi * (T_{1000})^2)/4 + (H_{1000} * \pi * B_{1000}) + (\pi * T_{1000} - \pi * B_{1000}) * H_{1000}$

$SA_{1000} = (3.14 * (16.5)^2)/4 + (3.14 * (18.375)^2)/4 + (18.375 * 3.14 * 16.5) + (3.14 * 18.375 - 3.14 * 16.5) * 18.375$

$SA_{1000} = 1538.96$

$$SA_{3000} = (\pi*(B_{3000})^2)/4 + (\pi*(T_{3000})^2)/4 + (H_{3000}*\pi*B_{3000}) + (\pi*T_{3000} - \pi*B_{3000})*H_{3000}$$

$$SA_{3000} = (3.14*(24.5)^2)/4 + (3.14*(27.5)^2)/4 + (26.5*3.14*24.5) + (3.14*27.5 - 3.14*24.5)*26.5$$

$$SA_{3000} = 3353.13$$

$$R = 3353.13 / (1538.96 * 3) = 0.726$$

Heat Loss Scale Factor = 3353.13 / 1538.96 = 2.18

JRS2c

APPENDIX III

Determination of Power Supply Requirements for a Production Facility

Bottom radius of a 235 ton ladle[*] = 140.9 cm (55.47 inches)

Top radius of a 235 ton ladle (at slag line)[*] = 168.9 cm (66.51 inches)

Height from bottom of ladle to slag line[*] = 322.58 cm (127.0 inches)

Surface area exposed to heat loss = 466,035 sq. cm (72,231.16 sq. in)

Temperature of last metal entering pouring box = 2770 F

Flow rate in lbs./min. = 2500

$(((2950 - 2770) * 2500 * 0.11)/1 \text{ minute}) / 56.92 = 870 \text{ KW}$

At 75% efficiency = 870 KW / 0.75 = 1160 KW

With four units = 1160 KW * 4 = 4640 KW total power required.

To determine the power required to preheat the box one needs to calculate the energy required to heat the steel from room temperature to molten steel over a six hour period. This method does not totally account for heat losses due to refractories, but, more stringent calculations are mute at this time, as the specific design of the pouring box, and the refractories used will have a large influence.

Size of steel heel to be heated = 3280 kg (7232.4 lbs.)

Initial temperature of steel heel = 24 degrees Celsius (75 F)

Final temperature of steel heel = 1454 degrees Celsius (2650 F)

Heat capacity of steel = 0.11 BTU/min.

KW required = ((2650 F - 75 F) * 7232.4 lbs* 0.11 BTU/F) / 360 minutes / 56.9 (conversion from BTU/min. to KW) = 100 KW

* - Data were taken from drawings of a 235 ton production ladle used at Armco Steel Company, L.P., Middletown Works.

JRS2d/jh
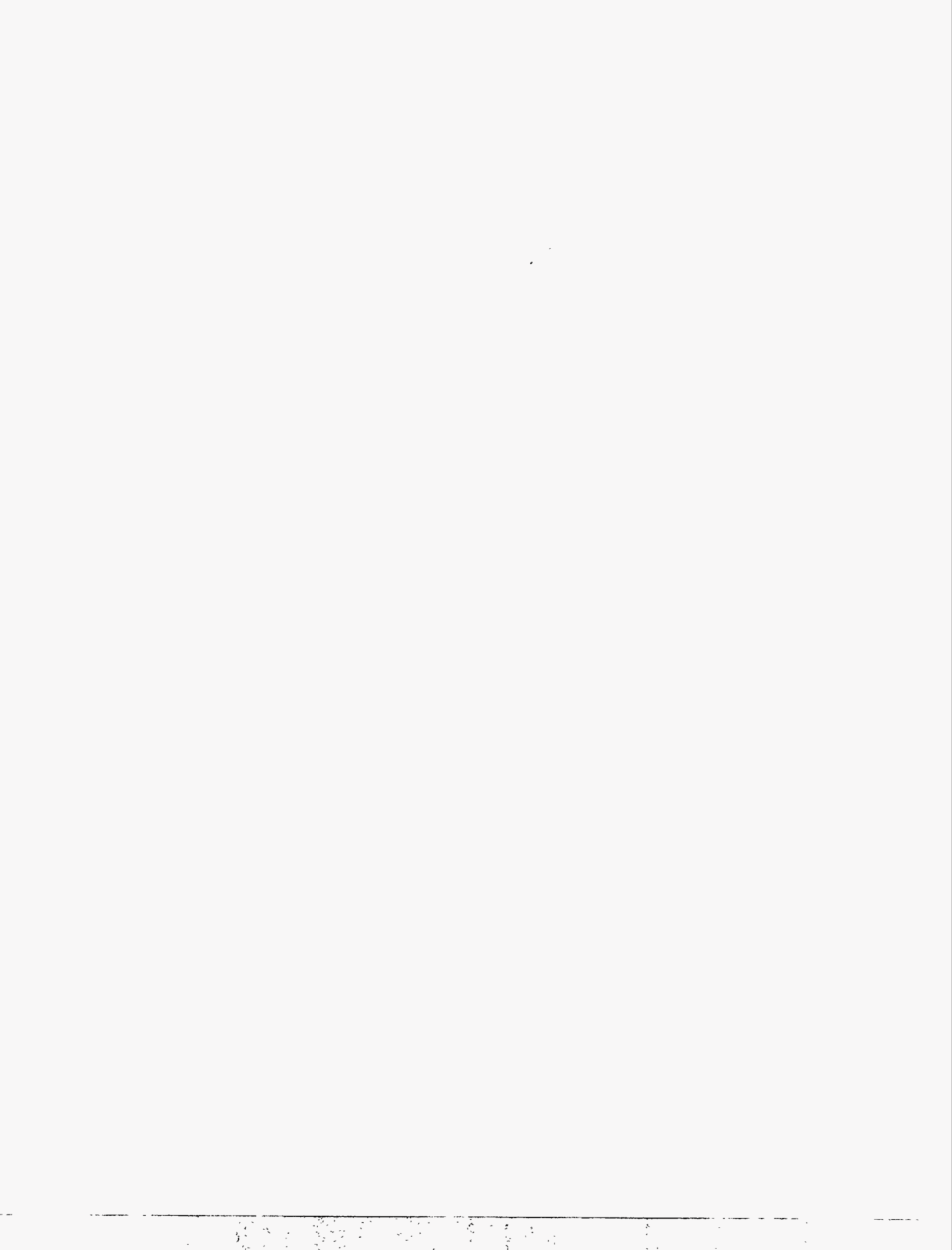
Appendix VI

Electromagnetic Enhancements
for Single Wheel Casting
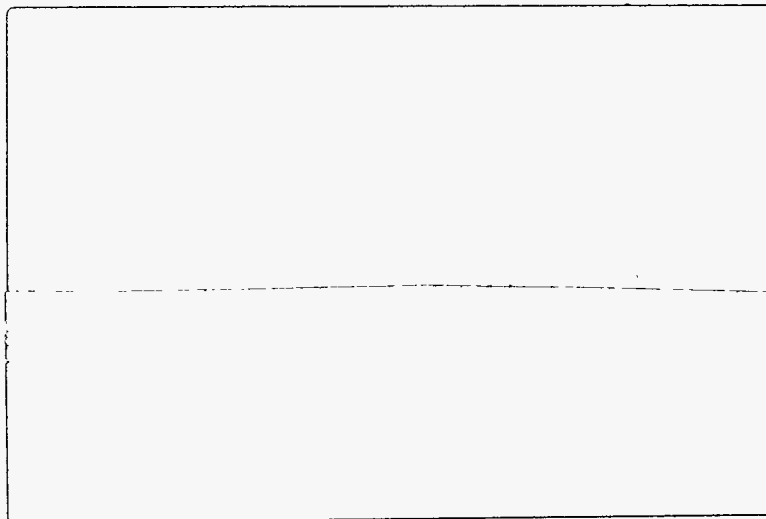
EM Enhancements for Single Wheel Casting

Magnetofluidynamic Feasibility Study

Final Report

ABSTRACT

The Department of Energy sponsored research into near net shape casting of carbon steels using the Single Wheel Casting Process. This effort, led by ARMCO Steel, was aimed at producing high-quality sheet steel of thicknesses up to 0.1 inch and widths of 60-80 inches. If successful, the resulting steel would go directly to cold rolling, eliminating the costly hot rolling step in the current sheet-steel making process. The present stage of development called for demonstrating feasibility in a 12-inch width and represents a 3-year, $6M program. Westinghouse was responsible for developing electromagnetic enhancements for the process which meant developing an electromagnetic seal for the nozzle/casting wheel interface (a 2-year, $650K program). This report describes concept generation and selection, analysis, and a scaled low melting-point liquid-metal experiment. Further development of the electromagnetic seal was not recommended. Shortly after the conclusion of the Westinghouse program, ARMCO elected to discontinue the overall program for strategic rather than technical reasons.

Table of Contents

List of Figures

List of Tables

EM Enhancements for Single Wheel Casting

Magnetofluidynamic Feasibility Study

Final Report

1.0 EXECUTIVE SUMMARY

The Department of Energy sponsored research into near net shape casting of carbon steels using the Single Wheel Casting Process. This effort, led by ARMCO Steel, was aimed at producing high-quality sheet steel of thicknesses up to 0.1 inch and widths of 60-80 inches. If successful, the resulting steel would go directly to cold rolling, eliminating the costly hot rolling step in the current sheet-steel making process. The present stage of development called for demonstrating feasibility in a 12-inch width and represents a 3-year, $6M program. Westinghouse was responsible for developing electromagnetic enhancements for the process which, for this program, meant developing an electromagnetic seal for the nozzle/casting wheel interface (a 2-year, $ 650K program).

The objective for Westinghouse during this phase in the development of single wheel casting was development of an electromagnetic seal for the nozzle/wheel gap. The moving casting wheel forms one side of an open box with the other four sides formed by the stationary nozzle and pour box. There is, by necessity, a physical gap between the wheel and the nozzle through which liquid steel can leak. If this steel leaks in the anti-casting direction and then freezes on the wheel, it is carried back underneath the nozzle and can do damage to the nozzle, perhaps terminating the cast. The amount of leakage is related to the gap size, liquid-metal head, liquid-metal surface tension, and wheel speed. Although care can be taken to minimize the physical gap, it is impossible to completely eliminate it, unless a rubbing seal is employed.

The major result of the feasibility study is a recommendation that the electromagnetic sealing option not be pursued. This conclusion was reached for two reasons. First, the technical risk remains very high. Although some indication of sealing potential were demonstrated, no significant improvement in sealing was present in the scaled experiment over that demonstrated without the electromagnetic shield. The lack of improvement is attributed to fluid dynamic effects which could be ameliorated through improvements in the pour box design and/or coil placement. Such improvements would require further analytical and experimental investigations, and any resulting sealing improvement is problematic. Second, the payoff for an electromagnetic seal has been dramatically reduced due to other developments of the strip casting program. During the course of the casting trials a rubbing seal between the nozzle and wheel was

developed. Further, the ability to control the relative position of the wheel and nozzle made it possible to keep the rubbing seal in contact throughout the cast. Given the high technical risk, the required work to attempt any significant risk reduction, and the reduced payoff, further work is not recommended.

Determining the lack of feasibility of any concept is much more difficult than proving feasibility. There is always the possibility that some other concept, design, or implementation will turn out to work. The structured process used in this program to select the sealing concept is designed to be inclusive, but ultimately is somewhat subjective, particularly in the selection of weights for rating categories. It is intended to produce the design with the lowest overall technical risk among alternatives. The process is not foolproof and the lack of positive sealing result is an indication of the high technical risk of the task, not an indictment of the process.

Shortly after the conclusion of the Westinghouse program, ARMCO elected to discontinue the overall program for strategic rather than technical reasons.

2.0 CONCEPT SELECTION

2.1 Introduction

The objective for Westinghouse during this phase in the development of single wheel casting is development of an electromagnetic seal for the nozzle/wheel gap. The moving casting wheel forms one side of an open box with the other four sides formed by the stationary nozzle and pour box. There is, by necessity, a physical gap between the wheel and the nozzle through which liquid steel can leak. If this steel leaks in the anti-casting direction and then freezes on the wheel, it is carried back underneath the nozzle and can do damage to the nozzle, perhaps terminating the cast. The amount of leakage is related to the gap size, liquid-metal head, liquid-metal surface tension, and wheel speed. Although care can be taken to minimize the physical gap, it is impossible to completely eliminate it, unless a rubbing seal is employed.

It has long been known[1,2] that magnetic fields can be used to support liquid metals, and the goal of this program is to use magnetic fields to seal the gap. The use of the electromagnetic seal will allow casting with a greater nozzle/wheel gap (simplifying mechanical design and reducing operating constraints), greater liquid metal heads (enlarging the casting envelope), or some combination of both. In addition to sealing the nozzle/wheel gap, the electromagnetic seal may have other benefits to the casting process, such as edge heating and melt pool stirring. Processes such as edge heating and melt stirring work to maintain a uniform temperature across the strip. Thus they reduce the likelihood of the strip tearing from internally developed thermal stresses.

Figure 2.1 shows a conceptual view of the single wheel casting process while Figure 2.2 shows a schematic of the nozzle/wheel area in more detail. Typical casting parameters will be a gap of 1 to 100 mils (.025- 2.5 mm), a liquid metal head on the order of 6 in. (152 mm) and a wheel speed of 5 fins (1.5 m/s).

The primary task of the electromagnetic enhancement is defined as providing a non-contacting seal of the gap between the moving casting wheel and the stationary nozzle. It is extremely difficult to control the gap size due to the large temperature change from room-temperature assembly through gas-fired preheating to steel casting conditions. The final gap dimension is set just before steel casting. Uniformity of
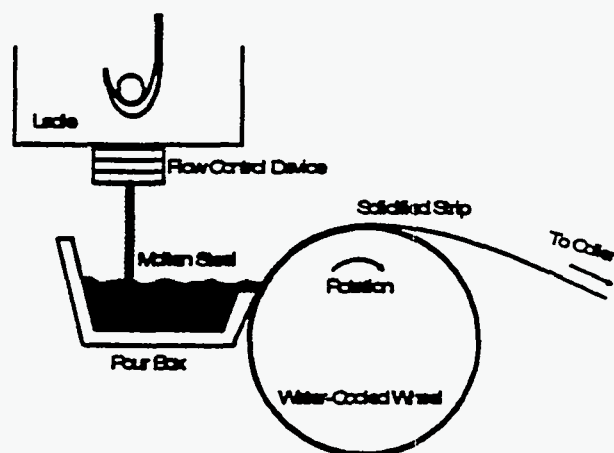
Figure 2.1 Simplified diagram of the single wheel casting process.

the gap across the width of the caster is difficult to maintain, especially as the cast width increases. In addition, the out-of-roundness of the wheel ensures that there is some variation about the nominal gap, although if in-place hot-dressing is used, the variation is small. Without electromagnetic enhancement there is only surface tension to withstand the leak: a gap of 10 mils (.25 mm) supports approximately 6 in (152 mm) of liquid steel.

There is a tendency of the liquid steel to leak against the direction of the wheel movement, i.e., back under the nozzle. The leaking tendency increases as the

Figure 2.2 Close view of the nozzle/wheel area showing the nozzle and pouring box.

ferrostatic head in the pour box is increased, as the gap is increased, or as the wheel speed is decreased. As the steel leaks backward, it begins to freeze on the wheel and is carried back up under the nozzle. If the frozen section is thicker than the nozzle/wheel gap, mechanical damage may result. This damage may ultimately result in premature ending of the cast. If the leak is sufficiently large, liquid steel may run to the lower quarter of the wheel and drip off, perhaps damaging other caster components.

The electromagnetic fields needed to seal the nozzle/wheel gap may have some benefits to other parts of the casting process. There will be heat added to the liquid steel in the melt pool, especially near the edges. As the seals will also be required to be effective on the sides of the nozzle, extra heating of the edges (thought to be beneficial) may be made to occur. Also, some stirring of the melt pool is likely, thereby increasing the uniformity of the superheat.

As shown in Figure 2.2, the wheel/nozzle area has little room for an electromagnetic seal. In addition, steel casting conditions (high temperatures, sparks and smoke, and vibrations) require rugged equipment and mechanically conservative designs. There are other considerations as well. Magnetic fields which are used to support the ferrostatic head may also induce heating in nearby caster components and may conceivably interfere with instrumentation and sensors. These undesirable side effects must be minimized. Both of these factors, steel casting environment and possible side effects, combine to make the design of the electromagnetic seal very challenging and add to the high degree of high risk inherent in the task of electromagnetically sealing the gap.

In summary, the electromagnetic device is to seal the physical gap between the nozzle and the casting wheel. This gap is expected to be less than 10 mils (.25 mm) without enhancement and up to 100 mils (2.5 mm) with the electromagnetic device. The liquid
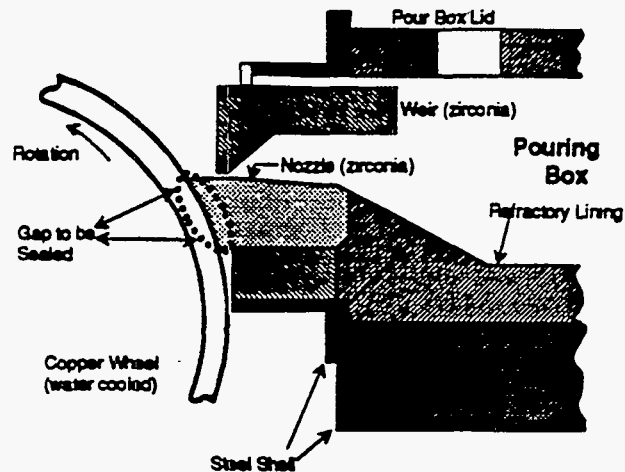
steel head which needs to be supported will be no more 6 in. (152 mm) while the wheel spins at approximately 5 fins (1.5 m/s). The electromagnetic seal must perform effectively while minimizing undesirable side effects such as caster heating and electromagnetic interference. The device will have to stand up to the harsh caster environment without overly complicating the design or manufacture of the balance of the casting equipment.

The remainder of this section presents the process whereby these recommendations were reached. A structured approach to problem solving was employed. The key steps to the process were brainstorming, concept grouping, concept evaluation, and concept selection (using a weighted selection matrix). Additional details are available in Reference [3].

2.2 Selection Process

2.2.1 Overview

As mentioned in the preceding section, a structured approach to problem solving was employed to select the sealing concept for the single wheel caster. In an investigation of this type where a new device is the intended result, a structured approach is recommended. The structured approach will ensure that the search will not be narrowed too soon and that due consideration is given to all factors. The principal steps of the approach were brainstorming, grouping, evaluation, and selection. Each of these steps are summarized below. The brainstorming took place in a single meeting called expressly for that purpose. Grouping was performed by a subset of the brainstorming meeting attendees which was familiar with sealing applications. Evaluation took place along two separate paths, one for electromagnetic phenomena and one for mechanical design caster integration. The results of the evaluations were combined using a weighted selection matrix. The final recommendations were reached after varying the weights in the selection matrix and examining the effects on the rankings.

The result of the concept selection process using the structured problem solving approach is the best concept among the ideas considered. In this context, 'best' implies most likely to meet all the selection criteria: it does not guarantee that all the criteria can be met. Thus the selected concept is the lowest-risk alternative identified, but the sealing task remains a high risk problem. Further, it is always possible that some other group of problem solvers would have identified other approaches that were not considered here.

2.3.2 Brainstorming

The brainstorming of ideas for the electromagnetic seal took place at a single meeting called for this purpose. Their were eight attendees at the meeting: 2 mechanical

designers, both with experience designing for liquid metal applications; two electro-magnetic analysts with general backgrounds; one electromagnetic analyst with liquid metal levitation experience, one induction heating specialist, and two liquid-metal MFD engineers with both theoretical and experimental backgrounds. After a short presentation explaining the single wheel casting task, concepts were solicited from each attendee until the flow of new concepts was exhausted. Care was taken not to critically evaluate any new concepts until all the concepts were put forth. There were seven concepts identified during the brainstorming: each is described below (in no particular order).

- **Current in Wheel Concept**
  - a high frequency current is injected into the casting wheel through some type of sliding brush system.
- **Current Sheet Concept**
  - sheet conductor carrying a uniform high frequency current
- **Single Turn "Pitchfork" Concept**
  - a single concentrated coil built into the face of the refractory nozzle
- **Current Injection in Pour Box Concept**
  - inject the current in the steel of the pour box
- **AC Current Injection in Liquid Steel**
  - currents injected into the liquid steel itself
- **DC Current in Steel and Behind Wheel**
  - current required in the molten steel in addition to and externally applied magnetic field
- **Single Turn "Loop" Concept**
  - a single conductor carrying high frequency current is used to provide the fields which support the liquid steel meniscus

2.2.3 Grouping

The seven concepts identified during the brainstorming process were examined by a subset of the attendees and similarities between different concepts were noted. It was possible to group together some of the different concepts and modify them slightly so that only four truly unique concepts emerged. By combining two of the unique concepts, a fifth concept for evaluation was obtained. The five grouped concepts are described in the following paragraphs.

2.2.3.1 Brush System A brush system can be used to inject currents into the belt in the vicinity of the liquid steel meniscus. It may be possible to use multiple electrodes to direct the steel both along the casting direction at the edges of the strip and across the width of the caster at the bottom of the melt pool. This technique uses the high conductivity of the wheel to carry the high currents required to provide support. The major difficulty of this approach is the tendency of the current to redistribute as it

traverses across the wheel. Segmenting the wheel would alleviate the current redistribution problem, but would greatly increase the mechanical complexity of the casting wheel. This approach is shown in Figure 2.3.

2.2.3.2 Current Sheet in Gap Another concept makes use of a current sheet in the gap between the pour box and the casting wheel, as shown in Figure 2.4. Both this approach and the previous one make use of high frequency currents. High frequency currents flowing in the liquid steel will be concentrated near the edge of the steel and the resulting forces will act as a surface pressure and provide more stable support of the liquid steel meniscus.
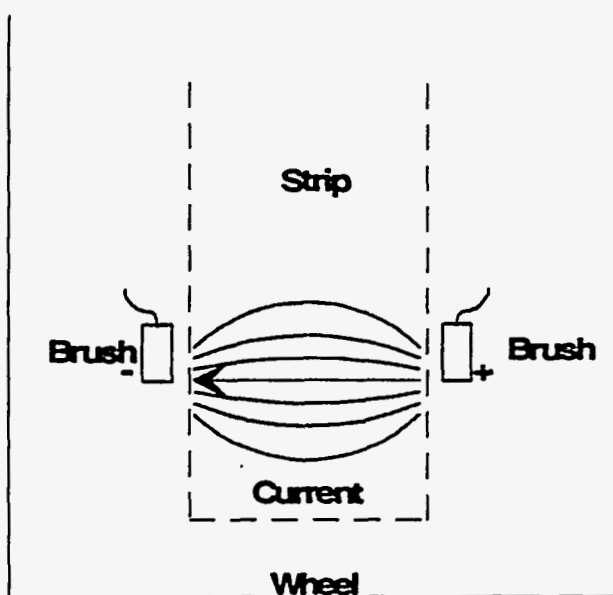
Figure 2.3 *Schematic of the brush system approach.*
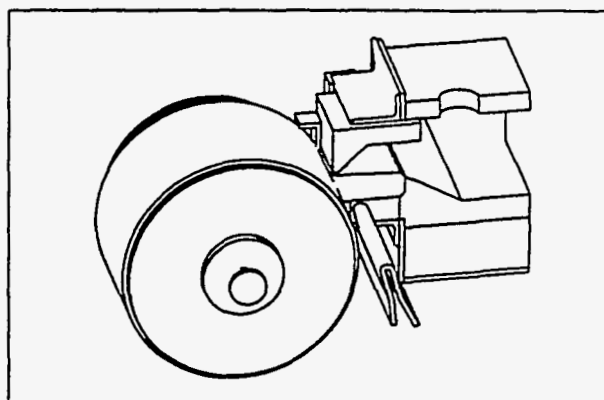
Figure 2.4 *Solid model of the current sheet approach.*

2.2.3.3 Low Frequency Coil in Wheel It is also possible to envision the use of a low frequency current, perhaps located on the inside of the casting wheel. Although originally proposed as part of a system which combined currents injected into the liquid steel, this approach expressly omits the liquid steel currents, which were felt to be too difficult to implement. Without the currents injected into the liquid steel, an AC field is required to produce the electromagnetic support. The use of a low frequency allows the field to more easily penetrate conducting material such as the copper wheel. Low frequency fields will, to an extent, provide support with low losses. The support, however, will not be concentrated at the surface as in the case with high frequency induced forces. The low frequency source of the fields for this approach need not be located inside the wheel. Figure 2.5 illustrates this approach.

2.2.3.4 Concentrated Coil This approach combines two of the concepts described in the brainstorming sections (single turn 'pitchfork' and single turn "loop" concepts). The single conductor system, shown in Figure 2.6, uses a liquid-cooled, hollow, copper conductor to carry high frequency currents in the vicinity of the meniscus. The return of the conductor to the supply could be a source of study during the design phase, but will most likely be between the pour box and the wheel. Although shown as a single conductor, the actual device may consist of several small conductors connected electrically in series. Cooling connections would be either series or parallel, depending on the cooling pump's flow characteristics.
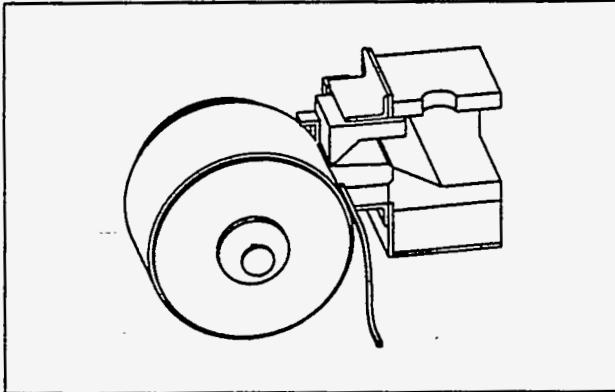
Figure 2.5 Solid model of the low-frequency in-wheel approach with two possible coil locations shown.
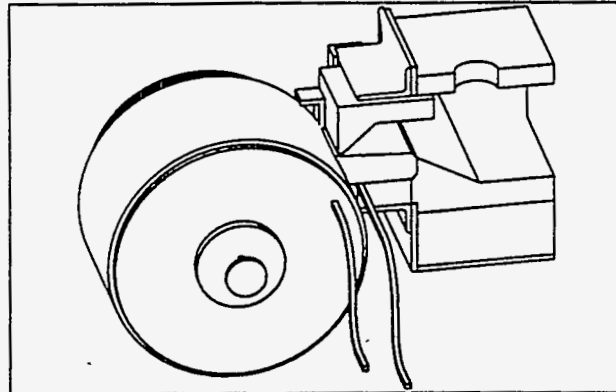
Figure 2.6 Solid model of the concentrated coil approach.

2.2.3.5 Two-Frequency Approach This design was the deliberate combination of the previous two concepts, combining the high support per unit current of the low frequency fields with the surface pressure nature of the high frequency approach. This concept is shown in Figure 2.7.
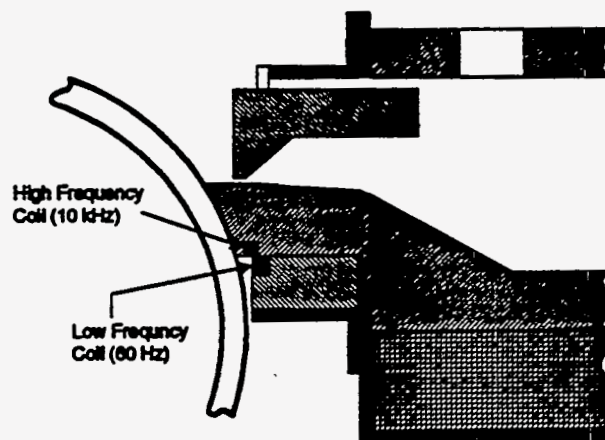
Figure 2.7 Drawing of the two-frequency approach.

2.3 Evaluation

The evaluation of the approaches described in the previous section proceeded primarily along two parallel tracks, one for electromagnetic phenomena and one for the study of mechanical design and caster integration. A third avenue of evaluation was a simple bench-top experiment to confirm the electromagnetic support of liquid metal for the conceptual arrangement. Each of these approaches to evaluation is briefly described in the following paragraphs.

The investigation of electromagnetic phenomena centered on the use of 2-D finite element electromagnetic (FEM) analysis using a commercially available package. An analysis was performed for each of the approaches, except the current sheet approach (which has the currents flowing in the wrong direction for the 2-D FEM package). The same model was used for all the FEM work so that all the approaches were evaluated on a common basis. Little attempt was made to optimize the FEM grid, geometry, or electrical frequency so that the analysis was only taken as indicating relative orders of electromagnetic support and induced heating and thus at this stage the results only reflect the relative capability of the different approaches. Each analysis resulted a solution for the magnetic field as illustrated by the plot of magnetic flux lines shown in Figure 2.8 (for the concentrated coil approach). From these FEM solutions, it is possible to estimated the currents required to support a desired liquid steel head as well as the induced heating in the liquid steel and caster components (primarily the casting wheel and the pour box). The numerical results are reflected in the rankings given in § 2.4. As mentioned above, the current sheet approach did not lend itself to FEM analysis so that a simple analytical expression was used to determine the required current. Induced heating effects were then based on comparison with FEM analysis of the other approaches.
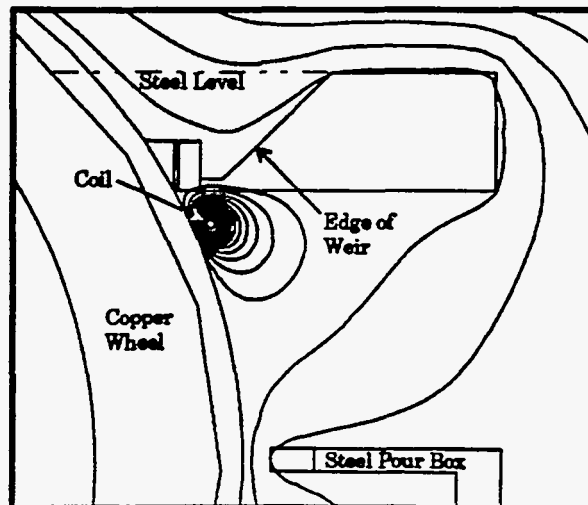
Figure 2.8 A plot of the magnetic flux lines for the concentrated coil approach.

The evaluation of mechanical-design and caster-integration issues was, by necessity, more qualitative. A list of critical issues was identified which applied to all of the approaches. This list included the following:

- Mechanical and Manufacturing Complexity
- Impact on Existing Caster Design
- Difficulty of Implementation
- Support Equipment Required
- Sensitivity to Mechanical Variations, Steel Grade, Wheel Surface Conditions
- Control During Start-up
- Applicability to Back and Side Seals
- Durability (life, wear, survivability from breakouts)

Approaches were considered in light of each criteria and evaluated as to their strengths and weaknesses. It was necessary to have a conceptual design in mind for each approach while carrying out the evaluation, but these designs were very preliminary. There was, however, an attempt to maintain the same level of detail and sophistication (or lack thereof) for each approach. The mechanical designers which performed the evaluation are well acquainted with steel casting conditions and half the evaluation team had witnessed trial casts at ARMCO. The results of the evaluation are reflected in the rankings of the selection matrix.

The final component of the evaluation was a bench-top experiment to demonstrate the capability of electromagnetic support of liquid metal. Using an existing power supply, tuning station and connecting bus, an experimental apparatus was designed and built. This apparatus, shown in Figure 2.9, consisted of four G-10 micarta panels arranged as a box in the center of a large copper plate which served as the box's bottom. The box was filled with liquid Indalloy 136, a lead-bismuth-tin eutectic, to a depth of one inch. A two-turn coil was built and positioned approximately 0.5 inch from both the copper plate and the G-10/Indalloy interface. The coil was energized with 3000 A at 8.5 kHz and support of 0.75 inch of the Indalloy was produced. The photograph of Figure 2.10 shows the support over nearly the entire width of the box (approximately 6 inches).
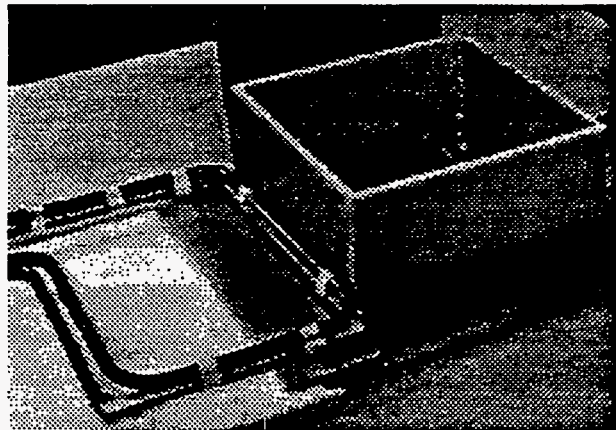
Figure 2.9 *A view of the bench-top experiment showing the two-turn coil and the G-10 micarta box holding the liquid metal.*

The Indalloy level before the coil is energized is shown by the short dark line in the inside center of the wall panel on the left-hand side of the box. The concentrated coil concept was used because of its ease of implementation for a bench-top experiment and its early identification as a strong contender for final selection. As part of an earlier DOE program on Thin Section Casting [3], a demonstration of the sealing ability of the brush approach (currents injected into the wheel) using a Gallium-Indium eutectic was produced. However, this approach does not scale to large cast widths.
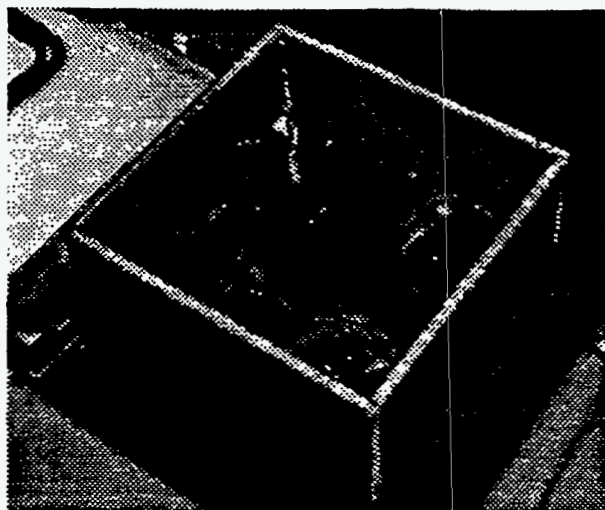
Figure 2.10 A view of the bench-top experiment in operation demonstrating support of the liquid metal. Indalloy level before energizing the coil is the short dark line in the center of the left-hand wall panel.

2.4 Selection Results

The final recommendation was based on the outcome of a weighted selection matrix process. Use of this technique provides a means quantifying some of the qualitative factors, at least in a relative sense. The matrix was developed by first selecting pertinent categories for both electric (or electromagnetic) and mechanical concerns. These categories, together with their respective weights, were selected by the evaluation teams before the actual scores were awarded.

All of the categories refer nominal casting conditions of 5 fins (1.5 Ms) casting rate, a 100 mil (25 mm) nozzle/wheel gap, and a 4 inch (102 mm) ferrostatic head. The categories are largely self explanatory, but a couple deserve some clarification. Stability of support refers to the tendency of the liquid steel to leak though force fields that are uniform. Unless the force increases as the fluid moves backwards down the wheel (anti-casting direction), there is no restoring force and the seal is unstable. Scalability to full width involves issues arising from differences between the 12 inch (.3 m) wide experimental caster and the final commercial sized caster which may have a width as great as 80 inches (2 m).

Within each category relative rankings were assigned by the evaluation groups with the general understanding that high scores were good. Before applying the category weights, category scores were normalized to 100 points so that category weights within a group were direct measures of category importance. Because the mechanical evaluators had higher average scores than their electrical counterparts, a group weight was added so that relative importance in the two groups could be adjusted. The categories, their weights, approach scores, and resulting ratings are shown in Table 2.1.

In order to determine the "robustness" of the resulting rankings, some weights were changed and differences to the rankings were noted. Changes included increasing the relative importance of the mechanical group compared to the electrical group. Within the electrical group, the importance of different loss components was changed while within the mechanical group, the importance of caster impact and auxiliary equipment was varied. None of these variations changed the primacy of the concentrated coil approach as the best concept, and the recommendation of the concentrated coil as the approach to pursue is therefore considered "robust." Some of the combinations of weights did move the dual frequency approach to a close second place so that it was considered a good alternative. As mentioned above, these rankings are relative so that although the recommended approach is judged the one with the lowest risk, it is by no means a low-risk solution to the sealing problem.

Table 2.1 The Filled in Selection Matrix

Raw Scores	Concepts	Electrical Categories				Weight: 3	Mechanical Categories				Weight: 2
		Required Current	Stability of Support	Total Losses	Losses in Steel	Scalability to Full Width	Design Complexity	Caster Impact	Durability	Use as Side Seal	Auxiliary Equipment
	Bush System	3	2	1	1	1	1	1	1	5	4
	Current Sheet in Gap	1	4	2	2	3	2	4	3	1	2
	Low Freq. Current Inside Wheel	3	1	3	3	3	4	3	4	2	4
	Concentrated Coil	2	4	2	2	3	5	5	3	5	4
	Two-Frequency Approach	4	3	4	4	3	3	2	3	2	2
	Total	13	14	12	12	13	15	15	14	15	16
	Weights	4	5	2	2	4	5	4	2.5	3	4
Normalized & Weighted Scores	Concepts										
	Bush System	92.3	71.4	16.7	16.7	30.8	33.3	26.7	17.9	100.0	100.0
	Current Sheet in Gap	30.8	142.9	33.3	33.3	92.3	66.7	106.7	53.6	20.0	50.0
	Low Freq. Current Inside Wheel	92.3	35.7	50.0	50.0	92.3	133.3	80.0	71.4	40.0	100.0
	Concentrated Coil	61.5	142.9	33.3	33.3	92.3	166.7	133.3	53.6	100.0	100.0
	Two-Frequency Approach	123.1	107.1	66.7	66.7	92.3	100.0	53.3	53.6	40.0	50.0

Selection Summary

Concepts	Electrical Score	Electrical Rank	Mech. Score	Mech. Rank	Total Score	Total Rank
Bush System	227.8	5	170.2	4	398.1	5
Current Sheet in Gap	332.6	3	181.9	3	514.5	4
Low Freq. Current Inside Wheel	320.3	4	260.2	2	580.5	3
Concentrated Coil	363.4	2	339.1	1	702.5	1
Two-Frequency Approach	455.9	1	181.9	3	637.7	2

3.0 Scaled Liquid-Metal Experiment

3.1 Scaling Study

3.1.1 Introduction

The difficulties inherent in a molten steel experiment with the required high temperatures necessitate the use of metals with lower melting points for initial testing of electromagnetic meniscus support concepts. The experiment with an alternate metal must be designed such that the observed results are valid when extrapolated to the molten steel system. This type of problem is addressed routinely in fluid dynamics by writing the governing partial differential equations in terms of dimensionless parameters which fully characterize the flow[4,5]. Results of a fluid flow experiment may be related directly to the actual system being designed if the dimensionless parameters and the physical arrangement are equivalent. It is rarely possible to maintain equality of all dimensionless parameters between experimental and prototypic systems. As such, the important phenomena of the physical situation must be extracted and used to design the experiment with similitude enforced on the dimensionless parameters involving these phenomena.

This section describes the rationale used to scale a single wheel casting magnetofluidynamic (MFD) experiment so that the results from the experiment are applicable to the design of a full-scale steel casting system[6]. The purpose of the MFD system is electromagnetic support of the molten metal in the gap between the pour box and casting wheel, as shown in the simplified schematic of Figure 3.1. The experiment will be used to understand the sealing capabilities and limitations of the proposed MFD sealing system as a function of various parameters. This scaling study identifies initial values for the five key parameters of the experiment: gap size, frequency, characteristic magnetic flux density, molten metal pool height, and velocity of the casting wheel. During testing, parameters in the experiment will be varied about the nominal values from this scaling study. Table 3.1 gives a complete list of all symbols used.
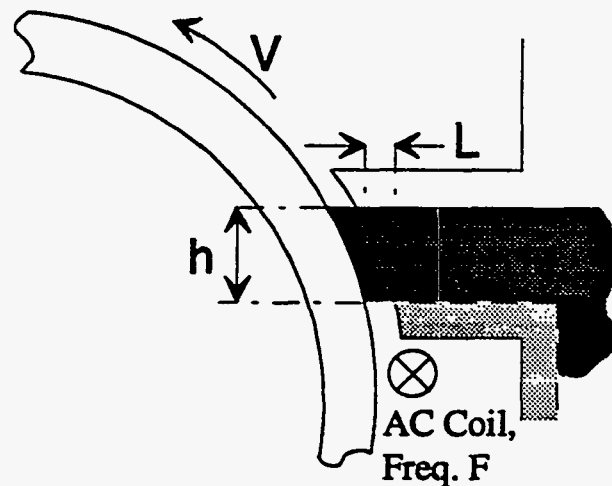
Figure 3.1 Simplified drawing of casting system which shows the gap L where the molten metal will be supported and the height h of the molten metal pool.

Table 3.1 Symbols used in Scaling Study

L	gap between wheel and pour box
h	height of molten metal pool
u	characteristic velocity of molten metal
B	flux density to support molten metal
J	induced current density
f	coil operating frequency
R	local radius of curvature on interface
δ	electromagnetic skin depth
ρ	mass density
ν	kinematic viscosity
μ_o	permeability of free space
σ	electrical conductivity
γ	surface tension
g	gravitational constant

3.1.2 Dimensionless Analysis

In terms of electrical and fluid properties, candidate molten metals are characterized by mass density, electrical conductivity, viscosity, and surface tension. These properties are given for steel, Indalloy 136 (a eutectic form of Wood's Metal), tin, sodium-potassium (NaK), and gallium-indium in Table 3.2.

Table 3.2 Material Properties for Candidate Materials

Material Properties	Steel	Indalloy	Tin	NAK	Ga-In
density (kg/m^3)	7170	9700	6900	870	6200
absolute viscosity (kg/m-sec)	6.40E-03	2.80E-03	1.75E-03	8.00E-04	1.40E-03
kinematic viscosity (m^2/sec)	8.93E-07	2.89E-07	2.54E-07	9.20E-07	2.26E-07
surface tension (N/m)	1.4	0.33	0.52	0.12	0.58
electrical conductivity (S/m)	7.10E+05	9.90E+05	2.30E+06	2.60E+06	3.70E+06

Supporting a molten metal interface using an ac coil involves solving for three unknowns which are coupled to each other in varying degrees: the magnetic field, the free surface shape, and the internal fluid motion. A time-varying magnetic field diffuses into surrounding molten and solid conductors approximately one skin depth, inducing eddy currents which result in a layer of Lorentz force density, J x B, with a magnitude on the order of:

$$\text{Lorentz Force Density:} \qquad \frac{B^2}{\mu_o \delta} \qquad\qquad (3.1)$$

The irrotational part of the force density can support the molten metal (the rotational part promotes stirring). When the skin depth is large, the force density exists

throughout a significant volume of the molten metal. In terms of stability, this means that downward movement of the meniscus is not accompanied by a strong restoring force. However, a low frequency system, with it lower power losses, may be practical due to the support or "dragging" effect of upward viscous shear forces from the casting wheel. The viscous forces will most likely play an important role in the experiment.

When the skin depth is small, the force density is confined to a thin layer at the molten metal interface. In this case, the Lorentz forces look like a magnetic surface pressure and can shape the interface in addition to supporting it due to the stronger coupling with the magnetic field. The basic equations are[7]

$$skin\ depth \qquad \delta = \sqrt{\frac{1}{\mu_o \sigma \pi f}}$$

$$magnetic\ pressure \qquad T_m = \frac{-1}{2\mu_o} B^2 \qquad (3.2)$$

$$static\ stress\ balance\ on\ interface \qquad \frac{\gamma}{R} + \frac{1}{2\mu_o} B^2 - \rho g h = 0$$

Due to the large mass densities of metals, support from surface tension will be one order of magnitude smaller than the magnetic and gravitational pressures. By writing a balance between magnetic pressure and gravitational head, one can solve for the B field required to balance a height (h) of liquid metal.

$$flux\ density\ required \qquad B = \sqrt{2\mu_o \rho g h} \qquad (3.3)$$

Looking at the fluid flow, the rotational part of the Lorentz force density acts as a source of vorticity at the surface which stirs the molten metal[8,9]. Hence, in addition to the three pressures of the static stress balance equation there is a dynamic pressure due to the fluid velocity. An upper limit on the velocity for a fully levitated volume of liquid metal, not contacting any solids, is obtained by equating the dynamic pressure with the gravitational head. Above this velocity the melt would tend to fragment due to centrifugal forces[10]. In single wheel casting, however, the majority of the molten metal in the gap is in contact with either the casting wheel or the pour box so this approximation is not valid. A better characteristic velocity for the scaling study is the casting wheel velocity.

From the discussion above, five order of magnitude pressures are:

dynamic (inertial)	ρu^2	
viscous	$\rho v u / L$	
magnetic	B^2 / μ_o	(3.4)
gravitational	$\rho g h$	
surface tension	γ / L	

These five order of magnitude pressures may be combined to create dimensionless parameters. The values of these parameters identify which phenomena dominate the physical process being studied.

Because the gap length is an order of magnitude smaller than the molten metal head, the dimensionless parameters are written in terms of two characteristic lengths: the gap length and the height of molten metal to be supported. Thus, the characteristic length is the gap length (L) everywhere except where the ratios involve gravity, and the height (h) of the metal pool is used there.

Combining various order of magnitude pressures gives the following dimensionless parameters[11,12]:

Bond, Bo (gravity / surface tension)	$\rho g h L / \gamma$	
Weber, We (inertila / surface tension)	$\rho u^2 L / \gamma$	
magnetic mach, Mm (inertial / magnetic)	$\sqrt{\rho \mu_o} u / B$	(3.5)
Reynolds, Re (inertial / viscous)	$u L / v$	
Froude, Fr (inertial / gravity)	$u^2 / g h$	

The last two dimensionless parameters fully characterize incompressible flow[1].

For a stability figure of merit, the ratio of the gap length to the skin depth can be defined as a dimensionless ratio.

Characteristic length / skin depth:	$L\sqrt{\mu_o \sigma \pi f}$	(3.6)

For the metals considered here, the Reynolds number is large, meaning that inertia dominates the flow, which may be turbulent. Additionally, the effect of fluid motion on the magnetic field is negligible if the magnetic Reynolds number (Rm), the ratio of magnetic diffusion time to transit time, is << 1.

Magnetic Reynolds, Rm $\qquad \sigma\mu_o L u \qquad$ (3.7)

This is the case for all systems considered.

3.1.3 Experiment Design

The above information may now be used to design the experiment. The parameters to be chosen for the experiment are frequency, gap length, height of the molten metal pool, characteristic magnetic flux density, and velocity of the casting wheel. Our goal is to choose the parameters for the experiment, based on the properties of each candidate metal, to match the dimensionless parameters for the steel casting case.

The project goal is stable support of gravitational head to seal the gap between pour box and casting wheel. To maintain the level of coupling between interface and magnetic field, the ratio of skin depth to gap length should be maintained. This puts a constraint on the frequency (f) and gap length (L). The second constraint is that the flux density be large enough to support the liquid metal pool, a constraint between h and B.

The Froude and magnetic numbers are equivalent within a constant factor because the flux density is defined such that the magnetic pressure can support the gravitational pressure. By definition, when the Bond and Weber numbers are kept constant, then the Froude and magnetic Mach number, and the length/skin depth ratio as constraints.

Keeping the Bond number constant along with the "L/skin depth" ratio means that the stabilizing effect of "surface pressure" and surface tension is equivalent for the full-scale steel system and experiment. The Reynolds number similitude assures that the fluid flow in the experiment is equivalent to the full-scale system.

Maintaining constant Reynolds, Weber and Bond numbers fully specifies velocity (u), gap (L), and height (h). The flux density is specified by requiring it to support the height (h) of liquid metal, and the frequency is specified by the gap to skin depth ratio.

Additionally, the power dissipated in the molten metal is approximated using an expression for the power input per unit surface area from a one-dimensional skin depth solution.

power / unit surface area $\qquad B^2 / 2\mu_o^2 \sigma\delta \qquad$ (3.8)

The power given by this approximation is obtained over an area defined by the gap length (L) and a six-inch width.

power to liquid metal $\qquad B^2 (0.15L) / 2\mu_o^2 \sigma\delta \qquad$ (3.9)

The high conductivity and low mass density of NaK scale the experiment parameters very nicely but the chemical reactivity of the metals make handling difficult and would

---

require that the experiment be run in a sealed atmosphere. The small gap lengths, large currents, and high frequencies required to scale the experiment with tin and gallium-indium make these metals unattractive. Indalloy 136 appears to be the best candidate metal for the experiment. The scaling ratios of experiment to steel system are given in Table 3.3.

Table 3.3 Steel/Experiment Scaling for Candidate Materials

Characteristic Variables	Indalloy	Tin	NAK	Ga-In
frequency (kHz)	1.99	7.06	0.12	10.75
characteristic length (inches)	0.60	0.21	1.50	0.13
cast velocity (ft/min)	0.54	1.36	0.69	1.89
gravitational head (inches)	0.29	1.85	0.47	3.59
gravitational pressure (psi)	0.39	1.78	0.06	3.10
flux density (Tesla)	0.63	1.33	0.24	1.76
magnetic field (amps/meter)	0.63	1.33	0.24	1.76
skin depth (inches)	0.60	0.21	1.50	0.13
power input (watts)	0 28	0.55	0.02	0.60
Dimensionless Parameters				
Reynolds number	1.00	1.00	1.00	1.00
Froude number	1.00	1.00	1.00	1.00
Bond Number	1.00	1.00	1.00	1.00
Weber number	1.00	1.00	1.00	1.00
magnetic Reynolds number	0.45	0.92	3.77	1.32
magnetic mach number	1.00	1.00	1.00	1.00
length/skin depth ratio	1.00	1.00	1.00	1.00

3.2 Experimental Apparatus

3.2.1 Overview

The mechanical components of the single wheel strip caster experiment[13] are designed to simulate, as closely as possible, the actual casting environment at ARMCO's casting research facility. To accomplish this goal, a single wheel caster featuring a 3-inch casting wheel assembly was procured from ARMCO (where it was used earlier in single wheel casting development) and was modified for use in the Westinghouse EM sealing experiment. The use of components from the 3-inch casting wheel assembly enabled Westinghouse to better simulate the strip casting machine. Considerable time and effort was saved by the incorporation of these components. The use of wheel assembly components allowed the study of dynamic effects which are induced into the EM field by a rotating wheel.

The main mechanical components of the experimental assembly are ARMCO's 3-inch wheel components, a liquid metal trough, concentrated current coil, adjustable weir and head gates, overflow/make-up reservoir, and supporting structure. These compo-

nents are shown in the solid model of the experimental apparatus, Figure 3.2. To simulate liquid steel, Westinghouse uses Indalloy 136, a eutectic lead-tin-bismuth alloy. This material is well suited to model the liquid steel as described in the scaling study memo[6]. The low melting point of Indalloy (136°F) relaxes temperature constraints during the experiment. The system contains heaters of both immersible and wrap-around styles to keep the Indalloy in the liquid state. The system is cost effective and reliable, and allows experimental results to be easily extrapolated to full scale casting of liquid steel.
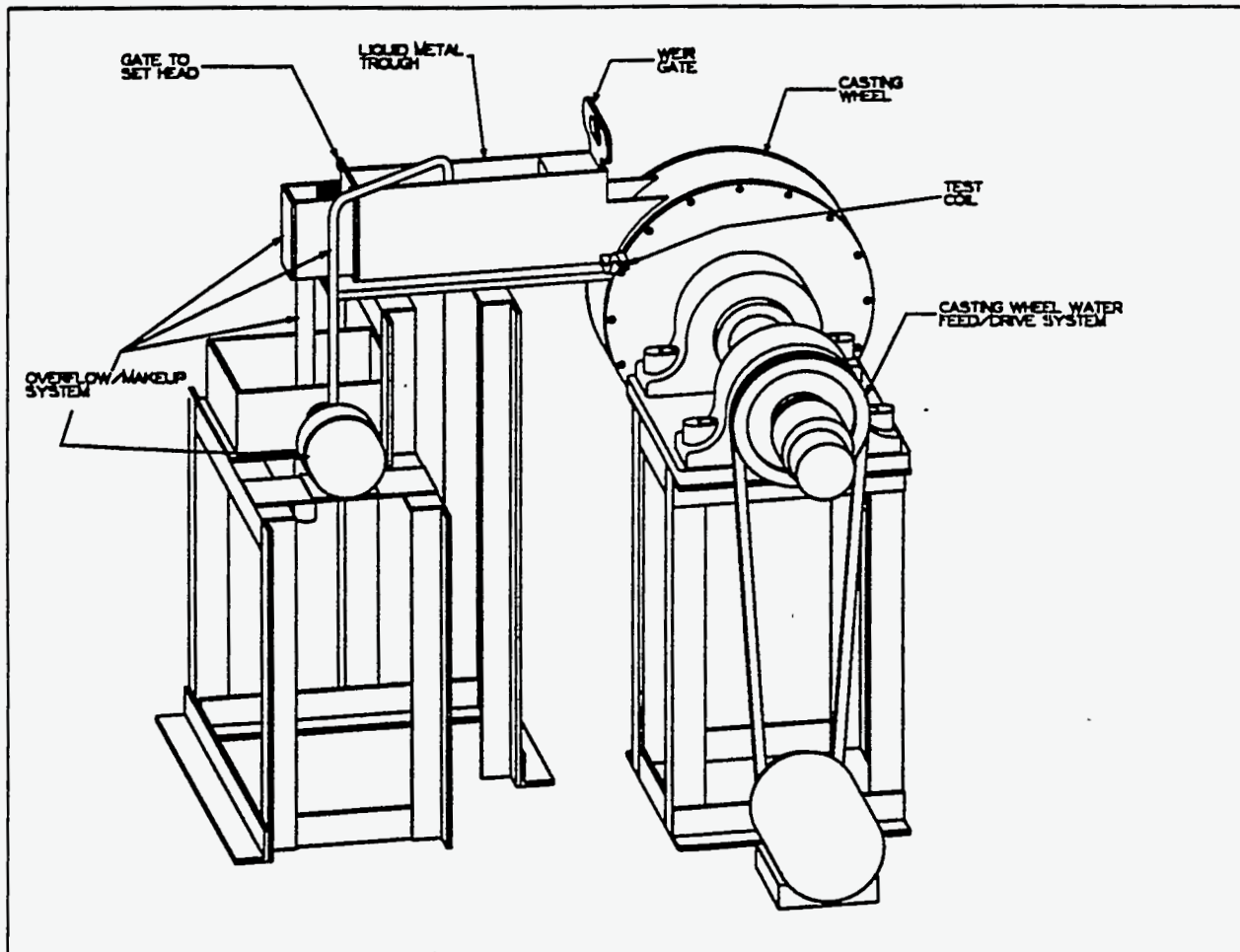
Figure 3.2 A solid model of the experimental apparatus showing major components.

3.2.2 Experimental Coil

The design of the experimental coil is based on work performed for the concept selection and the scaling study. During that work, a 2-D finite element electromagnetic analysis (FEM) of the concentrated coil seal was performed for the steel caster and solution were run at several frequencies. Based on these solutions (as seen in Figure 3.3), an operating frequency range of 1-5 kHz was chosen. A sample field analysis solution for

the 10 kHz case is shown here as Figure 3.4. For complete electromagnetic support of a 0.9 inch ferrostatic head (23 mm) with a gap of 0.1 inch (2.5 mm) and a cast width of 12 inches (305 mm), the seal's characteristics are the following:

- 49,000 Ampere-Turns
- 3 kHz
- Total Losses of 300 kW
  - 76 kW coil
  - 70 kW steel
  - 154 kW wheel
- 0.5" x 0.5" Coil (13 x 13 mm)
- 0.5 inch (13 mm) from wheel
- 0.5 inch (13 mm) from liquid metal
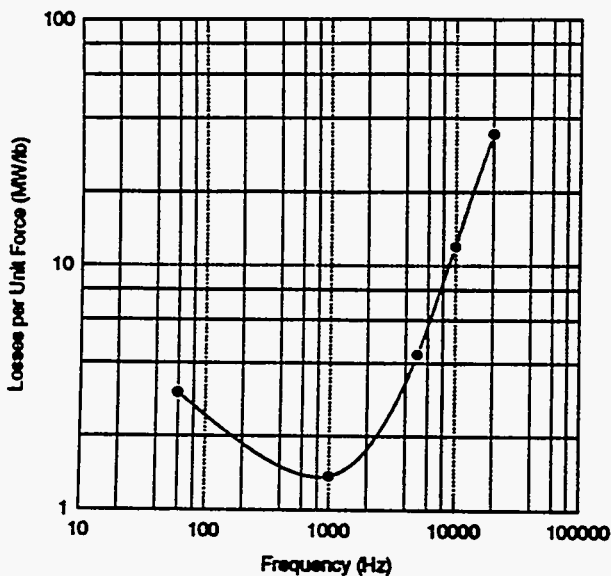
Figure 3.3 Plot showing the power required to support a 6-inch ferrostatic head as a function of frequency. Nominal conditions are given in the text.
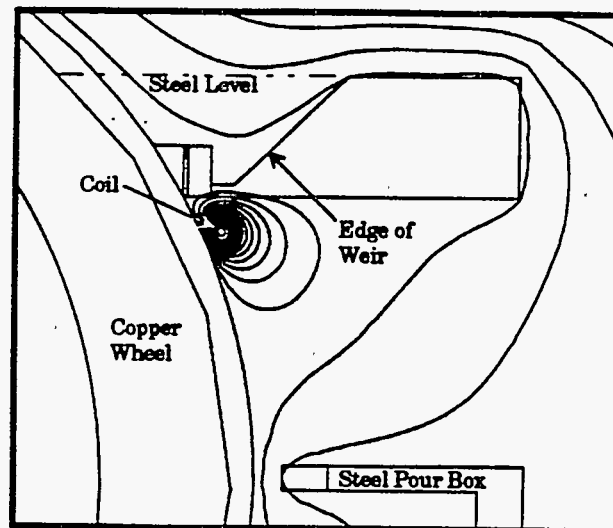
Figure 3.4 A plot of magnetic flux lines for the nominal seal design. Flux density is proportional to line spacing.

Using the results of the scaling study, the coil for the scaled experiment, operating at 2-10 kHz and carrying a total current of 30,000 ampere-turns will support a head which scales to a ferrostatic head of 1 inch (25 mm). In order to meet this goal, the test coil will have 6 turns of 0.375 inch (9.5 mm) copper conductor each carrying 25% of the total required current. The conductors will be water-cooled with up to 6 hydraulic paths, depending on the hydraulic resistance of the installed coil.

The amount of force required to prevent leaking is less than that required to completely support the static head. Both the drag of the wheel and the steel's high surface tension will aid in suppressing leaks. Another factor is the distribution of the electromagnetic forces within the liquid steel. The upward force is very concentrated in the lower portion in the pool and actually reverses in the upper portion of the melt pool. Only the net force is used in the calculations: actual support may be based on only the forces near the meniscus and may be an order of magnitude better. On the other hand, flow effects have been shown to reduce the effectiveness of electromagnetic support if oriented in the wrong direction[14] The scaled liquid-metal experiment should resolve this issue. In any event, the coil required to produce the system described above (49,000 AT) is extremely difficult to fit into the caster geometry, particularly at the distance required to achieve the indicated results.

3.2.3 Liquid Metal Trough

The liquid metal trough is designed to contain and direct the flow of molten Indalloy 136 toward the wheel. The weir area has the same geometry as ARMCO's existing 12-inch strip caster. The weir area has a vertically-adjustable gate for controlling flow through the weir opening. The weir gate adjustability allows various weir gap evaluations to be performed during the course of experimentation. Opposite the weir gate area, in the rear portion of the trough, various gates are located to control the liquid level and, hence, set the head. Each gate will be slotted at a different elevation to control the liquid level before allowing overflow into the liquid metal reservoir. The operation of the gate systems allows for controlled head height, and dross (oxide foam) control in the Indalloy 136. The trough is shown in Figure 3.5, a close up of one part of the complete solid model.

The liquid metal trough assembly is horizontally adjustable using linear bearings. The adjustment is done by mounting the trough on "Thomson" type linear rails and sets the nozzle to wheel gap. The adjustability of the head, weir gap, nozzle gap, and wheel speed allows these conditions to be examined in a systematic manner. Allowances for adjusting the test coil are also provided. The materials for fabrication of the liquid metal trough are G-10 micarta, teflon, and aluminum (away from the coil). The bottom plate, side walls, and weir components are fabricated from G-10 micarta. The weir gate and head setting gates are fabricated from teflon. These
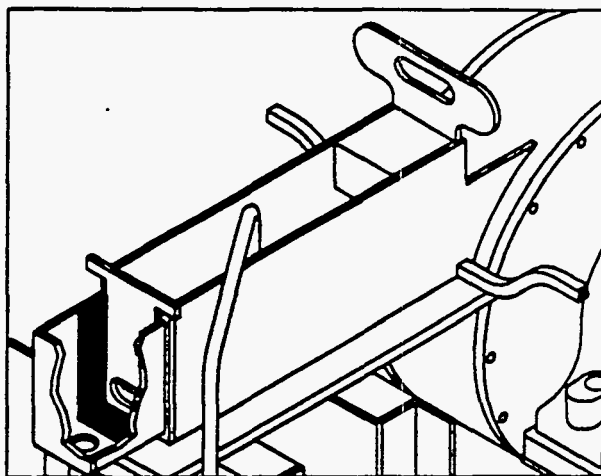
Figure 3.5 A close-up of the solid model of the experimental apparatus showing more details of the trough which holds the liquid metal.

materials allow ease of gate movements. Both G-10 micarta and teflon are well suited to withstand molten Indalloy 136. These materials also demonstrate good wetting characteristics with Indalloy 136. The rear, overflow portion of the trough is fabricated from aluminum, which is also be in contact with molten Indalloy. The aluminum allows for ease of movement of the teflon head control gates, and for a thermally efficient heater mount. The drain pipe into the reservoir is also aluminum and is also heated. In fact, all components of contacting the Indalloy are heated to maintain it in the liquid state.

3.2.4 Make-up System

The overflow make-up system (shown in Figures 3.6 and 3.7) consists of a reservoir, micro pump, and fill/drain piping. The body of the reservoir is fabricated from hot rolled carbon steel and contains a drain valve. The fill and drain piping are also carbon steel. Both the reservoir and piping are heated to keep the Indalloy 136 in a liquid state.

The pump is a magnetic drive pump rated at 2.5 GPM (0.16 l/s) driven by a fractional horsepower motor. The magnetic drive pump consists of two drive magnets (driver, driven) and teflon impellers. This type of pump almost entirely eliminates leaks and contamination. De-coupling occurs when the pump load exceeds the coupling torque between the magnets. This feature acts as a safety device to protect pump and motor from inadvertent damage. The teflon and teflon-encapsulated components are easily removed for maintenance or cleaning. Also, the teflon is compatible with liquid Indalloy 136, as previously described.
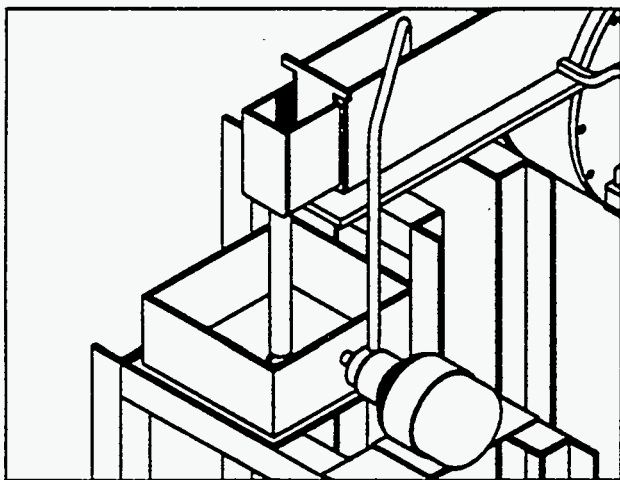
Figure 3.6 A close-up of the solid model of the experimental apparatus showing more details of the overflow pan and make-up pump.

Figure 3.7 A view of the experimental apparatus from the rear showing the liquid metal pump and the make-up reservoir (compare with Figures 3.5 and 3.6).

3.3 Test Plan

3.3.1 Test Plan Goals

The two goals of the scaled liquid-metal experiment are to demonstrate the electromagnetic sealing principle for single wheel casting and provide relevant information for the design of the caster seal. In order to meet these broad goals, there are three more specific goals. These goals are the following:

- Characterize the sealing capability of the single coil concept
  - Currents required to seal different gaps for different heads
  - Required power and distribution
  - Extrapolation to steel casting
- Perform sensitivity studies for selected design parameters
  - Position of coil relative to wheel (within expected coil placement window)
  - Operating frequency
  - Caster speed
  - Extrapolation to steel casting
- Evaluate effects of gross design changes
  - Use of additional coil/frequencies
  - Changing angle of attack

Characterization of the seal capability will be accomplished through experimentation where the wheel-to-nozzle gap and liquid-metal head are systematically varied. During these experiments, currents and powers required to stop leaks and prevent their initiation will be determined. The sensitivity studies will examine the effects of various system parameters, particularly coil position and operating frequency. The third goal addresses large changes in seal/caster design. It may not be required if the first two goals are successfully met and caster geometry remains essentially unchanged. The use of a carefully scaled experiment will allow these three detailed goals to address the broad goal of providing relevant design information for the caster version of the seal[15]. The test plan described in Sections 3.3.2, 3.3.3 and 3.3.4 was the preferred plan for the scaled liquid-metal test. As indicated in Section 3.4 on test results, circumstances forced significant departures from the original plan.

3.3.2 Test Plan Overview

As originally planned, three stages of testing are called for; one for each of the detailed goals. These stages are Gap/Head Characterization, Sensitivity Studies, and Gross Design Changes. It was hoped that completion of the first two stages would provide data leading to an adequate caster seal design. In the event that a good caster design was not indicated, other seal embodiments could be examined in the third stage of testing. During the first stage, wheel-to-nozzle gaps and liquid metal head were varied

systematically and for each gap/head point the currents required to stop an existing leak and prevent leak initiation were recorded. These tests were performed using a representative coil placement. In the second stage of testing the effects of coil placement, operating frequency, caster speed, and perhaps other parameters, were determined for several gap/head points. A statistically-based experiment design was considered for this stage.

The main components of the test system include power supply, tuning station, high-current bus, coil, casting wheel, test fixture, liquid metal make-up system, hot-water heating/cooling system, and cold-water cooling system. The electromagnetic seal system includes the coil, its excitation system, and the cold-water cooling system.

The test fixture, together with the casting wheel coil and liquid metal make-up system, is shown in Figure 3.8. The test fixture consists of a nonconducting basin, with weir, mounted on linear bearings. At the rear of the trough is the overflow-gate system which is used to set the liquid-metal head. This gating system allows the head to be set in discrete increments. The trough will be heated to set the temperature above the liquid metal's melting point. The liquid metal make-up system consists of a metal reservoir, small pump, and flexible tubing which is also heated. More details of all the test equipment will be found in the test report.
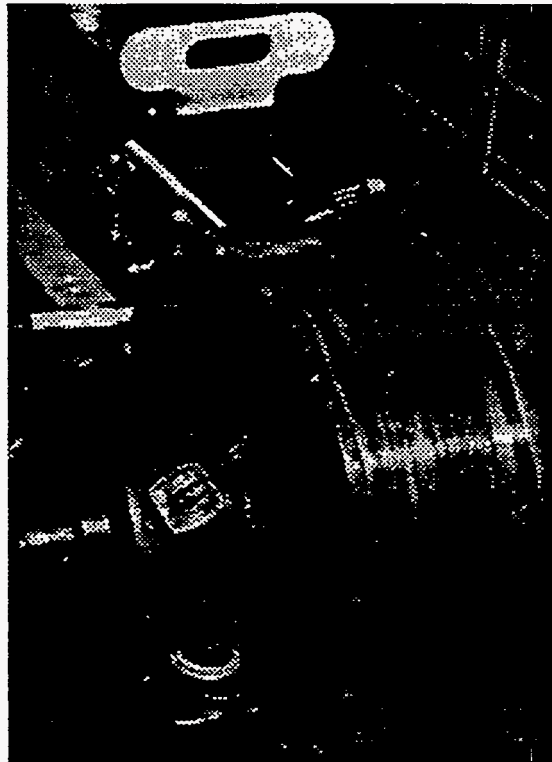
Figure 3.8 A view of the apparatus from the front showing the coil leads and the front of the liquid metal trough. The independent side shields are also shown.

The casting wheel, obtained from ARMCO, is connected to the hot water system to maintain the wheel temperature above the liquid metal melting point so that no casting takes place. The water system will also remove heat generated in the copper wheel while the coil is energized.

3.3.3 Planned Testing

This section describes the test plan as it was envisioned before testing actually was begun. Because this test description was written before the test apparatus was commissioned, it describes what was intended as the test program rather than as a description of the test program as carried out (see Section 3.3.4) and therefore is written in the future tense.

3.3.3.1 Gap/Head Characterization During the first stage of testing the test coil will be fixed in one position while the effects of current, casting gap (wheel-to-nozzle), and metallostatic head on leaking are investigated. Based on conceptual designs of the caster seal, a coil location that is reasonable will be chosen, perhaps 0.75 in below the pool and 0.75 in from the wheel. The test coil will then be accurately located with respect to the casting wheel and the liquid metal pool according to the experimental scaling laws.

Once the coil is positioned, a gap/head point will be selected and the test fixture will be adjusted accordingly. As described in the previous section, the gap can be continuously adjusted while the head can only be adjusted in discrete increments. After the fixture is adjusted, the casting wheel will be brought up to speed, liquid metal will be introduced to the system, and the presence of a leak will be established. If no leak develops, rotation will stop, liquid metal will be drained from the system, and a higher head will be set. One the leak is established, the coil will then be energized and current increased until the leak stops. The current will then be decreased until the leak reestablishes itself. It is expected that more current is required to stop an existing leak than is required to prevent a leak from starting due to dynamic and surface tension effects. This stage of testing will study gaps in the range of 5 to 100 mils and heads from 1 to 5 inches. The ranges will be completely covered in closely spaced intervals. In addition to monitoring coil current, quantitative measurements of power and system temperatures will be made.

In order to accomplish the tests described here, it may be necessary to run other tests to verify instrumentation, data collection, and operating procedures. These tests will be run at the discretion of the test engineer.

3.3.3.2 Sensitivity Studies During the second stage of testing the electromagnetic seal system will be examined for sensitivity to selected operating parameters about a nominal operating point. The nominal operating point is the gap/head point that seems most likely for caster operation. It will be selected by Westinghouse with advice from

ARMCO based on results of the casting trials. When the test fixture is adjusted to the nominal operating point, tests will be run to determine how the current required to stop an existing leak changes when selected operating parameters are systematically varied.

Operating parameters which will varied include position of the test coil (relative to the liquid metal and the casting wheel), operating frequency, and wheel speed. Other variables will be included at the discretion of the test engineer. Because some of these parameters may interact, a statistically-based experimental design may be appropriate and will be considered. For such experiments, the current (or power) required to stop a leak would be the continuous output variable.

3.3.3.3 Planned Departures from Test Plan A third stage of testing may be required under two different scenarios. In the first scenario, performance of the first seal system is not considered satisfactory. In this case the coil will be redesigned, perhaps to emphasize edge heating, perhaps with more physical turns, or perhaps with an additional coil operating at a different frequency. In the second scenario, changes in the steel casting conditions, determined during the ARMCO casting trials, may necessitate gross changes to the test apparatus. An example of this type of change would be a change in angle of attack.

Under either scenario, more testing is required. The most likely test for this phase would be repeats of all or portions of the previous two stages with the modified equipment. The exact form of these tests will be up to the discretion of the test engineer after consultation with program management, both at Westinghouse and ARMCO.

3.4 Test Results

This section describes the results of the tests carried out during the program. Tests were carried out using the coil shown in Figure 3.9. As carried out, the program did differ from that described in § 3.3.3 on planned testing. These differences were the results of three factors, one major and two relatively minor. The factor which lead to the most significant departure from the plan was the presence of catastrophic adhesion of the low-temperature liquid metal strip, Indalloy, to the copper wheel. Typical cast strip produced prior to adhesion is shown in Figure 3.10 This adhesion was strongly influenced by the wheel temperature; so much so that with no excitation of the EM seal, no adhesion occurred. Even when warm water was used in the wheel's water system (to keep the Indalloy molten) no adhesion was noted. When modest current was used (<10,000 A-t), adhesion took place in less than two minutes. With higher currents, desired for sealing purposes, the time before adhesion initiated was considerably less. The reduced useful casting time for each test made taking data difficult, with only the point where leaking first initiated able to be determined. Because of the modest currents which could be run, only a small effect was expected which added to the

difficulty of running the tests. In addition, the expense of each test was increased due to the clean-up efforts and wheel-redressing required after each test.

Figure 3.9 *The test coil shown by itself.*
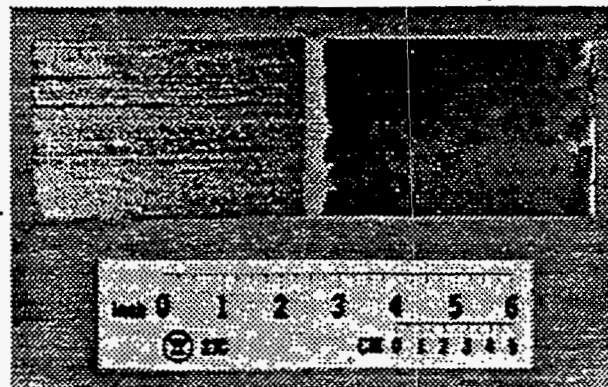
Figure 3.10 *Indalloy strip cast as part of the scaled liquid metal experiment. Both sides of the strip are shown, with the smoother side having been against the wheel.*

The two minor factors were wheel wetting and side shields. In order to mimic the steel/copper interface, the Indalloy must not wet the wheel. Visual observation indicated possible wetting of the wheel and an investigation of surface coatings was undertaken. Coatings of graphite, teflon and molybdenum diselenide were applied to sample copper plates. Drops of Indalloy were applied to the surfaces and drop shapes were examined. Temperatures of the plates ranged from room temperature to above the Indalloy melting point. The graphite coating was selected as the most non-wetting coating. In initial testing, sealing of the back joint was the focus and sealing of the sides was to be later. Sealing the sides during the investigation of the back joint was found to be necessary as metal which leaked out the side would sometimes cause shorting and would flow on the wheel, freeze, and be carried up under the rear joint disrupting the meniscus and initiating leaks. Developing seals was more involved than anticipated because of the relatively large variation in gap which had be accommodated (approximately 0.05 in). Eventually a spring loaded rubbing seal with a felt bearing surface was used. Both the wetting study and seal development were unanticipated efforts which diverted resources from actual testing.

The actual testing is summarized in Figure 3.11. Two presentations of the test data are shown on the graph: a curve showing the relation between metallostatic head and the gap which initiates a leak and a bar graph illustrating effect of coil current on the gap causing leakage. The first curve is taken at one wheel speed and corresponds to no coil current with warm water flowing in the casting wheel. The bar graph, which shows results for a one-inch Indalloy head, different coil water flows, and two current levels, indicates that no significant sealing was present. Indeed, there may be a slight

decrease in ability to withstand head although given the difficulty in making the tests and in ensuring identical surface conditions for subsequent tests, the decrease is not significant.

Given the lack of sealing, it is important to verify the predictions of magnetic field strength to determine if the lack of sealing is due to unanticipated shielding of nearby caster components or to a detrimental fluid dynamic effect. Figure 3.12 shows the results of magnetic field measurements together with a prediction from the finite element analysis. The agreement is quite good, both in magnitude of the peak field and in the rapid drop off in field away from the area of the peak. Based on this comparison, the predicted forces are certainly present on the liquid metal and the poorer than predicted support is due to fluid dynamic effects and not shielding effects of the copper wheel or other caster components.
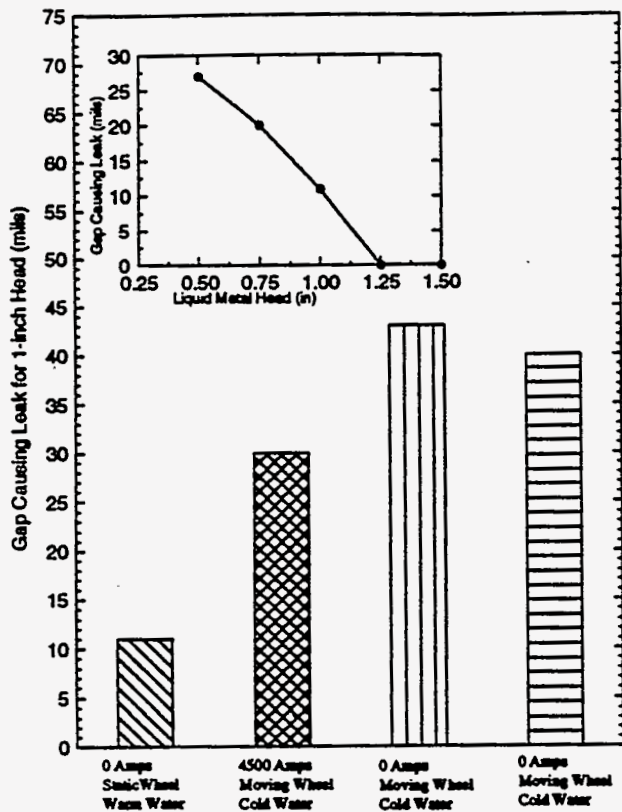
Figure 3.11 Results of the scaled experiment for a 1-inch liquid metal head with and insert showing static wheel result for a range of heads.
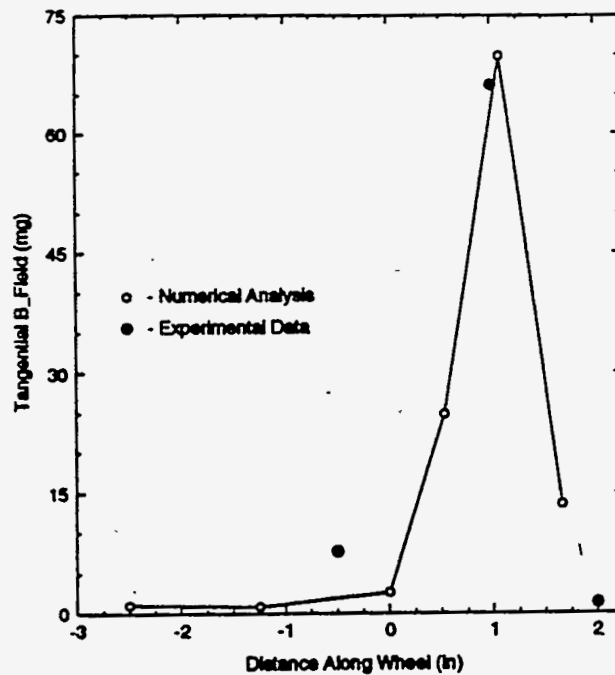
Figure 3.12 A comparison of actual magnetic field measurements and FEM predictions for comparable conditions showing good agreement.

A final test result is the power distribution graph of Figure 3.13. It is readily apparent that little of the total power is dissipated in the liquid metal. Thus the coupling to the liquid metal, which produces the supporting forces is relatively weak. Better coupling can be achieved by moving the current closer to the liquid metal. The coupling to the liquid metal is especially weak in comparison to the power dissipated in the wheel itself. The rather large proportion of power dissipated in the wheel is what led to the catastrophic adhesion condition, even at relatively modest currents.

Liquid Metal (1.9%)

Casting
Wheel
(19.8%)

Bus & System
(27.8%)

Coil
(57.3%)
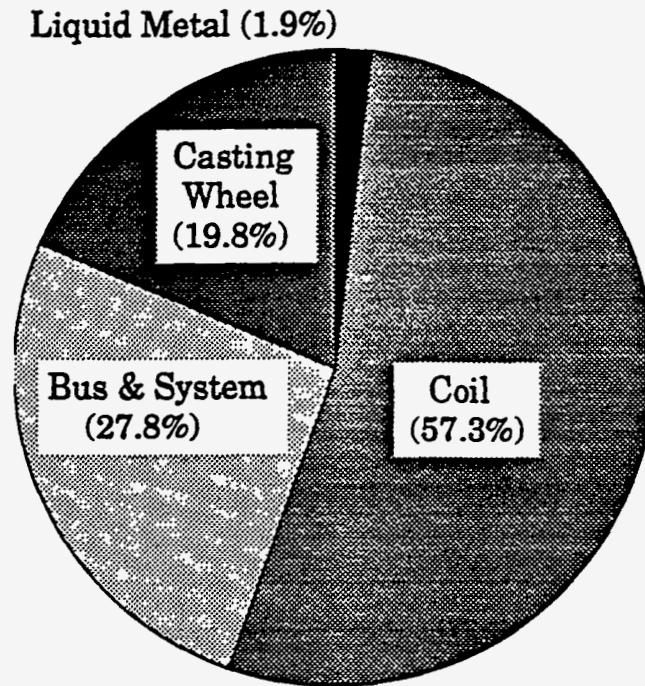
Figure 3.13 *Distribution of power among the components of the scaled experiment. Less than 2% of the power actually is used to support the liquid metal.*

4.0 Conclusions

The major result of the feasibility study is a recommendation that the electromagnetic sealing option not be pursued. This conclusion was reached for two reasons. First, the technical risk remains very high. Although some indication of sealing potential were demonstrated, no significant improvement is sealing was present in the scaled experiment. The lack of improvement is attributed to fluid dynamic effects which could be ameliorated through improved design in the pour box design and/or coil placement. Such improvements would require further analytical and experimental investigations and any resulting sealing improvement is problematic. Second, the payoff for an electromagnetic seal has been dramatically reduced due to other developments of the strip casting program. During the course of the casting trials a rubbing seal between the nozzle and wheel was developed. Further, the ability to control the relative position of the wheel and nozzle made keeping the rubbing seal in contact possible throughout the cast possible. Given the high technical risk, the required work to attempt any significant risk reduction, and the reduced payoff, further work is not recommended.

Determining the lack of feasibility of any concept is much more difficult than proving feasibility. There is always the possibility that some other concept, design, or implementation will turn out to work. The structured process used in this program to select the sealing concept is designed to be inclusive, but ultimately is somewhat subjective, particularly in the selection of weights for rating categories. It is intended to produce the design with the lowest overall technical risk among alternatives. The process is not foolproof and the lack of positive sealing result is an indication of the high technical risk of the task, not an indictment of the process.

Although the electromagnetic seal designed for this single wheel caster was not effective, the ability of magnetic fields to support liquid metal was demonstrated in the course of the program. The bench top experiment showed support as did some non-essential portion of the scaled experiment. In the bench top experiment support was clearly shown, although the support did not clear the metal completely from the simulated wheel (see §2.3). During the course of developing the side seals for the scaled experiments, small pools an/or dribbles of Indalloy which leaked very near the coil before it was excited were dramatically moved away from the coil when current was applied. That this positive indication of electromagnetic sealing was not duplicated with the rear seal is further evidence that fluid flow effects within the pour box may be influencing the sealing capability of the electromagnetic seal.

5.0 References

[1] E. C. Okress et al., "Electromagnetic Levitation of Solid and Molten Metals", Journal of Applied Physics, No. 23, p. 545, 1952

[2] Z. N. Getselev et al., US Patent 3,467,166, 1969

[3] R. M. Slepian, "Single Wheel Casting EM Seal: Concept Selection", 92-9TK1-SINGL-M1, Westinghouse Science & Technology Center, October 1992

[4] W. F. Hughes and J. A. Brighton, **Fluid Dynamics**, Schaum's Outline Series, McGraw-Hill Book Company, 1967, pp. 62-65.

[5] V. L. Streeter, Fluid Mechanics, McGraw-Hill, 1958, p. 216.

[6] R. M. Slepian and D. W. Fugate, "Single Wheel Casting EM Seal: MFD Scaling Study for the Liquid-Metal Experiment", 92-9TK1-SINGL-M2, Westinghouse Science & Technology Center, October 1992

[7] J. R. Melcher, **Continuum Electromechanics**, MIT Press, 1981, pp. 8.12-8.13.

[8] A. D. Sneyd, "Fluid flow induced by a rapidly alternating or rotating magnetic field", J. Fluid Mech., vol. 92, pp. 35-51, 1979.

[9] A. J. Mestel, "Magnet levitation of liquid metals", J. Fluid Mech., vol. 117, pp. 27-43, 1982.

[10] A. D. Sneyd and H. K. Moffat, "Fluid Dynamical Aspects of the levitation-melting process", J. Fluid Mech., vol. 117, pp. 45-70, 1982.

[11] W. F. Hughes and F. J. Young, **The Electromagnetodynamics of Fluids**, John Wiley & Sons, 1966, pp. 152-155.

[12] C. C. Alexion, et al., "Magnetofluidynamically enhanced feeding system for a thin section steel caster", 88-9E6-TCAST-R1, Westinghouse R&D Center, pp. 8-15 to 8-24.

[13] E. F. Docherty and R. M. Slepian, "Single Wheel Casting EM Seal: Experimental Apparatus for Liquid Metal Experiments", 92-9TK1-SINGL-M3, Westinghouse Science & Technology Center, October 1992

[14] "Thin Section Casting Joint Research Project", Final Report, USX and Bethlehem Steel Corporation, for DOE Cooperative Agreement No. DE-FC07-84ID12545, 1987

[15] R. M. Slepian, "Single Wheel Casting EM Seal: Test Plan and Procedures", 92-9TK1-SINGL-M4, Westinghouse Science & Technology Center, October 1992
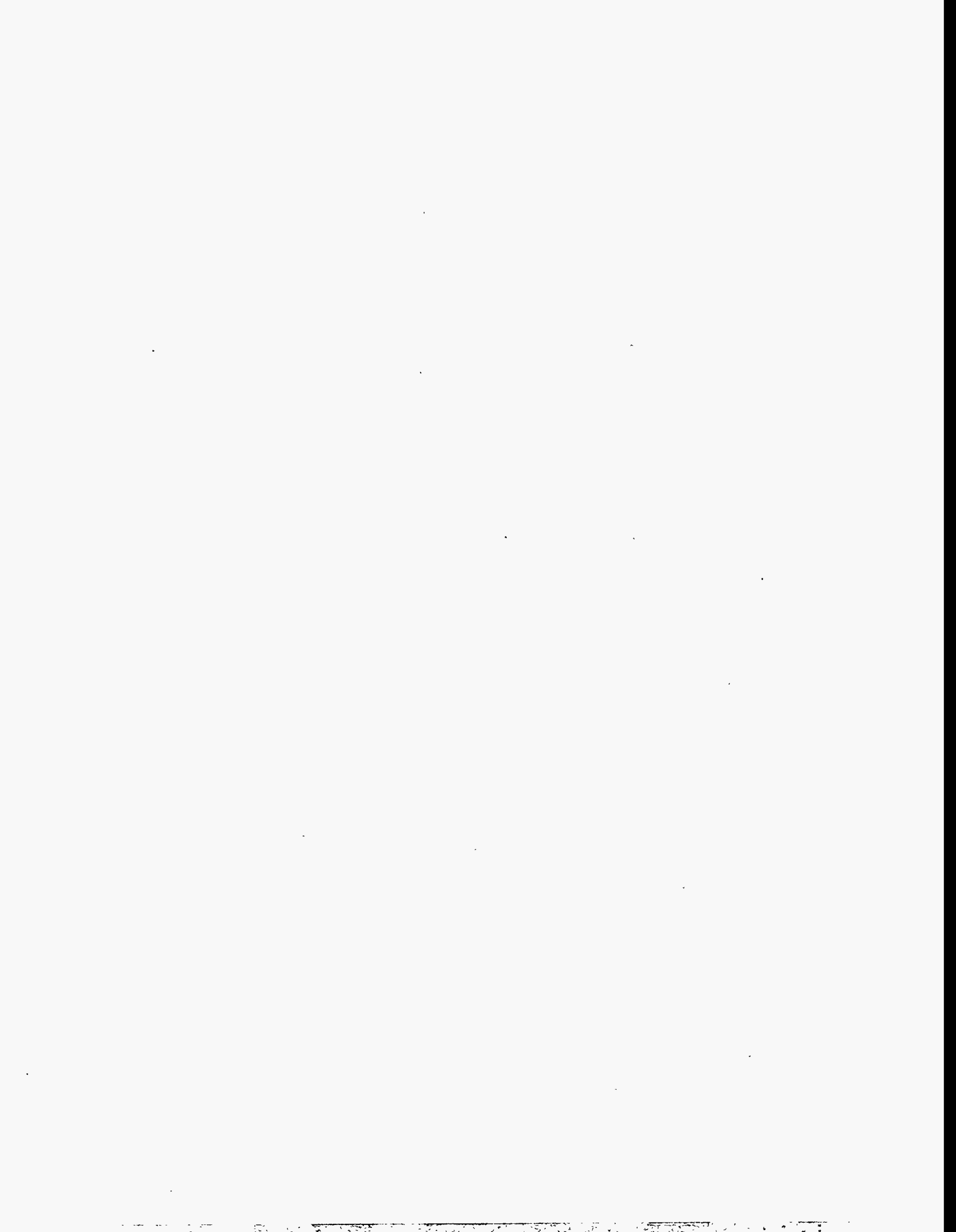
Appendix VII

Sensor Development for Thin Strip Casting
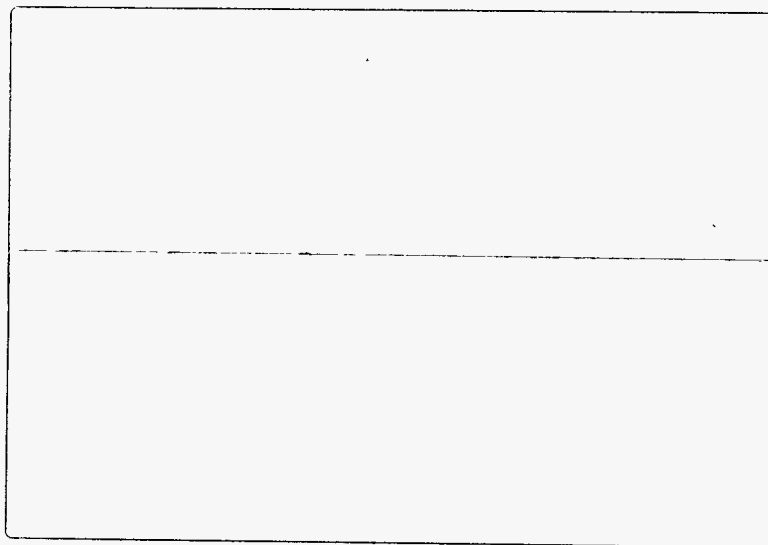
October 4. 1993

To: Mr. R. S. Williams
           Senior Staff Engineer
           Casting
           Research & Technology

From: J. W. Allen

Subject: Task 3.3 Of The Armco-D.O.E. Strip Casting Project

INTRODUCTION

Task 3.3 of this project covered sensor development and control. The subtasks were wheel-nozzle gap sensing and control, metal level sensing and control, substrate temperature sensing and control, melt temperature measurement, strip thickness measurement and substrate condition measurement. This report covers investigation and development work on these topics as well as on the topic of real time strip temperature measurement.

EXECUTIVE SUMMARY

The results of work on Task 3.3 are described in separate sections under the subtasks in the following paragraphs.

Task 3.3A: Gap Sensing-
A pneumatic gauge was developed for measurement of the wheel-nozzle gap that would withstand temperatures to 1300°C. The gauge could measure gaps of 0 to 0.2 cm with an accuracy of +-50 μm. The report on this concept was issued to DOE on October 22, 1992. A satisfactory insulated mounting of the gauge to the nozzle was developed for laboratory use but the mounting concept was never miniturized for use on the caster.

Other methods of measuring the gap at high temperatures were investigated. They were optical reflection, eddy current proximity gauges, capacitive proximity gauges, and optical imaging. The capacitance gauge showed promise. MTI Corp. had developed a gauge operable to 800°C and were in the process of developing one that would withstand temperatures to 1300°C.

Task 3.3B: Gap Control-
Four axis control (wheel up and down, in and out; box wag left or right, tilt left or right) drives and sensors were purchased. Software was developed to allow the nozzle to follow the shape of a distorted rotating casting wheel by using proximity sensors (mounted on the caster frame) to measure the wheel shape or by the use of four contact sensors buried in the corners of the nozzle. Contact sensors were not used in

... ... in the later casts. Only manual control of two axes was implemented due to lack of time and due to the mechanical complexity of adding two axis motion to the box support mechanism.

Task 3.3C: Metal Level Sensing and Control-
After investigation of a dozen methods of measuring mold level, an optical triangulation method used in equipment purchased from Selcom Inc. was used to measure and control level. The pneumatic rod movement mechanism was purchased separately and adapted to the control by Armco. Level measurement within +-. 1 cm and control within +-0.2 cm was achieved.

Task 3.3D: Substrate Temperature Sensing and Control-
Several methods of sensing were studied. They were infrared pyrometers, erodable surface thermocouples, buried thermocouples and sliding surface contact thermocouples. Infrared pyrometers would likely not work in this application. Due to the long delivery times and numerous wheel changes the erodable and buried thermocouple types were never used on a cast. The sliding contact thermocouple was used to determine wheel surface temperature and to control surface temperatures by controlling cooling water flow to the wheel.

Task 3.3E: Melt Temperature Measurement:
Contact and noncontact methods of determining melt temperature to the desired accuracy of +-5°C) were studied. Several kinds of immersion devices seemed feasible although response times were around 30 seconds. Many types of infrared pyrometers for the measurement of melt surface temperatures were analyzed. The best device seemed to be a short wavelength (0.65 μm) single wavelength pyrometer with a peak or valley picker. The present method of using a 0.5 cm fused silica tube encasing a platinum rhodium thermocouple worked well for the short cast times of these experiments. No new equipment for the measurement of melt temperature was purchased.

Task 3.3F: On-line Strip Thickness Measurement-
Noncontact methods were considered necessary for the measuring of the thickness of hot moving strip. The measurement accuracy needed to be +-25 μm and the response time <-0.5 seconds. The measurement accuracy was too stringent for ultrasound methods. Eddy current and capacitive proximity devices will not give accurate readings in strip that isn't flat. The only methods left were radiation methods and optical triangulation. X-ray gauges were too large to fit in the confines of this caster. Gamma gauges are rugged, compact and accurate (+- 6 μm). The avoidance of radiation sources led to the selection of a 3-point Selcom optical triangulation system with +- 25 μm accuracy and a response time of several milliseconds. These gauges were tested on cold strip but were never installed and tested on hot strip due to the termination of the project.

Task 3.3G: Substrate Condition

A method of measuring substrate condition using a scanning laser was tested in the laboratory on a static surface. The output clearly displayed the roughness features of the scanned surface. The best method of analyzing the output of the scanner was not determined. The method was not pursued due to the untimely demise of this project.

Task 3.3H: Thermal Imaging of the Strip-

A real time view of the temperature distribution on the strip surface just as it exited the melt pool was desired in order to determine the heat transfer conditions in the solidification region. A system was designed and installed by Xenas Communications Inc., under Armco supervision, that produced a false-color video with 16 temperature levels. The accuracy of this video was +-50 C and the resolution was 0. 1 cm.

RESULTS AND DISCUSSION

Task 3.3A: High Temperature Gap Gauges-
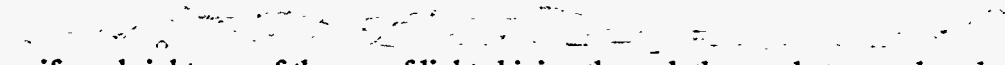
Several schemes other than the air gauge were investigated for gap measurements in high temperature environments. One method considered measures the gap by sending light through an optical fiber to one side of the gap, and sensing the reflected light through other optical fibers surrounding the sending fiber. The amount of light reflected into the pickup fibers is a function of the gap between the wheel and the optical fiber assembly. The most heat resistant optical fibers are fused silica. Fused silica fibers are usable to 800°C, beyond that temperature the fibers devitrify and lose their light transmission properties. This temperature limit could be avoided in our strip cast nozzles with sufficient wall thickness to lower the temperature at the sensor. The lack of a definitive edge on the wheel surface would complicate the measurement.

There are probes that work on magnetic fields (eddy probes) available that work up to 600°C. These consist of a coil through which alternating current flows. The fields around the coil are changed by the presence of magnetic or conductive materials. Electronics connected to the coil can be made to gauge distance between the coil and a conducting target. These probes contain soft magnetic materials that are used to form the field. Above 600°C the soft magnetic materials lose their magnetic properties. Probes made without magnetic materials need to be very stable dimensionally and electrically. Changes in coil resistance and coil dimensions with temperature make it very difficult to produce probes that work at high temperatures. Changes in the substrate with temperature make this nearly impossible.

Probes that work on capacitance looked very promising due to the mechanical simplicity of the design. A capacitance probe is an inner flat plate surrounded by an annular shield that is electrically isolated from it. The inner shield has an alternating voltage impressed on it. The voltage is between the inner flat plate and the grounded target. The amplifier drives the annular shield at the same voltage as the inner flat plate in order to isolate the inner flat plate from the effects of all of its surroundings except the target. Distance is measured by the current that flows from the inner flat plate to the target due to the capacitance of the plate-target gap. The electronics needed to do this is quite sophisticated : Very little current flows to the target; The detection amplifier must have very low common mode input capacitance --.02 pf, very high

common made input resistance and common mode rejection rates over 10,000 at operating frequency. The electronics is best left to someone else. MT1 Corp. had a research project on making high temperature sensors. Leakage from the inner conductor to the outer shield limited operating temperatures to under 800°C. Mechanically 1 050°C is possible. No sensors are commercially available as yet. Probes can be gas cooled but experiments with air gauges show that the cooling distorts the surrounding refractory so that insulation is needed between the gauge and the nozzle. These could be made to work if they were mounted in insulation like the ceramic air gauges. The insulated mounting arrangement was never adapted due to the limited space around the casting nozzles.

One can try to image the gap with a camera. This might work if sophisticated software is available to interpret the results. The high temperatures of the nozzle generate thermal distortion around the gap which makes it difficult to image a gap of a few mils at distances of inches.

A uniform brightness of the arc of light shining through the gap between the wheel and the nozzle was maintained by positioning the nozzle in horzontally and vertically. The arc was observed through a video camera positioned beside the nozzle. The desired intensity of the light was established by experience. This system could be readily automated using simple image analysis systems.

Task 3.3B: The Wheel Positioning Program-
The nozzle to wheel distance has to be held to a very close tolerance in order to keep the melt pool confined. The quality of the strip seems to be critically related to keeping even tighter tolerances on nozzle-wheel distances than melt pool confinement requires. One wants the ability to use bumpers (contact sensors in the nozzle) for automatic control of nozzle-wheel gap, and if the need arises, the ability to follow the wheel terrain with either proximity gauges mounted on the caster frame or with direct nozzle-wheel gauging. Manual control of positioning must be provided. Displaying and recording of position information is also necessary.

The bumper control and manual control will be described first. Bumpers are electrical contacts embedded in the nozzle that give elective indication of wheel contact by electrical shorting. The old positioning system used four bumpers on the nozzle corners for control of the wheel position (the wheel can move up or down and in or out). If either top bumper contacted the wheel, the wheel moved down, if either bottom bumper contacted the wheel the wheel moved out. The wheel could be moved manually in 75 μm steps--the bumpers would protect the nozzle by causing an overriding outward or downward motion whenever bumper contact was made. The wheel positioning was also controlled by limit switches in both directions (to avoid mechanical damage).

The new system can use the same four bumpers but has provisions for cast box movement as well. The cast box could be made to rotate about a vertical axis so that differences in left to right horizontal nozzle contact can be corrected. This is called wag. The differences in left to right vertical nozzle contact could be corrected by a left to right tilt control. Tilt is a rotation about an axis perpendicular to the vertical and

perpendicular to the wheel axis.

The wheel moves down in response to contact with either of the top two bumpers. The cast box wags right if the left bottom bumper makes contact without right bottom bumper contact and vice versa for wagging left. The cast box tilts left if the right top bumper makes contact without left top bumper contact and vice versa for tilting right.

The program is written so that the wheel continuously creeps upward and inward until bumper contact is made. This allows the wheel to move in and out, up and down, at the same time the cast box wags right or left, tilts right or left in response to the wheel nozzle gap. Motions are continuous until interrupted by changes in bumper contact, or contact with limit switches. The speed or motion at the nozzle edges is about 0. 1 cm/sec for all 4 axis of motion.

The manual control consists of X+, X-(out and in).Y+, Y-(down and up) buttons, W+W(left and right wag) lever and a T+, T- (left and right tilt) lever. Pushing a button causes a 75 μm/sec motion that exponentially increases in speed until bottom or lever release. This allows small or large motions to be made with no range switches. Manual control is overridden by bumper contact or limit switches. Wag and tilt were never implemented in the mechanical hardware due to mechanical complexity and lack of time.

Terrain Following Control Technique - Later casts were made on an abradable refractory without the use of bumpers. (Bumpers which must be embedded or attached to the nozzle tend to compromise the mechanical integrity of the nozzle.) All control during the cast was manual. There was a need for some automatic control for the purpose of keeping tighter nozzle-wheel clearances and reducing nozzle wear. Proximity gauges mounted on the caster frame can measure wheel radius on the left and right side. Those measurements (delayed by the time it takes for the area under the gauges to rotate under the nozzle) could be used to adjust the 4 axis for thermal expansion and distortion of the wheel. This leaves the manual control to adjust movement for nozzle changes. The manual correction becomes a slow correction not periodic with wheel rotation. Software was written and hardware was purchased for this wheel terrain following control but was not implemented due to lack of time.

Task 3.3C: Mold Level Sensing and Control-Mold Level Measurement Schemes-
Mold level sensing and control is necessary to having a stable and reproducible casting
process. The goal was to measure level to +-0. 1 cm and control level to +- 0.3 cm
with less than 1 cm overshoot on startup. More than a dozen schemes for measuring
mold level that were investigated, as discussed below. (A summation of the results is
shown in Chart I.)

Discrete electrodes - The gauge is an assembly of electrodes with lengths in
approximately 2 mm steps. The steel bath forms electrical contact with progressively
shorter electrodes as the metal level rises. Armco had a working discrete electrode
device on a galvanizing tank but operation in steel is much more difficult. This method
requires electrodes that can withstand liquid steel immersion for extended periods of
time. The electrode array must not cool the steel bath enough to cause skulling. The
only candidates for electrodes (must be electrically conductive) that are not likely to
melt, crack off or dissolve too quickly are refractory metals such as platinum,
molybdenum, tungsten and a few refractories that are resistant to thermal shock and
electrically conductive at high temperatures such as fused silica, alumina graphite and
zirconia. This method was not pursued because of the large number of leads required
(greater than 20) and the difficulty in keeping the electrodes from pulling excessive
heat out of the melt.

Bubbling gas back pressure - This method measures metal depth by measuring the
ferrostatic head. Gas is bubbled through a refractory tube. The back pressure is
proportional to the distance between the surface and the bottom of the tube. The gas
must not contaminate the melt--argon would work. The gas must also not cool the
tube enough to cause skulking. Due to the bubbling, there is some measurement noise
that probably can be made insignificant with electronic filtering and shaping of the end
of the tube. The bubbling technique was suggested by several people. It was felt that
cooling or changes in metal circulation caused by the bubbling could disturb the casting
process as could the presence of bubbles in the casting area. For this reason, the idea
was not pursued further.

Refractory float - Floats made of a material such as BN or ZrB_2 can withstand long
immersion times on molten steel. Floats made out of silica have been used in Europe
for mold level control. Two problems seem to plague these systems. The mechanical
mechanism attached to the float sees a dirty, extremely hot rugged environment. It's
hard to keep the level mechanisms working. The float itself is expensive - Armco's
experience was that an $80 float would last about 45 minutes. Having to replace floats
every 45 minutes adds high maintenance cost and makes it even more likely that the
mechanism would be frequently damaged.

Tundish scale - Weighing the casting box is a good indirect way of obtaining mold
level. Load cells can be placed underneath the box and away from the heat. The
biggest problem is that the casting box must stay mechanically isolated--nothing can
push or pull on the box in an unpredictable way. (This includes hoses, thermocouples
and their cables and any other wiring). Changes in flow rate into the cast box can
change the apparent weight. In this case, flow rates are changing slowly enough to be
easily compensated for in a mold level determination. Nozzle drag can be determined
as well as mold level by this method. The mechanics of cast box adjustment and the

very limited space under the cast box prevented this from being implemented. Detail of the weighing method is in Appendix A.

Optical methods - There are four optical methods that show promise for mold level determination. One approach uses a laser aimed nearly straight down at the melt pool. An optical system images the laser spot seen on the surface onto a line array. The position on the detector can be easily translated onto mold level. Another approach would use the specular reflection from a laser spot aimed at an angle to the metal surface. The position of the reflection determines mold level. This requires a lens or an optical detector at least half the size of the total range (which could be rather large). The surface must be kept clean. A slag layer would eliminate the specular reflection being used to detect mold level. A third approach is a laser time off light system. This calculates distance based on the time for the beam moving at the speed of light to travel to the surface and (after being reflected) travel back again. One big advantage to this system is that one hole slightly larger than the laser beam is all that is needed to view metal level. In tight locations or where extensive shrouding is needed this is quite an advantage. Finally, there is the imaging approach. One takes a video picture of the metal pool in the nozzle and judges metal level the same way a human operator would. The camera image can be analyzed to tell where the metal surface is. This requires a clear view of the metal level on the side of the nozzle. If the nozzle glows as brightly as the pool the metal level can't be determined. Some flexibility can be introduced to optical methods by the use of mirrors or fiber optics. The difficulty in doing this comes from protecting the optics from extreme heat and keeping optical surfaces clean in a smoky, dusty environment.

Microwave methods - The microwave methods are all time of flight methods. There are at least two mold level measurement-control instruments using microwaves in operation in Europe (made by INNSE-FALCK). These have the advantage that the microwaves can be pumped in and out of the caster area with waveguide or coax which is robust and dirt tolerant.

Radiation methods - A radiation source beams gamma radiation across the casting box through the refractory walls. (The radiation is low enough in energy that it doesn't make the refractory or the metal radioactive.) A detector on the other side measures the received radiation. If the box is full all of the radiation is blocked by the steel. The lower the metal level in the cast box the more radiation makes it to the detector. Many steel mills use this method. It is easy to beam the radiation by use of lead shutters so that no one is exposed to excessive radiation. The sources have doors that close completely and can be locked so that they can be safely handled when being moved for installation or achieved by the use of electronic detectors that are so sensitive that the limiting factor in level determination is background radiation . Also along the line of sight between the source and the detector, the refractory walls consisting of 10 cm of high density castable and 5 cm of low density castable would be replaced with 5 cm of high density castable and 10 cm of low density castable. This would reduce the necessary strength of the source by 20 times. The devices are inexpensive (working systems are available under $20,000) rugged, dirt proof and insensitive to temperature.

Ultrasound devices - Metal level measurement has been attempted using the time-of-flight of sound. The changes in sound speed caused by the wildly varying temperatures

of gases over the melt pool make the method difficult to apply from the top. One possibility is a sonar technique. Sound waves are sent upward through the bottom refractory and then through the melt pool. The resultant echoes (received by a detector on the cast box bottom) from the refractory-metal and metal-air interfaces will be received at a time separation equal to twice the pool depth divided by the speed of sound in liquid steel. One must be able to get sound through the refractory. In this caster, the layer of bubbled alumina looks like an excellent sound absorber.

Electrode contact - This method is a variation of the before mentioned discrete electrode method. An electrode is moved down toward the metal surface. If contact is made, the electrode is withdrawn a short distance. Then the electrode moves down again to repeat the process. When a slag layer is present, the electrode can be made to move up and down in such a manner as to keep a constant resistance between the electrode and the melt pool (the slag supplies the electrical resistance). Whatever electrode is used must withstand long periods of immersion in liquid steel or slag. A mechanical mechanism close to the metal pool surface (and thus able to withstand a hot dirty environment) is required. Kakogawa Works in Japan has successfully used this method of metal level measurement.

Eddy devices - There are three types of eddy devices all have been used in dozens of mill locations. One type is two coils in a canister that is located above the melt pool. Another type is a coil or two coils located in the refractory containing the melt pool. Billet casters use coils encircling the mold. All of these devices detect the change in magnetic field around a coil caused by changes in metal level. In a shallow pool as used in the Armco strip caster, the only practical eddy device is the canister. Canister devices with a 10 cm level range and a 0. 15 cm accuracy are commercially available at a cost of $60K to $100K.

Capacitive devices - The capacitance between a plate and the grounded melt pool is a function of metal level. A sensor for this would be 10 cm to 20 cm in diameter and probably 1 cm thick based on mechanical requirements and requirements of the sensor electronics. The sensor would be a flat disk ~10 cm diameter insulated from an annular disk surrounding it ~20 cm in diameter. Both parts of the sensor must be electrically isolated from ground and connected to electronics. The electrical conductivity of the hot gases above a melt pool might prevent it from working. Such a sensor would need to tolerate or be protected from extreme temperatures. The sensor size is a problem in the tight confines of our machine.

Thermocouples buried in the refractory box - Thermal methods of measuring metal level have been used in Japan on tundishes. Once the box reached thermal equilibrium changes in metal level can be measured if a 30 second time constant could be tolerated. In the present caster setup 2 second time constants are needed. The cast would be nearly over before the box would reach thermal equilibrium. Calibration, because of the short cast times, would be nearly impossible.

Task 3.3C: Mold Level Sensing and Control-Final Selection of Mold Level Measurement and Control Schemes
Armco Research already had a working laser gauge for metal level in development although it would take time to make it into a reliable mold level control system. A

system using imaging could be put together in-house but estimates of the delays due to development of image processing and stopper rod control discouraged its use. All of the methods requiring little development time (though they required significant mechanical engineering time) such as refractory float, bubbling, tundish weighing had been eliminated. The mold level schemes were then limited to immediately available commercial systems. This narrowed the choices to radiation devices, canister type eddy current systems and optical triangulation systems.

The Selcom device (optical triangulation) was selected due to its lower price ($50K for sensing and control intelligence versus $100K for the eddy canister devices.) The radiation devices required more room at the cast box sides than was available without major mechanical rework. It was also felt that the avoidance of radiation sources was desirable.

Task 3.3C: Mold Level Measurement and Control-Design and Modifications of the Optical Triangulation Mold Level System
The optocator uses a laser aimed straight down (or at a slight angle into the melt pool). This cameras aim line is at a 26 degree angle from the laser beam line. There is an imaging line camera that is aimed so that the laser spot image will be focused at the center of the detector when the melt level is in the middle of the range. The laser spot images on one end of the detector when the level is at the lowest end of the detector range and at the other end when the level is at the highest end of the detector range. The detector produces two analog signals. The difference of these signals divided by the sum of the signals determines spot position on the detector and thus mold level. This provides some immunity to signal level fluctuations from smoke, reflectivity changes. etc.

The measuring of the level of liquid steel is much more difficult than measuring the distance to a cold solid object. The Selcom system has several modifications from a simple laser distance gauge, and several additional modifcations were needed for our application. Our steel surface was several hundred degrees hotter than normal stainless steel or iron casting temperatures. There were spurious reflections off of nearby refractory (the weir face) that would not be present in normal installations. The instrument had to interface with existing caster data acquisition systems.

The modifications are as follows:

Several things were done to separate the laser spot from the incandescent background

1. The light images on a rectangular detector. Only light that comes from a patch on the surface 12.5 cm long and 0.4 cm wide can reach the detector. (The laser spot image is always in that patch if the melt level is within range.

2. The laser light is in the bandwidth of 815 to 825 nm. A filter was put in front of the detector that only allows 795 to 845 nm light to pass through. This includes all of the laser light and only background light in that 795 to 845 nm range. This turned out to be too little optical filtering. Two more flters were installed that only allowed light in the 815 to 825 nm region to pass through. This reduced background light on the detector by a factor of 5 while blocking little of the laser

light.

3. There was still enough background light coming into the detector to overload the input amplifers to the electronics. Selcom was able to reduce the gain of the input amplifers by a factor of ten without reducing the signal to noise ratio by an excessive amount.

4. The laser light is switched on and off at 16 kHz. The two outputs from the detector only contain mold level information around the frequency of 16 kHz. High pass filters eliminate much of the huge low frequency or d.c. background of the rippling incandescent pool of metal.

5. The two signals from the detector X_1 and X_2 are synchronously detected at the laser frequency of 16 kHz. That is, the electronics produces the difference in signal from when the laser is on to when the laser is off. The difference should only be the signal generated from the laser reflections.

6. The mold level information is in the difference of the X signals over the sum of the X signals. The circuitry adjusts the laser output to keep the sum of the X signals constant. This insures enough laser illumination to allow determination of metal level without shortening the life of the laser by running it at higher levels than necessary.

7. The electronics only counts mold level measurements that are taken when the laser output is in a normal range and enough signal is being received from the laser. This rejects spurious output caused by beam blockage or specular reflections into the detector.

8. The surface of the melt is turbulent--spurious reflections can image onto the detector when the laser beam is reflected onto the weir face. The laser beam is sometimes reflected on the weir face by the rippling metal surface. This spot on the weir face is seen by the detector (looking at the mirror like metal surface) as an extra laser spot indicating mold level. This caused enormous problems. The weir face was painted with Red Ruby mortar which reduced the infrared reflectance by a factor of three. The weir face was slanted away from the metal pool to minimize the laser reflections that could reach the weir face. Also the software was adjusted so that the level output (calculated 200 times a second from the difference of X signals over the sum) could not change more than 0.03 cm from one calculation to the next. This reflected dot moves very rapidly along the weir face (it is a function of rippling on the surface) so that ignoring any fast moving change in apparent metal level seemed to work.

9. The Selcom generated 200/sec. level signal produced garbage when sampled ten times per second by the analog input of the data acquisition system. To get good mold level readings into the analog I/O in the caster control booth required insertion of a 2 Hz bandwidth RC flter between the Selcom generated 200/sec output and the 10/sec sampling of the digital input of the data acquisition system. (Without the filter, one is sampling high frequency noise which is aliased into the 5 Hz. bandwidth of the digital board.)

Task 3.3C: Mold Level Measurement and Control-Operation of Mold Level Control - The mold level control consists of the Selcom Optocator head which measures level, an ajustable digital control loop within the Selcom computer, a pneumatic controller, and a pneumatic actuator.

The Selcom Optocator head measures level by optical triangulation which with an entered aim level and start up time determines the rod position. At the start of cast, the control system opens the stopper rod to a predetermined offset from the closed position. During this time the bottom of the cast box is filling with metal. When the system detects a rising metal level (the nozzle is now filling with metal) the level in the control loop is set at zero and the time clock is set at zero. The mold level control algorithm takes over. The aim level ramps up from zero to the true aim level over a specified time interval (TSTART). The rod position command consists of a linear combination of the difference between this internal aim level and the measured metal level and the integral (starting from time zero) of this difference.

The rod controller receives a rod command signal and an actual rod position signal. The valve opening is proportional to a linear combination of the difference between the command and the actual rod position and the time integral of that difference.

The valve operation for raising the rod feeds supply pressure into the bottom of the - cylinder and bleeds the top of the cyclinder to atmosphere. Reversing the action lowers the valve operation for the rod.

The control scheme including the pneumatic eficts has been modeled to allow the selection of optimal control parameter values to minimize metal level overshoot and avoid full rod closing under startup and change of metal level conditions. (Full rod closing can cause the stopper nozzle to freeze up.) The parameters of the system were TSTART, aim level, rod offset, rod maximum, rod minimum, rod mechanism friction, air supply pressure; multipiers on proportional rod position error, integral rod position error, proportional level error, integral level error; and integral level error limit.

Figure 1 shows a cast where mold level control was successful. Before the start of cast measurements on the ceramic wool and on the hot refractory imply a level measuring accuracy of +-0. 1 cm. There was a cobble in the beginning that makes the level appear to rise faster than the maximum fill rate (maximum rod opening) will allow. For a few seconds after the bottom fill the stopper rod was closed. The level was controlled within a standard deviation of+-0.2 cm for several minutes until a raise in the aim level was attempted. Mechanical binding or freeze off stopped operation on the change of level. The rod mechanism was known to bind and was subsequently modifed to eliminate the binding.

Figure 2 shows the results of optimal settings in a simulation of level control. On start of cast the rod opens to the rod offset. When the bottom of the box is full the gauge will begin to see the metal level rise. At this point the rod starts closing in order to slow the rate of metal rise to that needed to reach aim level at time TSTART. There is some level overshoot which one tries to minimize. Full closure of the stopper should be avoided to reduce the chance of nozzle freeze-up. Beyond the overshoot, a steady

level must be maintained. The stopper rod mechanism is modeled with friction so that the rod tends to move in jumps. Once the ladel is empty, the rod opens to rod max and the pool level starts to decrease since no new metal is available to replace the metal being cast. Eventually the metal level reaches zero.

Task 3.3D: Substrate Temperature

The substrate temperature is a diffIcult measurement to obtain. The periphery of the wheel is occupied with hot strip. the melt pool, structural, a grit blaster and various other sensors. The wheel is moving and hot (sometimes over 600°C). The obvious noncontact method of using an infrared pyrometer would be difficult to implement. The surface temperature is low enough to require using a long wavelength infrared sensor. The output of such a sensor is very sensitive to emissivity. Furthermore, the emissivity of some of our substrates such as copper can very over an order of magnitude depending on the degree of oxidation.

Three contact methods were investigated. Nanmac Corp. makes an erodable thermocouple assembly (that consists of over 99% of the base (wheel) material) that can be inserted into a tapered hole in the wheel. Only a thin film thermocouple less than 25 μm thick is not base material. These devices can produce accurate readings of the surface temperature until 0.5 cm of the device (and the wheel) has eroded or been machined away. Nanmac Corp. also produces a tapered plug assembly made of the base material that has small thermocouples buried at various depths from the surface Dip tests were done on both types in a heat transfer experiment. Frequent wheel changes and the long delivery time on thermocouples with the right lead placement prevented installation of these sensors. Nanmac Corp. also makes a thin film thermocouple that can slide across the surface of a rotating wheel. The surface temperature so obtained was used on several casts to control the wheel surface temperature by the switching of cooling water zones. The control method worked very well. The only problem was that the sliding thermocouples wore away in about 20 minutes. Fortunately, the thermocouples were quite inexpensive. A production system would require the embedded thermocouples or an optical pyrometer for where the wheel surface emissivity could be stabilized.

Task3.3E: MeltTemperature-Study of Ways to Measure Melt Temperature by Immersion Methods-

One of the parameters to be measured and controlled is melt temperature. The degree of accuracy needed is unknown but certainly it needs to be within +-25°C. A goal for this investigation was temperature measurement within +-5oC. The best measure of melt temperature would be from something that could be immersed in the melt bath. Presently a thermocouple sheathed in a quartz tube about 5 mm in diameter is used. This device has quick response time and good accuracy but its lifetime is limited to a few minutes. On a full sized caster one needs a refractory that will last somewhere close to an hour in liquid steel. It is felt that precise control of melt temperature ($\pm$ 5'C) may be needed and this will require quick response on the part of a ladle or cast box heater. Ladle temperature drops about 0.5°C per second on the present caster setup. The thickness and the thermal conductivity of the refractory must therefore be such that a thermal time constant of around 10 seconds (certainly under 30 seconds) is possible to provide the required control system response time.

Several commercial devices are workable. Mikron makes a device in which the infrared radiation from an immersed well is conducted through a filter optic to a temperature reading instrument. The well can be alumina, zirconia, silicon carbide or graphite. Only the frst two have any hope lasting in liquid steel immersion. Since the initial fill of the cast box takes under 10 sec., thermal shock properties are important--alumina graphite would be a better choice. The device is 0.25% accurate, and the manufacturer estimates the response to be 30 seconds.

There is a thermowell made by Vesuvius consisting of ceramic-cermet-molybdenum that has a 30 second response time and a life of 1-10 hrs. Several other types are available (and usually used for tundish temperature monitoring) using quartz or alumina-graphite. The cost of these devices is around $1000-$4000--the consumable parts are about $100-$500. An exotic immersion device developed by Nippon is a Pt/Rr thermocouple in an aluminum tube inside a ZrB_2 tube coated with a silica fiber that melts upon first contact. This device has less than a 30 second time constant and a 45 hr. life. The cost is unknown. A scaled up caster would need one of these devices. Because of the short cast times on the present machine, the old method of using at Pt. thermocouple in a quartz tube was used since these only cost several dollars and are easy to replace.

Task 3.3E: Melt Temperatures-Measurement of Melt Temperatures by Infrared Thermometers
All objects at temperatures between room temperature and the melting point of metals emit radiation that is primarily infrared. One can determine temperature by measuring the infrared power emitted by an object. Infrared thermometers work on this principle. Infrared thermometers that can be used to determine melt temperature come in 5 types (for my purposes).

One color -- This type measures total infrared power over a band width (usually 0.7-1 μm). The problem is that objects have different emissivities. Emissivity is the ratio of infrared power emitted at a given temperature to the maximum infrared power that can be emitted at that temperature by a perfect black body radiator. The emissivity of slag or oxidized steel is different from that of liquid steel. The error in temperature due to errors in emissivity is % Terror=% error x $T(°K)$ x $\lambda(pm)$ x $6.94x\ 10^{-5}$. For the smallest error, one should use the shortest wavelength at which an acceptable signal level can be obtained. For this temperature range the shortest usable wavelength is around 0.65μm. At that wavelength, 12% emissivity error at 1600°C translates to a 1% temperature error. To stay within 5°C would take an emissivity guess within 3%. Molten steel will have an emissivity ofaround 0.38. Iron oxide and most metal oxides have emissivities of 0.8 to 0.9. Since oxide islands float on the steel surface one can measure melt temperature by measuring oxide temperature using an emissivity of 0.85 and a peak picker. The oxides being thin are very close to the steel temperature and having the higher emissivity will radiate the most energy (and thus be detected as the peaks). The other approach is to use a valley picker on an instrument set for an emissivity of 0.38 and detect the lesser radiation from the clean steel surface to determine temperature.

Two color -- This measures infrared power at two bandwidths determining

temperature from the ratio of those powers. (This is similar to judging the temperature of a glowing object by its color.) One advantage of all two color instruments is that the target can be 90% obscured by smoke, oxide layer or dirt and an accurate reading can still be obtained. This is not true of one color instruments. The two color principle works if object is a grey body--that is the emissivities do not change with wavelength. Two color instruments use an emissivity slope adjustment to compensate for "non-grey" bodies. The error in temperature due to errors in emissivity slope is:

$$\% \text{ Terror} = \% \text{ slope error} \times T \, (°K) \times 6.94 \times 10^{-5}/(1/\lambda_2 - 1/\lambda_1) \, .$$

Two color instruments measure the infrared power almost universally in a narrow band around 1 μm and on a broadband of 0.7 to 1.0 μm. The effective wavelength is 0.85 μm, and a 1.4% slope error at 1600°C gives a 1% temperature error. A 5°C accuracy would limit the error in emissivity slope to .004, which is an order of magnitude better than the values commonly available.

Two Color Chopped -- Some instruments use one detector and alternate color filters to produce two color output to the electronics. This eliminates the need to build a stacked IR detector which expands the choices of wavelengths. If the object is non uniform and moving, the two colors signals may be from two areas of different temperature and emissivity. Error then becomes enormous. Armco has seen the effect when measuring the temperature of moving slabs. Since our pool (especially at the nozzle) has moving oxide islands, chopping devices should not be used.

Three color devices - These are an extension of two color devices. Temperature is determined by ratio as in a two color device. The third wavelength input is used to produce a temperature by the one color method. The output consists of a weighted average of these two temperatures. The weighting is determined by experiment (as one does emissivity on a one color instrument or emissivity slope on a two color instrument). Accurate temperatures can be obtained for such things as molten brass or aluminum which cannot be consistently measured with one or two color devices due to extremely variable emissivities and emissivity slopes (there is not an obvious reason this should work for aluminum and brass). It might work for the oxidized copper surface of some of our casting wheels or for the molten steel in the cast box.

Single Color Plus Laser -- This device uses a laser beam to measure emissivity by measuring distance to the object by time-of-flight and measuring the fraction of laser power that is reflected back into a sensor from the object surface. Pulsing the laser allows laser light to be distinguished from radiant light. At that same wavelength a one color measurement of infrared energy is made. One can then get temperature with some assurrance that the emissivity is correct. The device needs no fudge factors. Specular reflections must be avoided by shooting at an angle to the surface. This angle that must be input into the machine for accurate measurement. At too great of an angle, liquid metals radiate more infrared power than theory of diffuse reflection permits. Errors can result from this. The melt pool temperature continued to be monitored by a quartz encased platinum thermocouple.

Task 3.3F:Strip Thickness Measurement Methods-
There is a need to measure strip thickness a very short time after the material is cast.
The strip thickness coil will probably be used to control the metal level so that strip
thickness can be kept uniform. (High metal level gives thick strip, low metal level
gives thin strip). The strip is very hot (over 1200°C much of the time) and moving so
that noncontact methods should be used. Schemes for measuring strip thickness fall
into two categories--direct and indirect. Direct methods use the attenuation of x-rays
or gamma rays to determine the thickness. Both direct methods have an alloy
dependency. One may have to do several calibrations to cover the alloy ranges of
strip to be cast. The indirect methods measure the distance to the top and distance to
the bottom surface from fixed points and calculate thickness by subtraction of the sum
of the distances from the distance between the fixed points.

The x-ray gauge uses a source that is electrically generated. For this reason the source
is harmless when turned off. Accuracy can be maintained with passline variations of
several inches and air gaps of several feet. Response times of a few milliseconds are
typical. X-ray systems cost around ≈$100K for a C-frame system (which can scan
across the strip width) including environmental protection. The main disadvantage that
C-frame systems are very large. For the present caster a C-frame system would be 2.5
m high 0.6 m wide and 1.5 m deep. There is also the disadvantage of high
maintenance costs on the X-ray source.

The gamma gauges use a radioactive source. The source can be made very safe with
pneumatic shutters and lockouts but it is still active all of the time. Maintenance of the
source is minimal. High accuracy requires a radiation source with Gamma ray
energies in a certain range. If the energy is too high very little of the radiation is
blocked by the strip which means the detector signal has little variation with thickness.
If the energy is too low almost all of the radiation is blocked and the detector doesn't
get enough signal to discriminate thickness. This means that the source energies
available might not fit with the range of thickness needed to be measured. Fortunately,
Cs-137 is a good source for the caster thickness ranges. A single point system from
Berthold with the desired half second response with accuracy of ±6 μm for thicknesses
between .05 cm - .25 cm can be obtained for $20K including environmental protection.
Three of these (to cover the center and both edges) then would cost about $60K
including environmental protection. The air gap was kept to a minimum (10 cm) in
order to minimize the required source strength and minimize the possibility of someone
getting between the source and the detector.

The indirect methods include has eddy-current gauges, capacitance gauges, laser
gauges, μ-wave gauges, and ultrasonic gauges. For the ±25 μm desired accuracy, only
the first three gauge types are feasible. Eddy-current gauges and capacitance gauges
for an air gap of 2 cm to 10 cm (which is needed to accommodate strip handling, off-
flatness and cooling) have to be ~10 cm in diameter. The strip is not always flat over
10 cm so that the apparent measured thickness of the strip would be unacceptably
greater than the true thickness.

Laser gauges can be set up on pairs to read thickness. An air gap of 30 cm with a
passline variation of 2 cm is acceptable for accuracy of ±25 μm. The response time is

a few milliseconds. Of course, alloy dependence is not a problem. A three point system costs $66,000 for the gauges and electronics only. The C-frame (much smaller than for X-ray gauges) that the gauges are mounted on must be water cooled for dimensional stability. Unlike radiation gauges the source-detector separation must be held ±25 μm. The gauges and detectors (six in total) must be environmentally protected.

For compactness--the laser gauges and gamma gauges were good candidates. The installation costs was higher for the laser gauges because the Gamma gauges already have water cooled protection and did not require a water cooled C-frame. Laser gauges were chosen because of the desirability of not handling radioactive sources. I believe in a mill environment, the Gamma gauges would be more robust.

Task 3.3G:Substrate Condition-

Substrate condition is an important facet of single wheel casting. It could be crucial to continuously measure surface roughness, surface oxide and/or surface fluxing conditions. Because of the small features involved in roughness and the high surface temperature, it was felt than an optical approach is needed. The space available for any of these measurements is very limited. Around the wheel periphery one has the casting nozzle, the top of the wheel covered with white-hot strip, a runout table a metal stripper bar, part of the caster frame, a bead blaster and a row of wheel growth sensors. A method to do this was proposed (and tested on the laboratory) on a static surface by Gary Neiheisel of Armco Research. A laser beam is directed by a vibrating mirror (some feet away from the wheel) onto the wheel in a back and forth scan parallel to the wheel axis. The reflected light from the beam is picked up by a 2.5 cm diameter lucite rod placed about 2-5 cm from the wheel and channeled into a fast photomultiplier. The use of filtering on the light detector keeps any light other than that reflected off of the wheel by the laser from being detected. The electrical output from the photomultiplier at any instant corresponds to the light reflected from the spot that the laser beam is illuminating at that instant. When the detector output versus laser dot position was "plotted on an oscilloscope, " as in the lab demonstration, small roughness features such as circumferential scratches could be easily seen. Scanning the beam vertically by 1-4 cm at 30 times a second the output could be used to produce a video of the roughness over a 1-4 cm strip across the width of the caster wheel. Note that the frequency of change of reflectivity along the wheel width and circumference is similar to the width and height of surface roughness features. The degree of change of reflectivity is related to feature depth and the overall reflectivity over a small area is related to the amount of surface oxide. Determination of the method of analysis of the output has not been done. The use of two different laser colors might allow simultaneous analysis of fluxing and oxide conditions.

Task 3.3H: Thermal Imaging of the Strip

Thermal imaging works on the principle that all objects emit thermal radiation. (For room temperature to the melting point of metals this radiation is in the infrared to visible regions.) The amount of radiation emitted at a certain wavelength by a certain area of a certain temperature is proportional to $\varepsilon\lambda^{-5}\exp(-14400/\lambda T)$ where ε is the emissivity, λ is the wavelength in μm and T is the absolute temperature in degrees Kelvin. (Emissivity is the ratio of radiation at a certain wavelength emitted at all angles of a certain area at a certain temperature to the amount of radiation at a that same wavelength emitted at all angles by a perfect black body of the same size and shape at the same temperature. A perfect blackbody emits the theoretical maximum amount of radiation.)

If one can guess at the emissivity, the amount of radiation emitted by an certain area of an object can be used to determine its temperature. If an object is imaged on the pixel array of a video camera sensitive to the wavelengths at which radiation is emitted--one can produce the temperature distribution of an object as a function of time.

The system consisted of a camera, a computer, and video board that converted pixel brightness into a temperature which was then translated into a color. A real time, false color video results with different colors corresponding to different temperature ranges.

For the purposes of strip casting, a real time view of strip cooling just after formation was considered more important than the top pool temperatures in the nozzle. One needs a camera sensitive to wavelengths at which the cooling strip radiates. For strip temperatures on the wheel (1200°-1500°C), 99% of the thermal radiation lies in the wavelength region of 0.75 um to 20 um so the selection should be made in these wavelengths. The choice can be narrowed down by attempting to minimize the effect of error in emissitivy on the measured temperature. The % error of temperature is the % error of emissivity multiplied by $T\lambda/14400$. Obviously the shorter wavelength (smaller λ) the better, as long as enough radiation is received in the wavelength to overcome background noise, camera noise and background light. An infrared filter was used on the camera in order to narrow the bandwidth of the instrument to 0.70 μm to 0.30 um (the 1% response points) There was still enough signal to obtain good temperature readings. If there had been too much interference from ambient light one could shift the response curve further into the infrared.

The amount of infrared energy emitted in that bandwidth varies enormously with temperature. The effects of variable emissivity can be minimized because the temperature effect overwhelms the emissivity error effect. Theoretically one should receive thirteen times more radiation at 1500°C than at 1200°C in that 0.70 um to 0.30 um band. To measure temperature at 1200°C within 10°C requires the noise level to be less than 1% of the signal level at 1500°C so that one needs a signal to noise ratio of over 40 db in the temperature measurement system.

The selection of cameras was restricted to those with signal to noise ratios of over 50 db because the required range of temperature could not be specified since the caster design was continually evolving. (The brightness varies tremendously over the moving

strip.) The cameras were limited to ones with interframe transfer CCD detectors. A camera of this type with a signal to noise ratio of 56 db was obtained from Cohu. The signal to noise ratio of 630 to 1 was not the limiting factor. The limiting factor was the 8 bit quantitation limit (allows only 256 levels of infrared intensity) of the storage boards in the computer. (A gamma adjustment on the camera allows it to output a signal proportional to the 0.4 power of brightness rather than a signal linear with brightness. This would reduce the signal range out of the camera to about 4 to 1 for the range 1200°C to 1500°C and make the limiting factor the camera noise rather than the quantization noise. It turned out the gamma adjustment didn't effect the low level signals - so the signal range wasn't any smaller than before. For that reason the gamma adjustment was left at one). In actual practice if   1500°C was the highest temperature, 1125°C represented the calibration noise floor. At 1200°C an error of 8° C resulted from the noise floor.

Because of uncertainties in camera sensitivity with wavelength, lens absorption with wavelength and nonlinearities in the electronics and VCR it was felt necessary to use a blackbody source to do multiple point calibration. A blackbody calibrator is a variable temperature source that behaves almost like a perfect blackbody (emissivity >.99). A sixteen point calibration over the temperatures of 1125°C to 1500°C was used.

 The camera's pixels see a brightness from the strip and from the blackbody source that is independent of source angle or distance. Doubling the distance to a source causes a pixel to get the image from an area twice as big on each side (or 4 x the area). The light received at the pixel from a given area reduces as the square of the distance so that the pixel receives only 1/4 as much light per unit strip area. These two factors cancel each other. Thus there is no effect of distance from the blackbody source to the camera on the calibration. Viewing at a angle reduces the light received at the pixel by a given area by a cosine factor of the angle of tilt but the pixel "sees" 1/cos times more area. There is also no effect of the angle or of (due to geometric effects) the strip with respect to the camera or of the distance of the strip from the camera when taking measurements.

There are two sources of error other than electrical noise. One is an effect seen only on the unoxidized surface of the strip (or the molten metal pool). The radiation is emitted preferentially at low angles to the surface. This makes unoxidized strip viewed at a low angle look hotter that its emissivity and temperature would indicate. Most of the time the strip is oxidized sufficiently to minimize this effect within 4" of the pool and closer to the pool the strip looks like churning liquid. The second source of error is due to emissivity. The calibration results showed that 10% error in emissivity would result in 0.4% (at 1200°C) to 0.7% (at 1500°C) error in temperature. The camera is calibrated with a blackbody (emissivity of 1.0) source. A light oxide (emissivity of 0.8) should cause only a 1-1.5% error in the measured temperature. This error would apply to the oxidized strip and the oxide islands on the melt pool. The melt pool or unoxidized strip has an emissivity of 0.38 causing a temperature error of 5-7%.

The present system using the 16 point calibration produces a 16 color based temperature plot on real time of strip moving out of the pool onto the casting wheel. The possible 16 colors limit the accuracy of the temperature to ±25 C. On oxidized

strip the total error in temperature was ±50 C. The system turned out to be 1/5 the cost of a commercial video temperature measurement system.

Tundish Scale Method of Mold Control

A scheme was developed to measure nozzle drag and cast box metal level all at the same time using load cells on the three pair box mounts. The cast box would be mounted so that cables and hose connections don't apply a varying force on the box during casting. There would be very little motion in the load cells so that the stiffness of hoses and wires does not affect the measurement. The output of the load cells measured just before the stopper rod is opened could be used to mill out forces due to the cast box weight, the springs on the SEN holder, the weight or forces applied by hoses and wiring, and the weight of added items such as the bath thermocouple and the plug in the burner hole.

One problem was how to calibrate the cast box for mold level. It turns out that the inner dimensions of the box are constant enough during casting and measurable enough prior to casting to make this weighing method feasible. The rest is algebra easily done in real time on a computer.

Let $C(z)$ = cross sectional area of cast box at height z
        $G(z)$ = center of mass of sheet of metal of cross section of cast box at height z
        Xj, Yj = coordinates of load cell support j
        Wj = weight reading of load cell j
        Woj = weight reading of load cell j - cast box empty
        Xk, Yk = coordinates of center of nozzle side contact
        Nk = nozzle drag (K=4 North, K=5 South (bottom is ignored)

The equations for solving metal level and nozzle drag are:

Forces
$$W1-Wo1+W2-Wo2+W3-Wo3 = rho * \int C(z)dz + N4 + N5$$
Torques
$$(W1-Wo1)*x1+(W2-Wo2)*x2+(W3-Wo3)*x3 = rho * \int C(z)Gx(z)dz + N4*x4 + N5*x5$$
$$(W1-Wo1)*y1+(W2-Wo2)*y2+(W3-Wo3)*y3 = rho * \int C(z)Gy(z)dz + N4*y4 + N5*y5$$

The integrals can be evaluated by taking horizontal slices through the cast box whenever a change in the shape of the box sides occurs and at the zero and maximum design metal level. Since the side walls of the box, overflow, weir and nozzle are basically vertical one can assume that $C(z)$, $Gy(z)$, and $Gx(z)$ are linear in height between slices. That means that the mass of material between slices at z = h1, and z = h2 can be written as:
$$C1(z)=a1+b1*z \quad a1=[h2*C(h1)-h1*C(h2)]/(h2-h1) \quad b1=[C(h2)-C(h1)]/(h2-h1)$$
and the center of mass is
$$Gx1(z)=cx1+dx1*z \quad cx1=[h2*Gx(h1)-h1*Gx(h2)]/(h2-h1) \quad dx1=[Gx(h2)-Gx(h1)]/(h2-h1)$$
$$Gy1(z)=cy1+dy1*z \quad cy1=[h2*Gy(h1)-h1*Gy(h2)]/(h2-h1) \quad dy1=[Gy(h2)-Gy(h1)]/(h2-h1)$$
Using h1 as the floor bottom

        h2 as height where the nozzle runner slope changes
        h3 as height where metal level equals zero (lower lip of casting nozzle)

h4 as metal level design maximum
m as actual metal level

The formulas become:

W1-Wo1+W2-Wo2+W3-Wo3-N4-N5=rho*[a1(h2-h1)+a2(h3-h2)+a3(m-h3)] +
            rho*[b1(h2*h2-h1*h1)+b2(h3*h3-h2*h2)+b3(m*m-h3*h3)]/2

(W1-Wo1)*x1+(W2-Wo2)*x2+(W3-Wo3)*x3-N4*x4-N5*x5=
        rho*[a1*cx1(h2-h1)+a2*cx2(h3-h2)+a3*cx3(m-h3)]+
        rho*[(a1*dx1+b1*cx1)(h2*h2-h1*h1)+(a2*dx2+b2*cx2)(h3*h3-h2*h2)+
        (a3*dx3+b3*cx3)(m*m-h3*h3)]/2+
        rho*[b1*dx1(h2*h2*h2-h1*h1*h1)+b2*dx2(h3*h3*h3-h2*h2*h2)+
        b3*dx3(m*m*m-h3*h3*h3)]/3

and similarly for y.

One can predetermine everything but Wj's Wk's and m before the cast. The formulas
look like:

        W1-Wo1+W2-Wo2+W3-Wo3-N4-N5=
            A+B*m+C*m*m
        (W1-Wo1)*x1+(W2-Wo2)*x2+(W3-Wo3)*x3-N4*x4-N5*x5=
            C+D*m+E*m*m+F*m*m*m
        (W1-Wo1)*y1+(W2-Wo2)*y2+(W3-Wo3)*y3-N4*y4-N5*y5=
            G+H*m+I*m*m+J*m*m*m

When Wj are measured, a computer program determines the unknowns N4, N5 and m
from the three equations. Note: N4 and N5 are values of nozzle drag assuming drag
originates near the center of the side wings. What the bottom does is not
determinable. Basically, N4+N5 is the total drag on the nozzle. N4-N5 is an estimate
of the difference in nozzle drag between the North and South side.

        Jerry W. Allen
        Research Engineer
        Casting
        Research & Technology

JWA2jh

M maybe--can mount in swing away fashion or mount off of abort frame such that the abort doesn't cause mechanical interference.

CHART I

	Discrete Electrode	Bubbling Gas	Refractory Float	Load Cells	Laser Diffuse	Laser AT	µ Wave AT	Gamma Ray	Dip Electrode	IR Imaging	Eddy Suspended	Eddy Buried Coil
Commercially Available or Easy to Develop			X	X				X			X	X
Immune to Dust Smoke	X	X	X	X			X	X	X		X	X
Easy to Calibrate		X	X	X		X	X	X	X	X		
Measures at Lip					X	X				X	M	
One Set Up All Boxes	X	X	X	X	X	X	X	M	X	X	X	
One Set Up All Lids				X	X	X	X	X		X	M	X
Inexpensive	X	X	X	X	X	X			X	X		
No Extra Connections to Box Assembly					X	X	M	M		X	M	
No Delicate Mechanicals	X	X		X	X	X	X	X		X	X	X
No Metal Contact				X	X	X	X	X		X	X	X

Selcom Metal Level Control

Figure 1

Figure2-Mold Level Simulation

Position or Level in Meters

Time From Start Of Cast

Legend:
Ladle Level x 0.1
Aim Level
Actual Level
Rod Position

MOLDSIM.XLC
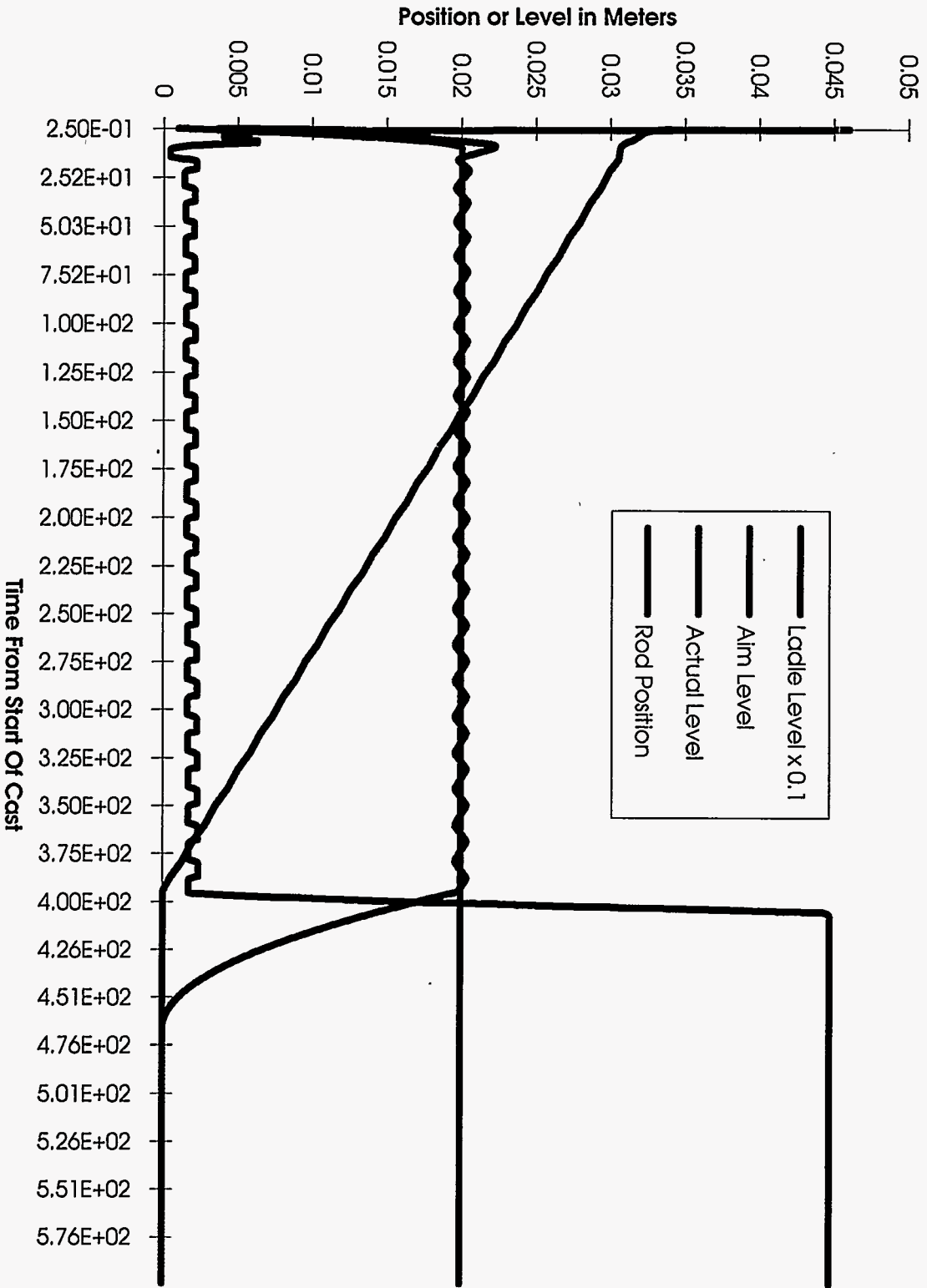
Appendix VIII

Summary of Refractory Development
for 12-Inch Strip Casting Nozzles
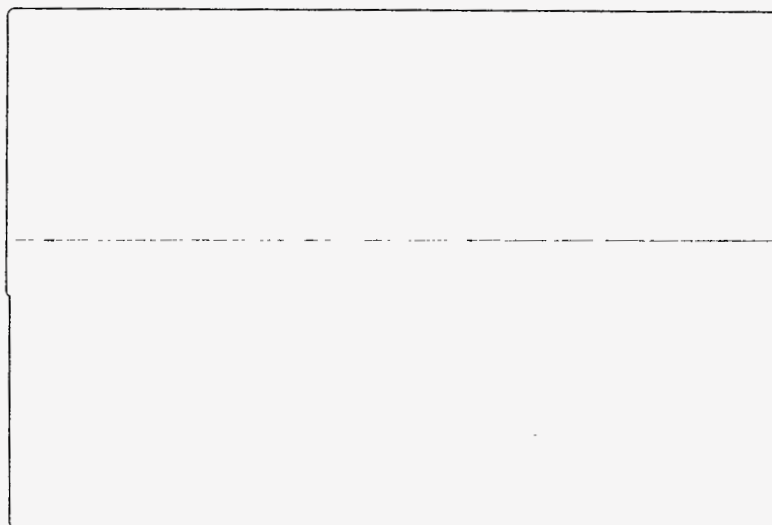
APPENDIX I

Zirconia Brick Sidewalls
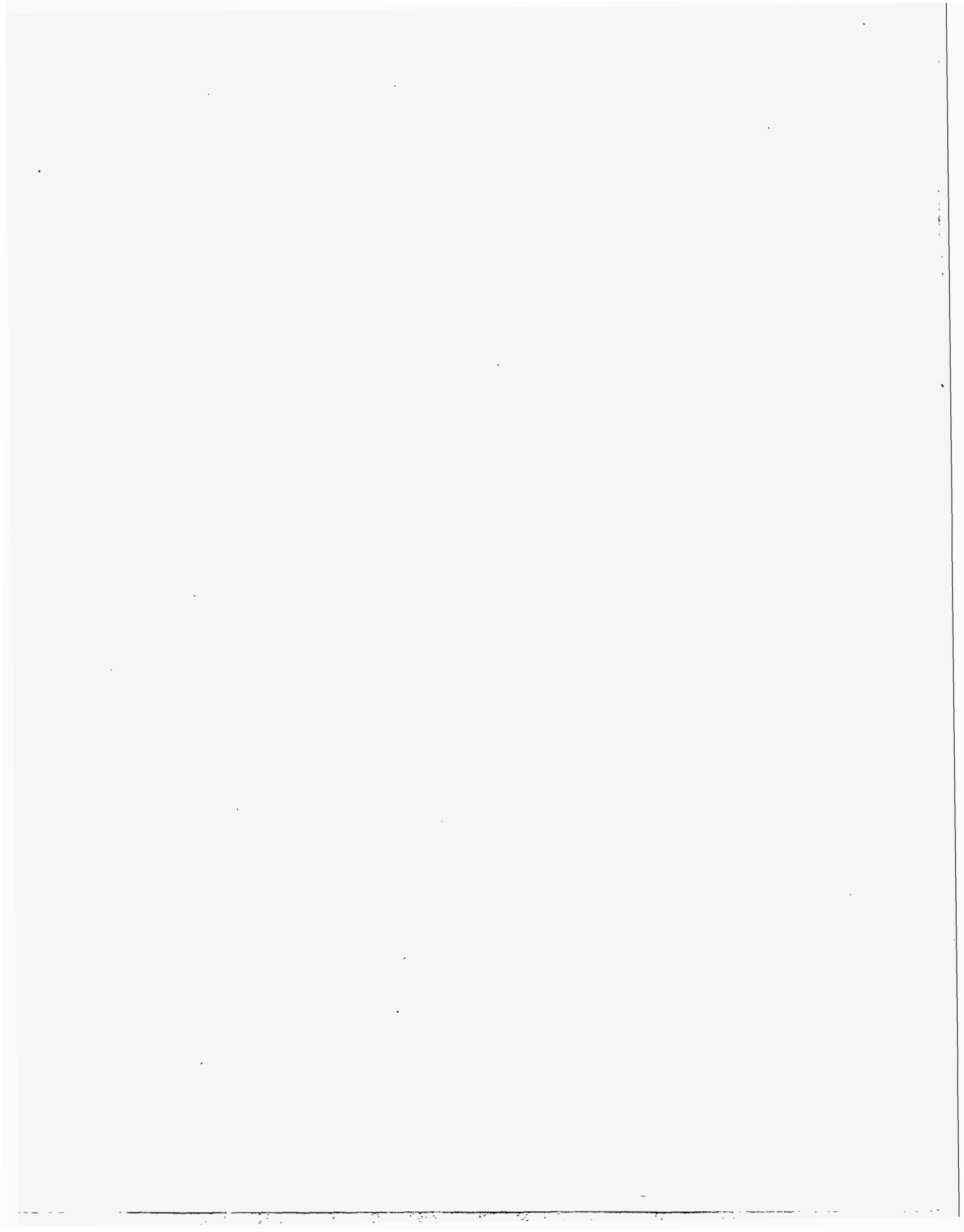
July 14, 1992

To: R. S. Williams
            Senior Research Engineer
            Casting Group - R&T

From: R. Engel

Subject: Comparison of Two Zirconia Brick for Nozzle Application
            D0204 - Report #1, Interim

SUMMARY

Two zirconia brick developed by Narco for use in the strip casting nozzle application were analyzed with the electron microprobe to determine the phases present. The only difference between the two brick was supposed to be the grain sizing with the one labeled 3006 being coarser than the Z-240 one. Microprobe work showed that the 3006 brick has the expected phases for a partially stabilized zirconia brick, while Z-240 has totally different ones present. An identification of these latter phases is being attempted.

A comparison of the Narco brick to the zirconia brick used for the qualifying runs of the original DOE contract shows 3006 to be very similar to it in percentage of tetragonal to monoclinic phases and chemistry.

INTRODUCTION

Work carried out under the previous DOE contract had shown that zirconia is not only a suitable, but a highly successful refractory for use as a nozzle for strip casting. Armco decided that in the new contract the most efficient way to operate was to have a refractory subcontractor which would develop and manufacture the zirconia nozzle brick and help in other refractory areas as well. North American Refractories Co. (Narco) was selected to be this refractory subcontractor.

In their capacity as subcontractors, Narco did laboratory testing of several mixes, whose main variation was the grain sizing. Of these mixes, two were deemed to be the most likely to fulfill

the requirements of good thermal shock resistance and good slag resistance. Bars used for dip tests in an induction furnace were given to Armco for determination of amount of zirconia stabilization. This report will document the findings. In addition, physical properties, as determined by Narco, of the mixes will also be presented.

BACKGROUND

The original DOE contract contained a clause which required success in 5 out of 7 consecutive strip casting attempts with success being defined as the production of strip in considerable quantity. To accomplish this feat, experimental zirconia brick manufactured by Didier of Cincinnati, Ohio was used. These brick were made out of Zettral 95 rework (rework is fired brick which is ground up and used in making a new brick, i.e., it is a way of recycling) which is a German mix produced overseas and send to the USA for pressing and firing. In addition, the brick underwent a special firing sequence. Due to the success achieved with these brick, more were requested. The next shipment did not work in service, although the claim was made that the brick were identical to the first batch. Two other attempts were made to duplicate service properties of the first batch with mixed results. The last one was the closest duplication and provided the basis for the Narco work.

DIDIER/NARCO AND ARMCO RELATIONSHIP

Didier is the largest refractory company in the world. Their headquarters are located in Wiesbaden, Germany. During the time the above mentioned work was being carried out, Didier bought Zircoa, a US company which specializes in the manufacture of zirconia products. At that time, no cross-fertilization between Didier, Cincinnati and Zircoa was allowed. At a later date, Didier bought Narco, a major US refractory company, which had no experience with the manufacture of zirconia parts. As part of the purchase agreement, Narco was to be in charge of all the North American refractory business as it pertained to steel. Soon after the purchase, dialog and interaction between Zircoa and Narco was approved. In addition, Didier ceased to be a refractory presence for the US steel industry. As the original DOE qualifying work was carried out using Didier's zirconia brick, a suitable replacement had to be found.

No relationship existed between Zircoa and Armco Research which meant that no knowledge of their capabilities was available to draw upon for possible cooperative work in strip casting. A trip was taken to Zircoa to determine the extend of their capabilities, amount of research and development which they could carry out and general willingness to work with Armco on this project. The evaluation was positive from Research's point of view and the possibility for Zircoa to become a subcontractor was discussed with them. At that time, Zircoa decided that they did not want to be the subcontractor, but that Narco should take on that role. Zircoa would do mix development for Narco when requested and also teach Narco to work with zirconias. Most of

stabilized zirconia in any given sample is generally determined via X-ray diffraction methods, which are not very accurate.

SAMPLE CHARACTERIZATION

Two different grain sizings were used to produce brick with the identifiers 3006 and Z-240. 3006 is the coarser of the two, but chemically they are the same. Table 1 is a listing of the physical properties of the samples as established by Narco. Figures 2 and 3 are dilatometer curves obtained from the mixes. Table 2 shows the chemical analysis and phases present of the same samples as determined by Zircoa.

MICROSCOPY

Brick pieces used in a dip test to determine slag/steel penetration were made into samples for the microprobe. Electron microprobe was picked because this tool is capable of very accurate compositional analysis of small areas. In addition, a technique using backscattered electrons for imaging purposes was discovered[4] to differentiate optically between partially and unstabilized zirconia.

Samples of suitable size for microprobe work were made from each brick type. Light microscopy was used to make an initial evaluation of the samples and new ones had to be made for the 3006 as all areas had been infiltrated with slag.

3006

As received: Figures 4 to 7 show the morphology of the sample in backscattered mode and the distribution (X-ray maps) of Si, Mg and Zr in the area shown in Figure 4. The Si is concentrated in the intergranular spaces and forms the glue which holds the zirconia grains together. The Mg can be found in great concentration with the silica and, in lower amounts, in the zirconia grains where it is the stabilizer. Optically, the zirconia grains containing Mg have a darker appearance than their pure counterparts and also have light and dark lines in them. The Zr is evenly distributed in the zirconia grains.

After dip test: Figures 8 to 11 show the changes in appearance of the brick due to its exposure to steel and the elemental distribution of Si, Mg and Zr. Optically (Fig. 8), the zirconia grains have been caught while destabilizing, white core vs. gray outer rim. Figure 10 shows that the core of the zirconia grains is devoid of Mg while some of it remains in the outer areas. Another telltale sign of the zirconia destabilizing is that the big grains are breaking down into multiple smaller ones. Note: magnification is only 500X while the previous set of pictures was done at

1000X. The Si (Fig. 9) stayed concentrated in the interstitial areas together with the Mg. The Zr is evenly distributed throughout the sample (Fig. 11).

Figure 12 shows the zirconia grain used to obtain EDS plots. Point 1 is in the interior of the grain and the plot shows only Zr present (Plot 1). When an edge point is analyzed (point 2) the EDS plot (Plot 2) shows the presence of a little Mg, but also Ca from the slag. Point 3 (Plot 3) contains typical slag making elements.

Z-240

As received: Microprobe work showed that this brick was made up of a different raw material than all previously studied zirconias (Fig. 13). The individual grains did contain areas with and without Mg (Fig. 14), but none showed the characteristic optical pattern associated with partially stabilized zirconia.

After dip test: Figure 15 shows the brick after exposure to slag/steel. The zirconia grains have broken down into many smaller ones with the areas lacking Mg expanding (Fig. 16), but again, no typical stabilized zirconia pattern could be found.

CONCLUSIONS

Mix 3006 is very similar in chemistry, percentage of monoclinic to tetragonal phases and porosity to the original good zirconia brick. Mix Z-240 is totally different and cannot be compared.

Although the chemical analysis and physical properties of the 3006 and Z-240 brick are very close, the microscopy work showed that they are totally different in crystallography. A hint of something unusual was provided during the hot strength testing where the Z-240 brick fell apart if left at high temperature overnight, while nothing happened to the 3006. As no data were generated, it was not reported in the data summary sheet.

The findings of this study show that many phases can be present in a brick which have the same chemistry, but behave very differently in service. In addition, the tests employed to determine physical properties may not be sensitive enough or may be the wrong tests to determine differences in the crystallography of the refractory.
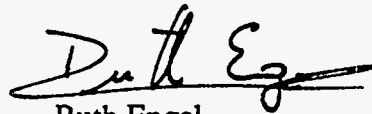
WORK IN PROGRESS

X-ray diffraction will be used to attempt to determine the nature of the phases present in the Z-240 brick. If this method is not sensitive enough, then transmission electron microscopy can be

used for this effect. If it is necessary to obtain this information, arrangements can be made to have the samples analyzed.

A different mix, 1936, will also be scrutinized with the microprobe to determine its phases as it showed some promise for nozzle application. This mix is another one which supposedly had the same chemistry as 3006, but different grain sizing.

Ruth Engel
Senior Research Engineer
RMI&R
Research & Technology

RE214

cc: J. W. Allen
       S. L. Campbell
       E. R. Case
       F. S. Cox
       D. W. Follstaedt
       S. W. Gilby
       K. Schneider
       J. R. Sauer
       R. C. Sussman

REFERENCES

1. Letter to R. Williams, June 23, 1992, "Summary of RPA RE928-7 Armco-DOE; Thin Strip Casting."
2. Thermoschockverhalten feuerfester Baustoffe aus Zirconiumdioxid, E. Protogerakis, Didier-Werke.
3. "High Temperature Materials and Technology," I. E. Campbell and E. M. Sherwood, John Wiley and Sons, Inc., 1967.
4. Letter to D. Follstaedt, Jan. 30, 1991, "Analysis of Used Zirconia Nozzle Brick."

TABLE 1

ZIRCONIA NOZZLE PROPERTIES

	3006	Z-240
Bulk Density, G/CC	4.60	4.49
Open Porosity, %	18.7	20.4
Specific Gravity	5.65	5.64
Flexural Strength @ Room Temp.		
MPa 15 Min. Preheat	28.4	23.8
PSi	4,220	3,460
Flexural Strength @ 1450 Deg. C		
MPa 15 Min. Preheat	10.9	N.D.
PSi	1,575	N.D.
Flexural Strength @ 1550 Deg. C		
MPa 15 Min. Preheat	4.3	N.D.
PSi	620	N.D.
Flexural Strength @ 1550 Deg. C		
MPa 15 Hours Preheat	2.1	5.5
PSi	300	790
Fracture Toughness @ RT MPaMexp-0.5	1.90	1.65
Elastic Modulus @ RT, GPA	46.7	44.1
PSi (X10EXP6)	6.8	6.4
Chemical Corrosion (Ind. Furnace)		
Eroded Area, In. SQR @ 1700C	0.13	0.16
Destroyed Area, In. SQR	4.98	5.13
Penetrated Area, In. SQR	0.13	1.66

RE214A/s

TABLE 2

CHEMICAL ANALYSIS, WT. %

	3006	Z-240
SiO_2	1.06	1.32
CaO	0.25	0.36
MgO	2.26	2.87
Fe_2O_3	0.13	0.12
Al_2O_3	0.54	0.07
TiO_2	0.13	0.07
$ZrO_2 + HfO_2$ (by diff.)	95.63	95.19

MONOCLINIC PHASE, %

3006	Z-240
50	43

RE214A/S
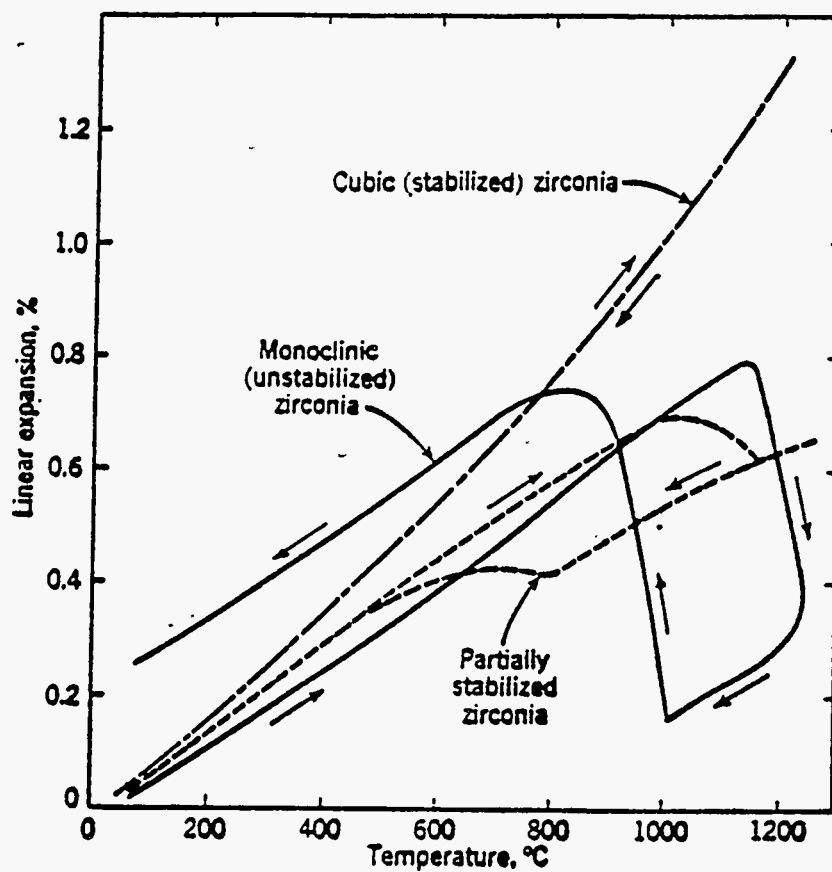
Figure 1. Dimensional changes as a function of temperature for different zirconias.

THERMAL EXPANSION
ZIRCOA 3006 BRAND
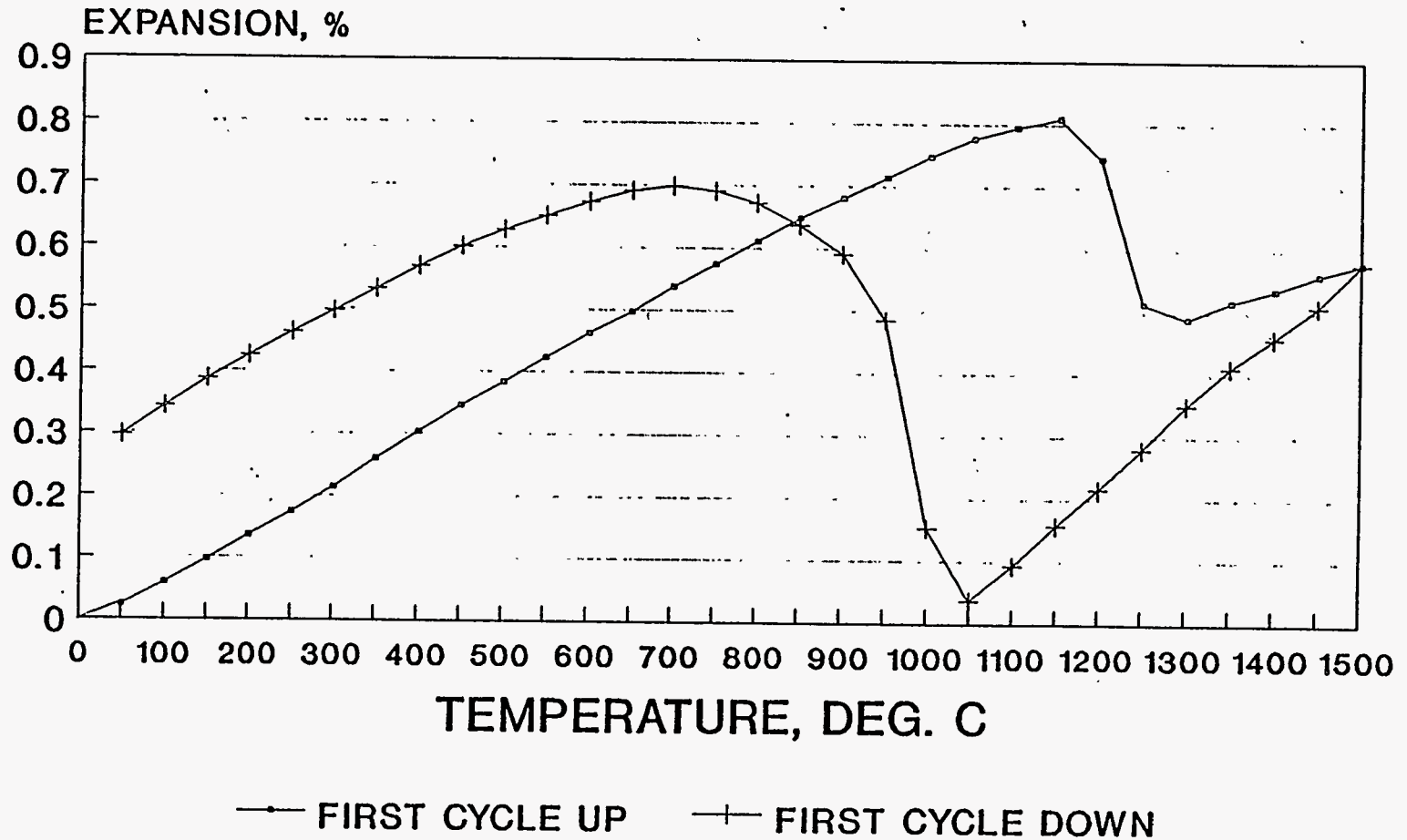
Figure 2

THERMAL EXPANSION
ZIRCOA Z-240 BRAND

EXPANSION, %

TEMPERATURE, DEG. C
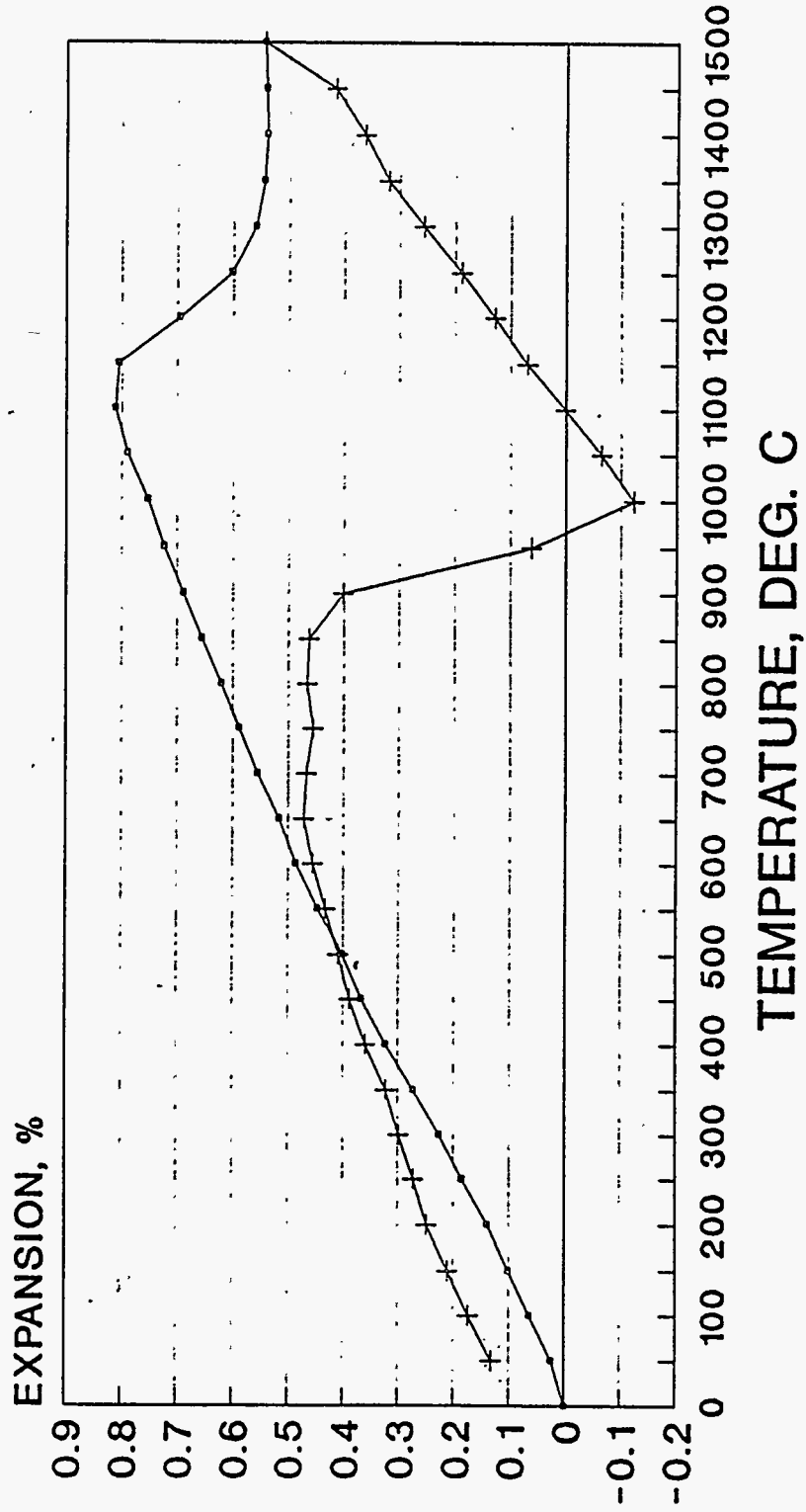
—□— FIRST CYCLE UP   —+— FIRST CYCLE DOWN

Figure 3
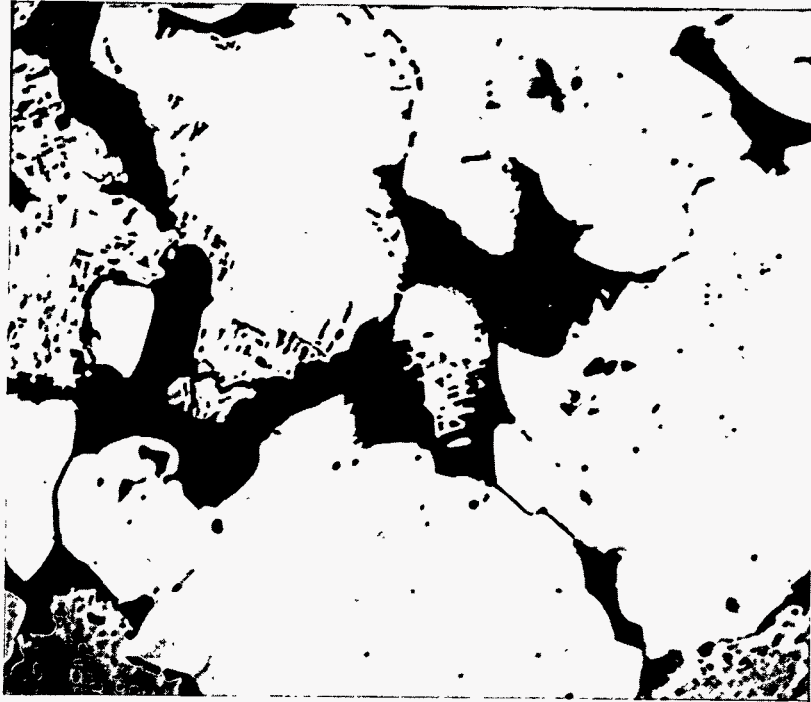
Figure 4. Backscattered electron microprobe photograph of a typical area of sample 3006 in the as-received condition. Magnification: 1000X.
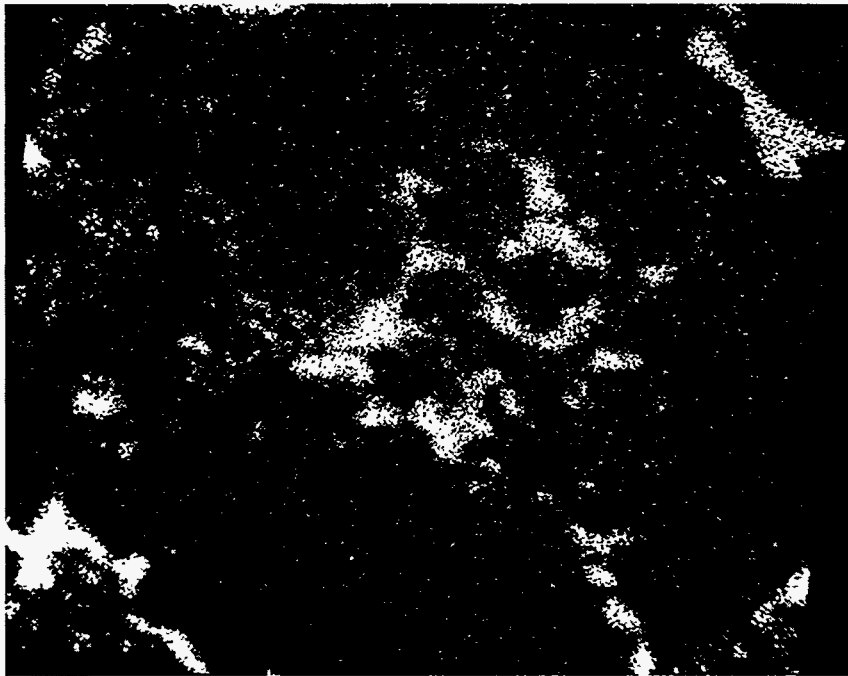
**Figure 5.** X-ray map of the distribution of Si in the area shown in Figure 4.
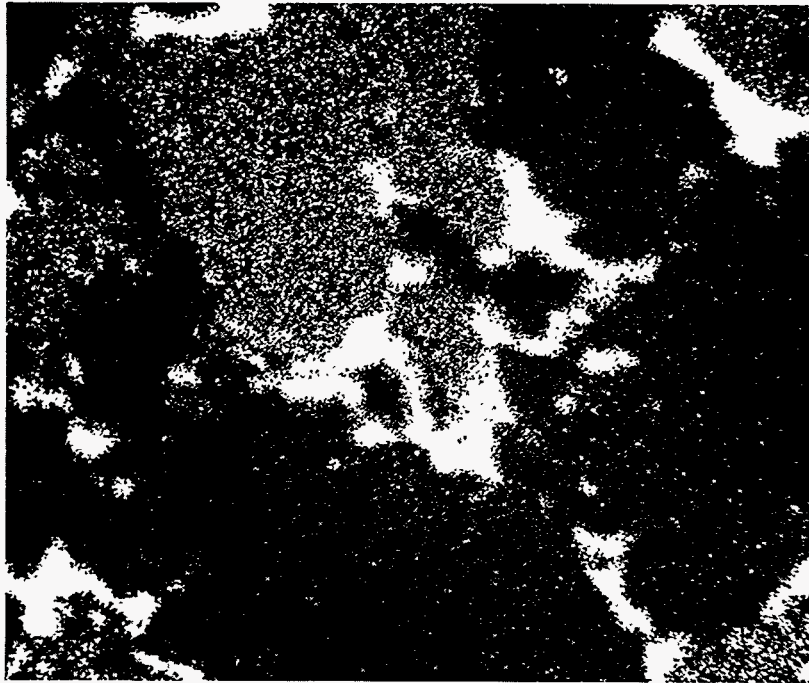
Figure 6. X-ray map of the distribution of Mg in the area shown in Figure 4.
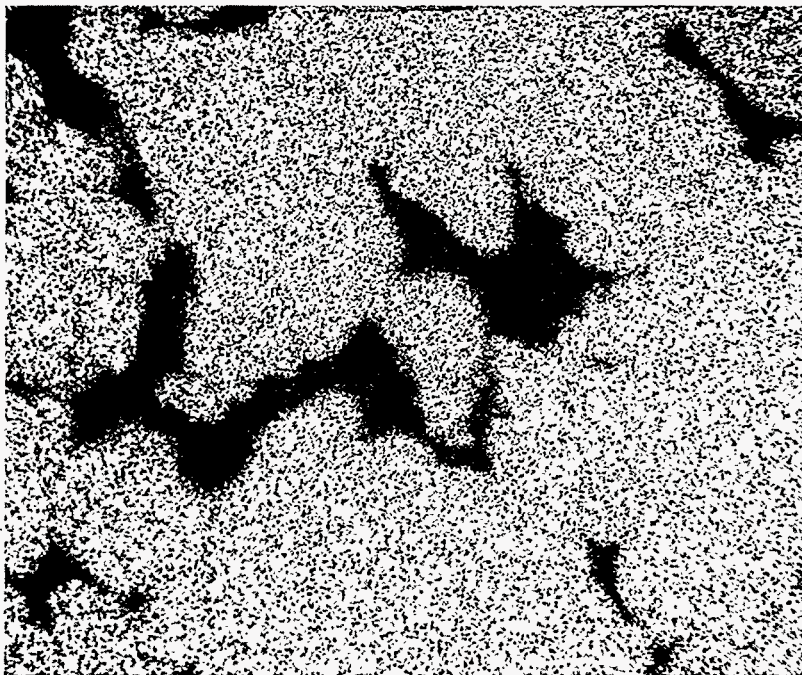
Figure 7. X-ray map of the distribution of Zr in the area shown in Figure 4.
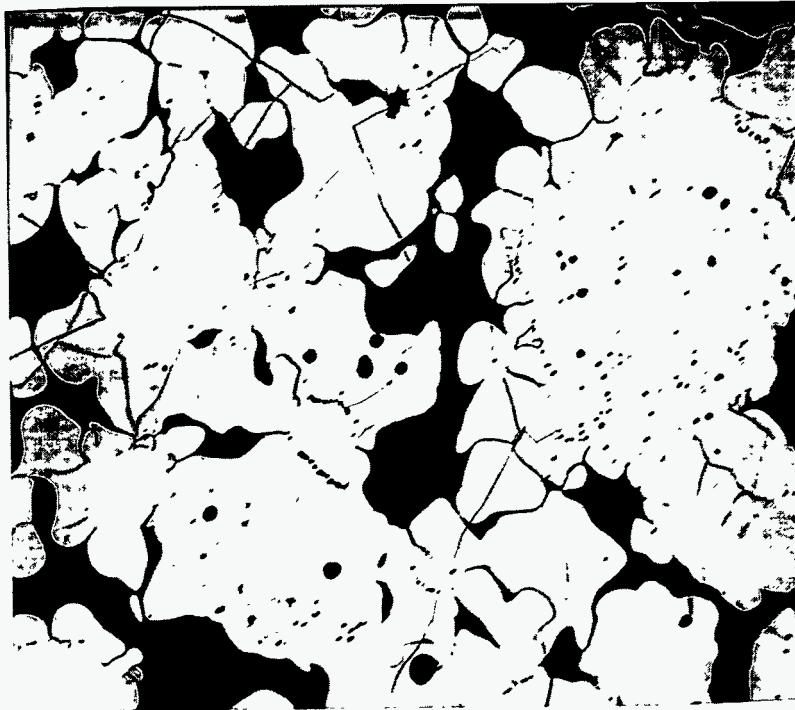
Figure 8.   Electron microprobe photograph of a typical area
             of sample 3006 after exposure to steel/slag.
             Magnification: 500X.
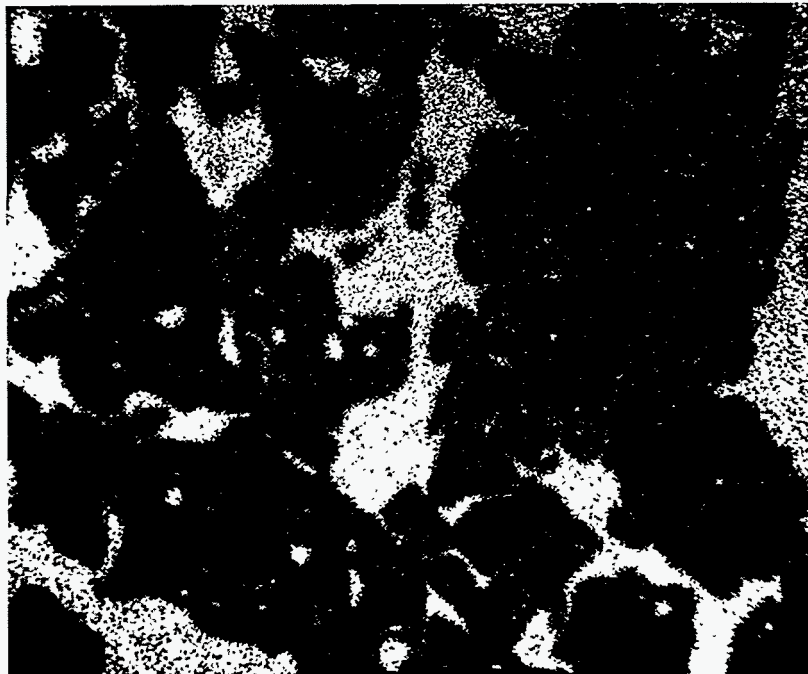
Figure 9.   X-ray map of the distribution of Si in the area
             shown in Figure 8.
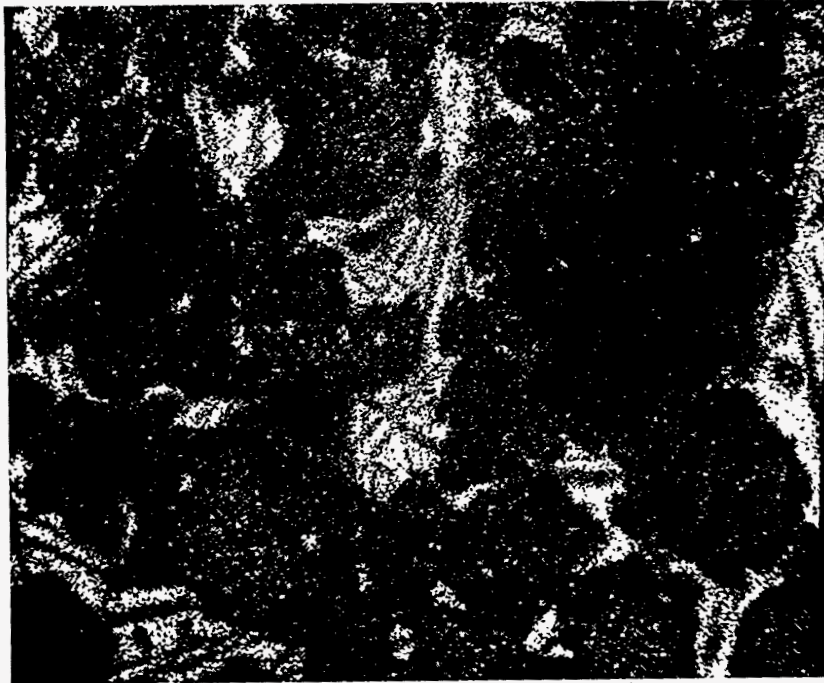
Figure 10. X-ray map of the distribution of Mg in the area shown in Figure 8.
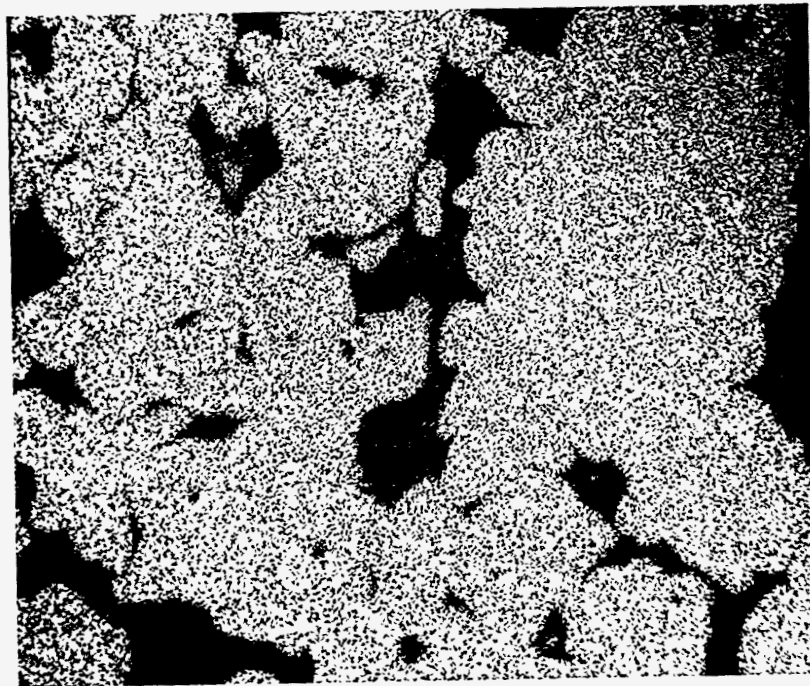
Figure 11. X-ray map of the distribution of Zr in the area shown in Figure 8.
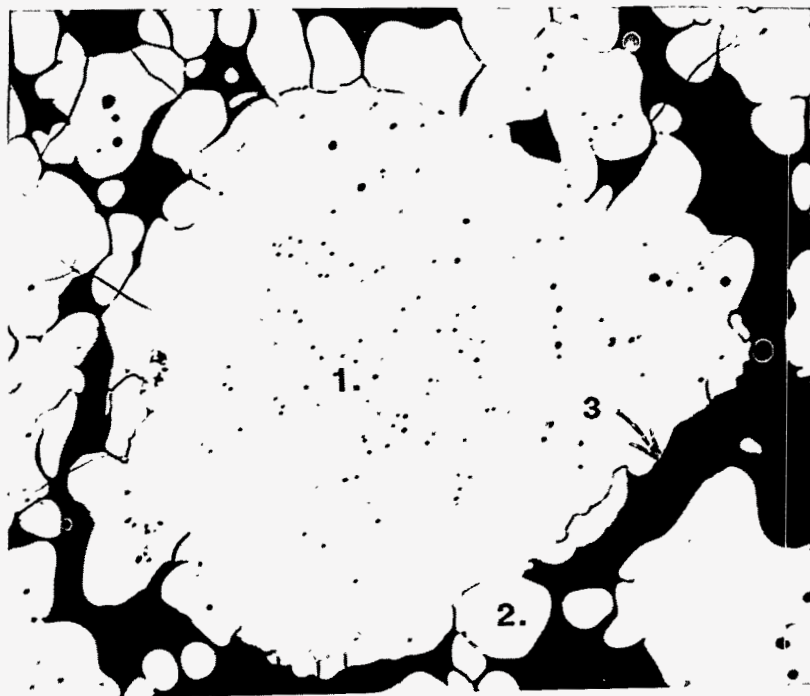
Figure 12. Zirconia grain used to generate EDS plots. Magnification: 500X.

21-May-1992 10:21:05

RUTH7
Vert= 3724 counts

Plot #1: Center of Grain in
Sample #2
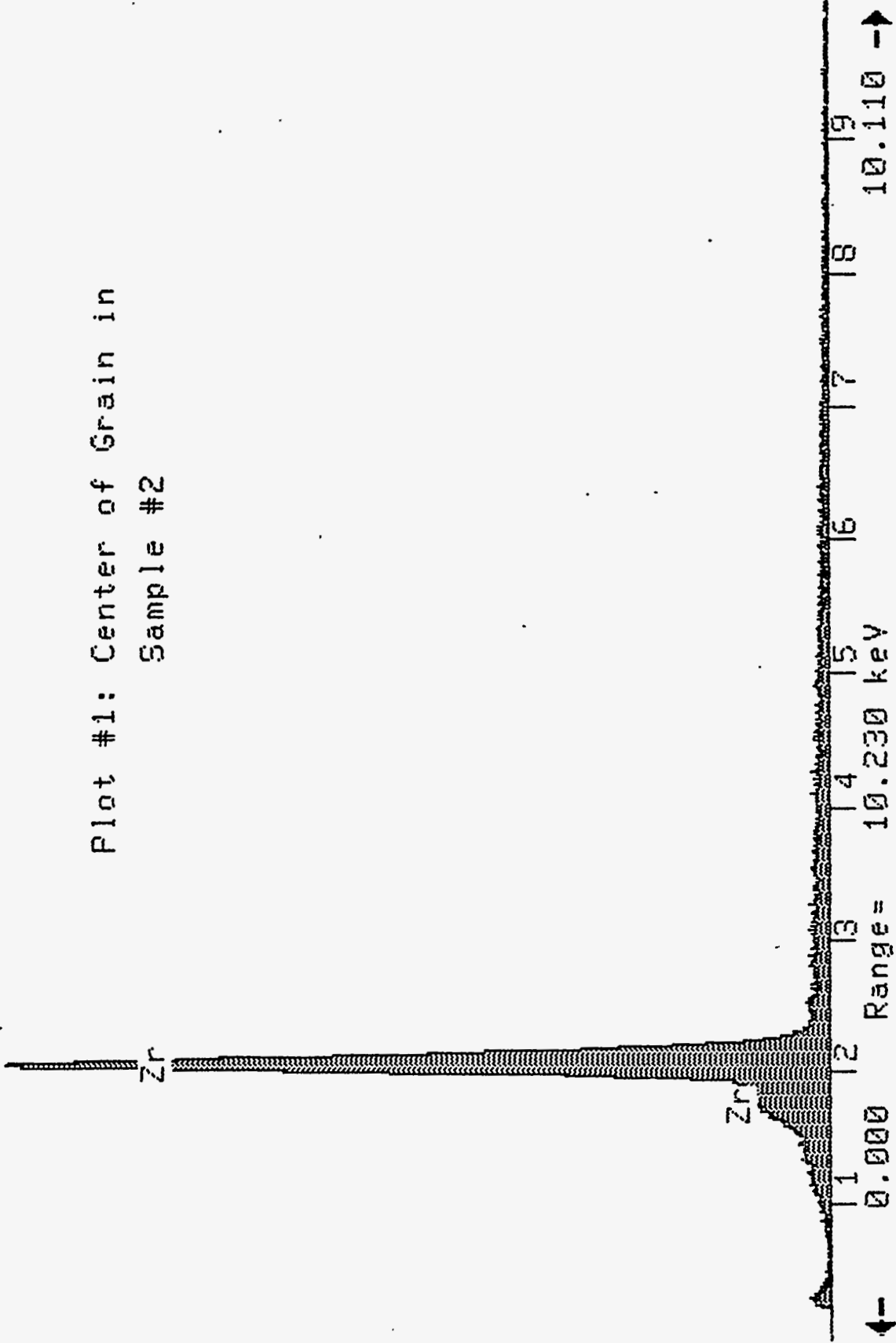
Zr

Zr

Zr
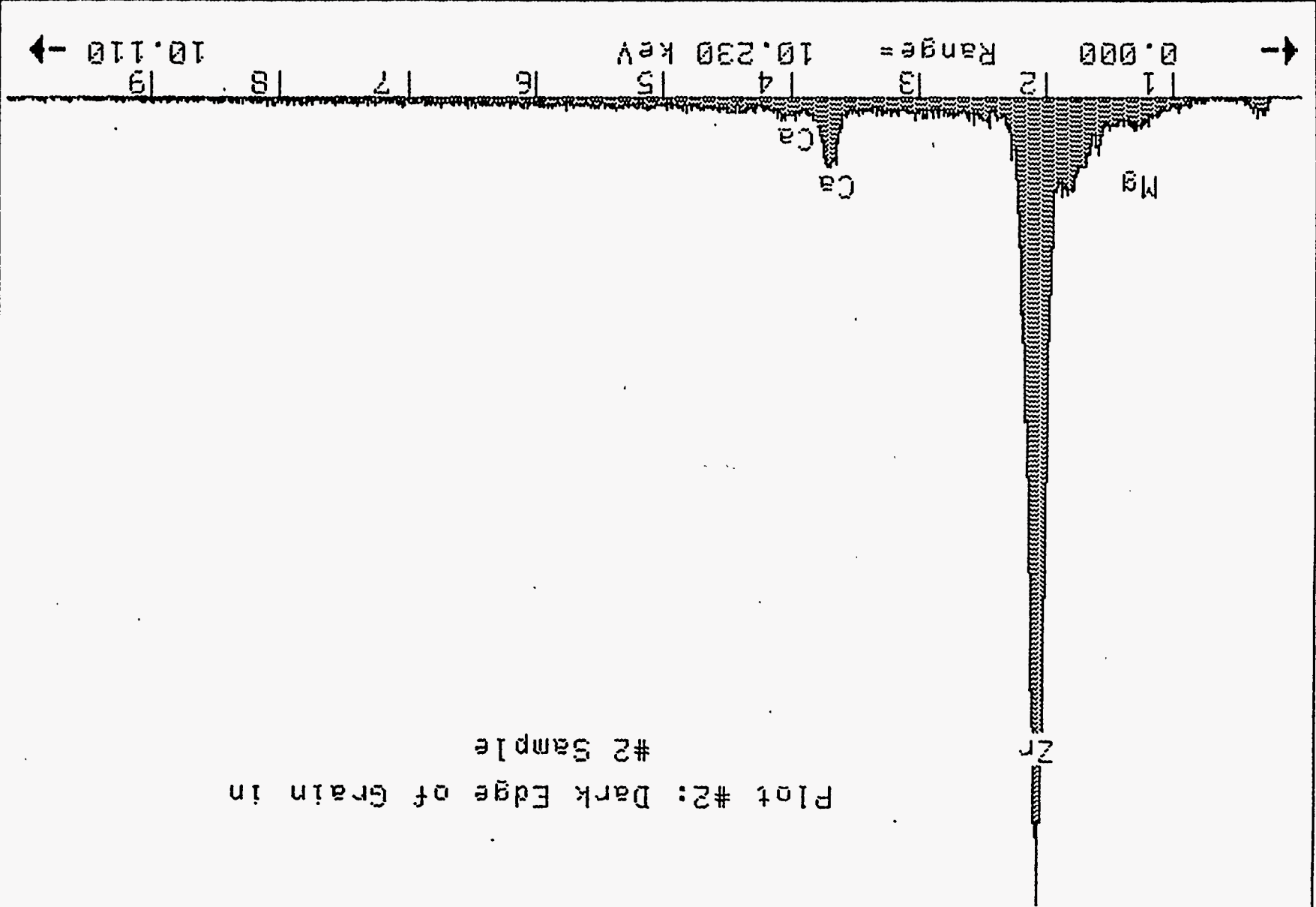
11   12   13   14   15   16   17   18   19
0.000   Range=   10.230 keV   10.110 →

21-May-1992 10:15:18

RUTH9
Vert= 904 counts

Plot #3: Dark Material Between
Grains in Sample #2

Si

Ca

Mg

Al

P

Ca

Ti

0.000 Range= 10.230 keV 10.110
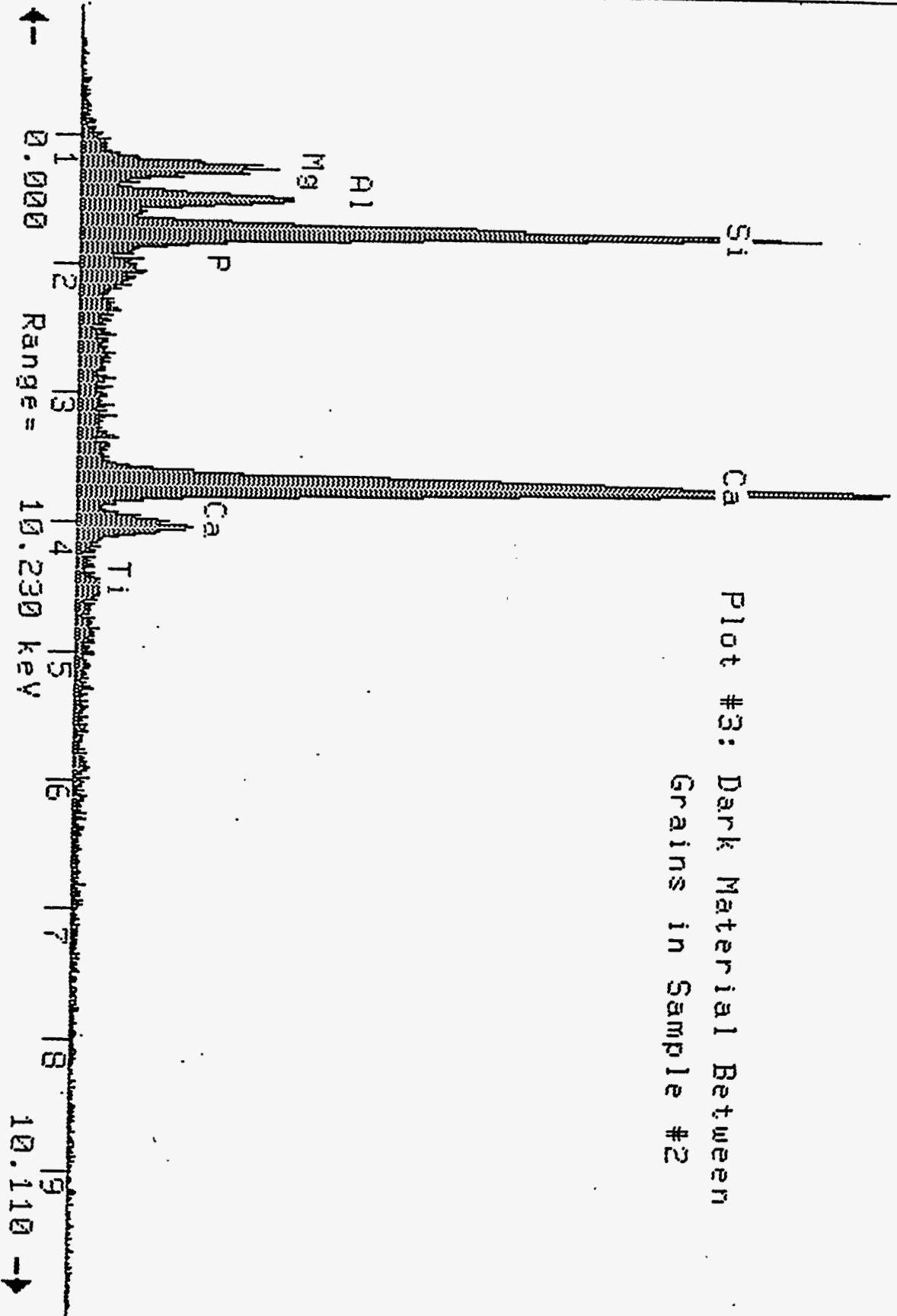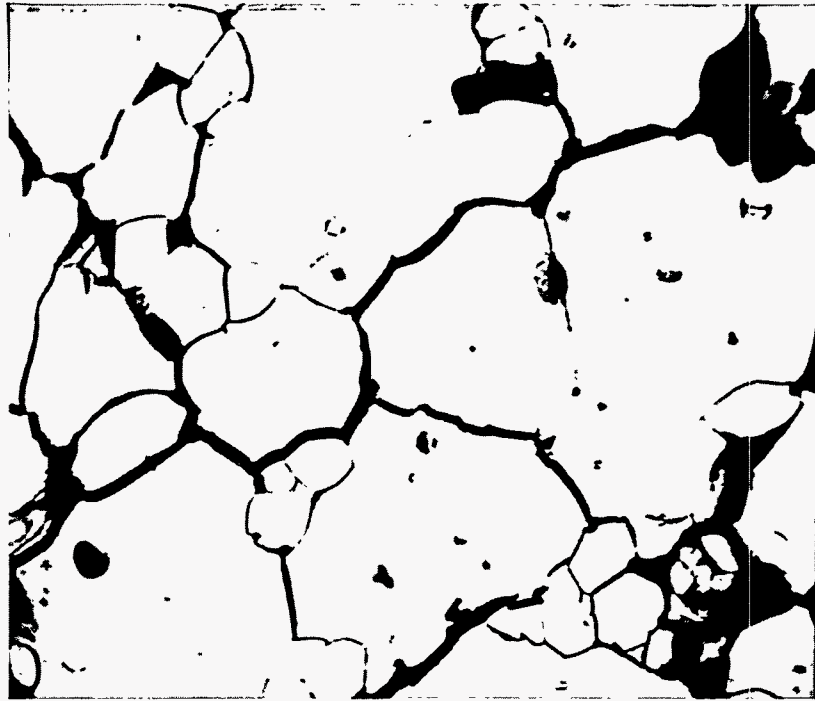
Figure 13. Backscattered electron microprobe photograph of a typical area of sample Z-240 in the as-received condition. Magnification: 1000X.
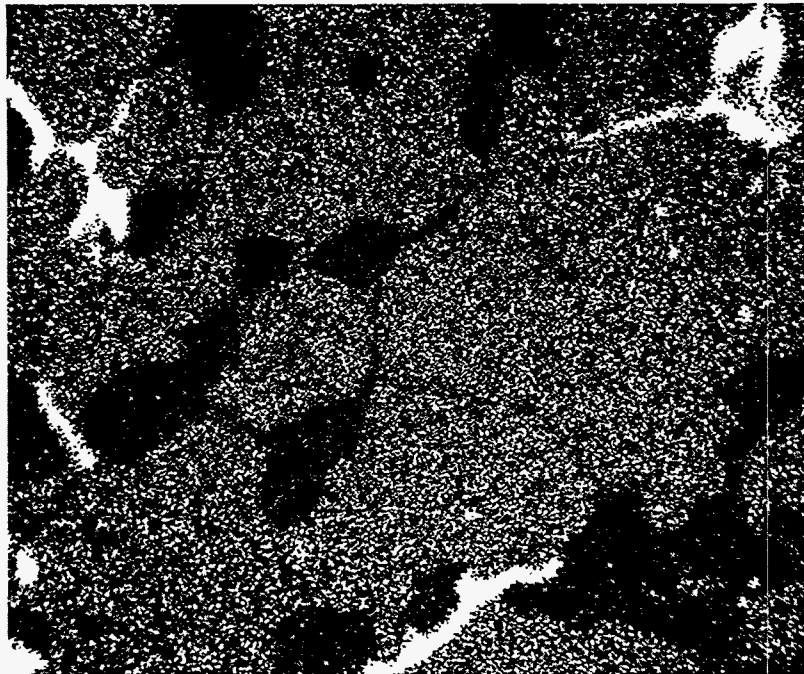
Figure 14. X-ray map of the distribution of Mg in the area shown in Figure 13.
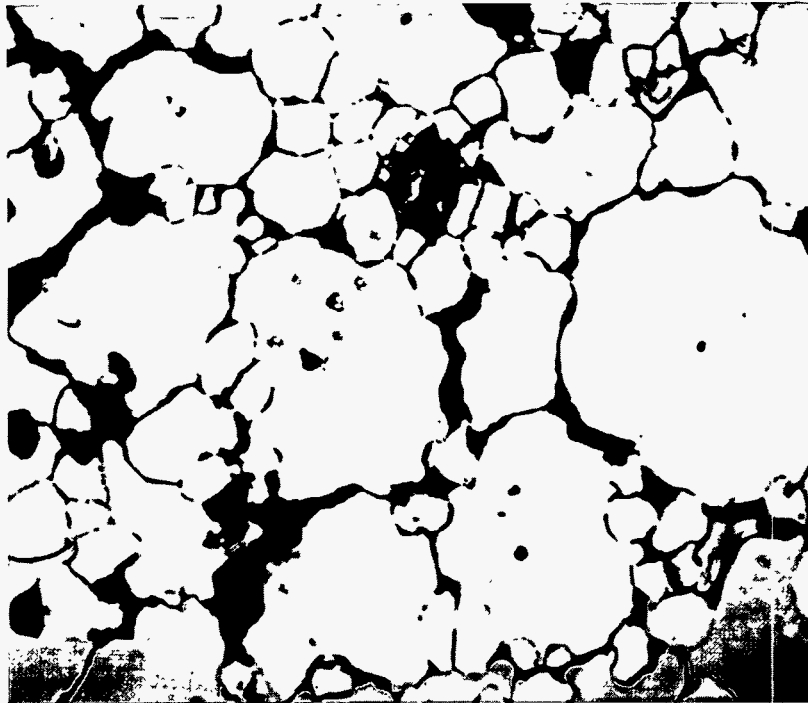
Figure 15:   Electron microprobe photograph of a typical area of sample Z-240 after exposure to steel/slag. Magnification: 1000X.
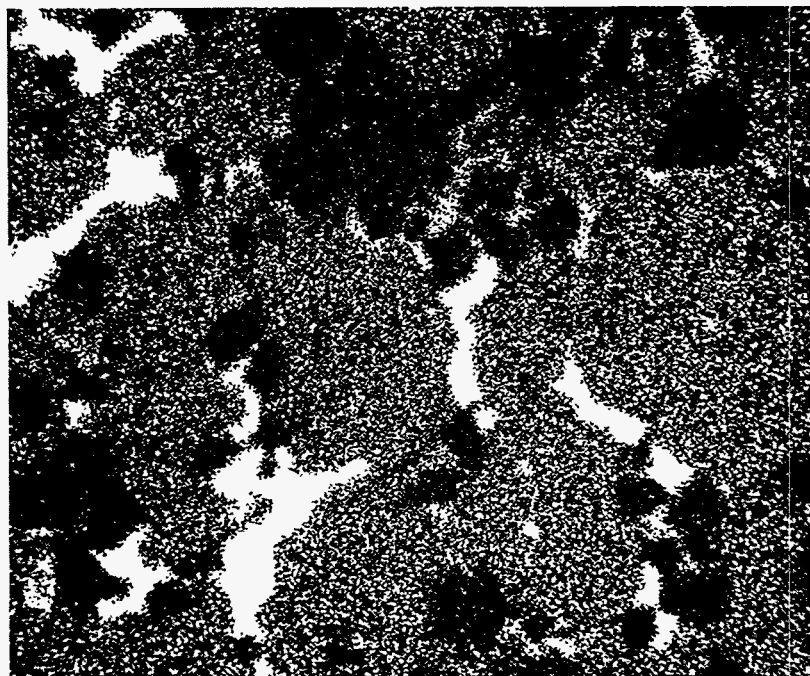
Figure 16.   X-ray map of the distribution of Mg in the area shown in Figure 15.

Appendix IX

Evaluation of Cracks In
As Cast Strip
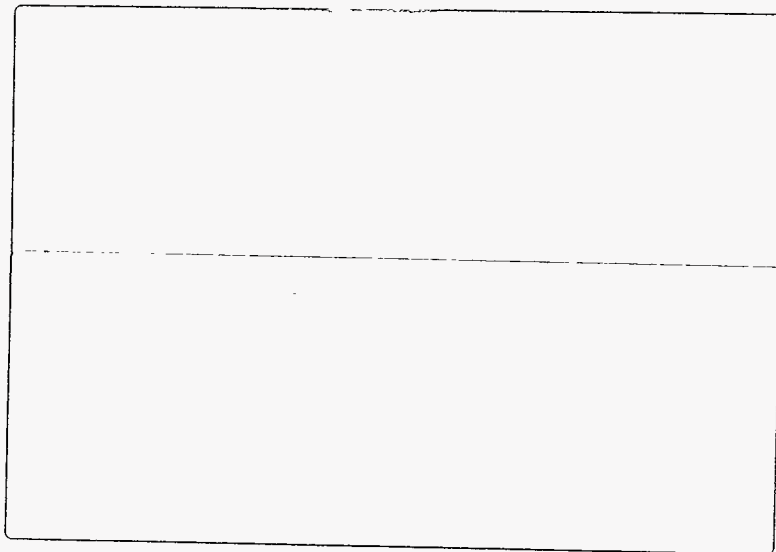
December 4, 1992

To:	Robert S. Williams	cc:	D. W. Follsteadt
	Senior Research Engineer		R. J. O'Malley
	Casting		R. C. Sussman
	Research & Technology		

From: R. E. Hook and P. J. Erfort

Subject: Evaluation of Cracks in As-Cast Strip

INTRODUCTION

The cracks which appear in the cast strip present a problem which must be overcome if strip casting of low-carbon steel is to be successful. The cracks are generally aligned in a longitudinal direction (parallel to the casting direction) or in a transverse direction. The cracks appear on both the bottom surface (wheel contact surface) and the top surface of the strip. Frequently the cracking does not penetrate through the entire thickness of the sheet. This study involved an examination of the cracks by various means in an effort to gain some insight into their origin.

SUMMARY AND CONCLUSIONS

The cracks which are found in the as-cast strip result from hot tearing caused by rupture at dendrite boundaries. There is also evidence presented which strongly indicates that there is a significant degree of local P segregation at dendrite boundaries. However, it cannot be concluded that the cracking is caused by the P segregation. Whether the inter-dendritic rupture occurred before or after these last to freeze regions had solidified could not be determined.

PROCEDURE

Pieces of 12 in. wide cast strip containing cracks were selected for examination from Cast No.000852 at 155 ft. into the cast and from Cast No. 000859 at 98 ft. into the cast. The former is a Si-killed low-carbon steel. The latter is also Si-killed and had alloy additions consisting of 0.05 wt pct Nb and 0.2 wt pct Ti made in an effort to improve the hot strength of the steel.

The cracks in the cast sheet were examined by light microscopy in the as-polished condition, after etching in 3 pct Nital which revealed the grain structure of the ferrite and after etching in Oberhoffer's reagent which revealed the as-cast dendritic structure. Both longitudinal and transverse cracks which occurred on the bottom and the top surfaces of the sheet were examined after polishing sheet punchings in the plane of the sheet. Also, cracks were examined for through-thickness sections taken normal to the crack path. In addition, a fracture surface was examined by SEM. Finally, the tip-end of three cracks were step-scanned in the electron microprobe in an attempt to identify any segregation of Si, P or S which might explain the

1

cracking. A traverse of 200 microns, 41 points at 5 microns per step, was performed with the crack tip at the center of the traverse.

RESULTS AND DISCUSSION

Figure 1 shows photographs of typical longitudinal (a) and transverse (b) cracks which, in this case, appear on the bottom surface of the strip. The series of finely spaced parallel lines shown are the finishing marks of the casting wheel which have been imprinted into the wheel contact surface of the strip. Occasionally longitudinal cracks which were non-collinear were joined by essentially transverse crack segments (not shown).

Figure 2 shows several cracks for the as-polished condition as viewed normal to the sheet surfaces for both the top and the bottom sheet surfaces. While not shown clearly here the surfaces of the cracks are coated with a thin film of iron oxide. On a microscopic scale the crack path is highly irregular. Even the shortest crack length segments are curvilinear as opposed to straight or linear. In Figure 2(c) we can see the discontinuous nature of the cracks which was frequently observed. The fracture morphology seen here is very suggestive of hot tearing associated with rupture occurring at inter-dendritic boundaries.

Figure 3(a) shows a through-thickness cross-section view of the top sheet surface oxide layer. The oxide thickness is on the order of 0.025 mm. Figure 3(b) shows a through-thickness cross-section view of a longitudinal crack showing the oxide layer on the crack surface. the oxide layer thickness is on the order of 0.0025 mm.

Figure 4 shows both through-thickness section and normal to the sheet views of the as-cast Widmannstaetten ferrite grain structure of the Si-killed steel of Cast No. 000852. Figures 4(a) and (b) show two through-thickness sections of appreciably different thickness, one at 0.032 in. and the other at 0.044 in. The thickness variations are appreciable and on a quite local scale. Figures 4(c) and (d) show the structure as viewed normal to the sheet surface at the bottom (wheel contact) surface and at the top surface. The scale of the Widmannstaetten ferrite lath structure is somewhat finer at the bottom surface.

Figure 5(a)-(d) shows a series of micrographs similar to those shown in Figure 4, but for a Si-killed steel containing additions of Nb and Ti, Cast No. 000859. The Widmannstaetten ferrite grain structure is notably finer than that for the steel shown in Figure 4. The Nb and Ti additions were made in this case to determine if these alloy additions would improve the cracking resistance.

Figure 6 shows micrographs of cracks where the Widmannstaetten ferrite grain structure is also revealed. The cracks were present prior to the formation of the ferrite by transformation from the parent austenite phase. The presence of a coarser ferrite bordering the cracks, particularly notable in Figure 6(b) and (c), is very likely a result of grain growth in regions along the cracks which are decarburized as a result of the oxide layer formed on the crack surface. Such a phenomenon is exhibited when cracking occurs in conventional strand cast low-carbon steel.

A specimen for examination of the fracture surface was cut from a sheet containing a full through-thickness transverse crack which is shown in Figure 1(b). The SEM micrographs of the fracture surface shown in Figure 7(a), (b) and (c) are consistent with inter-dendritic rupture. It must be pointed out that much of the detail or definition of the features of the fracture surface were undoubtedly obscured as a result of oxidation of the surface of the crack following rupture. In addition, the oxide was removed by lightly glass bead blasting which must have had some

2

effect in reducing the definition of the features. Figure 7(d) shows a polished through-thickness section which is etched to show the as-cast dendritic structure. The similarity in the appearance of this etched structure and that of the rupture surface in (c) is quite evident.
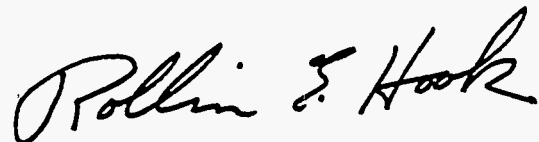
While the results of this study of the observed cracks support the conclusion that the cracks are in fact hot tears which occurred as a result of inter-dendritic rupture, it cannot be determined whether rupture took place through regions of the last to freeze liquid before or after full solidification. The expectation is that given the conditions associated with the strip casting process the strip would be the most susceptible to cracking by inter-dendritic rupture while the inter-dendrite boundary regions are yet liquid.

Electron microprobe step-scans across the crack tip of three cracks contained in as-polished samples, polished in the plane of the sheet, showed no remarkable results with respect to segregation of Si or S. The results with respect to P, however, are consistent with respect to expectations if appreciable inter-dendritic segregation of P is present. Figure 8 shows the step-scan results for P for the three 200 micron traverses at 5 micron per step. Bulk chemical analysis of the sheet by emission spectrography showed an average P level of 0.010 wt pct. The microprobe step-scan shows that locally the concentration of P can be 3 to 5 times this level. Since the average inter-dendritic boundary spacing appears to be on the order of about 25 microns, see Figure 7(c), one can say that the scale of the concentration fluctuations shown in Figure 8 are more or less consistent with expectations if the P is segregated in the inter-dendritic regions.
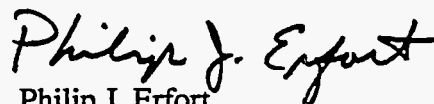
The evidence resulting from this study is that the cracks result from hot tearing caused by rupture at dendrite boundaries. There is also evidence presented which strongly indicates that there is a significant degree of local P segregation at dendrite boundaries. However, it cannot be concluded that the cracking is caused by the P segregation.
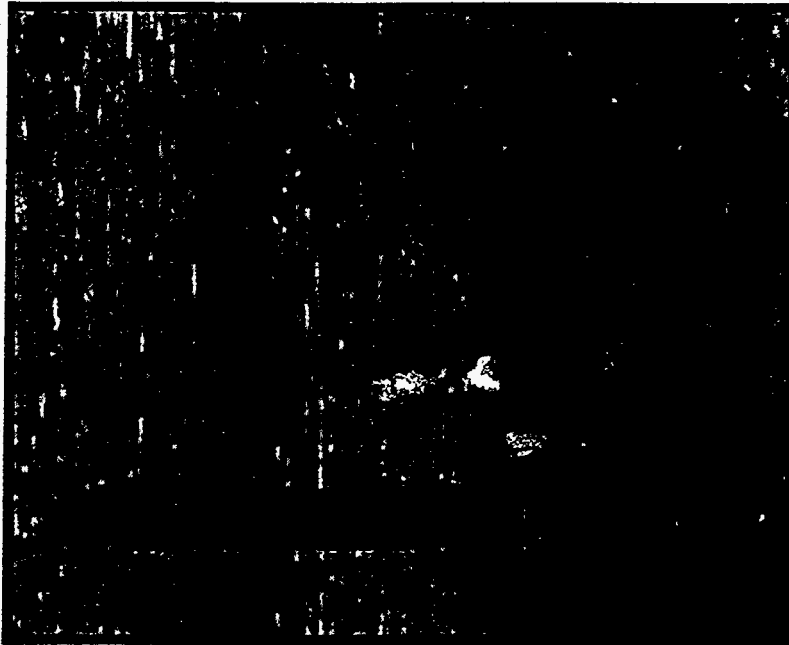

In the through-thickness section views of the strip shown in Figures 4(a), (b); 5(a), (b) and 7(a)—(d) the wheel contact side of the strip faces the bottom of the page.

Rollin E. Hook
Principal Research Metallurgist
Research & Technology

Philip J. Erfort
Master Research Technician
Research & Technology

3

Longitudinal Crack 1TT   (a)   N36272
Micro Mount 2007-1

Transverse Crack 2F   (b)   N36276
(Selected For SEM Fractography)

Casting Direction

Figure 1 - Typical (a) longitudinal and (b) transverse cracks on wheel contact surface of as-cast strip, Cast No. 00852 at 155 lineal feet. Cracking on the non wheel contact surface has the same appearance. Magn.= 3X.
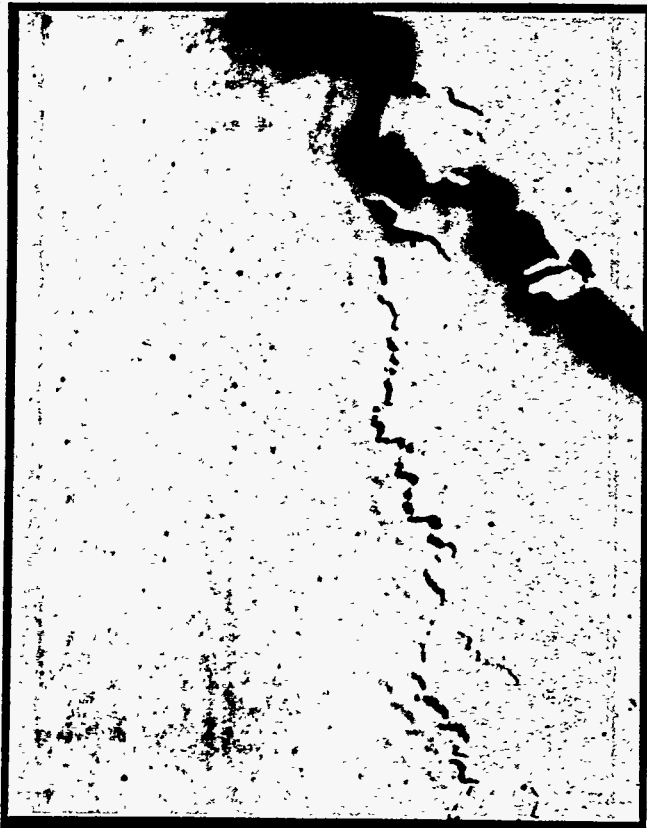
Transverse Crack (a) Wheel Contact Surface N 37637

Transverse Crack (b) Top Surface N 37638

(c) N37639

Transverse/Longitudinal Crack Junction Wheel Contact Surface

Casting Direction
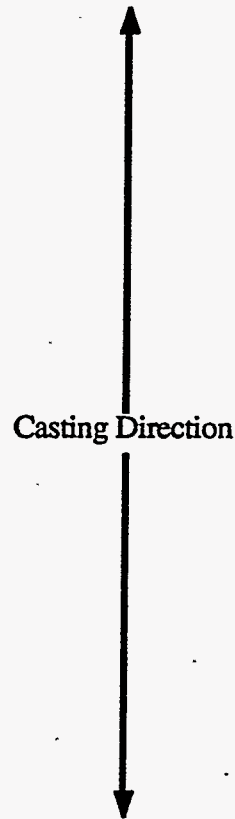
Figure 2 - View normal to sheet surfaces of as-cast cracks, as-polished condition. Magn.= 100X
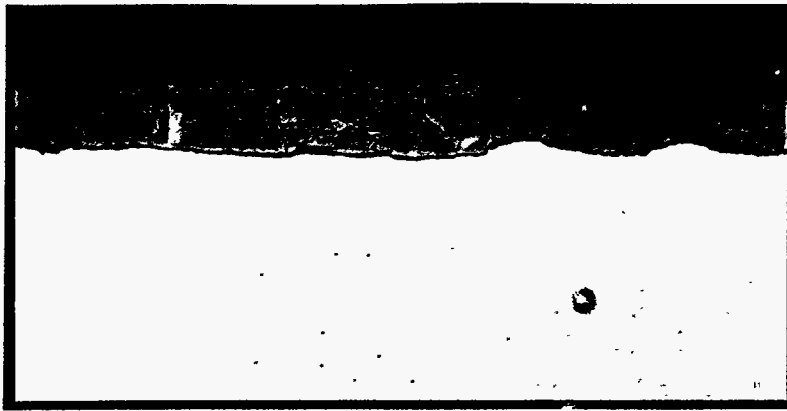
Micro Mount 2007-1   (a)   N 37640
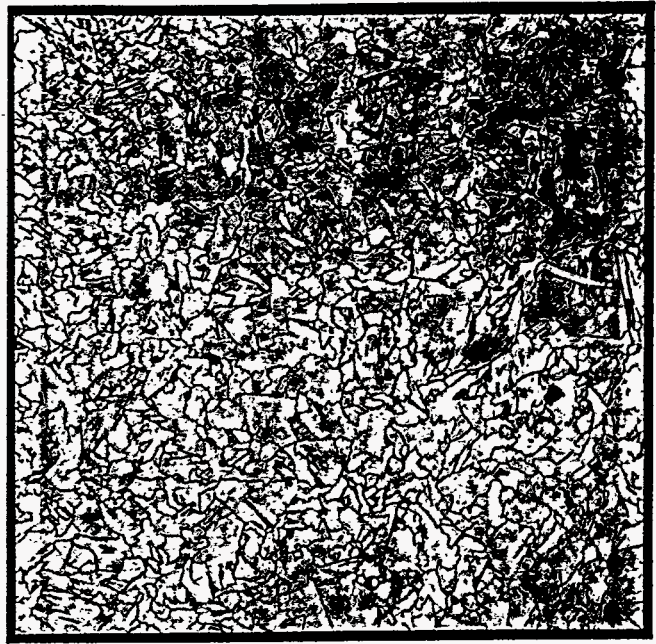Top Surface Oxide Layer, Thickness= 0.025 mm

Micro Mount 2007-1   (b)   N 37641
Oxide Layer On Crack Surface, Thickness= 0.0025 mm

Figure 3 - Through-thickness views showing relative oxide thicknesses of (a) sheet surface oxide on the top surface and (b) oxide layer covering the surface of a longitudinal crack on the wheel contact side of the sheet. Magn.= 500X.

(d) View Normal to Sheet, Top
Surface, Micro Mount 2007-4   N 37645

(c) View Normal to Sheet, Wheel
Contact Surface, Micro Mount 2007-2   N 37644
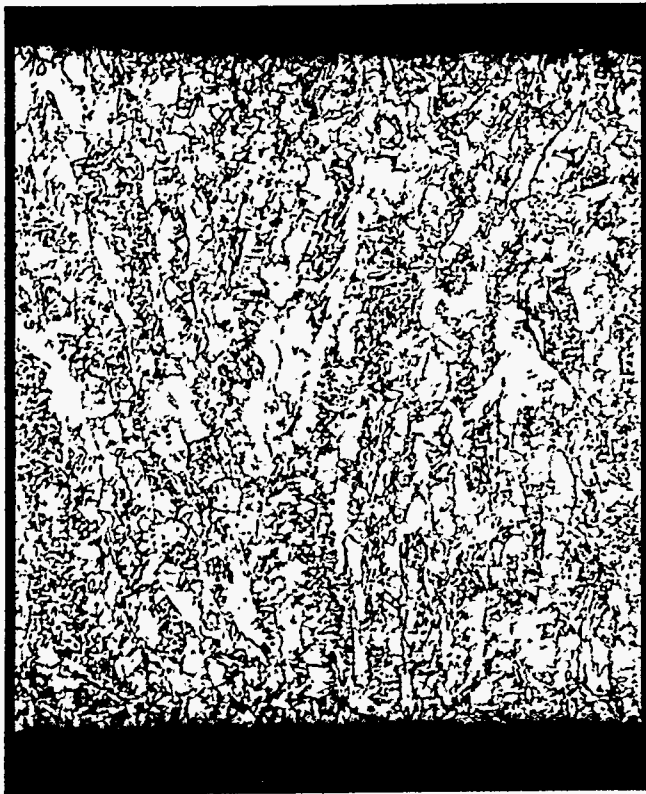
(b) Through Thickness Section
Micro Mount 2007-1   N 37643

(a) Through Thickness Section
Micro Mount 2007-1   N 37642

←——— Casting Direction ———→

Figure 4 - Through thickness and sheet normal views of the as-cast Widmannstaetten ferrite grain structure,
Cast No. 0008S2 at 155 lineal feet. Magn.= 100X
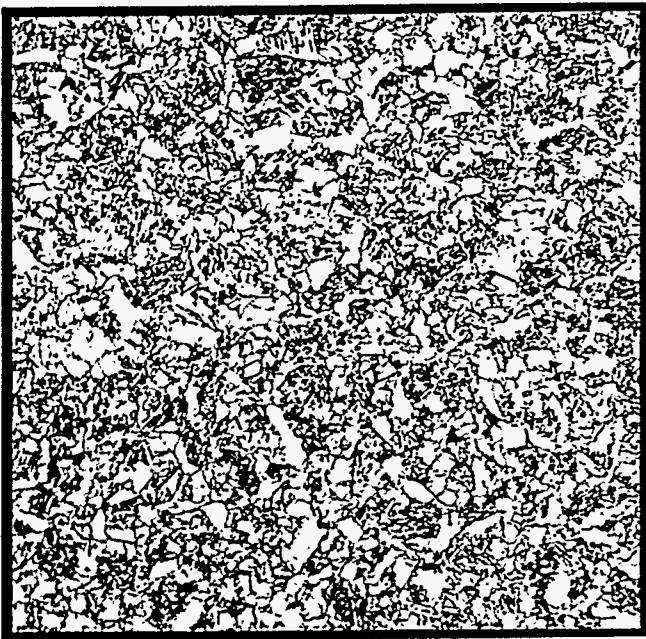
(a) Through Thickness
Longitudinal Section   N 37646
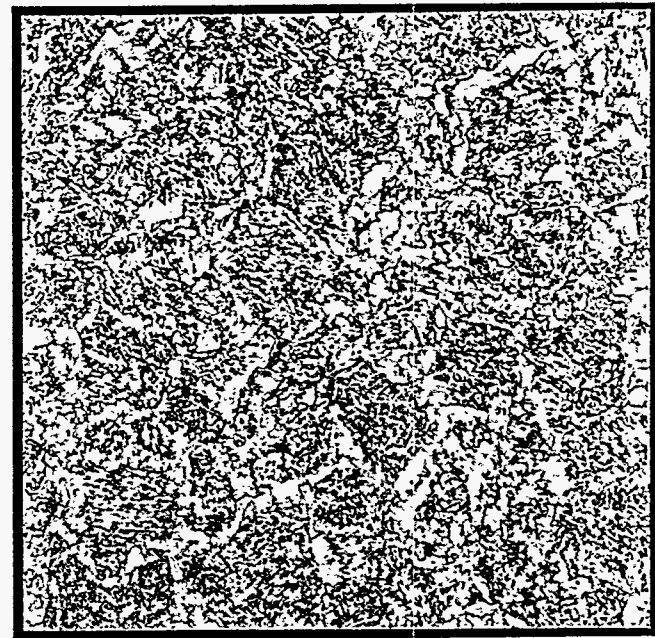
(b) Through Thickness
Transverse Section   N 37647

(c) View Normal to Sheet, Wheel
Contact Surface.   N 37648

(d) View Normal to Sheet, Top
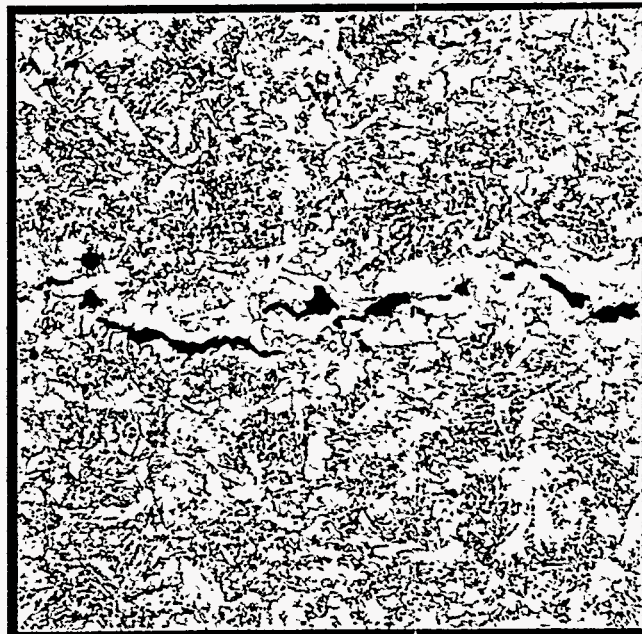Surface.   N 37649

Figure 5 - Through thickness and sheet normal views of the as-cast Widmannstaetten ferrite grain structure.
Cast No. 000859, steel containing 0.05 Nb, 0.2 Ti. Magn.= 100X

(a) Normal to Wheel Contact Surface   N 37650
Si-Killed Cast No. 000852

(b) Normal to Wheel Contact Surface   N 37651
Spyder Crack, Si-Killed Cast No. 000859
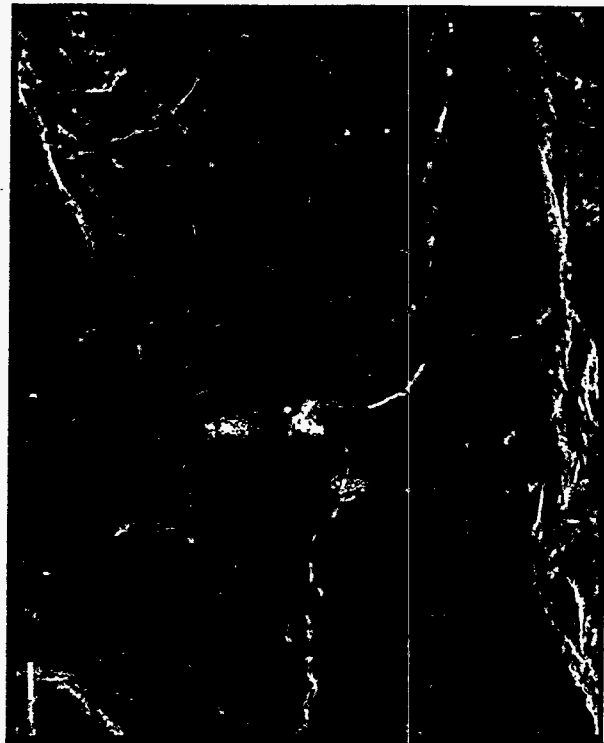Containing 0.05 Nb, 0.2 Ti

(c) Normal to Wheel Contact Surface   N 37652
Longitudinal Crack, Si-Killed Cast No. 000859
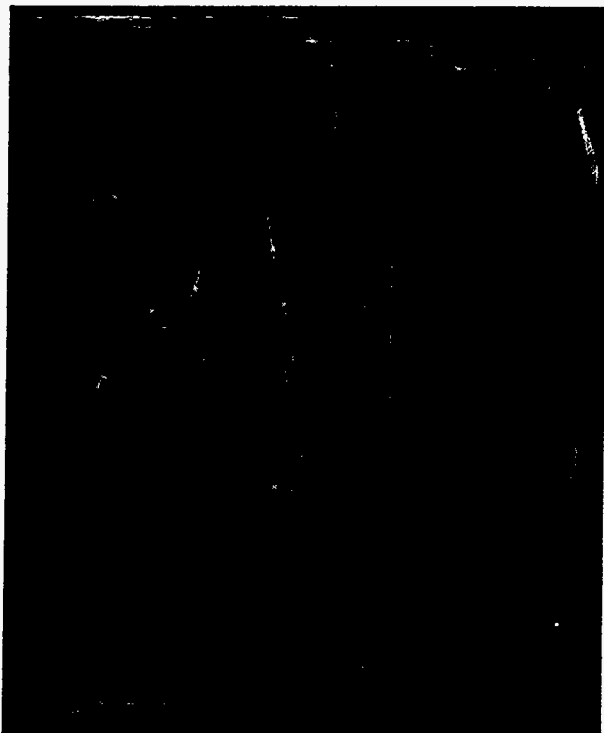Containing 0.05 Nb, 0.2 Ti

Figure 6 - A comparison of the crack and Widmannstaetten ferrite morphology of the as-cast steels, with and without a Nb+Ti alloy addition. Magn.= 100X

(a) Fracture Surface Showing   SM 78966
Partial Inter-Dendritic Rupture.   100 Magn.

(b) Enlarged View of Selected   SM 78965
Area Shown in (a).   500 Magn.

(c) Fracture Surface Showing   SM 78968
Complete Inter-Dendritic Rupture.   100 Magn.

(d) Polished and Etched   N 37653
Through Thickness Section Showing   100 Magn.
As-Cast Dendritic Structure.

Figure 7 - (a), (b) and (c) SEM fractographs of transverse crack shown in Figure 1(b), and (d) through thickness micrograph showing as-cast dendritic structure. Cast No. 000852 at 155 lineal feet.
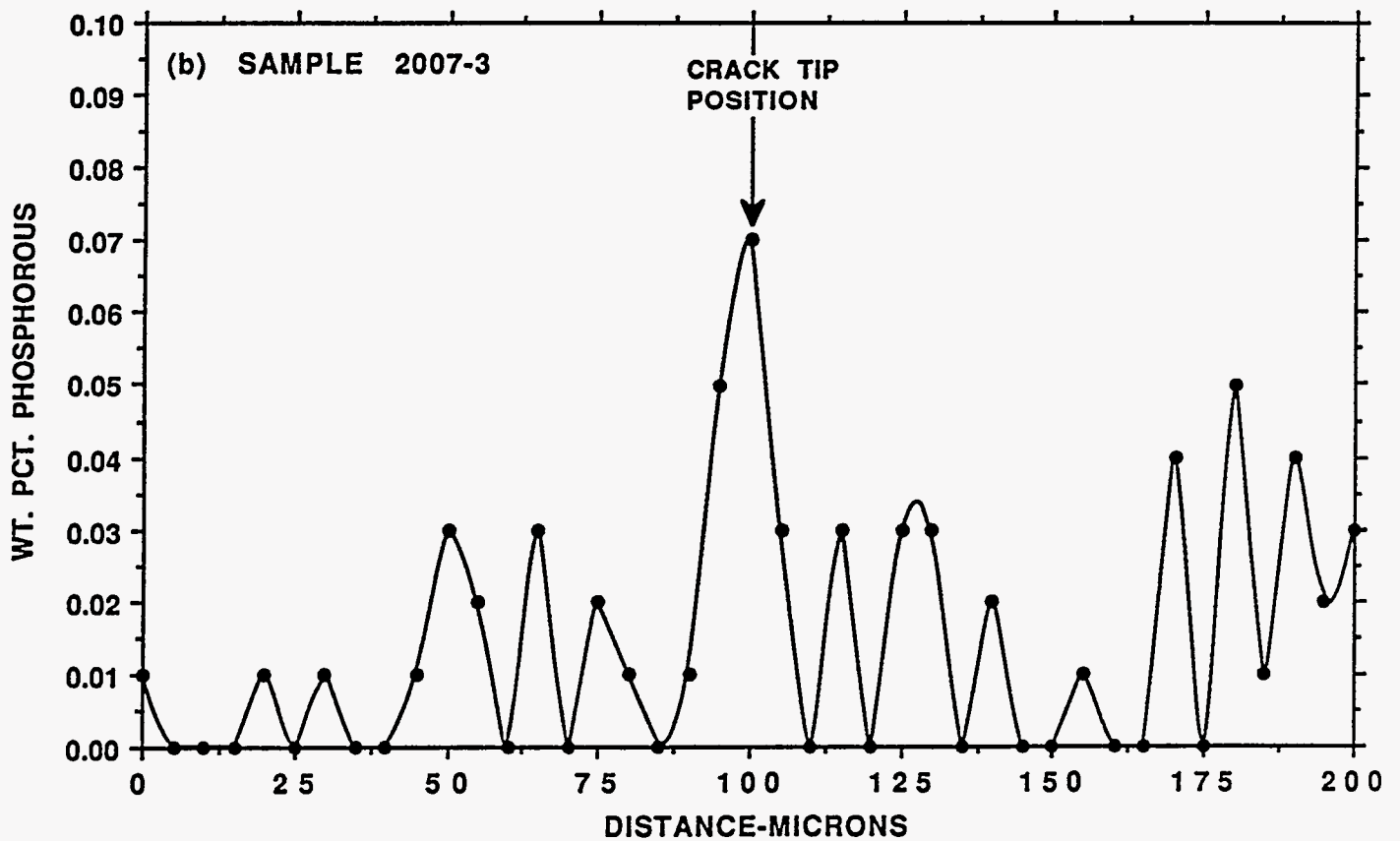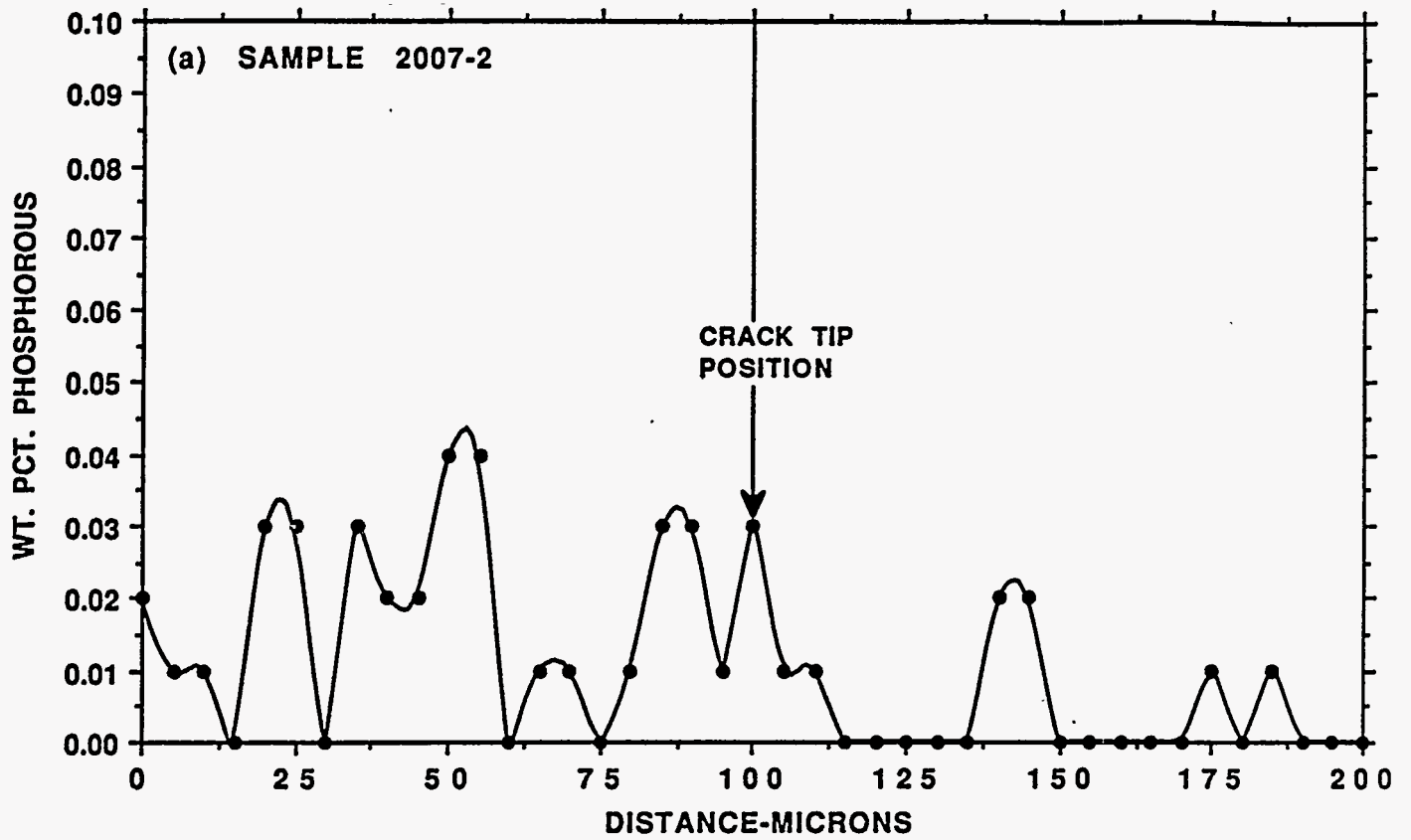
Figure 8 - Results of electron microprobe step-scan showing variation in P level.

Appendix X

Metallographic Investigation
of Cast Strip

TO: R. S. Williams

FROM: M. L. Lowry

SUBJECT: Metallographic Investigation of Cast Strip
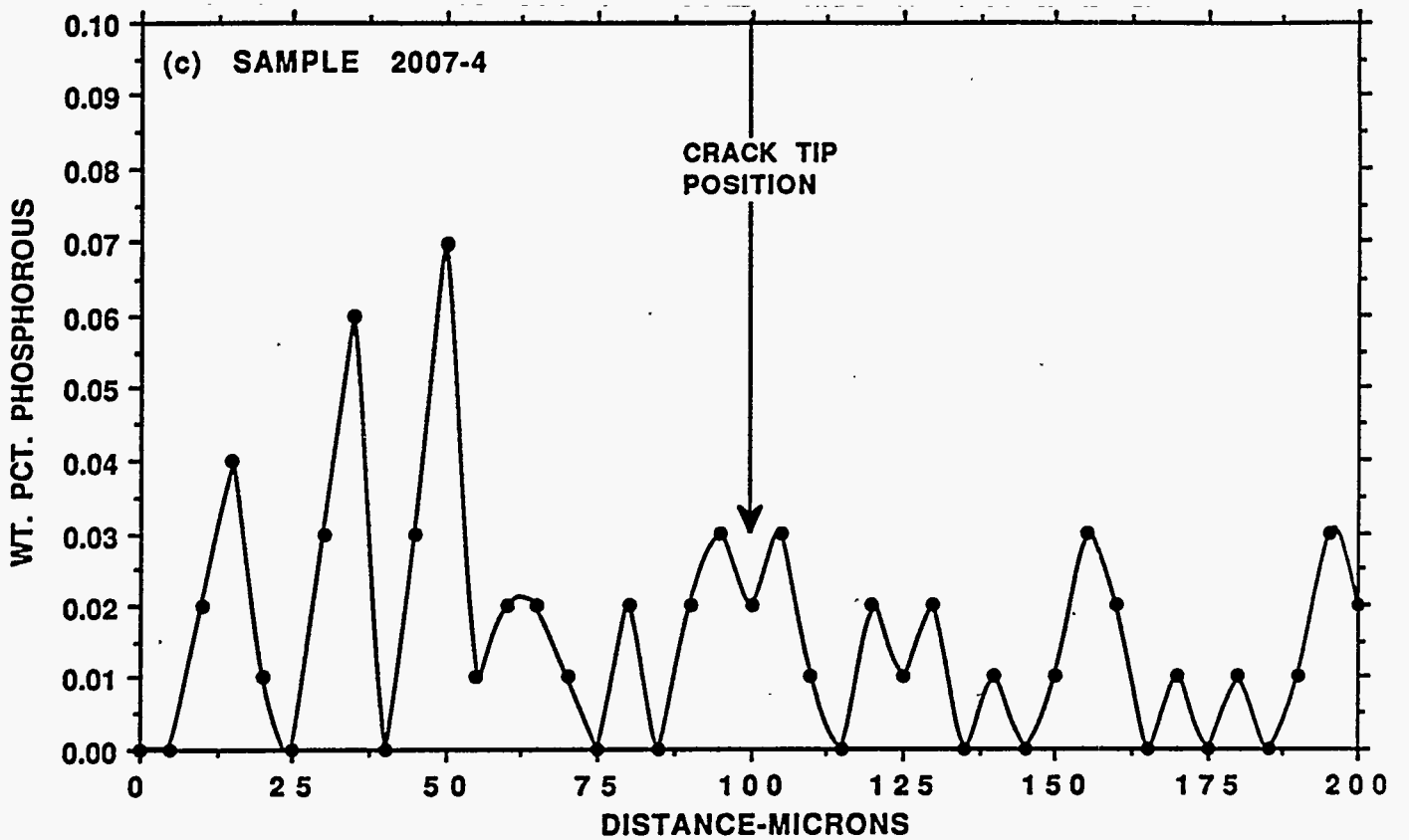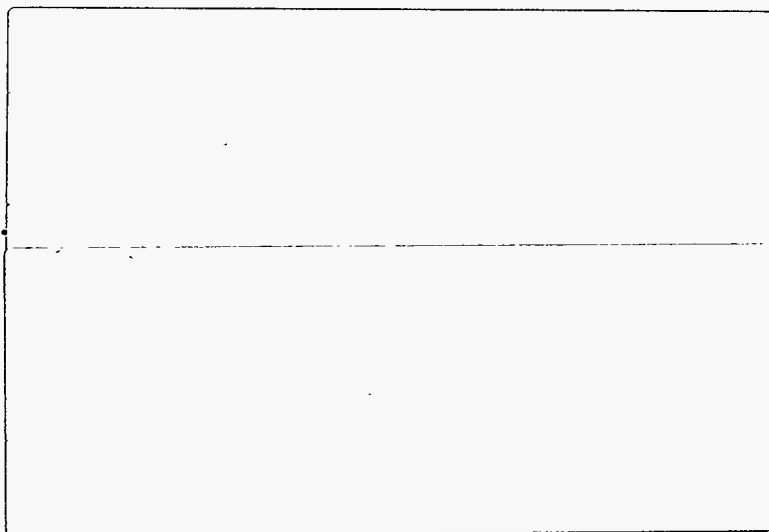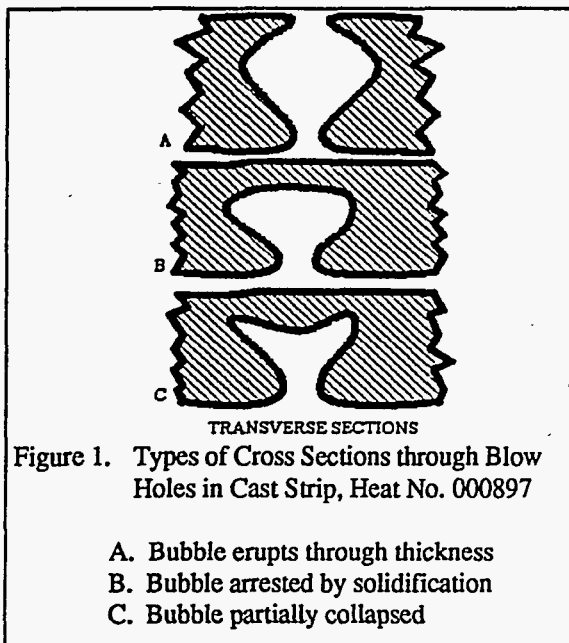

The results of a limited metallographic examination of the strip from two heats, Heat No. 000889 and Heat No. 000897 are summarized in the following paragraphs. Specific items of interest included the generation of blowholes, the composition of the non metallic inclusions, the surface condition of the strip including imperfections and scale, and finally the thickness and variation of the strip itself.
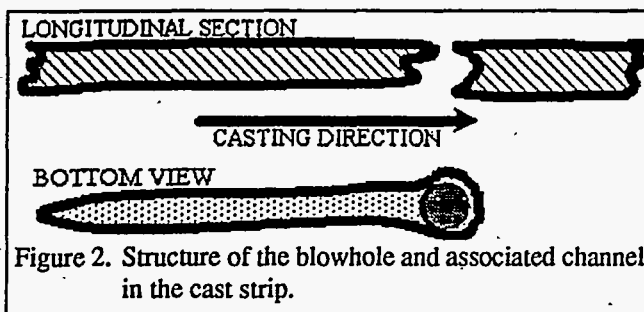
Blowholes

Steel strip solidified on the steel wheel contained numerous blowholes, many communicated through the entire strip thickness. Figure 1 shows the three general types of holes discovered in the metallographic examination. Figure 1A shows the cross section of the blowhole communicating through the entire thickness of the strip. This is a picture of an expanding gas bubble with sufficient volume to open to the top surface. Figure 1B describes a blowhole formed from a gas bubble which lacked volume or time to expand to the surface. Figure 1C shows a blow hole which lacked the volume necessary to expand and partially collapsed before solidification was complete.

TRANSVERSE SECTIONS

Figure 1.   Types of Cross Sections through Blow Holes in Cast Strip, Heat No. 000897

A. Bubble erupts through thickness
B. Bubble arrested by solidification
C. Bubble partially collapsed

Figure 2.   Structure of the blowhole and associated channel in the cast strip.

Associated with the blow hole itself is a channel extending downstream on the bottom only. Figure 2 diagrams the channel and blowhole. I propose the following hypothesis to explain this structure and the generation of the blowhole.

The proposed mechanism involves the reaction of melt carbon with iron oxide on the steel wheel to produce carbon monoxide gas. The bubble of gas and the reaction site travel with the solidifying strip but with the bubble also attached to the lip of the refractory nozzle. With the bubble attached to the nozzle lip, the bubble is stretched out as the strip passes through the melt pool. This last only as long as the gas pressure is maintained, and therefore stops as soon as the gas producing reaction stops or the bubble opens to the top surface as in Figure 1A. The gas producing reaction will stop because the reactants are depleted, either carbon or oxide; the solidification rate outstrips the bubble growth and confines it; or the decreasing temperature slows the reaction kinetically or makes the reaction thermodynamically unstable.

Inclusions

The inclusions formed in the strip produced in Heat No. 000897 were very small, on the order of 10 μm, and very sparsely distributed. All of the observed inclusions exhibited a single glassy phase composed without exception of 90% TiO_2 and 10% Al_2O_3. This is a direct result of the large titanium addition at tap. The inclusions exist in two forms in the solid strip; as single spherical particles and clusters of irregularly shaped particles. The inclusions give every appearance of being produced as a liquid phase. The liquidus temperature of the binary oxide of this composition is about 1800°C (3270°F)[1] which is much greater than any temperature experienced by the melt (and certainly after tapping when the titanium was added).

Gauge, Scale, and Imperfections

Extensive metallographic measurements of the strip gauge and scale layer from two samples produced on Heat No. 000897 exhibit a consistent base value with large deviations over short intervals. The deviations are numerous and consist of cracks, protrusions, and depressions. In particular, the gauge was quite uniform subject to sudden thickening or thinning, protrusions or dimples. Appendix A details the measurements, observations, and plots the results.

The mean gauge thickness was 0.62 mm with most variation between 0.70 mm and 0.55 mm. This, of course, does not include the scale but is the actual strip thickness.

The mean scale thickness was 0.011 mm and varied between 0.006 mm and 0.018 mm. The scale thickness on the strip is not a significant contributor to the variation in strip thickness. The calculation of the iron lost due to the scale on the strip is presented on Page A-11; the average iron lost in the scale amounts to 0.8%. A typical iron yield loss for a slab caster is 1.9%[2].

[1] Levin and McMurdie ,Phase Diagrams for Ceramists, 1975 Supplement (The American Ceramic Society, Columbus, OH, 1975) Fig. 4376.

[2] M. T. Burns, Armco Steel Co., LP, Private Communication.

APPENDIX A

METALLOGRAPHIC EXAMINATION OF CAST STRIP FOR HEAT NO. 000897

Sample A

Strip Length	519 ft.
Relative Width	27 %

Thickness Variation

Width Position	Thickness mm
1	0.54
2	0.55
3	0.55
4	0.56
5	0.57
6	0.68
7	0.67
8	0.71
9	0.68
10	0.58
11	0.59
Average	0.63
Std Dev	0.06
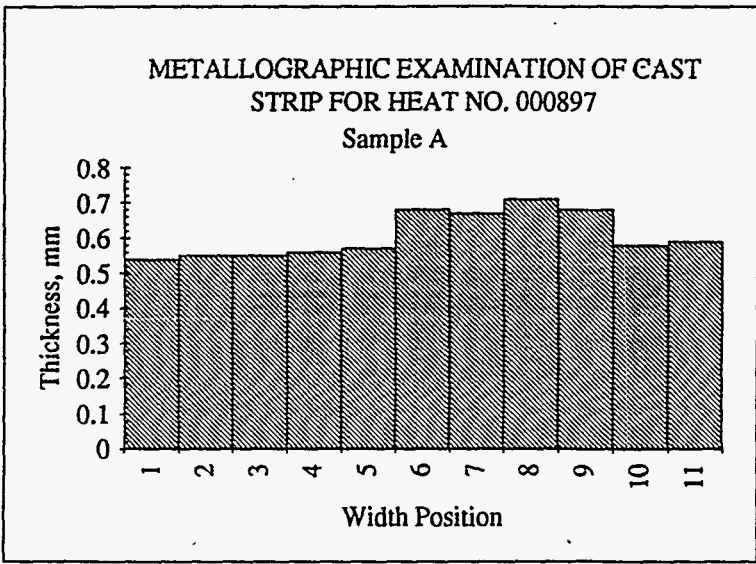
METALLOGRAPHIC EXAMINATION OF CAST STRIP FOR HEAT NO. 000897 — Sample A

Scale Thickness Variation

Width Position	Bottom Thickness mm	Top Thickness mm
1	0.0100	0.0086
2	0.0116	0.0124
3	0.0064	0.0140
4	0.0100	0.0220
5	0.0060	0.0120
6	0.0140	0.0090
7	0.0100	0.0150
8	0.0200	0.0122
9	0.0260	0.0100
10	0.0080	0.0124
11		0.0084
Average	0.0134	0.0126
Std Dev	0.0072	0.0043

CAST STRIP SCALE THICKNESS — Sample A
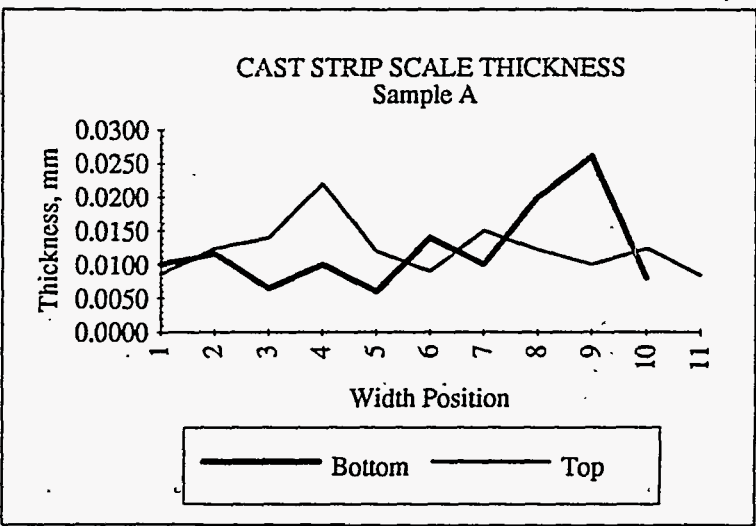
Observations

1 The thickness variation is all in the top surface.

2 0.008 mm below the top surface is a layer containing very small round inclusions and pores.

3 0.006 mm below the bottom surface is a similar layer of small inclusions and pores.

4 All of the inclusions are round and generally less than 0.002 mm in diameter.

Sample B

Strip Length   519 ft.
Relative Width   52.7 %

Thickness Variation

Width Position	Thickness mm
0	0.61
3	0.57
8	0.65
13	0.59
18	0.65
20.5	0.65
Average	0.62
Std Dev	0.03
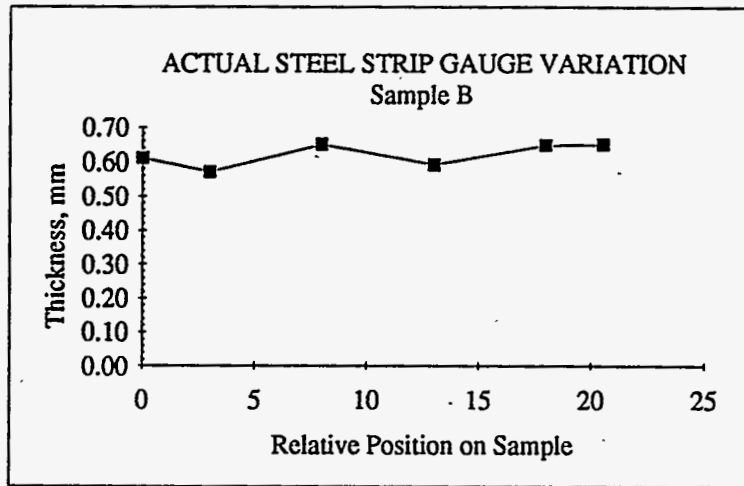
ACTUAL STEEL STRIP GAUGE VARIATION
Sample B

Scale Thickness Variation

Width Position	Bottom Thickness mm	Top Thickness mm
1	0.0100	0.0080
2	0.0116	0.0082
3	0.0120	0.0100
4	0.0050	0.0064
5	0.0080	0.0080
6	0.0100	
Average	0.0094	0.0081
Std Dev	0.0026	0.0013

CAST STRIP SCALE THICKNESS
Sample B
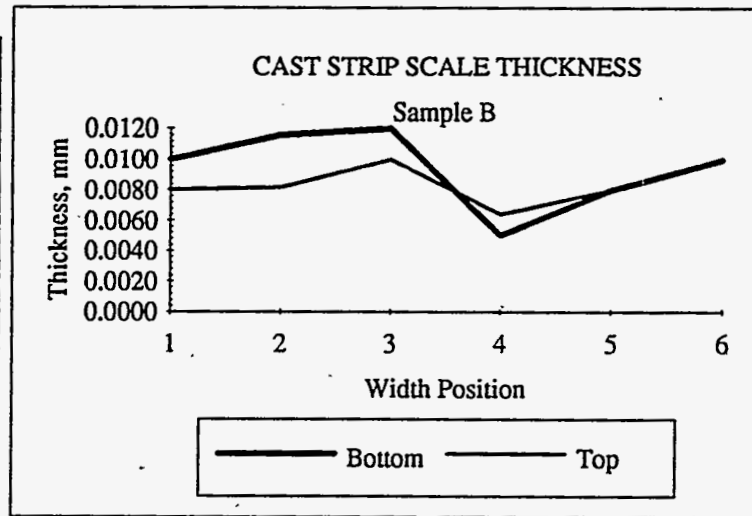
Observations

1 Small dimple on the bottom surface, depth =   0.02 mm
2 There is a thin layer just below the top surface containing small voids and inclusions
  Layer thickness =   0.04 mm
3 There are very shallow fissures in the top surface filled with oxide scale.
4 The top surface is rough in the intervals where the strip is thinner in gauge.

APPENDIX A

Sample C

Strip Length	519 ft.
Relative Width	76 %

Thickness Variation

Width Position	Thickness mm
0	0.622
1	0.621
4	0.611
9	0.508
14	0.630
15.2	0.800
19	0.612
Average	0.63
Std Dev	0.09

ACTUAL STEEL STRIP GAUGE VARIATION
Sample C
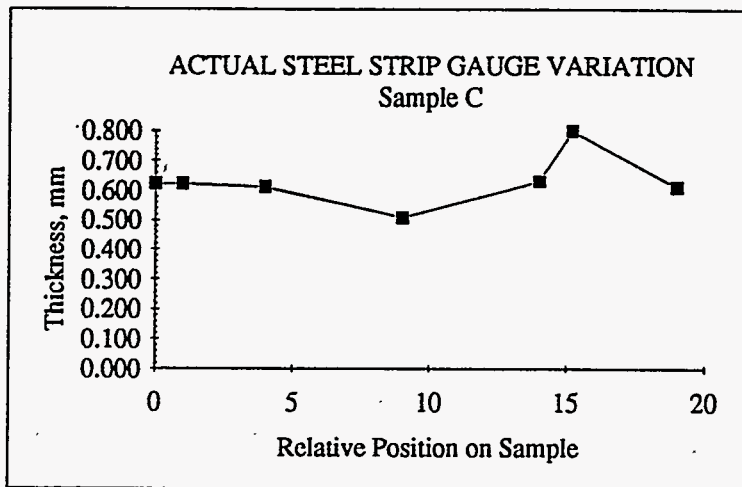
Scale Thickness Variation

Width Position	Bottom Thickness mm	Top Thickness mm
1	0.0172	0.0076
2	0.0162	0.0060
3	0.0158	0.0100
4	0.0200	0.0072
5	0.0196	0.0068
6	0.0116	0.0220
7	0.0120	0.0072
8	0.0164	
9	0.0160	
Average	0.0160	0.0099
Std Dev	0.0030	0.0061

CAST STRIP SCALE THICKNESS
Sample C
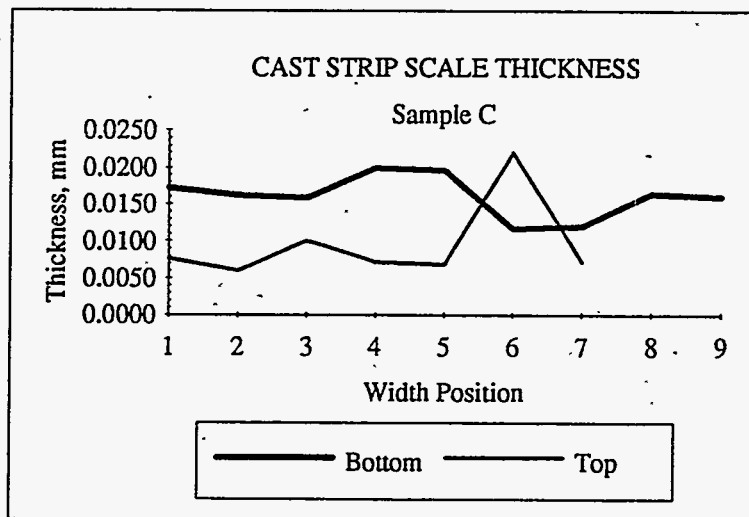
Observations

1 The strip gauge is fairly uniform except for a flattened protuberance.

2 The protuberance is 0.47 mm wide and rises suddenly 0.15 mm above the surface.
In 3-D this is a ridge on the surface of the strip.

3 There is a fissure on the bottom surface with a depth =   0.075 mm

APPENDIX A

11/1/93

Sample D

Strip Length	471	ft.
Relative Width	32.7	%

Thickness Variation

Width Position	Thickness mm
0	0.532
5	0.660
10	0.645
15	0.610
20	0.655
Average	0.62
Std Dev	0.05

ACTUAL STEEL STRIP GAUGE VARIATION
Sample D

Scale Thickness Variation

Width Position	Bottom Thickness mm	Top Thickness mm
1	0.0140	0.0080
2	0.0160	0.0070
3	0.0120	0.0076
4	0.0136	0.0060
5	0.0180	0.0092
6	0.0100	0.0080
7	0.0120	0.0124
8	0.0100	0.0080
Average	0.0132	0.0083
Std Dev	0.0028	0.0019

CAST STRIP SCALE THICKNESS
Sample D

Observations

1 A subsurface layer filled with intricate porosity of thickness = 0.08 mm

width = 7.9 mm

2 The porosity in #1 was grouped in clusters of channels.

Sample E

Strip Length	471 ft.
Relative Width	47.6 %

Thickness Variation

Width Position	Thickness mm
0	0.720
4	0.630
8	0.470
9.6	
10	0.470
14	0.735
19	0.670
21.5	0.580
Average	0.61
Std Dev	0.11
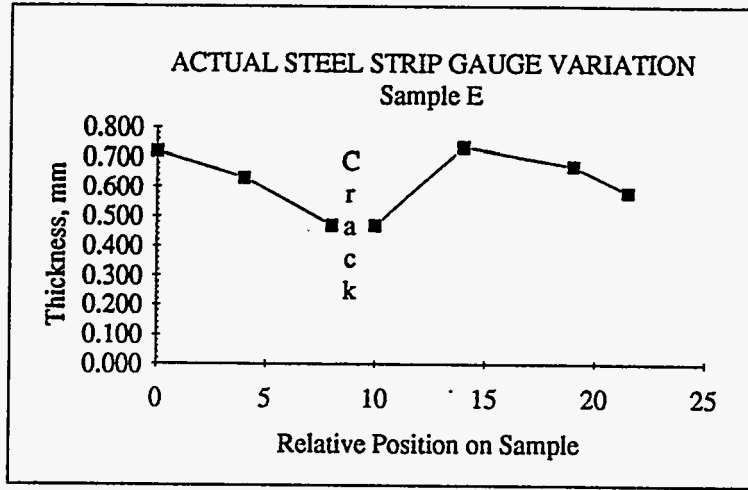
ACTUAL STEEL STRIP GAUGE VARIATION
Sample E

Scale Thickness Variation

Width Position	Bottom Thickness mm	Top Thickness mm
1	0.0140	0.0050
2	0.0104	0.0100
3	0.0150	0.0086
4	0.0160	0.0080
5	0.0184	0.0084
6	0.0100	0.0060
7	0.0100	0.0080
8	0.0140	0.0066
9	0.0196	0.0090
Average	0.0142	0.0081
Std Dev	0.0038	0.0013

CAST STRIP SCALE THICKNESS
Sample E
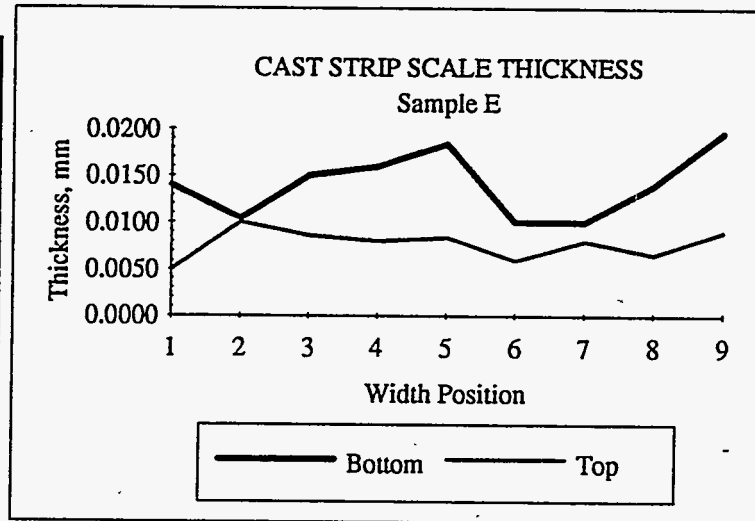
Observations

1 This sample was a cross section through a longitudinal crack.

2 Some rough surface on the top.

3 No obvious voids or cracks except for the major one.

Sample F

Strip Length	471 ft.
Relative Width	74.6 %

Thickness Variation

Width Position	Thickness mm
0	0.590
4	0.590
9	0.610
12.5	0.580
13	0.632
14	0.760
14.5	0.775
17	0.610
19	0.570
21	0.590
Average	0.64
Std Dev	0.08

ACTUAL STEEL STRIP GAUGE VARIATION
Sample F
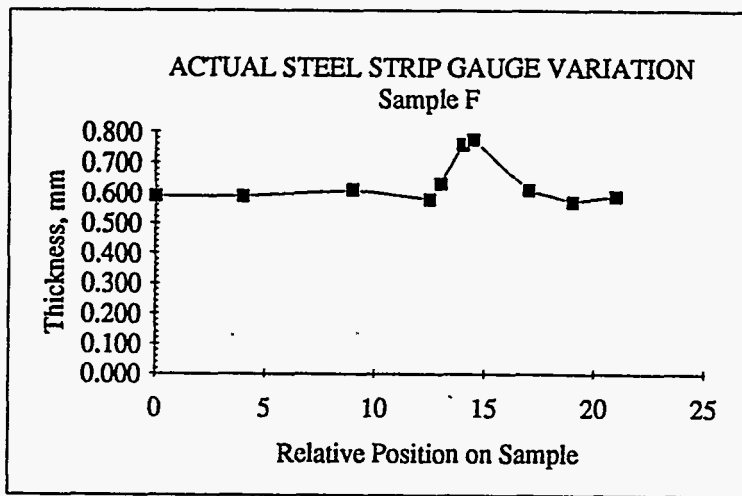
Scale Thickness Variation

Width Position	Bottom Thickness mm	Top Thickness mm
1	0.0144	0.0080
2	0.0150	0.0080
3	0.0120	0.0056
4	0.0020	0.0090
5	0.0020	0.0100
6	0.0200	0.0094
7	0.0120	0.0090
8	0.0160	0.0080
9	0.0100	0.0084
Average	0.0111	0.0084
Std Dev	0.0064	0.0013

CAST STRIP SCALE THICKNESS
Sample F
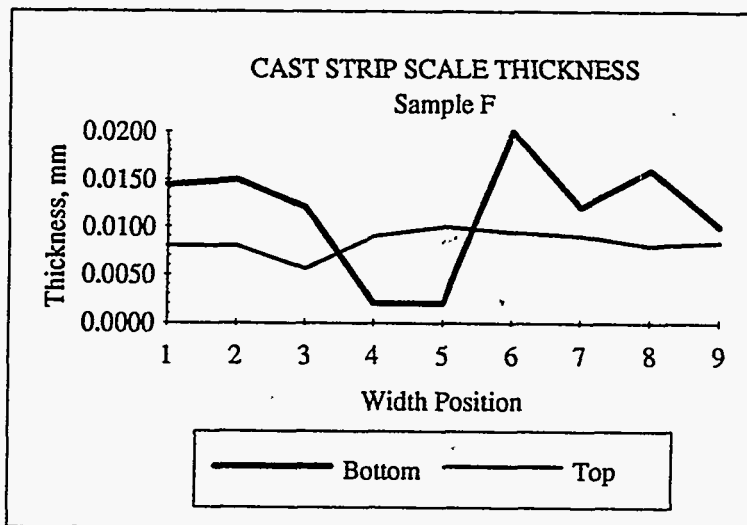
Observations

1 At the 0 width reference point there was a fissure, depth = 0.02 mm

2 At the 7 width reference point there was a deep fissure, depth = 0.27 mm
in a total thickness of 0.60 mm or 45% of the strip thickness.

APPENDIX A

Sample G

Strip Length   471 ft.
Relative Width   North Edge

Observations

1 This was an example of a dam formed by solidification on the casting nozzle which then pulled away and was frozen into the strip on the edge.
2 This dam contained a large glassy inclusion, thick =   0.48   length =   2.5 mm
3 Within the glass was a crystal inclusion showing evidence of dissolution.
4 Phase compositions

	Bulk Glass Phase	Inclusion Crystal Phase	Inclusion Glass Phase
Al2O3	21%	0%	47%
SiO2	29%	100%	0%
TiO2	12%	0%	1%
MnO	18%	0%	0%
FeO	14%	0%	0%
Cb2O3	6%	0%	2%
ZrO2	0%	0%	49%

by SEM-EDS analysis

Bulk Glass Phase is the melt slag increased in MnO and FeO by oxidation.
Inclusion is a piece of refractory.

Sample H

Strip Length   471 ft.
Relative Width   26.3 %

Thickness Variation

Width Position	Thickness mm
0	0.590
4	0.710
9	0.680
14	0.665
19	0.660
21	0.640
Average	0.66
Std Dev	0.04

ACTUAL STEEL STRIP GAUGE VARIATION
Sample H
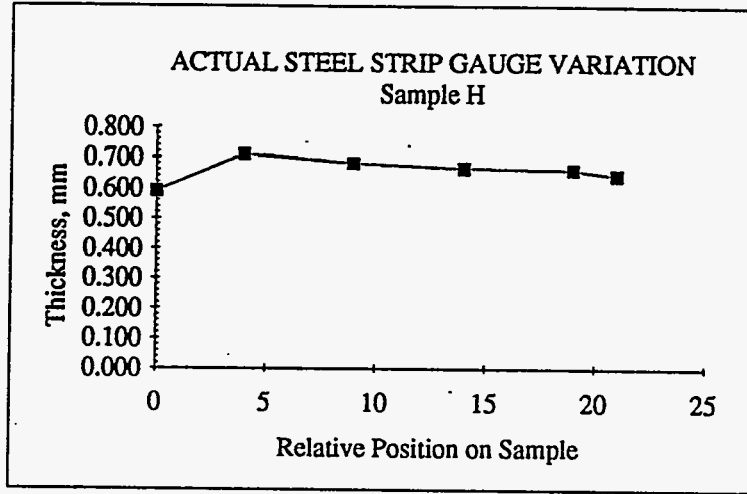
Scale Thickness Variation

Width Position	Bottom Thickness mm	Top Thickness mm
1	0.0080	0.0100
2	0.0100	0.0164
3	0.0080	0.0080
4	0.0070	0.0124
5	0.0100	0.0126
6	0.0100	0.0180
7	0.0080	0.0250
8	0.0080	0.0120
9	0.0110	0.0100
10		0.0080
Average	0.0089	0.0133
Std Dev	0.0015	0.0057

CAST STRIP SCALE THICKNESS
Sample H
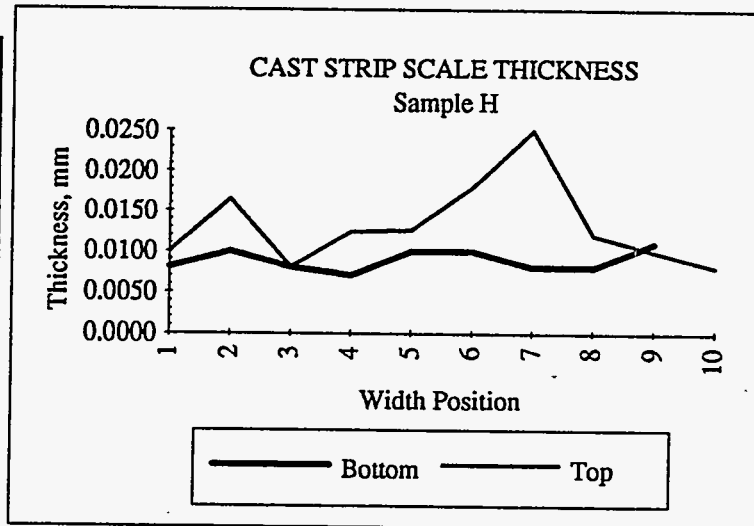
Observations

1 A cluster of internal porosity existed 0.14 mm from the bottom surface to 0.38 mm (approximately the strip center).

2 A string of pores began at the top surface and continued 0.27 mm into the strip or 38% of the strip thickness.

Summary of the Gauge and Scale Thickness Variation

| | Cast Length | Width Location from North | Strip Gauge | | Surface Scale Thickness | | | |
| | | | | | Bottom | | Top | |
			Av + sig.	Av - sig	Av + sig.	Av - sig	Av + sig.	Av - sig
Sample A	519	27.0%	0.69	0.57	0.0206	0.0062	0.0170	0.0083
Sample B	519	52.7%	0.65	0.58	0.0120	0.0068	0.0094	0.0068
Sample C	519	76.0%	0.72	0.54	0.0190	0.0129	0.0160	0.0038
Sample H	471	26.3%	0.70	0.62	0.0103	0.0074	0.0190	0.0075
Sample D	471	32.7%	0.67	0.57	0.0160	0.0104	0.0102	0.0064
Sample E	471	47.6%	0.72	0.50	0.0180	0.0104	0.0094	0.0068
Sample F	471	74.6%	0.72	0.56	0.0175	0.0047	0.0098	0.0071

Overall Average Values of All of the Measurements

| | Strip Thickness mm | Scale | |
		Bottom Thickness mm	Top Thickness mm
Mean	0.62	0.0123	0.0099
Std. Dev.	0.07	0.0046	0.0040

STRIP GAUGE VARIATION

SURFACE SCALE THICKNESS
Sample Length 519 ft

SURFACE SCALE THICKNESS
Sample Length 471 ft
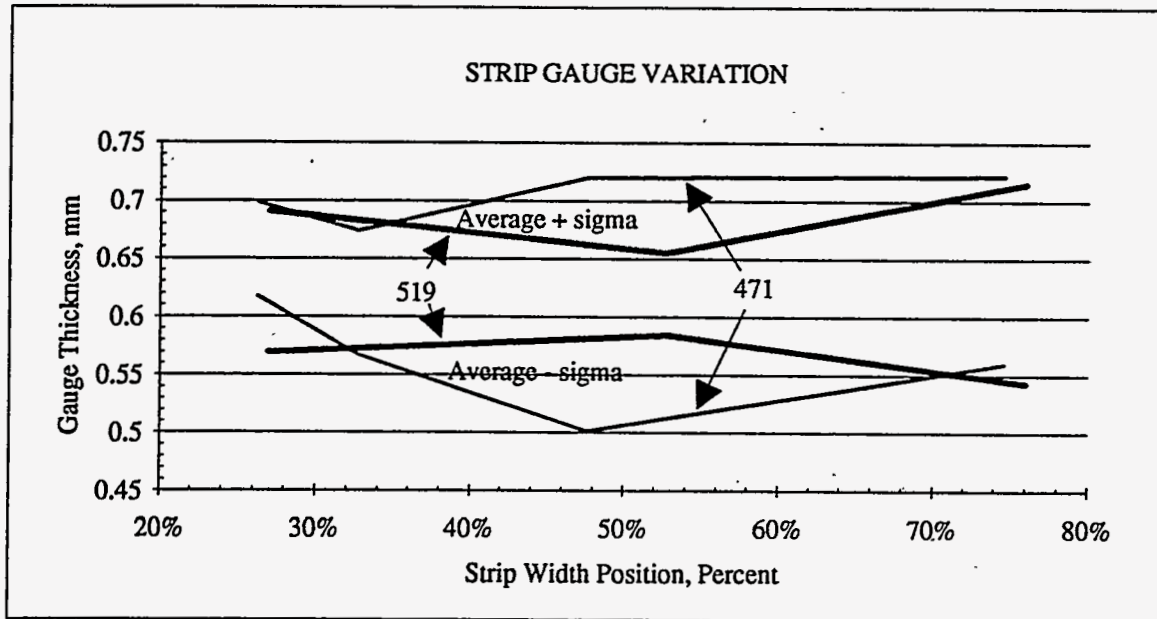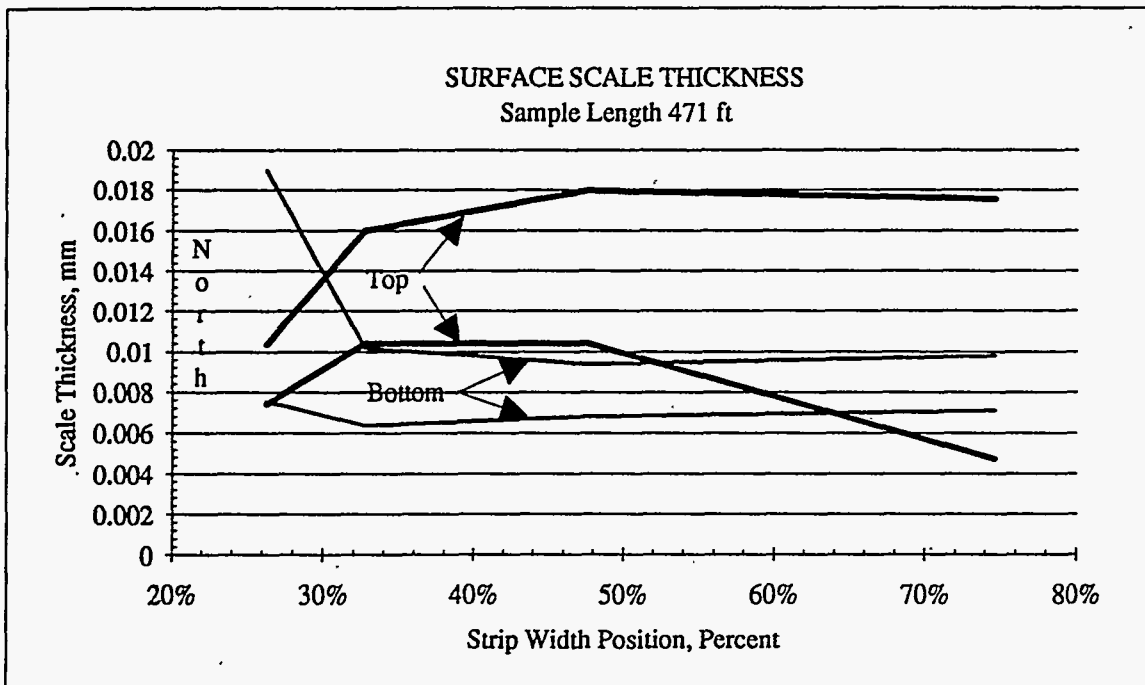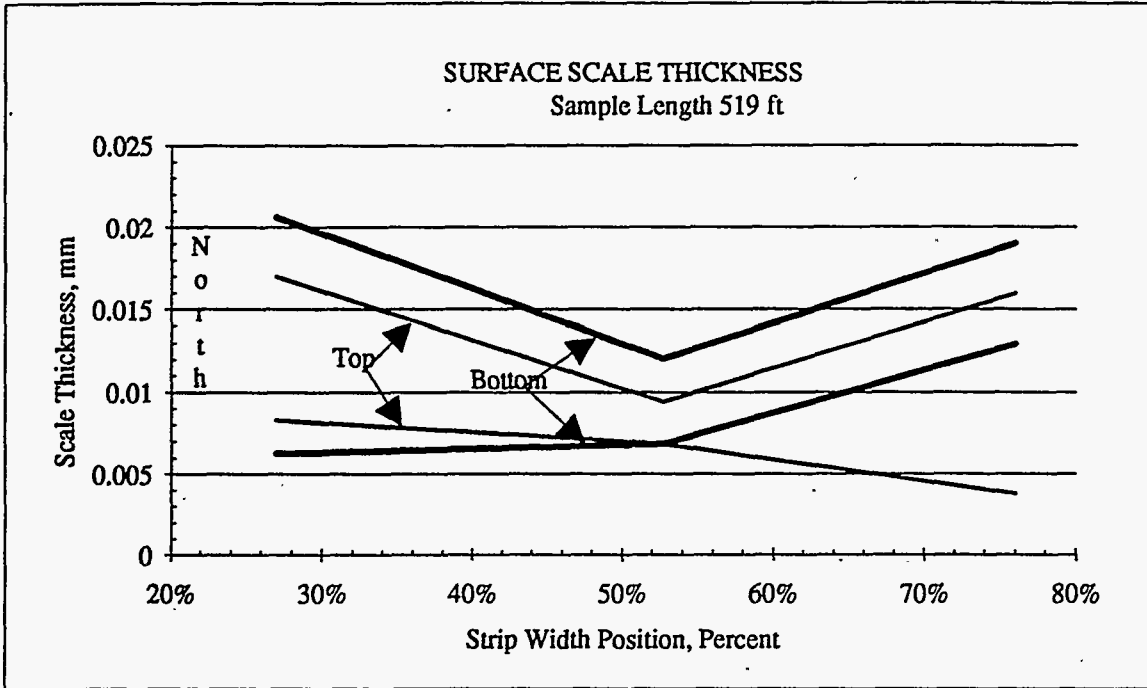
APPENDIX A

ESTIMATION OF IRON LOSS DUE TO SCALING

Density of Steel	490 lb/cf		
Density of Magnetite	322	Assumed composition of the hard grey scale	

			Amt Fe		
Average Steel Thickness	0.002066 ft		(Values converted from the averages of		
Average Scale Thickness	3.63E-05 ft		the above measurements)		
Weight of Steel per sq ft of strip	1.012	99.50%	1.007 lb Fe		
Weight of Scale per sq ft of strip	0.012	72.36%	0.008 lb Fe		

Portion of Iron Lost as Scale	0.83%

(a) Cast 1   NN 46333

Thickness
Direction

Longitudinal
Direction
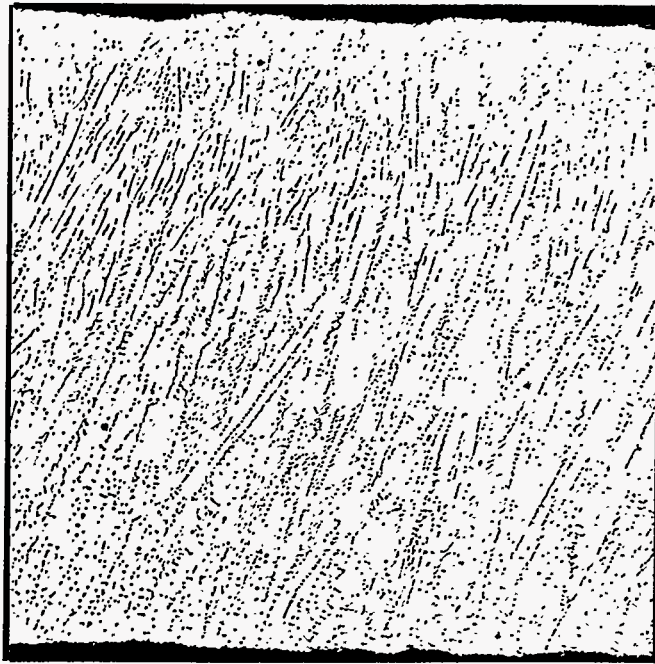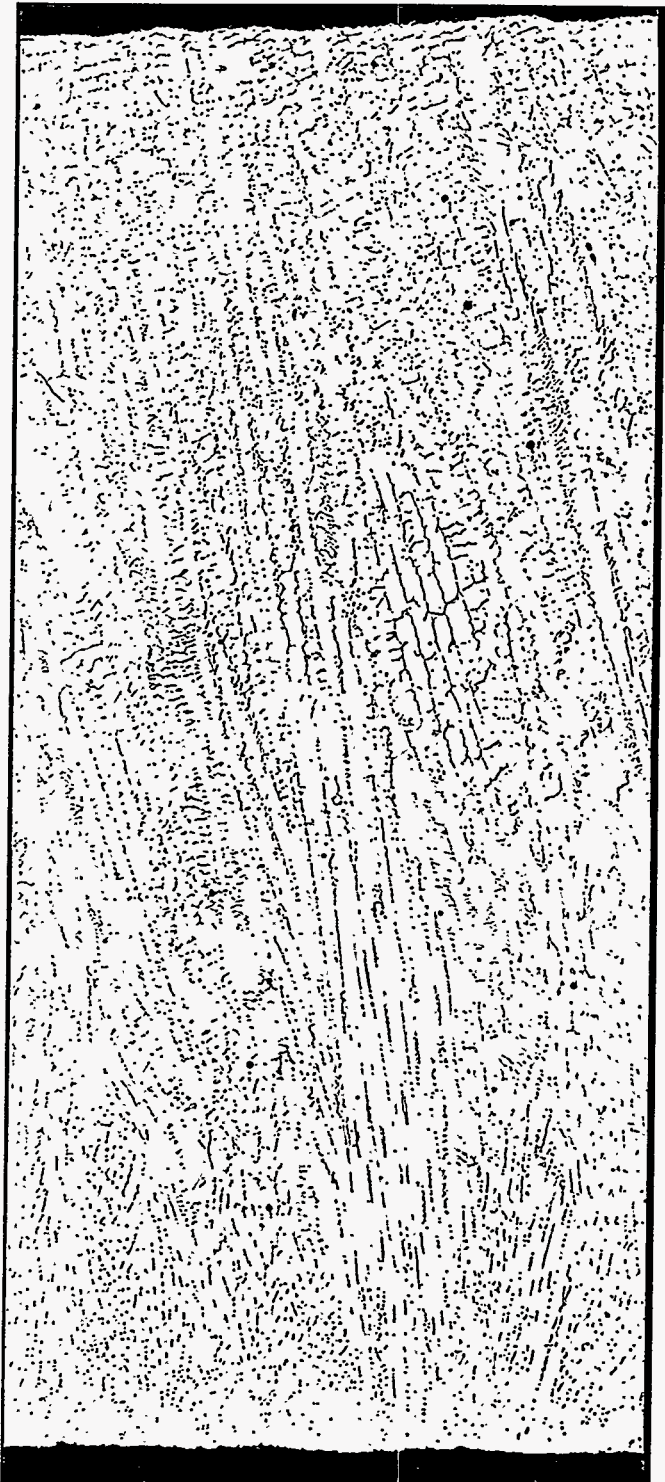
(b) Cast 2   NN 46334 & 46335
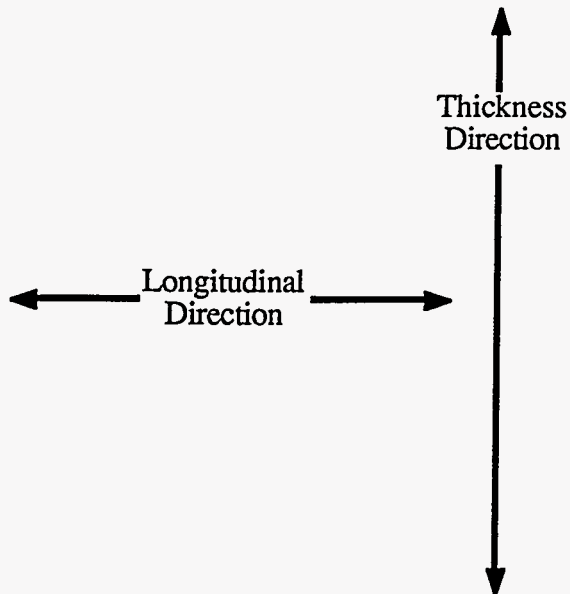
Figure 1 - As-cast microstructure consisting of austenite and a smaller fraction of delta - ferrite. 100 Magn.
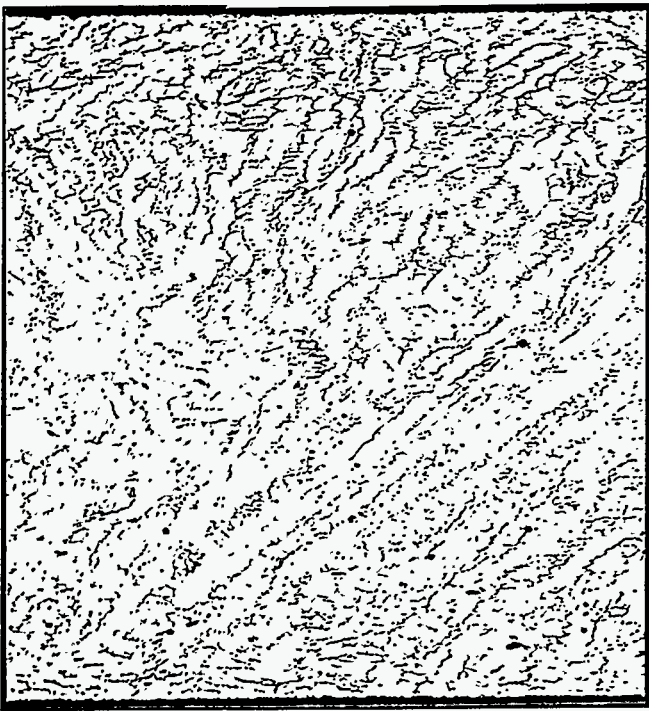
(a) Cast, Cold Rolled, Annealed   NN46343
100 Magn.
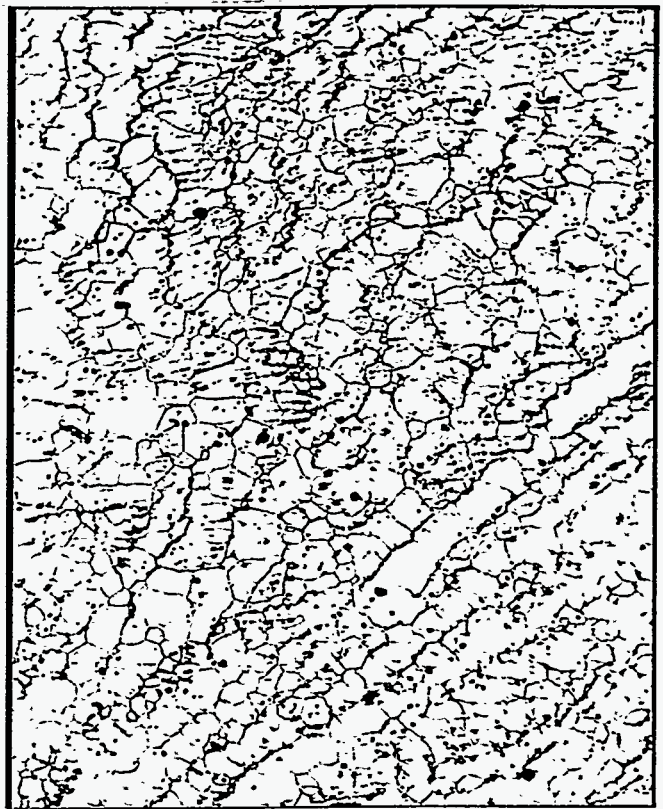
(c) Cast, Cold Rolled, Annealed   NN46344
200 Magn.
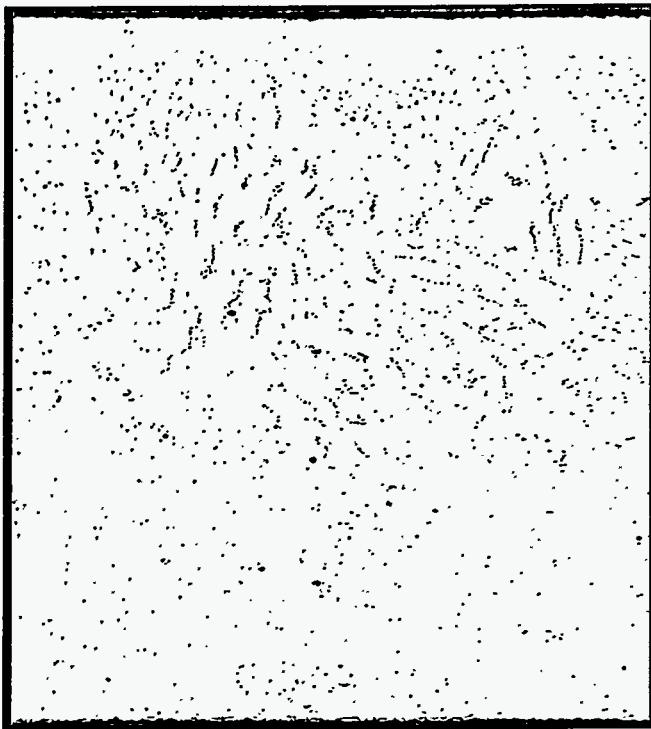
(b) Cast, Annealed   NN46345
Cold Rolled, Annealed   100 Magn.
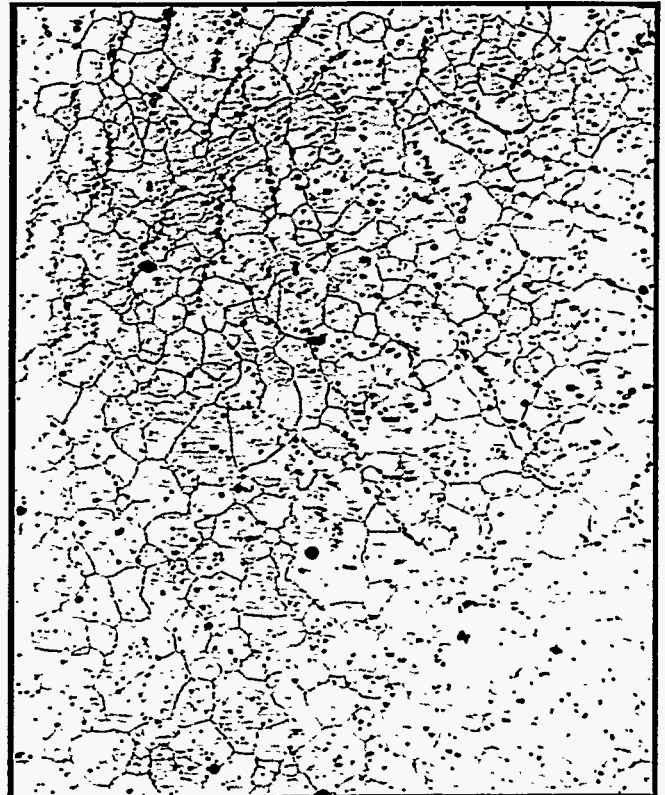
(d) Cast, Annealed   NN46346
Cold Rolled, Annealed   200 Magn.

Figure 2 - Longitudinal through thickness sections showing the microstructures of 50% cold rolled, annealed
Sheet, Cast 2.

(a) Cast 1 (1AC, L), 0.037 in., Longitudinal 100 Magn. N46329
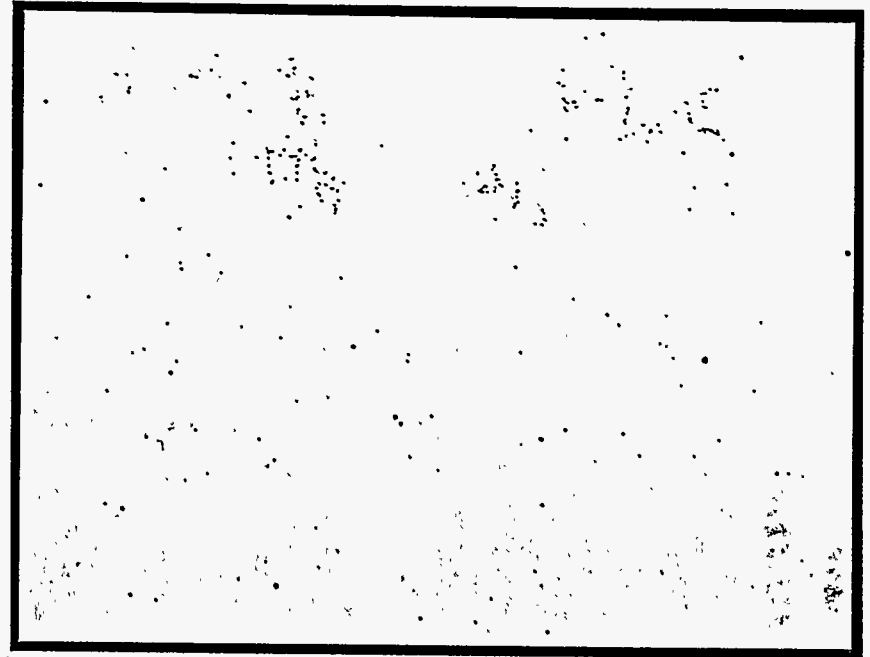
(b) Cast 1 (1AC, T), 0.037 in., Transverse 100 Magn. N46331
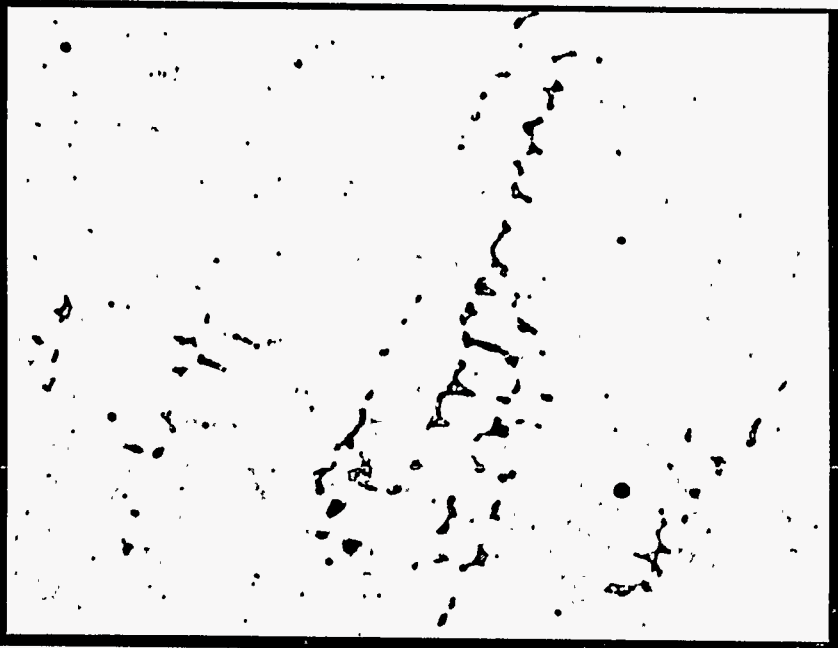
(c) Cast 1 (1AC, L), 0.037 in., Longitudinal 500 Magn. N46330
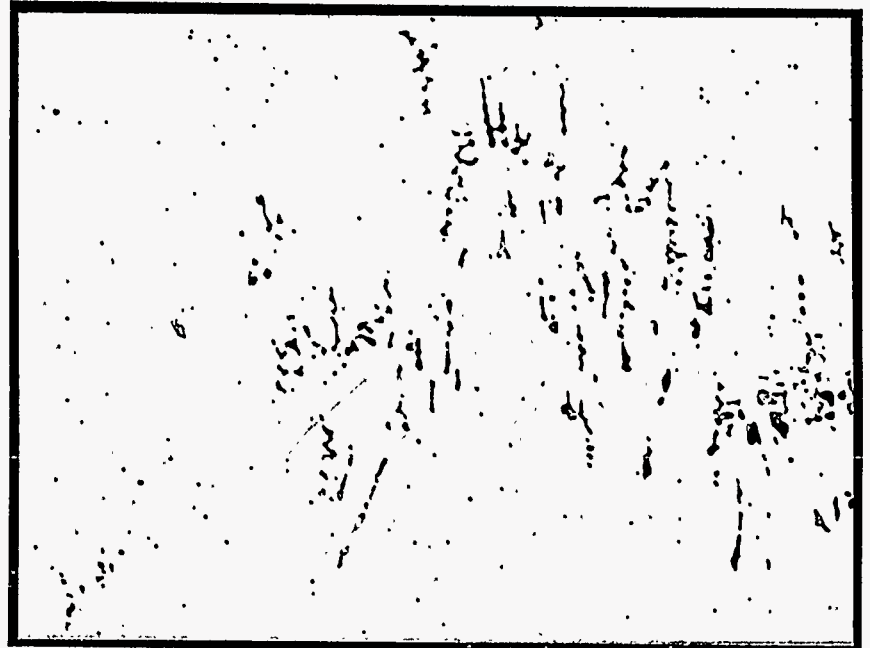
(d) Cast 2 (2AC, T), 0.074 in., Transverse 100 Magn. N46332

Figure 3 - As-cast interdendritic shrinkage porosity, single roll cast 304SS.

ROLLING DIRECTION

THICKNESS DIRECTION
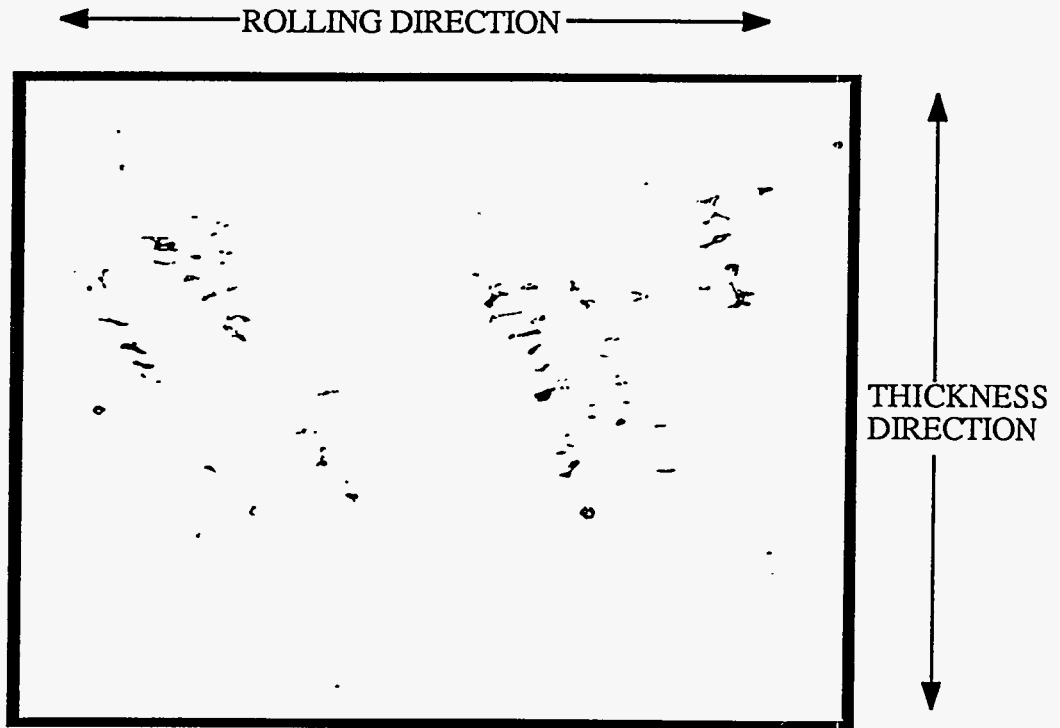
N46337

Figure 4 - Interdendritic shrinkage voids which persist in the cold rolled,
annealed sheet, single roll strip cast 304SS, Cast 1.
Sample (1AL), Longitudinal Section. 500 Magn.

N46336

Figure 5 - Surface rupture in the cold rolled, annealed sheet, single roll
strip cast 304SS, Cast 2.
Sample (2T), Transverse Section. 100 Magn.

Figure 6 - Fractographs of tensile specimen fracture surface of sample from cast 2 (2A-3, 0.074 in. cast, annealed 2050F, cold rolled 50%, annealed 2050F). Sample failed prematurely at 27% elong. in 2 in. as a result of the presence of interdendritic solidification shrinkage voids.

(a) Premature fracture initiation at site of a collection of voids.

(b) Fracture surface showing that the void morphology is consistent with that expected for interdendritic solidification shrinkage.

(c) Area of the fracture surface showing normal appearance consisting of ductile dimple rupture and void coalesence around silicate inclusions.

← Fracture Surface

← Intersection of Broad Face of Tensile Specimen and Fracture Surface.

← Broad Face of Tensile Specimen
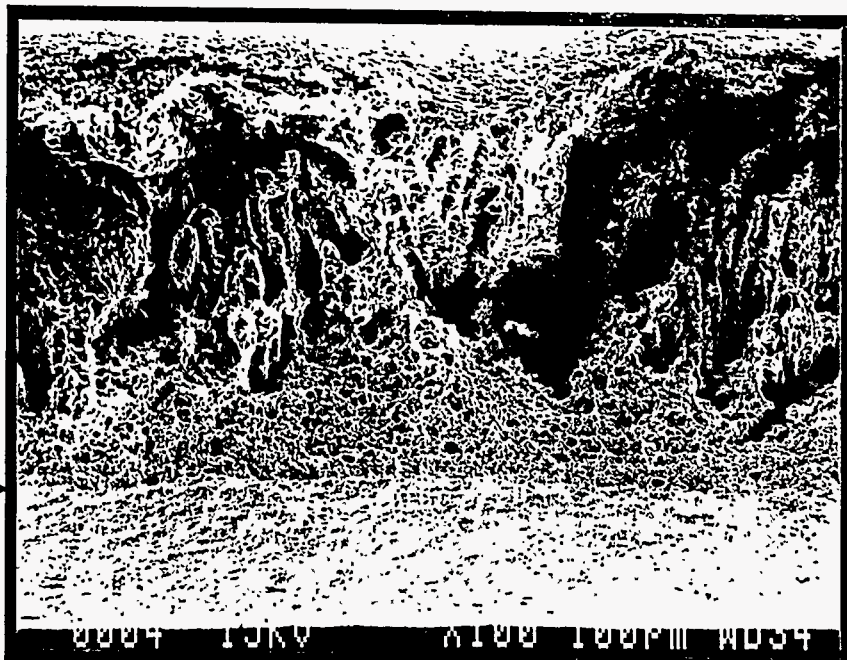
(a)   100 Magn. SM84022
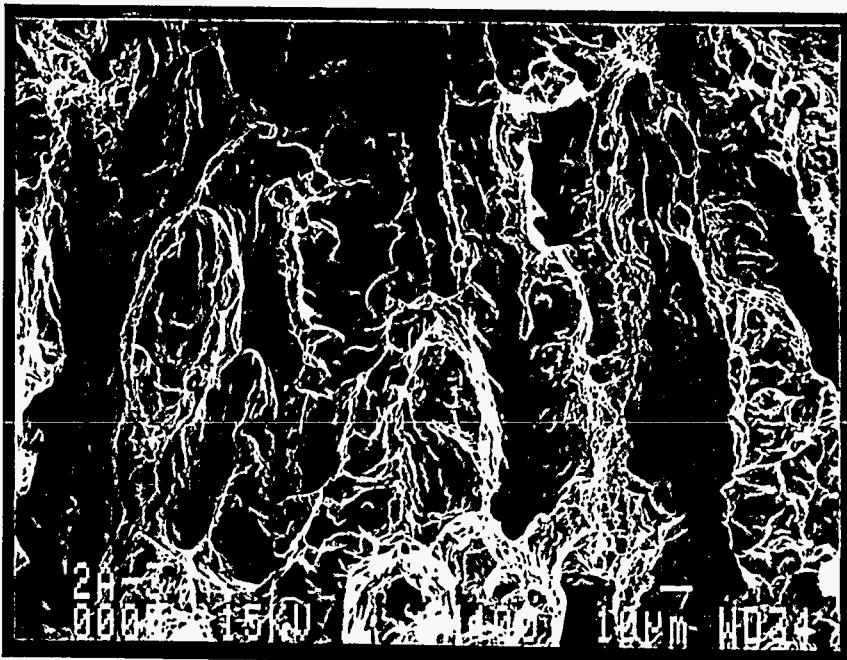
(b)   400 Magn. SM84023
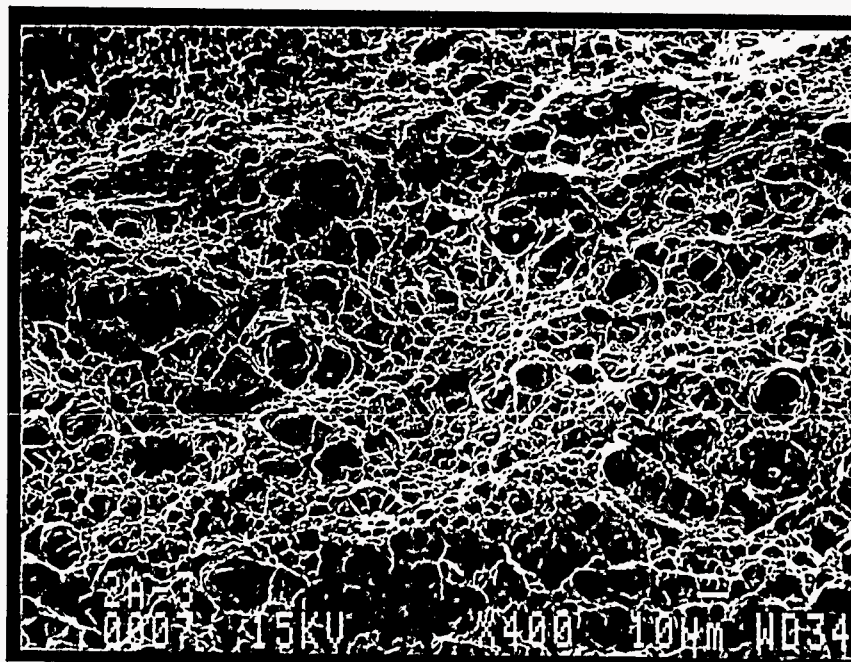
(c)   400 Magn. SM84025

Appendix XI

Evaluation of Strip Cast
304 Stainless Steel
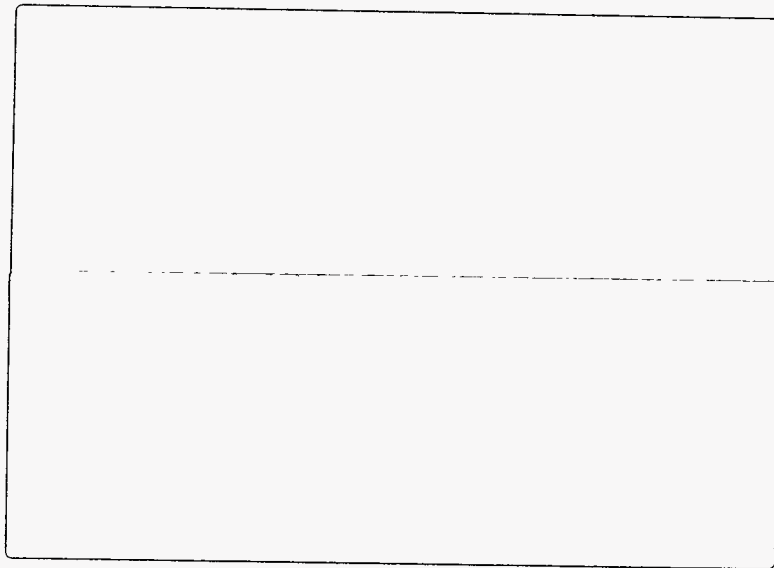
October 27, 1993

To:	Robert S. Williams	cc:	D. W. Follsteadt
	Senior Research Engineer		R. J. O'Malley
	Casting		R. C. Sussman
	Research & Technology		

From: R. E. Hook

Subject: Evaluation of Strip Cast 304 Stainless Steel

SUMMARY

The cold rolled, annealed properties of the strip cast 304 SS examined do not replicate well. Low elongation values (and fracture strengths) result from interdendritic shrinkage voids which persist after cold rolling and annealing. Since the voids do not "heal-up" as a result of cold rolling and annealing, the casting technology must be perfected to the point where interdendritic shrinkage voids are not present in the cast strip. For tensile test specimens free of these casting defects the properties were excellent. Elongation values in the range 56 to 61% were attained. It must be pointed out that due to circumstances and time constraints the three 304 SS casts made on the single roll caster were not conducted using all of features and best practices developed to date.

INTRODUCTION

Samples of 304 SS sheet from three casting trials were evaluated with respect to cast microstructure and cold rolled, annealed tensile properties and microstructure. The three materials are identified as CAST 1, CAST 2 and CAST 3 corresponding to the order in which the heats were cast. The cast strip samples received had nominal thicknesses of 0.037 in. (0.94 mm), 0.074 in. (1.88 mm) and 0.039 in. (0.99 mm), respectively.

PROCEDURE

Cast sheet samples which appeared to be free of cracks were selected for cold rolling and annealing for the purpose of evaluating the tensile properties. The surface oxide was removed from the sheets by a Kolene molten salt treatment followed by acid pickling in a nitric-hydrofluoric acid solution. Following removal of the surface oxide, numerous longitudinal cracks became evident on samples of the two lightest gage sheets from Cast 1 and Cast 3. The cracks were typically on the order of 1 in. (25 mm) in length. The sheet samples of the heaviest gage Cast 3 showed very little cracking.

After pickling, half of the cast sheet was annealed by placing the sheets in a furnace heated to 2050F (1120C) in an air atmosphere. Following exposure times in the furnace of 4 min. for the

1

light gage cast sheet and 7 min. for the heavy gage cast sheet, the sheets were air cooled, then pickled to remove the oxide. The purpose of annealing some of the cast sheet before cold rolling was to reduce, or eliminate, the delta-ferrite present in the cast microstructure. It is standard practice to anneal hot band coils of 304 SS rolled from conventional strand cast slabs for this purpose.

Sheet samples, both as-cast and cast plus annealed, were cold rolled. The light gage sheet from Cast 1 and Cast 3 was cold rolled 40% and the heavy gage sheet from Cast 2 was cold rolled 50%. The cold rolled samples were annealed by placing the sheets in a furnace heated to 2050F (1120C) in an air atmosphere. Following exposure times in the furnace of 3 min. for the light gage sheet and 4 min. for the heavy gage sheet, the sheets were air cooled, then pickled to remove the oxide. Replicate blanks were sheared from the sheets for machining into sheet tensile specimens according to specification ASTM A370. All testing was done in the longitudinal direction, i.e. parallel to the rolling direction which was parallel to the casting direction.

The microstructures of cast samples and of cold rolled, annealed samples were evaluated by optical microscopy. The tensile fracture surfaces of selected samples were examined by SEM.

RESULTS AND DISCUSSION

Tensile Properties Cold Rolled, Annealed Strip Cast Sheet

The cold rolled, annealed properties of the cast strip do not replicate well as shown in Table I. Low elongation values (an fracture strengths) result from interdendritic shrinkage voids which persist after cold rolling and annealing. Samples for which casting defects have not degraded the properties are shown in **bold face type.** These properties compare very favorably with those of conventionally produced 304 SS.

Microstructures

(1) Microstructures of Strip Cast Sheet

Figure 1 shows examples of the cast structures which consist of a two phase mixture. The major constituent is a Fe-Cr-Ni austenite while the minor phase is delta-ferrite.

Figure 3 shows examples of porosity found in samples of the cast strip. The porosity as it appears in both the longitudinal and the transverse section of the as-cast sheet is shown. It is clear from the morphology of the voids that they are interdendritic solidification shrinkage cavities.

(2) Microstructures of Cold Rolled, Annealed Strip Cast Sheet

Figure 2 (a) and (c) shows the microstructure of the cast strip that was cold rolled and annealed. An appreciable amount of delta-ferrite still remains in the structure following this processing. Figure 2 (b) and (d) shows that the amount of delta-ferrite is substantially less when the processing involved annealing the cast strip before cold rolling. However, the resulting tensile properties were the same for both processing routes (see Table I).

Figure 4 shows that the shrinkage voids in the cast strip persist after cold rolling and annealing. Figure 5 shows a surface rupture as it appears in a transverse section of a cold rolled, annealed sheet. It appears that the ruptured region may be associated with the presence of the shrinkage voids.

Figure 6 demonstrates that the cause of premature tensile failure, and the reduced tensile elongation values, is the presence of the interdendritic solidification cavities or voids.

2

REFERENCES

Research Laboratories Record Books
Mechanical Testing: BOOK MT055, thJOB 2486
Microstructure Lab.   BOOK 7135, PAGE 21
                           BOOK 7141, PAGE 25
                           BOOK 7139, PAGE 13

Research Daybooks
Microstructure Lab.   BOOK 6932, PAGES 15, 82

Rollin E. Hook
Principal Research Metallurgist
Research & Technology

3

Table I - Tensile Properties of Strip Cast, Cold-Rolled, Annealed 304 SS Sheet, Longitudinal Tests Only.

Gage (in.)	0.2% Offset YS (ksi)	UTS (ksi)	% Elong. (2 in.)	HRB
Cast 1 - 0.037 in. Cast. Cold Rolled 40 Pct. Annealed 2050F. (5 replicate test samples).				
0.0214	35.6	89.3	32.0	74.5
0.0230	35.9	95.7	44.0	74.5
0.0218	35.6	97.0	49.0	75.5
0.0217	37.2	**98.5**	**57.0**	76.0
0.0221	36.8	**98.3**	**61.5**	76.5
Cast 1 - 0.037 in. Cast. Annealed 2050F. Cold Rolled 40 Pct. Annealed 2050F. (4 replicate test samples).				
0.0226	35.2	92.1	fractured outside ga. marks	77.0
0.0222	33.4	**96.7**	**60.5**	73.5
0.0228	34.1	83.0	27.5	73.5
0.0222	34.2	73.1	20.0	75.0
Cast 3 - 0.039 in. Cast. Cold Rolled 40 Pct. Annealed 2050F. (4 replicate test samples).				
0.0245	35.8	75.0	17.0	75.0
0.0245	36.6	99.5	49.5	76.5
0.0238	36.4	**99.1**	**56.0**	76.5
0.0247	35.6	80.1	22.0	75.0
Cast 3 - 0.039 in. Cast. Annealed 2050F. Cold Rolled 40 Pct. Annealed 2050F. (5 replicate test samples).				
0.0234	33.7	94.0	43.0	74.4
0.0243	34.1	81,4	25.0	76.0
0.0244	33.3	72.2	20.0	74.5
0.0243	33.4	66.1	15.0	72.5
0.0232	34.3	**96.1**	**52.5**	72.5
Cast 2 - 0.074 in. Cast. Cold Rolled 50 Pct. Annealed 2050F. (4 replicate test samples).				
0.0353	36.6	**95.4**	**53.5**	76.5
0.0349	35.0	**95.2**	**58.5**	74.5
0.0346	36.1	**95.9**	**56.0**	80.0
0.0354	35.9	**95.0**	**56.0**	80.0
Cast 2 - 0.074 in. Cast. Annealed 2050F. Cold Rolled 50 Pct. Annealed 2050F. (5 replicate test samples).				
0.0364	35.6	**95.2**	**56.0**	80.0
0.0361	35.0	**94.4**	**56.5**	79.5
0.0352	34.9	84.5	27.0	81.0
0.0354	34.7	**94.9**	**55.0**	79.5
0.0352	34.8	93.6	42.5	79.5

Average Tensile Properties (180 Tests) of Cold-Rolled, Annealed Mill Produced 304 Stainless Steel Sheet

Gage (in.)	YS (ksi)	UTS (ksi)	% Elong. (2 in.)	HRB
longitudinal				
0.030/0.050	42.38	98.80	55.4	81.5
transverse				
0.030/0.050	41.85	94.80	59.5	

4

Appendix XII

Engineering Study for Strip Casting Pilot Plant
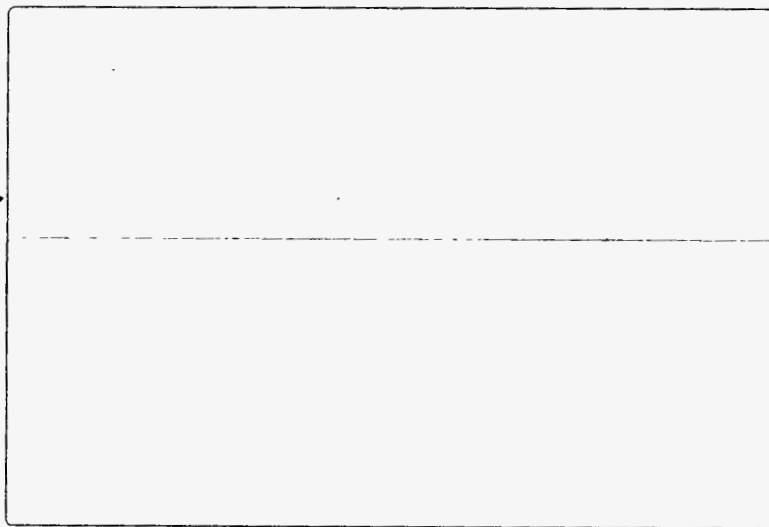
Specifications for Pilot Plant

The specifications for a Pilot Plant are based on the premise that four such casters, casting 80" wide, would have the productivity of a current slab casting shop. A Typical slab caster has a productivity of around 300 ton/hr. One fourth of that would be 75 ton/hr. A 48" wide Pilot Caster would therefore need a productivity of 45 ton/hr. to meet the above stipulation. In order to have a reasonable length of time to cast a heat, a 20 ton Melt Shop was chosen which would give at least a 25 min. casting time.

A 45 ton/ hr. rate would require a 48" wide strip by 1/8" thick running at 75 fpm. The Strip 1D model showed that the casting wheel would have to be 80" in diameter and use a 60_ arc of contact to meet these requirements. Casting on an 80" wheel from 75_ BTDC to 15_ BTDC would give the 60_ arc of contact which would require a liquid metal head of approximately 28".

The specifications for the Pilot Strip Caster would be:

Melt Shop:	20 Ton Induction Furnace w/Vacuum Degas or 20 Ton Vacuum Induction Furnace
Ladle Support:	A ladle support or car must be designed to support a 20 Ton capacity ladle over the Pouring Box and provide a shroud to protect the metal into the Pouring Box.
Pouring Box:	The Pouring Box Must be induction heated (preferred) and capable of melting a 1,000 lb. heel and maintaining the temperature of the heat exiting the box at a constant temperature. Total capacity of the box when filled to the 28" head exposed to the wheel would be approximately 4 1/2 ton. The Pouring Box must be capable of being accurately positioned in both the vertical and horizontal directions as well as tilt and wag. It must have an abort feature which quickly empties the molten steel in case of a nozzle failure.

Caster:		
Wheel Diameter		80"
Wheel Length	58"	
Arc of Contact	60_	
Head of Molten Steel (max.)		28 1/4"
Drive System	30 HP variable speed	
Wheel speed		25-200 fpm
Cooling Water - Wheel		2250 gpm @ 120_ F
Cooling Water - Other		250 gpm

Surface Conditioning   Grit Blasting

The Caster must have an exit conveyor which removes the strip at approximately TDC and conveys it to a set of pinch rolls which are synchronized with the casting wheel and/or capable of applying a slight tension to the strip coming off the wheel

Strip Handling: A 40' space should be provided between the Caster and the Coiler to allow for either a spray mist cooling or a Holding Furnace since the temperature treatment of the strip coming off the Caster has not been determined yet.

The strip collection system should include a set of pinch rolls, a shear and a 20 ton coiler.

The following estimate for a Greenfield site construction of a 20 ton Melt Shop and a 48" wide pilot strip caster was contracted to Belcan Engineering Group, Inc. Cincinnati, Ohio. Estimating was done using past engineering reports on similar installations, verbal estimates from vendors and educated ball park figures. The estimates should be accurate enough for budget planning.

BELCAN ENGINEERING GROUP, INC.

DATE   September 30, 1993   SHEET   1   OF   4

ENGINEERING ESTIMATE FOR
ARMCO RESEARCH & TECHNOLOGY, MIDDLETOWN, OHIO

PROJECT NO.   315-6640   BY: J.M. Torok

PROJECT: Strip Caster Pilot Plant   ESTIMATE NO.   1

Cost Account	Account Description	Quantity	Unit	Total Installation Cost Labor, Material, Equip. Usage, SubContract.	Engineered Equipment	Total Capital
1000	**SITE FACILITIES:**					
	Land	5.0	AC	50,000		50,000
	Plant Road	3,070	SY	49,000		49,000
	Fencing	1,900	LF	20,000		20,000
	Security	1	LS	10,000		10,000
	Water System	440	LF	17,600		17,600
	Sewage System	360	LF	18,000		18,000
	Storm Drainage	800	LF	35,000		35,000
	Gas System	200	LF	6,000		6,000
	132 KV Elect. Service and Substation	300	LS	350,000	375,000	725,000
	Site Improvements Fine Grade	24,200	SY	10,000		10,000
	Parking Area	300	SY	6,000		6,000
	Total Site Facilities:			571,600	375,000	946,600
2000	**BUILDING AND CRANES FACILITIES**					
	Scrap Prep. Bldg. 48'W x 40'H x 140'L	6,720	SF	806,400		806,400
	Shop & Coil Delivery Storage Bldg. 48'W x 34'H x 180'L	8,640	SF	881,300		881,300
	Melting Furnace & Caster Bldg. 56'W x 62'H x 120'L	6,720	SF	1,250,000		1,250,000
	MCC Room 20'W x 16'H x 60'L	1,200	SF	57,600		57,600
	Degasser 20'W x 48'H x 40'L	800	SF	115,200		115,200
	Cooling & Hydraulic Room 20'W x 16'H x 40'L	800	SF	76,800		76,800
	Fce., Degas, Caster Pulpit 8'W x 16'H x 60'L	480	SF	46,080		46,080
	Office, Rest & Lunch Room 22'W x 12'H x 80'L	1,760	SF	147,900		147,900
	Guard House	20	SF	5,120		5,120
	20T Shipping Crane and Electric	1	EA	65,000	500,000	565,000
	20/10T Scrap Crane and Electric	1	EA	65,000	550,000	615,000
	50/20T Ladle Crane and Electric	1	EA	90,000	1,000,000	1,090,000
	Total Building and Cranes Facilities			3,606,400	2,050,000	5,656,400

ENGINEERING ESTIMATE FOR
ARMCO RESEARCH & TECHNOLOGY, MIDDLETOWN, OHIO

PROJECT NO.   315-6640   BY: J.M. Torok

PROJECT: Strip Caster Pilot Plant   ESTIMATE NO.   1

Cost Account	Account Description	Quantity	Unit	Total Installation Cost Labor, Material, Equip. Usage, SubContract.	Engineered Equipment	Total Capital
3000	**SERVICES PIPING:**					
	Potable Water Piping	450	LF	11,250		11,250
	Make-Up Water Piping	600	LF	21,000		21,000
	Steam Piping	420	LF	14,700		14,700
	Oxygen Piping	370	LF	9,250		9,250
	Natural Gas Piping	1,220	LF	30,500		30,500
	Compressed Air Piping	1,050	LF	26,250		26,250
	Cooling Water	1,800	LF	72,050		72,050
	Argon Station and Piping & Instrumentation	1	LS	200,000	100,000	300,000
	Total Services Piping			**385,000**	**100,000**	**485,000**
4000	**MELTING FACILITIES:**					
	20 Ton Furnace (Induction) AJAX	COMP.		400,000	900,000	1,300,000
	Scrap Buckets & Scale	3	EA	10,000	110,000	120,000
	20 Ton Teeming Ladles	3	EA	40,000	82,000	122,000
	Ladle Repair Station & Drying	2	EA	40,000	73,000	113,000
	Ladle Preheat Station	2	EA	40,000	73,000	113,000
	Vacuum Tank Degasser 20 Ton	1	LS	1,500,000	1,500,000	3,000,000
	Water System For Machine & Ejection	1	LS	100,000	150,000	250,000
	Alloy Feed System & Handling	1	LS	40,000	60,000	100,000
	Ladle Preheat & Drying	1	EA	25,000	30,000	55,000
	Electric and Controls	1	LS	200,000	200,000	400,000
	Total Melting Facilities			**2,395,000**	**3,178,000**	**5,573,000**

BELCAN ENGINEERING GROUP, INC.

ENGINEERING ESTIMATE FOR

ARMCO RESEARCH & TECHNOLOGY, MIDDLETOWN, OHIO

PROJECT NO. 315-6640   BY: J.M. Torok

PROJECT: Strip Caster Pilot Plant   ESTIMATE NO. 1

Section	Account Description	Quantity	Unit	Total Installation Cost Labor, Material, Equip. Usage, SubContract.	Engineered Equipment	Total Capital
5000	**STRIP CASTER FACILITIES:**					
	48'W x 1/8" Strip Caster Complete	1	EA	800,000	900,000	1,700,000
	Ladle Stand	1	LS	40,000	80,000	120,000
	Operating Platform	200	SF	20,000	40,000	60,000
	Hydraulic System and Controls	1	EA	30,000	50,000	80,000
	Electric Controls	1	LS	200,000	200,000	400,000
	Cooling Water	1	LS	150,000	100,000	250,000
	Pinch Rolls Fnd. Frame w/Drive & Elec. Controls	1	EA	35,000	45,000	80,000
	Loop Pit Complete	1	LS	120,000	20,000	140,000
	Runout Table Complete & Elect. Controls	40	FT	25,000	38,000	63,000
	Holding Furnace Complete (Optional)	40	FT			
	Metal Level Control			100,000		100,000
	Pouring Box Heating			200,000		200,000
	Substrate Conditioning			100,000		100,000
	Thickness Measuring			100,000		100,000
	Data Collection System			120,000		120,000
	Total Strip Caster Facilities:			**2,040,000**	**1,473,000**	**3,513,000**
6000	**STRIP COLLECTION SYSTEM:**					
	Pinch Roll Complete	1	EA	35,000	45,000	80,000
	Shear Complete	1	EA	40,000	68,000	108,000
	Tension Reel Complete	1	EA	200,000	350,000	550,000
	Coil Storage Area 50' x 20'	1,000	SF	5,000		5,000
	Total Strip Collection System:			**280,000**	**463,000**	**743,000**

BELCAN ENGINEERING GROUP, INC.

ENGINEERING ESTIMATE FOR
ARMCO RESEARCH & TECHNOLOGY, MIDDLETOWN, OHIO

DATE September 30, 1993 SHEET 4 OF 4

PROJECT NO. 315-6640 BY: J.M. Torok

PROJECT: Strip Caster Pilot Plant ESTIMATE NO. 1

Section	Account Description	Quantity	Unit	Total Installation Cost Labor, Material, Equip. Usage, Subcontract.	Engineered Equipment	Total Capital
7000	MISCELLANEOUS					
	Cooling Tower 5,000 GPM	1	EA	90,000	90,000	180,000
	Pumps & Piping	4	EA	125,000	80,000	205,000
	Baghouse, Stack, and Fan	1	EA	200,000	475,000	675,000
	Dust Collector System	1	LS	110,000		110,000
	Air Comp. & Supply Piping & Dryer	1	LS	150,000	150,000	300,000
	Electric & Controls	1	LS	160,000	200,000	360,000
	Elect. Power 13.8 Sub.	1	LS	80,000	244,000	324,000
	Total Miscellaneous:			915,000	1,239,000	2,154,000
	TOTAL DIRECT COST:					19,071,000
9000	INDIRECTS					
	Engineering					1,000,000
	Construction Management					500,000
	Overhead & Profit					2,550,000
	Permits					50,000
	Taxes					350,000
	Contingency					3,479,000
	Total Indirect Cost:					7,929,000
	TOTAL PROJECT COST:					27,000,000